University of East Anglia

Stepwise synthesis of new porphyrinoid hybrids

Ibtesam Yehya A Mashnoy

Supervised by

Prof Andrew N. Cammidge

This thesis is submitted in partial fulfilment of the requirements of the degree of Doctor of Philosophy at the University of East Anglia

2025

Declaration

The research described in this thesis is, to the best of my knowledge, original except where due reference has been made.

Ibtesam Mashnoy

Abstract

This thesis aims to develop new synthetic strategies for stepwise, controlled construction of novel core-modified phthalocyanine hybrids – specifically diazabenzoporphyrin derivatives with one isoindole unit replaced by methine-linked thiophene ("tribenzodiazathiaporphyrins"). Treating benzamidine with 2,5-diethynylthiophene under copper-free Sonogashira cross-coupling reaction conditions led to the successful formation of bisaminoisoindoline thiophene as the required intermediate for the formation of the target macrocycles. Reaction of this intermediate with phthalonitrile gave the new macrocycles, and initial synthetic investigations involved substituting this top isoindole unit through using a range of phthalonitriles. The substituted phthalonitrile was reacted with the intermediate to form the desired macrocyclic structures. The different substituents on the top isoindole of the macrocycle has only a small effect on the absorption and emission properties; a slight red shift was observed in the Q band of the non-peripherally phenyl substituted derivative.

Modifying the synthetic route allowed substitution of both side isoindoles of the macrocycle so that the effect of modification on top and side fragments could be investigated. Again, a minimal effect was observed in the absorption and fluorescence emission properties across this series.

Isomeric macrocycles (*S*-confused, *cis*-diazatribenzothiophenyl porphyrins) were also synthesised using a similar approach, starting from 2,4-diethynylthiophene. However, in this case, we focused on the 2,4-positions of the thiophene moiety. The effect of modifying the position was also investigated in terms of the macrocycle's properties. This macrocycle, which is not aromatic, showed a significant blue shift of ~100 nm in comparison with tribenzodiazathiaporphyrins, where the longest wavelength peak appears around 644 nm.

Alternative reactants such as diamines, dicarbonyls and di-carboxylic acid chlorides, were also used to attempt macrocycle formation from our intermediate bisaminoisoindoline thiophene. Unfortunately, these attempts were unsuccessful and did not yield any of the desired macrocycles. The reaction of bisaminoisoindoline thiophenes with phthaloyl chloride formed a bisphthalimide derivative rather than the macrocycle. Replacement of the thiophene unit with bithiophene or pyridine was also investigated, but indicated no macrocycle formation.

The final part of the thesis describes an attempt to synthesis different macrocycles with distinct patterns of π-conjugation, specifically using triphenylene as a building block. A 2,11-diaminoisoindoline-triphenylene intermediate was produced by coupling triphenylene-2,11-diacetylene with bromobenzamidine using the same strategy that had been successfully used earlier. Attempts to produce a macrocycle by inserting a phthalonitrile unit were unsuccessful. However, attempts to cyclise the intermediate directly led to interesting new materials. We found evidence for intramolecular cyclisation, but the dominant product resulted from dimerization and spectroscopic (NMR) evidence suggests a complex, twisted conformation for this large macrocycle because there is a clear indication that symmetry is broken.

This thesis is dedicated to

My parents,

My husband, and

My beloved kids.

Acknowledgements

I would like to express my heartfelt gratitude to my supervisor, Professor Andrew N. Cammidge for his unlimited support, invaluable guidance, understanding and help throughout my journey as a PhD student. I am very appreciative of his patience, as well as his kindness and attentiveness.

I would also like to extend my thanks to Dr. Isabelle Fernandes for her advice and support. I would like to acknowledge her, Dr. Joseph Wright, and Dr. David Hughes for their assistance with X-ray crystallography processing. I extend my thanks to all past and current members of Cammidge's group for their support and for creating a brilliant working environment.

I want to extend my gratitude to everyone in the School of Chemistry, particularly those on the third floor. I am also thankful to the technical staff in the School of Chemistry for their assistance and for maintaining the instruments.

A special and massive thanks to my husband, Qasem, and my kids, Ariam, Rayan, Eyad, and Leen for their love, endless support, patience, and encouragement at every stage of my study. I would like to express my deepest gratitude to my parents and sisters for their constant support and encouragement throughout my study in the UK.

Lastly, I would also like to thank Najran University and the Saudi Culture Bureau for encouraging me to study abroad and funding my PhD research.

Abbreviations

Ac	acetate
br	broad
BINAP	2,2′-bis(diphenylphosphino)-1,1′-binaphthalene
DABCO	1,4-diazabicyclo[2.2.2]octane
DBU	1,8-diazabicyclo[5.4.0]undec-7-ene
DBN	1,5-diazabicyclo[4.3.0]non-5-ene
DCM	Dichloromethane
DDQ	2,3-dichloro-5,6-dicyano-1,4- benzoquinone
DIPEA	*N,N*-diisopropylethylamine
DMF	*N,N*-dimethylformamide
eq.	equivalent
MALDI-TOF	matrix-assisted laser desorption/ionisation-time-of- flight
MW	Microwave
NMR	Nuclear Magnetic Resonance
Pn	phthalonitrile
PE	Petroleum Ether
Pc	Phthalocyanine
Ph	Phenyl
r.t.	Room Temperature
TBDAP	TetraBenzoDiAzaPorphyrin
TBTAP	TetraBenzoTriazaPorphyrin
TCE	Tetrachloroethane
TEA	Triethylamine
THF	Tetrahydrofuran
TFA	Trifluoroacetic acid
TLC	Thin Layer Chromatography
TPP	Tetraphenyl porphyrin
UV-Vis	Ultraviolet-visible

Table of Contents

Chapter 1: Introduction

1 Introduction

1.1 Porphyrin

Porphyrin is a planar macrocyclic compound and natural pigment. It has four pyrroles linked together at α-positions that are fully conjugated with four methine carbons (also called *meso*-carbon bridges). The porphyrin structure displays 22 π-electrons, but only 18 of them form an aromatic system according to Huckel's rule (4n+2=18, n=4; pathways shown in bold in figure 1.1). The IUPAC numbering and nomenclature of the porphyrin structure is also given in figure 1.1. According to IUPAC rules, positions 5, 10, 15 and 20 are referred to as *meso*. Pyrrolic carbons (also called β-carbons) are found at positions 2, 3, 7, 8, 12, 13,17 and 18, while 21 and 23 indicate the two nitrogen atoms bonded to the hydrogen atoms.[1,2] The β-substituted porphyrins are commonly found in natural products, while *meso*-substituted porphyrins are artificially made.

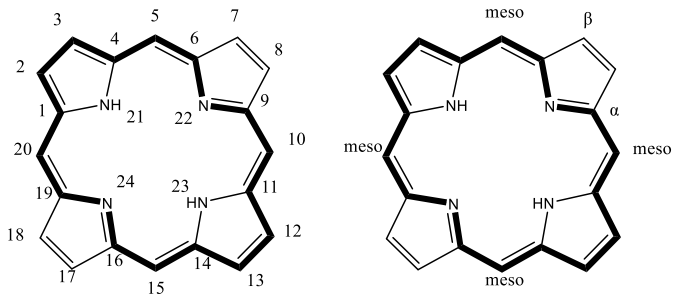

Figure 1.1: The IUPAC numbering system of porphyrin.

In plants, animals, and even bacteria, porphyrin molecules serve a variety of purposes. Natural porphyrins can be found in their metalled form, such as chlorophyll (magnesium porphyrin) and hemes (an iron porphyrin derivative), which play important roles to sustain life. Chlorophyll plays a vital role in the photosynthesis of plants by converting light energy into chemical energy,[3] while heme plays an important role as oxygen carrier in the blood.[4]

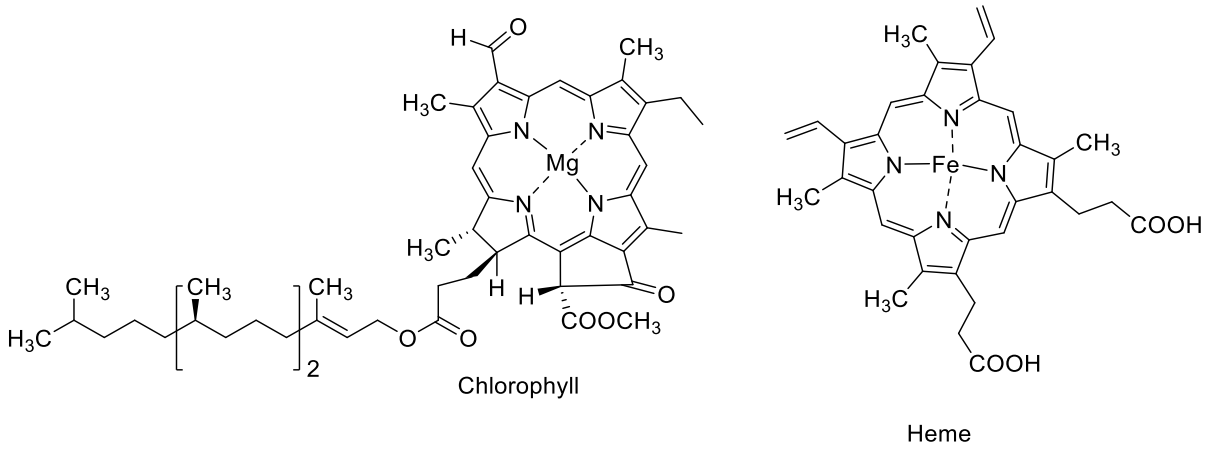

Figure 1.2: Chlorophyll and heme structures.

There are different synthetic strategies available to obtain porphyrins. The most common synthetic route to prepare the symmetric porphyrin, including the synthesis of tetraphenyl porphyrin (TPP), is by reaction of pyrrole with an aldehyde. The first method was described by Rothemund in 1941[5] and it was developed by Adler and Longo by using acidic conditions instead of more harsh conditions.[6] The yields of synthesised porphyrin were significantly enhanced under these acidic conditions with a yield of 30-40%, compared to less than 10% obtained using the Rothemund method.

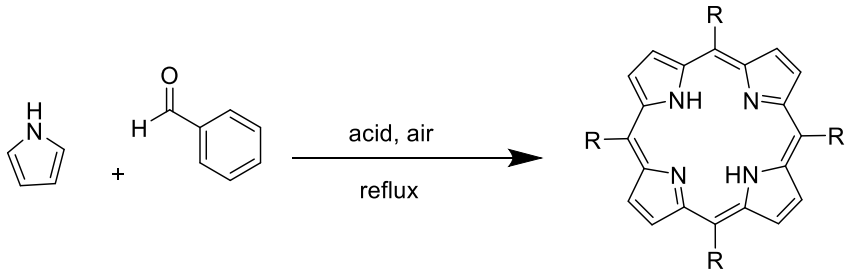

Scheme 1.1: Adler's procedure.

Lindsey improved on the previous two methods and utilized Lewis acids as a catalyst for carrying out TPP synthesis reactions under milder reaction conditions. The reaction requires a condensation of pyrrole with aldehydes in chloroform or dichloromethane in the presence of the acid catalyst, TFA or boron trifluoride etherate, at room temperature. DDQ or *p*-chloranil is added for oxidizing the initially obtained porphyrinogen into porphyrin[7] as shown in scheme 1.2.

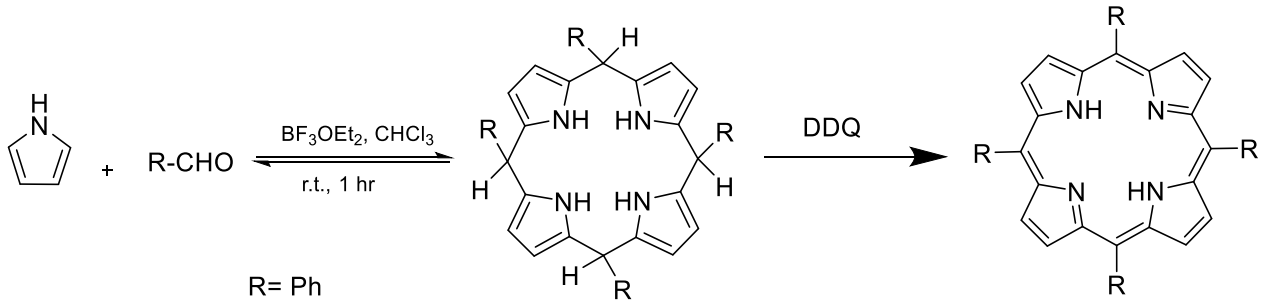

Scheme 1.2: The Lindsey synthetic route for the preparation of *meso*-substituted porphyrins.

Over the years, several synthetic strategies have been used to create artificial porphyrins and their derivatives. Examples include *meso*- and β-substitution, ring-contraction and ring expansion, isomerization and core-modification, with the main purpose of regulating their structural and electronic properties.[8]

These porphyrins find extensive applications in areas such as photodynamic cancer therapy and catalysis.[9] In addition, they are also used as photosensitizers to generate electrical energy in photovoltaic devices such as dye-sensitized solar cells (DSSCs).[10]

1.2 Phthalocyanines

Unlike porphyrins, phthalocyanines (Pc) are an exclusively man-made class of traditional industrial dye and the most important class of macroheterocyclic organic materials since its discovery by Braun in the early 1900s. Its structure contains a ring system of four isoindoline units linked together by nitrogen atoms known as aza-bridges (Figure 1.3). It can also be named tetrabenzotetraazaporphyrin. The aromatic 18- π electron conjugated system, consisting of four isoindole rings bridged by four imino nitrogen atoms at *meso*-position, leads to unique electrochemical and optical properties of these blue and green compounds such as their high chemical and thermal stability, and electronic absorption.[11,12] They have synthetic flexibility and ability to adapt to a broad variety of applications, such as catalysts, in photodynamic therapy and in solar cells.[13]

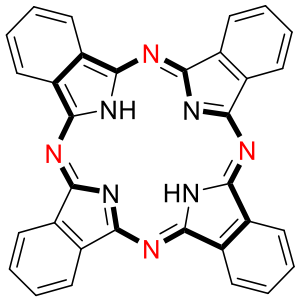

Figure 1.3: The structure of Pc

1.2.1 General synthetic procedure for the formation of phthalocyanines

Phthalocyanine, like porphyrin, can be formed by different methods. Generally, these methods are usually based on the cyclotetramerization reaction for several starting materials such as phthalic acid, phthalimide, phthalic anhydride, phthalonitrile and diiminoisoindoline in the presence of metal salts for metallated Pcs and in the absence of the metal salts for the metal-free Pcs as seen in scheme 1.3. [14,15]

The most popular method is based on phthalonitrile (1,2-dicyanobenzene) due to its ready production of phthalocyanine complexes in good yield. In the majority of syntheses, the phthalonitrile is simply heated in the presence of a metal salt in a high boiling solvent, such as alcohols.[16]

The Tomoda method was described in the 1980s as a straightforward and easy way to synthesise Pcs or metal Pcs in high yield. It involves heating phthalonitrile with a catalytic amount of DBU or DBN in the presence of metal salt for metal Pcs.[17,18]

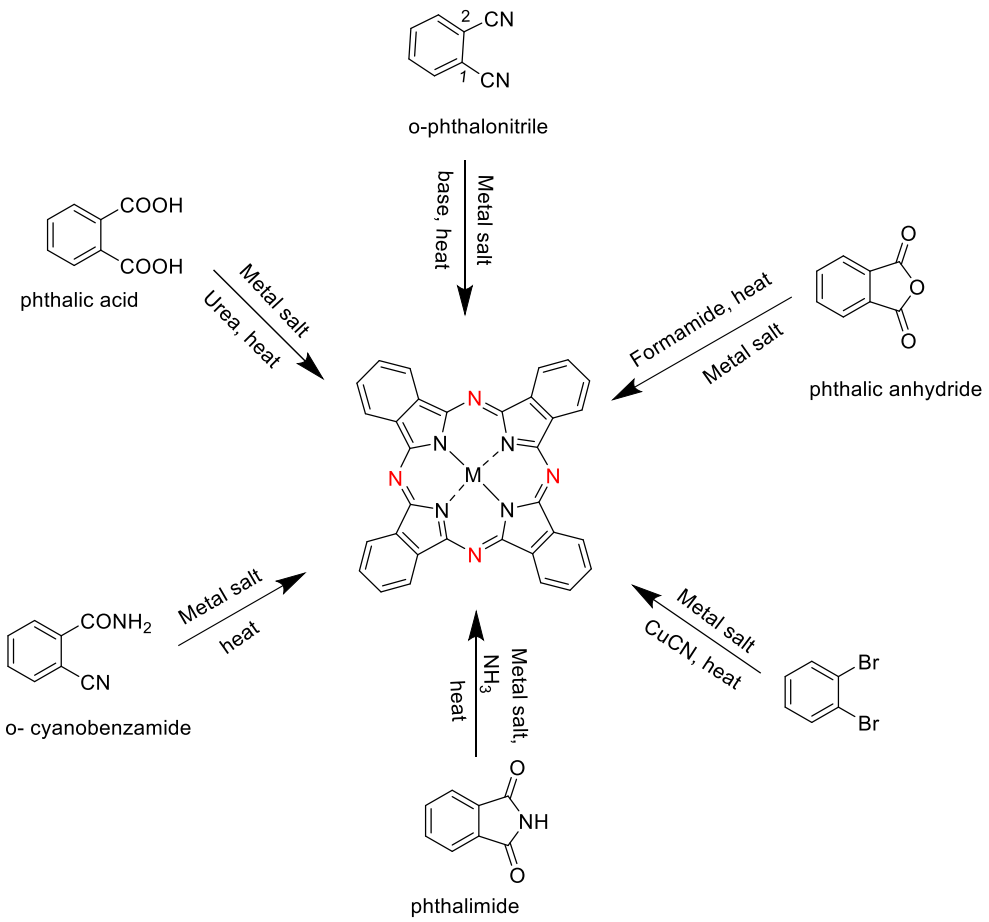

Scheme 1.3: Common synthetic precursors of phthalocyanine

1.3 Porphyrin-phthalocyanine hybrids

Porphyrin - phthalocyanine hybrids (tetrabenzo(aza)porphyrins) are a set of compounds that are related to the porphyrin and phthalocyanine macrocycles in their structure. Replacement of the bridging nitrogen atoms of phthalocyanine by one or more sp^2 carbon atoms leads to the formation of different types of hybrid macrocycles. The set of hybrid macrocycles are intermediate between Pcs and tetrabenzoporphyrins (TBP), as TBP is Pc with all four aza-nitrogen bridges replaced with methine (CH) bridges. The examples of the hybrid macrocycles are tetrabenzotriazaporphyrin (TBTAP), *cis*- and *trans* tetrabenzodiazaporphyrins (TBDAP), and tetrabenzomonoazaporphyrin (TBMAP), which are shown in figure 1.4.

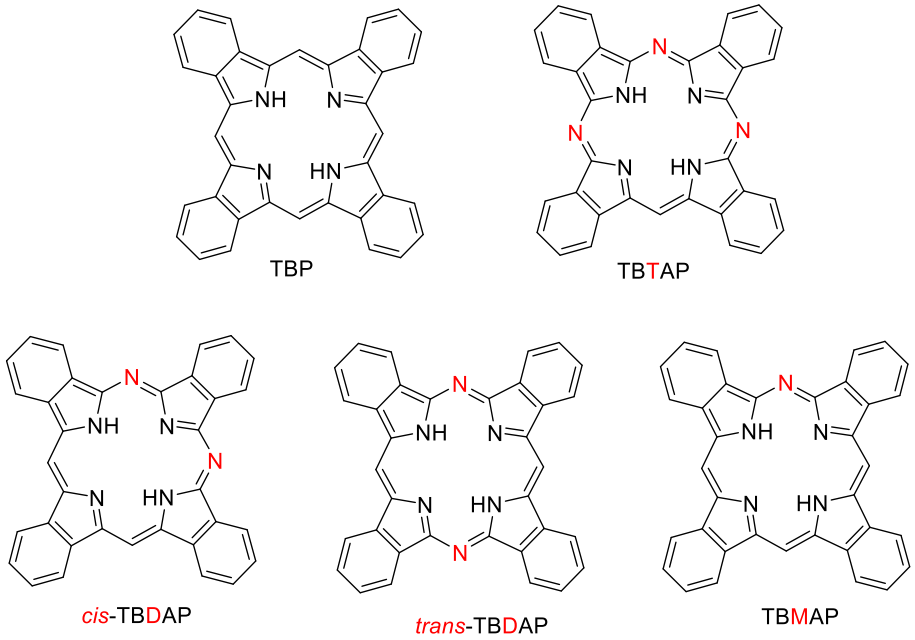

Figure 1.4: Molecular structures of Pc/TBP hybrid macrocycles.

The combination of aza and methine links within the 18π-electron core give interesting hybrid structures because they offer the potential to bridge the properties of the two systems and provide new chemistry within the field of macrocyclic chemistry. [19,20] Tetrabenzo(aza)porphyrin macrocycles are numbered as phthalocyanine Pc, as the atomic numbering scheme of the phthalocyanine type is more commonly used. Consequently, the tetrabenzotriazaporphyrin system's substituents on the benzene rings were numbered similarly to those of the phthalocyanine's system.

Both phthalocyanines and tetrabenzotriazaporphyrin hybrids have sixteen substitution sites on the macrocycle. Substituents which are located on the benzene rings at positions 2, 3, 9, 10, 16, 17, 23, and 24 are named as the peripheral (p) sites, whereas those at positions 1, 4, 8, 11, 15, 18, 22, 25, are known as the non-peripheral (np) sites[21] as shown in figure 1.5 as an example of these hybrids.

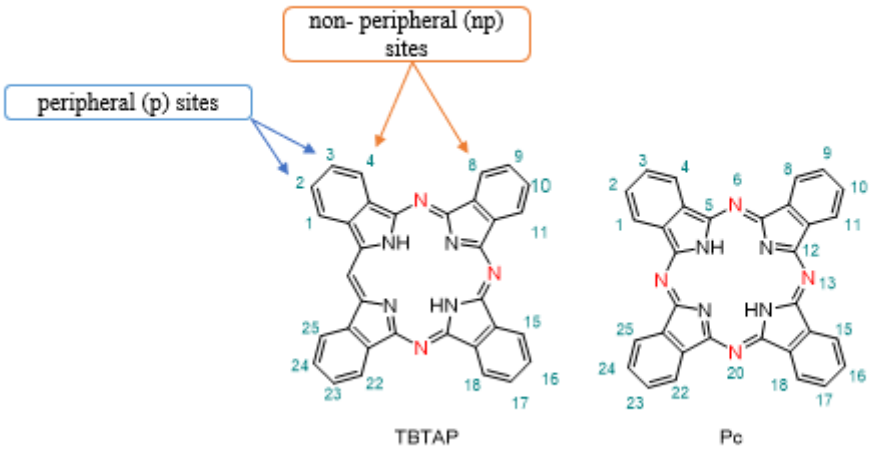

Figure 1.5: Structures and numbering of the atoms for Pc and TBTAP.

Although the first discovery of tetrabenzoazaporphyrin hybrids happened in 1930s by Dent,[22] and Linstead groups,[23] they are more rarely studied compared to the corresponding phthalocyanines. This is attributed to the difficulties in their synthesis and purification. Nevertheless, the interest in these compounds has increased over the last 2-3 decades though most of the syntheses depend on the original procedures with some improvements.[20,24] The original procedure was by reacting phthalonitriles with an organometallic reagent at high temperature as shown in scheme 1.4.

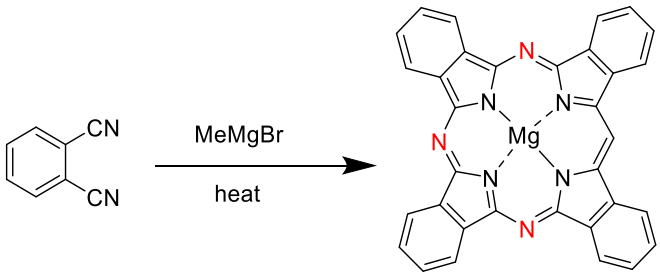

Scheme 1.4: Linstead's original strategy.[23]

The reaction of phthalonitrile with various ratios of Grignard reagents at high temperatures provides *meso*-carbon(s) and results in all hybrids. All reactions produce mixtures of products and generally low yields, with increased carbon incorporation from using higher numbers of equivalents of the Grignard reagent. [19] However, our group have developed and researched new synthetic strategies, effectively overcoming some of the initial issues.[20] This synthetic strategy involves the formation of TBTAPs using aminoisoindoline initiators, which are prepared following the procedure reported by Hellal and Cuny.[25]

The aminoisoindoline **1.2** was synthesised in two steps starting with 2-bromobenzonitrile. A solution of 2-bromo benzonitrile was treated with lithium bis(trimethylsilyl)amide (LiHMDS) in THF, followed by quenching with a mixture of isopropanol/HCl to produce the amidine salt **1.1** in a high yield. The amidine salt was then coupled with an aryl alkyne under copper-free Sonogashira coupling conditions (Scheme 1.5).

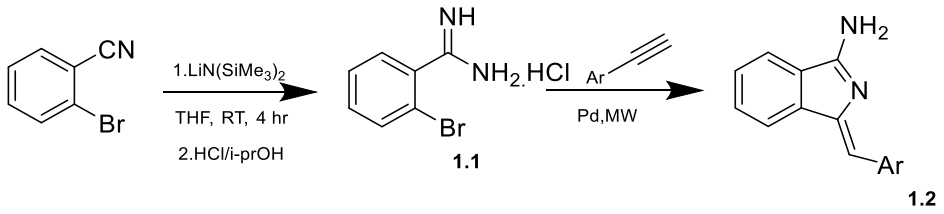

Scheme 1.5: Synthesis of aminoisoindolines **1.2**.

The first attempt to synthesise the TBTAP involved the reaction of diiminoisoindoline and aminoisoindolines **1.2**, in the presence of magnesium bromide as a template agent in high boiling solvents such as quinoline, DMEA, DMF or diglyme. The resultant reaction mixture contained a small amount of the desired *meso*-phenyl TBTAP, along with Pc and a self-condensation product of aminoisoindoline (**1.5**) as seen in scheme 1.6. This result prompted our group to modify the reaction strategy in order to increase the overall yield of the target compound and minimise the formation of side products (Pc and dimeric products). The modification involved the use of phthalonitrile as a less reactive precursor rather than diiminoisoindoline, controlling the addition of aminoisoindoline over the reaction and the addition of DABCO to the reaction mixture. This synthetic strategy showed a better yield (~40%) of the target *meso*-phenyl TBTAPs.

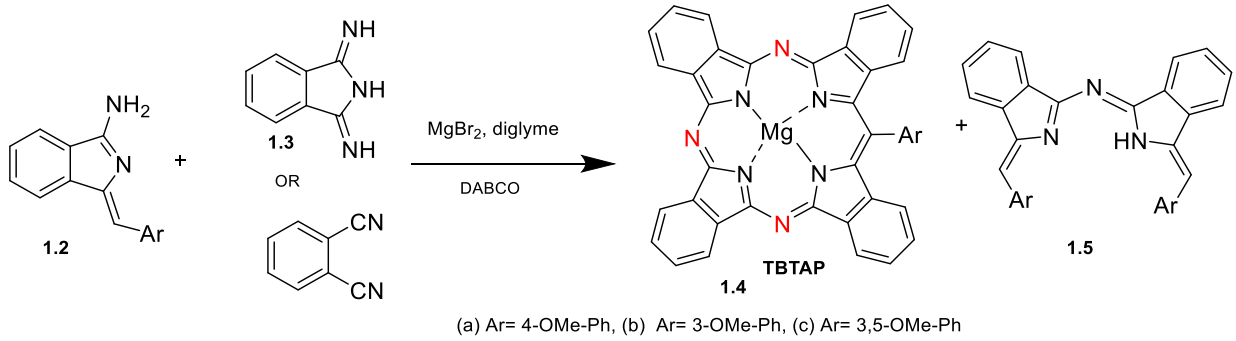

Scheme 1.6: Synthesis of *meso*-substituted magnesium TBTAP.

This synthetic method opens the way for designing and synthesising new families of *meso*-aryl TBTAPs, which can be developed into functional molecular materials. Recently, our group reported additional modification of *meso*-aryl TBTAP gives controlled access to functionalised *meso*-aryl TBTAPs and allow to a full range of complementary functionality.[26] In the study, the reaction was achieved by reacting three equivalents of substituted phthalonitrile with one equivalent of aminoisoindoline under the optimised conditions to yield the target compound Ar-ABBB TBTAP. However, two hybrid products were isolated, Ar-ABBB TBTAP as minor product and surprisingly the Ar-ABBA TBTAP as the dominant product. The aminoisoindoline fragment was functionalised to introduce substituents on rings close to the *meso*-Ar (blue ring). The same results were obtained, with ABBA Ar-TBTAP as major product. This result provides insight into the reaction pathways in TBTAP synthesis using aminoisoindolines.

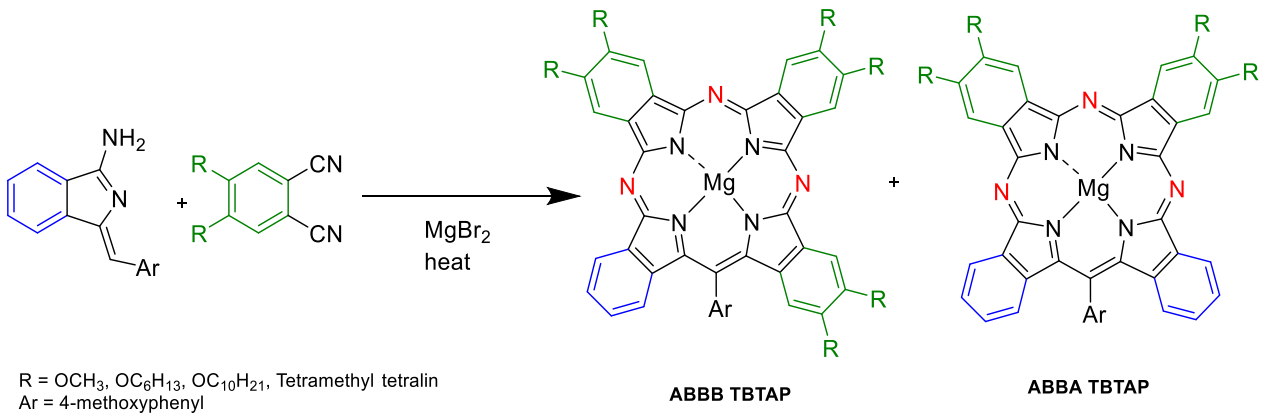

Scheme 1.7: The synthesis of *meso*-aryl ABBB and ABBA TBTAPs using phthalonitrile and aminoisoindoline.

Another example for selective synthesis of phthalocyanine hybrid was reported by Yamada *et al* in 2023 to synthesise metal-free 10,20-bis(triisopropylsilylethynyl) TBDAP by the metal-templated aza-annulation reaction, demetallation with TFA, and finally retro-Diels Alder reaction to get product in 14 % yield as seen in scheme 1.8.[27]

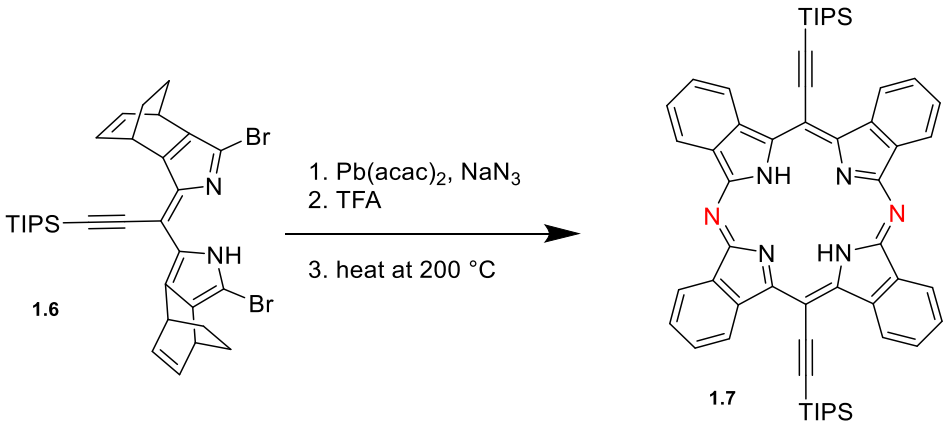

Scheme 1.8: The synthesis of TIPS-TBDAP.

1.3.1 Absorption Spectra of Phthalocyanines and Phthalocyanine hybrids

Phthalocyanine and related macrocycles possess a highly conjugated 18π-electron system, which results in the generation of low energy π-π* transitions. These transitions can be observed in UV-vis spectra in two different electronic absorption regions. The first region is in the near ultraviolet range (blue region) as a broad band of 300-400 nm, known as the B or Soret band. The second region is in the far-red range of the visible region, specifically in the range of 600-700 nm, referred to as the Q bands. The substitution of methine bridges for nitrogen atoms in Pc results in a reduction in the symmetry of the structure. This alteration induces changes in the UV-visible absorptions of each hybrid. Replacing a nitrogen bridge with a carbon atom leads to a hypsochromic shift towards shorter wavelengths and reduces the intensity of the Q band. However, the intensity of the porphyrin-like B band is increased, as seen in figure 1.6.[13,19,28,29]

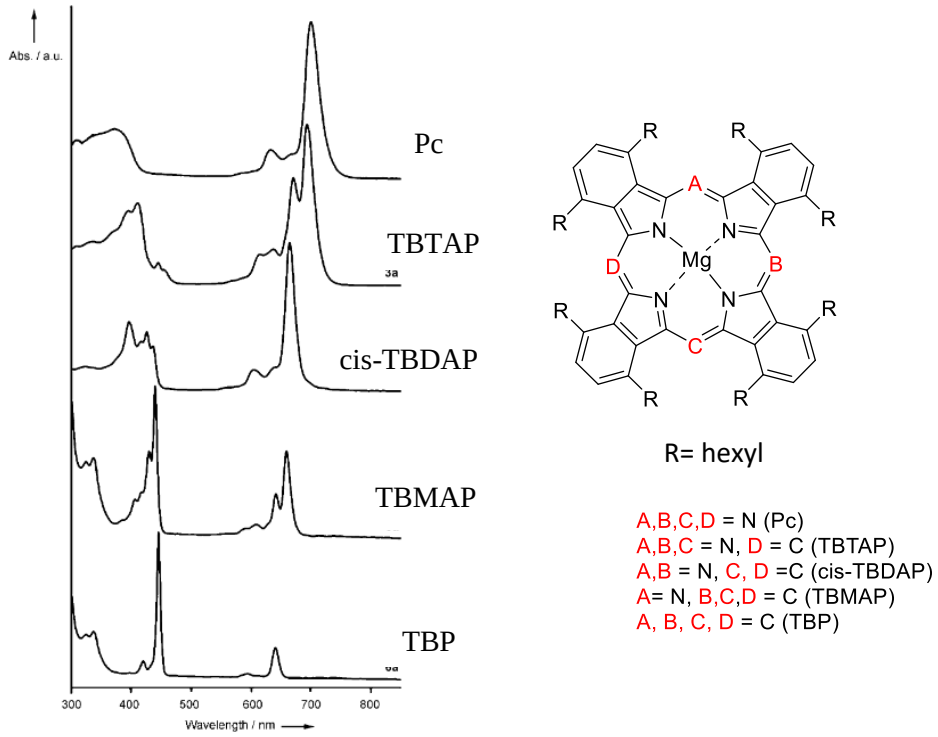

Figure 1.6: The UV-vis spectra of Pc and phthalocyanine hybrids.[19]

1.4 Porphyrin Derivatives

A significant area of research is investigating the various types of porphyrins that can be obtained by modifications to the heterocyclic core, extension of the macrocyclic ring, and changes in structural topology. These modifications provide an opportunity to design molecules for many applications within the fields of chemistry, biology, and material science.

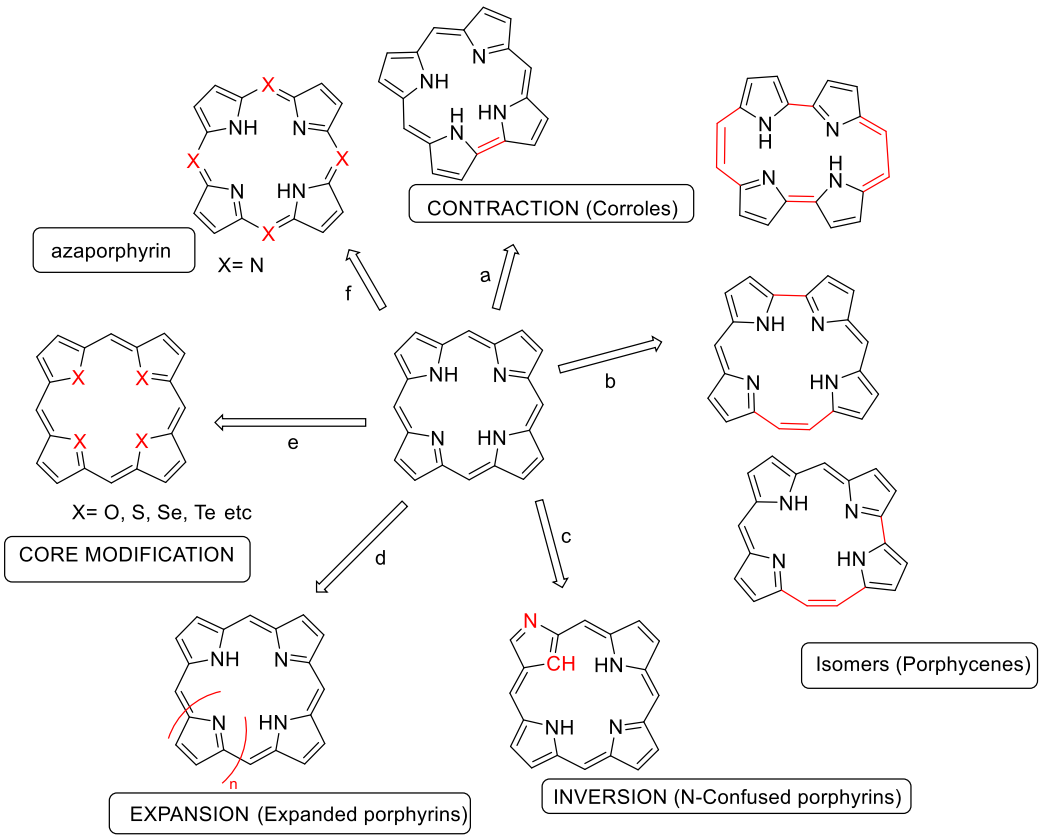

Figure 1.7: Structural modifications of the porphyrin core.[30]

(a) Contracted porphyrins: the analogues of contracted porphyrins that are produced by removing one of the *meso*-carbons, such as corroles.

(b) Isomeric porphyrins: porphyrins with the same chemical formula that are produced by rearranging the four bridging carbon atoms and the pyrrolic subunits.

(c) Inverted porphyrins: isomers of porphyrins which also known as *N*-confused porphyrins (NCP), where one or more of the core nitrogens extend outside from the ring.

(d) Expanded porphyrins: these are formed when the π-electron chromophores are expanded.

(e) Core-modified porphyrins: these are produced when heteroatoms such as O, S, Se, Te, etc. take the place of the pyrrolic nitrogens in the porphyrins.

(f) Azaporphyrin: these are produced when the *meso*-carbons of the porphyrin structure are replaced by nitrogen partially or completely.

1.5 Core-modified porphyrins

1.5.1 Core modification's structure and nomenclature.

Core-modified porphyrins result from the replacement of one or two inner pyrrolic nitrogens of porphyrin with other heteroatoms such as O, S, Se, P, Si and Te, which gives macrocyclic systems called heteroatom-substituted porphyrins or core-modified porphyrins. The introduction of C results in carbaporphyrins[31] that will be covered in detail later. The prefixes oxa- and thia were used to show that a nitrogen atom was replaced by chalcogen atoms. However, these terms usually mean replacing a carbon atom with oxygen or sulfur. Presently, this nomenclature is widely recognised to indicate the replacement of any element, such as oxygen (oxa-), sulphur (thia-), tellurium (tellural-), or selenium (selena-), for the nitrogen in porphyrin pyrrole.[32a]

1.5.2 Core modified porphyrin's properties:

Core modified porphyrins are macrocyclic aromatic compounds that support the aromatic character, in accordance with the presence of $(4n+2)\pi$ electrons (shown in bold in figure 1.8). Thus, these compounds possess interesting and special properties in terms of their optical and electrochemical properties, and their coordination environments for metals that are quite different from regular N4-porphyrins. Specifically, core-modified porphyrins have the potential ability to stabilize metals in unusual oxidation states, such as copper and nickel in the +1 oxidation state, which cannot be easily generated with regular porphyrins.[33–37] The crystal structures of heteroatom substituted porphyrins and metalloheteroporphyrins showed that the presence of large heteroatoms like S shrinks the macrocycle core size of mono and diheteroporphyrins. The Se atom shrinks the core size of the macrocycle, even further relative to thiaporphyrin. Their electronic properties are significantly altered by the structure variation of heteroporphyrins compared to regular porphyrins. Oxaporphyrins, on the other hand, are very similar to N4 porphyrins in terms of properties. This may be attributed to oxaporphyrin structures being almost the same as regular porphyrin structures due to the similar sizes of the 'N' and 'O'.[32a]

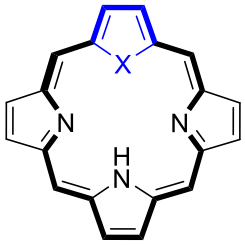

Figure 1.8: Monoheteroporphyrin structure.

1.5.3 Spectroscopic properties of porphyrin and heteroporphyrin:

1.5.3.1 NMR spectroscopy

^{1}H NMR spectra of porphyrins and heteroporphyrins confirm their aromatic character. The proton signals of β-pyrrole, *meso*- protons and heterocyclopentadiene moieties are deshielded due to the ring current deshielding effect. The internal N-H protons show a shift toward upfield as a result of the shielding effect of the ring current which shields the protons inside the macrocycle. The replacement of pyrrole nitrogen atoms with heteroatoms enforces the outer aromatic pathway, resulting in considerable downfield shifts of heterocycle proton signals. The deshielding was observed in monoheteroporphyrin to be more than in diheteroatom substituted porphyrin due to the presence of two large heteroatoms distorting the porphyrin macrocycle from planarity and thereby reducing the ring current. [33,38]

Porphyrin	NH proton	Pyrrole proton	Heterocycle protons
N_4P	-2.79	8.72	-
21-N_3SP	-2.66	8.64, 8.72	9.81
21-N_3OP	-1.65	8.49, 8.60	9.13
21,23-N_2S_2P	-	8.67	9.67
21,23-N_2O_2P	-	9.08	9.37

Table 1.1: ^{1}H-NMR chemical shifts of selected tetraryl heteroporphyrins δ in ppm.[32a]

1.5.3.2 UV-vis spectroscopy

Porphyrins display characteristic absorption in the UV-vis spectra because of their highly conjugated π system. As mentioned previously, they have intense absorption in the blue region between 390 and 425 nm, referred to as the B band or Soret band, in addition to two to four weaker absorption bands in the red region, called Q bands, between 480 and 700 nm.[39]

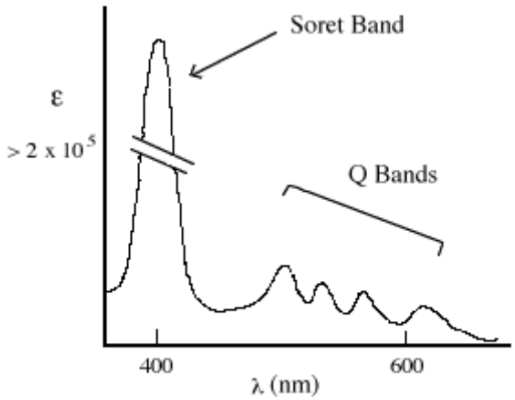

Figure 1.9: Typical UV-visible absorption spectrum of porphyrins.[40]

Likewise, heteroporphyrins exhibit an intense Soret band and 3-4 Q bands in the 700-450 nm region as in the regular porphyrin. Introducing a heteroatom other than nitrogen induces large red shifts of both Soret and Q (IV) bands in the visible spectrum. The strongest red shifts are observed with S, Se, and Te-containing heteroporphyrins, while O-containing heteroporphyrin showed minimum shifts. Similarly, diheteroatom substituted porphyrins are bathochromically shifted compared to those of the monoheteroatom analogues. Therefore, the energy levels of the macrocycle are significantly and additively affected by the quantity of heteroatoms. In addition, the heteroporphyrins' emission bands also showed a red shift, as shown in table 1.2, and their quantum yields decreased in comparison to N4 porphyrins.[32a,33,41,42]

Porphyrin	Soret λ_{max}/nm (log ε)	Q bands [λ_{max}/ nm (log ε)]				Emission nm
		Q(I)	Q(II)	Q(III)	Q(IV)	
N4P	419(5.67)	515(4.27)	548(3.93)	592(3.74)	647(3.39)	650
21-N_3SP	428(5.56)	514(4.47)	550(4.04)	618(3.62)	680(3.69)	685
21-N_3OP	422(4.97)	508(4.00)	540(3.34)	612(3.23)	672(3.26)	678
21,23-N_2S_2P	435(5.47)	515(4.47)	548(3.86)	635(3.35)	699(3.67)	706
21,23-N_2O_2P	416(4.99)	496(4.19)	526(3.67)	640(3.25)	704(3.54)	655

Table 1.2: Absorption and emission data of tetraaryl heteroporphyrins.[32a,33]

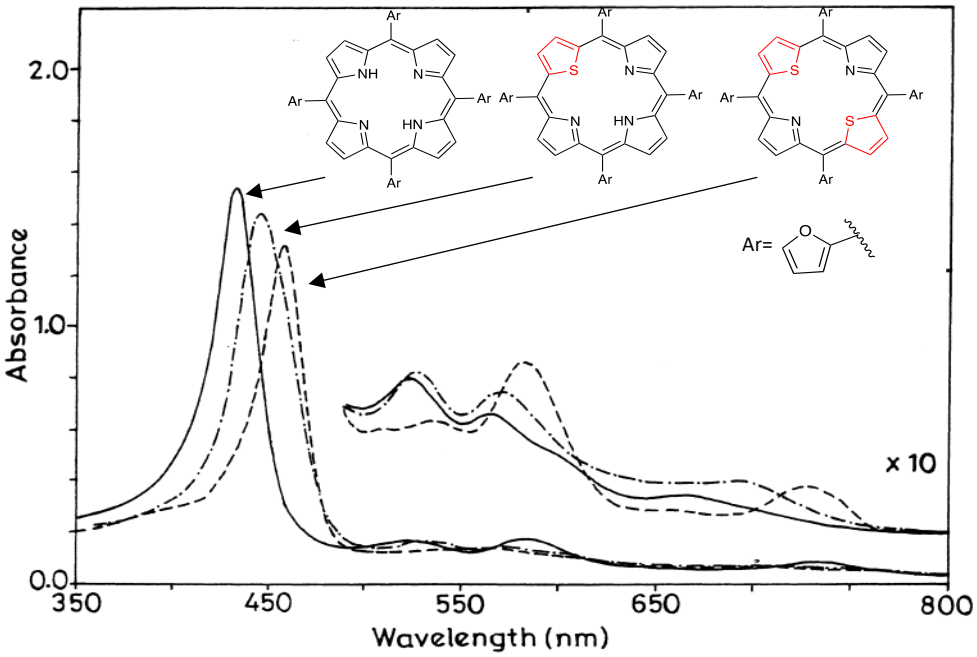

Figure 1.10: Comparison of the absorption spectra of porphyrin, monothiaporphyrin and dithiaporphyrin.[43]

1.5.4 Synthetic procedure for the formation of heteroporphyrin.

Several synthetic methods can be used to synthesise the monoheteroporphyrins that are produced when pyrrole was substituted with a variety of other five-membered heterocycles. Firstly, the "3 + 1" approach as reported by Broadhurst and Grigg[44] in 1971 and later by Lash[45] is one of the most versatile approaches for the synthesis of β-pyrrole alkylated and *meso*-unsubstituted 21-monoheteroatom substituted porphyrins. It involves the condensation of

dialdehyde **1.9** with readily available tripyrranes **1.8** in the presence of an acid catalyst (Scheme 1.9).

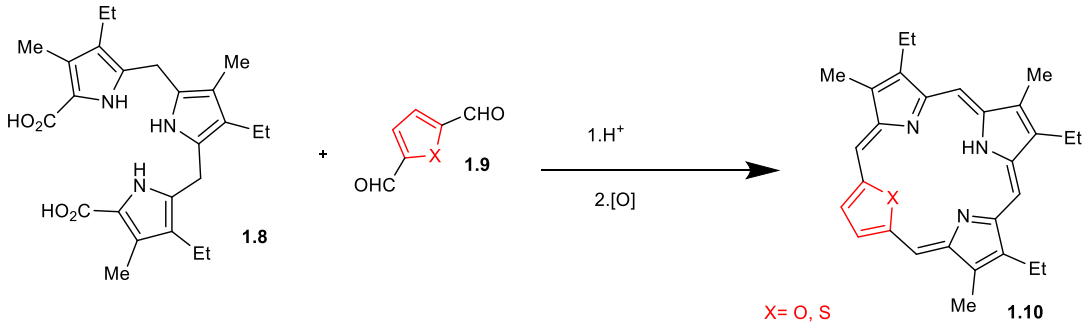

Scheme 1.9: "3+1" method towards heteroporphyrins

The investigation of porphyrins with fused aromatic rings has been extensive as the electronic absorption spectrum is significantly affected by modification of aromatic subunits. [46] A series of ring-fused heteroporphyrins have been synthesized to investigate the effect of ring fusion on heteroporphyrin chromophores.[47] The same "3+1" strategy was used to produce phenanthro-heteroporphyrins **1.12a–c** and acenaphtho-heteroporphyrins **1.14a–c** in 23–64% yield by condensing tripyrranes **1.11**, **1.13** with dialdehydes as seen in scheme 1.10. Phenanthroheteroporphyrins showed smaller shifts and relatively weak absorption Q bands at higher wavelengths, while acenaphthoporphyrinoids **1.14a–c** gave highly modified UV-vis spectra with multiple Soret bands and strong Q bands between 677- 684 nm (strong Q band of acenaphthoporphyrins at 658 nm). This result is attributed to the combined effect of acenaphthalene and the presence of larger core heteroatoms.[47] The same group recently reported the synthesis of phenanthroline-fused heteroporphyrins using the same methodology, which exhibit unusual spectroscopic properties with proton NMR spectra showing upfield shifts for internal and external protons compared to related structures.[48]

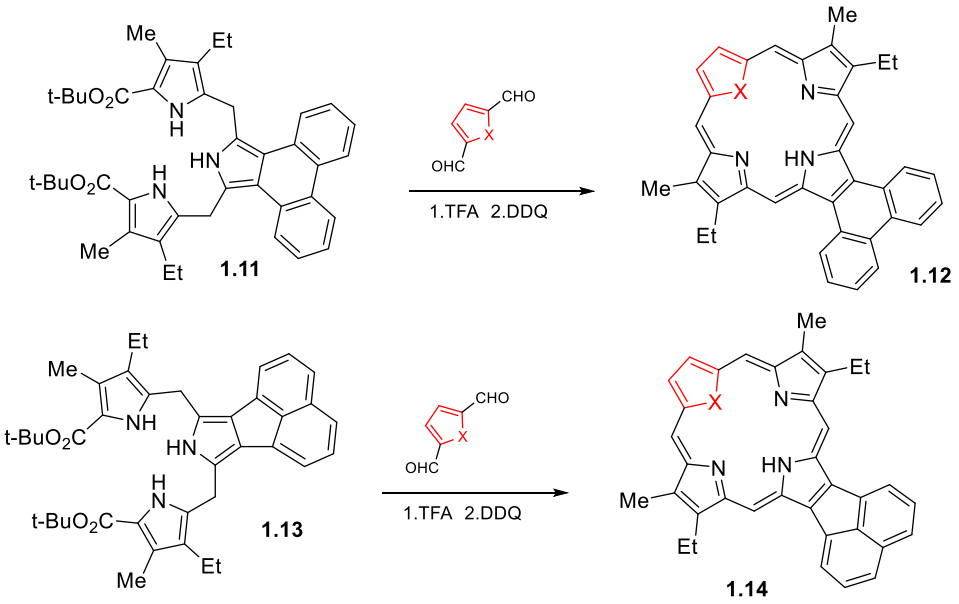

Scheme 1.10: Synthesis of heteroporphyrin fused to phenanthrene or acenaphthlene.

The previous approach was not found to be suitable for the synthesis of *meso*- tetraaryl heteroporphyrins. Ulman and Manassen first reported *meso*-tetrasubstituted heteroporphyrin syntheses in 1975,[49] and porphyrins with core modifications continue to be intensively investigated. The most common synthetic route to *meso*-tetrasubstituted heteroporphyrins involves heterocyclic dicarbinol. For example, 2,5-bis(arylhydroxymethyl)-heterocyclopentadiene reacted with 3 eq of pyrrole and 2 eq of the corresponding arylaldehyde under mild acid catalyzed conditions to give the desired monoheteroporphyrin (scheme 1.11). However, 21,23-diheteroporphyrins **1.17** were produced by reacting dicarbinol **1.15** with one equivalent of pyrrole in the presence of boron trifluoride etherate ($BF_3.Et_2O$). This methodology has been applied to the synthesis of oxa-, thia-, selena- and telluraporphyrins as well as dithia-, dioxa-, diselenaporphyrins.[31,50]

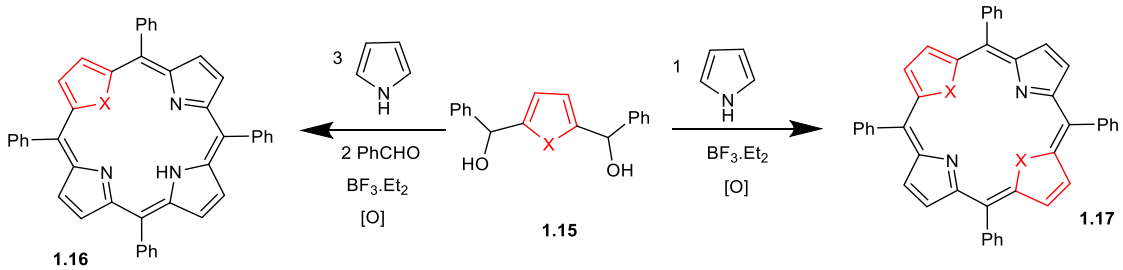

Scheme 1.11: Synthesis of heteroporphyrins from pyrrole and heterocyclic dicarbinols

This method gives access to synthesis of the functionalized monoheteroporphyrins where one or more functional groups are introduced at the *meso*-aryl group by using unsymmetrical dicarbinol.[31,51] The unsymmetrical dicarbinol method was also used to prepare mono-*meso*-unsubstituted 21-heteroaporphyrins. One *meso*-unsubstituted carbon porphyrin can be the starting point for the synthesis of other molecules, including *meso-meso* linked dimers.[52]

A rapid and simple synthetic route has been developed to synthesise heteroporphyrin by Gupta and Ravikanth using thiophene and furan mono-ols.[53,54] In this method, two equivalents of mono-arylhydroxymethyl furan or thiophene **1.18** were reacted with three equivalents of pyrrole and two equivalents of arylaldehyde under Adler's conditions[6] resulting in a mixture of porphyrins and the 21-thiaporphyrin, which were separated by column chromatography to isolate the N_3X (X = O, S) porphyrins in 2-6% yield (Scheme 1.12). This precursor can also be used to prepare the mono-trifunctionalized N_3S and N_3O porphyrin systems.

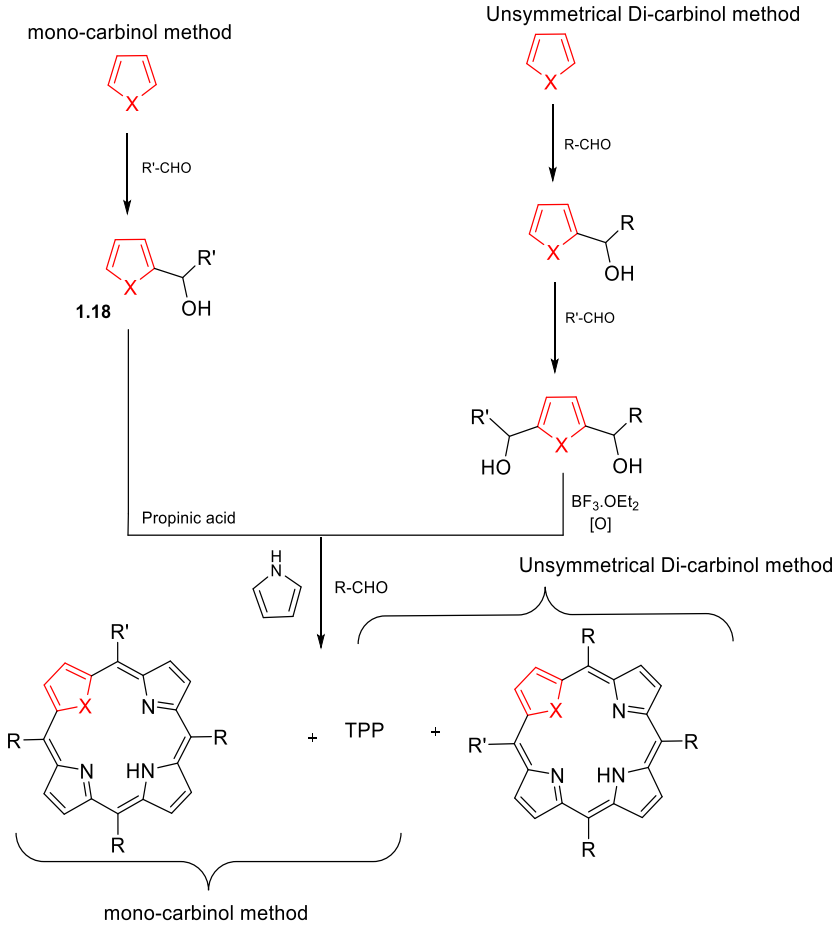

Scheme 1.12: General synthetic method for the synthesis of 21-heteroporphyrins using mono-ol and unsymmetrical di-ol.[34]

In 2024 Gupta *et al* [55] reported synthesis of 21-thiaporphyrins (A_3B and A_2B_2) type with carbazole/phenothiazine moieties at *meso*-positions employing diol and mono-ol methods. Because 21-thiaporphyrin shows significant absorption in the visible range and excellent electrochemical characteristics, the 21-thiaporphyrins could be used as photoredox catalysts for organic transformations. As mentioned earlier, red-shifted Soret and Q bands in thiaporphyrin (STPPH) were produced when sulphur was substituted for nitrogen in H_2TPP. This pattern was also seen in 21-thiaporphyrins **1.20** and **1.22a-d.** The presence of electron-donating heterocycles and electron-withdrawing aryl groups at the *meso*-positions showed bathochromic shifts of 12–34 nm for Soret band and 33–39 nm for Q(IV)-band compared to H_2TPP. This may be due to the conjugation between the porphyrin core and electron-rich heterocycles being extended at the *meso*-positions.

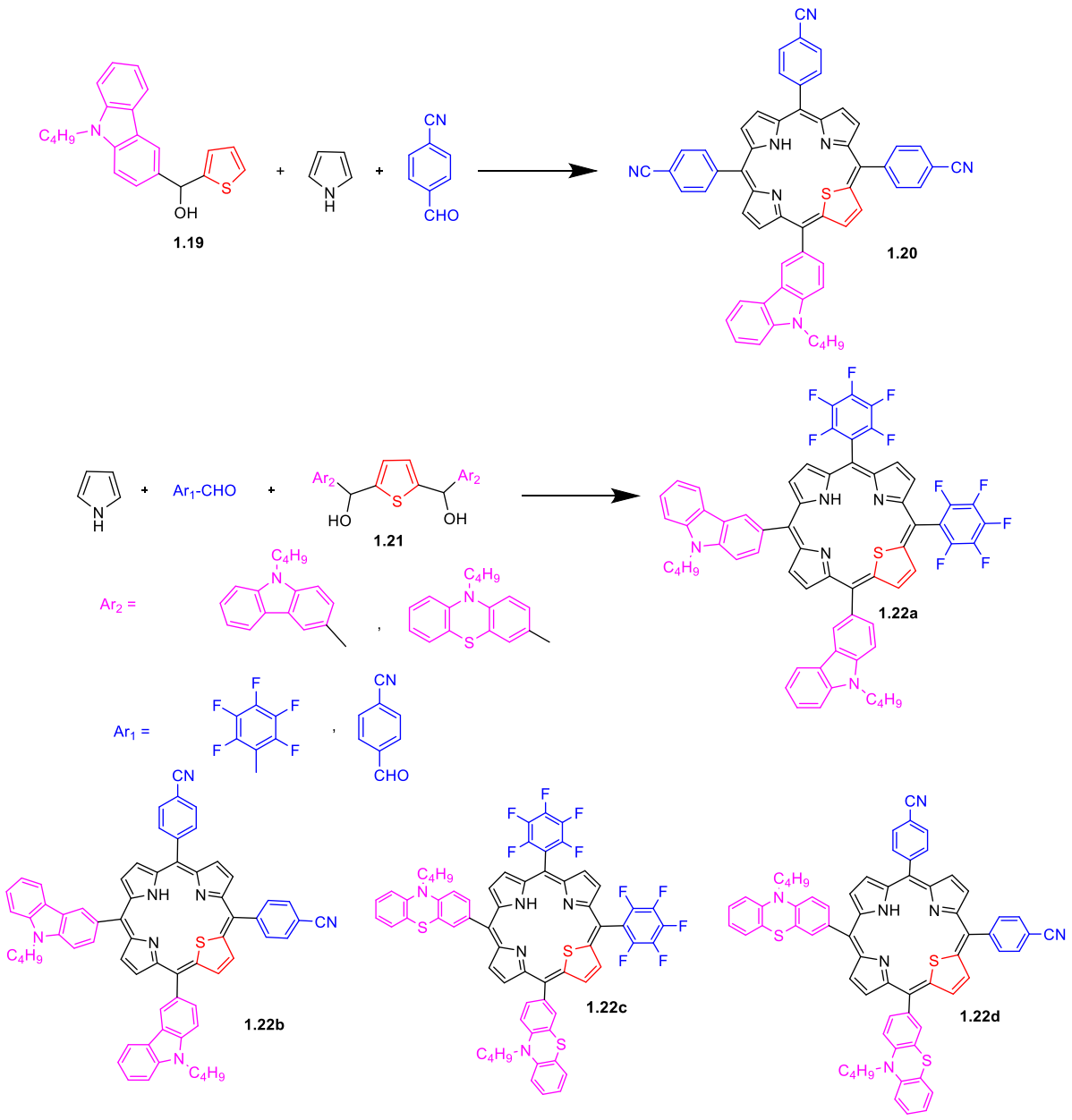

Scheme 1.13: General synthetic method for the synthesis of 21-thiaporphyrins (**1.20**, **1.22a-d**).

In this study, all thiaporphyrins **1.20**, **1.22a-d** were evaluated as photocatalysts for C-N borylation and C-H arylation as the chemistry of C-N borylation and C-H arylation are important in designing new pharmaceutical compounds. A catalyst loading of only 0.1 mol% of 21-thiaporphyrin was found to be efficient for the C-N borylation and C-H arylation of heteroarenes. For C-N borylation, the reaction mixture of *p*-nitroaniline, a boron containing compound and different porphyrin catalyst (**1.20**, **1.22 a-d**) was exposed to blue light to synthesise 4,4,5,5-tetramethyl-2-(4-nitrophenyl)-1,3,2-dioxaborolane. All thiaporphyrins **1.20** and **1.22 a-d** were shown to be effective as catalysts for this type of reaction, as seen in scheme

1.14, but **1.22d** exhibited the highest efficiency with 81% yield. When the reaction was carried out without the catalyst and light, no product was produced.

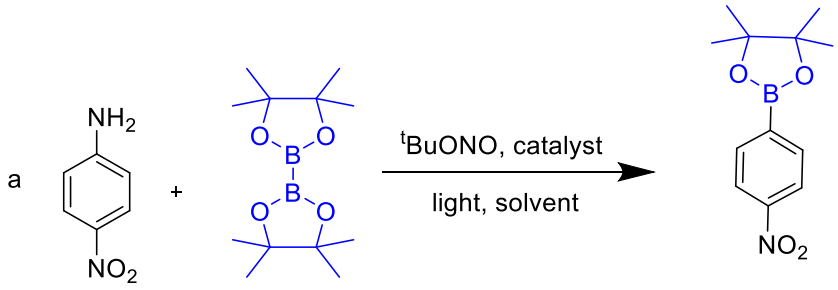

Entry	Solvent	Catalyst	Catalyst loading (mol %)	Yield (%)
1	ACN	1.20	0.1	65
2	ACN	1.22a	0.1	68
3	ACN	1.22b	0.1	70
4	ACN	1.22c	0.1	71
5	ACN	1.22d	0.1	81
6	ACN	1.22d	0.05	70
7	ACN	1.22d	0.2	80

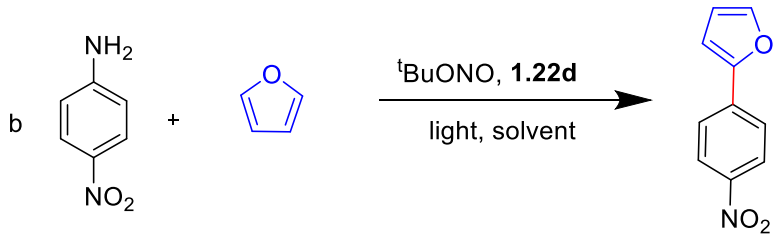

Scheme1.14: C-N Borylation and C-H Arylations of aniline using thiaporphyrin as catalyst.

Under the same conditions, 21-thiaporphyrin **1.22d** was also able to efficiently catalyse C-H arylation of furan with 67% yield (Scheme 1.14b). This study aligns with the work of Derksen and co-workers, who demonstrated the use of thiaporphyrins in photocatalytic dehalogenation reactions. Using *meso*-5,10,15,20-tetraphenyl-21-monothiaporphyrin (STPP), when combined with Hantzsch ester (HEH) and DIPEA, could efficiently dehalogenate α-functionalized carbonyl compounds under red light (λ > 645 nm). While the method worked exceptionally well for bromine- and iodine-containing substrates (75–98% yields), it was less effective for chloro ketones (12–40%) and failed for α-bromo esters and amides.[56,57]

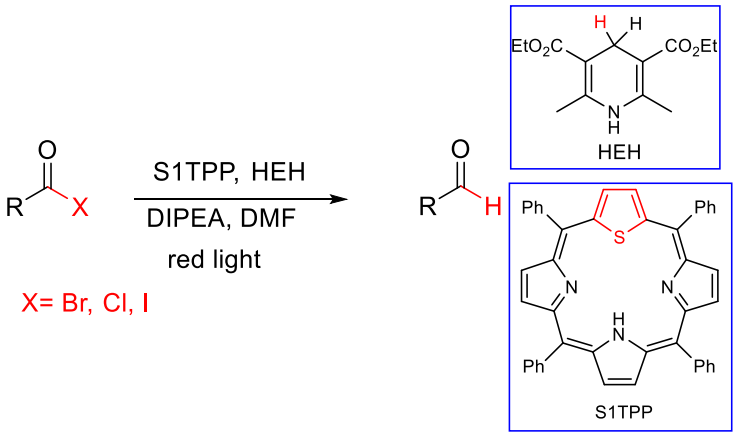

Scheme 1.15: Dehalogenation using thiaporphyrin.

Using the diol procedure, Hsiung Hung and co-workers[58] synthesised novel A_3B and A_2B_2 systems with mono or dual anchoring groups with different linkers and effectively used them in dye-sensitized solar cells (DSSCs). Thiaporphyrins **1.23-1.28** were synthesised by condensation of symmetrical and unsymmetrical diol with pyrrole and appropriate aldehydes in the presence of boron trifluoride–diethyl etherate as catalyst, followed by oxidation with DDQ.

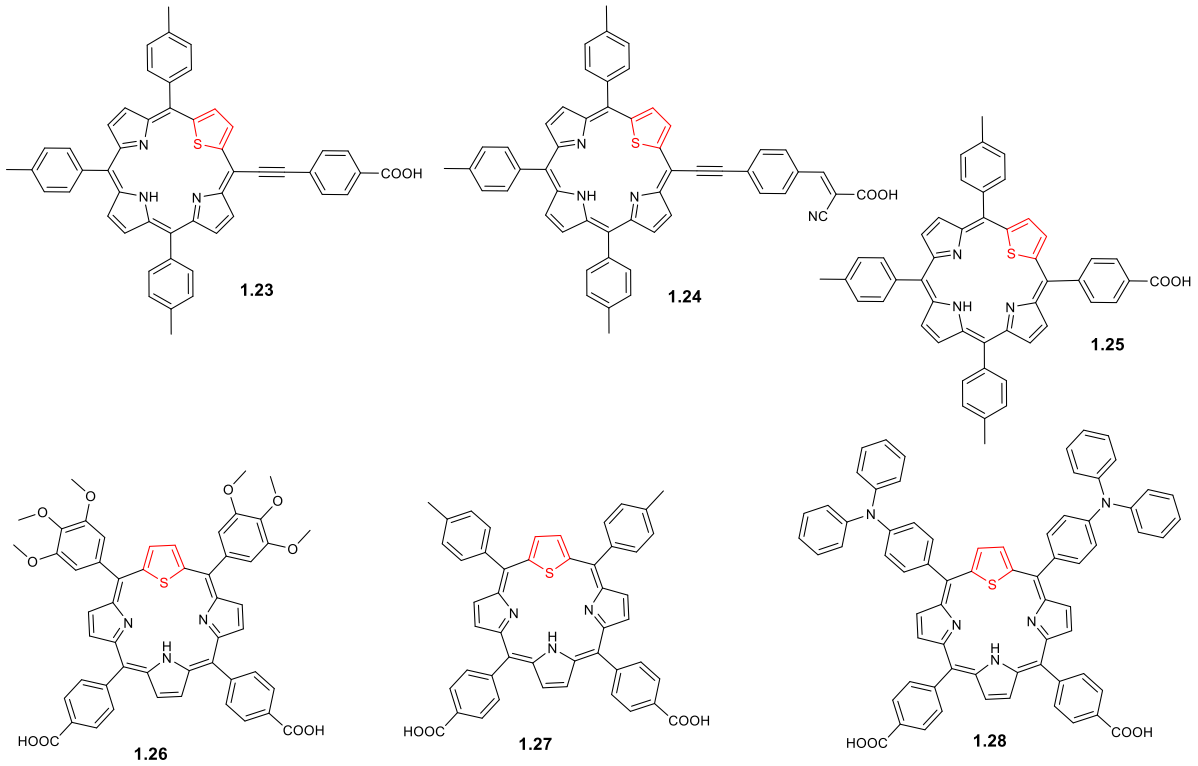

Figure 1.11: Thiaporphyrins with different *meso*-substituents.

Based on typical porphyrin sensitiser examples, it was expected that near-infrared (NIR) absorption could improve the solar to current conversion efficiency of DSSCs, and heteroporphyrins are an effective method for enhancing the photophysical properties of porphyrins without affecting the macrocycle's aromaticity.[59] Ethynylphenyl substitution effectively enhanced the absorption wavelengths towards the near infra-red region for A_3B thiaporphyrins compared to those without an ethynylphenyl linkage. Studies showed thiaporphyrin **1.24**, having an ethynylphenyl linker and a cyano acrylic acid, achieved the highest conversion efficiency of 1.69% among other thiaporphyrin dyes while, in the previous work by the same group,[60] the efficiency of DSSC of **1.23** was 0.22%. Theoretical calculations (DFT) for zinc dithiaporphyrin supported the conclusion that effective sensitizers can be achieved by replacing the appropriate substituents, giving efficient conversion of solar energy in DSSC applications. [61]

Heteroporphyrins were also synthesised by modified conditions of the "3+1" method. In this method, the diol was condensed with a *meso*-aryl tripyrrane **1.29** under mild acidic conditions followed by oxidation with DDQ[62,63] (Scheme 1.16). Similarly, dioxa-, dithia- and oxathiaporphyrins were prepared by reacting oxa- and thiatripyrranes **1.30** with dicarbinols in the presence of TFA, followed by oxidation as also shown in scheme 1.16.

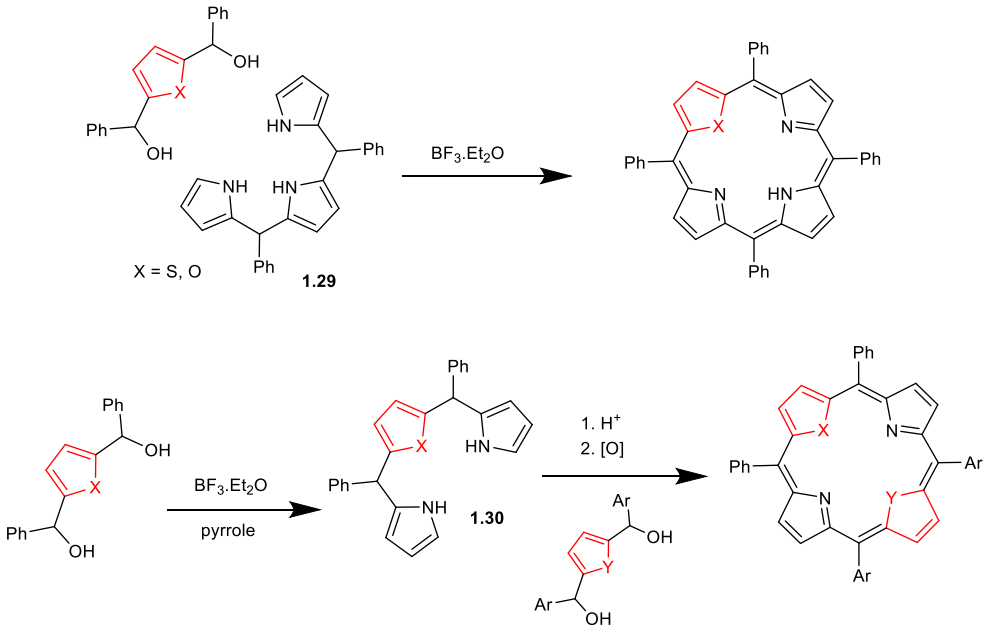

Scheme 1.16: Syntheses of heteroporphyrins from tripyrrane.

Furthermore, 21-oxa and 21-thiatetraphenylporphyrins can also be prepared in high yields (8-21%) by condensing the corresponding furan or thiophene diols, respectively, with dipyrromethane under mild acid catalyzed conditions as reported by Chandrasheker[64] (Scheme 1.17).

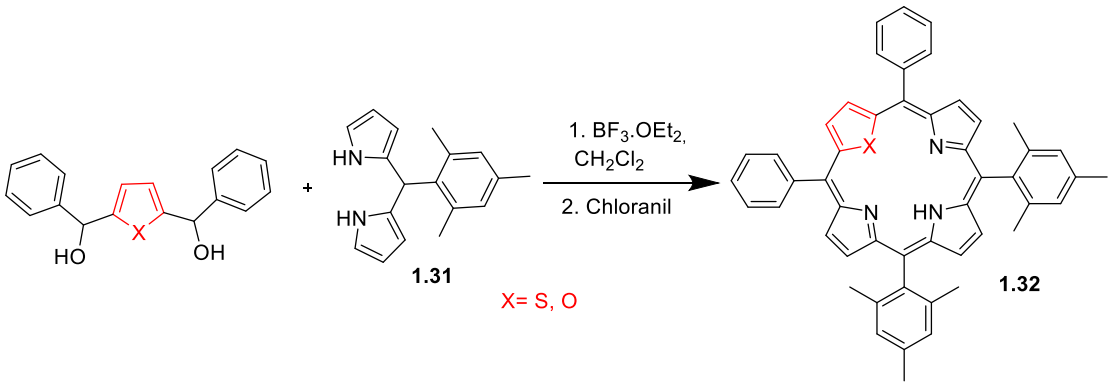

Scheme 1.17: Syntheses of heteroporphyrins from dipyrromethane.

Meso-aryl functionalized dipyrromethane was used also by Lee and co-workers[65] to synthesise regular and monofunctionalized 21-heteroporphyrins. This reaction was carried out by condensing thienylpyrromethane diol/furylpyrromethane diol with *meso*-aryl functionalized dipyrromethane under mild acid-catalyzed conditions. The disadvantage of their synthetic method is the necessity for multi-step precursor synthesis, even though it allows control over the heteroatom placement in the core and the *meso* substituents. Several covalent and non-covalent unsymmetrical porphyrin dyads and higher arrays have been synthesised using mono-functionalized heteroporphyrins, which offer interesting properties and unusual electronic structure.[41,51,52]

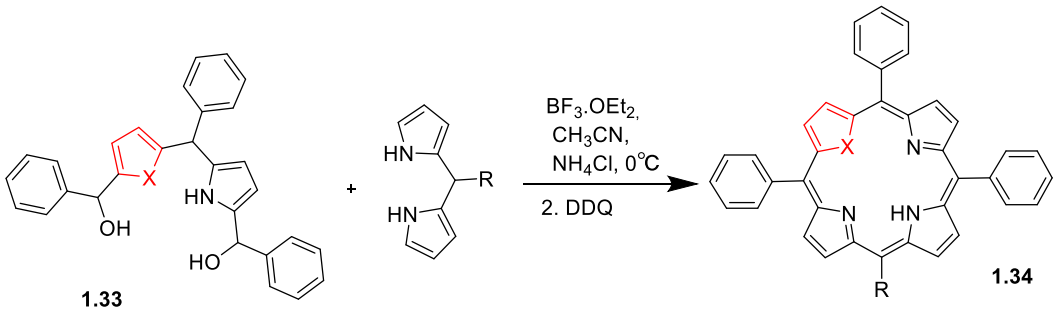

Scheme 1.18: Syntheses of heteroporphyrins from dipyrromethane.

Step-by-step replacement of nitrogen atoms in porphyrins with chalcogen atoms produces a series of macrocycles with an increasing number of heteroatoms such as tetraheteroporphyrin dications with the first reported examples in the 1980s and 1990s. [32a]

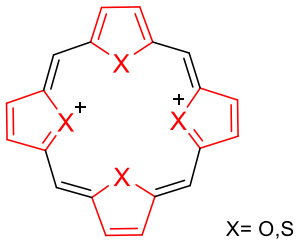

Figure 1.12: Tetraheteroporphyrin dications.

Kaur *et al.*[66] synthesised *N*-methyl-*meso*-tetraaryl-21-thiaporphyrins, and the *N*-methyl derivatives kept highly aromatic properties and 23-methyl resonance appeared at δ -3.3 ppm. When compared to 21-thiaporphyrins, the presence of the internal methyl unit resulted in notable bathochromic shifts of four Q bands and one strong Soret band. The tetraphenylthiaporphyrins (Ar = Ph), showed a Soret band at 428 nm and Q bands at 514, 547, 618 and 675 nm. After alkylation to give **1.35**, these bands exhibited a red shift to 444 (Soret band), and 532, 572, 632 and 698 nm (Q bands).

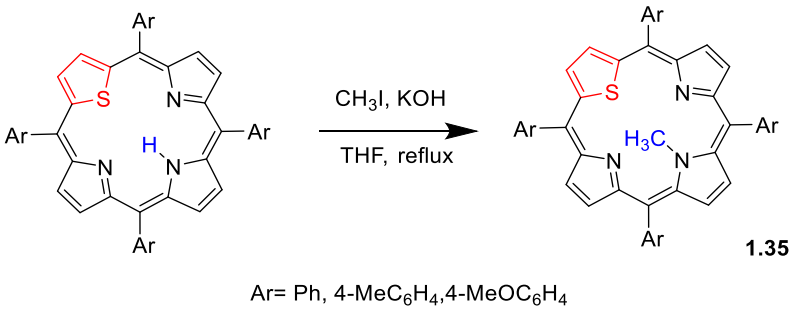

Scheme 1.19: Alkylation of thiaporphyrins.

Heteroporphyrins are generally soluble in organic solvents, such as $CHCl_3$, CH_2Cl_2, and THF. However, their solubility in polar solvents like methanol and water requires the introduction of polar substituents at their periphery. Water-soluble porphyrin derivatives are of interest given their significant applications in biology and medicine. In particular, they show promise as photosensitizers for photodynamic therapy (PDT). Heteroatom substituted porphyrins absorb in longer wavelength region (650–700 nm) compared to N4 porphyrins so water-soluble derivatives can be useful photosensitizers to allow access to deeper tissues that are best activated by light that penetrates in the 650–800 nm range.

Chandrashekar and co-workers were the first to synthesise water-soluble tetrasulfonated 21-thiaporphyrin by sulfonating porphyrins with chlorosulfonic acid under mild reaction conditions. [33,67–70]

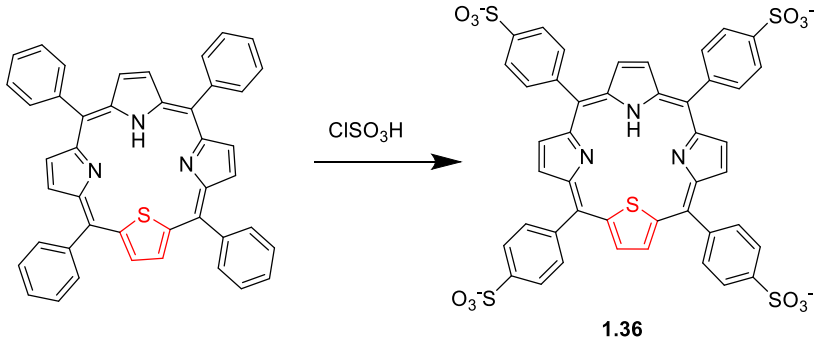

Scheme 1.20: Sulfonation of thiaporphyrins.

Detty and colleagues[70] produced water-soluble tetrasulfonated 21,23-dithiaporphyrin, and 21,23-diselenaporphyrin as tetrasodium salts in 85 % yield by sulfonating the porphyrins with sulfuric acid and then treating with sodium hydroxide.

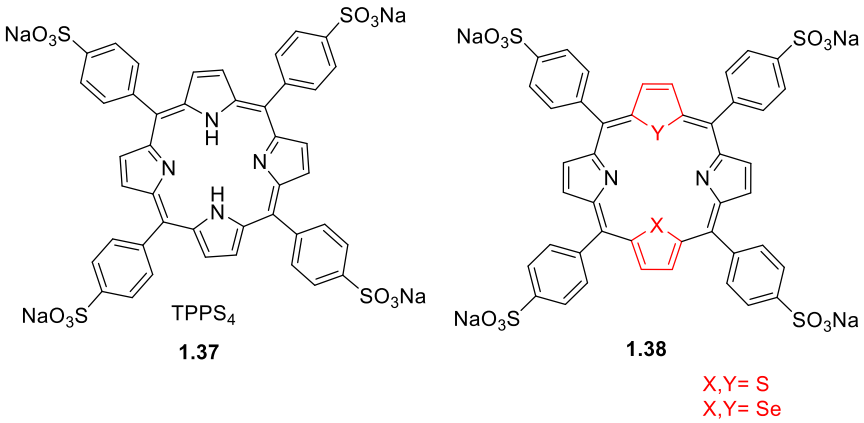

Figure 1.13: Structures of tetrasulfonated porphyrins.

The sulfonated dithia derivative and diselena derivative both exhibit absorption maxima in water at 695 nm, which is 65 nm longer than that of sulfonated porphyrin ($TPPS_4$) **1.37**. The sulfonated dithiaporphyrin derivative behaved as an effective photosensitizer *in vitro* against Colo 26 cancer cells, demonstrating greater efficacy than $TPPS_4$ at comparable light dose and concentrations.

1.5.5 Metalloheteropophyrins

Porphyrins are effective dianionic ligands for transition metal ions. In contrast to tetrapyrrolic porphyrins, core-modified porphyrins exhibit poor coordination chemistry and are less reactive chemically and geometrically to metal ions. This is attributable to incorporating larger heteroatoms such as S, Se and Te into the porphyrin core, which alters the cavity size in addition to the nonplanar orientation of the heteroatoms in comparison to the typical porphyrin rings. [31] However, in some cases, the heteroporphyrins are able to form stable metal complexes that could stabilize the metal in an unusual oxidation state. As monoheteroporphyrins contain only one internal hydrogen, they require axial ligands to stabilize metal ion in +II/+III oxidation states, whereas the diheteroporphyrins have none, so they act as neutral ligands.[71] The first synthesis of Cu(II), Fe(II), and Ni(II) complexes of 21-thiaporphyrin Fe(II) / Cu(II) /Ni(II) **1.39** was reported by Latos-Grazyski, and coworkers.[72] This was achieved by reacting free base 21-thiaporphyrin with corresponding anhydrous metal chloride salts under reflux conditions and chloride is the axial ligand in all three metal complexes.

Both complexes (Fe(II) and Ni (II) **1.39**) show spectral properties similar to porphyrins, with strong absorption near 400 nm attributed to Soret bands and weaker features in the visible region linked to Q bands. However, the lower symmetry of thiaporphyrin complexes results in a more complex low-energy absorptions compared to regular metalloporphyrin complexes.

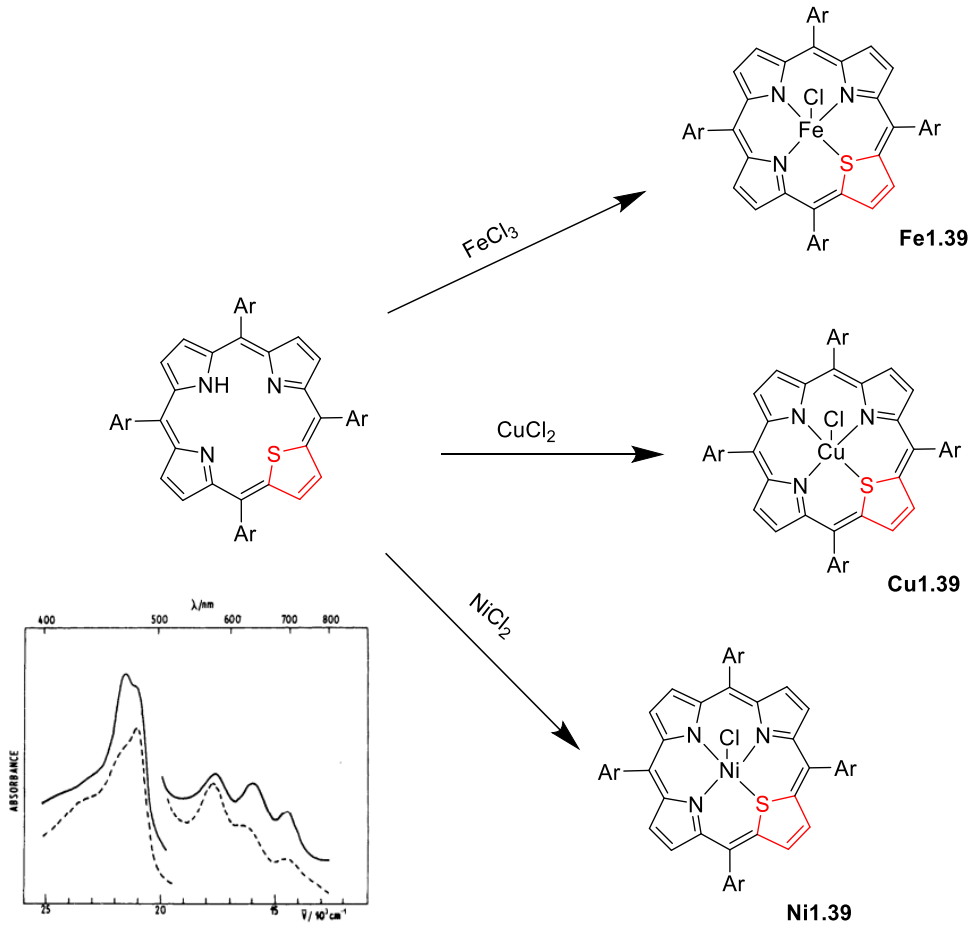

Scheme 1.21: Metal complexes of 21-thiaporphyrin; inset, absorption spectra of (STPP)Fe^{II}Cl (solid line) and (STPP)Ni^{II}Cl (dash line).

1.6 Carbaporphyrinoid systems

Carbaporphyrinoid systems are porphyrin analogues that contain one or more carbon atoms instead of the nitrogen atoms in the central core.[73] These molecules show great potential in synthesising organometallic derivatives and in stabilising uncommon oxidation states. Moreover, these porphyrin analogues display atypical reactivity and usually exhibit intense absorptions above 700 nm, making them potentially valuable as photosensitizers in photodynamic therapy applications.[74] These porphyrinoids vary in their aromaticity from highly aromatic systems to borderline aromatic or nonaromatic macrocycles, and the proton NMR spectroscopic data give important information on the boundaries of porphyrinoid aromaticity.[75,76]

There are various examples of carbaporphyrin, such as *N*-confused porphyrin, carbaporphyrins, azuliporphyrins, benziporphyrins, and oxybenziporphyrins as shown in figure 1.14.[50,77]

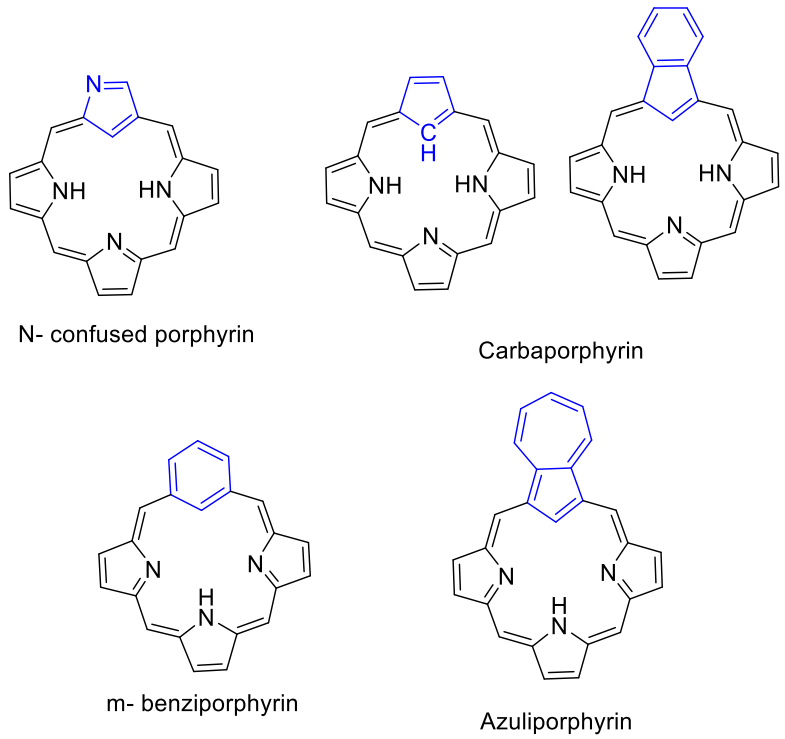

Figure 1.14: The Structures for some common of carbaporphyrinoids.

Carbaporphyrins include cyclopentadiene units instead of a pyrrole moiety which show that the system's aromatic characteristics are not significantly reduced when a cyclopentadiene or indene unit replaces a single pyrrole molecule.

The carbaporphyrins were mainly produced by the utilisation of "3 + 1" acid catalyzed MacDonald condensation. Lash and Hayes reported that benzocarbaporphyrin **1.41** was prepared from diformylindene **1.40** with tripyrrane in the presence of TFA, followed by neutralization with triethylamine and oxidation with DDQ to get benzocarbaporphyrin in 43% yield. [75,78]

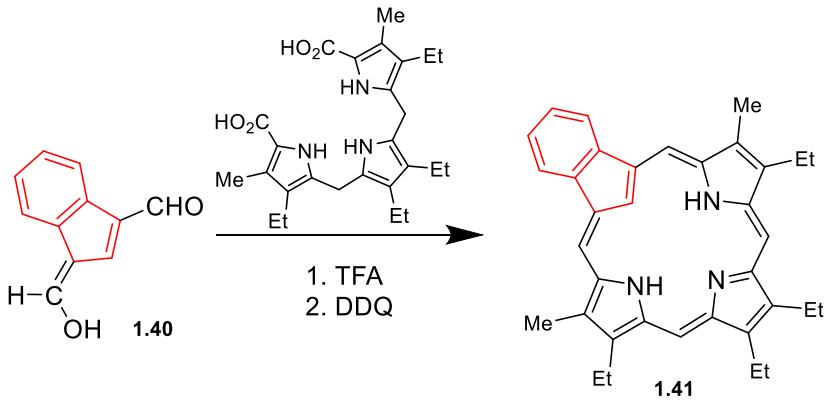

Scheme 1.22: Synthesis of benzocarbaporphyrins **1.41**.

Benziporphyrins are a class of carbaporphyrinoid compounds in which the pyrrolic unit has been replaced with a benzene ring. The synthesis of *meta*-benziporphyrin **1.43** was achieved by condensation of pyrrole, an aryl aldehyde, and diol **1.42** under the conditions described by Lindsey (Scheme 1.23). The reaction was catalyzed by $BF_3 \cdot Et_2O$ in CH_2Cl_2, followed by oxidation with DDQ. After purification by chromatography, the macrocycle **1.43** was isolated in a yield of 15%. To synthesise the *para*- benziporphyrin **1.45,** the same method was used, but with diol **1.42** replaced by its *para* isomer, **1.44** (Scheme 1.23). However, this reaction gave a significantly lower 1–3% yield. The procedure is notably less efficient for the *para* isomer, most likely due to steric factors caused by the incorporation of two sp^2 carbon atoms from the para-phenylene unit into the macrocyclic core, leading to an unfavourable geometry that hinders efficient ring closure.[79]

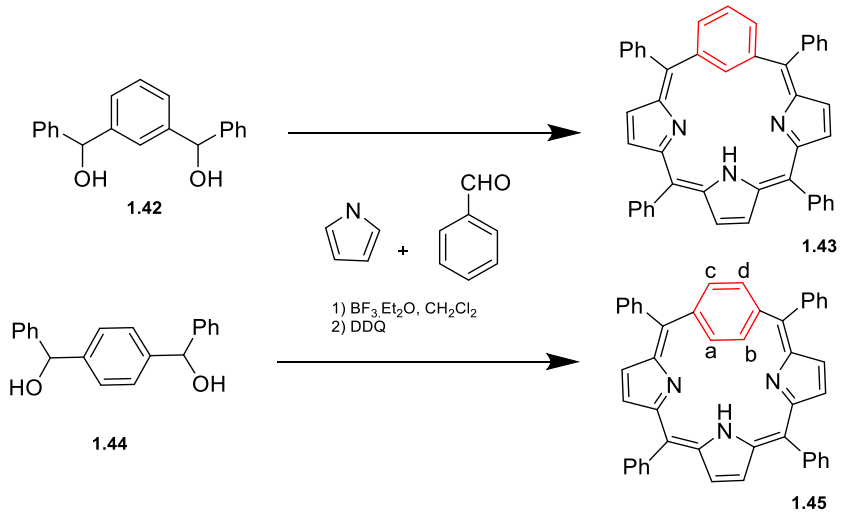

Scheme 1.23: Synthesis of *meta* and *para*- benziporphyrin.

When benzene is incorporated into a porphyrin framework, the local aromaticity of the benzene typically affects the overall π-conjugation of the macrocycles. In *m*-benziporphyrin, the benzene unit was connected to the tripyrrolic fragment through the 1,3-positions. This caused a loss of π-electron delocalisation in the whole molecule, resulting in a non-aromatic structure. The modification of benzene's connecting mode to the 1,4-position produced *p*-benziporphyrin. Unlike the case of *m*-benziporphyrin, the linkage between the tripyrrolic unit and the *p*-phenylene moiety allows effective π-electron conjugation. The chemical shifts of the inner CH protons, a and b, were observed upfield at 2.32 ppm. while, the outer CH protons, c and d, were observed at 7.68 ppm, indicating the presence of a diatropic ring current as reported by Latos-Grazynski. [8,80]

1.7 Inverted (confused) porphyrins

The term "confusion" refers to the modification of the linkage position of the pentacyclic ring (pyrrole) in the porphyrin structure from the regular α−α to the unusual α−β′ position.

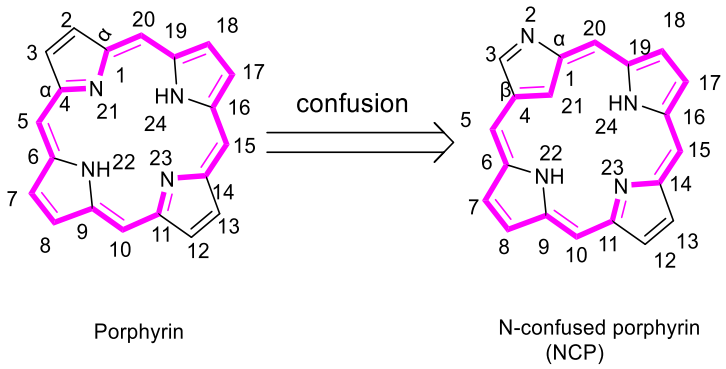

Figure 1.15: porphyrin and N-confused porphyrin.

The first *N*-confused porphyrin (NCP) was reported by Latos-Grazyński *et al*[81] and Furuta *et al*[82] in 1994. It is also called 2-aza-21-carbaporphyrin or inverted porphyrin, as shown in figure 1.15, and is a group of regular porphyrin isomers that have an inverted pyrrole which contains the inner CH, external and internal N atoms. Interestingly, NCP shows NH tautomerism in solution, allowing the proton to migrate between the inner and outer nitrogen and the tautomeric equilibrium is controlled mainly by the solvent. For example, an inner 3-H tautomer is found in nonpolar solvents like $CHCl_3$; the solution is red, which is the most stable and aromatic. Meanwhile, an inner 2-H tautomer is found in polar solvents such as DMF, and the solution is green, with an incomplete aromatic system.[83]

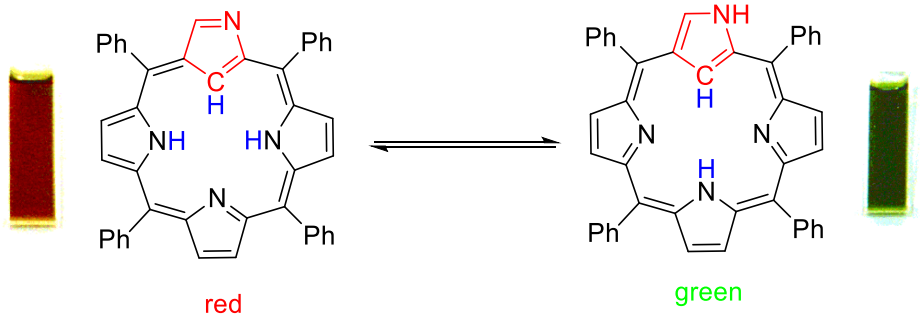

Scheme 1.24: NH tautomerism of NCTPP.

N-confused porphyrins were first discovered unexpectedly by Furuta *et al* and Latos-Grazynski *et al*, as by-products of standard one-pot porphyrin syntheses. Latos Grazynski synthesized

NCP using *p*-tolylaldehyde and pyrrole in CH_2Cl_2, catalysed by $BF_3{\cdot}Et_2O$, resulting in the production of NCP in low yield (4%) and the major product was a regular porphyrin.[81,84] Lindsey then reported the synthesis of NCPs in better yield 39% by condensation of pyrrole with aryl aldehyde, like the process used to prepare porphyrins, but using a different acid catalyst (methanesulfonic acid).[83,85]

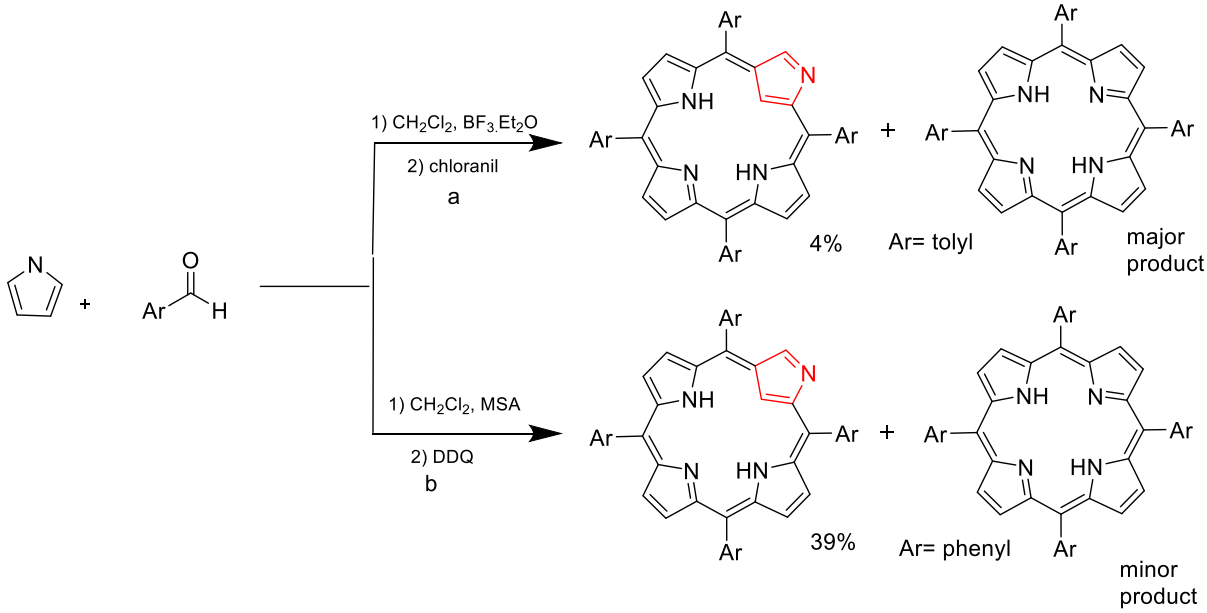

Scheme 1.25: Synthetic procedures for generation of H_2NCTPP: (a) Latos-Grazynski *et al*. (b) Lindsey *et al*.

The organometallic chemistry of these systems has attracted a lot of attention because of the potential to stabilise uncommon oxidation states and produce new catalytic systems (acting as dianionic ligands and trianionic ligands). [86,87]

The core modification of *N*-confused porphyrins involves the replacement of one or two pyrrole nitrogens within the porphyrin with other heteroatoms, such as S, O, and Se. The confusion can occur with the pyrrole ring or with the other heterocycle like furan, thiophene and selenophene. As a result, *N*-confused heteroporphyrins and heteroatom-confused heteroporphyrins are thus the sub-classifications of the confused heteroporphyrins. These compounds showed very interesting metal coordination properties because the presence of inner CH along with external and internal nitrogens helped in the formation of inner and outer coordination complexes and supramolecular structures.[84,88]

1.7.1 Heteroatom-Confused Heteroporphyrins

Latos-Grazynski and co-workers[89] also synthesized the first *S*-confused porphyrin (5,10,15,20-tetraphenyl-2-thia-21-carbaporphyrin) via 2,4- bis(phenylhydroxymethyl) thiophene as a key building block. The synthesis involved two methods: a one-pot, two-step reaction involving the condensation of 2,4-thiadicarbinol with benzaldehyde and pyrrole, or a reaction between 2,4-thiacarbinol and 5,10-diphenyltripyrrane, as outlined in scheme 1.26.

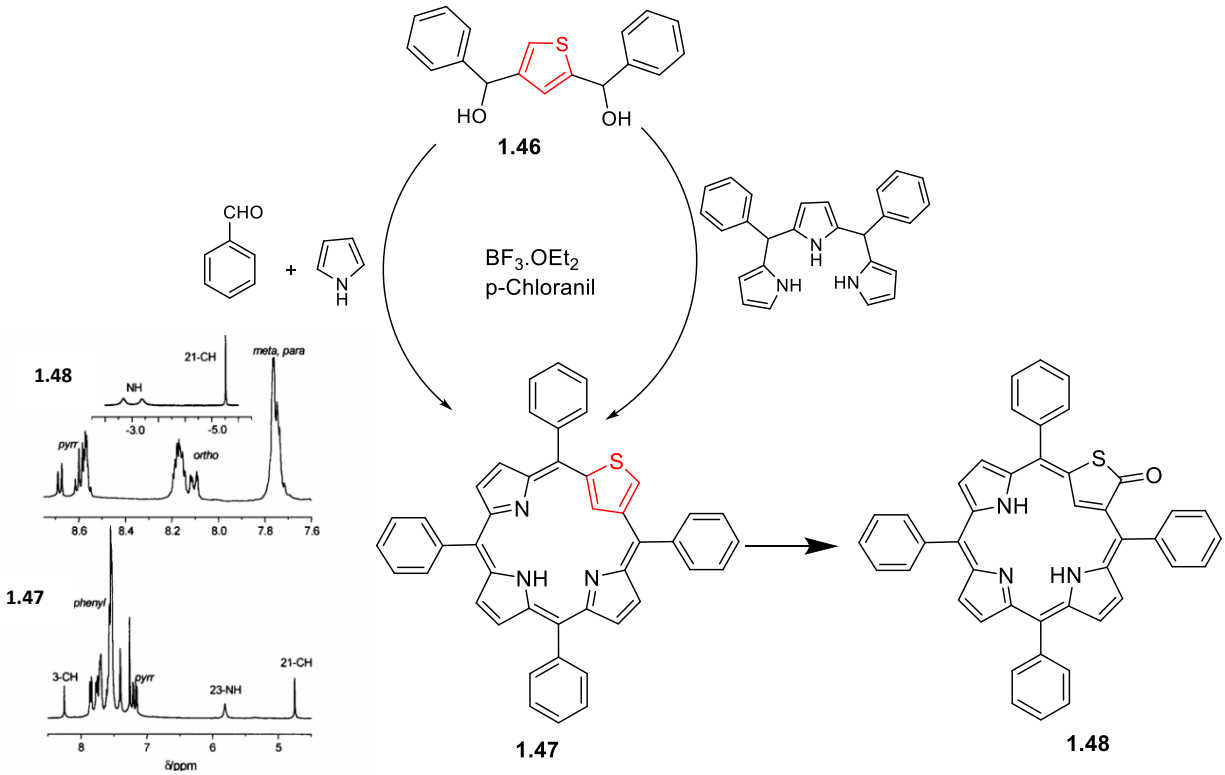

Scheme 1.26: Synthesis of *S*-confused porphyrin.

This porphyrinoid **1.47** showed borderline aromaticity, as confirmed by NMR spectroscopy with the inner NH resonating at δ 5.81 ppm while the inner thiophene CH resonated at δ 4.76 ppm. Oxidation of **1.47** with DDQ or with an excess of p-chloranil gave compound **1.48**, which exhibited typical aromatic features with inner CH and two inner NH resonances appearing at δ −5.31, −3.37, and −2.93 ppm.

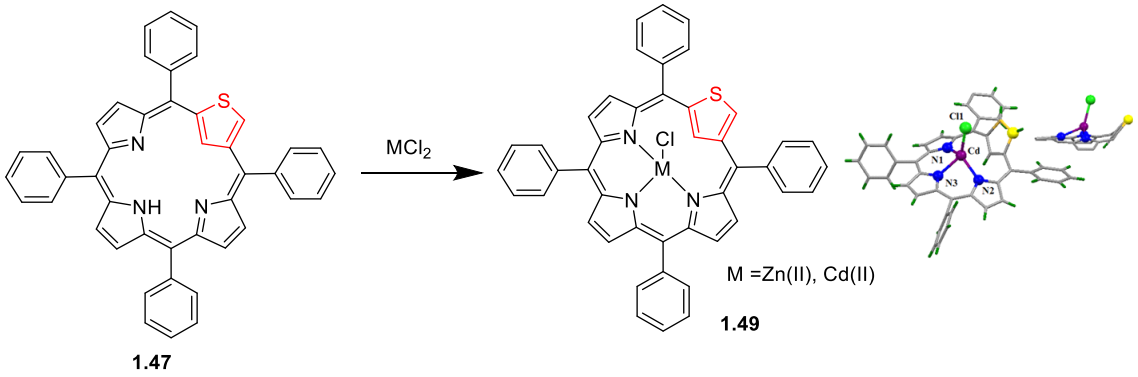

Scheme 1.27: Synthesis of zinc and cadmium complexes of *S*-confused porphyrin and the crystal structure of Cd **1.49**.[31]

Zinc and cadmium complexes of *S*-confused porphyrin were reported.[90] In these complexes, the metal ion binds to three nitrogen atoms and one axial chloride ligand and interacts with the C(21)H group of the inverted thiophene. So, this macrocycle acts as a monoanionic ligand. The interaction between the C(21)H group and metal ion was clear in the ^{13}C NMR spectrum, which showed significant changes in the chemical shifts of the C(21) carbon atom (92.9 ppm of Zn**1.49** and 88.7 ppm of Cd**1.49**, while 123.7 ppm for the starting macrocycle **1.47**). The X-ray crystallographic analysis of the Cd(II) complex, Cd **1.49**, showed that the Cd(II) ion is coordinated by three pyrrolic nitrogen donors and an apical chloride ligand. The coordination properties of X-confused heteroporphyrins have been less extensively investigated compared to *N*-confused porphyrins.[91]

1.7.2 *N*-Confused Heteroporphyrins

In this class, the isomer of 21-heteropophyrins has an inverted pyrrole ring positioned *cis* or *trans* to the hetero rings and they combine characteristics of the standard heteroporphyrins and inverted porphyrins.[92] For example, *N*-confused 21-selenaporphyrin **1.50** was synthesized by Latos-Grazyński and co-workers in 1% yield as a side product in a typical acid-catalyzed condensation of 2,5-selenadicarbinol with azatripyrrane to produce 21-selenaporphyrin. *N*-confused 21-selenaporphyrin showed a UV-vis spectrum that is porphyrin-like, with a Soret band that is bathochromically shifted (~20 nm) in comparison to the standard 21-selenaporphyrin (The UV-Vis spectrum of **SeC-DPDTPH 1.50 (**5,10-diphenyl-15,20-bis(p-tolyl)-2-aza-21-carba-22 selenaporphyrin) showed absorption peaks at 451, 541, 578, 618, and 666 nm, while **SeDPDTPH (**5,20-diphenyl-10,15-bis (p-tolyl)-21-selenaporphyrin) exhibited peaks at 433, 518, 552, 618, and 667 nm).[92,93]

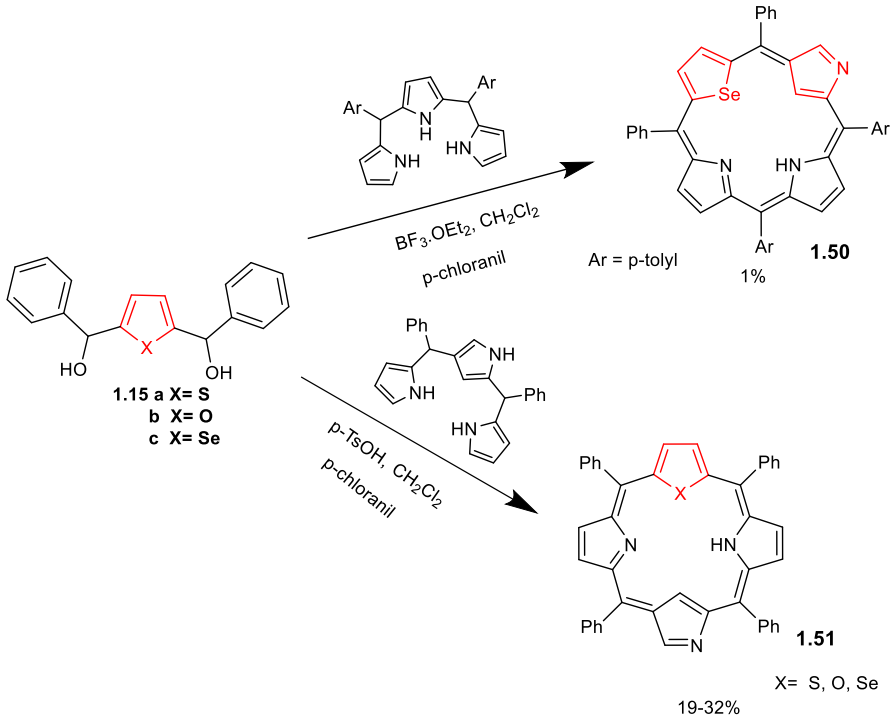

Scheme 1.28: Synthesis of *N*-Confused Heteroporphyrins**.**

Chandrashekar and co-workers prepared *N*-confused 21-heterporphyrin **1.51**, which has a confused pyrrole opposite to the heterocycle, employing different precursors in 19-32% yields. A modified tripyrrane containing the *N*-confused ring was condensed with the corresponding heterodicarbinol under mild acid-catalyzed conditions to afford the *N*-confused 21-heteroporphyrin.[94]

1.8 Expanded porphyrins:

Expanded porphyrins are a class of conjugated macrocyclic compounds in which pyrrole rings are linked to each other in a cyclic fashion through *meso*-carbon bridges. Unlike porphyrins, which have 18 π-electrons, the expanded porphyrins have more than 18 π-electrons in their conjugated route. An increase in the number of π-electrons can be achieved either by increasing the conjugated double bonds between the four pyrrole rings or by expanding the total number of pyrrole rings to five or more. Figure 1.16 displays some examples of expanded porphyrins such as Sapphyrin, Pentapyrin, Rubyrin and Hexapyrin.[8,95]

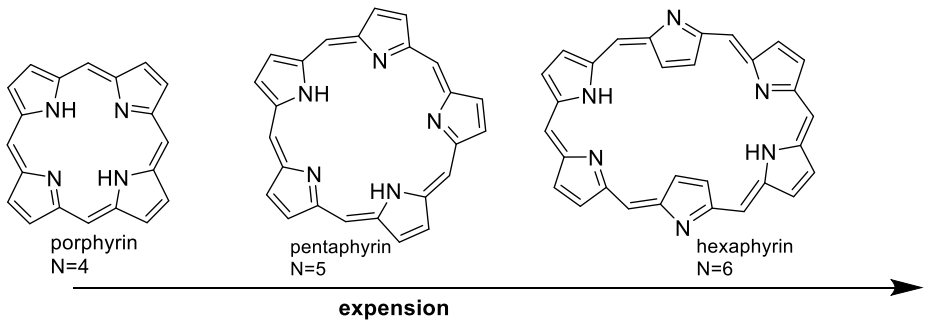

Figure 1.16: Porphyrin and expended porphyrins, where N= number of pyrrole subunits.[95]

1.8.1 Sapphyrin

Sapphyrin, the first reported example of an expanded porphyrin, is identified by its penta-azaheterocyclic core, which contains the building blocks 2,2'-bipyrrole and tripyrrane.[96] Decaalkyl-substituted sapphyrin was discovered by Woodward and co-workers during their attempt to synthesise vitamin B. Sapphyrin macrocycles have 22 π-electrons and they consist of a single direct α-α linkage, like corrole, and four methine bridges connecting the pyrrolic moieties.

The Soret-like absorption of sapphyrins is red-shifted and usually more intense (456 nm of decamethylsapphyrin) compared to porphyrins (414 nm of octamethylporphyrin) and corrole (413 nm of diethylhexamethylcorrole).[97] It has been demonstrated that these conjugated penta-pyrrolic macrocycles hold great promise for medical uses, such as photodynamic therapy[98] in addition to acting as catalysts for phosphate hydrolysis.[99] In addition, sapphyrins have been employed for the photodynamic inactivation of the herpes simplex virus.[100]

Sessler and co-workers[101] synthesised decaalkylsapphyrin based on the MacDonald-type [3 + 2] condensation approach using the acid catalysed condensation of diformyl bipyrrole and diacid tripyrrane in the presence of O_2.

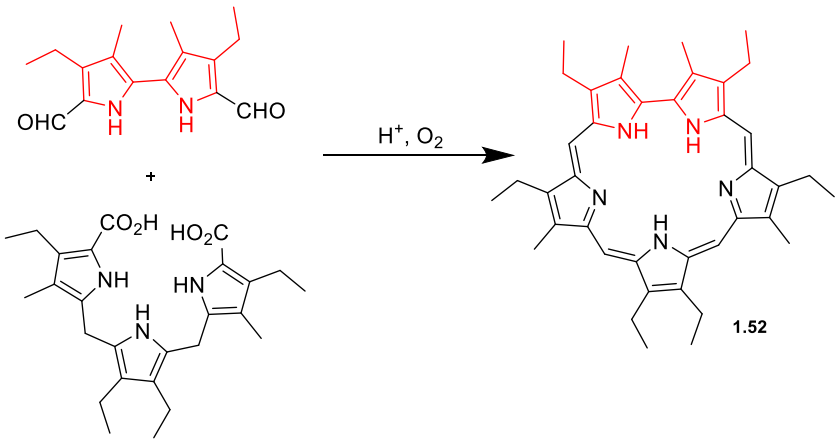

Scheme 1.29: Synthesis of sapphyrin.

However, a multistep synthesis is needed to prepare such a substituted bipyrrolic precursor. The same research group developed the [3 + 1 + 1] approach to synthesise β-alkyl sapphyrin.[102] In this methodology, the final step involves the production of a direct pyrrole–pyrrole bond. The bisformyl tripyrromethane underwent an acid-catalyzed condensation reaction with 2 eq of β-substituted pyrrole. Subsequent oxidation resulted in the formation of the β-substituted sapphyrin with a yield of 34%. This synthetic approach provided an alternative pathway to the [3 + 2] strategy, resulting in improved overall yield and a reduced number of synthetic steps for the preparation of β-alkyl azasapphyrin.[103]

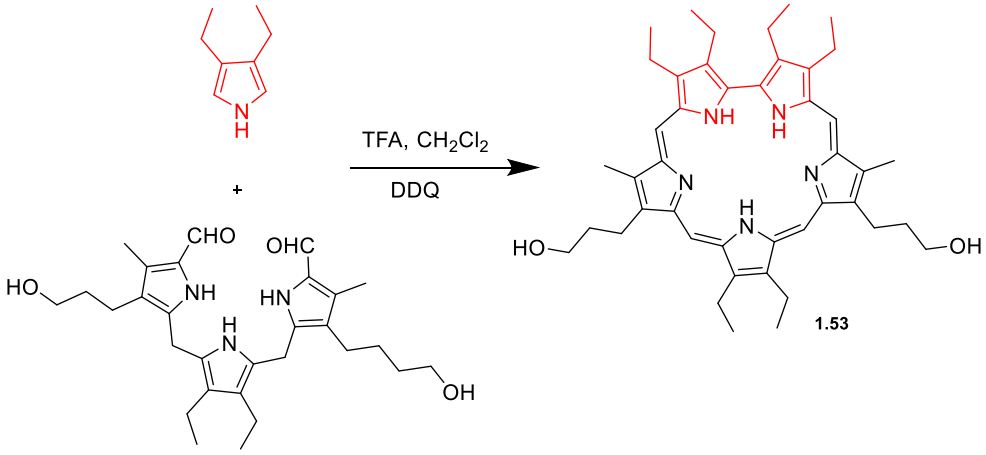

Scheme 1.30: Synthesis of β-Alkyl Sapphyrin using (3+1+1) procedure.

To modify the electrical, photochemical, and optical properties of expanded macrocycles with retained aromatic character, the core of porphyrins can be adjusted by substituting heteroatoms like O, S, Se, or Te for pyrrole NH. As discussed previously, this results in "core-modified expanded porphyrins".[104,105] Johnson and coworkers have developed the synthesis of the first

heteroatom analogues of sapphyrin when they discovered them as side products during their attempt to produce heteroatom analogues of corroles. Tripyrrane was condensed with diformylbifuran, following by oxidation to synthesise dioxa sapphyrin in 10% yield.[101,106]

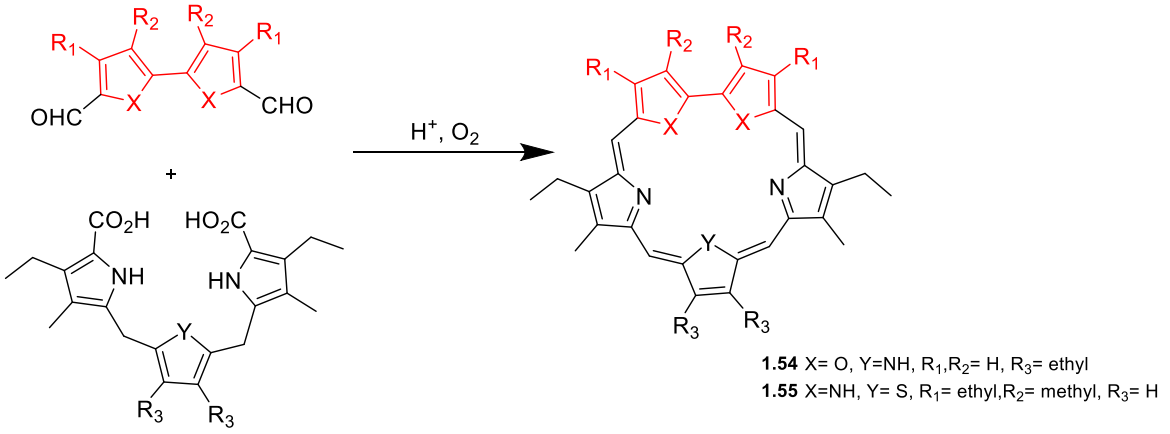

Scheme 1.31: Synthesis of heterosapphyrin.

Dioxasapphyrin **1.54** absorbs at a shorter wavelength, with Soret band at 442 nm compared to the absorption of the all-nitrogen sapphyrin (456 nm). In contrast, thiasapphyrin **1.55** absorbs at a longer wavelength at 463 nm.[101]

1.8.1.1 Anion-Binding Interactions

Molecular receptors are host molecules that selectively recognize and bind to neutral species, cations, or anions. Of these, receptors or hosts for anions are rare. The ability of a molecular receptor to bind and select guests depends largely on the size of its cavity coupled to appropriate non-covalent interactions. Expanded porphyrins, with their unique structures containing more than four pyrrole rings, show exceptional versatility as macrocyclic receptors. While this is common for coordinating metal cations in the porphyrin cavity, anion binding began with Sessler and Ibers' unexpected discovery that sapphyrin could bind fluoride ions.[107] In 1990, the first X-ray structural analysis of the diprotonated sapphyrin through a counterion-exchange reaction revealed unexpected findings. The structure instead showed a fluoride ion bound within the sapphyrin core. The discovery of fluoride binding in sapphyrin led to the question of whether other anions could bind in the same way. In 1992, X-ray analysis showed that larger chloride ions couldn't fit within the sapphyrin core. Instead, they attached to opposite faces of the macrocycle through hydrogen bonds. Further studies demonstrated their high specificity for phosphate-containing anions. The anion-recognition properties of sapphyrin have been examined over the past decades and open a wide range of potential applications in chemistry

and biological contexts, including separation science, DNA binding and cleavage and membrane transport.[97,103]

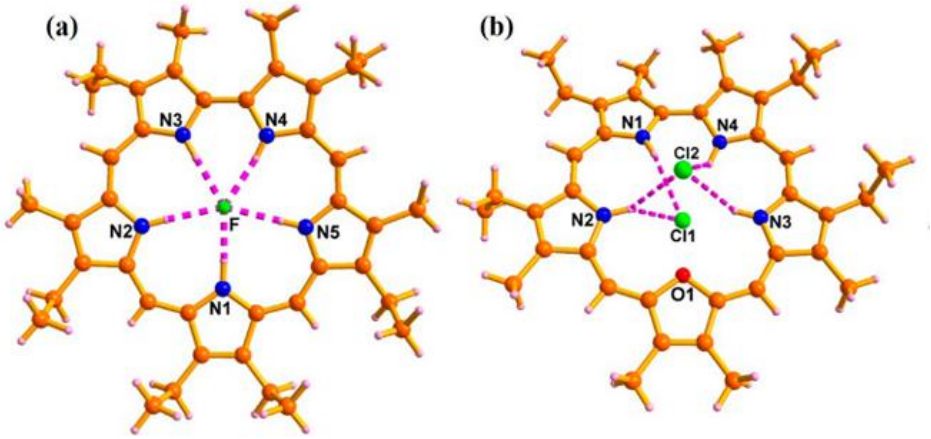

Figure 1.17: Crystal structures of Sapphyrins binding different anions.[103]

Chapter 2: Results and Discussion

2 Results and Discussion

2.1 The aims of the project:

Phthalocyanines (Pcs) and their derivatives have garnered a lot of interest because of their technological applications. Simple phthalocyanines are constructed through macrocyclization of four isoindole units linked by nitrogen bridges. The isoindole units are typically identical (leading to the parent Pc or symmetrical Pcs) but can be different (Figure 2.1, left). Most commonly, the properties of Pcs whether chemical, optical, coordination, electrochemical, and others can be adjusted in three ways: altering the phthalocyanine ring's periphery through pi-extension and/or introduction of substituents, changing the *meso*-atoms, and replacing the central atom. Another more drastic but promising pathway for modifying Pcs and their derivatives is through modification of the core itself, for example by changing the isoindole nitrogen(s) for other elements (Figure 2.1, right).[108]

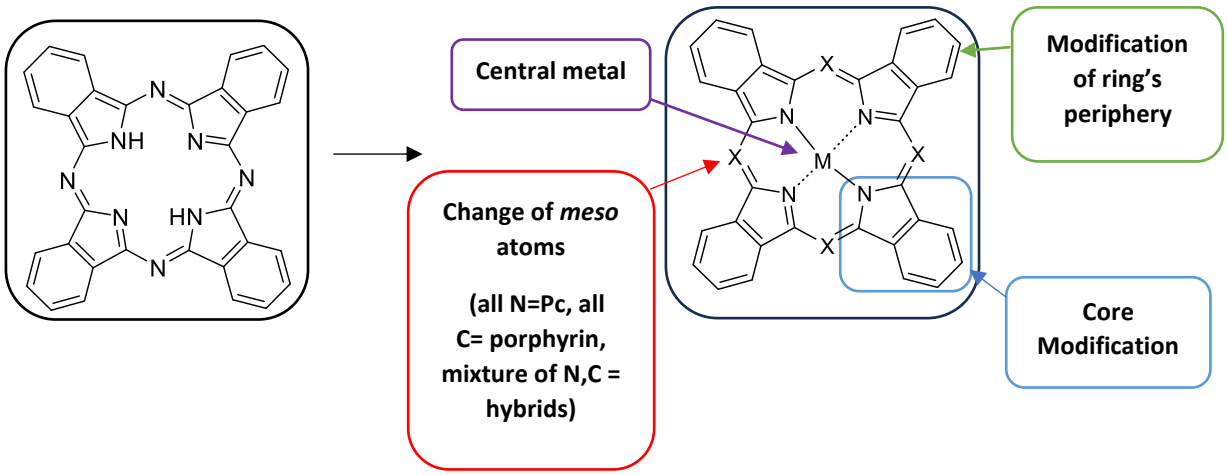

Figure 2.1: Phthalocyanine structure.

This project aims to combine all modification pathways to produce a unique class of macrocycle - "Tribenzodiazathiaporphryin hybrids". The target macrocycles are related to phthalocyanine hybrids, specifically diazatetrabenzoporphyrin (TBDAP) derivatives with replacement one of the isoindole groups with thiophene.

The method that we will follow to synthesise phthalocyanine hybrids will be based on a stepwise synthesis that has been recently developed in our group. Over the last 10 years or so our group's interest in the synthesis of hybrids led to development of a modern synthesis of the tetrabenzotriazaporphyrins, TBTAPs.[26] The synthesis employs aryl-aminoisoindolines (as

initiator fragment) and phthalonitrile co-reactants. Aminoisoindolines are readily synthesised from amidines and aryl acetylenes by a Sonogashira coupling followed by a 5-*exo*-dig cycloisomerization domino reaction.

Our proposed synthetic strategy involves the utilization of a diacetylene instead of monoacetylene (as used in TBTAP synthesis) to produce a bisaminoisoindoline, which subsequently undergoes reaction with phthalonitrile to yield our desired macrocyclic compound. The outline synthetic scheme is shown below (Scheme 2.1), illustrating tribenzodiazathiaporphryin for the 2,5-linked thiophene derivative. Our TBDAP hybrid skeleton can be considered as constructed from 4 units; one diaminoisoindoline fragment is retained (red), but C-bridges are introduced through incorporation of other indoline fragments (green and blue). Our investigation will seek to exchange the green fragment, specifically with thiophene derivatives as shown, and study the effect of modification (substitution) at red and blue fragments.

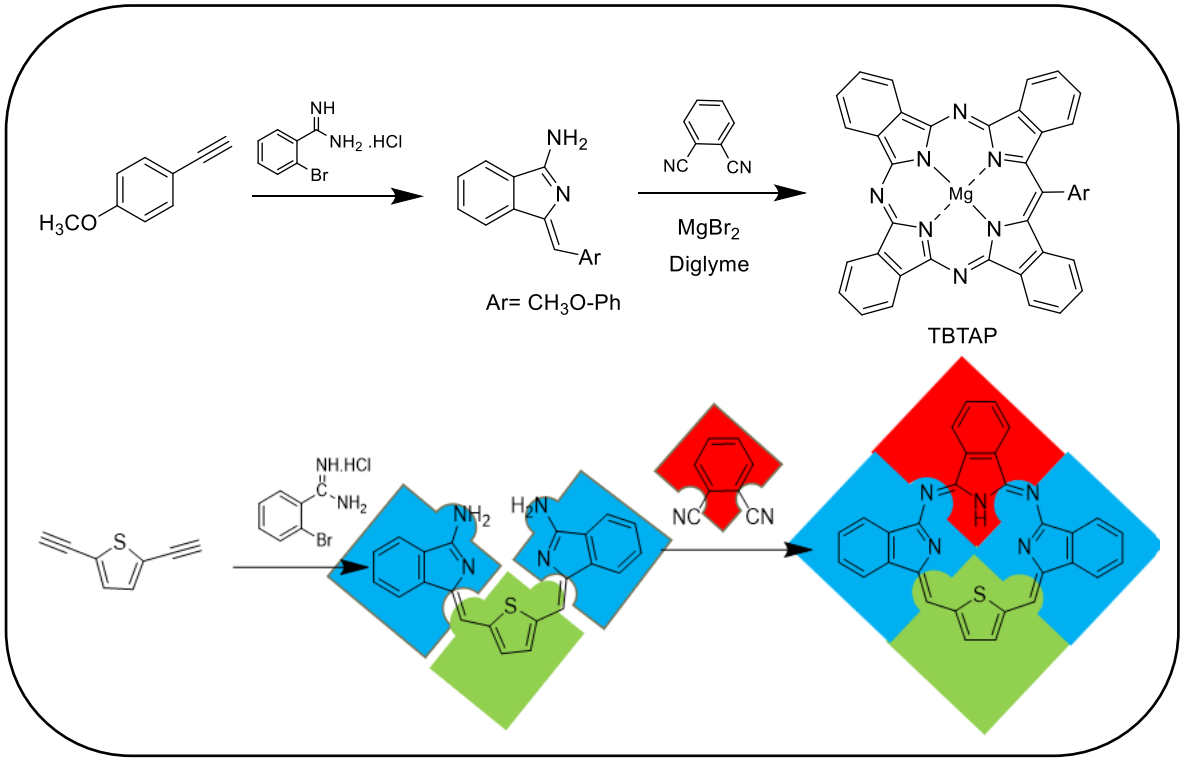

Scheme 2.1: Standard TBTAP sequence (top), and planned tribenzodiazathiaporphryin synthesis (bottom).

The main focus of this project is to evaluate the scope of the synthesis for modifying the four pieces and to compare the influence of each building block on the optical properties.

2.2 Synthesis of the first series of tribenzodiazathiaporphyrins.

In the first series, our objective focused on synthesising the first tribenzodiazathiaporphyrin structures and altering the top isoindoline moiety, employing substituted phthalonitriles in the synthesis.

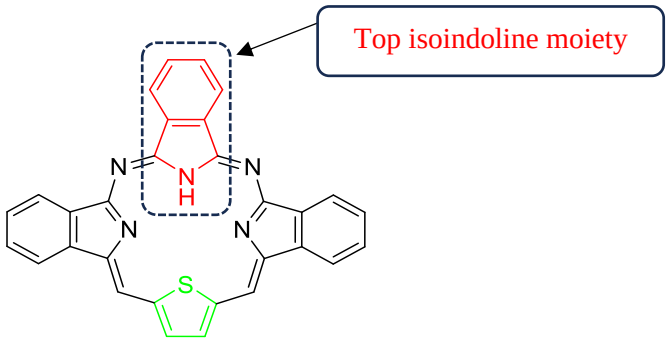

Figure 2.2: Tribenzodiazathiaporphyrin structure.

2.2.1 Synthesis of intermediate 2.2:

The first challenge in this project was the synthesis of bisaminoisoindoline thiophene **2.2,** as it was required before the macrocyclization can be achieved. At the heart of the strategy lies bromobenzamidine **2.1** and thiophene diacetylene as intermediates to form **2.2**.

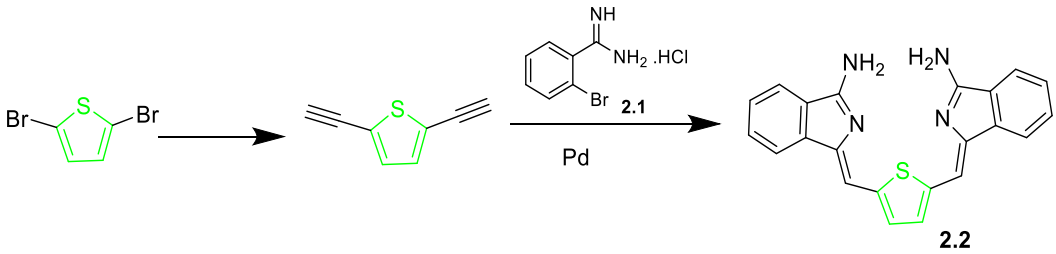

Scheme 2.2: Proposed synthesis of intermediate **2.2**.

The required intermediate **2.2** was to be synthesised by following a similar sequence to that used for the synthesis of aminoisoindoline **2.3**,[20] which was prepared from bromobenzamidine via a copper-free Sonogashira coupling followed by a 5-*exo*-dig cycloisomerization domino reaction (Scheme 2.3). We started our investigation by reproducing the conditions from the literature used to prepare aminoisoindoline **2.3**.

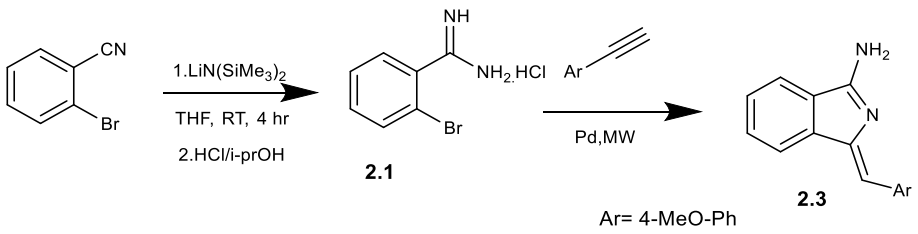

Scheme 2.3: Synthetic route to aminoisoindolines **2.3**.

The synthesis of aminoisoindoline **2.3** begins with the synthesis of amidine **2.1** by treating a solution of 2-bromobenzonitrile in THF with lithium bis(trimethylsilyl)amide. The $LiN(SiMe_3)_2$ behaves as a nucleophile, attacking the electrophilic carbon next to the nitrogen. Then, the reaction mixture was treated with a solution of 5M hydrochloric acid in isopropanol to remove the silyl protecting groups. 2-Bromobenzamidine hydrochloride salt **2.1** was produced as a white solid in 85% yield.[109]

The next step in the synthesis of the aminoisoindoline **2.3** followed the procedure developed by Hellal and Cuny,[25] which involves a one-pot palladium catalysed, copper-free Sonogashira cross-coupling followed by a cycloisomerisation reaction to give easy access to the derivative **2.3**. The one-pot synthesis was carried out by reacting amidine **2.1**, 4-methoxyphenyl acetylene, catalytic amounts of a palladium catalyst and BINAP as ligand, in the presence of DBU as a base and employing DMF as a solvent for the reaction. The reaction was most conveniently performed in a microwave reactor. After work-up and purification by column chromatography and recrystallisation, the aminoisoindoline product **2.3** was isolated as yellow needles. The identity of the product was confirmed by ^{1}H NMR spectroscopy which showed the characteristic alkene proton at ~ 6.78 ppm. Aminoisoindoline **2.3** had already been synthesised by our group with excellent success by applying the same procedure.

We were now confident to reproduce the efficient synthesis of aminoisoindolines like **2.3**, and ready to shift our focus towards our new target molecule **2.2**. The proposed intermediate **2.2** was synthesised in a stepwise fashion, starting by introducing the bis-aminoisondoline to thiophene via a Sonogashira coupling between bromobenzamidine and thiophene diacetylene by following the procedure published by Hellal *et al.*, as explained previously**.** However, in the previous syntheses of aminoisondolines like **2.3**, an excess of acetylene was required to compensate for the formation of unwanted homocoupling byproduct from acetylene. This approach was not possible for our double reaction. Fortunately, other work in the group had refined the synthesis of thiophene methylene aminoisoindoline **2.4**, revealing that using TMS-

protected acetylene, instead of acetylene itself, effectively minimizes the formation of unwanted homocoupling byproduct and improved the yield.

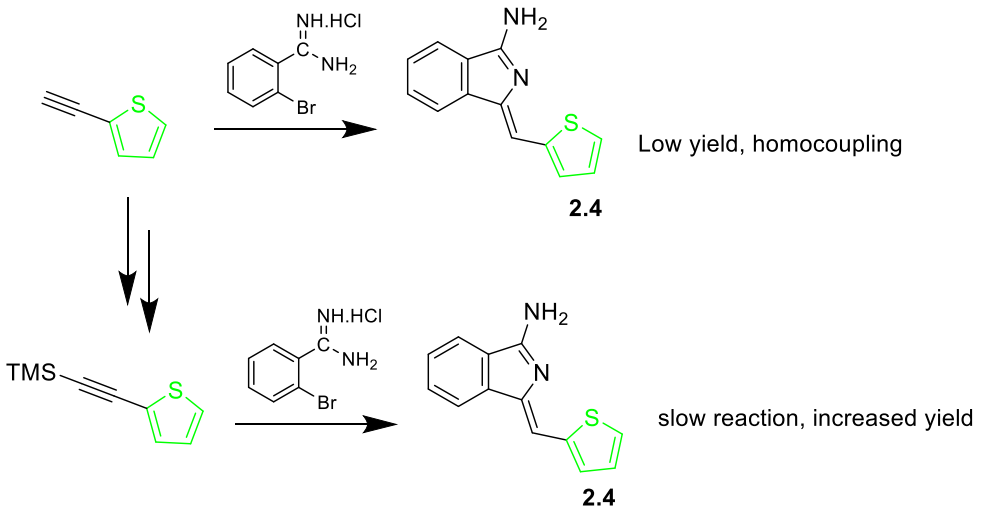

Scheme 2.4: Synthesis of compound **2.4**.

Thus, we prepared **2.2** by directly using the TMS protected diacetylene, which relied on a copper free Sonogashira coupling methodology as shown in scheme 2.5.

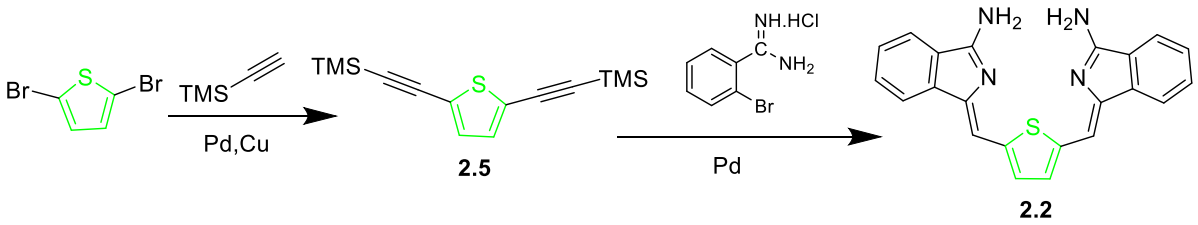

Scheme 2.5: Synthesis of compound **2.2**.

To synthesise the desired intermediate **2.2**, it was required to synthesise bis(trimethylsilylethynyl) thiophene **2.5** according to the reported method.[110] A solution of 2,5-dibromothiophene and (trimethylsilyl)acetylene was refluxed in the presence of bis[triphenylphosphine]palladium dichloride and copper(I) iodide in triethylamine and THF overnight. After purification, the product was obtained in good yield (91%) as a yellow solid**.** The compound was characterised, and the structure was confirmed by NMR spectroscopy.

To prepare bis-aminoisoindoline **2.2** (Scheme 2.5), 2 eq of amidine hydrochloride and 1 eq of bis(trimethylsilylethynyl) thiophene **2.5** were coupled using catalytic palladium/BINAP in a microwave reactor at 120 °C for 1h. The isolation process proved challenging and time consuming. The resultant red solid was subjected to column chromatography, using a high

polarity system with a solvent mixture of (THF: PE) in a 2:1 ratio for effective separation to obtain the title compound as a red solid.

The ^{1}H NMR spectrum of intermediate **2.2** in deuterated methanol is shown in figure 2.3. As expected, the spectrum shows a symmetrical structure. A singlet around 7 ppm, integrating to two protons, probably corresponds to protons of alkene, and a singlet peak at 7.28 ppm probably corresponds to thiophene protons. The peaks of benzene protons are also as expected. This compound's solubility was insufficient for ^{13}C NMR spectroscopy.

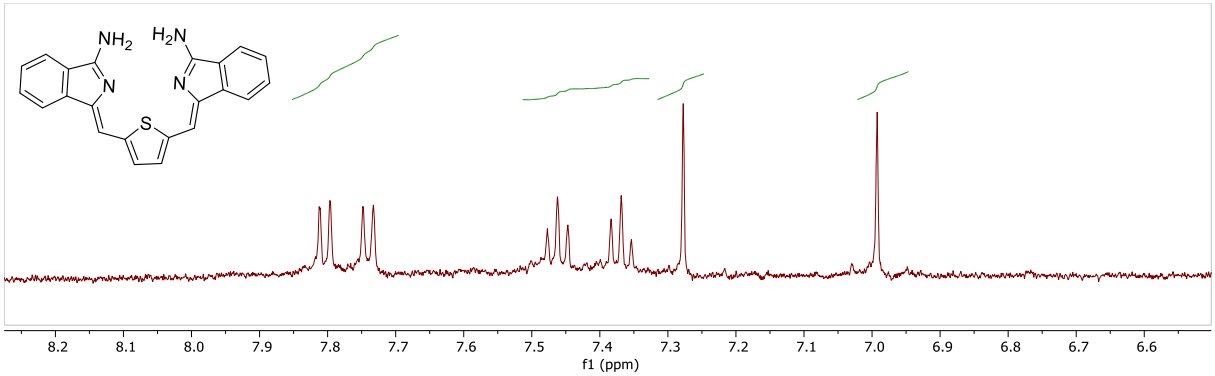

Figure 2.3: ^{1}H NMR spectrum of compound **2.2**.

2.2.2 Synthesis of the first series of macrocycle

Once the intermediate **2.2** was synthesised, it was employed in the preparation of tribenzodiazathiaporphyrin.

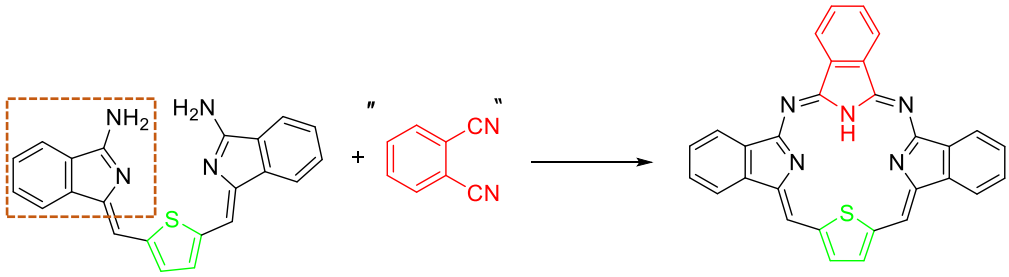

2.2

Scheme 2.6: Proposed synthesis of tribenzodiazathiaporphyrin.

Our initial plan for the reaction involved combining compound **2.2** with phthalonitrile and refluxing in a high-boiling solvent to produce our macrocyclization product. However, it was recognised that harsh conditions would likely lead to cyclization of phthalonitrile itself to give Pc, prompting us to avoid them. We aimed to investigate conditions conducive to the formation

of a more reactive intermediate. Fortunately, some parallel work in our group was already exploring related conditions, which helped us in this investigation. This study demonstrated increased reactivity of activated phthalonitrile derivatives like **2.6**, easily prepared from the reaction of phthalonitrile with methanol and sodium methoxide.[111] In related reactions, it was found that compound **2.7** was successfully synthesised through the refluxing of aminoisoindoline **2.3** and dimethoxyisoindoline **2.6** in methanol (aminoisoindoline would undergo homocondensation in higher boiling solvents such as toluene). It was subsequently found that isolation of **2.6** was not needed, and the reaction could be achieved in a single operation. The reaction involving compound **2.3** was similar to our intermediate compound **2.2** on one side**,** so we decided to employ these conditions for the synthesis of tribenzodiazathiaporphyrin**.**

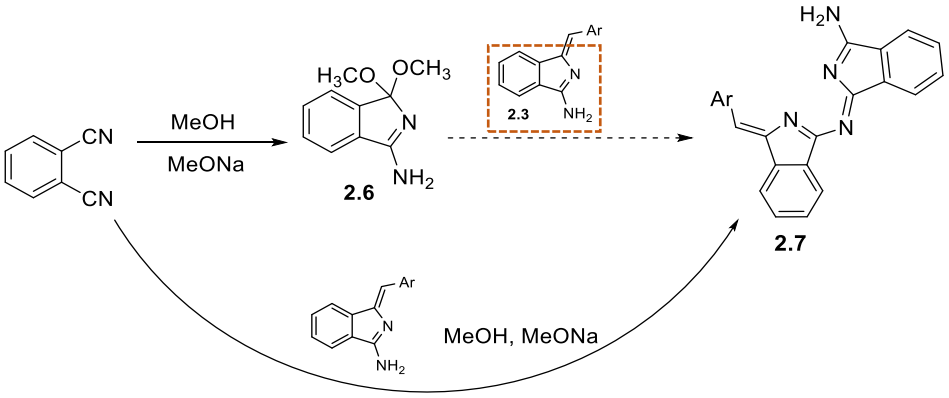

Scheme 2.7: Synthesis of product **2.7**.

The formation of tribenzodiazathiaporphyrin was achieved using one subunit of compound **2.2** with one subunit of phthalonitrile in methanol with sodium methoxide acting as nucleophile/initiator. Initial investigation using unsubstituted phthalonitrile indicated that the reaction product showed limited solubility. Therefore, we chose to employ a derivative bearing solubilising functionality. The first phthalonitrile used in the research was the *tert*-butyl phthalonitrile derivative due to its commercial availability, which reduced the initial steps needed to obtain our compound (Scheme 2.8).

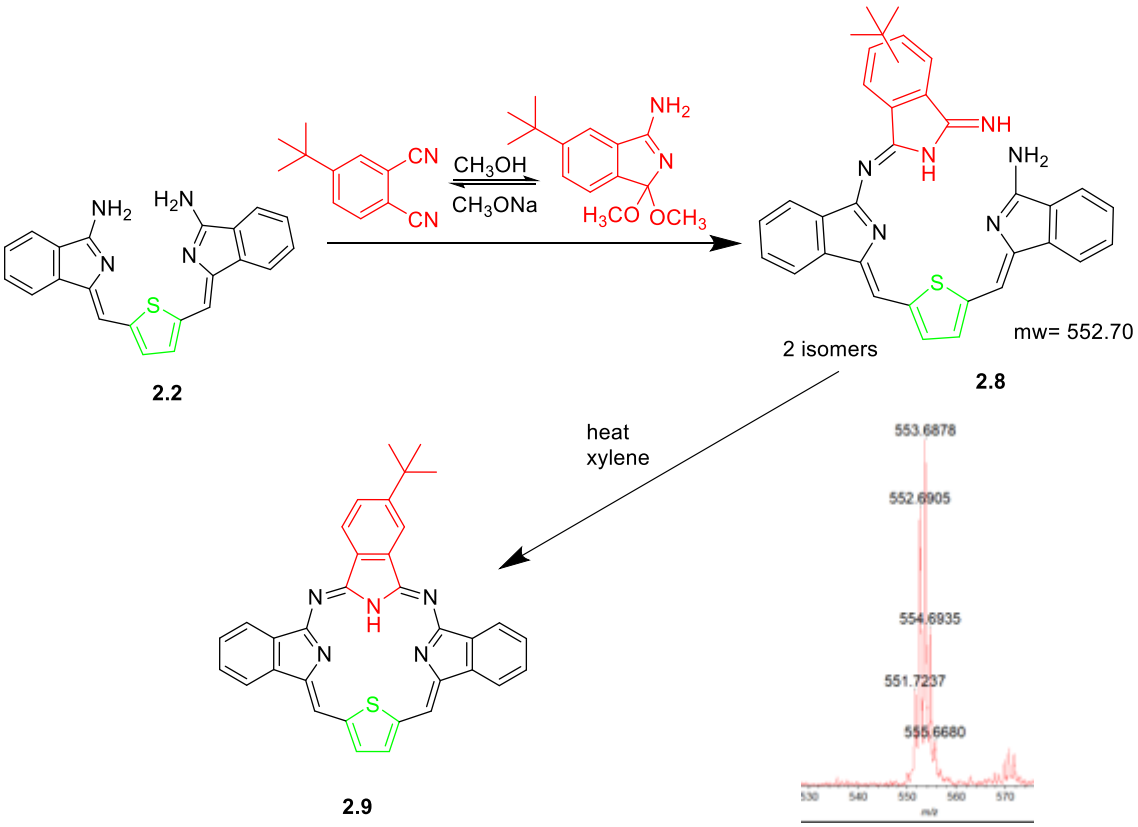

Scheme 2.8: Synthesis of compound **2.9**; inset, MALDI-TOF-MS spectrum of **2.8**.

We reasoned that the reactive intermediate (dimethoxyisoindoline) can be prepared in the reaction itself, in equilibrium with phthalonitrile. Therefore, to synthesise the target product **2.9**, as well as the proposed intermediate **2.8**, a mixture of *tert*-butyl phthalonitrile, compound **2.2** and sodium methoxide was stirred in refluxing methanol overnight. TLC showed a new deep purple spot close to a baseline that was expected to correspond to the intermediate **2.8**. Isolation of this fraction was performed by column chromatography using THF and PE and the material was characterised by MALDI-TOF MS, which confirmed the formation of intermediate **2.8** with a molecular ion peak at (m/z 553). The NMR spectroscopic analysis of this product showed complicated spectra, suggesting the potential presence of isomers, which were not easy to separate. While the reaction was performed under mild conditions to avoid Pc formation, its formation still occurred to some extent, resulting in a reduction of the desired compound yield.

Intermediate **2.8** was heated in refluxing *p*-xylene and the reaction was monitored by TLC. The cyclized compound **2.9** was easily observed through TLC due to intense pink emission exhibited under a 365 nm UV lamp and this proved a valuable aid distinguishing between

macrocyclized compound **2.9** and the open compound **2.8**. Separation of the component was achieved by column chromatography followed by recrystallisation from DCM/methanol to give the target compound **2.9**. The identity of compound **2.9** was confirmed by ^{1}H NMR and MALDI-TOF MS spectroscopies.

The ^{1}H NMR spectrum in deuterated chloroform for **2.9** gave all signals corresponding to all protons of the compound and showed a reduction in symmetry of the compound due to the presence of a *tert*-butyl group which was found at 1.7 ppm (Figure 2.4). Assignment of all signals was assisted by COSY. The H-H COSY played a crucial role in identifying protons of benzene rings, and the absence of a cross peak in the region around 9.5 ppm indicates that the signals present there correspond to two singlets, which are for the alkene protons, as shown in figure 2.4. NOESY NMR spectroscopy contributes significantly to assigning the peak at 9.5 ppm to the alkene protons, which demonstrates a correlation with both the benzene and thiophene protons.

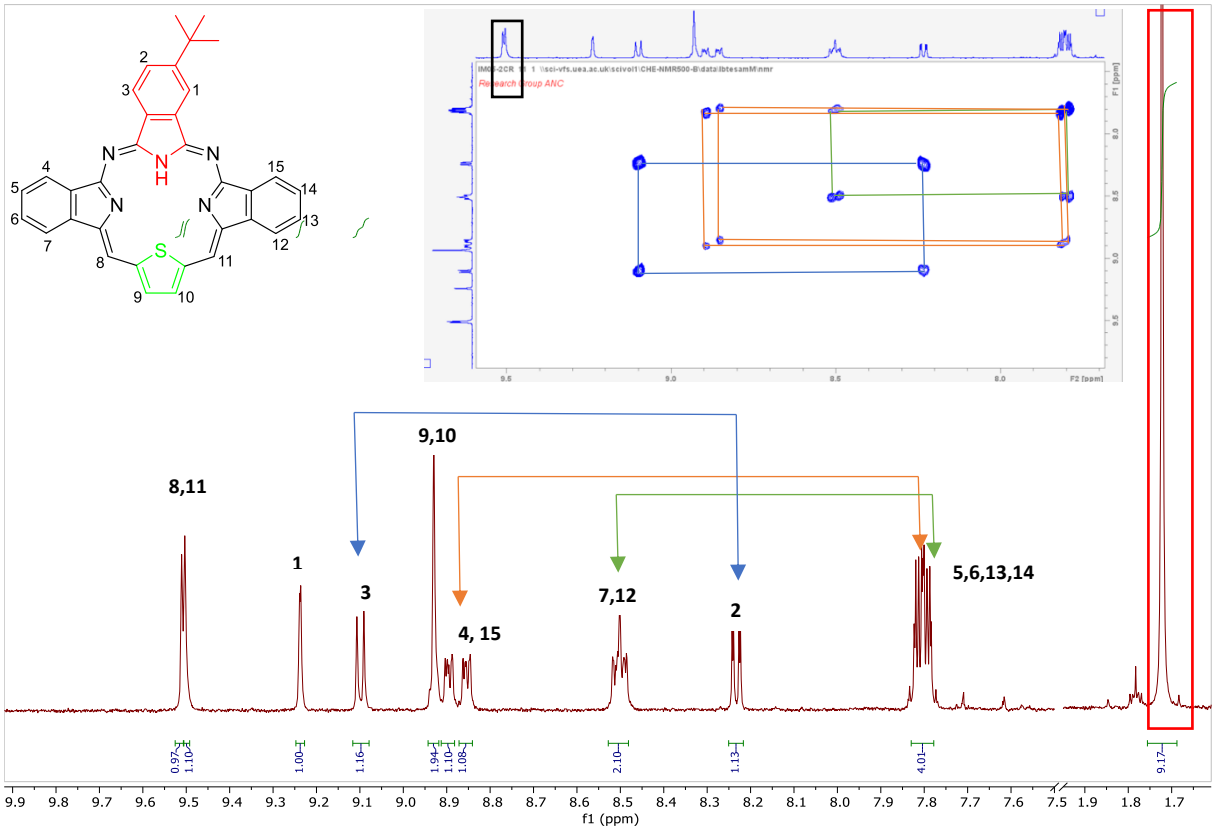

Figure 2.4: ^{1}H NMR spectrum and H-H COSY NMR spectrum of compound **2.9**.

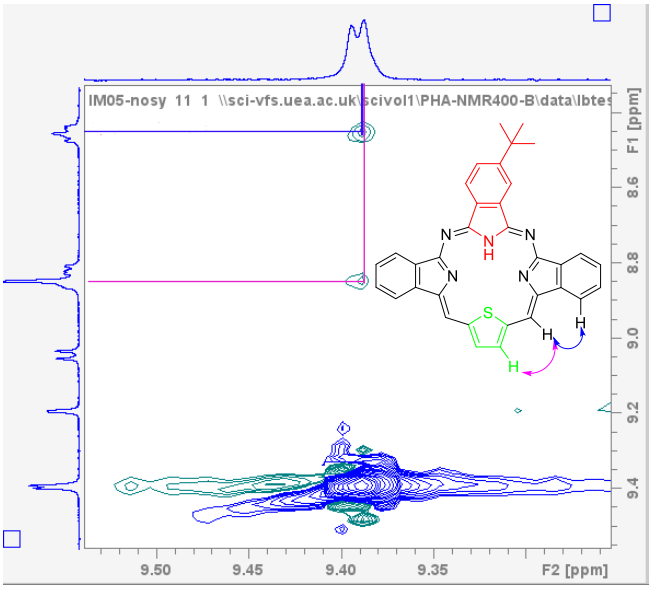

Figure 2.5: NOESY NMR spectrum of compound **2.9**.

The reduction of symmetry in the prior compound prompted the investigation of an alternative derivative. Among various potential phthalonitriles, 6,7-dicyano-1,1,4,4-tetramethyl-tetralin was chosen due to our expectation that the product would be soluble and stable due to the bulk of the system and NMR spectra are expected to be simplified. The confirmation of solubilising effect in the substituted 6,7-dicyano-1,1,4,4-tetramethyl-tetralin was verified by the Cammidge group during the synthesis of TBTAPs with this substituted compound.[26] The synthesis of phthalonitrile **2.14** is shown in scheme 2.9.

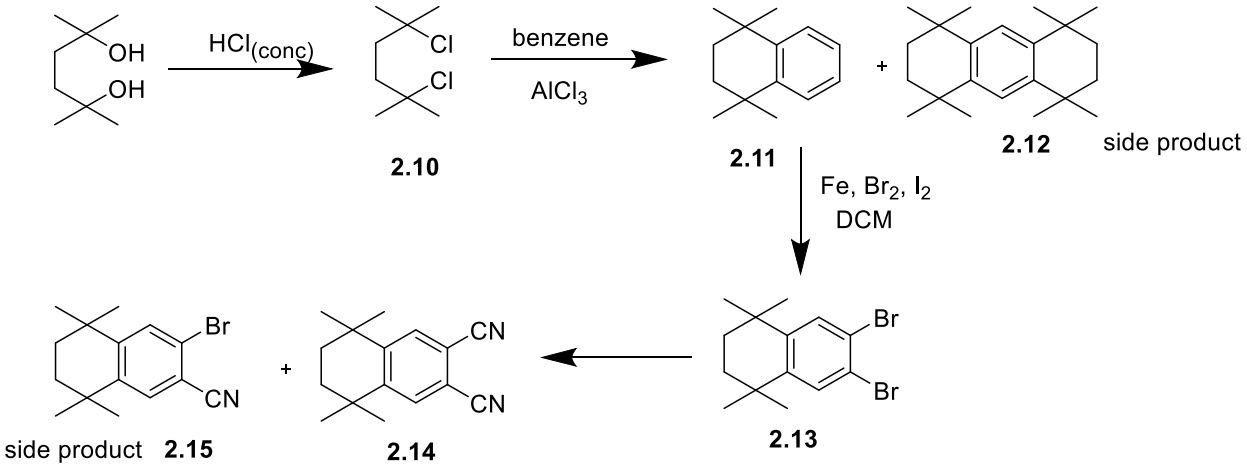

Scheme 2.9: Synthesis of 6,7-dicyano-1,1,4,4-tetramethyltetralin **2.14**.

This route started with the conversion of 2,5-dimethyl hexane-2, 5-diol to the 2,5-dichloro-2,5-dimethylhexane[112,113] **2.10** using concentrated hydrochloric acid. The acid was added to the diol in an ice bath and then left to stir at room temperature overnight. Work-up and crystallisation from methanol gave the 2,5-dichloro-2,5-dimethylhexane in a good yield. In the second step 1,1,4,4-tetramethyl-1,2,3,4-tetrahydronaphthalene **2.11** was prepared through Bruson's procedure via Friedel-Crafts reaction.[112] 2,5-Dichloro-2,5-dimethylhexane was dissolved in benzene and heated to 50°C, and anhydrous aluminium chloride was added in small portions over 30 min and was then left stirring for 24 h at 50°C. It was observed that the reaction produced two products, a liquid mono- and a solid di-cycloalkylation product, **2.11** and **2.12**. After work-up, the solvent was removed and column chromatography using PE as an eluent solvent was applied to remove the side product **2.12**. The next reaction was bromination of 1,1,4,4-tetramethyl-1,2,3,4-tetrahydronaphthalene **2.11**. Iron powder and iodine were added to a solution of 1,1,4,4-tetramethyl-1,2,3,4-tetrahydronaphthalene **2.11** in DCM. Then, the mixture was cooled to 0°C and Br_2 was added dropwise over 30 min and left stirring at room temperature overnight. The reaction was checked by ^{1}H NMR spectroscopy to ensure the total consumption of the starting material. The last step to prepare the desired phthalonitrile **2.14** was achieved by following the Schareina *etal.* cyanation reaction[114,115] which has been developed by our group, which uses non-toxic cyanide source potassium hexacyanoferrate (II), copper as a catalyst and a ligand system based on 1-alkyl-1H-imidazoles to convert aryl halides into nitriles. A mixture of 6,7-dibromo-1,1,4,4-tetramethyl-1,2,3,4- tetrahydronaphthalene **2.13**, $K_4[Fe(CN)_6]$, CuI and 1-butylimidazole was refluxed in anhydrous *p*-xylene under an argon atmosphere and the reaction was monitored by TLC. TLC showed three spots for the crude mixture; the two first spots were related to the starting material **2.13** and the mono nitrile product **2.15**, and the third spot was the dinitrile product **2.14**. With column chromatography, we effectively recovered unreacted starting material and isolated both the mono- and di-nitrile products from the crude mixture. The Rosenmund–von Braun synthesis was also followed to prepare dinitrile product **2.14** as briefly discussed in the next section. The yield of dinitrile was higher when Schareina *etal.* cyanation reaction[114,115] was used compared with the Rosenmund–von Braun synthesis.[116]

A reasonable amount of phthalonitrile **2.14** had been accumulated at this stage and was used to prepare tribenzodiazathiaporphyrin **2.18.**

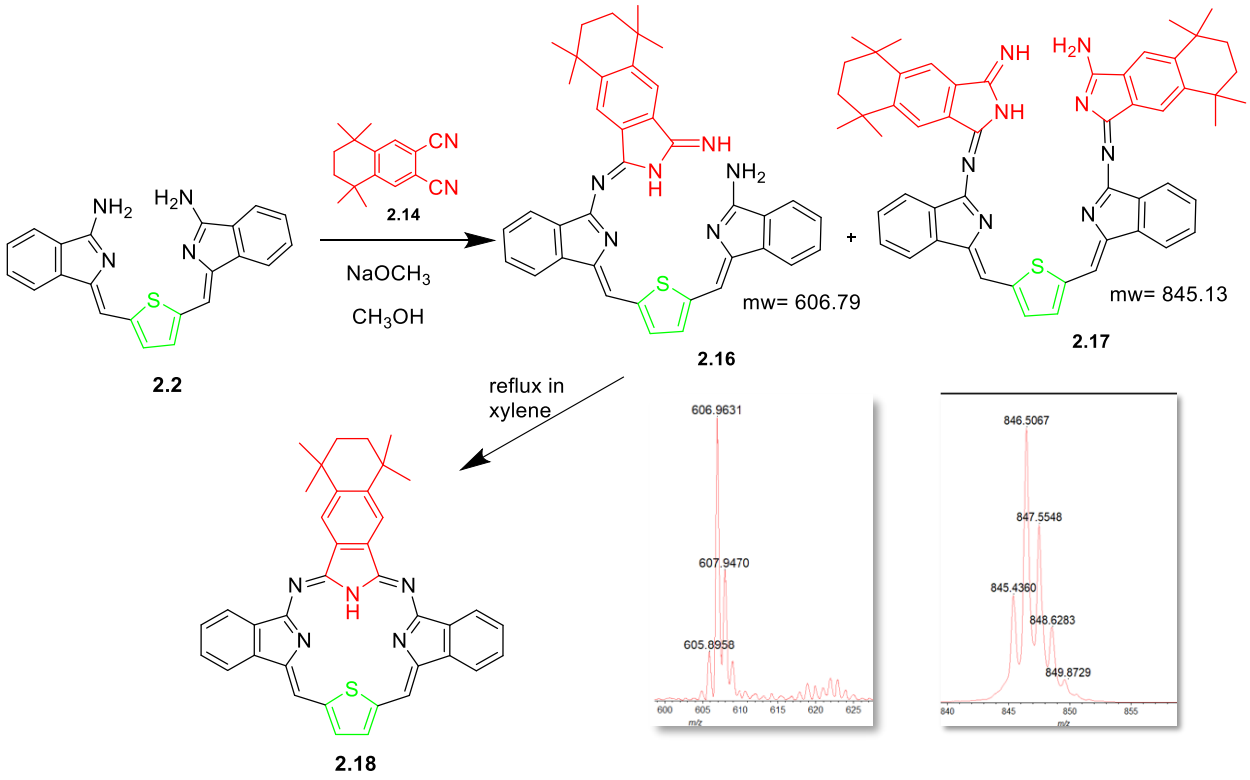

Scheme 2.10: Synthesis of tribenzodiazathiaporphyrin **2.18**; inset, MALDI-TOF-MS spectra of **2.16** and **2.17**.

Tribenzodiazathiaporphyrin **2.18** was synthesised by reacting phthalonitrile **2.14** with bis(aminoisodoline) thiophene **2.2**. The reaction was carried out at reflux in methanol with $NaOCH_3$ as base overnight. The crude mixture was analysed by TLC and showed the total consumption of the phthalonitrile component. After the reaction, TLC showed spots related to Pc, a trace of a green spot, a deep purple spot which corresponded to the expected intermediate **2.16**, as well as a spot that was related to the starting material **2.2**. Additionally, there was a black fraction that remains on the baseline, suggesting that polymerisation or decomposition might have occurred. separation of these fractions was achieved by column chromatography and MALDI-TOF-MS was checked for the fractions. The expected peak at 606 m/z was observed for the deep purple fraction, which corresponded to open compound **2.16**, and a peak at 846 m/z for the green fraction corresponded to the double addition of Pn **2.17** as shown in scheme 2.10. Once isolated, compound **2.16** was verified via MALDI-TOF MS and ^{1}H NMR spectroscopic analysis, and we proceeded to the next step to synthesise our target macrocyclic molecule **2.18**.

The following stage involved producing the macrocycle by refluxing **2.16** in a high boiling solvent (*p*-xylene). While refluxing compound **2.16** in *p*-xylene, an unexpected decomposition occurred in the initial attempt, potentially due to a reaction involving the THF stabilizer, which might still have been present after column chromatography using THF and PE. To address this, precipitation of intermediate **2.16** was induced before proceeding to this step to remove any residual stabiliser, leading to the successful preparation of compound **2.18** as a purple solid.

Figure 2.6 displays the ^{1}H NMR spectrum of **2.18** in DCM at r.t. and TCE at 70 ˚C, and both showed that all aromatic peaks were broad, which is because of the aggregation of the compound. The NMR spectrum showed splitting and less broad peaks in deuterated chloroform.

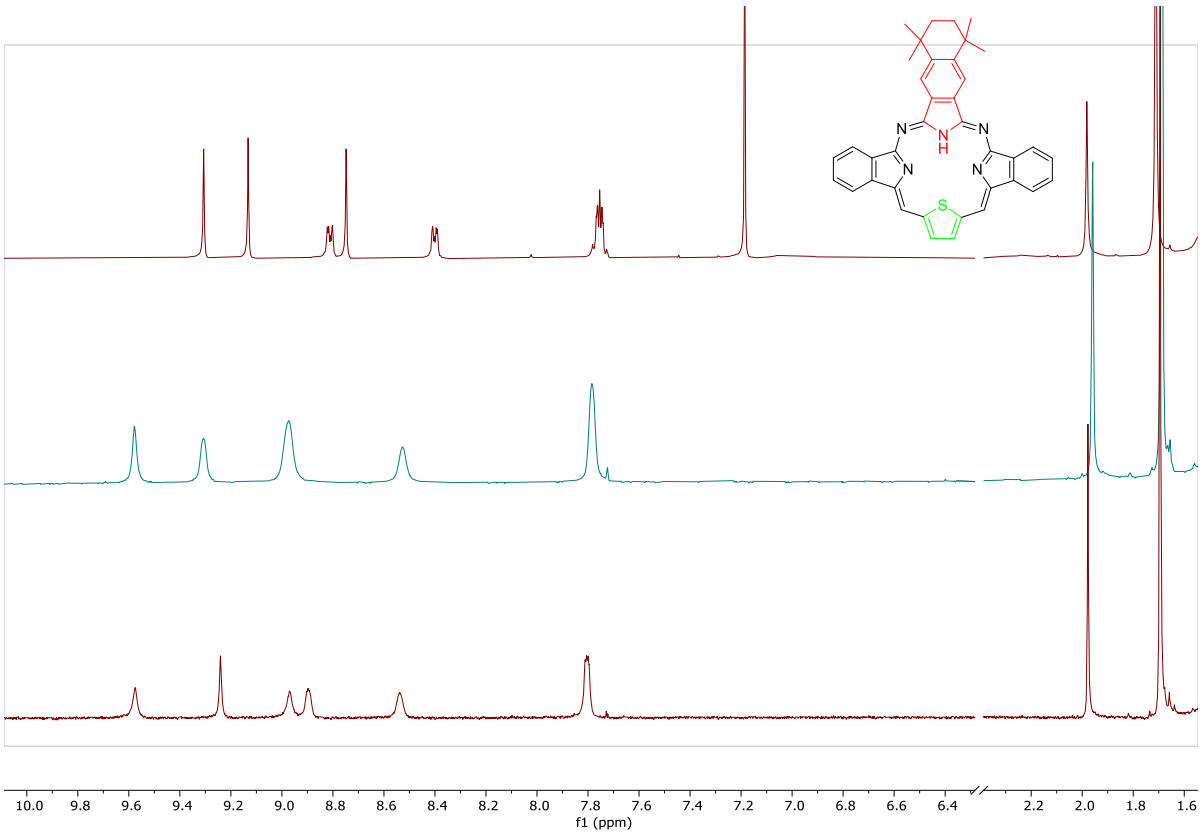

Figure 2.6: ^{1}H NMR spectra of compound **2.18** in $CDCl_3$ (top), TCE-d_2 at 70 °C (middle), and in DCM-d_2 (bottom).

The MALDI-TOF-MS analysis provides evidence for the structure with a molecular ion peak (m/z 589). The compound gave suitable crystals for X-ray diffraction analysis which further confirmed the structure. As expected, the core exhibits a planar structure. In contrast, X- ray analysis of 21-thaiporphyrin shows a slight saddle shaped distortion in the macrocyclic core. [32a,b] The C-S bond lengths in compound **2.18** (1.722 and 1.731) Å, closely matching those

observed in 21-thiaporphyrin (1.733 and 1.740 Å). This small variation is likely due to crystal packing, as the molecule is symmetrical. Similarly, the C_α-C_β bonds within the thiophene ring in **2.18** (1.406 Å) are comparable to the range reported for 21-thiaporphyrin (1.421 Å), suggesting similar aromatic character.[32b] Further detail of the X-ray analysis, which was carried out by Dr. David Hughes, can be found in the appendix.

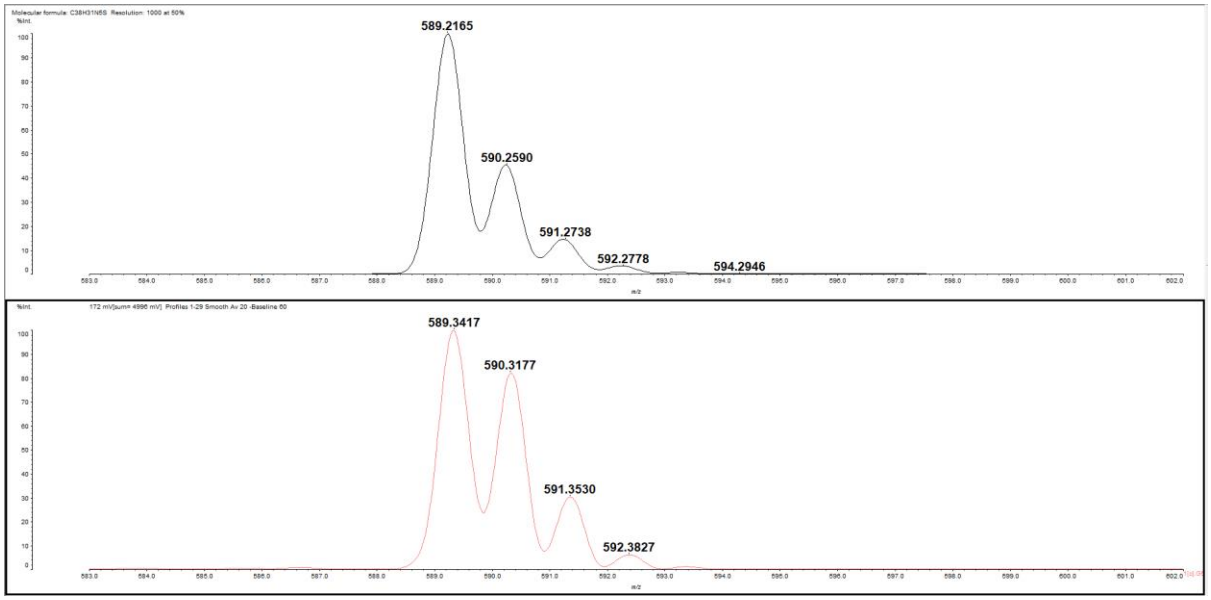

Figure 2.7: MALDI-TOF-MS spectrum of **2.18** with its theoretical prediction (top).

a)

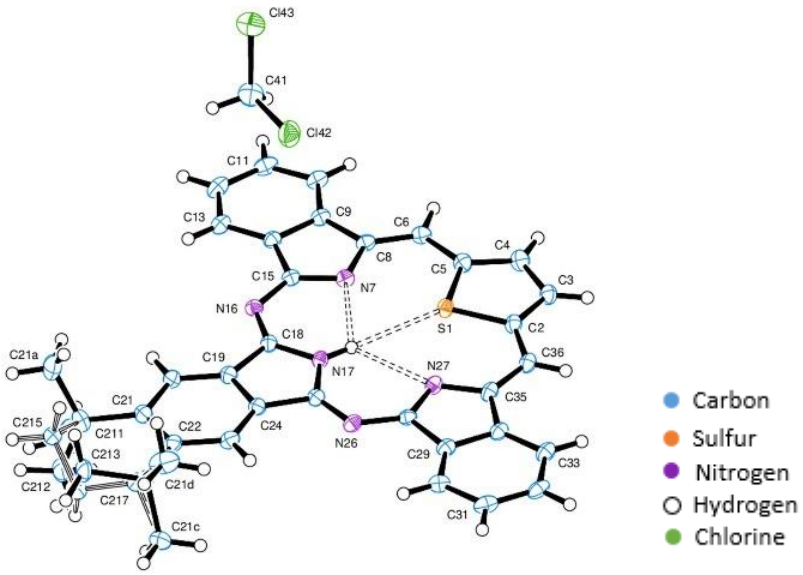

b)

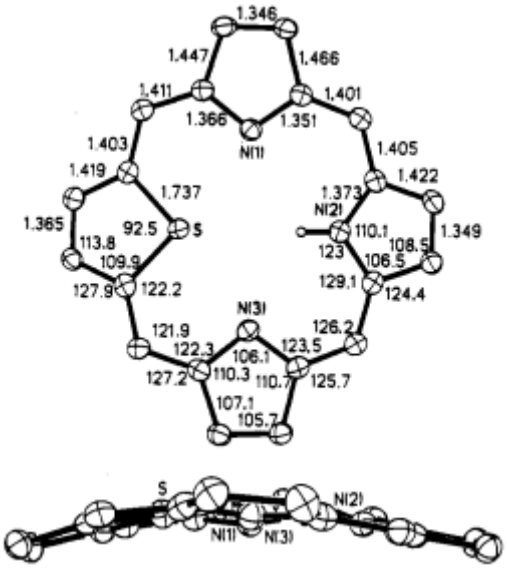

Figure 2.8: a) X-ray crystal structure of compound **2.18, b**) provides relevant structural data for the thiaporphyrin core.[32b]

The nature of the substituents not only influences the solubility of our macrocycles but also their physical and chemical behaviour. As a result, attention was switched to 4,5 diphenoxy phthalonitrile bearing electron donating groups, and similar short and long-chain 4,5-dialkyloxy phthalonitriles. In addition, one example of a 3,6-di-substituted phthalonitrile was investigated as well to study the effect of this substitution position on our compounds. The synthesis required 4,5-alkoxysubstituted phthalonitrile, as shown in scheme 2.11.

The first step was bromination of 1,2-dialkoxy benzenes by the dropwise addition of bromine to a solution in DCM at 0°C. After work up, 1,2-dibromo-4,5-dialkoxybenzenes were isolated in good yield. 4,5-Dialkoxyphthalonitriles were then easily synthesised by the Rosemund-von Braun cyanation which used CuCN as a cyanide source in dry DMF at 150-153°C.[116]

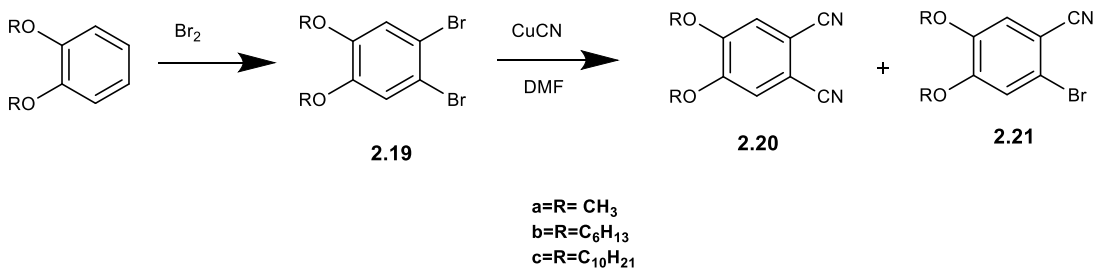

Scheme 2.11: Synthesis of 4,5-alkoxysubstituted phthalonitriles.

Despite the toxicity of the reagents and challenges associated with purification and formation of several side products in this reaction, it was to our benefit to separate the monosubstituted product as well as the phthalonitrile because both were to be used in this project. The reaction was left to reflux for a maximum of 3 h and monitored by TLC. Temperature and time were carefully controlled to minimize copper phthalocyanine formation and give access to the substituted 2-bromobenzonitrile. At the end of the reaction period, the mixture was filtered to remove the copper salts. The filtrate was then washed with water to remove the excess of DMF and was extracted with Et_2O. It was also washed with an aqueous solution of ammonia until no blue colour from copper salts was obtained. The crude product was purified using column chromatography and the structure of the compounds was confirmed by ^1H NMR spectroscopy.

Synthesis of peripherally and non-peripherally substituted tribenzodiazathiaporphyrins were then performed, as seen in scheme 2.12.

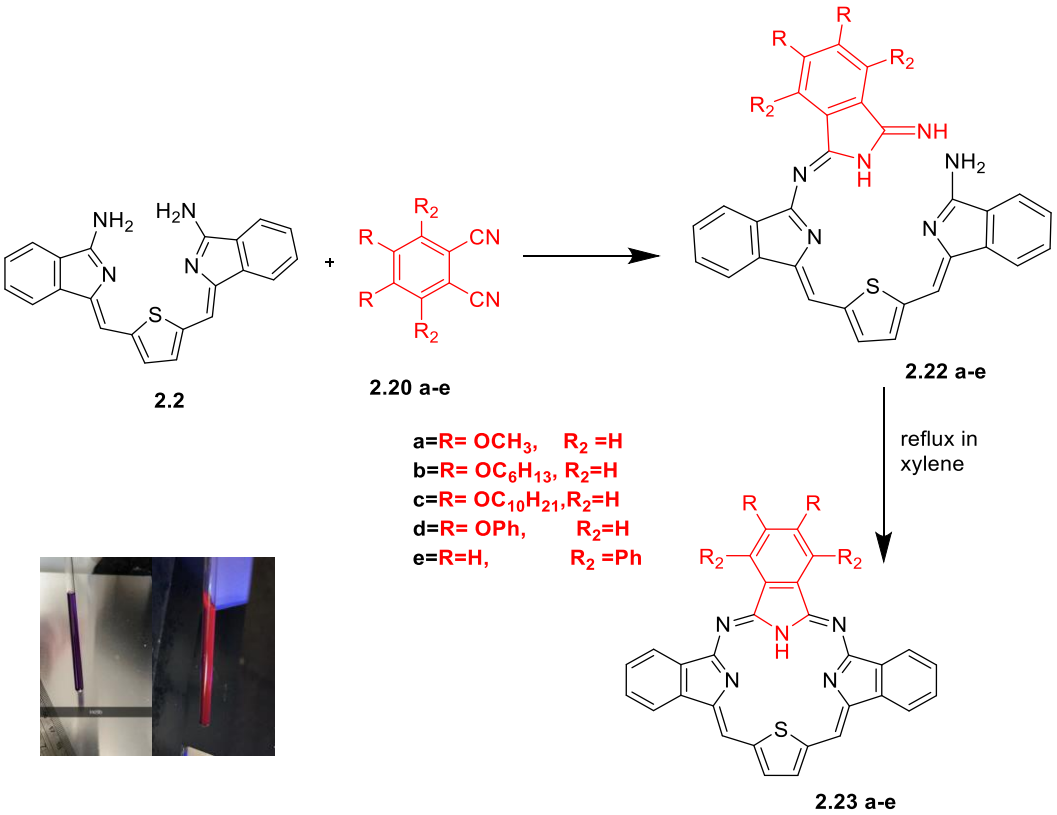

Scheme 2.12: Synthesis of tribenzodiazathiaporphyrins **2.23 a-e**; inset, highly coloured product **2.23d** under normal light (left) and the same compound under irradiation with a 365 nm light (right).

The macrocycle synthesis was performed again as a two-step reaction using previously described conditions. The first step refluxed phthalonitrile derivatives **2.20a-e** with compound **2.2** in methanol in the presence of $NaOCH_3$ and the progress was monitored by TLC. Open compounds (**2.22a-d**), Pc and traces of green fraction were formed in this step. Notably, using 3,6-di-substituted phthalonitrile for synthesising open compound **2.22e** took longer time (4 days) than usual for 4,5-di-substituted phthalonitriles and no notable Pc was formed with this derivative. The resultant deep purple solid was subjected to column chromatography aiming to separate compounds **2.22 a-e** from other fractions.

The green fraction was isolated in the case of reaction with **2.20b**. MALDI-TOF MS shows a peak cluster at 1026 m/z that is related to double addition of phthalonitrile **2.24** as seen in figure 2.9. The isolated product was also analysed by ^1H NMR spectroscopy, which revealed a symmetric structure with two peaks at 4.13 and 3.66 ppm corresponding to the methylene groups (OCH_2) from the alkyloxy groups, confirming the structure **2.24**. The UV-vis spectrum is shown in figure 2.11 and exhibited broad UV-visible absorption.

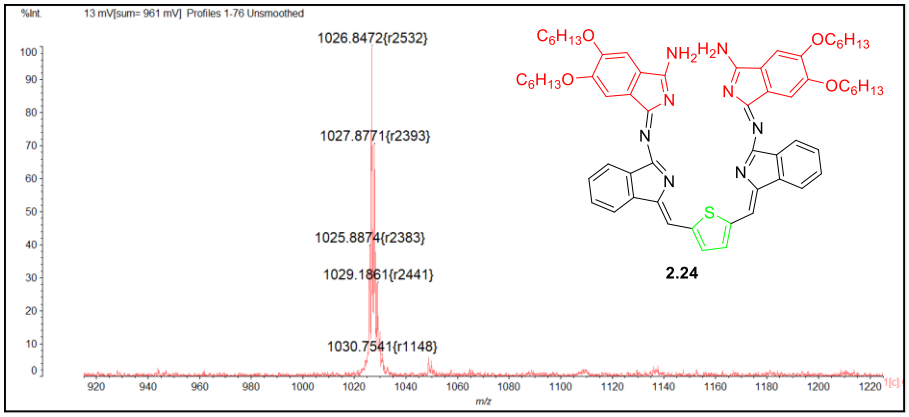

Figure 2.9: MALDI-TOF-MS spectrum of **2.24**.

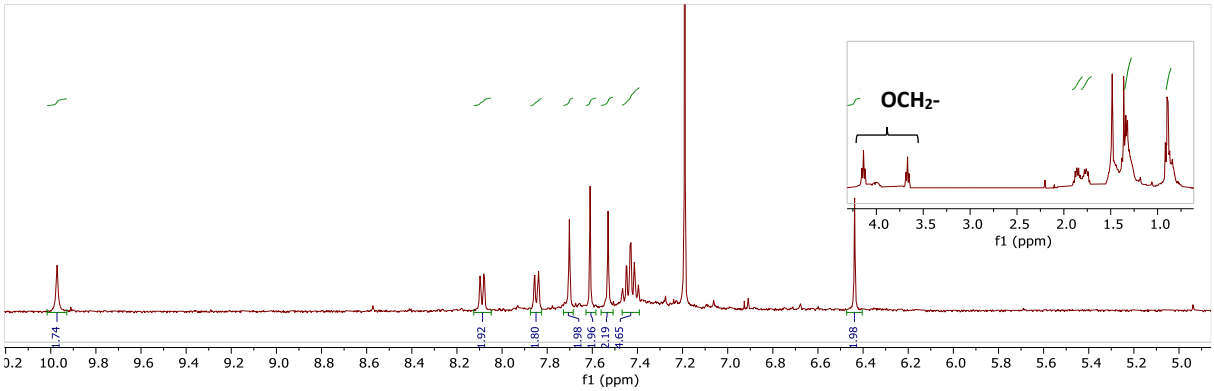

Figure 2.10: ^{1}H NMR spectrum of **2.24**.

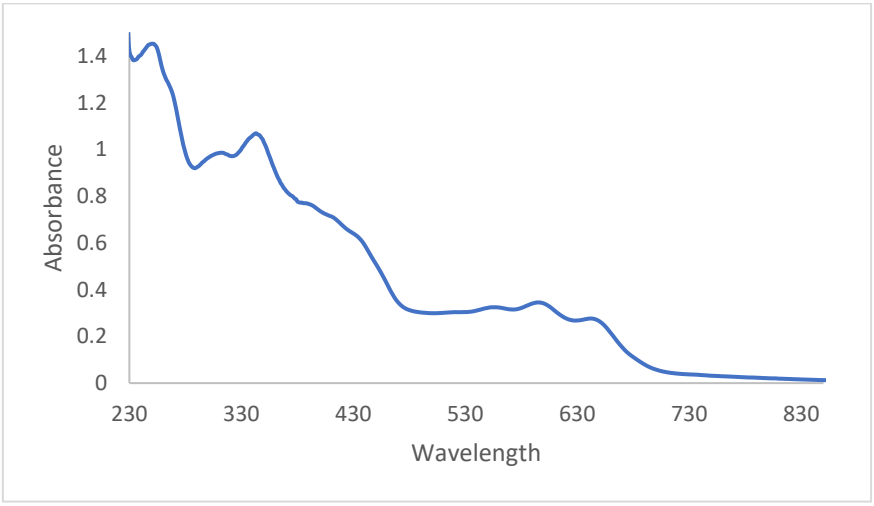

Figure 2.11: UV-vis spectrum of **2.24**.

The next step was the macrocyclization of open compounds **2.22 a-e**, which was carried out by refluxing in xylene overnight; harsh conditions are needed to accomplish macrocyclization. TLC showed a spot for cyclized compounds **2.23 a-e** as purple compounds that exhibit a pink fluorescence under irradiation with a UV lamp at 365 nm. After the reaction period, the crude residues were separated by column chromatography and then recrystallization from DCM: MeOH. Tribenzodiazathiaporphyrin with non-peripheral substitution gave significantly reduced yield due to incomplete consumption of starting materials, and no notable Pc was formed.

The identities of the cyclized products were confirmed by NMR and MALDI-TOF-MS analysis. The ^{1}H NMR spectra provided every signal matching to every proton in the molecule. ^{1}H NMR spectra were recorded for both of open **2.22c** and cyclized compound **2.23c,** and evidence of the reduction of symmetry in the open compound **2.22c** (Figure 2.12) is clear

compared to the **2.23c** (Figure 2.13). The aliphatic region is also complicated in the **2.22c** spectrum due to the reduction in symmetry. Furthermore, the spectrum of **2.23c** showed a peak at – 0.25 ppm that is related to the inner NH proton, indicating a diatropic ring current effect that disappears after leaving the sample in chloroform-d for a while, whereas the **2.22c** showed the distinctive singlet at 12.5 ppm characteristic for (NH).

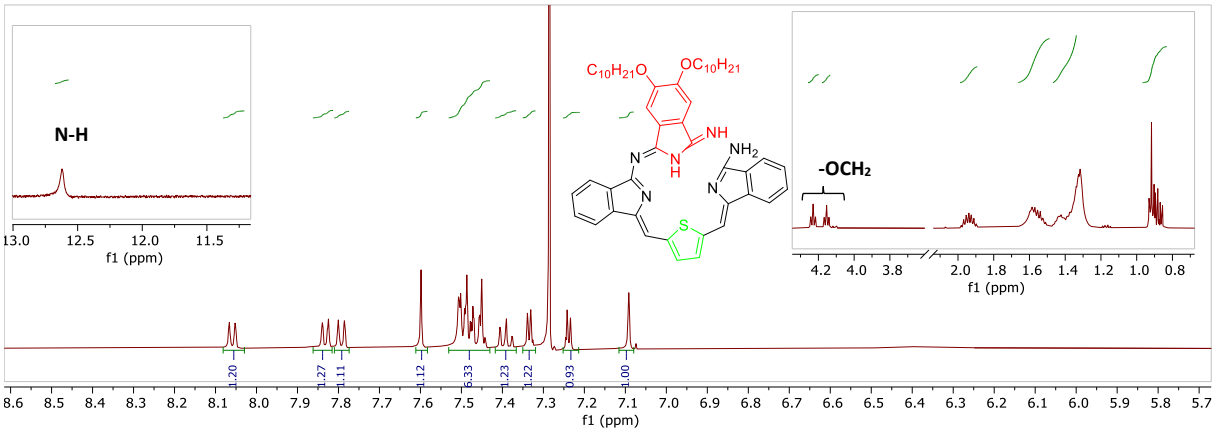

Figure 2.12: ^{1}H NMR spectrum of compound **2.22c,** with an expansion of the aliphatic region.

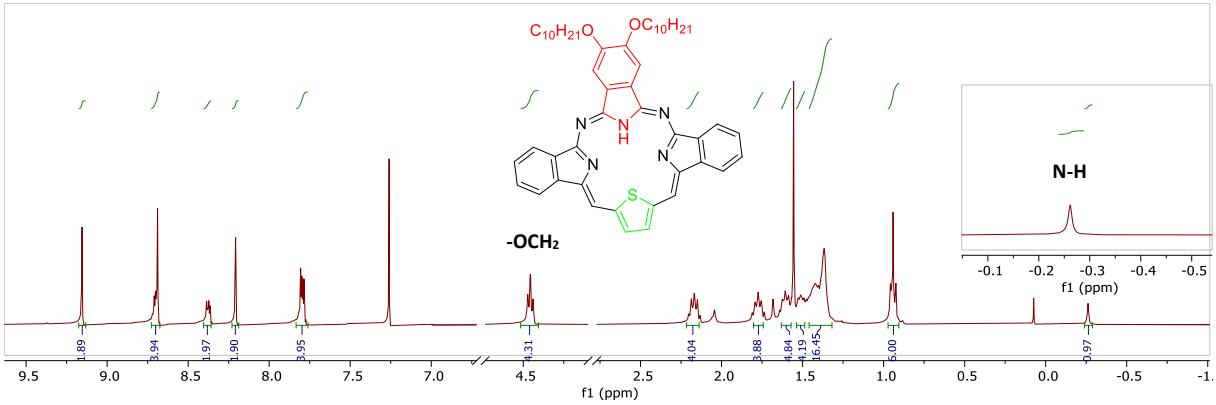

Figure 2.13: ^{1}H NMR spectrum of compound **2.23c**.

In this series, naphthalene-2,3-dicarbonitrile was chosen as the subsequent phthalonitrile based on the extension of the molecule's π -system. The synthesis of **2.25** included an optimisation study that will be briefly discussed later. Confirmation of the compound formation was achieved by MALDI-TOF-MS which showed a peak at 528 m/z. However, the product's solubility proved to be an issue for NMR spectroscopic analysis.

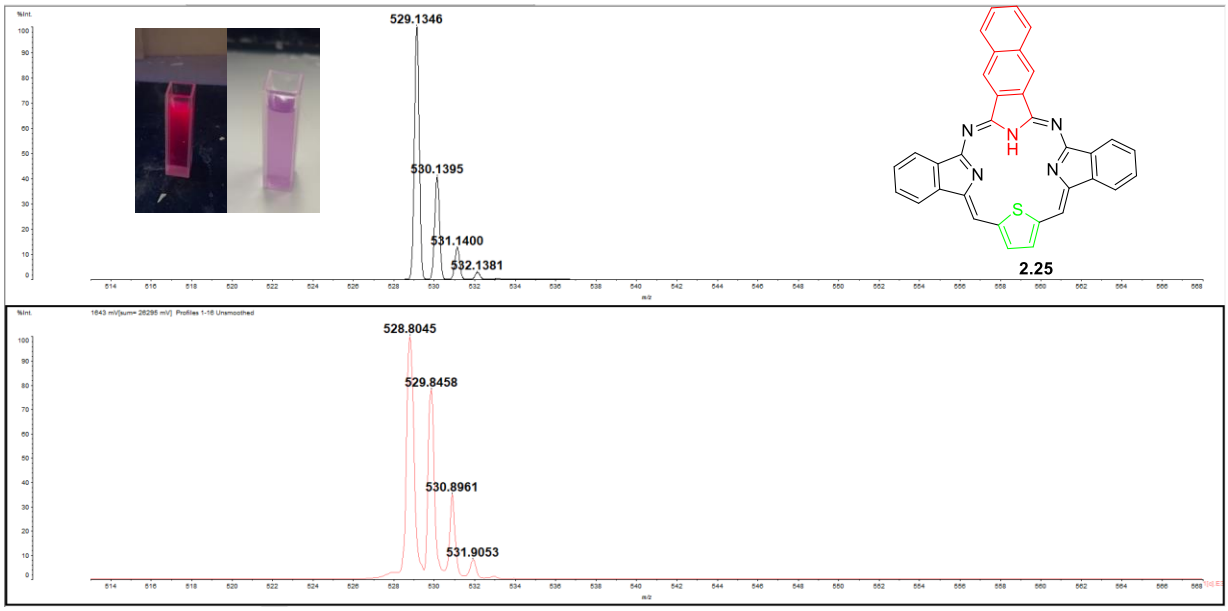

Figure 2.14: MALDI-TOF-MS spectrum of **2.25** with its theoretical prediction (top); inset, highly coloured product **2.25** under normal light (right) and the same compound under irradiation with a 365 nm light (left).

2.2.3 Optical properties of the 1st series:

The UV-visible absorption spectra of the 1st series in dichloromethane, except **2.25** in THF, are shown in figure 2.15. They display strong Soret-like bands around 415 nm and a set of four lower energy Q-like bands between 510 and 665 nm. There is close similarity in absorbance between tribenzodiazathiaporphyrins with different substituents on the top isoindoline, with slightly red shifted Q bands of phenoxy derivative and the non-peripherally phenyl substituted derivative observed. Unexpectedly, it is notable that the π-extended derivative **2.25** shows minimal change in its lowest energy transition, but the main "Q" band around 550 nm is significantly shifted.

A similar situation was observed for the fluorescence emission spectra. Whereas tribenzodiazathiaporphyrin with non-peripheral phenyl substituents exhibited slightly bathochromic shift, with the main emission band at 663 nm, other derivatives within the series, emitted around 650 nm, with exceptions noted for **2.18**, which demonstrated slight blue shift.

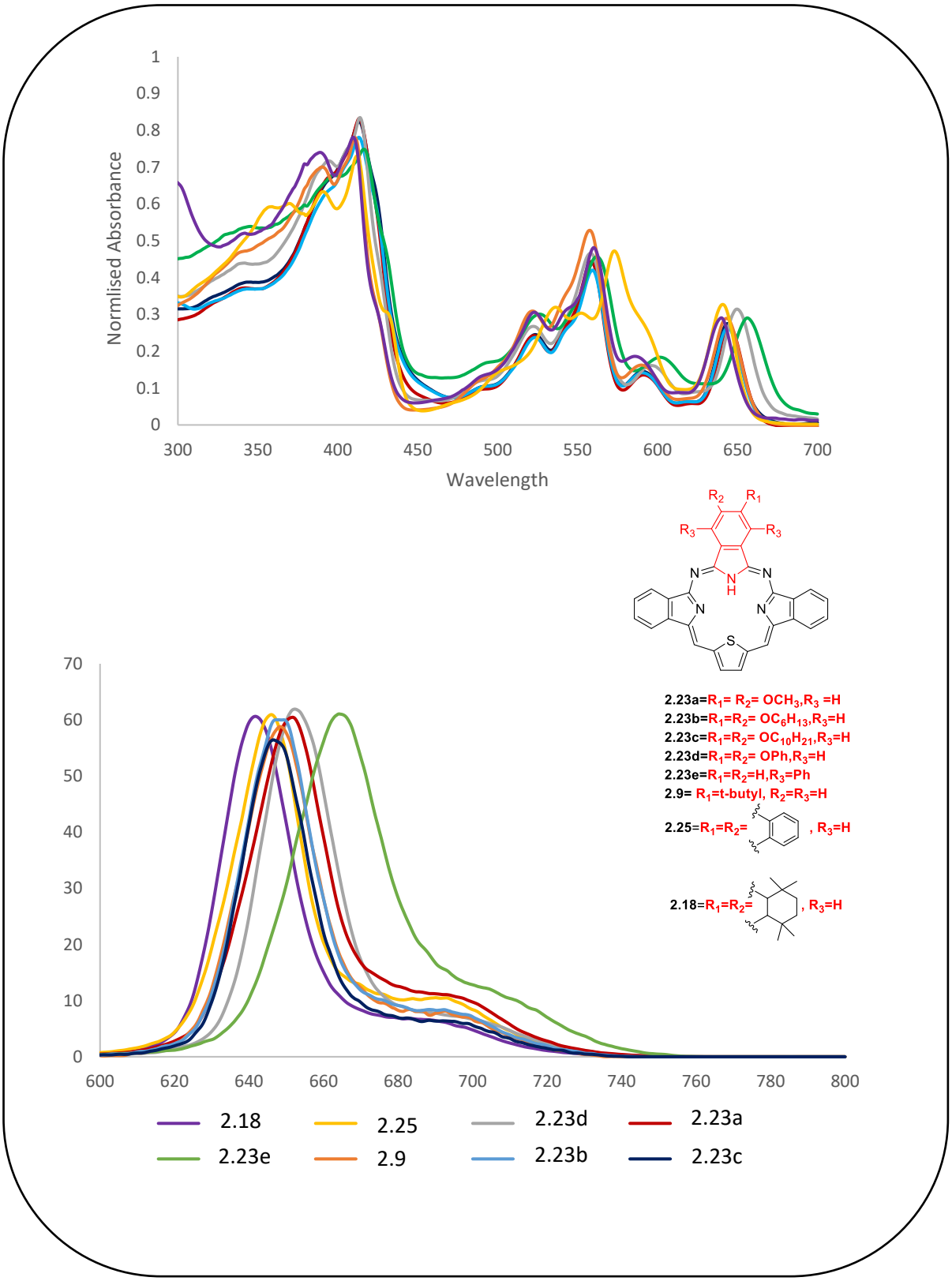

Figure 2.15: UV-vis absorption and fluorescence spectra of the 1st series compounds.

On the other hand, the UV-Vis spectra of open and cyclized compounds are shown in figure 2.16 and illustrate a red-shifted Soret band of **2.23c** compared to **2.22c.** Moreover, the cyclized compound **2.23c** displays a resolved, split "Q"-band, contrasting with the broad band observed in the open form. Overall, however, it is noteworthy that the cyclization itself does not significantly shift the absorbance to lower energy.

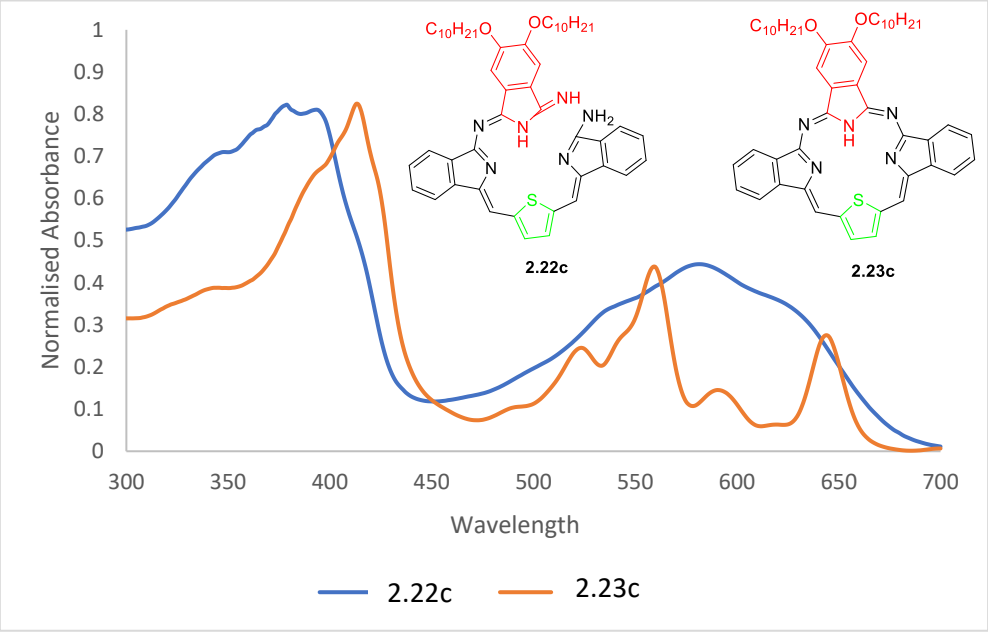

Figure 2.16: UV-vis spectra of **2.22c** and **2.23c**.

The attempted metallation of examples of these macrocyclic compounds was carried out by another member of our research group. The results indicated that tribenzodiazathiaporphyrins are not amenable to metal complexation.

2.3 Synthesis of the second series of Tribenzodiazathiaporphyrins

The first series of tribenzodiazathiaporphyrins were prepared using substituted phthalonitriles to change the "top" unit of the macrocycle. In this subsequent series, we focused on the additional modification of the side isoindoline moieties (in conjunction with the top isoindoline moiety in some compounds) via employing both substituted intermediates (bis-aminoisoindoline thiophenes from substituted amidines) and substituted or unsubstituted phthalonitriles, resulting in the alteration of all isoindoline moieties within the phthalocyanine derivative. For this series, the synthesis of substituted bis(aminoisoindoline)thiophene was the required initial challenge.

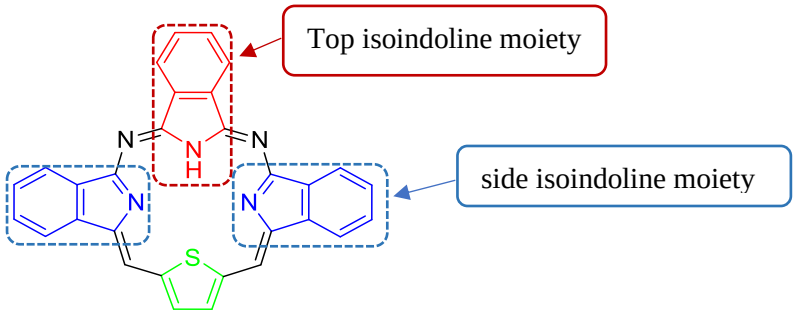

Figure 2.17: Tribenzodiazathiaporphyrin structure.

2.3.1 Synthesis of the substituted bis-(aminoisoindoline)thiophenes

To form substituted intermediates, the first step required was a synthesis of substituted amidine as shown in scheme 2.13. It starts with 2-bromobenzonitrile derivatives to convert them to the corresponding amidine derivatives, followed by utilization in a coupling reaction to yield the targeted substituted intermediates.

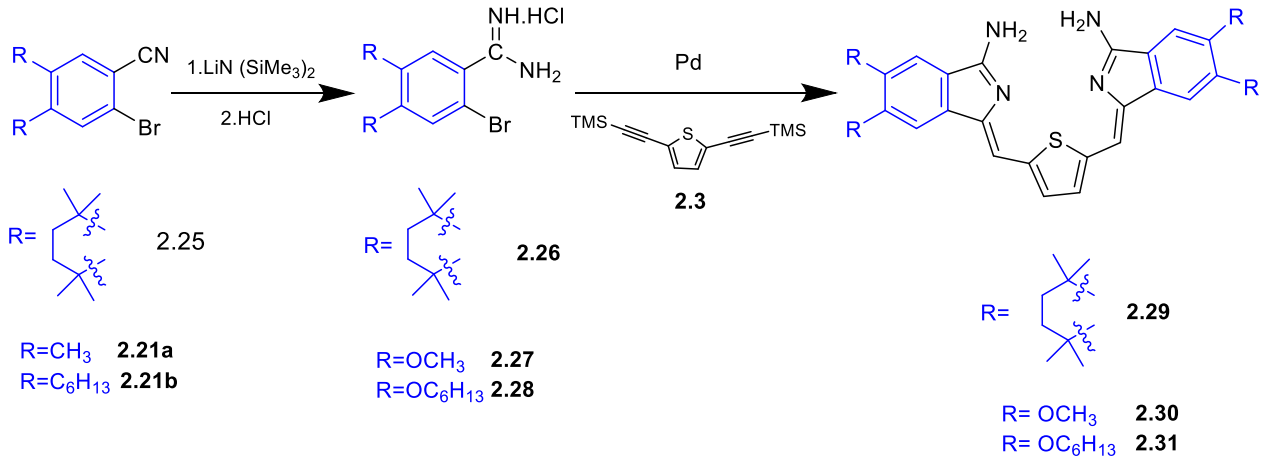

Scheme 2.13: Synthesis of substituted bis-aminoisoindoline thiophene.

It was difficult to find suitable 2-bromobenzonitrile derivatives from commercial sources and they required prior synthesis. As mentioned previously, all 2-bromobenzonitrile derivatives were isolated as side products from cyanation reactions discussed in the synthesis of phthalonitrile precursors. Bromobenzonitriles were converted into the corresponding amidine derivatives by reacting a solution of $LiN(SiMe_3)_2$ in THF and 2- bromobenzonitrile derivatives. The reactions were stirred for 4h under a N_2 atmosphere. The mixture was cooled and hydrolysed using solution of hydrochloric acid in 2-propanol to give the amidine hydrochlorides. The resulting precipitates were filtered off and washed several times with diethyl ether, then recrystallised from methanol.[26,109] The structures of these compounds were confirmed by ^{1}H NMR spectroscopy. ^{1}H NMR spectra gave two singlet peaks of one proton integration in aromatic range corresponding to the benzene ring protons in addition to the peaks corresponding to the aliphatic protons.

The same process that was used for unsubstituted bis-aminoisoindoline thiophene was employed to prepare substituted bis-aminoisoindoline thiophenes. The 2-bromobenzamidine hydrochloride derivatives (2 equivalents) underwent a coupling reaction with bis(trimethylsilylethynyl)thiophene (one equivalent) in the presence of a palladium catalyst, BINAP as the ligand, DBU as base, and DMF as solvent. The reaction was carried out in a microwave reactor at 120°C for an hour. All reactions were performed similarly without any alteration to the original and typical conditions. After work up, these polar compounds were tricky to purify. Further purification attempts by column chromatography using silica gel or aluminium oxide or recrystallisation were unsuccessful. Thus, these compounds were characterised by mass spectrometry. The resulting peak from the MALDI-TOF MS spectra

showed 589 m/z for **2.29** (Figure 2.18 top), 488 m/z for **2.30** and 768 for **2.31** (Figure 2.18 bottom).

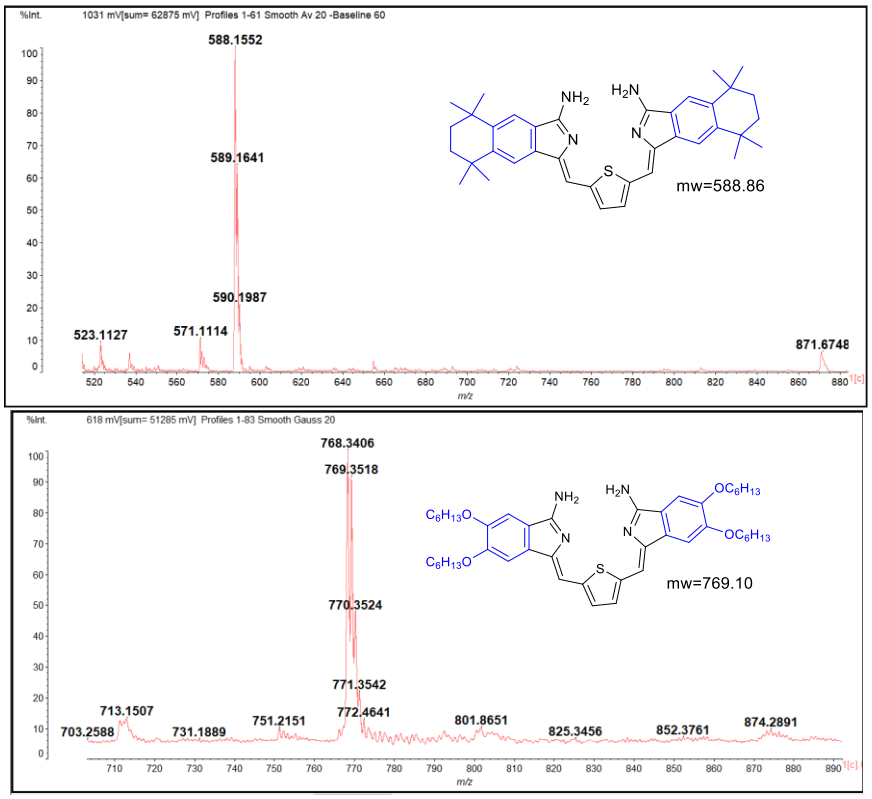

Figure 2.18: Intermediate **2.29**, **2.31** identified by MALDI-TOF-MS with a m/z of 589 (top)and 768 (bottom) respectively.

2.3.2 Tosylation of the intermediate

Due to the challenging isolation of the intermediates, we decided to functionalise them in order to prove their identity before carrying out the next steps. We wanted a derivative that was easy to make, and that would make characterization more straightforward. We selected tosylation as our method and initially returned to simple unsubstituted intermediate **2.2** to develop the chemistry.

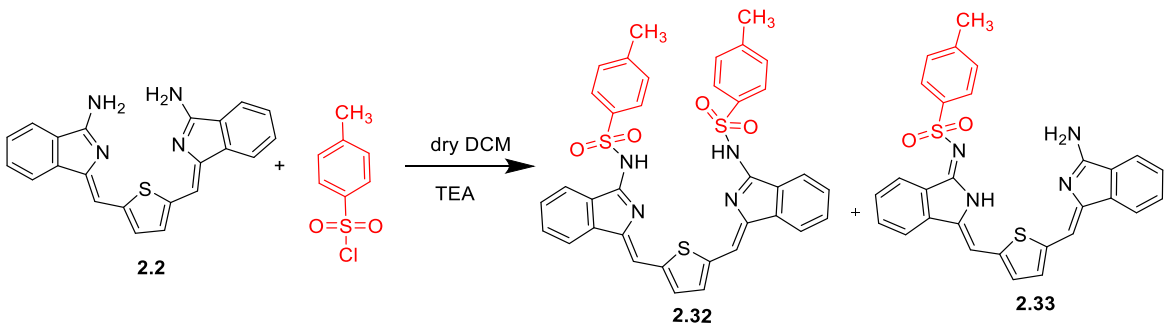

Scheme 2.14: Synthesis of mono- and di-tosylate of compound **2.2**.

The intermediate **2.2** was reacted with *p*-TsCl in dry DCM in the presence of TEA as seen in scheme 2.14. The reaction was monitored by TLC, and new spots were observed after 3 h. The reaction mixture was stirred overnight to ensure all reactants were consumed. TLC analysis showed that the reaction mixture consisted of two components which corresponded to the mono- and di-tosylate. The crude product mixture was then chromatographed on a silica gel column and recrystallised from DCM and hexane to yield the products as orange (di-) and red (mono-) solids of the tosylates of intermediate **2.2**. They show fluorescence under a UV lamp, as shown in below figure 2.19.

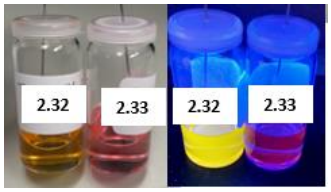

Figure 2.19: Picture of **2.32, 2.33** under normal light (left) and the same compounds under irradiation with a 365 nm light (right).

^{1}H and ^{13}C NMR spectroscopic analyses confirmed mono and di tosylates of unsubstituted intermediate. The ^{1}H NMR spectrum for the di-tosylate showed symmetrical characteristics in the aromatic region and a peak at 2.4 ppm with an integration of 6 attributed to two methyl groups that were attached to the tosyl groups. In contrast, the mono-tosylate compound exhibited reduced symmetry in the aromatic region and a peak at 2.35 ppm with an integration of 3 attributed to the one methyl group that was attached to the tosyl group as seen in figure 2.21. Homonuclear COSY spectroscopy played a significant role in the identification of protons associated with the tosyl groups within the molecular structure.

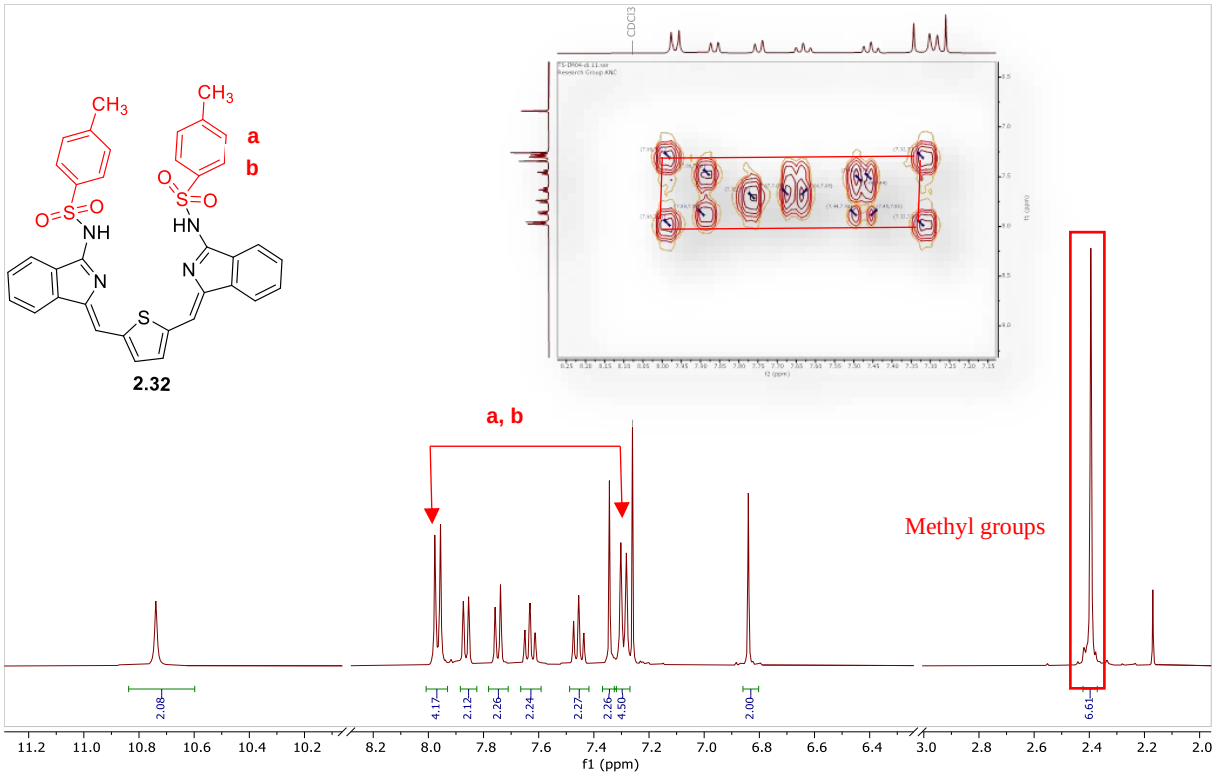

Figure 2.20: ^{1}H NMR and H-H COSY NMR spectra of compound **2.32**.

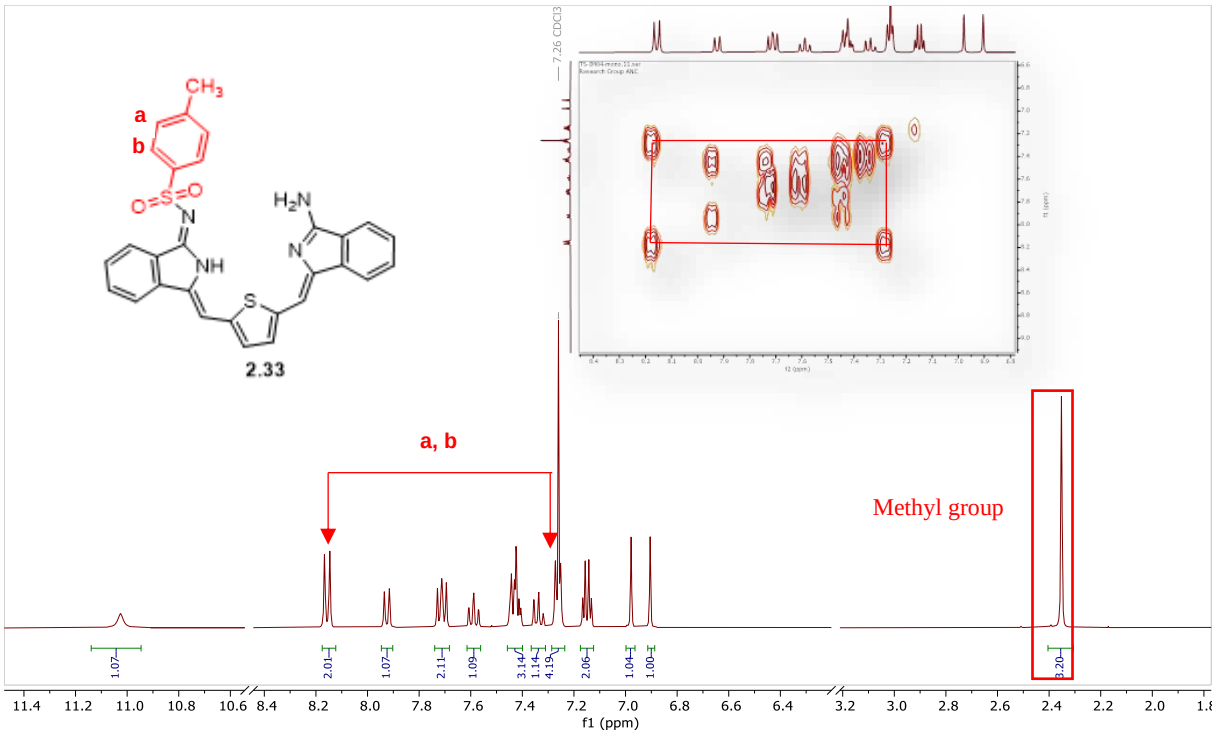

Figure 2.21: ^{1}H NMR and H-H COSY NMR spectra of compound **2.33**.

The NMR spectroscopic analyses could not prove beyond doubt that the indicated nitrogens had been functionalised, but fortunately the full confirmation of the mono-structure was possible after suitable crystals were grown slowly from DCM. Single-crystal X-ray diffraction revealed that the central isoindole-thiophene-isoindole (ITI) unit is planar, from N(20) through N(1), S(1), N(21), to N(30). The attached phenyl ring was also found to be planar but oriented almost perpendicular to the ITI unit (angle ~87.9°). Within the ITI structure, two C=N double bonds (C(2)-N(20) and C(29)-N(21)) were clearly identified, with both showing shortened bond lengths (1.319 Å and 1.317 Å, respectively).

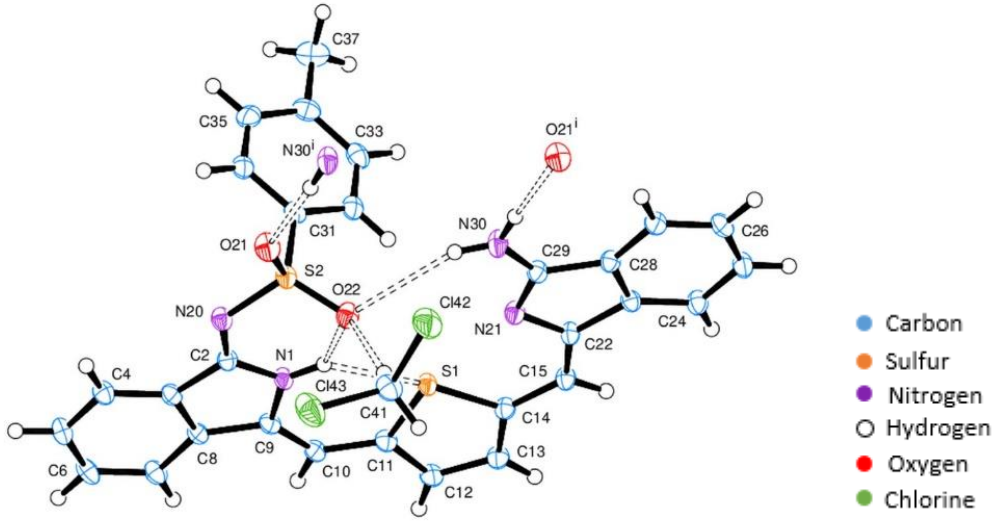

Figure 2.22: X-ray crystal structure of compound **2.33**.

Figure 2.23 depicts a comparison of UV-vis absorption spectra of derivatives **2.32**, **2.33** in DCM and **2.2** in THF. Surprisingly, a blue shift is present for the di- compared to mono-tosylates of unsubstituted intermediate. Additionally, the UV-vis absorption of di- tosylate **2.32** was quite similar to starting material **2.2.** A similar observation was noted in the fluorescence spectra.

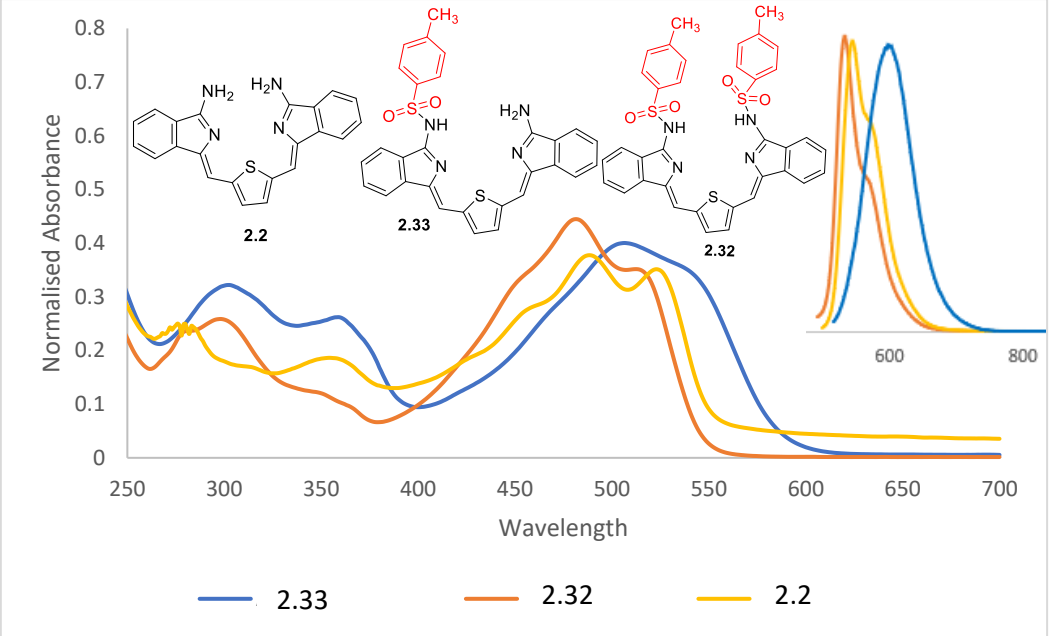

Figure 2.23: Comparison UV-vis spectra of **2.2, 2.32, 2.33**; inset, fluorescence spectra.

The same tosylation strategy was then applied to substituted intermediates for the purpose of isolating the compound and characterising its structure through NMR spectroscopic analysis. The same methodology for one pot tosylation reaction of an unsubstituted intermediate was followed using *p*-TsCl. To do so, the substituted intermediate was stirred in dry DCM at room temperature under an argon atmosphere in the presence of TEA as a base overnight. The solvent was evaporated and the crude products were purified by column chromatography to isolate the di-tosylate of the substituted intermediate. Both products **2.34**, **2.35** were obtained in good yield (40- 43 % yield) as red solids. These products were fully characterised by NMR, UV-vis spectroscopies and MALDI-TOF MS. A low yield of mono-tosylation of the substituted intermediate was also found.

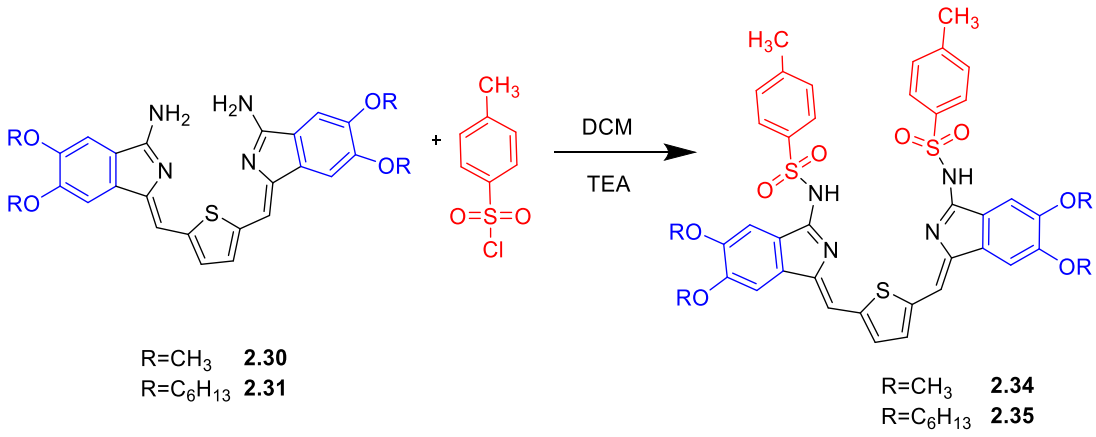

Scheme 2.15: Synthesis of di-tosylate of the substituted intermediates.

The identification of di-tosylate intermediates via MALDI-TOF-MS is challenging due to concurrent existence of shared fragmentation peak of mono-tosyl compounds as seen in figure 2.24. In contrast, ^{1}H NMR spectroscopy provides a clear spectral analysis, thereby enabling the effective identification of di-tosyl compounds. The integration of the peaks matches with the expected number of protons of the depicted compounds and both compounds **2.34** and **2.35** displayed identical integration values in the aromatic region. Although the alkyl chains of compounds **2.34** and **2.35** differed, their absorption and fluorescence maxima were similar (as expected) as we see in figure 2.25.

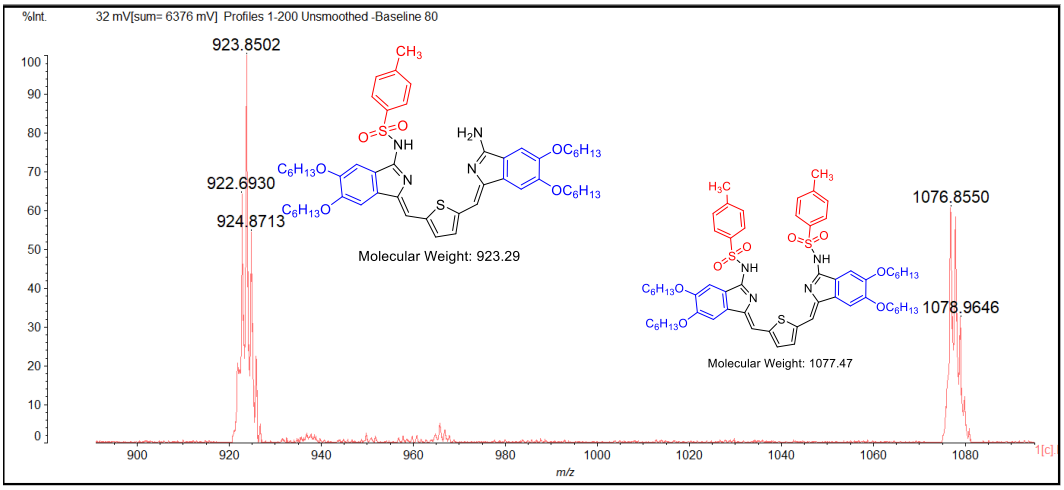

Figure 2.24: MALDI-TOF-MS of di-tosylate intermediate.

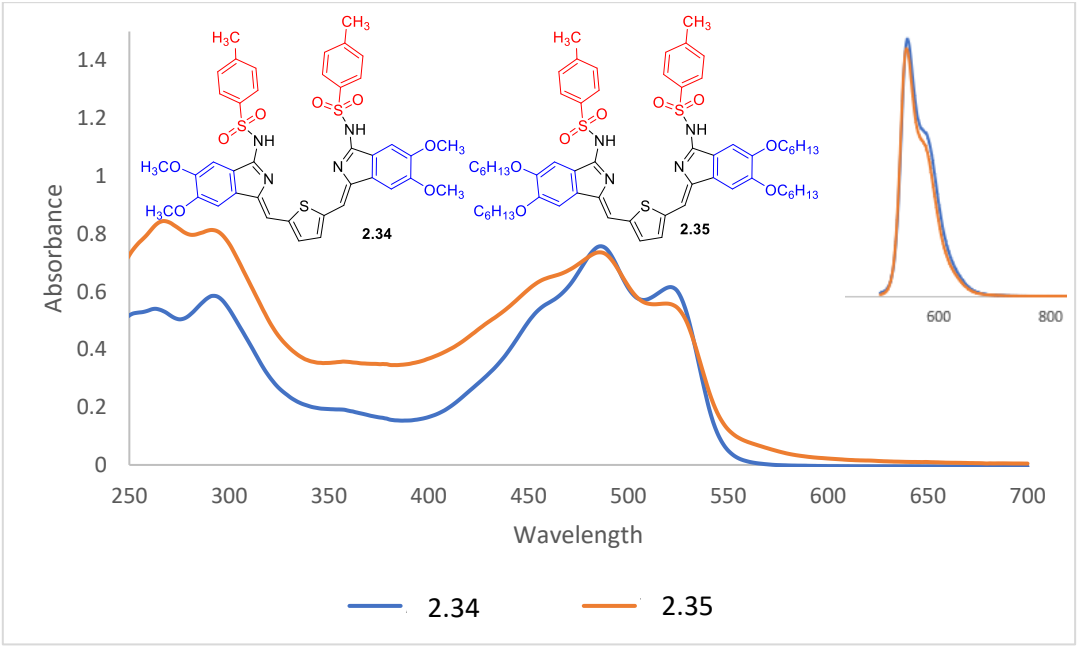

Figure 2.25: Comparison UV-vis spectra of **2.34, 2.35**; inset, fluorescence spectra.

2.3.3 Synthesis of the second series of macrocycle

Following the synthesis of intermediates **2.29**, **2.30** and **2.31** and subsequent confirmation of their structures by tosylation, we proceeded to prepare the second series of tribenzodiazathiaporphyrin. Throughout this series, all substitutions were directed towards the β-peripheral position.

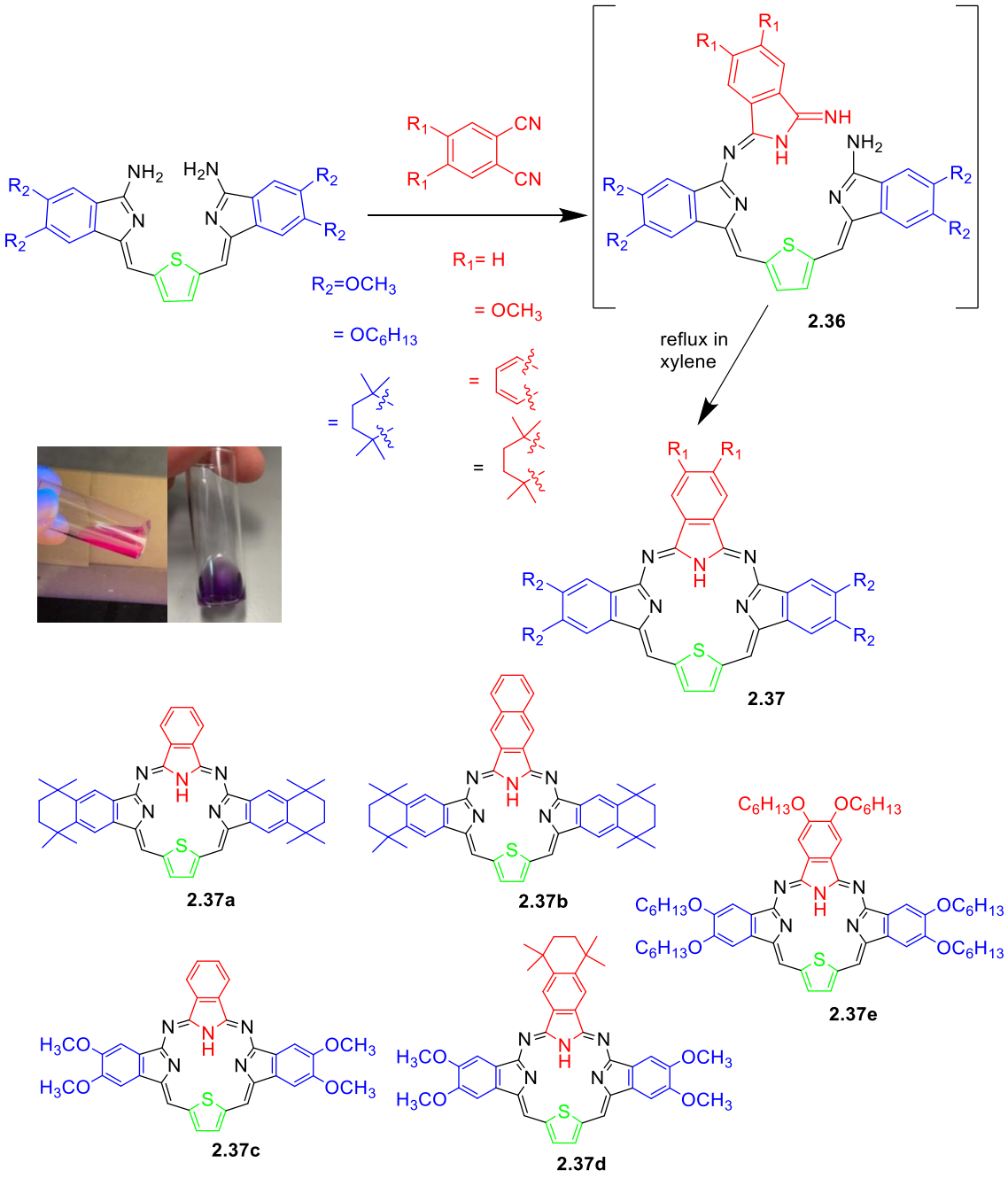

Scheme 2.16: Synthesis of the second series of tribenzodiazathiaporphyrins; highly coloured product **2.37b** under normal light (right) and the same compound under irradiation with a 365 nm light (left).

After the substituted intermediates were prepared, it was then used to prepare tribenzodiazathiaporphyrins **2.37a-e** by reacting the substituted intermediate with unsubstituted or substituted phthalonitriles in methanol in the presence of $NaOCH_3$ as base, as shown in scheme 2.16. Reactions were monitored by TLC. The first investigation of compound **2.37a** was conducted under atmospheric air conditions and resulted in a low yield. Notably, running the reaction in an argon atmosphere significantly improved the yield. Consequently, all reactions were conducted under an argon-controlled environment. After the reaction, the solvents were removed under vacuum and the resulting mixture was purified using silica gel chromatography followed by precipitation to collect the products as deep purple solids. The deep purple compounds were identified using MALDI-TOF-MS, indicating successful formation of compounds **2.36**, as expected. The deep purple intermediate compounds were then refluxed in *p*-xylene and reactions monitored by TLC. The cyclized compounds **2.37a-e** were easily observed through TLC because of the bright pink emission that was seen under UV lamp, as mentioned previously. MALDI-TOF-MS proved the formation of the desired compounds, again as purple solids. All compounds required column chromatography and recrystallisation to afford purified materials. Compound **2.37e** was particularly challenging to isolate due to the presence of a brown side product alongside the desired compound after column separation. The TLC analysis revealed only a small difference in R_f values between them. To achieve effective separation, the compound underwent preparative TLC separation. The yield of **2.37e** was notably the lowest within this series of compounds with the yield 5%.

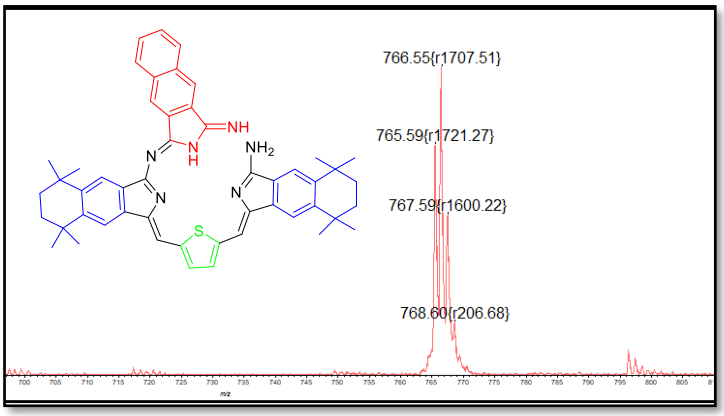

Figure 2.26: MALDI-TOF-MS spectrum of compound **2.36b**.

Crystals of the tribenzodiazathiaporphyrin **2.37a** were grown from a mixture dichloromethane and isopropanol and subjected to X-ray analysis. The resulting structure is shown in figure

2.27. The crystal quality was poor, confirming the molecular structure but a better crystal is needed for detailed structural analysis.

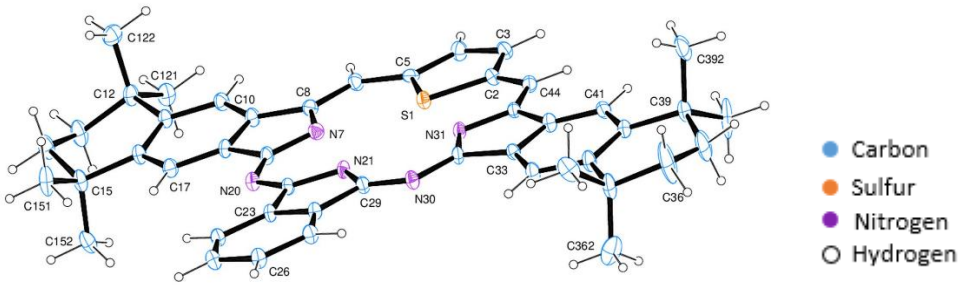

Figure 2.27: X-ray crystal structure of compound **2.37a.**

2.3.4 Optical properties of the 2nd series and 1st series

The effects of introducing substituents to the macrocycle's aromatic system and the variations in their molecular structures and their position on the Q band's maximum absorption and emission will be compared in this section. Table 2.1 shows absorption and emission bands of the 2nd series and some compounds from 1st series. As observed in the table, the effects are small, but it is evident that the substituents on the side (rings A) isoindolines have greater effect than on the top (ring B) in terms of inducing bathochromic shift.

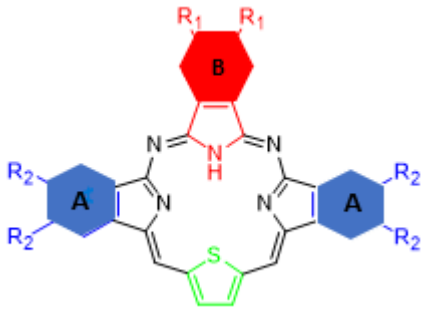

	R_1	R_2	Abs bands λ_{max} (nm) Q bands	Emission bands λ_{max} (nm)
2.18		H	523, 560, 586, 639.	641
2.25		H	536, 552, 573, 641.	646

2.23a	OCH_3	H	523, 558, 591, 645.	652
2.23b	OC_6H_{13}	H	523, 559, 590, 644.	648
2.37a	H	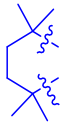	523, 560, 600, 656.	665
2.37b		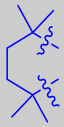	539, 560, 578, 654.	660
2.37c	H	OCH_3	523, 560, 595, 650.	657
2.37d		OCH_3	525, 564, 590, 645.	652
2.37e	OC_6H_{13}	OC_6H_{13}	526, 563, 597, 652.	656

Table 2.1: Absorption and emission data for compounds of the 2nd series.

As mentioned previously, comparing between **2.37a** and **2.37b** to study effect of top ring fused to the macrocycle in **2.37b**, we find nearly no effect on the longest wavelength band, while bands between 520-580 exhibit significant change. Overall, therefore, we conclude that changing the top ring has no discernible influence on the longest wavelength absorption.

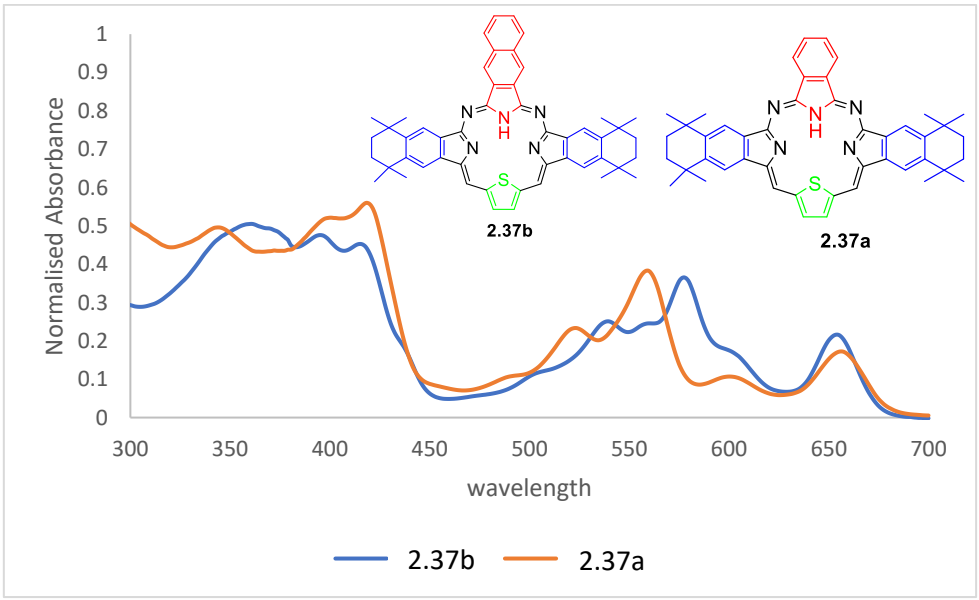

Figure 2.28: UV-vis spectra of **2.37a**, **2.37b** in DCM.

2.4 Optimisation of reaction conditions for tribenzodiazathiaporphyrin formation.

While the tribenzodiazathiaporphyrins described previously were synthesised to investigate the influence of substituents on the various positions, they were generally achieved in low yields. A short optimization study was performed, and conditions were tested to try to improve the yield. Table 2.2 summarises the results obtained during this process. Notably, the type of base, solvent and temperature all influence this reaction.

.

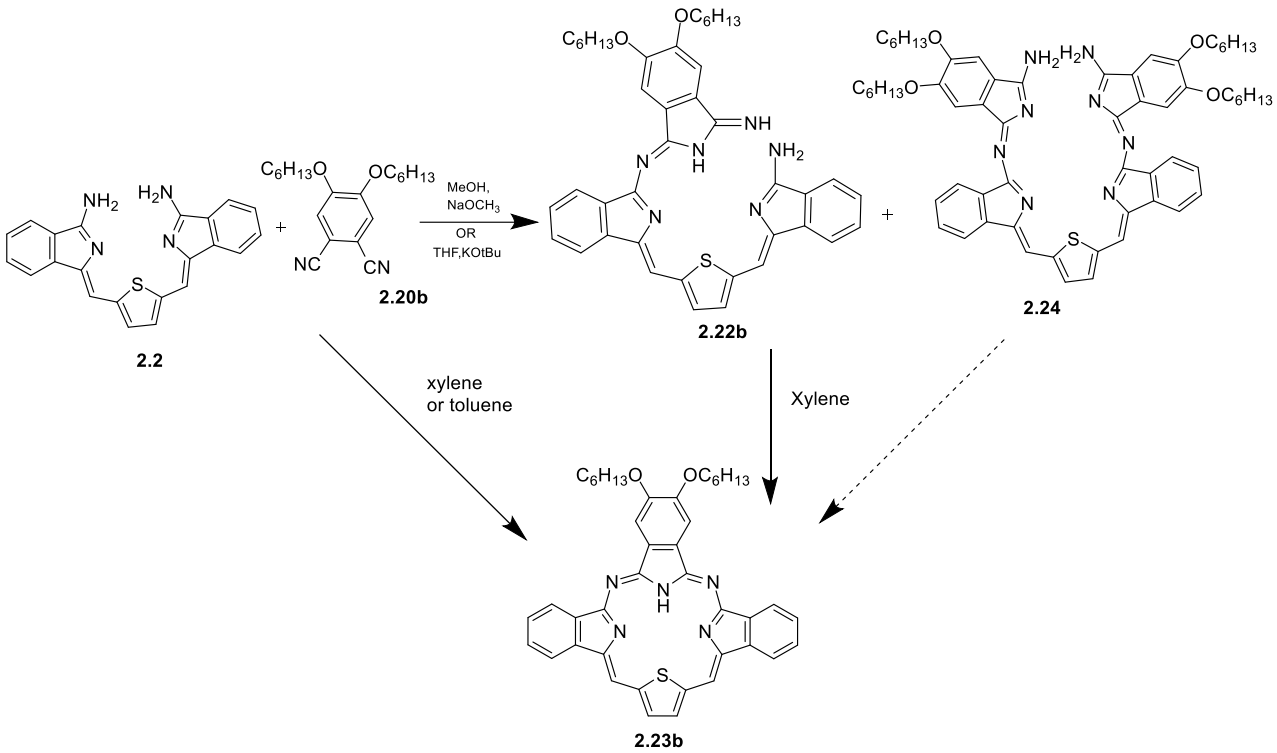

Entry	equivalents		base	solvent	Yield%	time	notes
	Compound 2.2	Pn 2.20b					
1	1	1	$NaOCH_3$	MeOH then xylene	9%	2 days	Two steps
2	1	1	potassium tert-butoxide	THF then xylene	18%	5 days	Two steps
3	1	2	-	toluene	36%	4 days	One step
4	1	2	-	xylene	23%	4 days	One step

Table 2.2: Optimisation of tribenzodiazathiaporphyrin synthesis with different reaction conditions.

The previous approach to synthesise tribenzodiazathiaporphyrin used, i.e. reflux in methanol with $NaOCH_3$, followed by reflux in xylene, and did not fully consume starting material **2.2**. Also, a side-product formed (Pc) rather than our desired product. We aimed to improve

efficiency and yield by changing the strategy. The first change was to use THF instead of methanol with potassium *tert*-butoxide as a base. The reaction was carried out at reflux and monitored by TLC. We noted the formation of **2.22b,** which was then refluxed in xylene to produce **2.23b**. Although this approach avoided the formation of Pc, the reactants were still not completely consumed.

According to the previous two methods, neither completes the consumption of starting material. Therefore, we aimed to increase overall yield and ensure the reactants are used up by using a solvent with a high boiling point beginning with toluene. The reaction was refluxed in toluene without the presence of a base for two days. TLC indicated the formation of **2.23b** directly, as a purple spot with strong pink fluorescence with a green spot which corresponded to **2.24**. TLC also revealed that the starting material **2.2** was still present, so Pn **2.20b** was added and refluxed for two more days until the double addition compound (green fraction) **2.24** was no longer visible on TLC. For the purification of crude reaction products, toluene was removed, and a short column was enough to separate the final product **2.23b** from the rest of the reaction products. In this strategy, the tribenzodiazathiaporphyrin **2.23b** was obtained in one step in a higher yield of 36%, without using a base, making the purification process simpler. In the rest of the reaction mixture, unreacted compound **2.2** and open compound **2.22b** were observed. Subsequently refluxing the remaining reaction solution in *p*-xylene with added 1 eq of Pn resulted in a 4% increase in the yield of the desired compound. A significant amount of dark side product was formed beside the product. So, the reaction was repeated in toluene and initially stirred at r.t. for two days, but the reaction did not occur. Subsequently, the temperature was increased to 60 °C over two days without any product formation. Finally, the reaction was performed under reflux, yielding the product in 36%, consistent with the results from the first attempt in toluene.

According to the results we obtained, the reaction improved significantly with a rise in temperature. Thus, an additional optimization attempt of the reaction was conducted with the aim of enhancing yield within the shortened duration of the reaction. 1.2 eq of Pn **2.20b** with 1 eq of compound **2.2** were refluxed in *p*-xylene overnight. TLC results showed a spot for the desired compound **2.23b** and a green spot of **2.24**; Pn **2.20b** was absent from TLC. Then, 0.08 eq of Pn **2.20b** was added to the mixture and refluxed for 3 days until no double addition compound **2.24** was left and mostly consumption of the starting materials was achieved. However, the dark side product was also again noticed under this condition and the desired product was formed but the yield had significantly reduced to 23%.

2.5 Reaction to toyslate-compound

In this section, we aimed to confirm the structure of the open compound **2.38** with naphthyl substitution since the macrocyclized compound **2.25** exhibits poor solubility. Therefore, we decided to synthesise compound **2.40a** given previous studies have proven that the presence of a tosylate group enhances solubility and facilitates isolation. This approach also demonstrates a controlled sequential strategy of producing unsymmetric derivative **2.40a** without the complication of double addition of phthalonitrile.

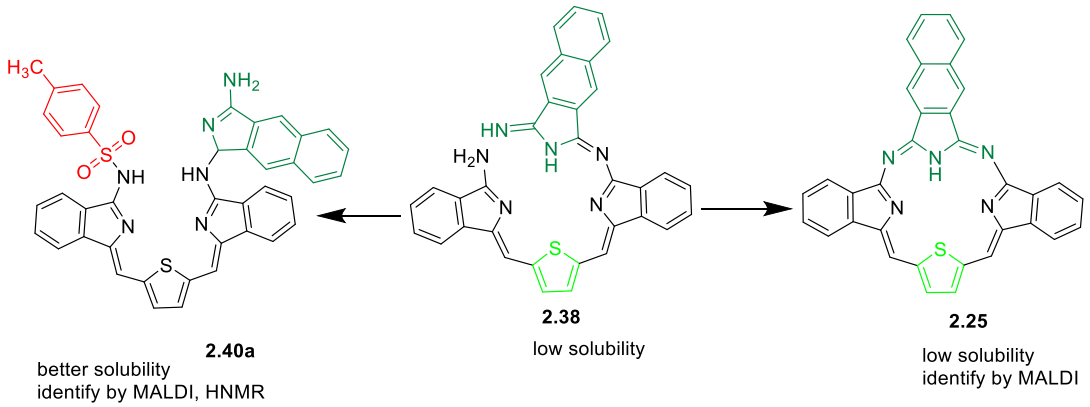

Scheme 2.17: The structure of **2.38, 2.25**.

To synthesise the target condensation product **2.40a**, dimethoxyisoindoline synthesis is required due to its high activation towards nucleophilic attack. It is easily synthesised following procedures previously developed at UEA[111] as shown in scheme 2.18. Naphthalonitrile was added to a solution of sodium methoxide, that was produced using methanol and sodium metal, and stirred at 35 ˚C for 6 h. The resulting reaction mixture was poured onto ice water then filtered and washed with cold water to obtain the required dimethoxyisoindoline **2.39** in good yield.

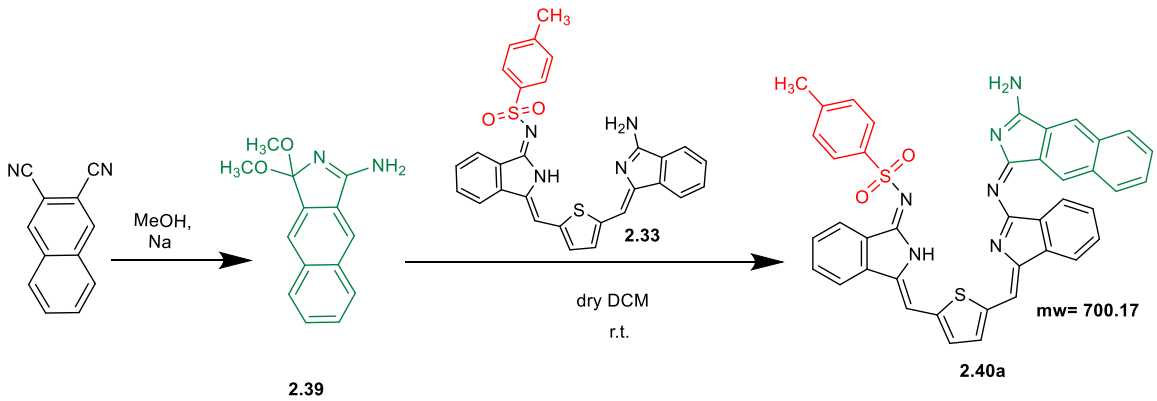

Scheme 2.18: Synthesis of compound **2.40a**.

Following the synthesis of the dimethoxyisoindoline **2.39**, the next step was a condensation reaction between **2.39** and mono tosylate of intermediate **2.33.** The reaction was carried out by stirring the reactants in dry DCM. Initial TLC results seemed promising, with a new purple spot observed. The reaction was continued overnight, and upon completion, the reaction mixture was checked by MALDI-TOF-MS, revealing a peak at 700 m/z which corresponded to the target compound **2.40a** (Figure 2.29).

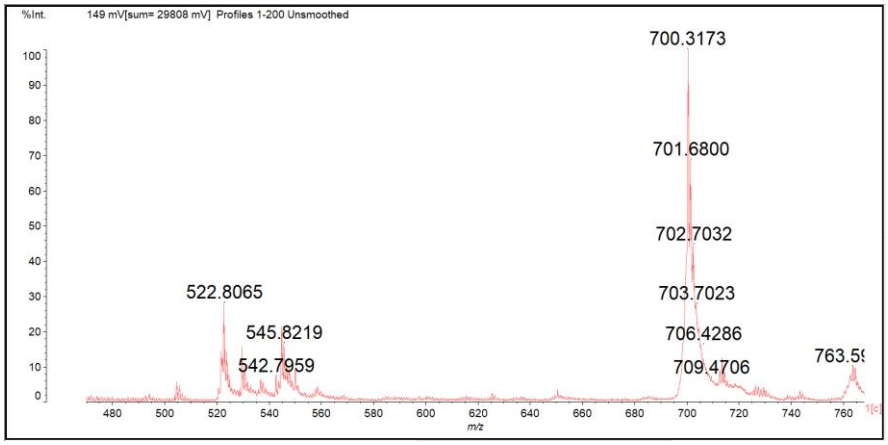

Figure 2.29: MALDI-TOF spectrum of mixture reaction of **2.40a**.

The desired compound was isolated using column chromatography then recrystallisation to yield **2.40a** as a purple solid (23%). MALDI-TOF-MS analysis conducted after purification revealed a peak at 702 m/z rather than the expected mass at 700 m/z that was observed before the purification (Figure 2.30). The mass was checked by running the instrument calibrated with different known compounds that have close molecular weights, and it was confirmed that there was no instrument issue. Therefore, it is more likely that the compound underwent hydrolysis during purification by column chromatography.

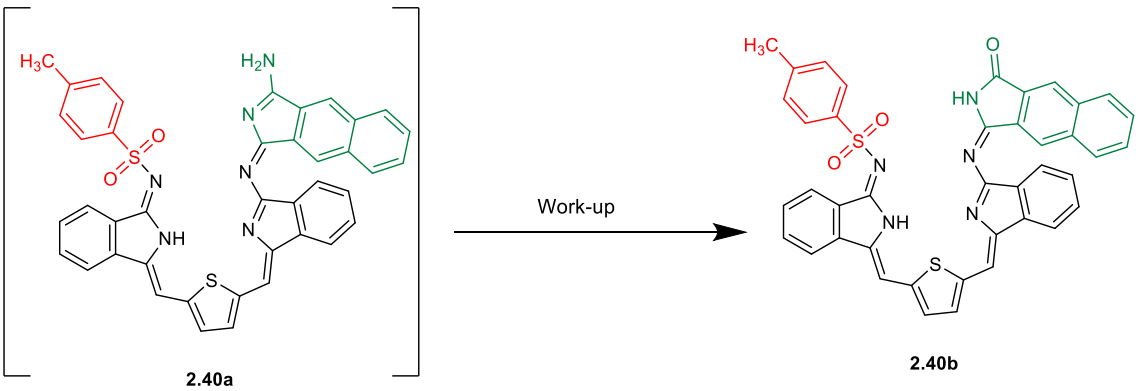

Scheme 2.19: Hydrolysis of compound **2.40a**.

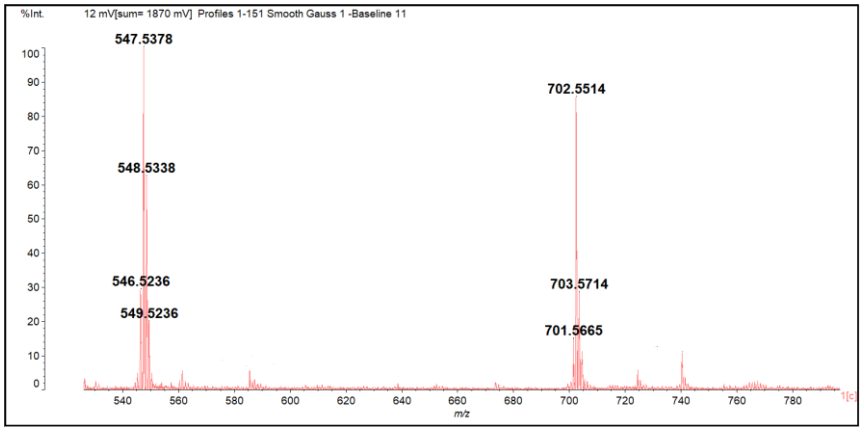

Figure 2.30: MALDI-TOF-MS spectrum of **2.40b**.

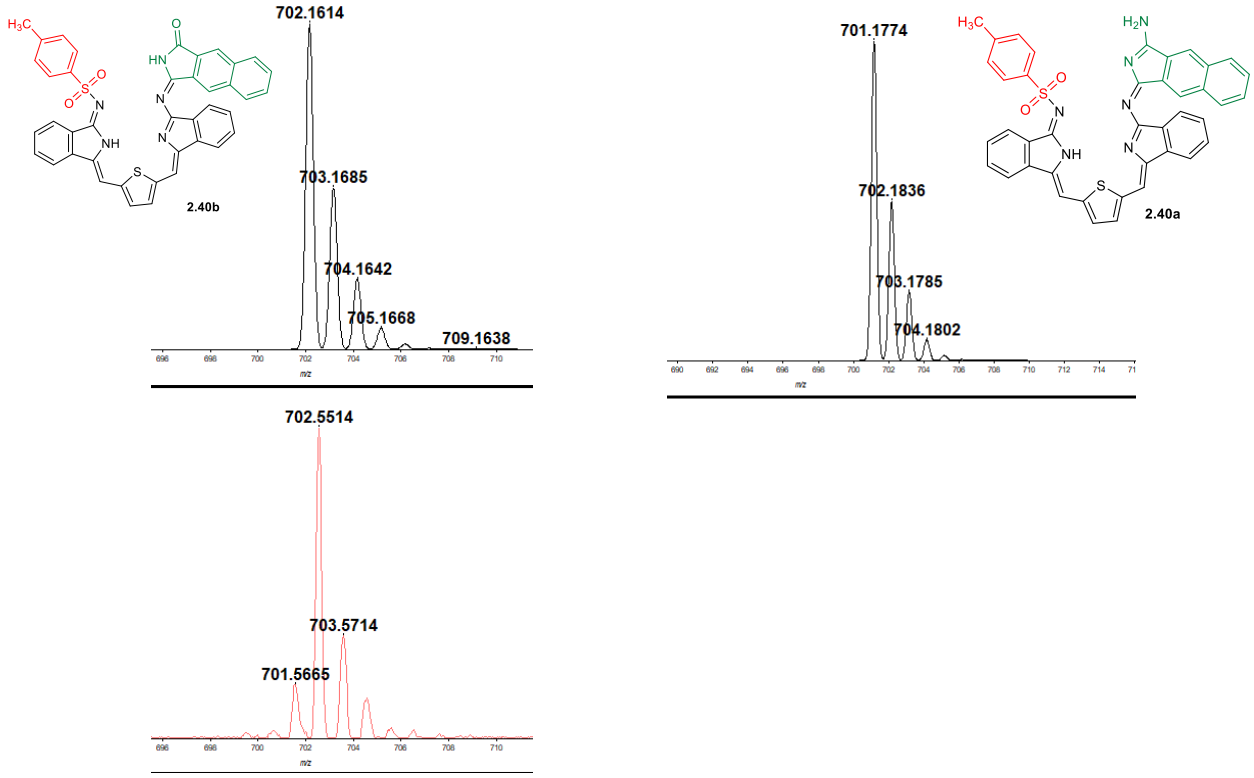

Figure 2.31: MALDI-TOF mass spectrum of **2.40b** with theoretical prediction (M+1) for both **2.40a** and **2.40b** (top).

Closer inspection of the MALDI-TOF-MS data revealed a peak at 547 m/z beside 702 m/z that corresponded to the compound without a tosyl group as seen in the figure 2.30. This obtained result was confusing, suggesting the presence of two compounds. Thus, TLC was conducted in different systems, but they confirmed that it was a single compound, and the MS peak is therefore a result of hydrolysis on the plate or during the measurement (fragmentation).

The ^{1}H NMR spectra is concordant with the structure proposed and shows a peak at around δ 11 ppm with the integration of 1, which is attributed to the NH of the isoindole unit that is connected to the tosyl group (highlighted in green). This peak is also observed in the starting material **2.33**. Another peak around 12 ppm, again with an integration of 1, likely corresponds to NH within isoindole group (highlighted in pink). These observations suggest that the compound is more likely to be **2.40b**. Further evidence supporting this structure was provided by infrared spectroscopy, which revealed a signal at 1734 cm^{-1}, corresponding to the carbonyl group. Comparison of the absorption spectra of **2.40b** with the starting material **2.33** is shown in figure 2.33, a significantly longer wavelength absorption band was observed, as expected due to the extension of the molecule's π-system. Due to these results, no further investigation was conducted.

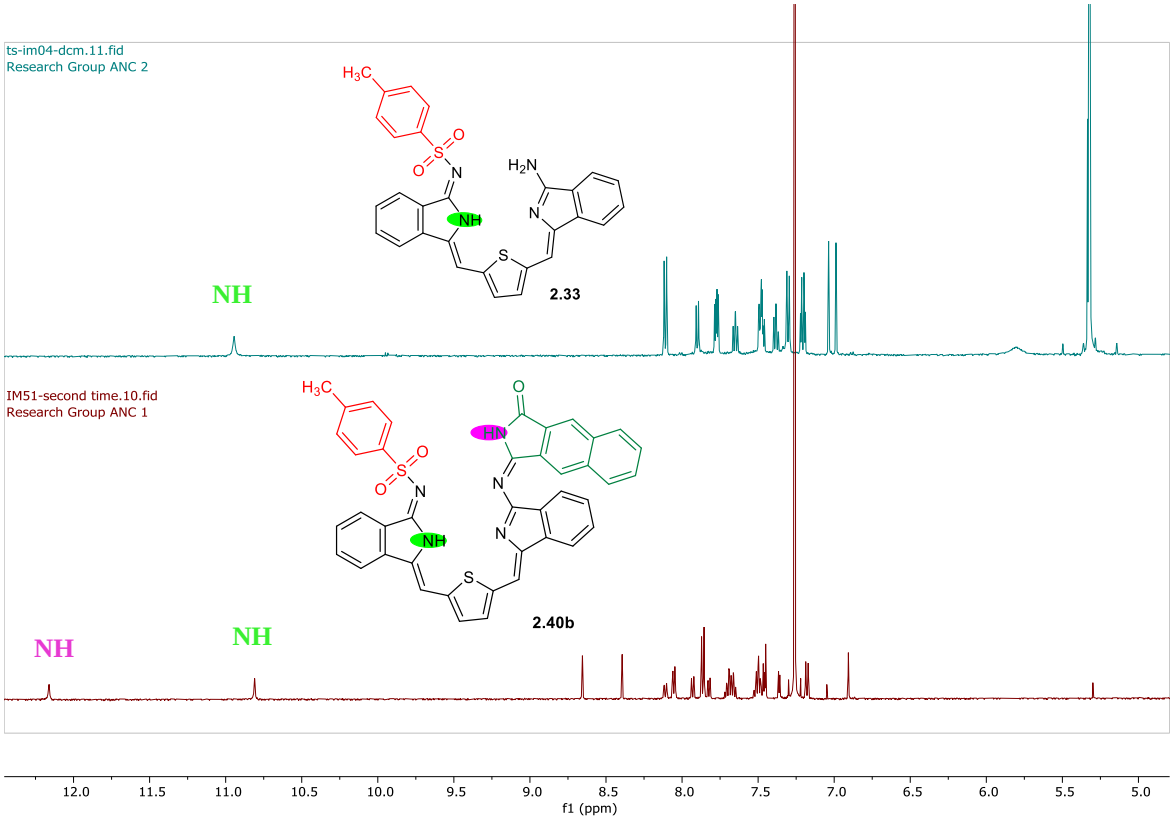

Figure 2.32: ^{1}H NMR spectra of compounds **2.40b, 2.33**.

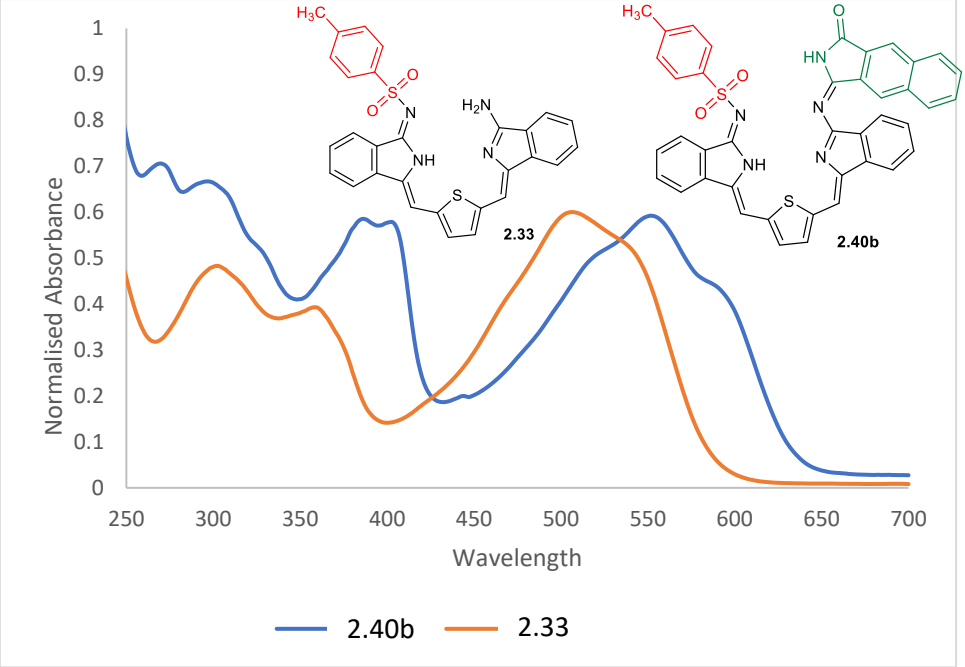

Figure 2.33: Comparison of UV-vis spectra of **2.40** and **2.33**.

2.6 The third series - *S*-confused *cis*-diazatribenzothiaporphyrin.

The previous studies focused on using the intermediate bisaminoisodoline thiophenes like **2.2** linked through positions 2,5- within the thiophene structure. This presents a sulfur atom inside the macrocyclic structure in a manner that bears close similarity to porphyrin and phthalocyanine structures. Within this section, our attention was on the synthesis of *S*-confused *cis*-diazatribenzothiaporphyrin distinguished by the presence of inner CH alongside an external (outer) sulfur atom within the macrocyclic structure. The change also disrupts the formal cyclic conjugation pathway (aromaticity).

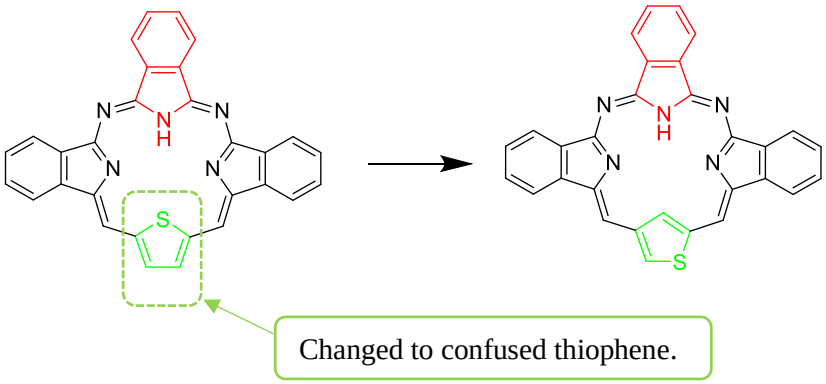

Figure 2.34: Tribenzodiazathiaporphyrin structure with indicated change in thiophene bonding.

2.6.1 Synthesis of the *S*-confused intermediate:

The key to *S*-confused *cis*-diazatribenzothiaporphyrin synthesis was using an isomeric bisaminoisoindoline thiophene **2.42** as an intermediate. This intermediate was prepared by direct utilization of TMS- protected acetylene at positions 2 and 4 of the thiophene molecule. 2,4-Dibromo thiophene was cross-coupled with trimethylsilylacetylene under Sonogashira conditions to give the bis(trimethylsilylethynyl) thiophene as shown in scheme 2.20.

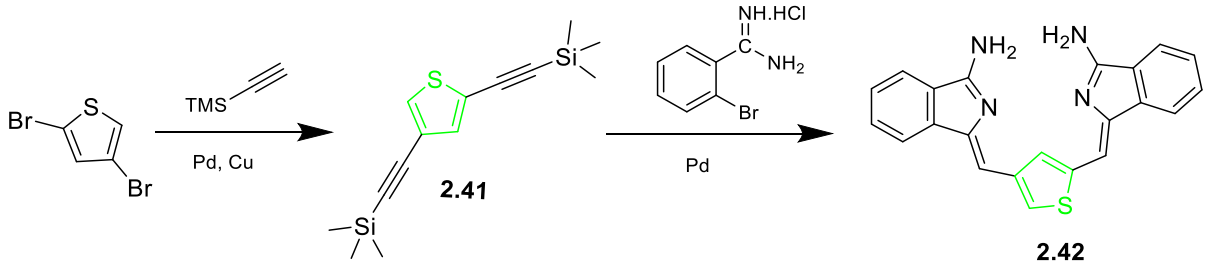

Scheme 2.20: Synthesis of 2,4 bis(trimethylsilylethynyl)thiophene and compound **2.42**.

The synthesis of bisaminoisoindoline thiophene **2.42** required investigation before the macrocyclization could be achieved. The same method as mentioned previously to prepare bisaminoisoindoline **2.2** was used to prepare bisaminoisoindoline **2.42**. Treatment of amidine **2.1** with acetylene **2.41** under palladium catalysis leads to cross-coupling and cyclization, thus yielding the product **2.42** directly as a green solid. Since this compound consistently stays at the baseline in various TLC systems without movement, it was difficult to isolate it by column chromatography. Alternative purification methods were employed to improve its purity. The dried solid was dissolved in acetone and, after filtration through a bed of Celite, a few drops of conc. HCl was added. The solid was filtered off, and CH_3OH/ CH_3ONa were added to the solid. The product was stirred for 5 min and then poured into water to give the title compound as a green powder.

The proton NMR spectrum of compound **2.42** showed four peaks at 6.78, 7.04, 7.8 and 7.9 ppm as singlets with integration of 1 proton, which correspond to alkene and thiophene protons, as well as 4 multiplet signals, which correspond to aromatic protons. Structure **2.42** is a green compound with broad UV-visible absorbance as shown in figure 2.36. Additionally, its fluorescence emission spectra provide a peak at 489 upon excitation at 388 nm.

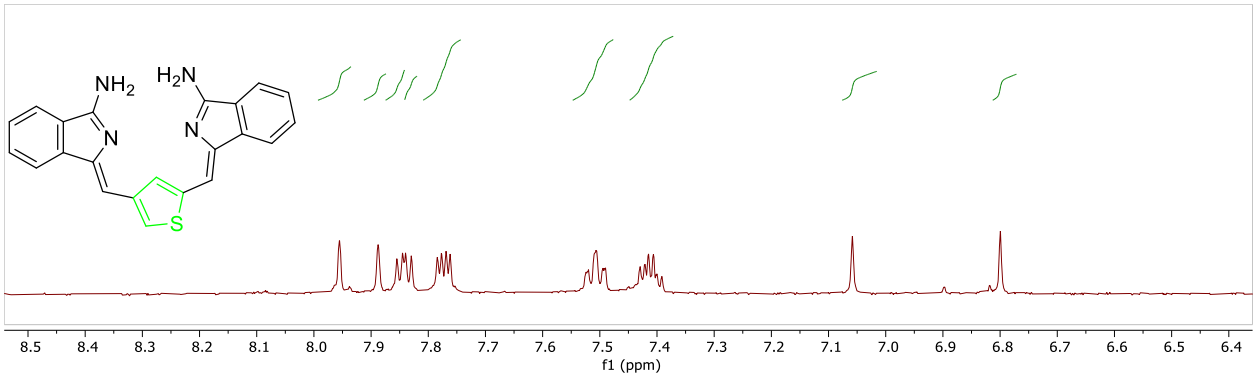

Figure 2.35: ^{1}H NMR spectrum of intermediate **2.42**.

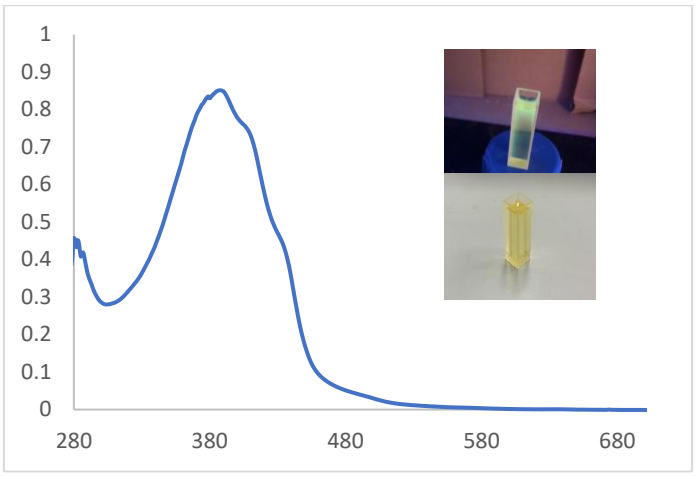

Figure 2.36: UV-vis spectrum of **2.42**.

2.6.2 Synthesis of the third series of macrocycle

Once the syntheses of the intermediate bisaminoisodoline **2.42** was achieved successfully, we were in a position to use it to prepare S-confused cis-diazatribenzothiaporphyrin. Since 4-*tert*-butylphthalonitrile is a commercially accessible derivative, it was the subject of the first investigation in this series.

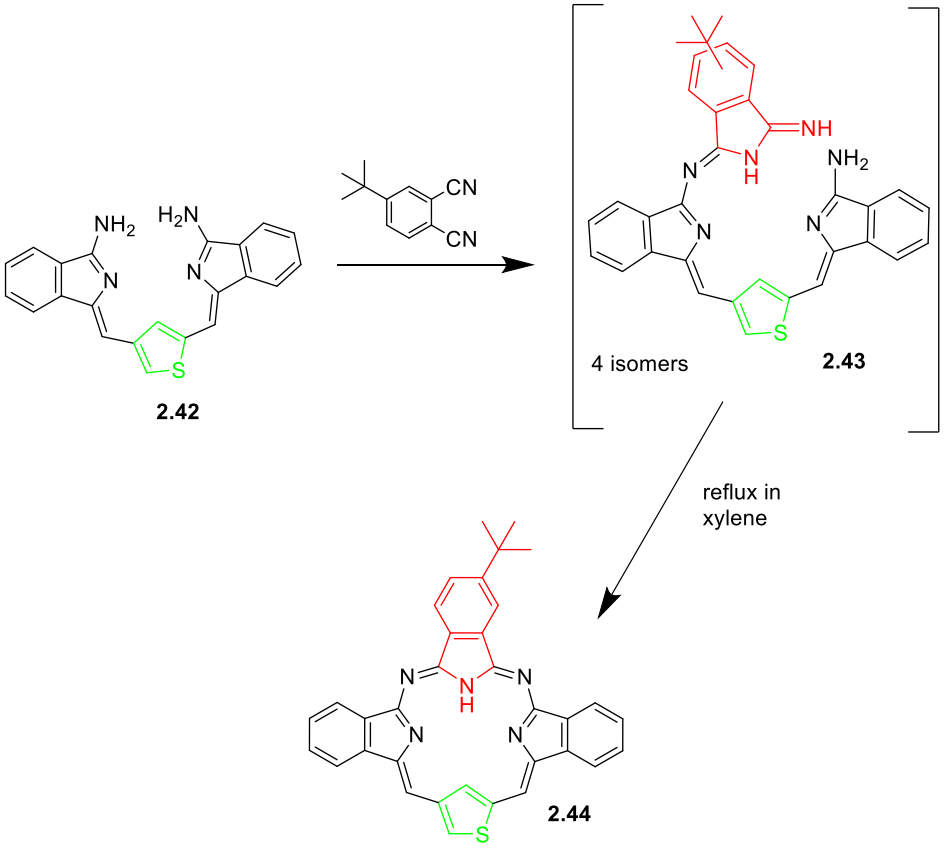

Scheme 2.21: Synthesis of the *S*-confused *cis*-diazatribenzothiaporphyrin **2.44**.

S-confused *cis*-diazatribenzothiaporphyrin was synthesised employing the same two step standard procedure utilized in the synthesis of tribenzodiazathiaporphyrins. The compound **2.44** was obtained by refluxing (1 equivalent) of intermediate **2.42** with 4-*tert*-butylphthalonitrile (1 equivalent) in methanol in the presence of $NaOCH_3$ under a nitrogen atmosphere. After the reaction period (when TLC did not show a spot for Pn), the crude residue was isolated as a mixture of isomers of the open compound **2.43** and employed in the next step which involved refluxing the mixture in *p*-xylene. The reaction appeared promising, with a red spot possessing the characteristic strong red fluorescence visible by TLC analysis. Then, the crude solids were separated using silica gel chromatography, followed by recrystallisation to collect the red product **2.44** as the isolated compound.

As expected, the ^1H NMR spectroscopic characterisation is complicated due to the reduction in symmetry and isomer formation. Integration of the proton NMR spectrum in the typical aromatic region, revealed a “missing” proton, but an additional broad peak around 6.5 ppm. Consequently, in response to this observation, a few drops of deuterium oxide (D_2O) were added to the NMR sample and shaken, aiming to confirm whether this peak belongs to the

previously missed C-H proton of the compound or due to the proton of the inner NH group. Notably, the sharpness exhibited by this peak implies it is related to C-H in the compound. In addition to HSQC NMR shows a cross peak corresponding to this specific signal, confirming it belonged to a proton connected to a carbon.

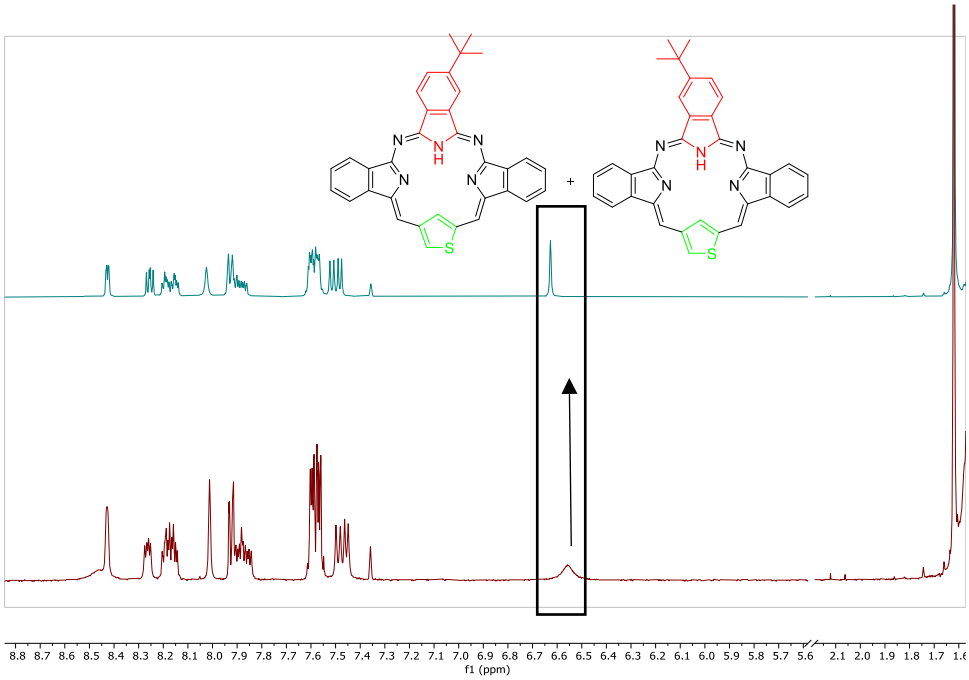

Figure 2.37: ^{1}H NMR spectra of compound **2.44** in DCM-d_2, and DCM with added D_2O (top).

The COSY NMR spectrum (Figure 2.38) gave a clear indication that the molecule is an equal mixture of two isomers as expected. Signals between 7.4-7.5 ppm show no cross peak in the COSY, indicating the 4 singlets that likely correspond to alkene protons (2x signal for each isomer).

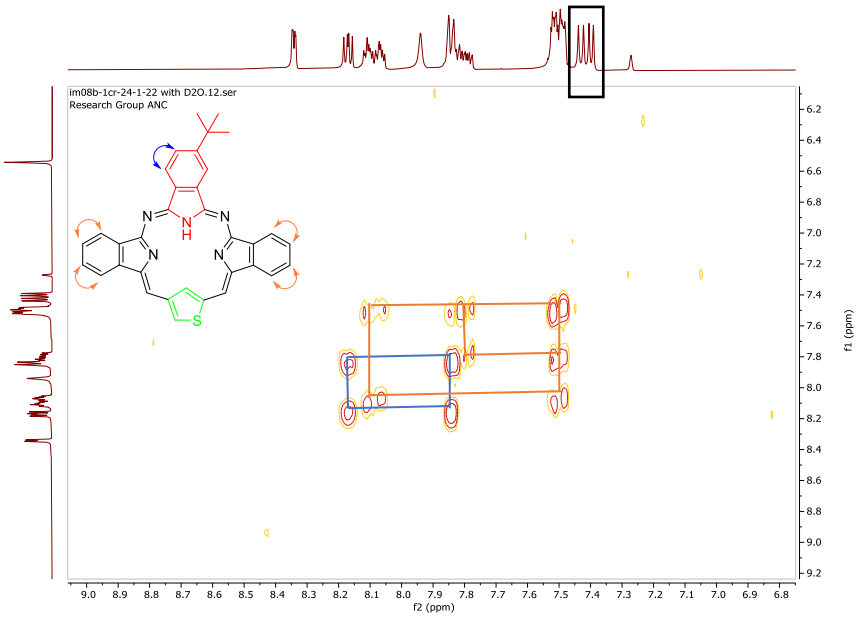

Figure 2.38: COSY experiment showing cross peaks in compound **2.44**.

Due to the challenging NMR spectra of the previous compound with *tert*-butyl derivative, the decision was made to use an alternate derivative in order to facilitate a more straightforward NMR spectroscopic analysis. As result, the 6,7-dicyano-1,1,4,4-tetramethyl-tetralin was selected and synthesised as described previously, with the aim to synthesise *S*-confused derivative **2.46** (Scheme 2.22).

The *S*-confused *cis*-diazatribenzothiaporphyrin **2.46** reaction was carried out in two steps, as described in the previous section. The first process produced a deep red substance that was identified by MALDI-TOF-MS that indicated it to be the open compound **2.45**. This compound was not easy to identify by ^{1}H NMR spectroscopy due to isomeric forms (there are two different nitrogens that can attack Pn to form an intermediate). The isomeric mixture was refluxed in *p*-xylene and monitored by TLC, and the completion was observed in 24h. A clear indication of the cyclized compound **2.46** was visible on TLC, with the formation of a strongly coloured red spot with bright red fluorescence under UV lamp. Purification was performed by using column chromatography and recrystallisation to obtain the macrocycle as a single compound, thereby simplifying the NMR spectra analysis.

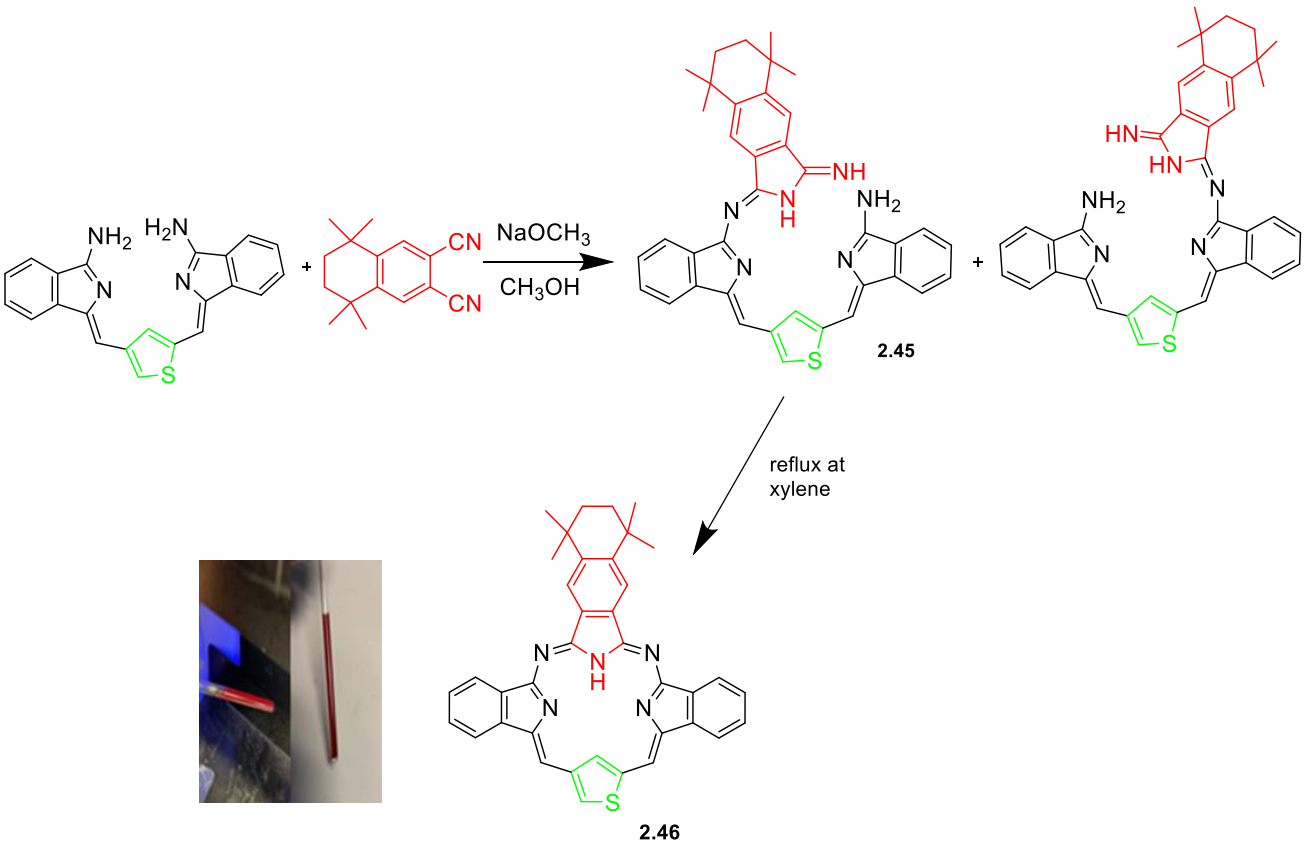

Scheme 2.22: Synthesis of the *S*-confused *cis*-diazatribenzothiaporphyrin **2.46**; inset, highly coloured product **2.46** under normal light (right) and the same compound under irradiation with a 365 nm light (left).

Despite the enhanced clarity of the ^{1}H NMR spectrum of the compound **2.46** compared to preceding compound **2.44**, the reduction of symmetry is still observed. Interestingly, the ^{1}H NMR study on compound **2.46** showed that the inner NH appeared as a singlet at 9.1 ppm, as seen in figure 2.39, consistent with the structure not showing aromaticity in the full macrocycle. The single crystal X-ray structure of **2.46** was solved by our collaborator Dr David Hughes, and his comments on the detail of the structure can be found in the appendix. As shown in figure 2.40, it reveals a planar molecule; the only significant deviations from the central 16-membered ring are in the cyclohexenyl ring C(5)-C(10). There is also disorder in the thiophene ring, where the sulfur atom is in either the S(27) or S(28) site; the occupation ratio here is 0.63:0.37. Bond lengths in the 16-membered ring indicate clearly the double-bonds in the C(13)-N(14), C(16)-N(15) and C(23)-C(24) bonds and in the corresponding bonds on the opposite side of the ring; the bonds about N(1) and C(25) are all quite similar at ca 1.39 Å, as in the aromatic rings. The hydrogen atoms on N(1) and C(25) both form shared weak hydrogen

bonds to both N(15) and N(31) within the 16-membered ring. Full details are included in the appendix.

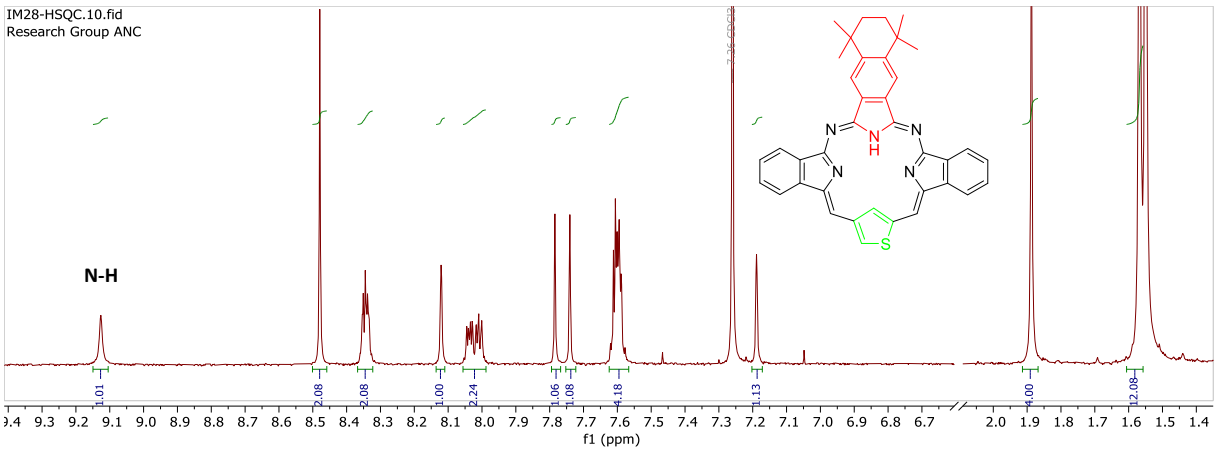

Figure 2.39: ^{1}H NMR spectrum of compound **2.46**.

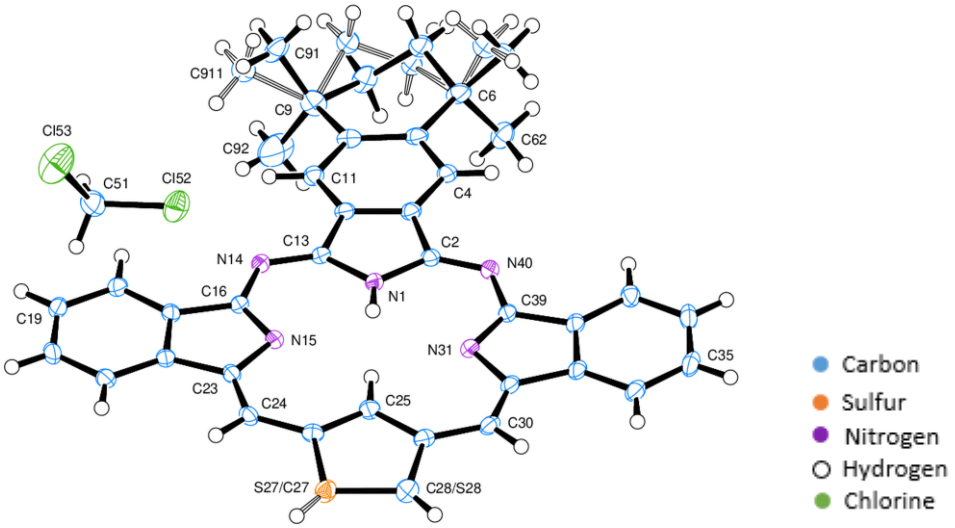

Figure 2.40: X-ray structure of compound **2.46**.

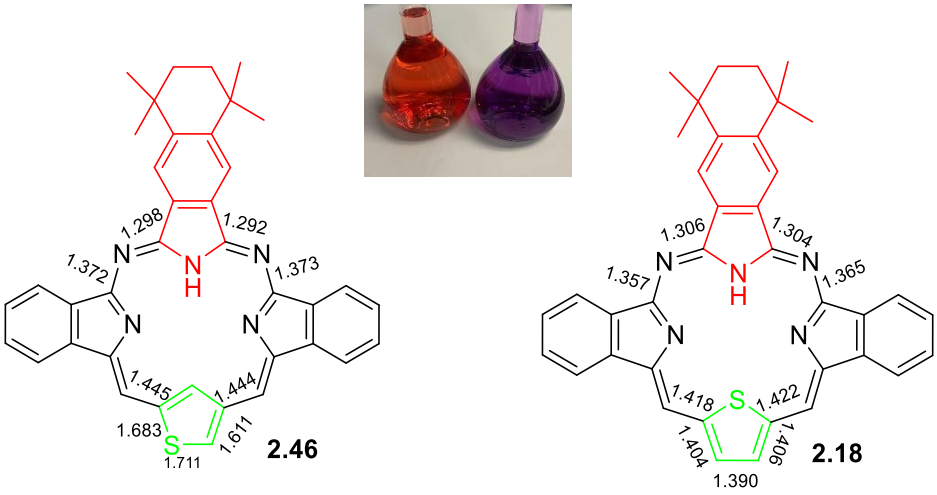

Figure 2.41: The structures for **2.46** and **2.18** with selective bond lengths.

According to the crystal structures for **2.46** and **2.18,** the non-aromatic system of **2.46** was observed. As shown in the crystal structure of **2.46** with selected bond lengths, the bond alternation is more pronounced. In contrast, the bond lengths shown in structure **2.18** provides evidence of aromaticity.

The substituents influence not just the solubility of the macrocycle but also its physical and chemical properties. So, a selection of the same substitutions utilized in tribenzodiazathiaporphyrin synthesis were employed in the preparation of *S*-confused *cis*-diazatribenzothiaporphyrin series.

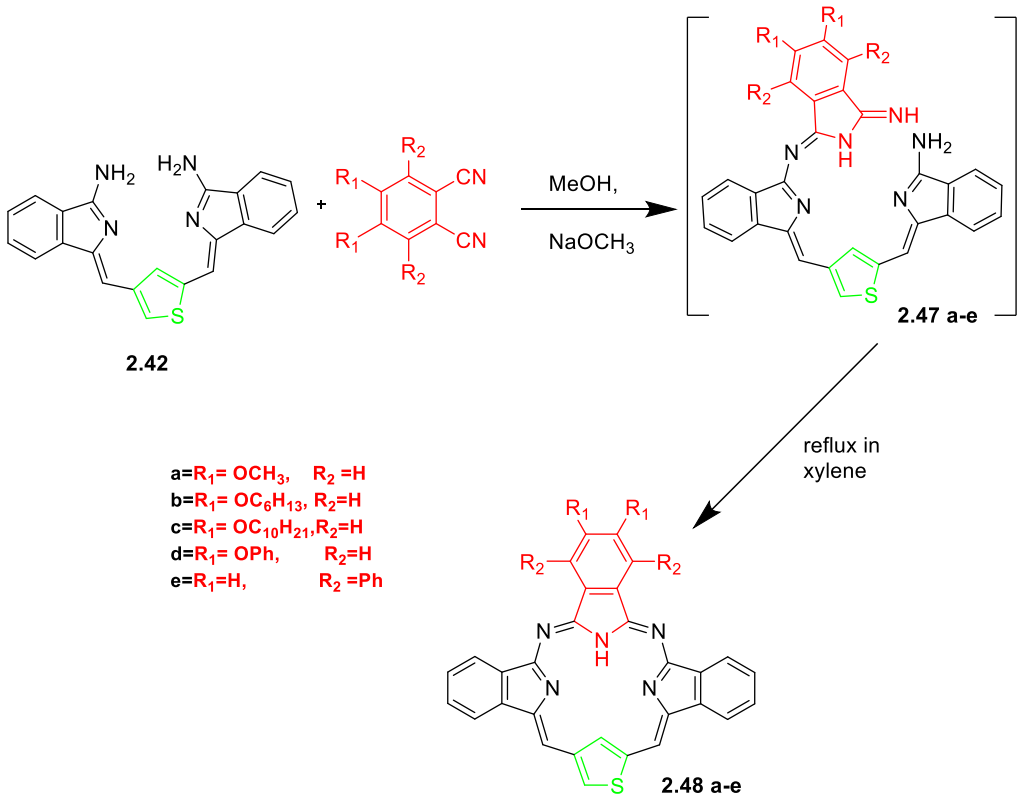

Scheme 2.23: Synthesis of the *S*-confused *cis*-diazatribenzothiaporphyrins **2.48**.

The majority of synthesised derivatives were prepared following a two-step procedure, as outlined previously. However, in the case of compound **2.48e**, the product did not form, and notably there was no exhibited consumption of the starting material using this method. Therefore, an alternative approach was used based on the optimisation strategy. Initially, the reaction was conducted via reflux in toluene, resulting in the formation of the cyclized product as confirmed by MALDI-TOF-MS; however, both starting materials remained evident from TLC analysis. Subsequently, the solvent was switched to *p*-xylene and subjected to reflux conditions, leading to the complete consumption of the starting material and this resulted in the desired product in 14% yield. This was a notably higher yield compared to other derivatives obtained through the previous approach. The improvement is general, and by this changed method derivative **2.48a** was isolated in 21% yield compared to 7% previously achieved.

Isolation of these compounds **2.48 a-e** was performed using column chromatography, followed by recrystallization from DCM and methanol, and they were characterised by MALDI-TOF-MS and ^{1}H NMR spectroscopy.

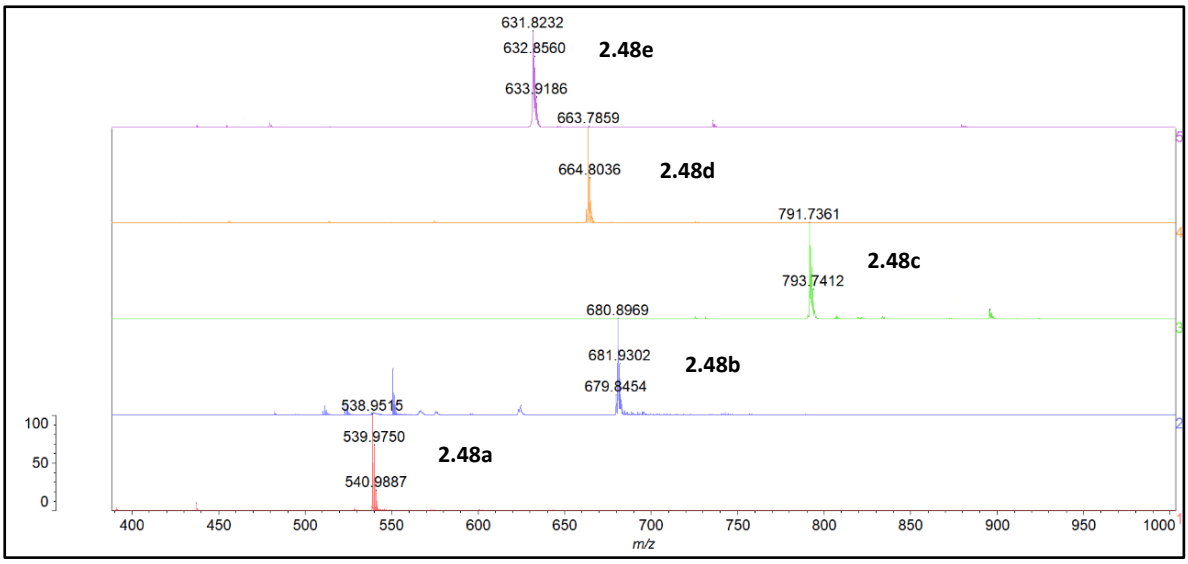

Figure 2.42: MALDI-TOF-MS of some of the *S*-confused *cis*-diazatribenzothiaporphyrin products.

The π -extended napthalo-derivative was next targeted to see if a red-shift would be observed (noting napthalocyanine's 100 nm shift compared to phthalocyanine,[117]). Naphthalene-1,2-dicarbonitrile was therefore chosen as the next phthalonitrile in this series and employed in a two-step synthesis to obtain our target product. The compound formation was confirmed by MALDI-TOF-MS, which displayed a peak at 529 m/z. The product's solubility continued to be an issue for NMR spectroscopic analysis, however, and clear spectra could not be obtained.

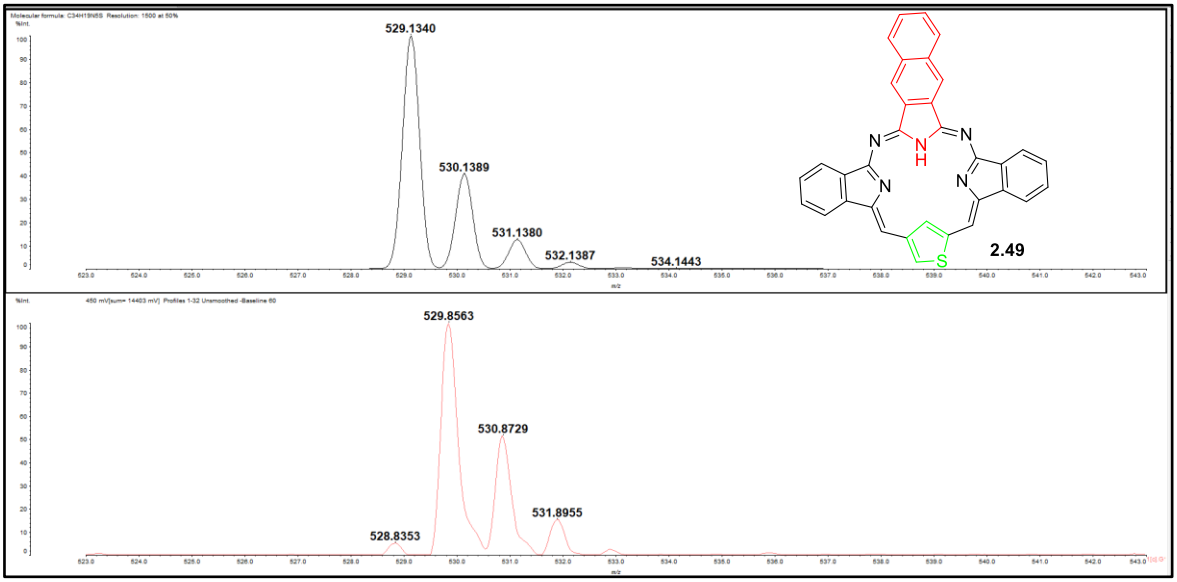

Figure 2.43: MALDI-TOF-MS of compound **2.49** with its theoretical prediction (top).

Oxidation of the *S*-confused derivatives was briefly investigated because related work on *S*-confused porphyrins has shown that the thiophene can be oxidised at carbon with potential to produce a fully conjugated macrocycle.[118] However, the experimental attempt to oxidize the compound **2.43b**, employing conditions analogous to those reported in the literature for porphyrin systems using DDQ, yielded no observable reaction.

Due to earlier work[90] that successfully inserted metals into *S*-confused porphyrin, insertion of Pd(II) into *S*-confused *cis*-diazatribenzothiaporphyrin **2.48b** was attempted. The reaction was carried out by stirring palladium acetate with compound **2.48b** in ethyl acetate at room temperature. MALDI- TOF MS analysis was used to monitor the reaction over 10 days and a peak corresponding to the Pd complex was observed after 24h.

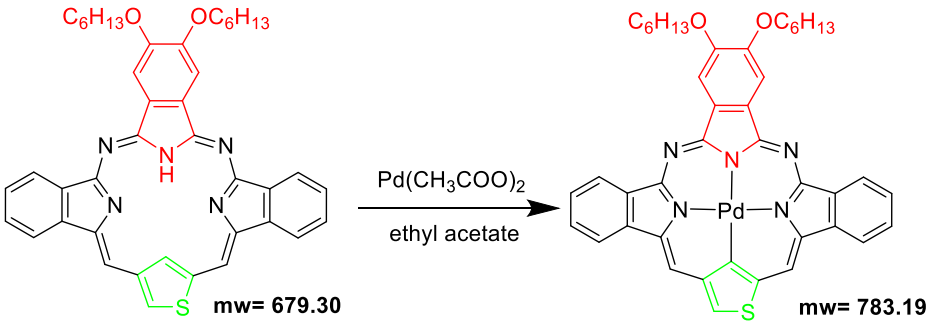

Scheme 2.24: Pd complex synthesised attempt.

As seen in figure 2.44, the reaction did not show further progression with an increase time. The reaction was then stopped, and column chromatography was employed to separate the mixture. However, the Pd complex could not be separated from the starting material and there is no conclusive evidence that Pd is inside the macrocycle because of the failure of the reaction to proceed to completion. It is likely that Pd binds to the external nitrogen (or sulfur) of the macrocycle and complexation was not the further investigated.

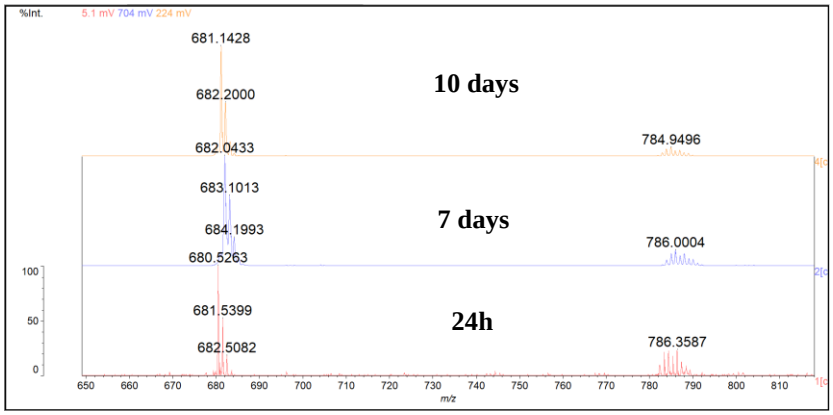

Figure 2.44: MALDI-TOF-MS of Pd complex reaction.

Additionally, it is worth noting that a trace of green material was observed in the previous reaction and analysis of this fraction indicated a peak corresponding to dimerization of two molecules of macrocycles that are directly linked to each other by a covalent bond. We suggested the bond was in the external single carbon of the *S*-confused thiophene as observed in Chmielewski's work[119] on the synthesis *N*-confused dimer. We therefore used coupling conditions to see if we could achieve dimerization of the starting material. DDQ and TFA were added to a solution of **2.48b** in DCM and the reaction was monitored by MALDI-TOF MS. No evidence for dimerization was observed but there was an indication of hydrolysis.

2.6.3 Optical properties of the of the 3rd series:

The UV/Vis absorption spectrum of **2.48d**, shows a very strong and split band at 341 nm, and a broad band at 516 nm with a shoulder peak at 560 nm. It also exhibits red fluorescence at 610 nm upon excitation at 514 nm. *S*-confused *cis*-diazatribenzothiaporphyrin therefore showed a blue shift as we expected, reflecting the complete π -delocalization pathway for the entire macrocycle in the normal series that is absent in the *S*-confused cases.

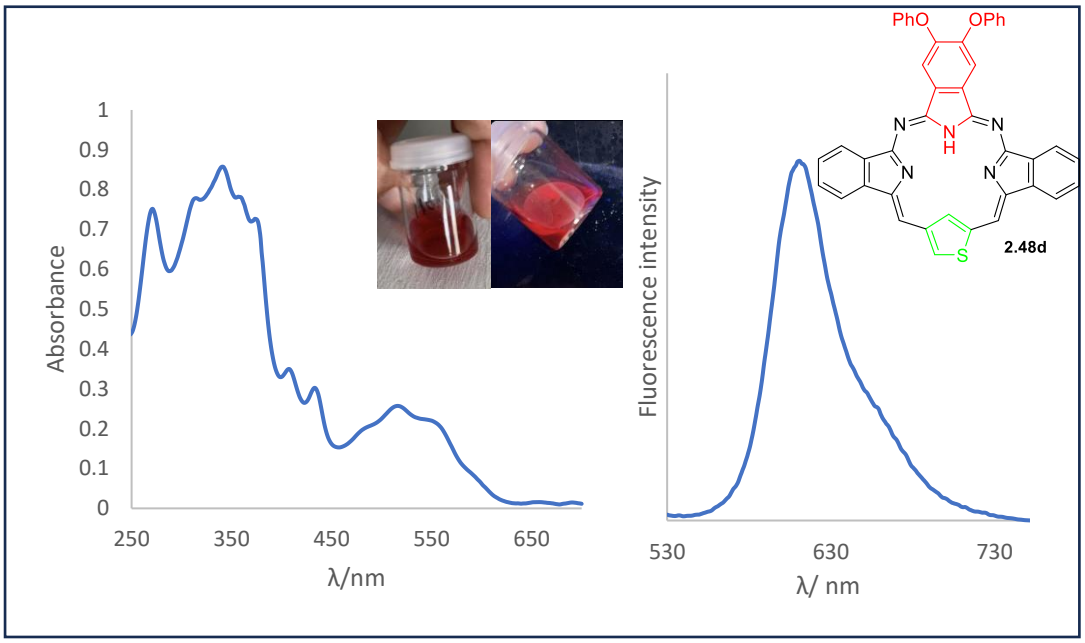

Figure 2.45: UV-vis absorption and fluorescence spectra of **2.48d**.

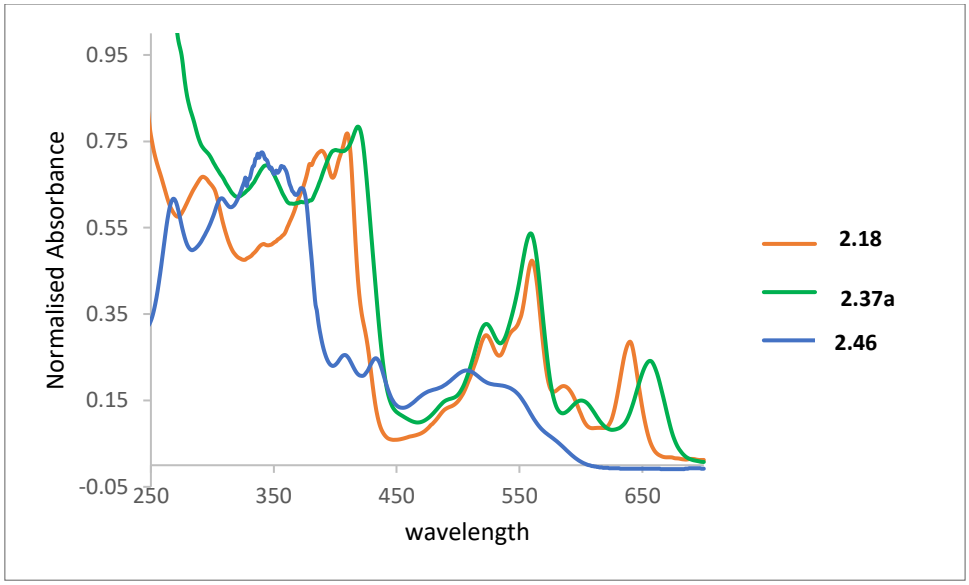

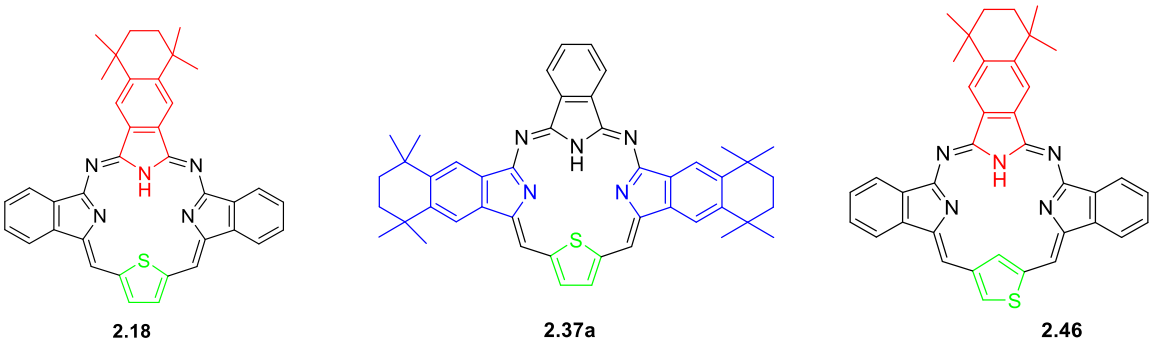

Figure 2.46: UV-vis absorption spectra of **2.18**, **2.37a**, **2.46**.

2.7 Attempts to prepare macrocycles and derivatives with other functional groups:

The successful synthesis and structural characterization of core modified phthalocyanine derivatives, specifically TBDAP between diaminoisoindoline thiophene intermediate and phthalonitrile, has motivated our investigation into further functionalization instead of through phthalonitrile. This includes studying acid chlorides, carbonyl and amine groups, aiming to expand the potential applications of these compounds.

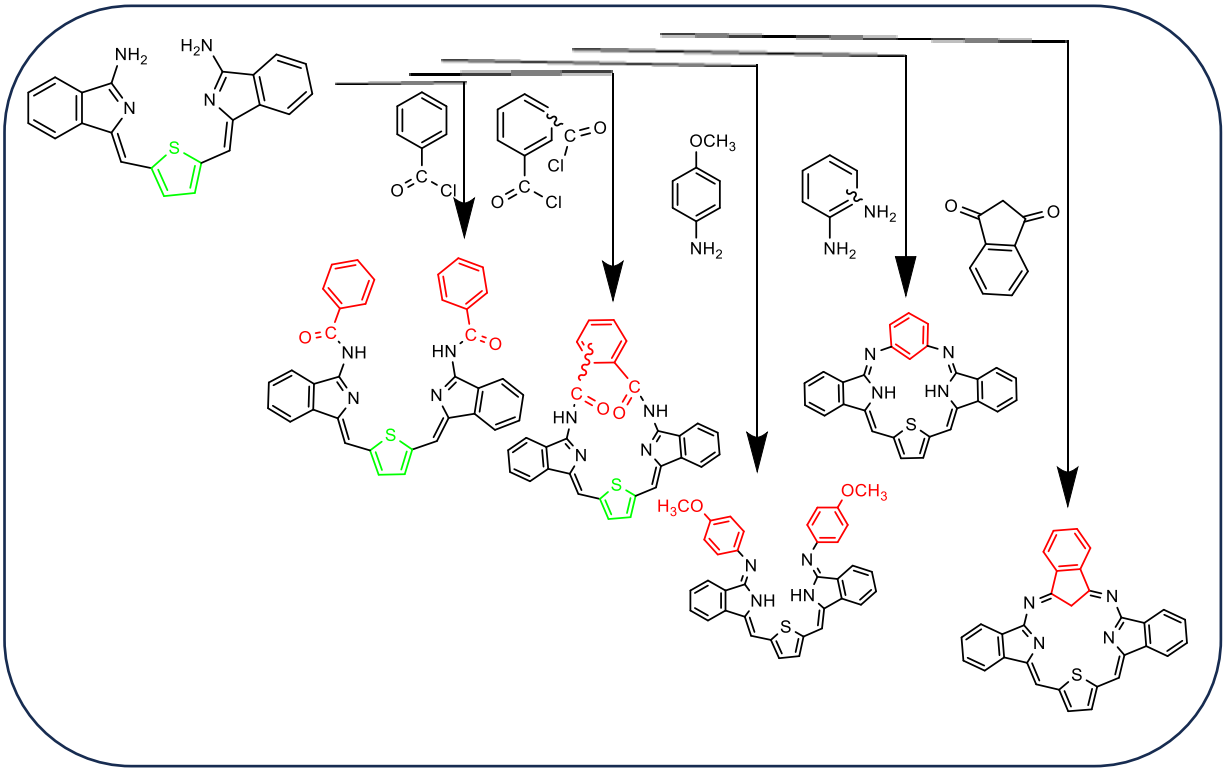

Scheme 2.25: The synthesis plan for macrocyclic compounds from various functionalized compounds.

2.7.1 Attempt with acid chloride:

Our investigation started with simple mono acid chloride compounds in order to evaluate their reactivity and potential in the reaction. Benzoyl chloride was added to a solution of **2.2** or **2.42** in dry DCM in the presence of TEA as a base, and the reaction mixture was stirred at room temperature overnight. The MALDI-TOF-MS showed that both amines react with acid chloride to give the bisamide compounds **2.50**, and **2.51**. The products were isolated by column chromatography using THF: PE, then recrystallized from DCM and pet ether to give the products as a red solid of **2.50**, and a yellow solid of **2.51** (Scheme 2.26).

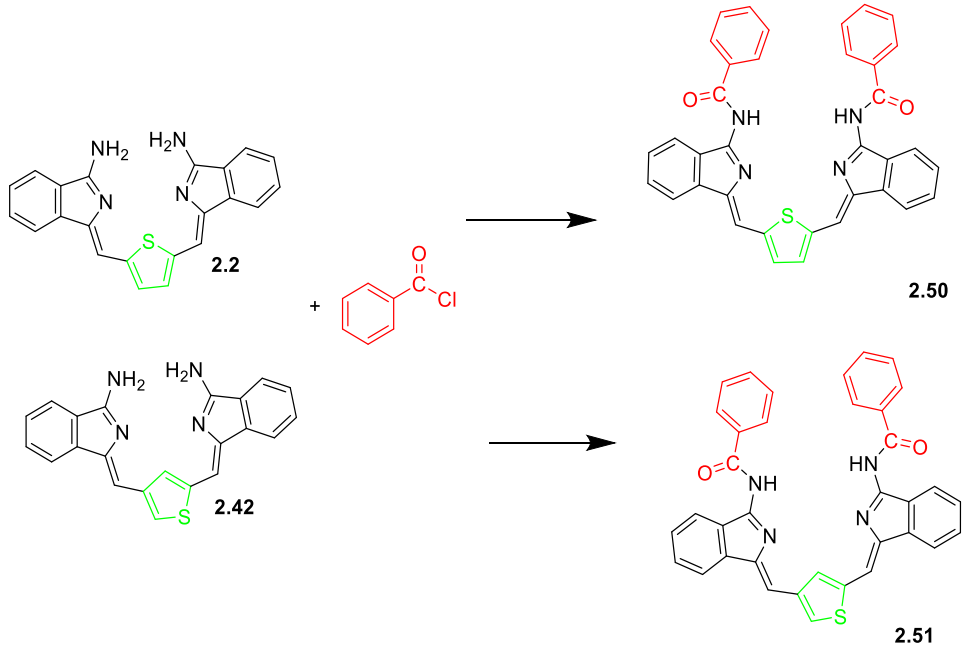

Scheme 2.26: Synthesis of the compounds **2.50**, **2.51**.

Following the successful reaction with benzoyl chloride, our focus turned towards di-acid chloride compounds with the aim of forming macrocyclic product **2.52**. 1 eq of **2.2** and 1 eq of phthaloyl chloride were stirred at room temperature in dry THF and TEA. The reaction was followed by TLC. After around 4 h, a new spot was observed by TLC, while **2.2** was not all consumed. After around 12 h the TLC was still showing the same outcome as the previous result.

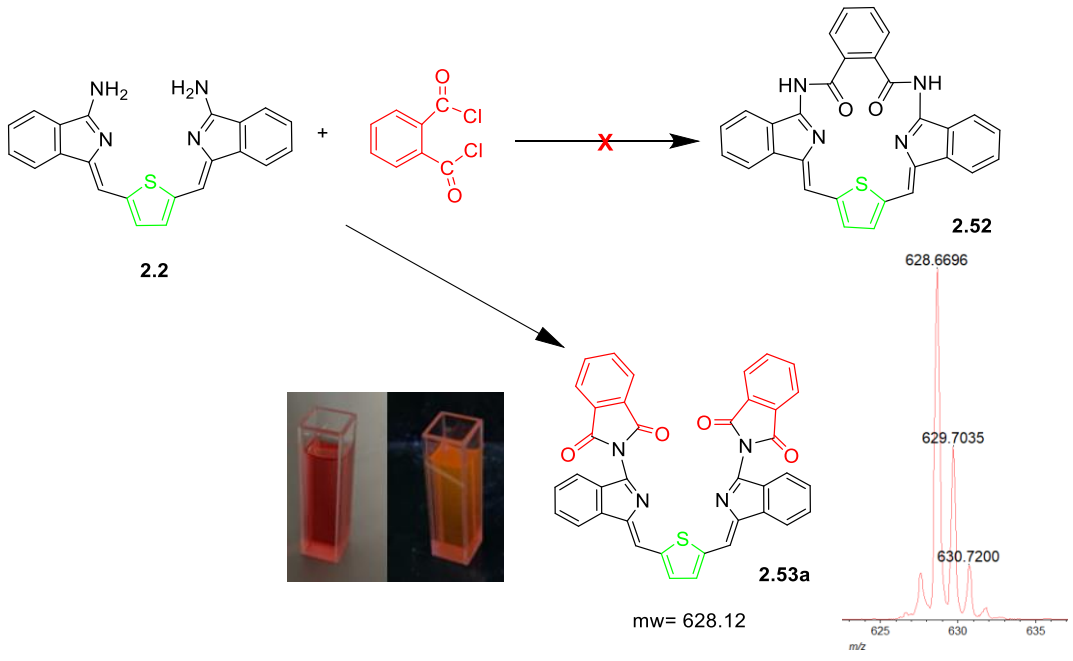

Scheme 2.27: Attempt to synthesise compound **2.52**; inset, MALDI-TOF-MS of **2.53a**.

The new spot was analysed by MALDI-TOF-MS. The obtained results show a cluster of peaks at m/z = 628. This peak may be due to the formation of the product **2.53a**. The product has a bright colour and is fluorescent under a UV lamp, as shown in the picture (Scheme 2.27).

The synthesis of the isomeric analogue **2.54** was also attempted in order to see if the same results could be obtained from intermediate **2.42**. The compound **2.54** was synthesised using the same methodology of the one-pot procedure for the formation of **2.53a**. Following the reaction, the MALDI-TOF-MS was checked, and a peak at 628 m/z was again observed, which indicated formation of compound **2.54**. This compound was isolated as a yellow solid and confirmed by MALDI-TOF-MS and ^{1}H NMR spectroscopy.

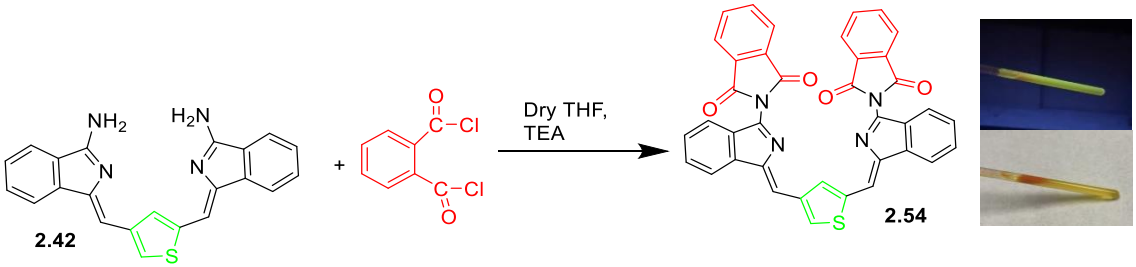

Scheme 2.28: Synthesis of the compounds **2.54**.

With the unexpected result **2.53a**, the reaction was repeated by altering the position of the acid chloride groups, aiming at formation of a macrocyclic compound. Attempts were made at positions 1,3 (isophthaloyl chloride) and 1,4 (terephthaloyl chloride), but unfortunately, the MALDI-TOF-MS analysis of both reactions did not exhibit any peak corresponding to the macrocycles.

Following the production of compound **2.53a** in the preceding reaction, we formulated the product as depicted in scheme 2.27. However, it was recognised that it could also correspond to the less likely doubly bridge structure, **2.53b** (Figure 2.47).

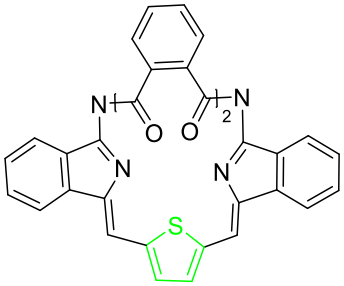

Figure 2.47: Structure of **2.53b**.

Our objective was to verify the identity of this compound by subjecting phthaloyl chloride to a reaction involving the mono-tosyl compound. This experimental approach aimed to confirm the nature and composition of the previously obtained product. Mono-tosylate intermediate **2.33** and phthaloyl chloride were stirred in dry DCM in the presence of TEA and monitored by TLC. The mixture was purified by column chromatography and recrystallised from DCM/PE to yield the desired compound as a red solid.

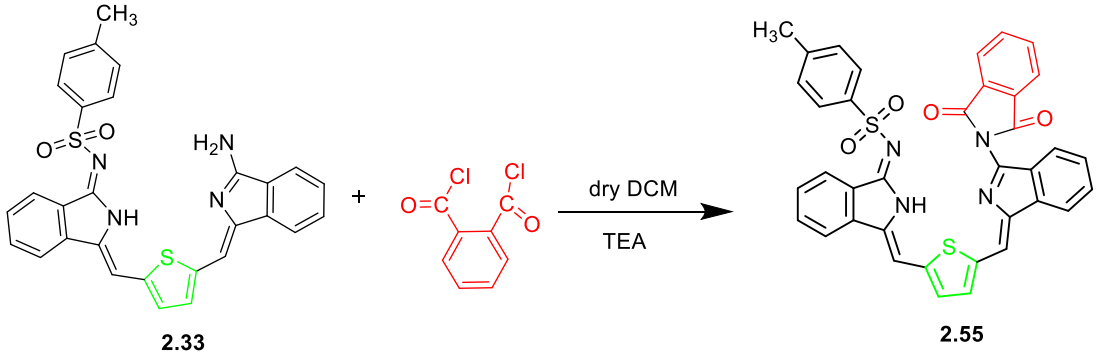

Scheme 2.29: Synthesis of the compounds **2.55**.

The ^{1}H NMR spectrum is concordant with the structure proposed, as seen in figure 2.48 (middle). The rapid formation of **2.55** indicates that the compound **2.53a** is most likely to be the structure. The comparison between spectra of **2.55**, **2.53a** and **2.32** to identify phthaloyl fragment was difficult, however, and the reasons can be seen when the crystal structure (figure 2.49; solved by our collaborator Dr David Hughes - his comments on the detail of the structure can be found in the appendix) is examined. We can see clear overlap of the aryl termini which will lead to unpredictable peak shifts. The X-ray structure of this compound shows that the central part of the molecule, from the isoindole group of N(21), through the thiophene ligand, to the isoindole group of N(2), is approximately planar. However, rotations about the C(29)-N(30) and C(1)-N(41) bonds are observed which take the tosyl group of S(3) and the isoindole group of N(41) out-of-plane and into an almost parallel arrangement of these aromatic groups. Extensive intermolecular π–π stacking involving all the aromatic rings is observed.

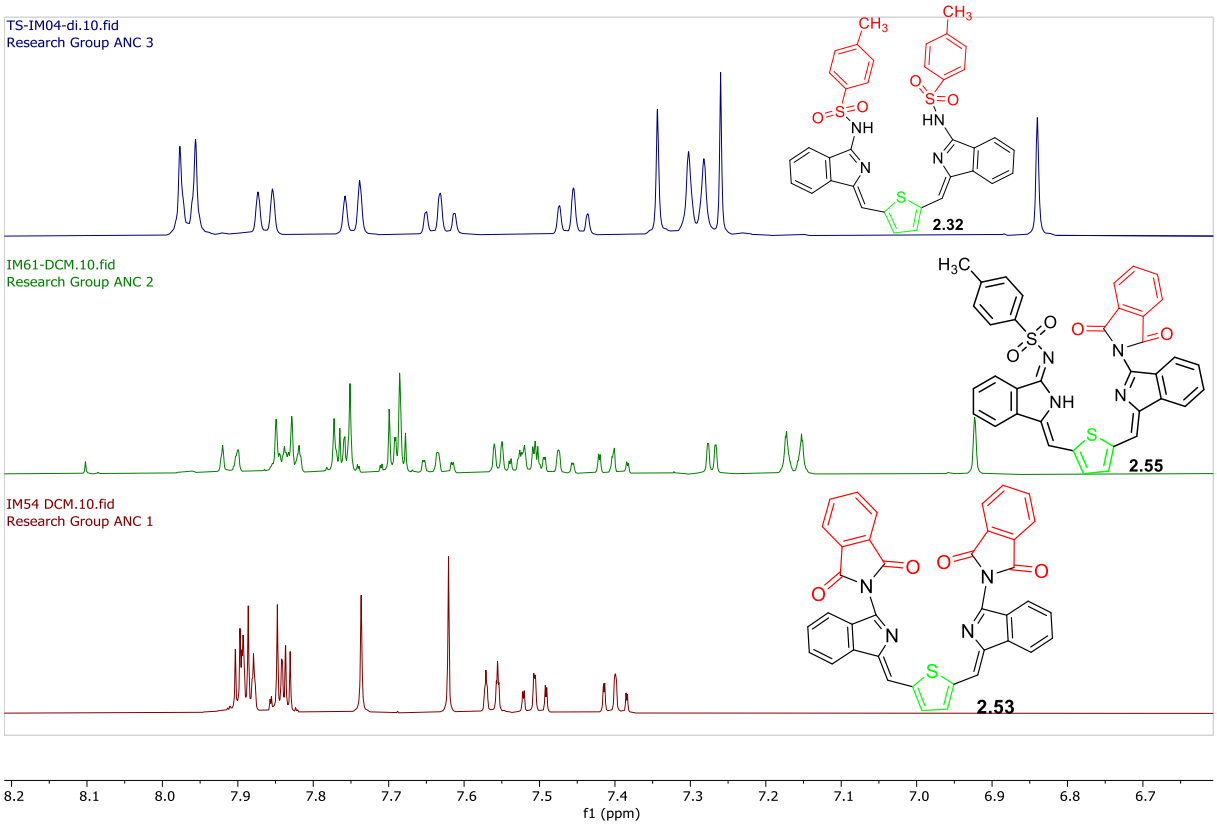

Figure 2.48: NMR spectra of compounds **2.32**, **2.55** and **2.53a**.

The crystals suitable for X-ray diffraction were grown by slow diffusion of hexane into a dichloromethanesolution of the compound, and showed the *Z*, *Z* configuration, as seen in below figure 2.49.

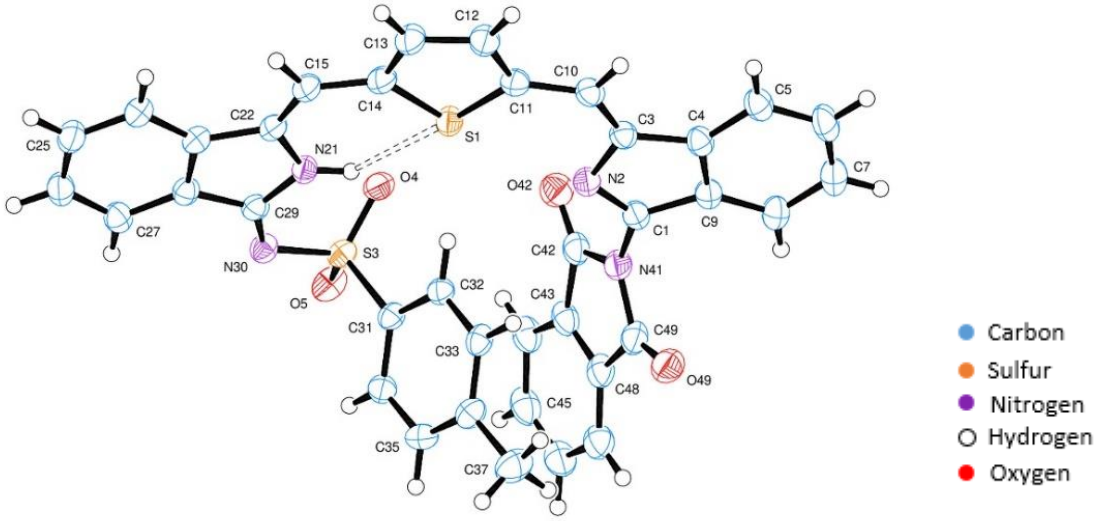

Figure 2.49: X-ray crystal structure of compound **2.55**.

Substituted derivative **2.56** was also then synthesised, following the same reaction conditions previously mentioned. The ^{1}H NMR spectroscopy data clearly matched with the isolated product **2.56**.

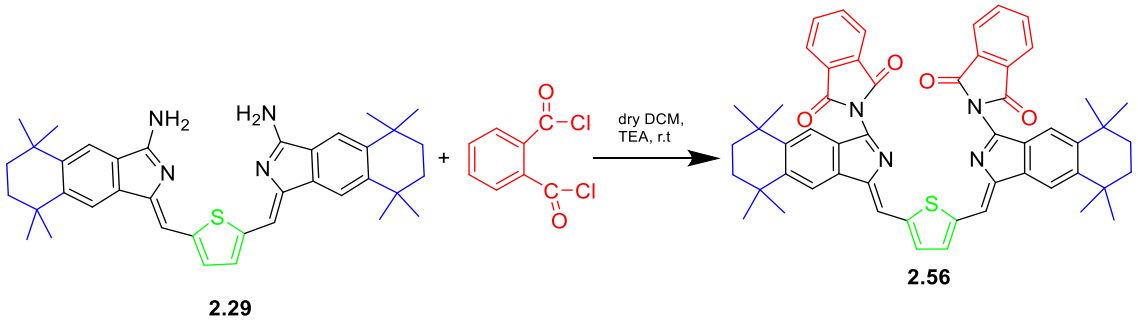

Scheme 2.30: Synthesis of the compounds **2.56**.

2.7.2 Attempt with amine group:

In this part, we shifted our focus to the amine group, initiating with a monoamine compound to investigate the reactivity with our "open" intermediates. Compound **2.2** and *p*-anisidine were refluxed in *p*-xylene for 3 days under an argon environment. The reaction appeared promising, with two new spots visible by TLC analysis. After the reaction period, the crude residue was separated by column chromatography. MALDI-TOF-MS analysis was performed for isolated products, which indicated the formation of **2.57**, and **2.58**. The reaction is summarised by scheme 2.31.

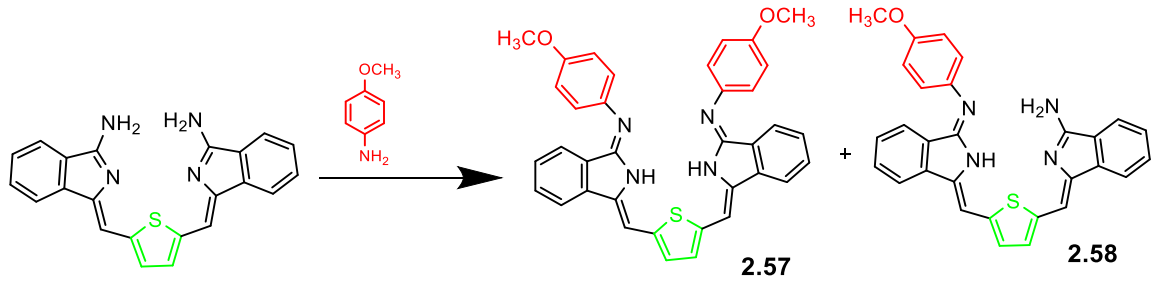

Scheme 2.31: Synthesis of the compounds **2.57, 2.58**.

While isolated product **2.57** was identified by MALDI-TOF-MS, as seen in figure 2.50, the ^{1}H NMR spectrum was complicated, so it could not be fully characterised, possible due to mixtures on isomers. On the other hand, compound **2.58** showed clear ^{1}H NMR spectra, which displayed the reduction in symmetry in the aromatic region, as we expect, with two doublet peaks of two protons each at 7.06 and 8.38 ppm, which may relate to the benzene ring of the anisidine

fragment. In addition, the methoxy group protons appeared at 3.83 ppm, as shown in the figure 2.51.

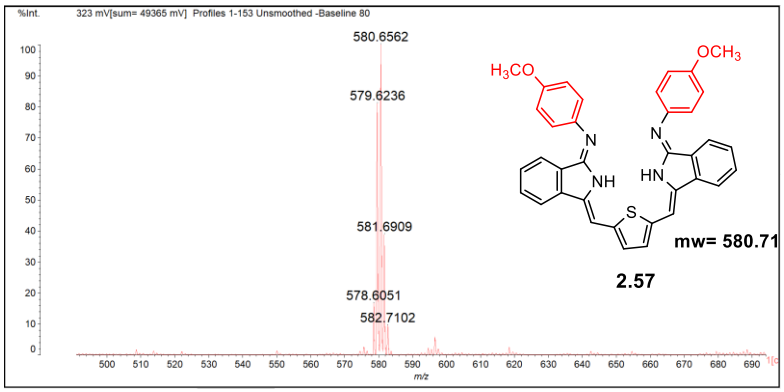

Figure 2.50: MALDI-TOF-MS of compound **2.57**.

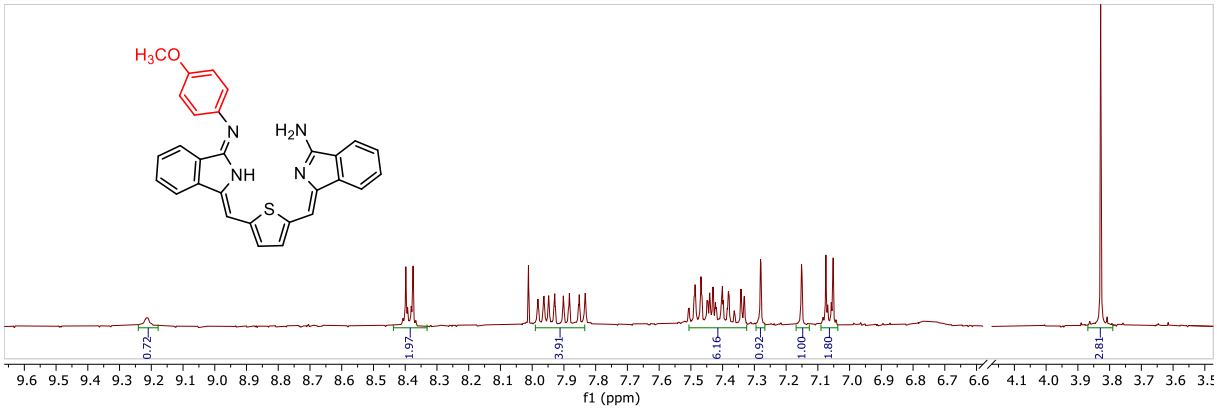

Figure 2.51: ^{1}H NMR spectrum of compound **2.58**.

Our focus therefore moved to introducing benzene to our macrocycles by using diaminobenzene instead of phthalonitrile, following a successful reaction with *p*-anisidine. Benziporphyrins have attracted significant attention due to their structural and spectroscopic properties, and potential to stabilise organometallic derivatives. For example, benzene-containing phthalocyanines were synthesised by reacting diiminoisoindoline with 1,3-diaminobenzene and the metallation of these systems was also investigated, yielding some derivatives resembling benziporphyrin.[120] So, we started our investigation with 1,3-diaminobenzene, and a solution of **2.2** in dry xylene was refluxed for 20 min, and then 1,3-diaminobenzene was added. A new purple colour appeared in TLC, while compound **2.2** was not all consumed. This product was analysed by MALDI-TOF-MS. The obtained result showed a peak at m/z = 550. This peak may be due to the formation of a double addition of 1,3-diaminobenzene **2.60**. However, there was no obvious result indicating the formation of the

target compound **2.59**, which is expected to be m/z = 442, even after increasing time and temperature. While compound **2.60** was possibly identified by MALDI-TOF-MS, not enough could be isolated successfully to facilitate recrystallisation and thus reliable NMR and UV-vis spectroscopic characterisation.

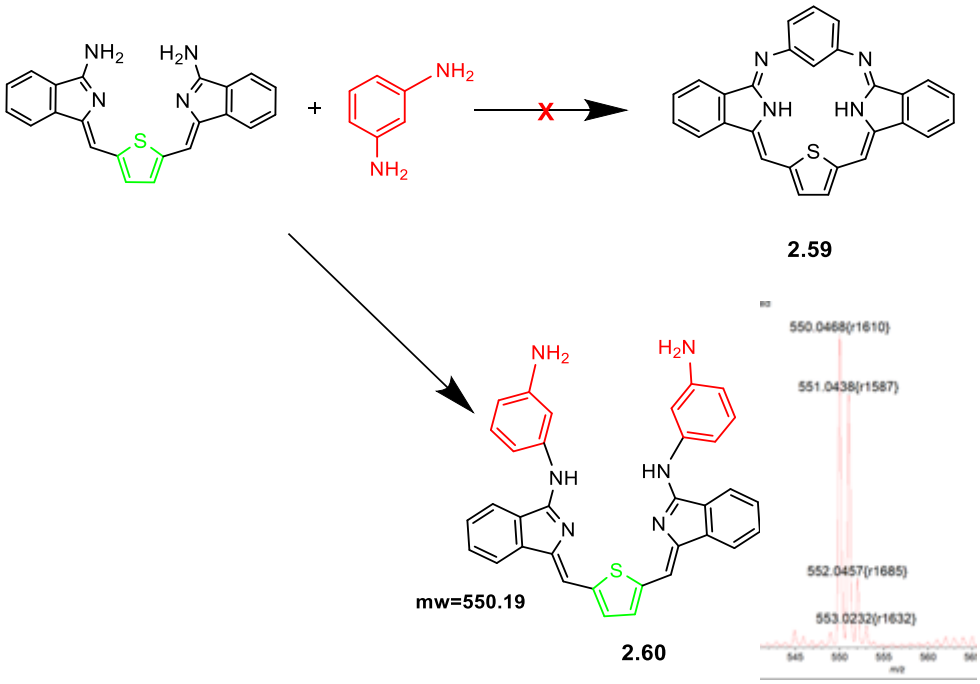

Scheme 2.32: Attempted synthesis of compound **2.59;** inset, MALDI-TOF-MS indicating possible formation of compound **2.60**.

We also attempted synthesis with 1,2-diaminobenzene, and the same conditions were followed. The solution colour changed from red to brown. It was found that the colour change may indicate the polymerisation of the amine, and the desired product was not formed in this reaction according to analysis by MALDI-TOF MS.

2.7.3 Attempts with dicarbonyls.

Carbaporphyrins are porphyrin analogues in which a cyclopentadiene ring has replaced the one of the pyrrolic subunits, and these systems show highly aromatic characteristics and unique properties (acting as trianionic ligands and forming stable silver(III) and gold(III) organometallic derivatives).[76,87]So, in this part, we decided to attempt to produce heterocarbaporphyrins using 1,3-indandione.

A solution of **2.2** and 1,3-indandione in dry toluene in the presence of molecular sieves and a catalytic amount of *p*-toluene sulfonic acid was placed in the microwave reactor at 100°C and monitored by TLC each hour. After 8h, we noticed no indandione starting material was left.

The complicated crude mixture was checked by MALDI-TOF-MS and there was no evidence for the formation of a macrocyclic product **2.61**.

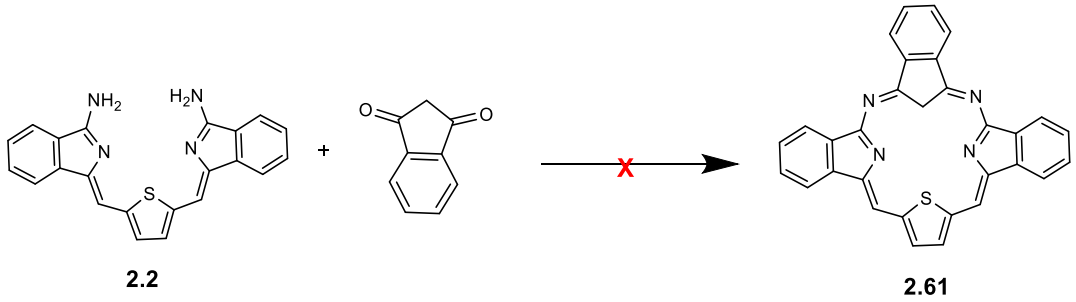

2.2 **2.61**

Scheme 2.33: Attempted synthesis of the compounds **2.61**.

2.8 Attempt to extend the macrocycle:

Expanded porphyrinoids have become more popular in the last few years due to their relatively larger ring size and extended π -electron conjugation pathways compared to naturally occurring tetrapyrrolic macrocycles, such as porphyrins. Expanded porphyrinoids show remarkable coordination chemistry, physicochemical characteristics, and a variety of applications in fundamental and applied research areas.[121,122]

Sapphyrins, the first examples of expanded porphyrin systems, have the replacement of a pyrrole subunit by a bispyrrole in porphyrin. Sapphyrins have received considerable attention due to aromaticity in large conjugated systems and its ability to bind anions.[97]

At this point, it was decided to expand our macrocycle using bithiophene following the same pathway that we used to produce tribenzodiazathiaporphyrins (Scheme 2.34).

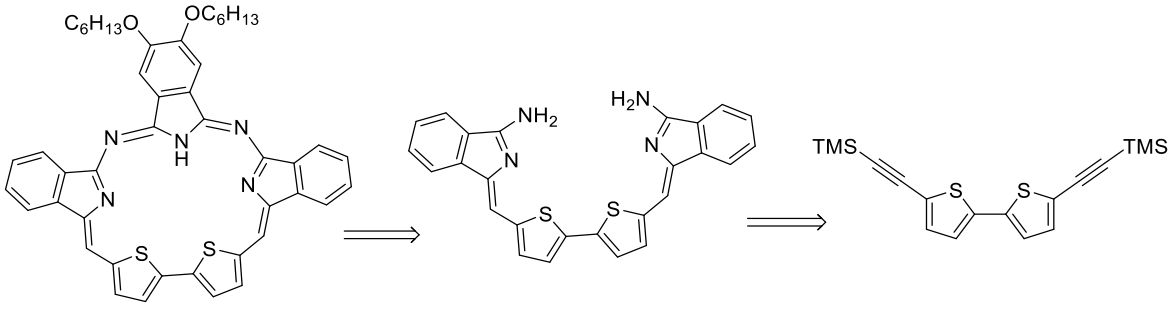

Scheme 2.34: Retrosynthetic route of our expanded macrocycle.

It was necessary to do an investigation into the synthesis of bisaminoisoindoline bithiophene **2.63** prior to attempting macrocyclization.

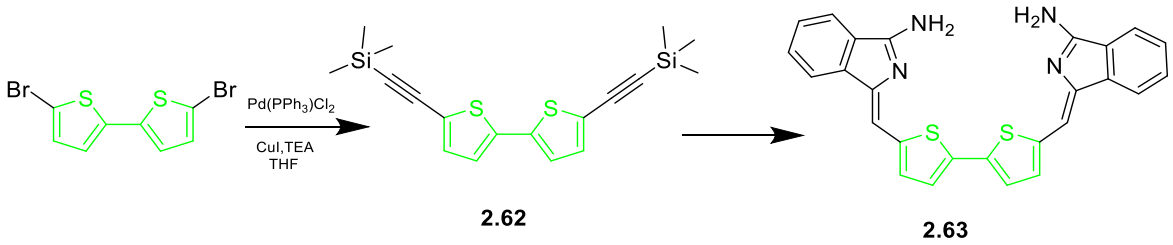

Scheme 2.35: Synthesis of the compound **2.63**.

The synthetic route to diaminoisoindoline bithiophene **2.63** is shown in scheme 2.35. It starts with the preparation of bis(trimethylsilylethynyl) bithiophene **2.62** from 5,5`-dibromo-2,2`-bithiophene under the Sonogashira reaction conditions. The intermediate **2.62** underwent a coupling reaction with 2-bromobenzamidine hydrochloride **2.1**, synthesised previously, by following the method mentioned previously to prepare **2.2** in the presence of a palladium catalyst. The ^{1}H NMR spectrum of the isolated product **2.63** was concordant with the structure proposed (Figure 2.52).

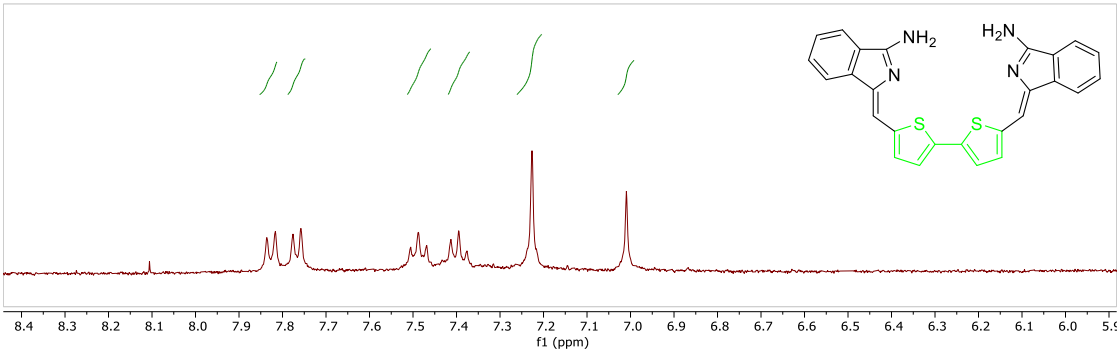

Figure 2.52: ^{1}H NMR spectrum of product **2.63**.

In light of previous evidence indicating that the presence of a tosyl group enhances solubility, we chose to tosylate compound **2.63**. This decision aimed to simplify the characterization process to confirm the compound structure and investigation of its reactivity. The compound **2.63** was treated with *p*-TsCl in dry DCM and TEA to produce ditosylate compound **2.64** in good yield. The product was fully characterised by UV-Vis, NMR spectroscopies and MALDI-TOF-MS.

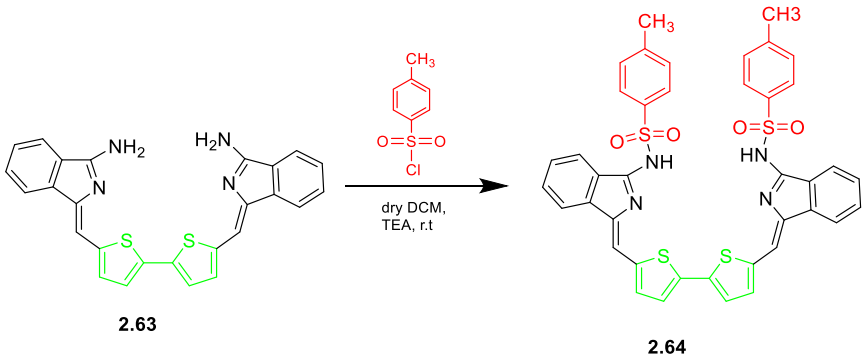

Scheme 2.36: Synthesis of the compound **2.64**.

After preparing intermediate **2.63** and confirming its structure, we moved on to the investigation of macrocyclization.

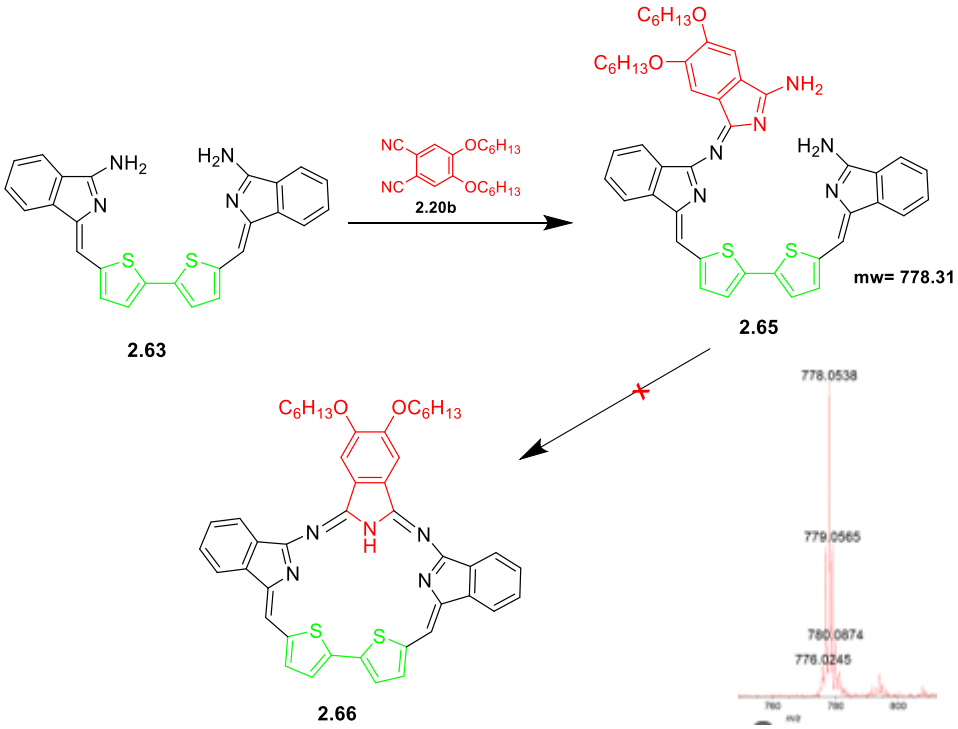

Scheme 2.37: Attempt to synthesise the compound **2.66**; inset, MALDI-TOF-MS of compound **2.65**.

Refluxing of the intermediate **2.63** with Pn **2.20b** in MeOH with $NaOCH_3$ yielded the product **2.65** as a purple solid**,** with side product formation (Pc). Analysis by MALDI-TOF-MS confirmed the formation of an open intermediate **2.65**, with a peak at 778 m/z. The next step utilised a higher boiling point solvent, *p*-xylene, at reflux as a higher temperature was expected to be required to achieve macrocyclization of the open intermediate **2.65** with the elimination

of ammonia. Unfortunately, despite several attempts under various conditions, no macrocyclic product **2.66** was observed on the TLC or by MALDI-TOF-MS.

The synthesis of substituted intermediate **2.67** was also achieved by the same method that we used to synthesise unsubstituted intermediate **2.63**. The reaction was easy to perform and fast; the reagents were heated up to 120 ºC under microwave irradiation for 1 h as illustrated in scheme 2.38. The MALDI-TOF-MS analysis confirmed the formation of the substituted intermediate **2.67**, promoting the investigation of the subsequent reactions.

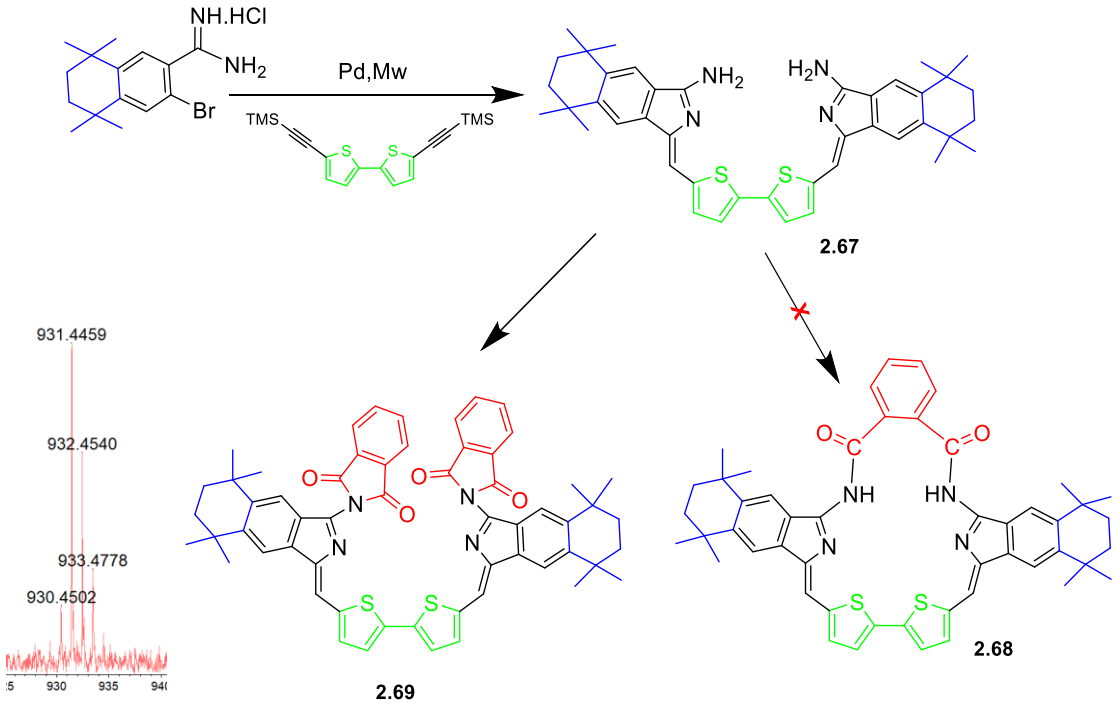

Scheme 2.38: Attempt to synthesise compound **2.68**.

Following the unsuccessful macrocyclization to yield product **2.66** with phthalonitrile, phthaloyl chloride was chosen with substituted intermediate **2.67** to investigate the potential to afford the macrocyclization product **2.68**. A solution of phthaloyl chloride in dry DCM was added to a solution of bisaminoisoindoline **2.67** in dry DCM and stirred at room temperature in the presence of TEA. Upon completion, the MALDI-TOF-MS spectrum was again concordant with the structure of bisphthalimide compound **2.69**, with a peak visible at 931m/z instead of the desired macrocycle **2.68**. The same result was obtained when intermediate **2.2** with one thiophene ring was reacted with phthaloyl chloride as described previously. The isolated product of **2.69** was also analysed by ^{1}H NMR spectroscopy, which revealed a symmetric structure (Figure 2.52). The methylene protons appeared together at 1.79 ppm, with

an integration of 8 protons, while methyl protons showed as expected as two singlets with an integration of 12 protons each between 1.45-1.30 ppm.

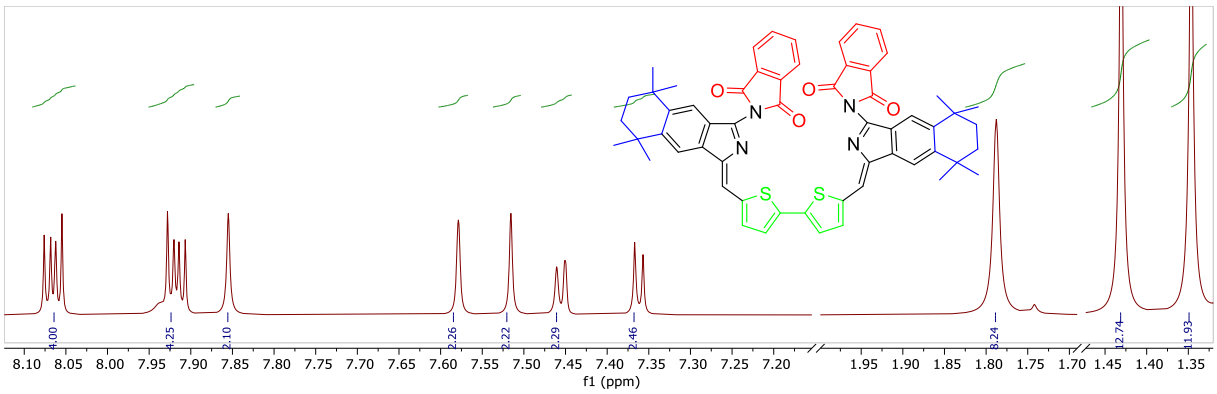

Figure 2.52: ^{1}H NMR spectrum of **2.69**.

The UV-vis spectra of compounds **2.56** and **2.69** are shown in figure 2.53. The spectra indicate a small but expected red shift for compound **2.69,** which presents two thiophene rings in its structure, compared to **2.56,** which contains only one thiophene ring. The fluorescence spectrum is also red shifted for the compound with two thiophene rings compared to the compound with a single thiophene ring.

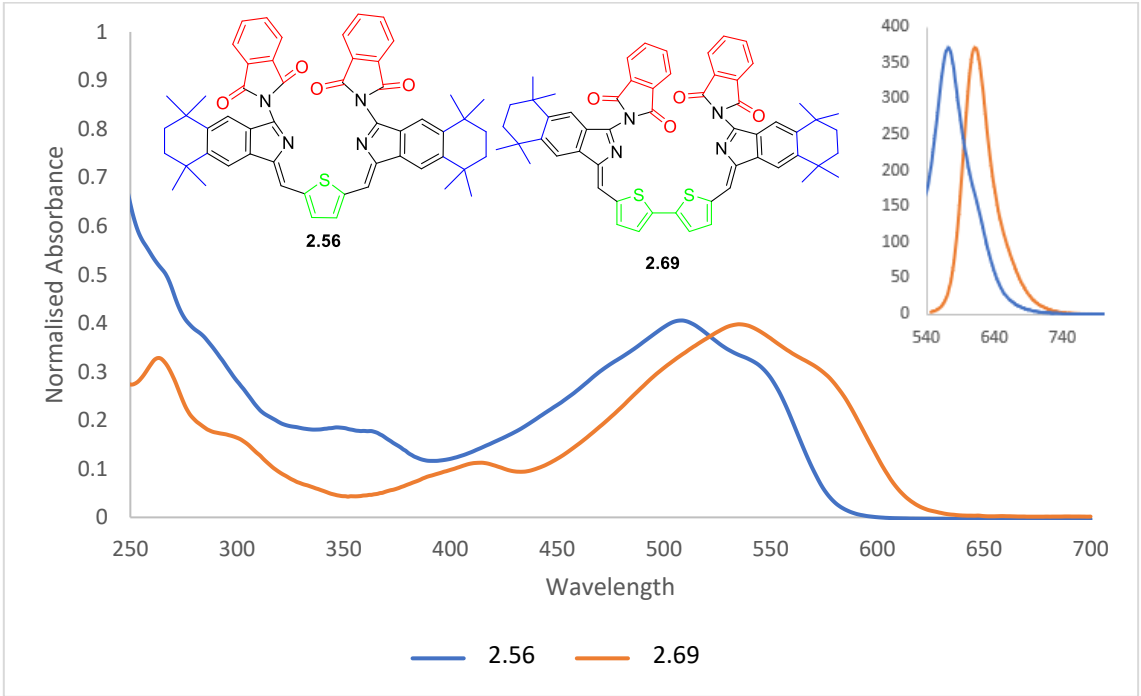

Figure 2.53: UV-vis and fluorescence spectra of **2.56** and **2.69** with their structures.

2.9 Attempted synthesis of core modified TBMAP using intermediate 2.2.

In our group's work,[20] the formation of TBTAP can be hypothesised through a reaction between phthalonitrile and aminoisoindoline, as shown in scheme 2.39, to form 4- membered open chain oligomer which can cyclises with loss of an ammonia.

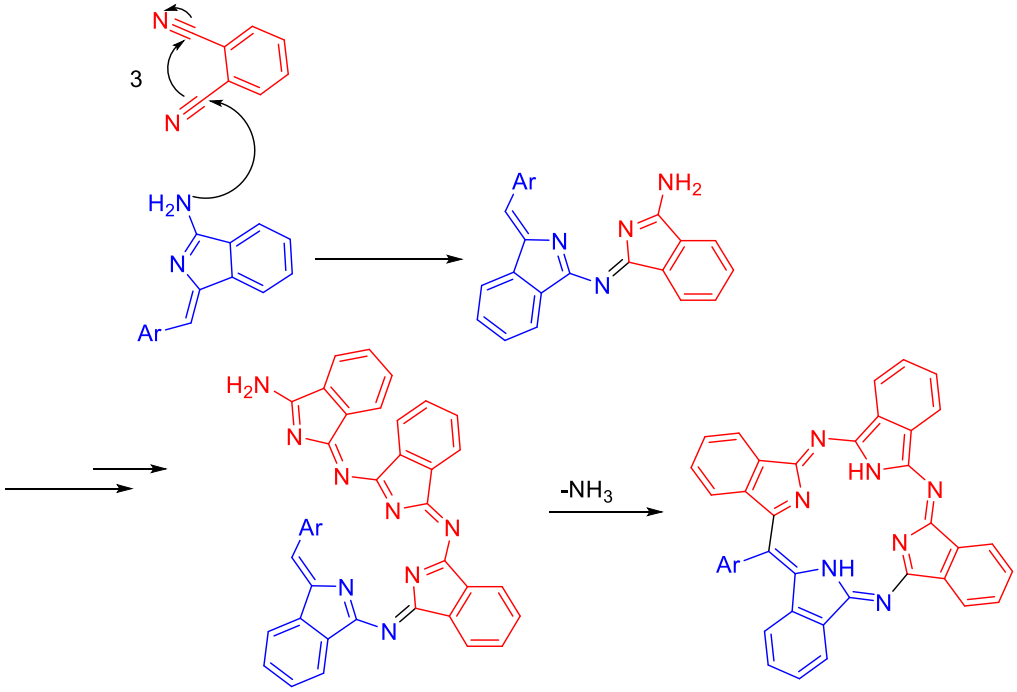

Scheme 2.39: Hypothesised TBTAP macrocyclization pathway.

Assuming that the proposed mechanism of TBTAP macrocyclization with phthalonitrile is correct, we reasoned that an intermediate like **2.2** may react with aminoisoindoline to produce a similar intermediate that could cyclise to give tribenzomonoazathiaporphyrins **2.70** (Scheme 2.40).

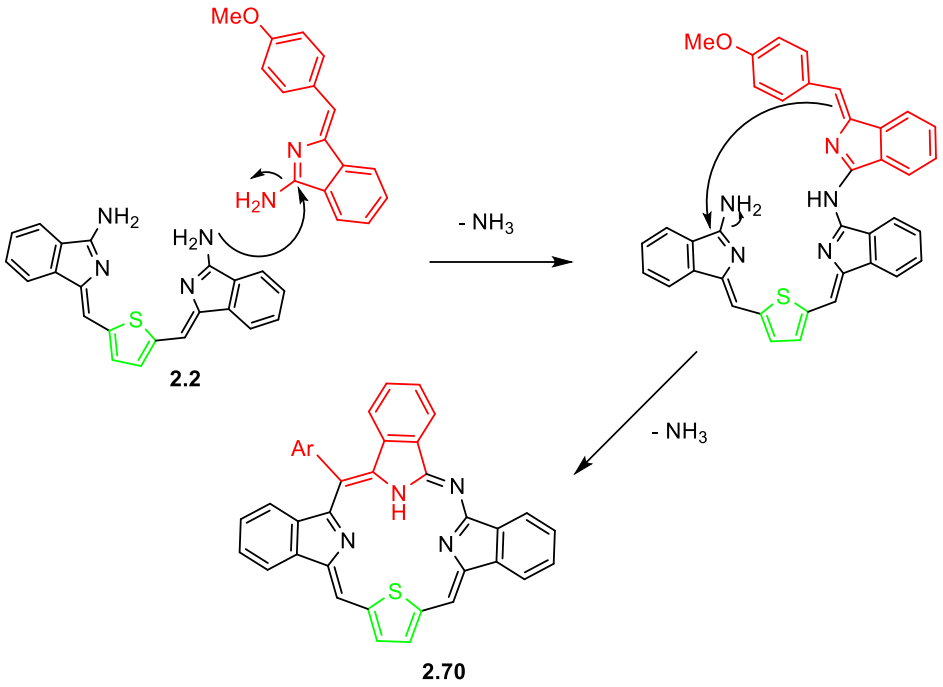

Scheme 2.40: Proposed mechanism for tribenzomonoazathiaporphyrins **2.70** formation.

Scheme 2.41 shows a pathway for the first attempted tribenzomonoazathiaporphyrins **2.70** synthesis, utilizing aminoisoindoline and intermediate **2.2**, then refluxing in *p*-xylene. The reaction was monitored by TLC which indicated the presence of a significant quantity of a red spot, which may be related to the expected dimer **2.73**. As well as a green material that was likely to be the product **2.71**, a trace amount of the purple material which is related to compound **2.23b** and brown material **2.72** in addition to an unknown dark brown material which stays on the baseline of TLC. These fractions were separated using column chromatography, and MALDI-TOF-MS was used to characterise the materials. In this experiment, the major product formed was dimer **2.73**, yielding 42% of the total product. A trace amount of purple material was detected using MALDI-TOF-MS and TLC analysis. To confirm its identity as **2.23b**, comparison TLC and MALDI-TOF-MS were performed, including of mixed samples with authentic. Formation of **2.23b**, as previously described, suggested the elimination of an aromatic fragment of **2.72** upon macrocyclization.

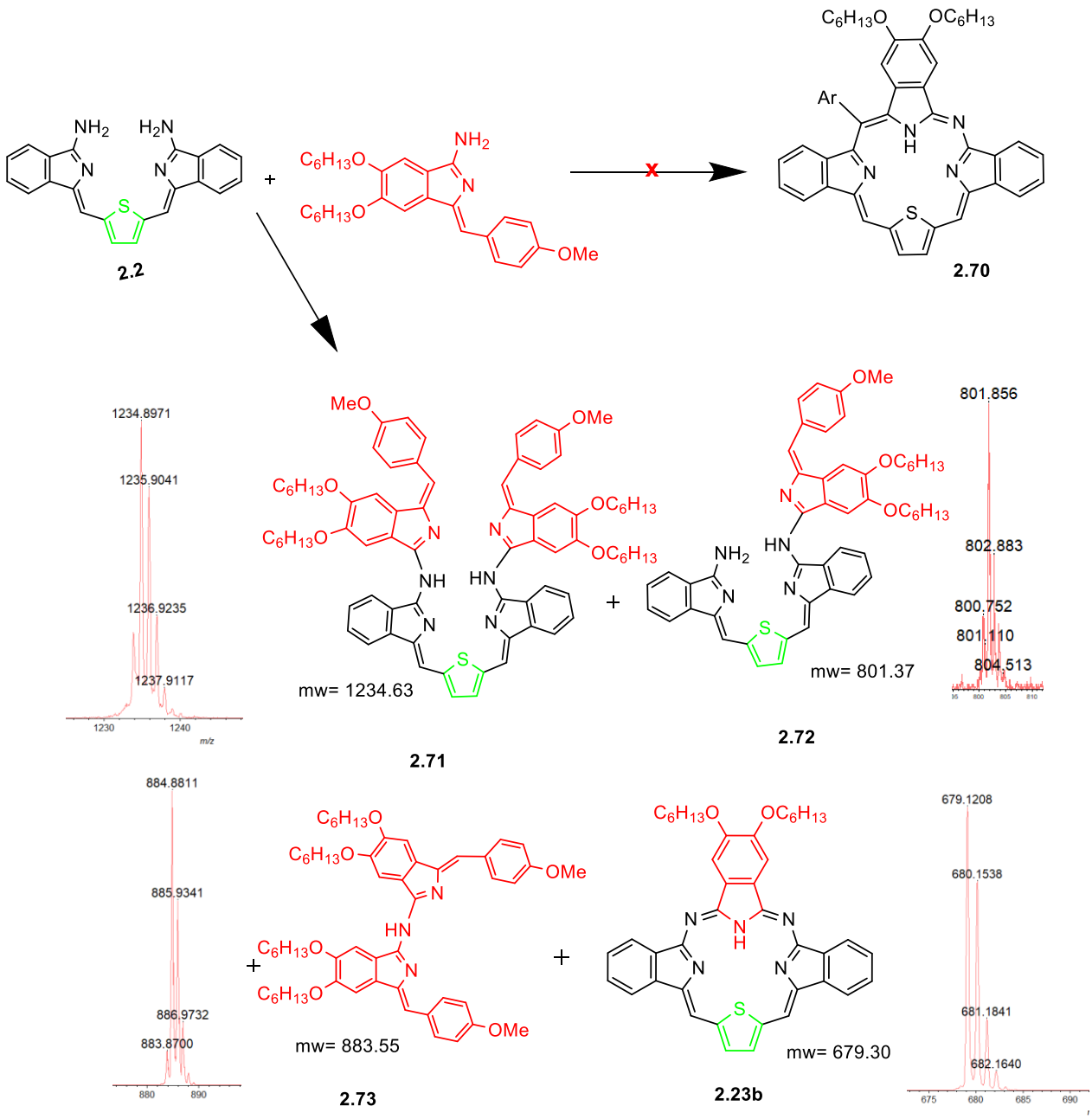

Scheme 2.41: Attempted synthesis of the compound **2.70**, including MALDI-TOF MS of **2.23b** isolated from this reaction.

The interesting compound **2.71** was identified and isolated from the reaction mixture, and its structure was characterised by ^{1}H NMR spectroscopy. It revealed a structure with higher symmetry that is concordant with the structure shown in figure 2.54. Two doublets at 6.55 and 5.42 ppm correspond to protons on the phenyl ring attached methoxy groups, as confirmed by COSY experiments. The UV-vis spectrum of **2.71** is shown also in figure 2.55 and exhibited broad absorbance. The compound gave suitable single crystals for X-ray diffraction analysis,

which confirmed its molecular structure. The crystals were grown by slow diffusion of hexane into a dichloromethane solution of the compound (Figure 2.56). The X-ray crystal structure was solved by our collaborator, Dr David Hughes, and detailed information on the structure is provided in the appendix. Evidence of π…π stacking was observed, where the phenyl groups incorporating C(27) and C(57) overlap with the isoindole groups incorporating N(37) and N(7) respectively, but the pairs of rings are rather distorted from parallel.

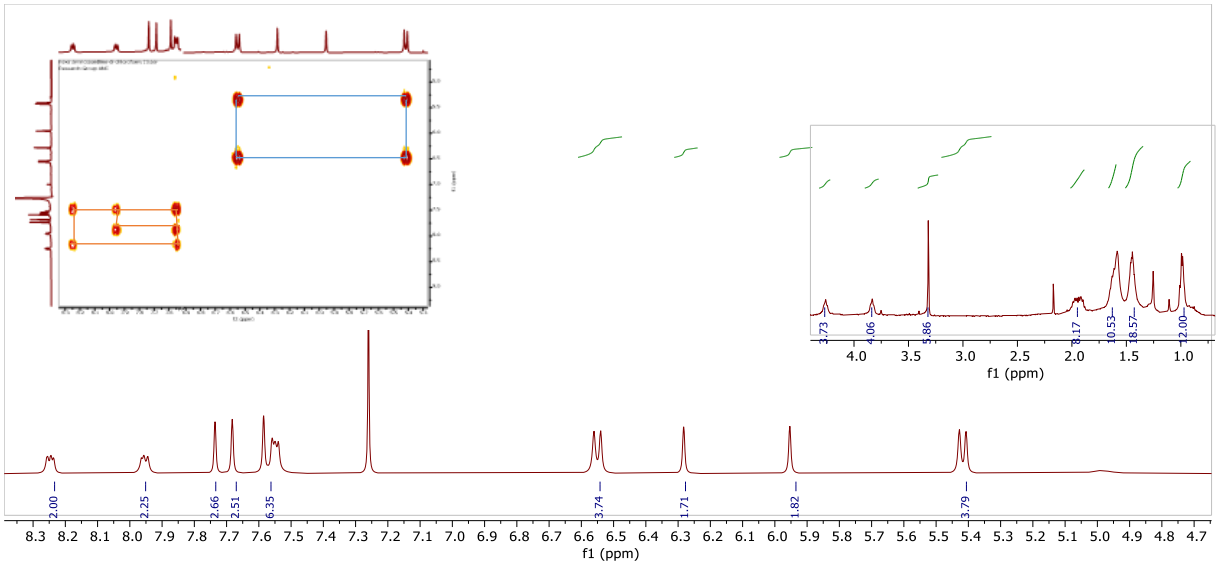

Figure 2.54: ^{1}H NMR spectrum of **2.71**.

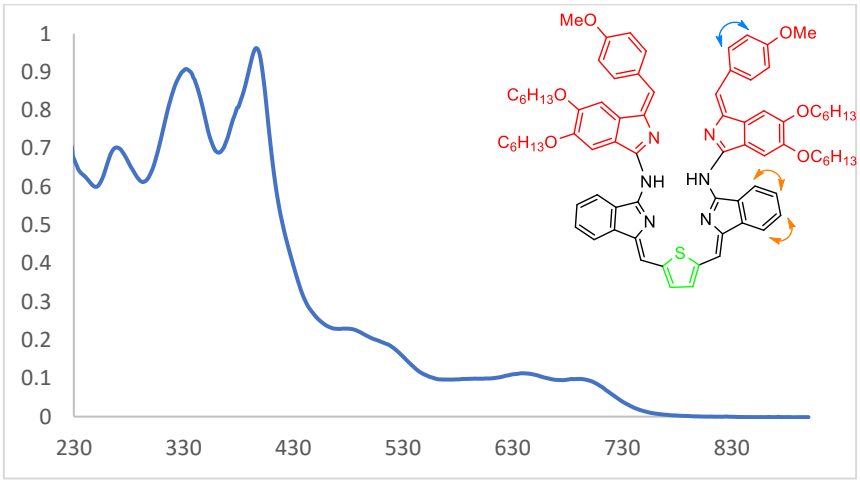

Figure 2.55: UV-visible spectrum of product **2.71** in DCM.

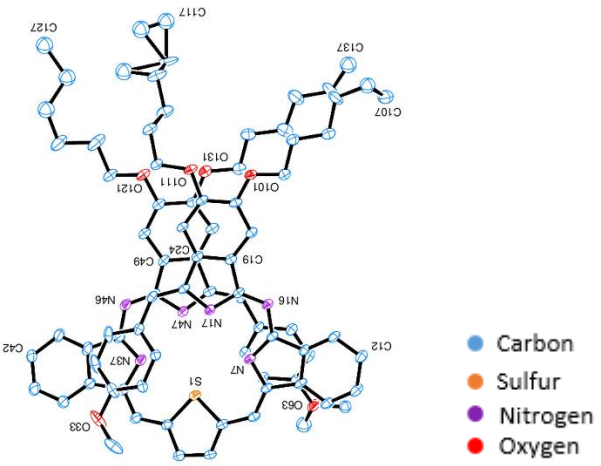

Figure 2.56: X-ray structure of compound **2.71**.

2.10 Attempt to synthesise macrocycle with pyridine:

After achieving success in preparing core-modified phthalocyanine derivative, TBDAP, with thiophene moiety, our focus shifted towards substituting thiophene with pyridine, another type of heterocyclic ring. This change aims to investigate how replacing thiophene with pyridine affects the characteristics and potential applications, particularly because pyridine provides a good ligand for metal binding in the cavity of the macrocycle.

Synthesis of the macrocycle began with the formation of the required intermediate **2.75**. We started with the preparation of **2.74** through the Sonogashira coupling methodology with an overall yield of over 92%. Then, the synthesis of the intermediate **2.75** was readily achieved from benzamidine and acetylene **2.74** under copper-free Sonogashira cross-coupling condition followed by a 5-*exo*-dig cycloisomerization domino reaction.

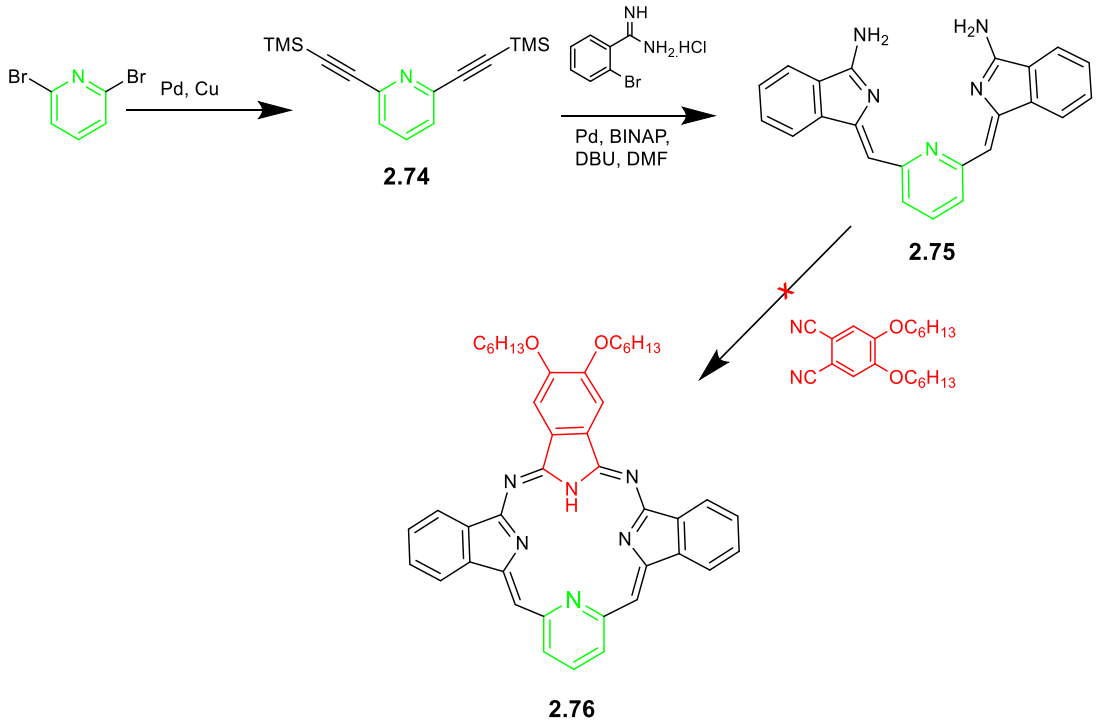

Scheme 2.42: Synthesis of the intermediate **2.75** and **2.76**.

The identity of product **2.75** was confirmed by ^{1}H NMR spectroscopy and MALDI-TOF-MS, as ^{1}H NMR showed a symmetrical structure, with singlet at 6.53 ppm, which may correspond to alkene protons.

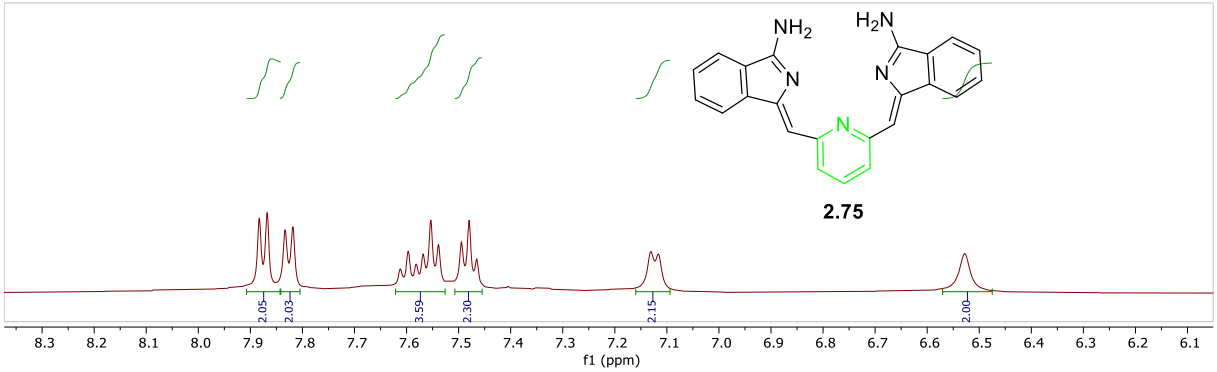

Figure 2.57: ^{1}H NMR spectrum of **2.75**.

After the intermediate **2.75** was prepared successfully, it was then used in an attempt to prepare **2.76**. Unfortunately, despite several attempts under various conditions, such as changing the solvent and temperature, and adding zinc acetate, no macrocyclic product **2.76** was observed on TLC or by MALDI-TOF-MS. The lack of reactivity is presumably due to the electron withdrawing character of the pyridine.

2.11 Synthesis of porphyrinic macrocycles incorporating triphenylene:

Following the successful diacetylene approach using thiophene, the focus of the research was moved on to attempt to prepare different macrocycles using the same strategy. Triphenylene was chosen due to its extended π-conjugation, and ease of synthesis. Regarding its properties, it has been extensively researched in the literature for more than a century. Its aromatic structure and multiple functionalization sites make it versatile, with a wide range of potential applications. [123–125]

Our plan involved using key intermediate **2.81**, which is similar to the previously prepared intermediate with a thiophene structure. However, the intermediate **2.81** has a larger gap between the isoindoline units. It was thought that the macrocycles could be completed either by incorporating one Pn unit (**2.83**) or by losing ammonia (**2.84**).

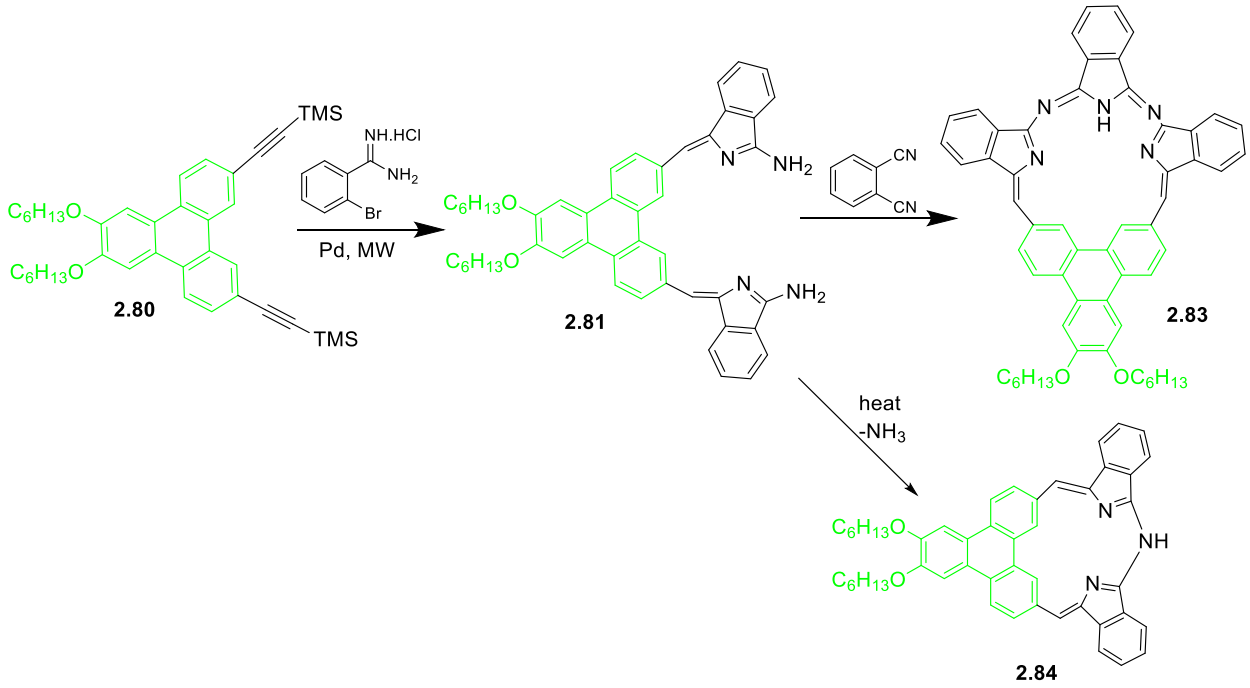

Scheme 2.43: Plan to synthesis compounds **2.83**, **2.84**.

To synthesise triphenylene bisaminoisoindoline, the necessary starting material, trimethylsilylethynyl triphenylene **2.80** was prepared. It was prepared in four steps starting from 1,2-dibromo-4,5-bishexyloxybenzene as illustrated in scheme 2.44.

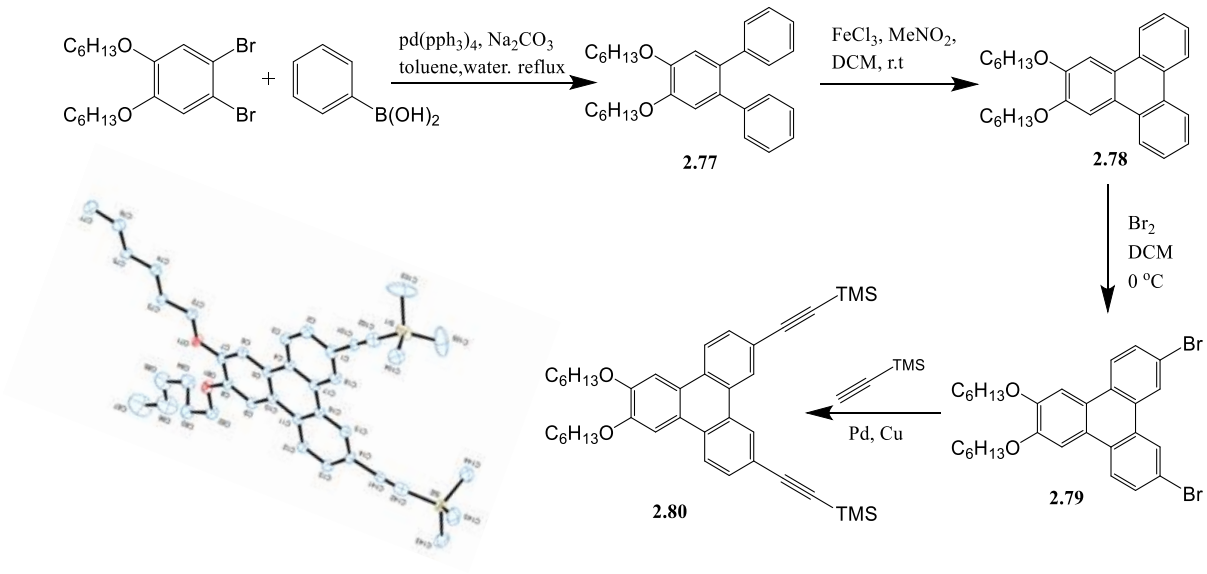

Scheme 2.44: Synthesis of the trimethylsilylethynyl triphenylenylene **2.80**; inset, X-ray crystal structure of compound **2.80.**

1,2-Dibromo-4,5-bishexyloxybenzene underwent a Suzuki coupling reaction with phenyl boronic acid in the presence of $Pd(PPh_3)_4$ and Na_2CO_3 to give **2.77** in 96% yield.[126] The next step consisted of a cyclodehydrogenation of **2.77** by treatment with ferric chloride in the presence of nitromethane to give 2,3-dihexyloxytriphenylene **2.78**.[126] Then, bromination of **2.78** by bromine afforded dibromo-6,7-bis(hexyloxy)triphenylene in 95% yield.[127] Compound **2.80** was prepared by a palladium catalysed cross-coupling reaction. A solution of 2,11-dibromo-6,7-bis(hexyloxy)triphenylene and (trimethylsilyl)acetylene was refluxed in the presence of bis[triphenylphosphine]palladium dichloride and copper(I) iodide in triethylamine and THF overnight. The following day, we noticed the starting material was not completely consumed, so [triphenylphosphine]palladium dichloride and (trimethylsilyl)acetylene were added again, and the reaction continued until all of the starting material was consumed. The product obtained a reasonably good yield (70 %) as a yellow solid**.**

Subsequently, we moved on to synthesising the triphenylene-bisaminoisoindoline **2.81**, using the conditions previously employed for bisaminoisoindoline synthesis from thiophene diacetylenes. This reaction was notably influenced by the concentration, highlighting its crucial role in achieving the desired outcome. In the first attempt for compound **2.81** the synthesis was conducted in a diluted solvent 6 mL for an hour (**2.80**= 130 mg, **2.1**= 100 mg). The reaction yielded a tiny amount of product, and a significant quantity of starting materials remained even after extending the reaction time to 4 h. Subsequently, the experiment was replicated at the

same scale with a decrease of solvent to 2 mL, resulting in the complete reaction within an hour. The compound formed good quality single crystals suitable for X-ray analysis. The crystal structure showed two very similar and mostly planar molecules, except for slight differences in the $SiMe_3$ and O-hexyl groups. Full details of the X- ray structure data, carried out by our colleague Dr. David Hughes, are provided in the appendix.

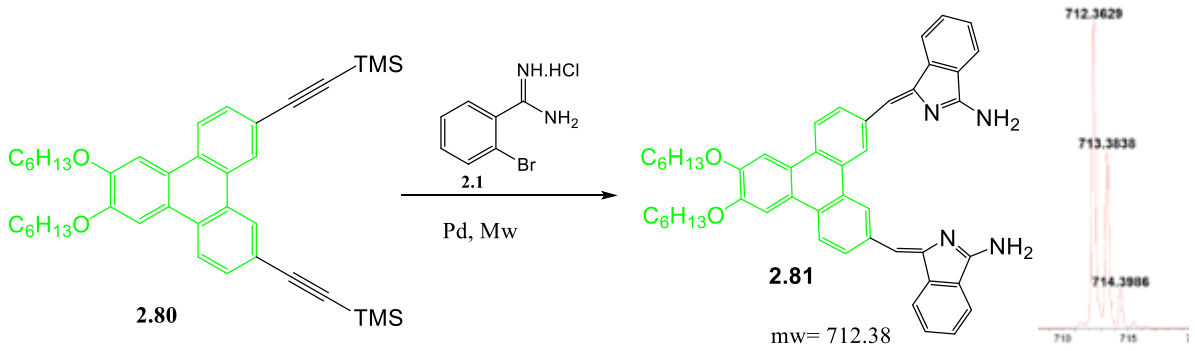

Scheme 2.45: Synthesis of the intermediate **2.81** and its MALDI-TOF-MS.

MALDI-TOF-MS analysis of the reaction mixture revealed the formation of the target triphenylene-bisaminoisoindoline product **2.81**. However, its isolation and characterisation proved to be challenging, so our investigations moved to tosylate this compound, aiming to enhance the isolation process and confirm the structure. Previous evidence indicates that the presence of a tosyl group enhances isolation and solubility. The compound **2.81** and *p*-toluenesulfonyl chloride were stirred in dry THF in the presence of TEA at room temperature overnight. The solvent was removed under vacuum and then the resulting solid was purified by column chromatography and recrystallised from DCM and hexane to get the di-tosylated product as an orange solid.

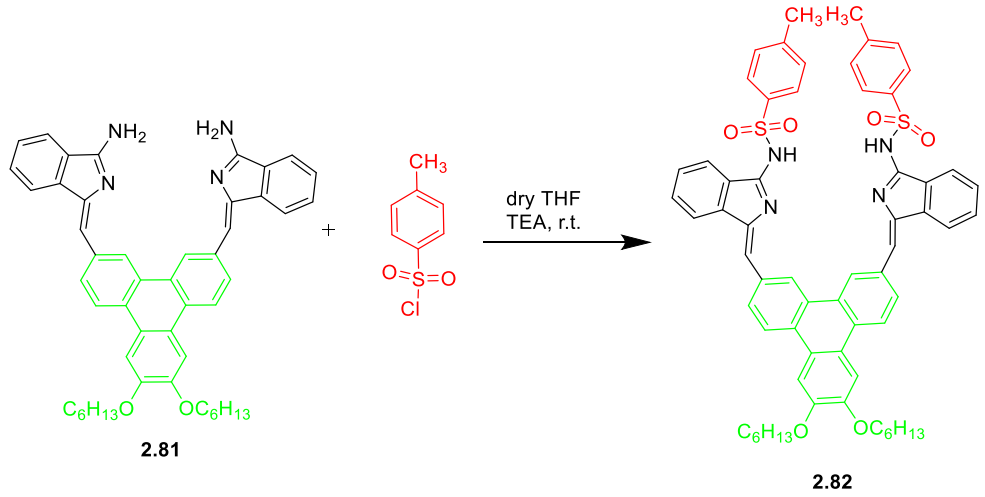

Scheme 2.46: Synthesis of the tosylate compound **2.82**.

The product identity was confirmed using ^{1}H NMR spectroscopy, which revealed a highly symmetric structure that confirmed that the Ts group is indeed coupled on both amine groups of the bisaminoisoindoline triphenylene, as illustrated in figure 2.58. The Ts group protons appeared as doublets at 7.25 and 7.98 ppm with the integration of 4 each. The protons in the triphenylene fragment (a, b) appeared at 7.66 and 8.37 ppm. COSY NMR analysis supports this assignment by showing the cross peaks for these protons. Methyl group protons appeared as a singlet at 2.35 ppm.

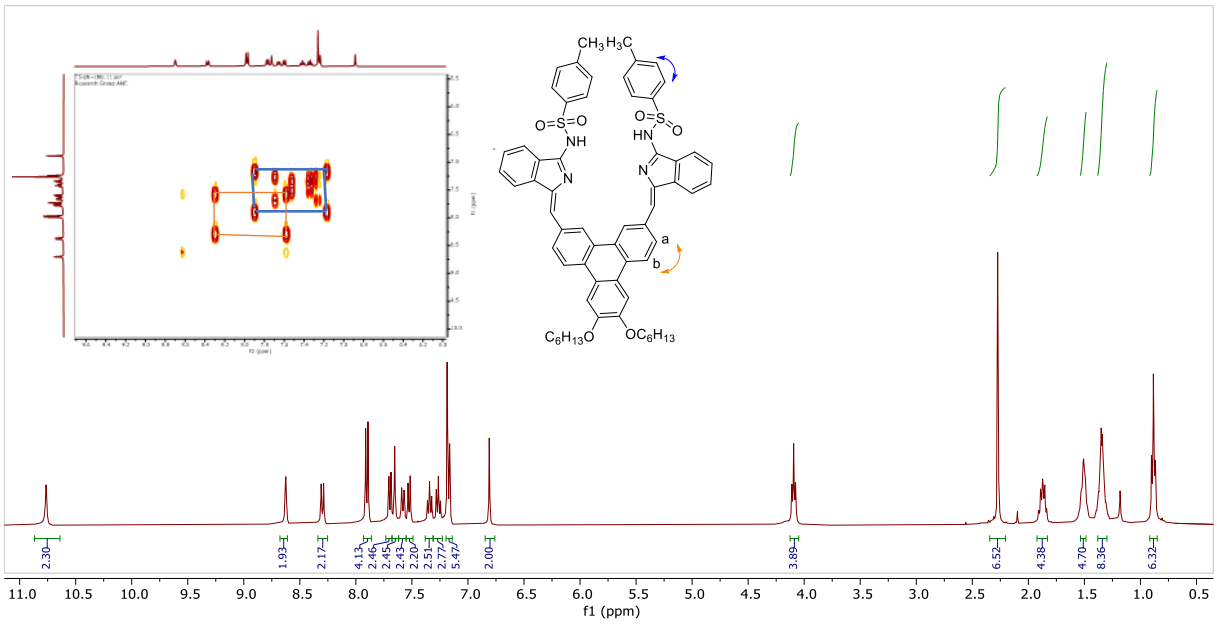

Figure 2.58: ^{1}H NMR and H-H COSY spectra of **2.82**.

After the intermediate was successfully synthesized and its structure was confirmed, our attempts to produce the first potential macrocycle could proceed.

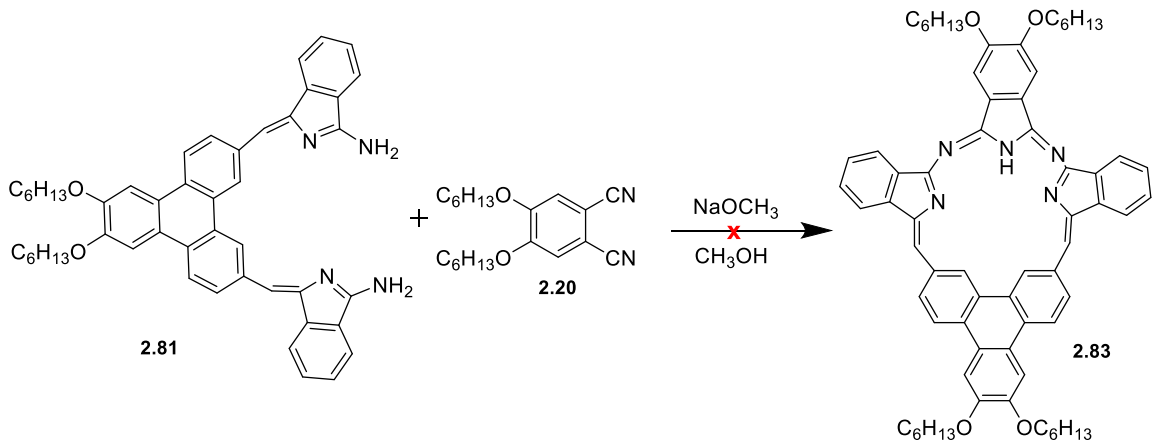

Scheme 2.47: The attempted synthesis of compound **2.83**.

Pn **2.20** and compound **2.81** were refluxed in methanol with sodium methoxide ($NaOCH_3$) for 4 days. After this period, some yellow material remained at the baseline of the TLC, which was presumed to be the starting material **2.81**, along with a blue spot corresponding to Pc and an additional unidentified spot. MALDI-TOF-MS analysis showed no peak for the macrocycle **2.83**. We also tried different reaction conditions, such as refluxing the starting material in *p*-xylene. However, the same result was obtained: no desired product **2.83**.

Due to this failure in our attempt to produce the macrocycle **2.83** by adding Pn unit, our focus shifted to exploring other potential macrocyclic structures **2.84**. The reaction was performed by refluxing the intermediate **2.81** in 3 mL of *p*-xylene overnight.

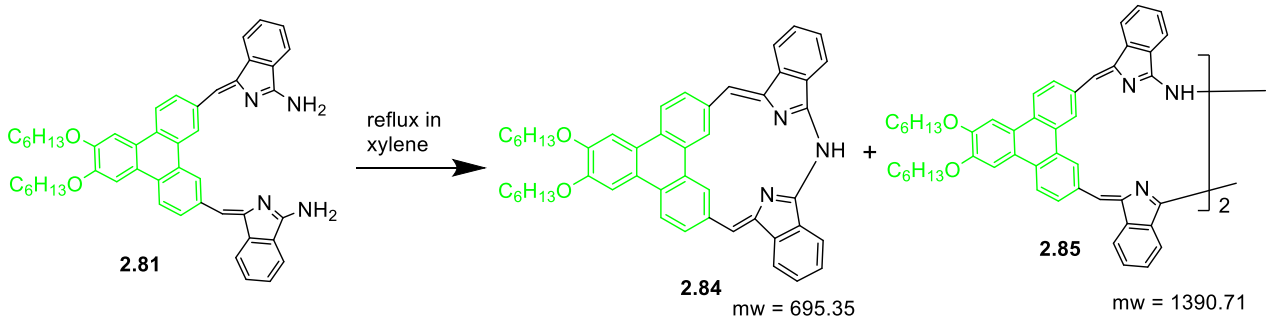

Scheme 2.48: Synthesis of compound **2.84**.

The desired compound **2.84** was obtained in tiny quantities (MALDI-MS evidence only), and a different major product, a brown product, was observed on TLC. The MALDI-TOF-MS analysis for this product displayed a peak m/z 1390, indicating dimerization of the compound **2.81**. We also noticed this spot in TLC in the earlier reaction (Scheme 2.47) in the attempted synthesis **2.83**. We rechecked the MALDI data from this reaction again and found the same mass peak related to dimer **2.85**.

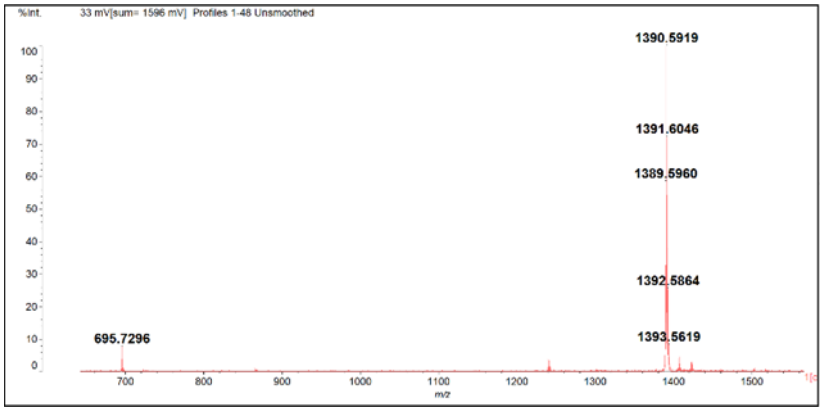

Figure 2.59: MALDI-TOF MS analysis of the reaction mixture showing peaks related to **2.84** and **2.85**.

The dimer was easily isolated by column chromatography, and ^{1}H NMR spectroscopy also confirmed its identity. The integration of the peaks matches with the expected number of protons with a peak at 10.09 ppm. A few drops of deuterium oxide (D_2O) were added to the sample in an NMR tube to determine if the peak at 10.09 ppm corresponds to protons attached to carbon within the compounds. After adding D_2O, we noticed that the peak at 14.38 ppm disappeared, while the peak at 10.09 ppm remained. So, the peak at 14.38 ppm was from an exchangeable proton, likely from the amino group, whereas the peak at 10.09 ppm corresponds to a C-H in the compound's structure.

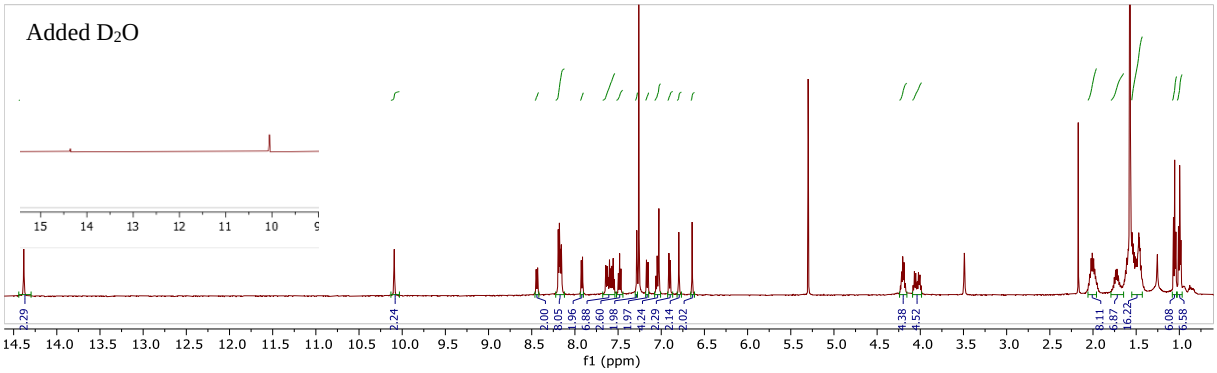

Figure 2.60: ^{1}H NMR spectrum of **2.85**.

The ^{1}H NMR spectrum of the dimer **2.85**, however, showed lower symmetry than expected for structure (A) depicted in figure 2.61. The highly symmetrical conformation A is unlikely to be realistic due to bond angle strain and steric hindrance. So, it is unsurprising that we get a break in symmetry that is seen in NMR spectroscopy. Initial analysis suggests that the arrangement or orientation in strain-free conformation (B) with the isoindoles positioned in opposite

directions would be preferred. This is the arrangement reduces angle strain, and is similar to the arrangement we have observed before in related dipyrromethene structures.[125]

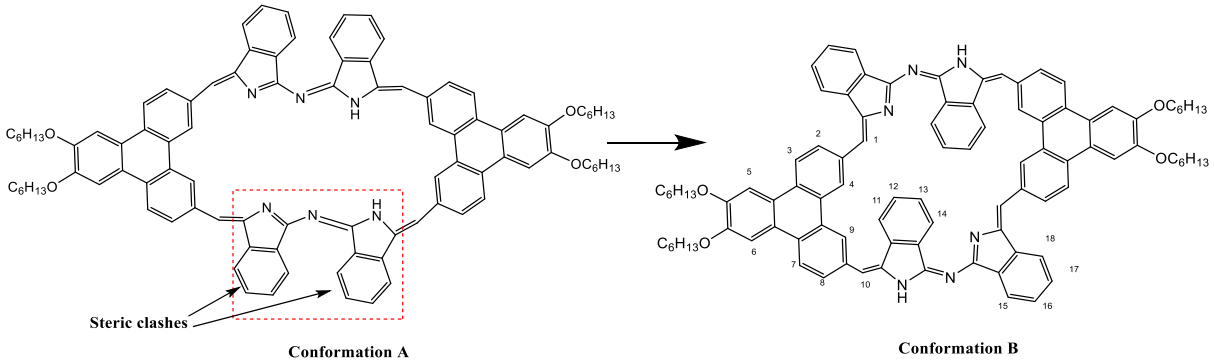

Figure 2.61: Strain-free structure of compound **2.85.**

However, closer analysis of the ^{1}H NMR spectrum indicated that even this is an oversimplification. In the region corresponding to the OCH_2, where we expect two simple triplet signals, the observed spectrum is much more complex, likely due to diastereotopic methylene protons, indicating that the molecule may not be planar. 2D experiments are also complicated and do not give any answer to the molecule's arrangement. One possibility is that the structure may adopt an aromatic Möbius configuration, which has been observed in simple dibenzihexaphyrin (Figure 2.63).[120,128] Additionally, our attempts to obtain a crystal for X-ray crystallography have so far been unsuccessful.

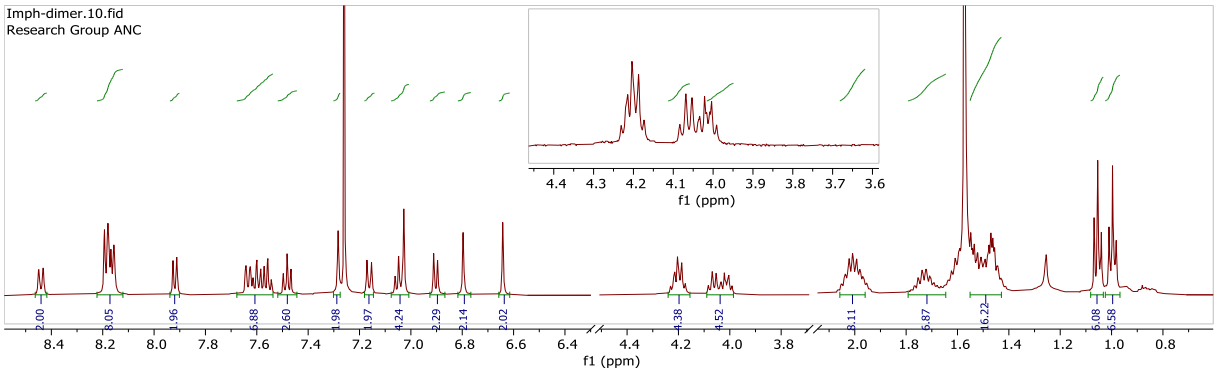

Figure 2.62: ^{1}H NMR spectrum of **2.85,** with an expansion of OCH_2 region.

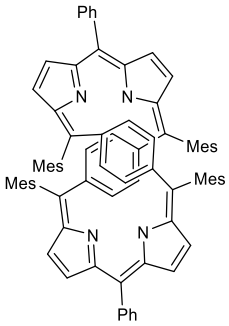

Figure 2.63: Möbius conformation of dibenzihexaphyrin.[120]

Figure 2.64 shows the UV-vis spectra of **2.85** and **2.82** in DCM. Compound **2.85** shows a new weak absorption peak appearing at lower energy at 564 compared to compound **2.82**. Interestingly, its fluorescence data reveal two emission bands at 506 and 663 nm. Our photophysics colleagues are currently investigating this compound. The dimer structure shows promising characteristics, making it an interesting compound for future investigation.

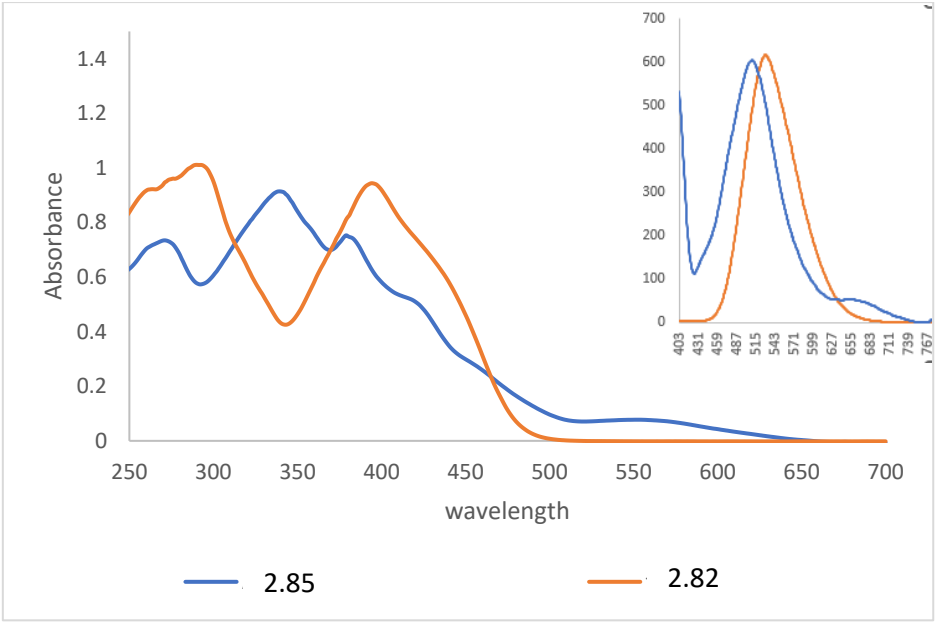

Figure 2.64: UV-vis spectra of **2.82**, **2.85**; inset, fluorescence spectra.

2.12 Conclusion

This work represents the successful synthesis of a variety of new peripherally and non-peripherally substituted tribenzodiazathiaporphyrins. Treating unsubstituted and substituted amidine with 2,5-bis(trimethylsilylethynyl)thiophene under Sonogashira copper-free cross

coupling reaction conditions led to the formation of bisaminoisoindolines, which subsequently undergo reaction with unsubstituted and substituted phthalonitriles to yield our desired macrocyclic compounds. A similar approach was employed to synthesise the novel isomer of tribenzodiazathiaporphyrins, *S*-confused *cis*-diazatribenzothiaporphyrins, using 2,4-bis(trimethylsilylethynyl)thiophene instead of the previously used 2,5-bis(trimethylsilylethynyl) thiophene. Due to the thiophene moiety's different bonding mode in the macrocyclic structure, the thiophene subunit reduces conjugation pathways in *S*-confused *cis*-diazatribenzothiaporphyrin while giving the highly effective π 18 delocalization paths for tribenzodiazathiaporphyrins.

The macrocycle's aromatic system based on 2,5-diacetylene thiophene showed strong Soret-like bands around 415 nm and a set of four lower energy Q-like bands between 510 and 665 nm. The effects of introducing substituents on the top or side isoindolines were investigated. A small effect was noticeable in both the Q-band's maximum absorption and fluorescence emission. In contrast, the *S*-confused *cis*-diazatribenzothiaporphyrin, which is based on 2,4-diacetylene thiophene, showed a blue shift as we expected in comparison with tribenzodiazathiaporphyrins, suggesting that this porphyrinoid showing no, or weak, aromaticity, unlike the tribenzodiazathiaporphyrins which demonstrate the strong aromatic structure with a complete π -delocalization pathway for the entire macrocycle.

The optimised synthetic method involves treating the reaction mixture of bisaminoisoindoline thiophene and phthalonitrile with high boiling solvents such as toluene and *p*-xylene without using base, and this led to improvement in the yields.

The bisaminoisoindoline, formed from the reaction between thiophene diacetylene and amidine, was further reacted with other electrophiles in an attempt to synthesise new macrocycles. The reaction of this bisaminoisoindoline with phthaloyl chloride indicated no macrocyclic product was formed; instead, it resulted in the formation of bisphthalimide compounds. The reaction of the same intermediate with diamine indicated no macrocyclic product with MALDI evidence for double addition. In addition, we attempted to synthesise tribenzomonoazathiaporphyrins using aminoisoindoline instead of previously used phthalonitrile. Remarkably, this attempt led to the formation of the tribenzodiazathiaporphyrins again (loss of an aryl fragment) along with the double addition of aminoisoindoline; there was no indication for the formation of tribenzomonoazathiaporphyrins.

The final work aimed to synthesise different macrocycles with distinct patterns of π-conjugation, specifically using triphenylene as a building block. The same synthetic strategy that had been successful in our earlier work with thiophene based macrocycles was applied. The reaction with diaminoisoindoline-triphenylene led to the formation of a unique dimeric compound. This structure seems to have some special characteristics and could be interesting for further investigation.

2.13 Future Work

In this project, the synthesis and structural investigation of new macrocyclic compounds (*S*-confused *cis*-diazatribenzothiaporphyrin **2.48b**) were carried out, including to insert palladium (pd) into the macrocyclic core. However, metal insertion was unsuccessful under the condition used. A related compound (*S*-confused thiaporphyrin) has been reported in the literature[90], where successful metal insertion was achieved. Based on that study, it appears that metal coordination is possible with our similar macrocyclic systems, suggesting that further efforts with modified conditions or different metals could lead to successful incorporation.

Another promising area of research is the continued investigation of the triphenylene-based macrocycles, as their structural features suggest the potential to form a Möbius- type topology. Möbius macrocycles are of particular interest due to their ability to exhibit stable distinct aromatic characters, depending on their conformation and the number of π electrons. Unlike typical planar systems that follow Hückel's rule, Möbius structures can support aromaticity with 4n π electrons, and their conformational flexibility enables switching between aromatic and antiaromatic behaviour. These features make them valuable systems for exploring how molecular conformation and π-electron delocalization influence electronic structure.[95]

Chapter 3: Experimental

3 Experimental

3.1 General Methods

Solvents and reagents were obtained from commercial suppliers and used without any further purifications. Water refers to distilled water. Organic layers were dried using anhydrous magnesium sulphate. The solvent was evaporated on a Büchi rotary evaporator at reduced pressure or by blowing argon, as reported in the corresponding experimental procedures.
Thin layer chromatography (TLC) was performed with aluminium sheets coated with Alugram® Sil G/UV254 (Macherey-Nagel) and the compounds were visualised by viewing under short-wavelength UV light at 254 nm or long-wavelength at 365 nm. Column chromatography was carried out using silica gel 60Å mesh 70 – 230 (63 – 200 μm) eluting with the solvent system stated under regular conditions. Solvent ratios are given as v: v.
^{1}H NMR spectra were recorded either at 400 MHz on Ultrashield PlusTM 400 spectrometer or 500 MHz on a Bruker AscendTM 500 spectrometer in 5 mm diameter tubes. The residual solvent peaks were used as references. ^{1}H NMR signals are reported in ppm and the coupling constants *J* are given in Hertz. ^{13}C spectra were recorded at 101 MHz or 126 MHz. NMR spectra were performed in solution using deuterated chloroform, methanol, and dichloromethane at room temperature or TCE at 70°C. NH peaks were broad or not observed in many cases. In some cases, the low solubility or the aggregation of compounds prevented the acquisition of spectra.
MALDI-TOF mass spectra were carried out using a Shimadzu Biotech AXIMA instrument (no matrix was used). Ultraviolet-visible absorption spectra were recorded on the Hitachi U-3310 Spectrophotometer in solvent as stated, and emission spectra were recorded using the Hitachi F-4500 fluorescence spectrophotometer. Melting points were recorded on a Reichart Thermovar microscope with a thermopar based temperature control system. Microwave reactions were carried out using a Biotage Initiator+ system.

3.2 2-Bromobenzamidine hydrochloride (2.1)

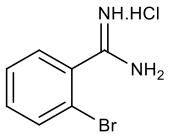

2.1

Following the method reported by Dalai,[109] a solution of 2-bromobenzonitrile (9 g, 49.4 mmol, 1 eq) in THF (6 mL) was added to a solution of $LiN(SiMe_3)_2$ in anhydrous THF (1M, 54 ml, 54 mmol, 1.1eq). The reaction mixture was stirred at room temperature for 4 h. Then, the reaction was cooled down on an ice bath, and HCl (5 M, 15 ml) solution in isopropanol was added dropwise to the cooled mixture. The reaction mixture was left to stir at room temperature overnight. The resulting precipitate was filtered, and the solid was washed with Et_2O to give the title compound as a white solid (9.9 g, 85.3%).

^{1}H NMR (500 MHz, Methanol-*d*$_4$) δ 7.82 – 7.79 (m, 1H), 7.61 – 7.52 (m, 3H).

3.3 (Z)-1-(4-Methoxyphenylmethylene)-1H-isoindol-3-amine (2.3)

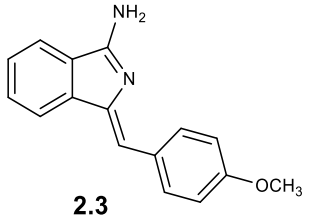

2.3

Following the method reported in the literature,[25] a mixture of 2-bromobenzamidine hydrochloride **2.1** (706.5 mg, 3 mmol, 1eq), BINAP (102 mg, 0.165 mmol, 0.055 eq) and $PdCl_2(MeCN)_2$ (39 mg, 0.15 mmol, 0.05 eq) was sealed in a microwave vessel with a magnetic bar and then purged with N_2. Then, a solution of 4-ethynylanisole (0.467 mL, 0.476 g, 3.6 mmol, 1.2eq) and DBU (1.12 mL, 1.14 g, 7.5 mmol, 2.5eq) in dry DMF (12 mL) was added. The mixture was stirred under N_2 for 5 min at room temperature to give a clear yellow solution with a white solid. Finally, the mixture was irradiated in a microwave reactor at 120°C for 1 h. After cooling, ethyl acetate (50 mL) was added, and the mixture was washed with a saturated solution of $NaHCO_3$ (3 x 75 mL). The organic layer was dried with $MgSO_4$, filtered and concentrated. The residue was finally purified by column chromatography using PE: EtOAc (1:1) and then EtOAc as a solvent gradient. The resulting solid was recrystallised from a mixture of DCM: PE (1:1) to yield the title compound as yellow needles (297 mg, 40%).

^{1}H NMR (500 MHz, Chloroform-*d*) δ 8.03 (d, *J* = 8.7 Hz, 2H), 7.79 (d, *J* = 7.8Hz, 1H), 7.57 (d, *J* = 7.6 Hz, 1H), 7.51 (td, *J* = 7.5, 1.0 Hz, 1H), 7.39 (td, *J* = 7.4, 0.9 Hz, 1H), 6.96 (d, *J* = 8.9 Hz, 2H), 6.78 (s, 1H), 3.85 (s, 3H).

3.4 2,5-Bis(trimethylsilylethynyl)thiophene (2.5) [110]

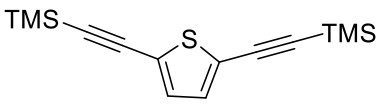

2.5

To a dry round bottomed flask, (trimethylsilyl)acetylene (2.40 g, 25 mmol) was added to a mixture of 2,5-dibromothiophene (1.2 g, 5 mmol), CuI (190 mg, 1 mmol), and $Pd(PPh_3)_2Cl_2$ (352 mg, 0.5 mmol) in triethylamine (10 mL) and THF (20 mL) under an argon atmosphere, and the mixture was heated to reflux overnight at 70 °C. After cooling, the solution was filtered through a bed of Celite. Then, the filtrate was evaporated under reduced pressure and the residue was finally purified by silica-gel column chromatography using petroleum ether. After purification, a yellow solid was obtained (1.26 g, 91%).

^{1}H NMR (500 MHz, Chloroform-*d*) δ 7.04 (s, 2H), 0.24 (s, 18H).

3.5 Bisaminoisoindoline thiophene (2.2)

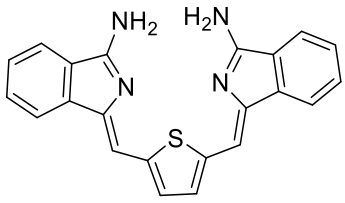

2.2

A mixture of amidine **2.1** (0.5 g, 2.1 mmol, 2 eq), BINAP (0.0725 g, 0.12 mmol) and $PdCl_2(MeCN)_2$ (0.0275 g, 0.11 mmol) was sealed in a microwave vessel with a magnetic bar and purged with N_2. A solution of 2,5 bis[2-(trimethylsilyl) ethynyl]thiophene (0.293 g, 1.1 mmol, 1 eq) and DBU (0.8 mL) in dry DMF (6 mL) was added. The reaction mixture was stirred at room temperature for 5 min. After that, the reaction mixture was irradiated in a microwave reactor at 120 °C for 1h. After cooling, the solution was poured onto water. A red precipitate formed, which was filtered off and washed with water. Finally, the solid was purified by column chromatography using THF: PE (2:1) and then recrystallised from THF/ PE to give the title compound as a red powder (0.19 g, 47%).

MP > 300°C

^{1}H NMR (500 MHz, Methanol-d_4) δ 7.80 (d, J = 7.7 Hz, 2H), 7.74 (d, J = 7.5 Hz, 2H), 7.46 (t, J = 7.5 Hz, 2H), 7.37 (t, J = 7.4 Hz, 2H), 7.28 (s, 2H), 6.99 (s, 2H).

MALDI-TOF-MS$(C_{22}H_{16}N_4S)^+$ m/z $[M]^+$ calcd: 368.10 found: 368.06.

UV-vis (THF): λ_{max} (nm) (ε (dm^3. mol^{-1} .cm^{-1})) = 489 (0.231 x10^5), 523 (0.215 x10^5).

Fluorescence (THF, Excitation at 488 nm): 544 nm.

3.6 Tribenzodiazathiaporphyrin (2.9)

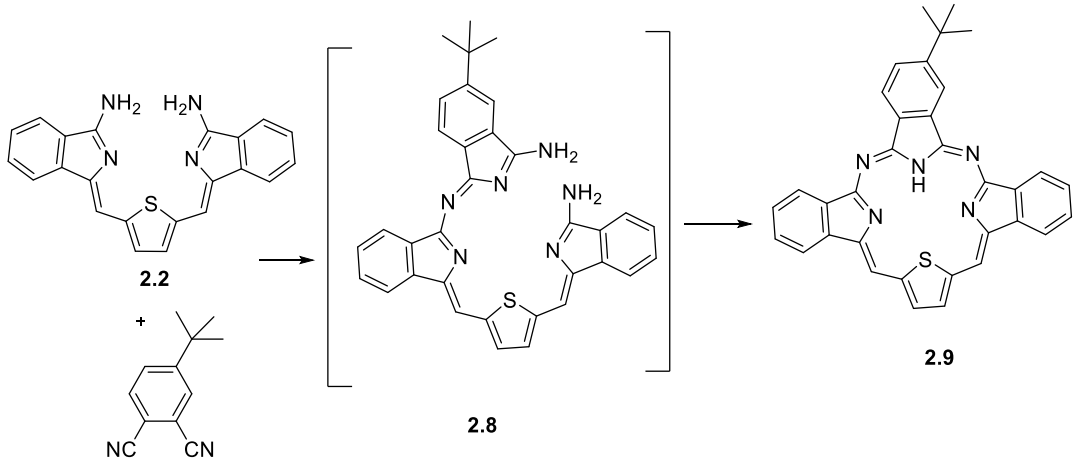

To a dry round bottomed flask, a mixture of bisaminoisoindoline thiophene **2.2** (160 mg, 0.43 mmol, 1eq) and 4-*tert*-butylpthalonitrile (80 mg, 0.43 mmol, 1 eq) was added and then refluxed with stirring in methanol (10 mL) for 24 h in the presence of sodium methoxide (approximately 3 mg). The solvent was evaporated under reduced pressure. The resulting purple crude product was purified by column chromatography eluting with THF/PE (1:1) and precipitated to give the desired intermediate product **2.8** as a deep purple-blue product. Then, the intermediate **2.8** was refluxed in *p*-xylene (3 mL) overnight. Then, the solvent was removed under an argon atmosphere while cooling and the residue was purified by silica-gel column chromatography (THF: PE = 4:10) then recrystallisation using DCM: PE to give a purple-magenta solid (25 mg, 11%).

MP 261°C

^{1}H NMR (500 MHz, Chloroform-*d*) δ 9.51 (s, 1H), 9.50 (s, 1H), 9.24 (s, 1H), 9.10 (d, J = 8.0 Hz, 1H), 8.93 (s, 2H), 8.91 – 8.88 (m, 1H), 8.87 – 8.84 (m, 1H), 8.53 – 8.48 (m, 2H), 8.23 (dd, J = 8.0, 1.7 Hz, 1H), 7.83 – 7.78 (m, 4H), 1.72 (s, 9H).

^{13}C NMR (126 MHz, Chloroform-*d*) from HSQC NMR δ 114.88, 120.07, 123.31, 131.09, 122.66, 122.66, 120.07, 129.47, 128.17, 31.58

MALDI-TOF-MS$(C_{34}H_{25}N_5S)^+$ m/z $[M]^+$ calcd: 535.18 found: 535.27.

UV-vis (DCM): λ_{max} (nm) (ε (dm^3. mol^{-1} .cm^{-1})) = 388 (0.263 x10^5), 411 (0.280 x10^5), 521 (0.105 x10^5), 558 (0.165 x10^5), 590 (0.598 x10^4), 643 (0.980 x10^4).

Fluorescence (CH_2Cl_2, Excitation at 590 nm): 648, 694 nm.

3.7 2,5-Dichloro-2,5-dimethylhexane[112,113]

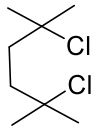

2.10

A solution of 2,5-dimethylhexane-2,5-diol (10 g, 68.38 mmol) in concentrated hydrochloric acid (50 mL) was stirred in an ice bath for 30 min. The mixture was stirred overnight at room temperature. The solid was filtered off and washed with water. Then, the solid was dissolved in DCM, washed again with water and extracted with DCM (3 × 50 mL). The organic extracts were dried ($MgSO_4$), and the solvent removed under reduced pressure to afford the product as a white solid which was recrystallised from methanol to give the desired compound as white crystals (10.56 g, 84%).

^{1}H NMR (500 MHz, Chloroform-*d*) δ 1.95 (s, 4H), 1.60 (s, 12H).

3.8 1,1,4,4-Tetramethyl-1,2,3,4-tetrahydronaphthalene

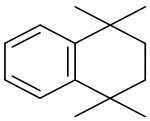

2.11

Following Bruson's procedure, [112] a solution of 2,5-dichloro-2,5-dimethylhexane (10 g, 54.60 mmol) in benzene (125 mL) was stirred at 50°C for 10 min. Anhydrous aluminium trichloride (2.92 g, 21.9 mmol) was added in portions over 30 min and was then left stirring for 24 hat 50°C. The resulting solution was cooled to room temperature, poured into dilute hydrochloric acid (50 mL) and extracted with DCM (3 × 50 mL). The organic layer was washed with water and dilute sodium carbonate solution before being dried over $MgSO_4$. The solvent was evaporated under vacuum. The resulting material was purified by column chromatography using 100% PE as eluent to yield the product as a colourless oil (6.7 g, 65.7%).

^{1}H NMR (500 MHz, Chloroform-*d*) δ 7.31 (dd, *J* = 5.9, 3.4 Hz, 2H), 7.13 (dd, *J* = 5.9, 3.4 Hz, 2H), 1.69 (s, 4H), 1.29 (s, 12H).

3.9 6,7-Dibromo-1,2,3,4-tetrahydro-1,1,4,4-tetramethylnaphthalene[129]

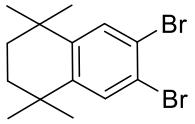

2.13

1,1,4,4-Tetramethyl-1,2,3,4-tetrahydronaphthalene (5.76 g, 0.0302 mol) was dissolved in DCM (50 mL). Iron powder (0.202 g, 0.0037 mol) and iodine (0.077 g, 0.00031 mol) were added to the mixture and cooled to 0ºC. Bromine (3.18 mL, 0.0612 mol) was added dropwise to the stirring mixture over 30 min. After that, the reaction mixture was allowed to warm up to room temperature and stirred for 24 h. The resulting solution was washed with a saturated solution of sodium metabisulfite and then with sodium bicarbonate to remove the excess of bromine. Water and brine (50 mL) were added, and the mixture extracted with DCM (3×50 mL). Organics were combined, dried with $MgSO_4$ and the solvent was evaporated under reduced pressure. The crude product was purified by column chromatography over silica gel using PE as eluent to give the title compound as a white solid (8.33 g, 79%).

^{1}H NMR (500 MHz, Chloroform-*d*) δ 7.50 (s, 2H), 1.66 (s, 4H), 1.25 (s, 12H).

3.10 6,7-Dicyano-1,2,3,4-tetrahydro-1,1,4,4-tetramethylnaphthalene.[115]

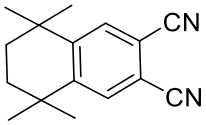

2.14

6,7-Dibromo-1,1,4,4-tetramethyl-1,2,3,4-tetrahydronaphthalene (6.0 g, 17.33 mmol) was dissolved in anhydrous *p*-xylene (20 mL) under N_2. CuI (330 mg, 1.733 mmol) was added, followed by 1-butylimidazole (5.4 g, 43.32 mmol), and the solution stirred. Finely ground and dried $K_4[Fe(CN)_6]$ (2.85 g, 8.665 mmol) was added, and the solution was heated to reflux. The reaction was monitored by TLC until completion (48-96 h). The reaction was cooled to room temperature. EtOAc (50 mL) was added, and the solution was filtered. The filtrate was transferred to a separating funnel and washed with H_2O (3 x 50 mL). The organic phase was dried ($MgSO_4$), and the solvent was removed to yield a white solid. The crude product was purified by silica gel chromatography (EtOAc: PE,1:7) to yield the title compound as a yellow solid (2.23 g, 54%).

^{1}H NMR (500 MHz, Chloroform-*d*) δ 7.71 (s, 2H), 1.72 (s, 4H), 1.30 (s, 12H).

3.11 6-Bromo-7-cyano-1,2,3,4-tetrahydro-1,1,4,4-tetramethylnaphthalene[26]

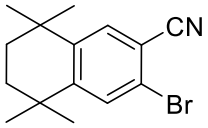

2.15

The title compound was obtained as a side product from the dicyanation of 6,7-dibromo-1,1,4,4-tetramethyl-1,2,3,4-tetrahydronaphthalene. Alternatively, the title compound may be selectively synthesised using the next method.

A mixture of 6,7-dibromo-1,1,4,4-tetramethyl-1,2,3,4-tetrahydronaphthalene (1.52 g, 4.39 mmol) and CuCN (1 g, 10.99 mmol) was refluxed in dry DMF (15 mL) under an argon atmosphere for 3 h. The reaction mixture was cooled to room temperature, and Et_2O (50 mL) was added. The solid was filtered to remove copper salt and the filtrate was washed with water (3 x 50 mL) and with an aqueous ammonia solution until no blue colour was obtained in the aqueous layer. The organic layer was then washed with a saturated solution of $NaHCO_3$, dried over $MgSO_4$ and filtered. The filtrate was evaporated under reduced pressure to give the crude product. The crude product was purified by column chromatography (EtOAc: PE,1:7) to yield the product as a yellow solid (0.9 g, 70%).

^{1}H NMR (500 MHz, Chloroform-*d*) δ 7.57 (s, 1H), 7.55 (s, 1H), 1.68 (s, 4H), 1.27 (s, 6H), 1.26 (s, 6H).

3.12 Compound (2.16)

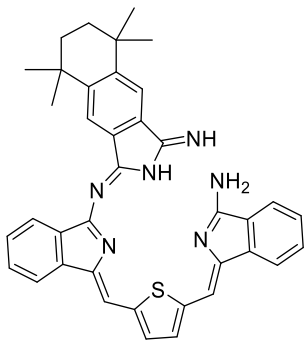

2.16

A mixture of bisaminoisoindoline thiophene **2.2** (200 mg, 0.543 mmol) with 6,7-dicyano-1,2,3,4-tetrahydro-1,1,4,4-tetramethylnaphthalene (120 mg, 0.543 mmol) was stirred in refluxing methanol (10 mL) in the presence of sodium methoxide (approximately 3 mg) under N_2 atmosphere overnight. The solvent was removed under vacuum, and the crude compound

was purified by column chromatography using THF: PE (1:4) and then precipitated using THF: PE (1:3) to yield **2.16** as a deep purple-blue solid (46 mg, 14%).

MP > 300°C

^{1}H NMR (400 MHz, Chloroform-*d*) δ 12.7 (s, 1H, NH), 8.11 (s, 1H), 8.07 (d, *J* = 6.1 Hz, 1H), 8.02 (s, 1H), 7.84 – 7.78 (m, 1H), 7.75 (d, *J* = 7.5 Hz, 1H), 7.52 – 7.41 (m, 5H), 7.38 – 7.35 (m, 1H), 7.31 (d, *J* = 3.9 Hz, 1H), 7.21 (d, *J* = 4.0 Hz, 1H), 7.05 (s, 1H), 1.78 (s, 4H), 1.44 (s, 6H), 1.39 (s, 6H).

MALDI-TOF-MS $(C_{38}H_{34}N_6S)^+$ m/z $[M]^+$ calcd: 606.25 found 606.14.

UV-vis (DCM): λ_{max} (nm) (ε (dm^3. mol^{-1} .cm^{-1})) = 338 (0.341 x10^5), 579 (0.146 x10^5).

3.13 Tribenzodiazathiaporphyrin (2.18)

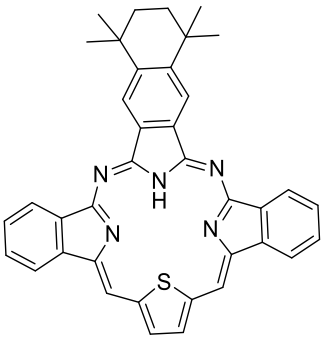

2.18

The dried compound **2.16** (46 mg, 0.075 mmol) was refluxed in *p*-xylene (3 mL) overnight under an argon atmosphere. Then, the solvent was removed by blowing argon while cooling. Finally, the crude material was purified by column chromatography using DCM:PE (3:1) and then recrystallised from DCM and methanol to give the title compound as a purple-magenta solid (29 mg, 66%).

MP > 300°C

^{1}H NMR (500 MHz, TCE-d_2) δ 9.58 (br-s, 2H), 9.31 (br-s, 2H), 8.97 (br-s, 4H), 8.53 (br-s, 2H), 7.78 (br-s, 4H), 1.96 (s, 4H), 1.69 (s, 12H).

^{1}H NMR (400 MHz, Chloroform-*d*) δ 9.38 (s, 2H), 9.21 (s, 2H), 8.92 – 8.86 (m, 2H), 8.82 (s, 2H), 8.51 – 8.43 (m, 2H), 7.87 – 7.75 (m, 4H), 2.06 (s, 4H), 1.79 (s, 12H).

^{13}C NMR (101 MHz, Chloroform-*d*) δ 160.09, 149.99, 148.53, 148.05, 145.47, 141.20, 139.28, 133.43, 130.77, 128.59, 127.67, 122.67, 121.88, 120.17, 115.03, 35.90, 32.73, 29.71.

MALDI-TOF-MS $(C_{38}H_{31}N_5S)^+$ m/z $[M]^+$ calcd: 589.22 found 589.34.

UV-vis (DCM): λ_{max} (nm) (ε (dm^3. mol^{-1} .cm^{-1})) = 389 (0.317 x10^5), 410 (0.342 x10^5), 523 (0.133 x10^5), 560 (0.217 x10^5), 586 (0.874 x10^4), 639 (0.131 x10^5).

Fluorescence (CH_2Cl_2, Excitation at 650 nm): 641, 691 nm.

3.14 1,2-Dibromo-4,5-dimethoxybenzene [130]

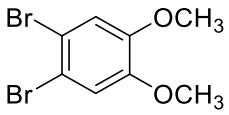

2.19a

Veratrole (1,2-dimethoxybenzene) (20 g, 0.145 mol) was dissolved in DCM (150 mL) and stirred at 0 ̊C. Bromine (16.3 mL, 50.97 g, 0.319 mol) was added dropwise while stirring. The reaction mixture was then stirred at room temperature for 1h. The mixture was washed with a saturated solution of sodium thiosulphate, brine, and water and the organic layer was dried with $MgSO_4$ and filtered. The solvent was removed, and the residue was recrystallised from MeOH to give colourless crystals (41 g, 97%).

^{1}H NMR (500 MHz, Chloroform-*d*) δ 7.06 (s, 2H), 3.85 (s, 6H).

3.15 2-Bromo-4,5-dimethoxybenzonitrile[26,116,131]

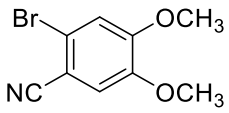

2.21a

A mixture of 1,2-dibromo-4,5-dimethoxybenzene (2.6 g, 8.8 mmol) and CuCN (1.6 g, 17.6 mmol) was refluxed in dry DMF (15 mL) under an argon atmosphere for 3 h. The mixture was cooled to room temperature, and DCM was added. The solid was filtered to remove copper salt and the filtrate was washed with H_2O and with an aqueous solution of ammonia (5%) until no blue colour was obtained in the aqueous layer. The organic layer was washed with a solution of $NaHCO_3$, then dried over $MgSO_4$ and filtered. The solvent was removed, and the crude material was purified by column chromatography using DCM: PE (1:1) and then DCM to get the product as a colourless solid (1.38 g, 65%).

^{1}H NMR (500 MHz, Chloroform-*d*) δ 7.07 (s, 1H), 7.04 (s, 1H), 3.93 (s, 3H), 3.88 (s, 3H).

3.16 1,2-Dicyano-4,5-dimethoxybenzene

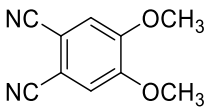

2.20a

This compound was isolated as a side product from the cyanation reaction above (0.35 g, 21%).

^{1}H NMR (500 MHz, Chloroform-*d*) δ 7.15 (s, 2H), 3.97 (s, 6H).

3.17 Tribenzodiazathiaporphyrin (2.23a)

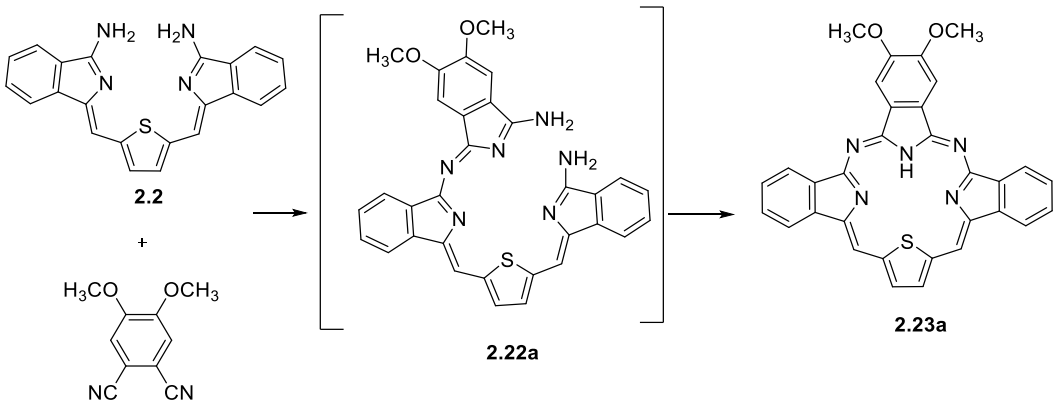

A mixture of bisaminoisoindoline thiophene **2.2** (100 mg, 0.272 mmol, 1 eq) and 4,5-dimethoxyphthalonitrile (51 mg, 0.272 mmol) was stirred in refluxing methanol (10 mL) in the presence of sodium methoxide (approximately 3 mg) overnight under an argon atmosphere. The solvent was removed under vacuum, and the crude compound was purified by column chromatography using THF: PE (1:2), then precipitated using THF: PE to get the intermediate **2.22a** as a deep purple-blue solid. The intermediate **2.22a** was refluxed in *p*-xylene (3 mL) overnight under an argon atmosphere. Then, the solvent was removed by blowing argon while cooling. Finally, the crude material was purified by column chromatography using DCM: EtOAc (150:5), then recrystallised from DCM and methanol to give the title compound as a purple-magenta solid (16 mg, 11%).

MP > 300°C

^{1}H NMR (400 MHz, Chloroform-*d*) δ 9.19 (s, 2H), 8.75 (s, 2H), 8.63 – 8.58 (m, 2H), 8.41 – 8.35 (m, 2H), 7.96 (s, 2H), 7.84 – 7.76 (m, 4H), 4.25 (s, 6H), -0.60 (s, 1H).

MALDI-TOF-MS $(C_{32}H_{21}N_5O_2S)^+$ m/z $[M]^+$ calcd: 539.14 found 539.75

UV-vis (DCM): λ_{max} (nm) (ε (dm^3. mol^{-1} .cm^{-1})) = 413 (0.360 x10^5), 523 (0.105 x10^5), 558 (0.189 x10^5), 591 (0.595 x10^4), 645 (0.113 x10^5).

Fluorescence (CH_2Cl_2, Excitation at 558 nm): 651, 697 nm.

3.18 1,2-Dibromo-4,5-bis(hexyloxy)benzene[127]

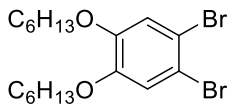

2.19b

1,2-Bis(hexyloxy)benzene (18 g, 0.065 mol) was stirred in DCM (150 mL) at -10°C**.** Bromine (9 mL, 27 g, 0.17 mol) was added dropwise, and the mixture was stirred for 1 h. After that,

the reaction mixture was washed with a saturated solution of sodium metabisulphite solution ($Na_2S_2O_5$) (100 mL). The organics were combined and dried over $MgSO_4$ and filtered. The solvent was evaporated in a vacuum to give the product as an orange oil.

^{1}H NMR (500 MHz, Chloroform-*d*) δ 7.06 (s, 2H), 3.94 (t, *J* = 6.6 Hz, 4H), 1.85 – 1.73 (m, 4H), 1.51 – 1.40 (m, 4H), 1.38 – 1.27 (m, 8H), 0.94 – 0.84 (m, 6H).

3.19 1,2-Dicyano-4,5-bis(hexyloxy)benzene[26,116]

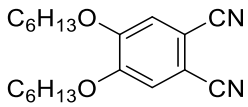

2.20b

A mixture of 1,2 dibromo-4,5-bis(hexyloxy)bezene **2.19b** (5.79 g, 0.013 mol) and CuCN (5.82 g, 0.0659 mol) was refluxed in dry DMF (45 mL) under a nitrogen atmosphere for 3 h. The reaction mixture was cooled to room temperature, and Et_2O was added. The reaction mixture was filtered to remove the copper salts. Then, the filtrate was washed with H_2O (3 × 50 mL) and with an aqueous ammonia solution until no blue colour was obtained in the aqueous layer. The organic layer was washed with a solution of $NaHCO_3$, dried with $MgSO_4$ and filtered. The solvent was removed, and the crude product was purified using column chromatography (PE/ Et_2O, 5:1) to yield the product as a white solid (1.4 g, 33.3%).

^{1}H NMR (500 MHz, Chloroform-*d*) δ 7.11 (s, 2H), 4.05 (t, *J* = 6.5 Hz, 4H), 1.90 – 1.80 (m, 4H), 1.52 – 1.42 (m, 4H), 1.41 – 1.29 (m, 8H), 0.95 – 0.87 (m, 6H).

3.20 2-Bromo-4,5-bis(hexyloxy)benzonitrile

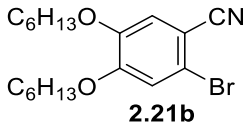

2.21b

This compound was isolated as a side product from the above cyanation reaction (2 g, 40%).

^{1}H NMR (500 MHz, Chloroform-*d*) δ 7.03 (s, 1H), 7.03 (s, 1H), 4.01 (t, *J* = 6.6 Hz, 2H), 3.96 (t, *J* = 6.6 Hz, 2H), 1.89 – 1.75 (m, 4H), 1.51 – 1.41 (m, 4H), 1.39 – 1.27 (m, 8H), 0.94 – 0.84 (m, 6H).

3.21 Tribenzodiazathiaporphyrin (2.23b)

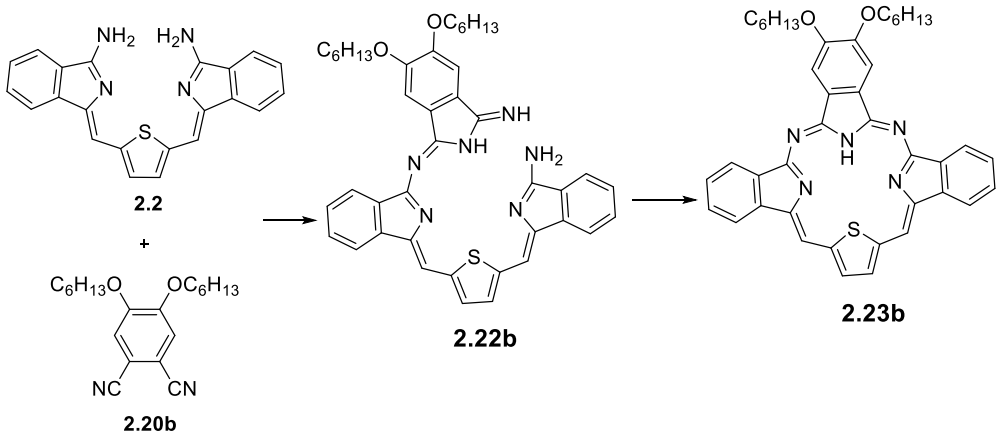

Method A

To a dry round bottomed flask, a mixture of bisaminoisoindoline thiophene **2.2** (160 mg, 0.43 mmol, 1 eq) and 1,2-dicyano-4,5-bis(hexyloxy)benzene (140 mg, 0.43 mmol, 1 eq) was stirred in refluxing methanol (10 mL) for 24 h in the presence of sodium methoxide (approximately 3 mg). The solvent was then removed under vacuum, and the resulting dark purple crude product was purified by column chromatography eluting with THF/PE (1:1) and precipitated from THF and PE to give the desired intermediate product **2.22b** as a deep purple-blue product (38 mg, 13%).

MP 245℃

^{1}H NMR (400 MHz, Chloroform-*d*) δ 12.49 (s, 1H, NH), 8.02 (d, *J* = 7.1 Hz, 1H), 7.80 (d, *J* = 7.2 Hz, 1H), 7.76 (d, *J* = 7.6 Hz, 1H), 7.56 (s, 1H), 7.42 – 7.35 (m, 5H), 7.41 (s, 1H), 7.36 (t, *J* = 7.4 Hz, 1H), 7.30 (d, *J* = 3.9 Hz, 1H), 7.20 (d, *J* = 3.9 Hz, 1H), 7.05 (s, 1H), 4.20 (t, *J* = 6.6 Hz, 2H), 4.12 (t, *J* = 6.5 Hz, 2H), 1.96 – 1.87 (m, 4H), 1.56 – 1.50 (m, 4H), 1.41 – 1.36 (m, 8H), 0.97 – 0.90 (m, 6H).

MALDI-TOF-MS $(C_{42}H_{45}N_6O_2S)^+$ m/z $[M+H]^+$ calcd: 697.33 found: 697.78.

UV-vis (DCM): λ_{max} (nm) (ε (dm^3. mol^{-1} .cm^{-1})) = 393 (0.270 x10^5), 581 (0.151 x10^5).

2.22b (38 mg) was refluxed in *p*-xylene (3 mL) overnight under an argon atmosphere. Then, the solvent was evaporated under reduced pressure, and the product was purified by silica-gel column chromatography (DCM: hexane = 3:1) and then recrystallised using DCM: MeOH to give the title compound **2.23b** as a purple-magenta solid (26 mg, 9% from **2.2**).

MP 217℃

^{1}H NMR (500 MHz, TCE-d_2) δ 9.49 (s, 2H), 8.95 (s, 2H), 8.91 – 8.86 (m, 2H), 8.60 – 8.53 (m,

4H), 7.90 – 7.85 (m, 4H), 4.56 (t, *J* = 6.4 Hz, 4H), 2.21 – 2.12 (m, 4H), 1.85 – 1.77 (m, 4H), 1.61 – 1.57 (m, 8H), 1.13 – 1.06 (m, 6H).

^{1}H NMR (400 MHz, Chloroform-*d*) δ 9.05 (s, 2H), 8.69 – 8.58 (m, 4H), 8.37 – 8.29 (m, 2H), 8.12 (s, 2H), 7.83 – 7.72 (m, 4H), 4.43 (t, *J* = 6.6 Hz, 4H), 2.24 – 2.11 (m, 4H), 1.86 – 1.72 (m, 4H), 1.61 – 1.55 (m, 8H), 1.08 (t, *J* = 7.1 Hz, 6H), -0.50 (s, 1H, NH).

^{13}C NMR (101 MHz, Chloroform-*d*) δ 159.03, 152.78, 148.10, 146.73, 145.23, 141.18, 139.35, 130.44, 128.94, 128.31, 127.40, 122.48, 120.09, 114.32, 105.60, 69.69, 32.00, 29.55, 26.16, 22.97, 14.34.

MALDI-TOF-MS($C_{42}H_{41}N_5O_2S$)$^{+}$ m/z $[M]^{+}$ calcd: 679.29 found: 679.30.

UV-vis (DCM): λ_{max} (nm) (ε (dm^3. mol^{-1} .cm^{-1})) = 413 (0.433 x10^5), 523 (0.133 x10^5), 559 (0.233 x10^5), 590 (0.808 x10^4), 644 (0.146 x10^5).

Fluorescence (CH_2Cl_2, Excitation at 558 nm): 648, 692 nm.

Method B

A mixture of bisaminoisoindoline thiophene **2.2** (30 mg, 0.08 mmol, 1 eq) and 1,2-dicyano-4,5-bis(hexyloxy)benzene (26 mg, 0.08 mmol, 1 eq) was stirred in refluxing THF (6 mL) in the presence of potassium *tert*-butoxide (approximately 3 mg) for 4 days. The solvent was then removed under vacuum and the resulting crude product was purified by column chromatography eluting with THF/PE (1:1) and precipitated to give the intermediate (open compound) product **2.22b** as a deep purple-blue product. Then, intermediate **2.22b** was refluxed overnight in *p*-xylene (3mL) and the reaction was monitored by TLC. Then, the solvent was evaporated under reduced pressure and the product was purified by silica-gel column chromatography (DCM: hexane = 3:1) then recrystallised using DCM: MeOH to give the title compound as a purple-magenta solid (10 mg, 18%).

Method C

A mixture of bisaminoisoindoline thiophene **2.2** (30 mg, 0.08 mmol, 1 eq) and 1,2-dicyano-4,5-bis(hexyloxy)benzene (26 mg, 0.08 mmol, 1 eq) was stirred in refluxing toluene (1 mL) for 48 h. 26 mg of **2.20b** and 2 mL of toluene were then added again, and the mixture refluxed two more days. The solvent was then removed under vacuum, and the resulting product was purified by column chromatography eluting with DCM/PE (3:1) and then recrystallised using DCM: MeOH to yield the desired product **2.23b** directly as a purple-magenta product (20 mg, 36%).

Method D

A mixture of bisaminoisoindoline thiophene **2.2** (30 mg, 0.08 mmol, 1 eq) and 1,2-dicyano-4,5-bis(hexyloxy)benzene (32 mg, 0.097 mmol, 1.2 eq) was stirred in refluxing *p*-xylene (3 mL) overnight and **2.20b** (21 mg, 0.08 eq) was then added to the mixture and refluxed for 4 days. The solvent was then removed under vacuum, and the resulting product was purified by column chromatography eluting with DCM/PE (3:1) and recrystallised from DCM/MeOH to give the desired product **2.23b** as a purple-magenta product (12.8 mg, 23%).

3.22 Compound (2.24)

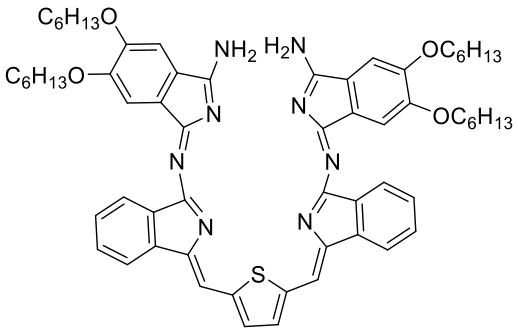

2.24

This compound was isolated as a side product from the previous reaction (Method A) as a green solid (3 mg, 1%).

MP > 300°C

^{1}H NMR (400 MHz, Chloroform-*d*) δ 10.04 (s, 2H, NH), 8.16 (d, *J* = 6.7 Hz, 2H), 7.92 (d, *J* = 6.6 Hz, 2H), 7.77 (s, 2H), 7.68 (s, 2H), 7.60 (s, 2H), 7.54 – 7.46 (m, 4H), 6.51 (s, 2H), 4.21 (t, *J* = 6.7 Hz, 4H), 3.74 (t, *J* = 6.4 Hz, 4H), 1.98 – 1.87 (m, 8H), 1.88 – 1.77 (m, 8H), 1.42 – 1.35 (m, 16H), 0.98 – 0.93 (m, 12H).

MALDI-TOF-MS($C_{62}H_{73}N_8O_4S$)$^+$ m/z $[M+H]^+$ calcd: 1025.54 found:1026.05.

UV-vis (DCM): λ_{max} (nm) (ε (dm^3. mol^{-1} .cm^{-1})) = 305 (0.281 x10^5), 343 (0.302 x10^5), 434 (0.168 x10^5), 556 (0.888 x10^4), 595 (0.938 x10^4), 642 (0.761 x10^4).

Fluorescence (CH_2Cl_2, Excitation at 350 nm): 444 nm.

3.23 1,2-Dibromo-4,5-bis(decyloxy)benzene[132]

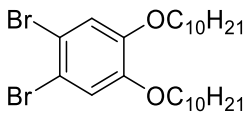

2.19c

1,2-Bis(decyloxy)benzene (10 g, 0.025 mol) was stirred in DCM (100 mL) at -10°C. Bromine (3.38 mL, 10.56 g, 0.066 mol) was added dropwise, and the mixture was stirred for 1 h. On completion, the mixture was washed with sodium metabisulphite solution ($Na_2S_2O_5$). The organic layer was extracted with DCM and dried over $MgSO_4$. The solvent was removed, and the residue was recrystallised from methanol to give a colourless solid (13.1 g, 95%).

^{1}H NMR (400 MHz, Chloroform-*d*) δ 7.06 (s, 2H), 3.94 (t, *J* = 6.6 Hz, 4H), 1.87 – 1.73 (m, 4H), 1.51 – 1.39 (m, 4H), 1.38 – 1.17 (m, 24H), 0.93 – 0.82 (m, 6H).

3.24 1,2-Dicyano-4,5-bis(decyloxy)benzene[26]

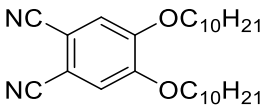

2.20c

1,2-Dibromo-4,5-bis(decyloxy)benzene (2.5 g, 0.00455 mol) and CuCN (2.039 g, 0.0227 mol) were refluxed in dry DMF (15 mL) under an argon atmosphere for 3 h. The mixture was cooled to room temperature and Et_2O was added and the solid formed was filtered off to remove copper salt. The filtrate was washed with H_2O and with an aqueous solution of ammonia (5%) until no blue was obtained in the aqueous layer. The organic layer was washed with a solution of $NaHCO_3$ then dried over $MgSO_4$ and filtered. The solvent was removed, and the crude product was purified by column chromatography using DCM:PE (1:1) then DCM to afford the product as a colourless solid (0.60 g, 30%).

^{1}H NMR (400 MHz, Chloroform-*d*) δ 7.11 (s, 2H), 4.04 (t, *J* = 6.5 Hz, 4H), 1.91 – 1.78 (m, 4H), 1.54 – 1.40 (m, 4H), 1.41 – 1.13 (m, 24H), 0.95 – 0.79 (m, 6H).

3.25 Compound (2.22c)

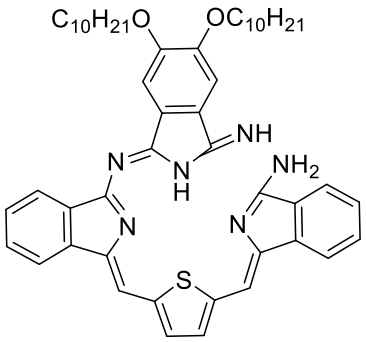

2.22c

A mixture of bisaminoisoindoline thiophene **2.2** (100 mg, 0.272 mmol, 1 eq) and 4,5-

bis(decyloxy)benzene-1,2-dicarbonitrile (120 mg, 0.272 mmol, 1 eq) was stirred in refluxing methanol (10 mL) in the presence of $NaOCH_3$ (approximately 3 mg) for 24 h under an argon atmosphere. The solvent was removed under vacuum, and the resulting solid was separated by column chromatography using (THF: PE (1:4)) and then recrystallised from DCM: MeOH to afford the product as a deep purple-blue solid (0.045 g, 20%).

MP 160°C
^{1}H NMR (500 MHz, Chloroform-*d*) δ 12.62 (s, 1H, NH), 9.46 (br-s, 1H, NH), 8.06 (d, *J* = 7.5 Hz, 1H), 7.83 (d, *J* = 7.4 Hz, 1H), 7.79 (d, *J* = 7.5 Hz, 1H), 7.60 (s, 1H), 7.53 – 7.43 (m, 6H), 7.42 – 7.37 (m, 1H), 7.34 (d, *J* = 4.1 Hz, 1H), 7.24 (d, *J* = 4.0 Hz, 1H), 7.09 (s, 1H), 6.35 (br-s, 2H, NH_2), 4.23 (t, *J* = 6.6 Hz, 2H), 4.15 (t, *J* = 6.7 Hz, 2H), 1.99 – 1.89 (m, 4H), 1.66 – 1.49 (m, 12H), 1.47 – 1.31 (m, 16H), 0.93 – 0.88 (m, 6H).
MALDI-TOF-MS $(C_{50}H_{61}N_6O_2S)^+$ m/z $[M+H]^+$ calcd: 809.45 found 809.94.
UV-vis (DCM): λ_{max} (nm) (ε (dm^3. mol^{-1} .cm^{-1})) = 378 (0.139 x10^5), 394 (0.311 x10^5), 581 (0.177 x10^5).

Fluorescence (CH_2Cl_2, Excitation at 378 nm): 428 nm.

3.26 Tribenzodiazathiaporphyrin (2.23c)

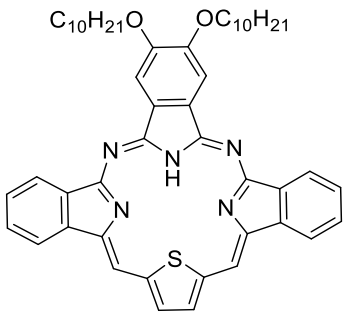

2.23c

The compound **2.22c** (45 mg, 0.055 mmol) was heated in refluxing *p*-xylene (3 mL) overnight. The solvent was removed under an argon stream while cooling. The crude mixture was purified by column chromatography using THF: PE (1:10) as eluent. Recrystallisation from DCM: MeOH gave the title compound as a purple-magenta solid (30 mg, 68%).

MP 153°C
^{1}H NMR (400 MHz, Chloroform-*d*) δ 9.15 (s, 2H), 8.73 – 8.67 (m, 4H), 8.40- 8.36 (m, 2H), 8.21 (s, 2H), 7.83 – 7.76 (m, 4H), 4.46 (t, *J* = 6.6 Hz, 4H), 2.22 – 2.14 (m, 4H), 1.80 – 1.74 (m, 4H), 1.63 – 1.57 (m, 4H), 1.54 – 1.49 (m, 4H), 1.46 – 1.39 (m, 16H), 0.97 – 0.91 (m, 6H), -0.26 (s, 1H, NH).
^{13}C NMR (101 MHz, Chloroform-*d*) δ 159.10, 152.74, 148.11, 146.82, 145.20, 141.12, 139.27, 130.43, 128.92, 128.26, 127.35, 122.41, 120.02, 114.35, 105.58, 69.60, 32.04, 29.87, 29.77, 29.71, 29.51, 29.47, 26.36, 22.78, 14.19.
MALDI-TOF-MS $(C_{50}H_{57}N_5O_2S)^+$ m/z $[M]^+$ calcd: 791.42 found 791.31.

UV-vis (DCM): λ_{max} (nm) (ε (dm^3. mol^{-1} .cm^{-1})) = 413 (0.546 x10^5), 524 (0.168 x10^5), 559 (0.291 x10^5),591 (0.103 x10^5),644 (0.188 x10^5).

Fluorescence (CH_2Cl_2, Excitation at 559 nm): 646, 695 nm.

3.27 Tribenzodiazathiaporphyrin (2.23d)

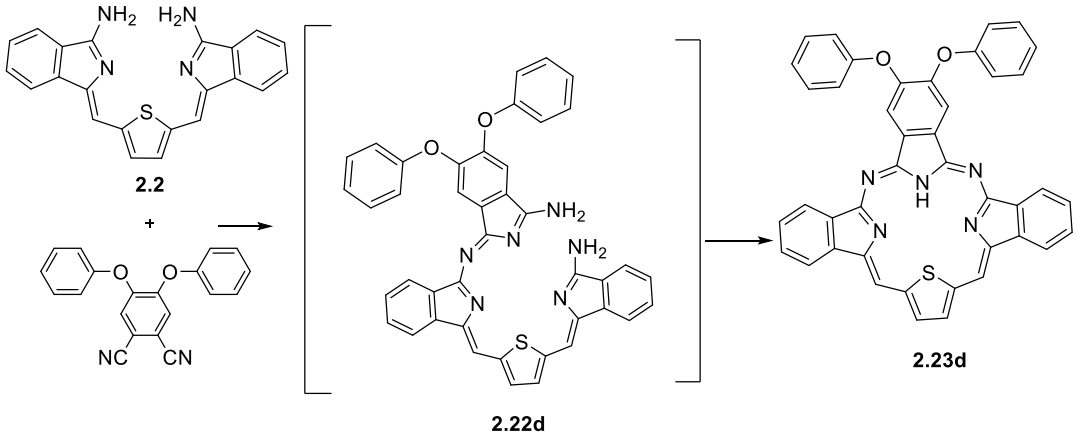

A mixture of bisaminoisoindoline thiophene **2.2** (120 mg, 0.341 mmol) and 4,5-diphenoxybenzene-1,2-dicarbonitrile (90 mg, 0.341 mmol) was stirred in refluxing methanol (10 mL) in the presence of sodium methoxide (approximately 3 mg) under argon atmosphere overnight. The solvent was removed under vacuum, and the crude compound was purified by column chromatography using THF: PE (1:2) and then precipitated using THF: PE. Analysis of the crude solid by MALDI-TOF MS showed a peak at m/z 681 that corresponds to the expected mass of the open compound **2.22d**. The intermediate **2.22d** was refluxed in *p*-xylene (3 mL) for 24 h. Then, the solvent was removed while cooling under argon. The reaction mixture was purified using column chromatography using DCM: PE (3:1) as eluent and then recrystallised from DCM: MeOH to give the title product as a purple-magenta solid (21 mg, 10%).

MP > 300°C

^{1}H NMR (500 MHz, TCE-d_2) δ 9.89 (s, 2H), 9.25 (s, 2H), 9.06 (s, 2H), 8.93 (d, *J* = 7.1 Hz, 2H), 8.71 (d, *J* = 7.2 Hz, 2H), 7.94 – 7.85 (m, 4H), 7.54 (t, *J* = 7.8 Hz, 4H), 7.37 – 7.26 (m, 6H).

MALDI-TOF-MS $(C_{42}H_{25}N_5O_2S)^+$ m/z $[M]^+$ calcd 663.17 found 662.86.

UV-vis (DCM): λ_{max} (nm) (ε (dm^3. mol^{-1} .cm^{-1})) = 394 (0.237 x10^5), 414 (0.279 x10^5), 522 (0.863 x10^4), 558 (0.155 x10^5), 596 (0.500 x10^4), 650 (0.105 x10^5).

Fluorescence (CH_2Cl_2, Excitation at 557 nm): 653, 699 nm.

3.28 Tribenzodiazathiaporphyrin (2.23e)

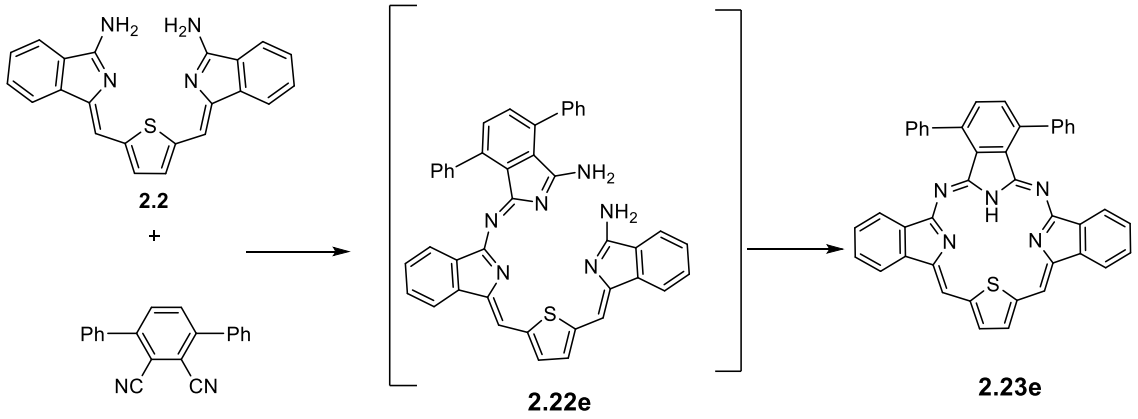

A mixture of bisaminoisoindoline thiophene **2.2** (100 mg, 0.27 mmol, 1 eq) and 3,6-diphenylbenzene-1,2-dicarbonitile (76 mg, 0.27 mmol, 1 eq) was heated in refluxing methanol in the presence of $NaOCH_3$ (approximately 3 mg) for 4 days. The solvent was removed under vacuum, and the product was isolated by column chromatography, eluting with THF: PE (2:1), then precipitated using THF: PE. The MALDI-TOF MS showed a peak at m/z 648, which corresponds to the expected mass of the open compound **2.22e**. The intermediate **2.22e** was then refluxed in *p*-xylene (3 mL) and the reaction monitored by TLC. The solvent was removed under an argon atmosphere while cooling. The resulting solid was purified by column chromatography eluting with THF/PE (1:4) and then recrystallised by slow evaporation from DCM: MeOH to give the title product as a purple-magenta solid (12 mg, 7%).

MP > 300°C

^{1}H NMR (500 MHz, Chloroform-*d*) δ 9.85 (s, 2H), 9.20 (s, 2H), 8.60 (d, *J* = 7.5 Hz, 2H), 8.14 (s, 2H), 8.10 – 8.05 (m, 4H), 7.88 (d, *J* = 7.4 Hz, 2H), 7.84 – 7.76 (m, 8H), 7.67 (t, *J* = 7.5 Hz, 2H).

MALDI-TOF-MS $(C_{42}H_{26}N_5S)^+$ m/z $[M+H]^+$ calcd: 632.19 found 632.55.

UV-vis (DCM): λ_{max} (nm) (ε (dm^3. mol^{-1} .cm^{-1})) = 416 (0.294 x10^5), 526 (0.115 x10^5), 562 (0.189 x10^5), 601 (0.670 x104), 656 (0.124 x10^5).

Fluorescence (CH_2Cl_2, Excitation at 562 nm): 663, 710 nm.

3.29 Tribenzodiazathiaporphyrin (2.25)

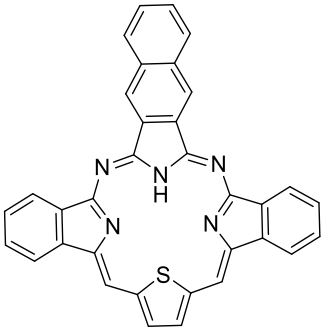

2.25

A mixture of bisaminoisoindoline thiophene **2.2** (100 mg, 0.272 mmol, 1 eq) and naphthalene-1,2-dicarbonitrile (0.9 mg, 0.543 mmol, 2 eq) was stirred in refluxing toluene (3 mL) under an argon atmosphere and monitored by TLC (4 days). The solvent was removed under vacuum, and the product was purified by column chromatography using THF: hexane (1:3) as eluent. The title compound was isolated as a purple-magenta solid (40 mg, 28%).

MP > 300°C

^{1}H&^{13}C NMR The compound is poorly soluble, even in THF solvent.

MALDI-TOF-MS $(C_{34}H_{19}N_5S)^+$ m/z $[M]^+$ calcd: 529.13 found 528.80.

UV-vis (THF): λ_{max} (nm) (ε (dm^3. mol^{-1} .cm^{-1})) = 359 (0.124 x10^5), 370 (0.125 x10^5), 391 (0.130 x10^5), 412 (0.149 x10^5), 536 (0.654 x10^4), 552 (0.626 x10^4), 573 (0.955 x10^4), 641 (0.666 x10^4).

Fluorescence (THF, Excitation at 572 nm): 646, 695 nm.

3.30 6-Bromo-1,1,4,4-tetramethyl-1,2,3,4-tetrahydronaphthalene-7-imidamide hydrochloride[26]

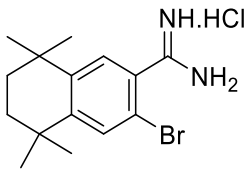

2.26

A solution of 2-bromobenzonitrile (1.43 g, 4.89 mmol) in dry THF (1 mL) was added to a solution of $LiN(SiMe_3)_2$ in anhydrous THF (5.38 ml, 5.38 mmol, 1.1 eq) and the reaction mixture was stirred at room temperature for 4 h. A 5 M HCl solution in isopropanol (15 mL) was added to the cooled mixture. The crude reaction mixture was left to stir at room temperature overnight. The precipitated product was filtered off and washed with diethyl ether to yield the title compound as colourless crystals (1.1g, 65%).

^{1}H NMR (500 MHz, Methanol-d_4) δ 7.70 (s, 1H), 7.54 (s, 1H), 1.74 (s, 4H), 1.31 (s, 6H), 1.30 (s, 6H).

3.31 Tribenzodiazathiaporphyrin (2.37a)

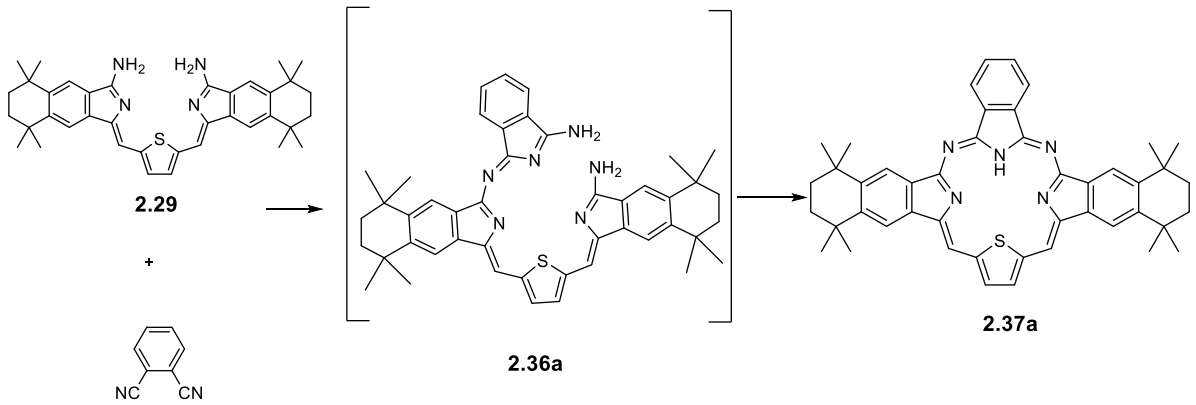

A mixture of 6-bromo-1,1,4,4-tetramethyl-1,2,3,4-tetrahydronaphthalene-7-imidamide hydrochloride (0.5 g, 1.446 mmol), BINAP (0.0495 g, 0.079 mmol), $PdCl_2(MeCN)_2$ (0.018 g, 0.072 mmol) and 2,5-bis [2-(trimethylsilyl)ethynyl] thiophene (0.19 g, 0.723 mmol) was sealed in a microwave vessel with a magnetic bar and then purged and refilled with N_2. Then, DBU (0.8 mL) in dry DMF (6 mL) was added, and the reaction mixture was stirred under N_2 for 5 min. Finally, the mixture was irradiated in a microwave reactor at 120℃ for 1 h. The mixture was poured into water (20 mL), and a red precipitate formed, which was filtered and washed with water. The title dried compound **2.29** as a red powder (0.52 g) (MALDI-MS: m/z 588.15) was used without further purification.

A mixture of bisaminoisoindoline **2.29** (100 mg) with phthalonitrile (21 mg, 0.17 mmol) was stirred in refluxing methanol (10 mL) in the presence of $NaOCH_3$ (approximately 3 mg) overnight under an argon atmosphere. After cooling, the solvent was evaporated under reduced pressure. The reaction mixture was purified by column chromatography using THF: PE (1:4) and then precipitated to afford the intermediate **2.36a** as a deep purple-blue solid. Then, a solution of intermediate **2.36a** in *p*-xylene (3 mL) was heated at reflux under an argon atmosphere and monitored by TLC (overnight). The solvent was removed, and the product was purified by column chromatography using DCM: PE (2:1) and then recrystallisation from DCM: MeOH to afford the desired compound as a purple-magenta solid (16 mg, 16% over two steps).

MP > 300℃

^{1}H NMR (400 MHz, Chloroform-*d*) δ 9.69 (s, 2H), 9.39 – 9.34 (m, 2H), 9.08 (s, 2H), 8.89 (s, 2H), 8.59 (s, 2H), 8.27 – 8.16 (m, 2H), 1.98 (s, 8H), 1.71 (s, 12H), 1.66 (s, 12H).

^{13}C NMR (101 MHz, Chloroform-*d*) δ 160.55, 149.44, 147.44, 146.54, 145.80, 145.76, 139.18, 137.54, 135.98, 131.43, 130.87, 123.99, 120.71, 118.49, 114.81, 35.58, 32.77.

MALDI-TOF-MS $(C_{46}H_{45}N_5S)^+$ m/z $[M]^+$ calcd: 699.33 found 700.09.

UV-vis (DCM): λ_{max} (nm) (ε (dm^3. mol^{-1} .cm^{-1})) = 395 (0.225 x10^5), 415 (0.247 x10^5),

523 (0.120 x10^5), 560 (0.213 x10^5), 600 (0.492 x10^4), 656 (0.995 x10^4).

Fluorescence (CH_2Cl_2, Excitation at 559 nm): 665, 711 nm.

3.32 Tribenzodiazathiaporphyrin (2.37b)

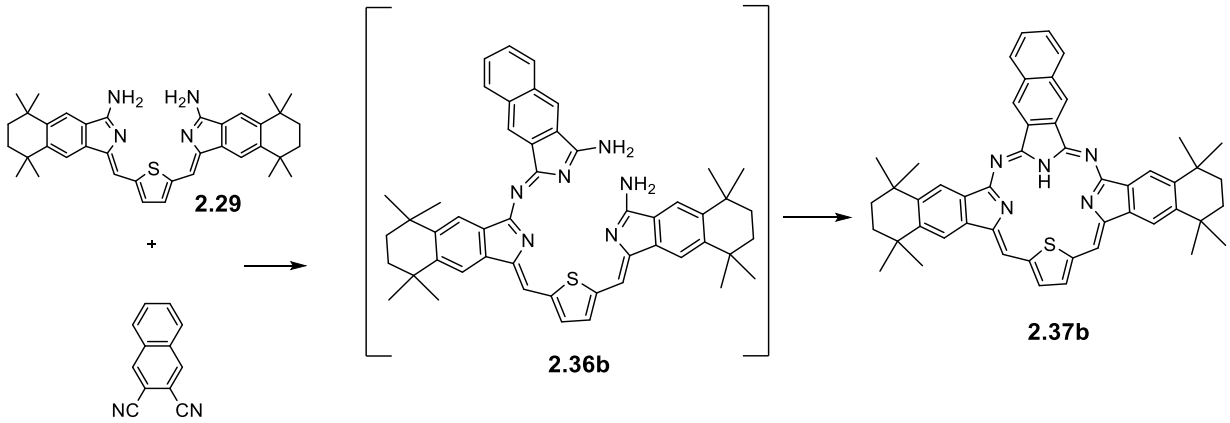

A mixture of bisaminoisoindoline thiophene **2.29** (100 mg) and naphthalene-2,3-dicarbonitile (30 mg, 0.171mmol) was heated in refluxing methanol in the presence of sodium methoxide (approximately 3 mg) under an argon atmosphere for 24h. The solvent was removed under vacuum, and the crude product was then purified by column chromatography using THF/PE (1:4) and then precipitated to separate the required intermediate **2.36b** (MALDI-MS: m/z 767). After that, intermediate **2.36b** was refluxed in *p*-xylene (3 mL) overnight. The solvent was removed under an argon atmosphere while cooling. The crude product was purified by column chromatography eluting with THF/PE (1:8) and then recrystallised using DCM: MeOH to afford the title product as a purple-magenta solid (14 mg, 13% over two steps).

MP > 300°C

^{1}H NMR (500 MHz, Chloroform-*d*) δ 9.78 (s, 2H), 9.42 (s, 2H), 8.83 (s, 2H), 8.81 (s, 2H), 8.52 – 8.48 (m, 2H), 8.44 (s, 2H), 7.84 – 7.80 (m, 2H), 1.88 (s, 8H), 1.62 (s, 12H), 1.54 (s, 12H).

^{13}C NMR (126 MHz, Chloroform-*d*) from HSQC NMR δ 124.60, 114.88, 130.44, 120.72, 130.12, 118.45, 127.85, 35.14, 32.55, 32.22

MALDI-TOF-MS $(C_{50}H_{47}N_5S)^+$ m/z $[M]^+$ calcd: 749.35 found 749.61.

UV-vis (DCM): λ_{max} (nm) (ε (dm^3. mol^{-1} .cm^{-1})) = 361 (0.422 x10^5), 395 (0.395 x10^5), 415 (0.376 x10^5), 539 (0.214 x10^5), 560 (0.208 x10^5), 578 (0.313 x10^5), 654 (0.183 x10^5).

Fluorescence (CH_2Cl_2, Excitation at 577 nm): 660, 710 nm.

3.33 2-Bromo-4,5-dimethoxybenzamidine hydrochloride[26]

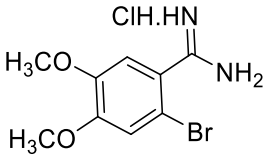

2.27

A solution of 2-bromo-4,5-dimethoxybenzonitrile (1.17 g, 4.8 mmol) in dry THF (1 mL) was added to a solution of $LiN(SiMe_3)_2$ in anhydrous THF (1M, 5.2 mL, 1.1 eq). The mixture was stirred for 4h at room temperature. After that, a 5M HCl solution in isopropanol (15 mL) was added to the cooled mixture. The reaction mixture was left to stir at room temperature overnight. The resulting solid was filtered off and washed with diethyl ether to afford the desired compound as colourless crystals (1.25 g, 88%).

^{1}H NMR (500 MHz, DMSO-*d_6*) δ 7.32 (s, 1H), 7.23 (s, 1H), 3.84 (s, 3H), 3.80 (s, 3H).

3.34 Compound (2.34)

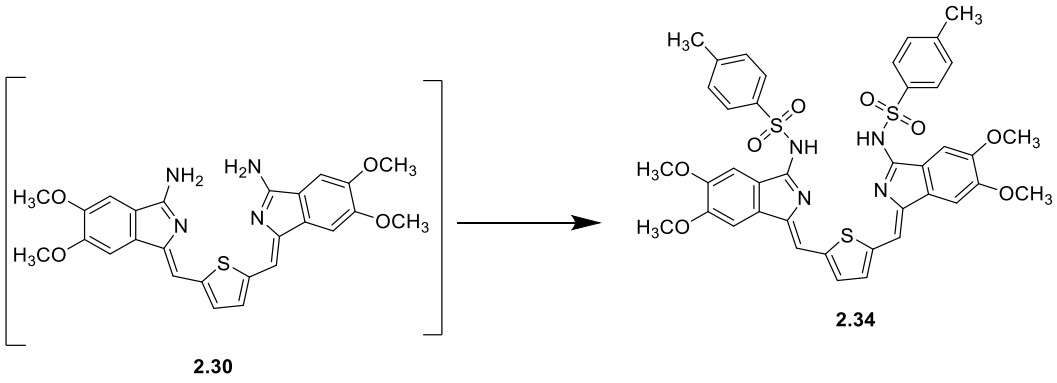

2.30 **2.34**

A mixture of 2-bromo-4,5-dimethoxybenzamidine hydrochloride **2.27** (0.5 g, 1.69 mmol), BINAP (0.058 g, 0.0930 mmol), $PdCl_2(MeCN)_2$ (0.0219 g, 0.084 mmol) and 2,5-bis [2-(trimethylsilyl)ethynyl] thiophene (0.23 g, 0.845 mmol) was sealed in a microwave vessel with a magnetic bar and then purged with N_2. Then, DBU (0.8 mL) and dry DMF (6 mL) were added, and the reaction mixture was stirred under N_2 for 5 min. The reaction mixture was irradiated in a microwave reactor at 120℃ for 1 h then the mixture was poured in 20 mL of water after cooling. A red precipitate is formed which was filtered and washed with water. The dried compound **2.30** (0.34 g) (MALDI-MS: m/z 487.77) as a red powder was used without further purification.

A mixture of crude **2.30** (50 mg) with 4-toluenesulfonyl chloride (38 mg, 0.20 mmol) was stirred in dry DCM (10 mL) and TEA (1 mL) overnight at room temperature. The reaction

mixture was diluted with H_2O, extracted with DCM, dried over $MgSO_4$ and filtered. The solvent was removed under reduced pressure then the crude material was purified by column chromatography using DCM: EtOAc (4:1) to afford product **2.34** as a red solid (33 mg, 33% over two steps).

MP > 300°C
^{1}H NMR (400 MHz, Chloroform-*d*) δ 10.30 (s, 2H, NH), 8.00 (d, *J* = 8.3 Hz, 4H), 7.32 (d, *J* = 8.1 Hz, 4H), 7.28 (s, 2H), 7.13 (s, 2H), 6.95 (s, 2H), 6.78 (s, 2H), 4.07 (s, 6H), 3.86 (s, 6H), 2.40 (s, 6H).
^{13}C NMR (101 MHz, Chloroform-*d*) δ 158.94, 153.94, 150.77, 143.42, 139.22, 138.84, 133.11, 129.94, 129.60, 129.48, 126.73, 123.23, 104.17, 101.74, 101.49, 56.59, 56.15, 21.58.
MALDI-TOF-MS $(C_{40}H_{36}N_4O_8S_3)^+$ m/z $[M]^+$ calcd: 796.16 found 796.57.
UV-vis (DCM): λ_{max} (nm) (ε (dm^3. mol^{-1} .cm^{-1})) = 264 (0.269 x10^5), 292 (0.262 x10^5), 485 (0.295 x10^5), 520 (0.229 x10^5).

Fluorescence (CH_2Cl_2, Excitation at 489 nm): 542 nm, shoulder peak 576 nm.

3.35 Tribenzodiazathiaporphyrin (2.37c)

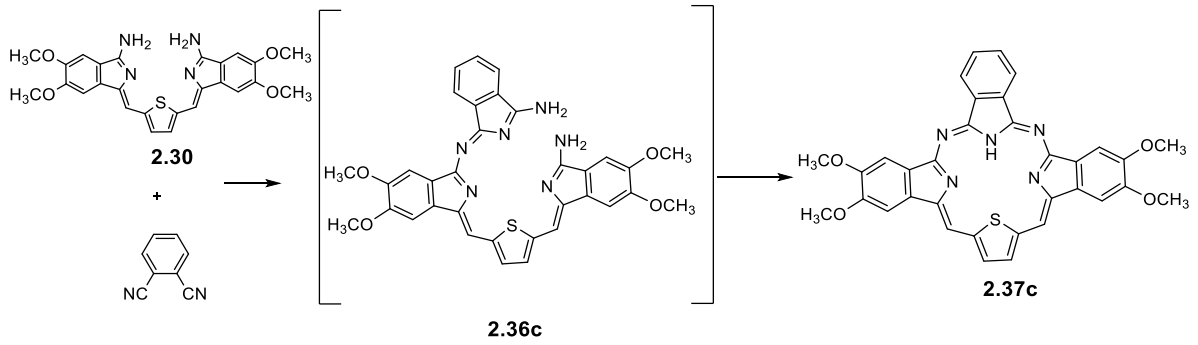

A mixture of crude bisaminoisoindoline thiophene **2.30** (0.10 g) and phthalonitrile (0.12 g, 0.204 mmol) was stirred in refluxing methanol (10 mL) in the presence of $NaOCH_3$ (approximately 3 mg) overnight under an argon atmosphere. Upon completion, the solvent was removed under vacuum, and the crude mixture was purified by column chromatography using (THF: PE (1:4)) then precipitated to get intermediate **2.36c** as confirmed by MALDI-TOF MS. The intermediate **2.36c** was refluxed in *p*-xylene (3 mL) overnight. Then, the solvent was removed under an argon stream while cooling. The residue was purified by column chromatography using THF: PE (1:8) as eluent. Recrystallisation from DCM and methanol gave the title compound as a purple-magenta solid (11 mg, 7% over two steps).

MP > 300°C
^{1}H NMR (500 MHz, Methylene Chloride-d_2) δ 9.36 (s, 2H), 9.25 – 9.19 (m, 2H), 8.86 (s, 2H), 8.27 – 8.21 (m, 4H), 7.93 (s, 2H), 4.29 (s, 6H), 4.22 (s, 6H).

MALDI-TOF-MS $(C_{34}H_{25}N_5O_4S)^+$ m/z $[M]^+$ calcd: 599.16 found 599.34.
UV-vis (DCM): λ_{max} (nm) (ε (dm^3. mol^{-1} .cm^{-1})) = 388 (0.269 x10^5), 408 (0.308 x10^5), 523 (0.112 x10^5), 560 (0.19663 x10^5), 595 (0.5816 x10^4), 650 (0.108 x10^5).

Fluorescence (CH_2Cl_2, Excitation at 559 nm): 657, 705 nm.

3.36 Compound (2.36d)

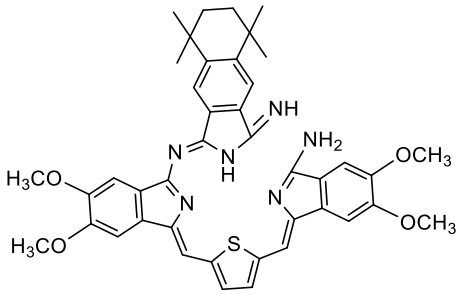

2.36d

A mixture of crude bisaminoisoindoline thiophene **2.30** (100 mg) with 6,7-dicyano-1,2,3,4-tetrahydro-1,1,4,4-tetramethylnaphthalene (48 mg, 0.272 mmol) was stirred in refluxing methanol (10 mL) in the presence of sodium methoxide (approximately 3 mg) overnight under an argon atmosphere. Upon completion, the solvent was removed under vacuum and the crude solid was purified by column chromatography using THF: PE (1:4) and then recrystallised from DCM and methanol to give the title compound as a deep purple-blue solid (26 mg, 14% over two steps).

MP > 300°C
^{1}H NMR (500 MHz, Methylene Chloride-d_2) δ 8.03 (s, 1H), 7.94 (s, 1H), 7.41 (s, 1H), 7.25 (s, 1H), 7.23-7.19 (m, 2H), 7.15 (s, 1H), 7.11 (d, *J* = 4.0 Hz, 1H), 6.97 (s, 1H), 6.85 (s, 1H), 3.94 (s, 3H), 3.91 (s, 3H), 3.89 (s, 3H), 3.83 (s, 3H), 1.71 (s, 4H), 1.37 (s, 6H), 1.32 (s, 6H).
MALDI-TOF-MS $(C_{42}H_{43}N_6O_4S)^+$ m/z $[M+H]^+$ calcd: 727.30 found 727.79.
UV-vis (DCM): λ_{max} (nm) (ε (dm^3. mol^{-1} .cm^{-1})) = 354 (0.437 x10^5), 367 (0.442 x10^5), 582 (0.199 x10^5).

3.37 Tribenzodiazathiaporphyrin (2.37d)

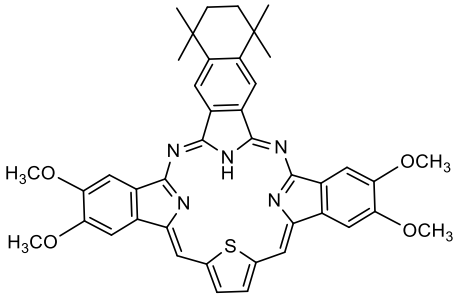

2.37d

A solution of the intermediate **2.36d** (24 mg, 0.033 mmol) in *p*-xylene (3 mL) was heated to reflux overnight under an argon atmosphere. Upon completion, the solvent was removed under an argon stream while cooling. Finally, the crude material was purified by column chromatography using THF: PE (1:8) then recrystallised from DCM and methanol to give the title compound as a purple-magenta solid (13 mg, 52%).

MP > 300°C

^{1}H NMR (500 MHz, Methylene Chloride-d_2) δ 9.55 (s, 2H), 9.29 (s, 2H), 8.99 (s, 2H), 8.37 (s, 2H), 8.01 (s, 2H), 4.22 (s, 6H), 4.14 (s, 6H), 1.98 (s, 4H), 1.71 (s, 12H).

MALDI-TOF-MS $(C_{42}H_{39}N_5O_4S)^+$ m/z $[M]^+$ calcd: 709.27 found 709.03.

UV-vis (DCM): λ_{max} (nm) (ε (dm^3. mol^{-1} .cm^{-1})) = 377 (0.322 x10^5), 406 (0.316 x10^5), 525 (0.118 x10^5), 564 (0.205 x10^5), 590 (0.7216 x10^4), 645 (0.118 x10^5).

Fluorescence (CH_2Cl_2, Excitation at 564 nm): 652, 696 nm.

3.38 2-bromo-4,5-bis(hexyloxy)-benzamidine hydrochloride[26]

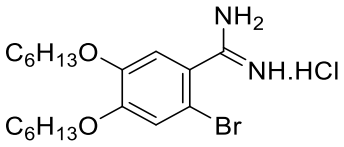

2.28

A solution of 2- bromo-4,5-bis(hexyloxy)-benzonitrile (1.4 g, 3.7 mmol) in dry THF (3 mL) was added to a solution of $LiN(SiMe_3)_2$ in anhydrous THF (1M, 4 mL, 4 mmol, 1.1 eq). The reaction was stirred at room temperature for 4h. A 5M HCl solution in isopropanol (15 mL) was added to the cooled mixture and stirred overnight. The precipitate was filtered and washed with diethyl ether to yield the desired compound as colourless crystals (1.46 g, 91%).

^{1}H NMR (500 MHz, Methanol-d_4) δ 7.27 (s, 1H), 7.14 (s, 1H), 4.08 – 3.97 (m, 4H), 1.86 – 1.69 (m, 4H), 1.56 – 1.43 (m, 4H), 1.39 – 1.28 (m, 8H), 0.97 – 0.85 (m, 6H).

3.39 Compound (2.35)

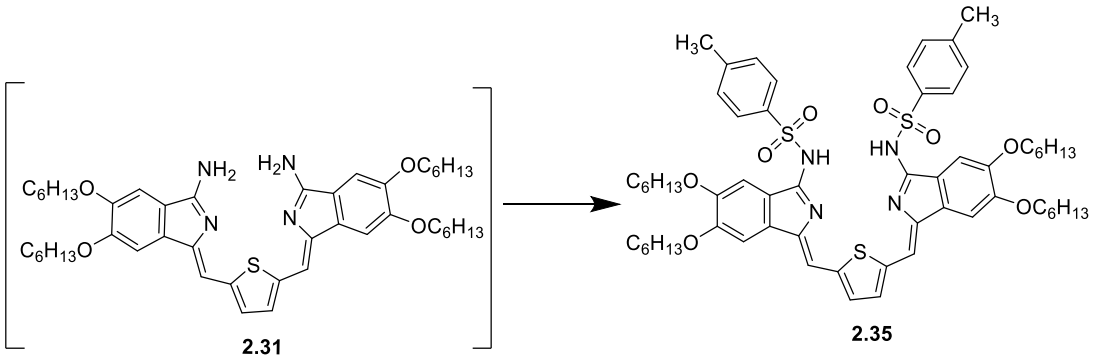

A mixture of 2-bromo-4,5-bis(hexyloxy)-benzamidine hydrochloride **2.28** (0.4 g, 0.917 mmol), BINAP (0.031 g, 0.050 mmol), $PdCl_2(MeCN)_2$ (0.011 g, 0.045 mmol) and 2,5-bis [2-(trimethylsilyl)ethynyl] thiophene (0.126 g, 0.458 mmol) was sealed in a microwave vessel with a magnetic bar and then purged with N_2. Then, DBU (0.8 mL) and dry DMF (6 mL) were added, and the reaction mixture was stirred under N_2 for 5 min. The mixture was then irradiated in a microwave reactor at 120 ˚C for 1 h. After cooling, the mixture was poured into water (20 mL), and a red precipitate formed, which was filtered and washed with water. The title dried compound **2.31** (0.32 g) (MALDI-MS: m/z 768.34) was used without further purification.

A mixture of crude **2.31** (50 mg) with 4-toluenesulfonyl chloride (24 mg, 0.13 mmol) was stirred in dry DCM (10 mL) and TEA (1 mL) overnight at room temperature. The reaction mixture was diluted with H_2O, extracted with DCM, dried over $MgSO_4$, and filtered. The solvent was removed under reduced pressure and then purified by column chromatography using DCM: EtOAc (4:1) to afford the product **2.30** as a red solid (21 mg, 28% over two steps).

MP 210°C

^{1}H NMR (400 MHz, Chloroform-*d*) δ 10.52 (s, 2H, NH), 7.96 (d, *J* = 8.4 Hz, 4H), 7.32-7.27(m, 6H), 7.24 (s, 2H), 7.13 (s, 2H), 6.71 (s, 2H), 4.12 (t, *J* = 6.6 Hz, 4H), 4.01 (t, *J* = 6.6 Hz, 4H), 2.40 (s, 6H), 1.92 – 1.79 (m, 8H), 1.53 – 1.43 (m, 8H), 1.39 – 1.31 (m, 16H), 0.95 – 0.87 (m, 12H).

^{13}C NMR (126 MHz, Chloroform-*d*) δ 159.08, 154.15, 151.07, 143.27, 139.15, 139.07, 133.55, 129.91, 129.50, 129.08, 126.65, 123.38, 106.21, 102.54, 101.12, 69.48, 69.36, 53.43, 31.51, 28.97, 28.94, 25.64, 25.62, 22.58, 21.56, 18.45, 14.00, 13.97.

MALDI-TOF-MS $(C_{60}H_{76}N_4O_8S_3)^+$ m/z $[M]^+$ calcd: 1076.48 found: 1076.85.

UV-vis (DCM): λ_{max} (nm) (ε (dm^3. mol^{-1} .cm^{-1})) = 265 (0.405 x10^5), 293 (0.406 x10^5), 487 (0.393 x10^5), 523 (0.318 x10^5).

Fluorescence (CH_2Cl_2, Excitation at 485 nm): 544 nm.

3.40 Tribenzodiazathia porphyrin (2.37e)

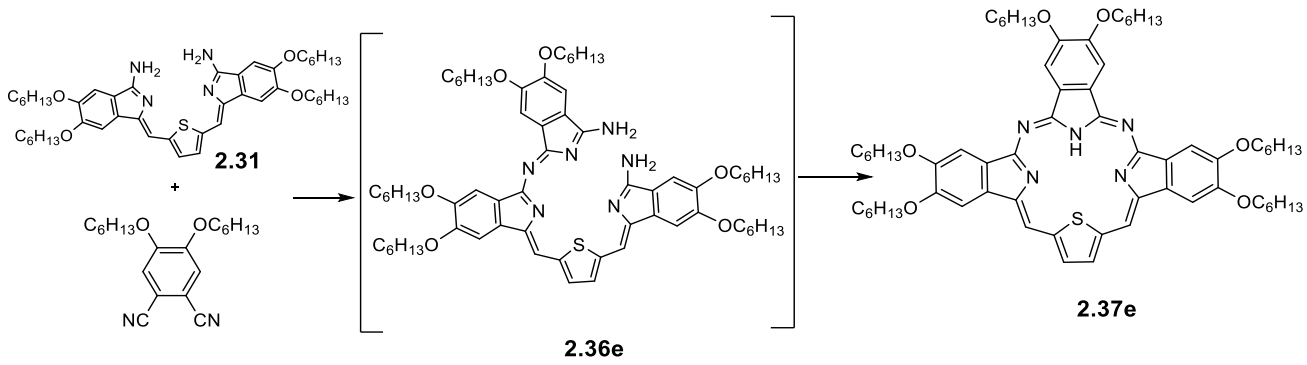

A mixture of crude bisaminoisoindoline thiophene **2.31** (100 mg) and 1,2-dicyano-4,5-bis(hexyloxy)benzene (42 mg, 0.13 mmol) was stirred to reflux in methanol (10 mL) under an argon atmosphere in the presence of sodium methoxide (approximately 3 mg) overnight. After cooling to room temperature, the solid was filtered and washed with methanol several times to afford a deep purple-blue product (MALDI-MS: m/z 1098) that is assumed to be the open compound **2.36e**. Then, the resulting solid was heated to reflux in *p*-xylene (3 mL) overnight to get the desired compound that was purified by column chromatography using DCM: PE (3:1) to afford the title compound as a purple-magenta solid (7.7 mg, 5% over two steps).

MP 142°C

^{1}H NMR (500 MHz, TCE-d_2 at 70°C) δ 9.52 (s, 2H), 8.96 (s, 2H), 8.75 (s, 2H), 8.44 (s, 2H), 8.01 (s, 2H), 4.50 (t, J = 6.4 Hz, 4H), 4.38 (t, J = 6.5 Hz, 4H), 4.31 (t, J = 6.5 Hz, 4H), 2.07 – 1.93 (m, 12H), 1.70 – 1.58 (m, 12H), 1.46 – 1.37 (m, 24H), 1.01 – 0.86 (m, 18H).

MALDI-TOF-MS $(C_{66}H_{89}N_5O_6S)^+$ m/z $[M]^+$ calcd: 1079.65 found: 1079.46.

UV-vis (DCM): λ_{max} (nm) (ε (dm^3. mol^{-1} .cm^{-1})) = 411 (0.456 x10^4), 526 (0.136 x10^4), 563 (0.242 x10^4), 597 (0.744 x10^3), 652 (0.1388 x10^4).

Fluorescence (CH_2Cl_2, Excitation at 563 nm): 656, 703 nm.

3.41 Compound (2.32)

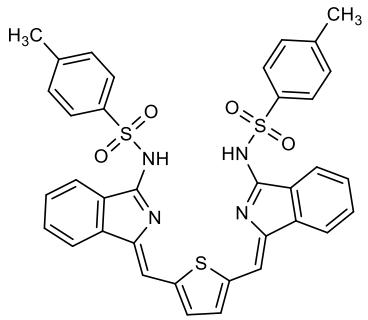

2.32

Following the general procedure of tosylation,[133] a mixture of **2.2** (300 mg, 0.81 mmol, 1 eq) and 4-toluenesulfonyl chloride (310 mg, 1.6 mmol, 2 eq) was stirred in dry DCM (20 mL) and TEA (1 mL) overnight at room temperature. The reaction mixture was diluted with H_2O, extracted by DCM, dried over $MgSO_4$, and filtered. Then, the solvent was removed under reduced pressure, and the resulting solid was purified by column chromatography using DCM: PE (1:2) and then DCM to afford the product as a red solid (200 mg, 36%).

MP 266℃

^{1}H NMR (400 MHz, Chloroform-*d*) δ 10.74 (s, 2H, NH), 7.97 (d, *J* = 8.3 Hz, 4H), 7.86 (d, *J* = 7.8 Hz, 2H), 7.75 (d, *J* = 7.7 Hz, 2H), 7.63 (t, *J* = 7.6 Hz, 2H), 7.45 (t, *J* = 7.5 Hz, 2H), 7.34 (s, 2H), 7.29 (d, *J* = 8.1 Hz, 4H), 6.84 (s, 2H), 2.39 (s, 6H).

^{13}C NMR (101 MHz, Chloroform-*d*) δ 158.67, 143.46, 139.26, 138.74, 135.83, 133.31, 133.01, 130.89, 129.72, 129.53, 129.38, 126.74, 124.27, 119.91, 102.04, 21.57.

MALDI-TOF-MS $(C_{36}H_{28}N_4O_4S_3)^+$ m/z $[M]^+$ calcd: 676.12 found 676.64.

UV-vis (DCM): λ_{max} (nm) (ε (dm^3. mol^{-1} .cm^{-1})) = 297 (0.266 x10^5), 481 (0.114 x10^5), 512 (0.358 x10^5).

Fluorescence (CH_2Cl_2, Excitation at 481 nm): 533, 569 nm.

3.42 Compound (2.33)

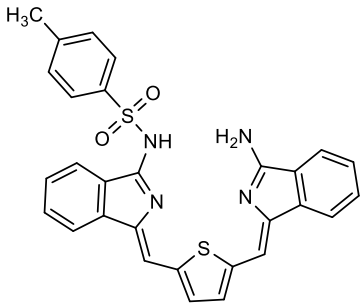

2.33

This compound was isolated from the previous reaction as a side product and was obtained as a dark red solid (50 mg, 12%).

MP 152℃

^{1}H NMR (500 MHz, Methylene Chloride-d_2) δ 10.94 (s, 1H, NH), 8.11 (d, *J* = 8.4 Hz, 2H), 7.90 (d, *J* = 7.7 Hz, 1H), 7.79-7.75 (m, 2H), 7.65 (td, *J* = 7.6, 1.1 Hz, 1H), 7.51 – 7.45 (m, 3H), 7.38 (td, *J* = 7.4, 1.0 Hz, 1H), 7.30 (d, *J* = 7.8 Hz, 2H), 7.23 – 7.21 (m, 1H), 7.121-7.18 (m, 1H), 7.04 (s, 1H), 6.99 (s, 1H), 5.80 (s, 2H, NH), 2.37 (s, 3H).

^{13}C NMR (126 MHz, $CDCl_3$) δ 164.10, 158.49, 149.00, 144.75, 143.31, 141.40, 140.78, 139.15, 136.49, 132.56, 132.49, 131.16, 130.48, 129.83, 129.60, 129.10, 128.55, 128.14, 127.26, 126.90, 124.25, 119.97, 119.56, 119.50, 108.51, 105.25, 21.51.

MALDI-TOF-MS $(C_{29}H_{22}N_4O_2S_2)^+$ m/z $[M]^+$ calcd: 522.11 found 522.51.

UV-vis (DCM): λ_{max} (nm) (ε (dm^3. mol^{-1} .cm^{-1})) = 300 (0.871 x10^4), 361 (0.672 x10^4), 503 (0.965 x10^4), 549 (0.698 x10^4).

Fluorescence (CH_2Cl_2, Excitation at 505 nm): 597 nm.

3.43 1-Amino-3,3-dimethoxybenzoisoindoline[111]

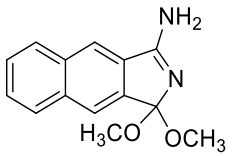

2.39

2,3-Dicyanonaphthalene (0.1 g, 0.55 mmol) was added to a solution of methanol (10 mL) and sodium metal (0.06 g, 2.8 mmol). The solution was stirred at 35 ˚C for 6 h. The reaction mixture was poured into ice water and then filtered, and the solid was washed with cold water to afford the title compound as a yellow solid (0.09 g, 67%).

^{1}H NMR (500 MHz, Chloroform-*d*) δ 7.97 – 7.90 (m, 3H), 7.82 (s, 1H), 7.61 – 7.53 (m, 2H), 3.46 (s, 6H).

3.44 Compound (2.40)

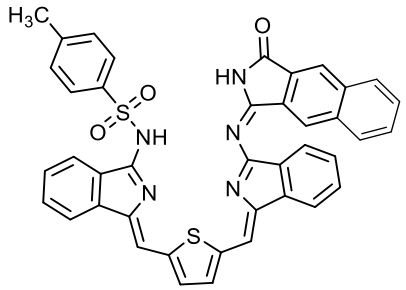

2.40

The mixture of **2.33** (0.2 g, 0.38 mmol) and amino-3,3-dimethoxybenzoisoindoline (0.09 g, 0.38 mmol) was stirred in dry DCM (10 mL) under an argon atmosphere and the reaction was monitored by TLC. Upon completion, the solid was filtered off and washed with methanol. The final product was isolated by column chromatography (DCM: Pet ether: THF (1:1:0.2)) and then recrystallised by slow evaporation from DCM: MeOH to obtain the title product as a purple solid (60 mg, 23%).

MP > 300°C
^{1}H NMR (500 MHz, Chloroform-*d*) δ 12.09 (s, 1H, NH), 10.74 (s, 1H, NH), 8.59 (s, 1H), 8.32 (s, 1H), 8.04 (d, *J* = 7.7 Hz, 1H), 7.98 (d, *J* = 7.4 Hz, 2H), 7.86 (d, *J* = 7.7 Hz, 1H), 7.79 (d, *J* = 8.3 Hz, 2H), 7.75 (d, *J* = 7.3 Hz, 1H), 7.66 – 7.57 (m, 3H), 7.47 – 7.37 (m, 6H), 7.29 (d, *J* = 4.3 Hz, 1H), 7.11 (d, *J* = 8.1 Hz, 2H), 6.84 (s, 1H), 2.23 (s, 3H).
MALDI-TOF-MS $(C_{41}H_{28}N_5O_3S_2)^+$ m/z $[M+H]^+$ calcd: 702.16 found 702.10.
UV-vis (DCM): λ_{max} (nm) (ε (dm^3. mol^{-1} .cm^{-1})) = 386 (0.172 x10^5), 402 (0.170 x10^5), 551 (0.174 x10^5), 590 (0.128 x10^5).

Fluorescence (CH_2Cl_2, Excitation at 550 nm): 625 nm.
FT-IR (liquid, cm^{-1})**:** 1734 (C=O)

3.45 2,4-Bis(trimethylsilylethynyl)thiophene (2.41) [134]

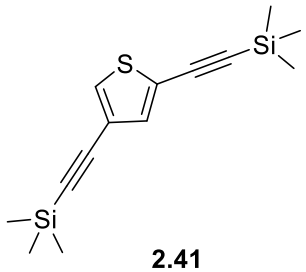

2.41

To a dry round bottomed flask, (trimethylsilyl)acetylene (1.23 g, 12.5 mmol) was added to a mixture of 2,4-dibromothiophene (0.60 g, 2.5 mmol), Cul (0.095 g, 0.5 mmol), and Pd $(PPh_3)_2Cl_2$ (0.176 g, 0.25 mmol) in triethylamine (5 mL) and THF (10 mL) under an argon

atmosphere, and the mixture was heated to reflux overnight. The cold solution was filtered through a bed of Celite. The filtrate was evaporated under reduced pressure and the residue was finally purified by silica gel column chromatography using petroleum ether to afford the desired product 2.41 as yellow oil (0.64 g, 93%).

^{1}H NMR (500 MHz, Chloroform-*d*) δ 7.33 (d, *J* = 1.3 Hz, 1H), 7.21 (d, *J* = 1.3 Hz, 1H), 0.24 (s, 9H), 0.23 (s, 9H).

3.46 Bisaminoisoindoline thiophene (2.42)

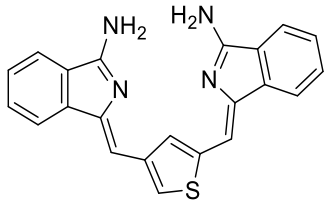

2.42

A mixture of amidine **2.1** (0.5 g, 2.1 mmol, 2 eq), BINAP (0.0725 g, 0.12 mmol) and $PdCl_2(MeCN)_2$ (0.0275 g, 0.11 mmol) was sealed in a microwave vessel with a magnetic stirrer bar and purged with N_2. A solution of 2,4 bis-[2-(trimethylsilyl)ethynyl]thiophene (0.293 g, 1.1 mmol, 1 eq) and DBU (0.8 mL) in dry DMF (6 mL) was added. The reaction mixture was stirred at room temperature under N_2 for 5 min. After that, the reaction mixture was irradiated in a microwave reactor at 120 °C for 1h. After cooling, the solution was poured into water, and a green precipitate formed, which was filtered and washed with water. The dried solid was dissolved in acetone, the solution filtered through a bed of Celite, then 2-3 drops of conc. HCl was added, causing a precipitate. The solid was filtered off, and CH_3OH (20 mL)/ CH_3ONa (10 mg) were added to the solid. The product was stirred for 5 min and then poured into water to give the title compound as a green powder (0.16 g, 40%).

MP > 300°C
^{1}H NMR (500 MHz, Methanol-d_4) δ 7.94 (s, 1H), 7.87 (s, 1H), 7.84 – 7.80 (m, 2H), 7.77 – 7.74 (m, 2H), 7.51 – 7.47 (m, 2H), 7.41 – 7.37 (m, 2H), 7.04 (s, 1H), 6.78 (s, 1H).

MALDI-TOF-MS$(C_{22}H_{16}N_4S)^+$ m/z $[M]^+$ calcd: 368.10 found: 368.23.
UV-vis (THF): λ_{max} (nm) (ε (dm^3. mol^{-1} .cm^{-1})) = 387 (0.229 x10^5).

Fluorescence (THF, Excitation at 388 nm): 494 nm.

3.47 *S*-confused *cis*-disazatribenzothiaporphyrin (2.44)

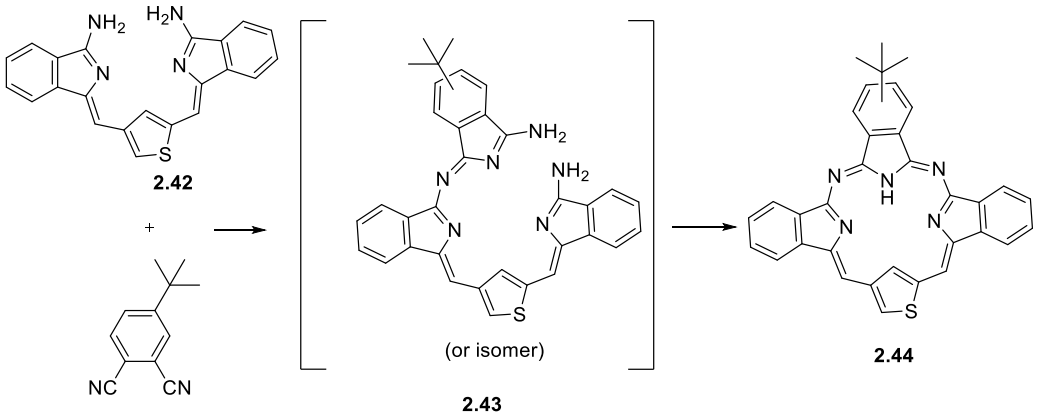

A mixture of **2.42** (160 mg, 0.434 mmol, 1 eq) and 4-*tert*-butylphthalonitrile (80 mg, 0.434 mmol, 1 eq) was stirred in refluxing methanol (10 mL) in the presence of sodium methoxide (approximately 3 mg) under an argon atmosphere for 24h. The solvent was removed under vacuum, and the crude product was purified by column chromatography using THF/ PE (1:4) then THF/ PE (1:1) to collect the dark red fraction (MALDI-MS: m/z 552) that identified as the open compound **2.43**. The dark red fraction was precipitated with THF/ PE (1:3) and filtered off. Then, the solid was heated overnight in refluxing xylene (3 mL). Upon completion, the solvent was removed under an argon atmosphere while cooling. The crude product was purified by column chromatography eluting with THF/ PE (1:4) and then recrystallised by slow evaporation from DCM: MeOH to give the title product as a red solid (16 mg, 7%).

MP > 300°C

^{1}H NMR (500 MHz, Methylene Chloride-d_2) δ 8.35 (d, *J* = 1.7 Hz, 1H), 8.34 (d, *J* = 1.6 Hz, 1H), 8.28-8.23 (m, 2H), 8.21 – 8.12 (m, 4H), 8.02 (s, 2H), 7.95 – 7.85 (m, 6H), 7.62 – 7.54 (m, 8H), 7.52 (s,1H), 7.50 (s, 1H), 7.48 (s,1H), 7.47 (s, 1H), 6.63 (s, 2H), 1.62 (s, 18H) for two isomers.

MALDI-TOF-MS($C_{34}H_{25}N_5S$)$^+$ m/z $[M]^+$ calcd: 535.18 found: 535.78.

UV-vis (DCM): λ_{max} (nm) (ε (dm^3. mol^{-1} .cm^{-1})) = 270 (0.225 x10^5), 339 (0.267 x10^5), 407 (0.101 x10^5), 432 (0.971 x10^4), 511 (0.783 x10^4), 553 (0.599 x10^4).

Fluorescence (CH_2Cl_2, Excitation at 509 nm): 604 nm.

3.48 *S*-confused *cis*-diazatribenzothiaporphyrin (2.46)

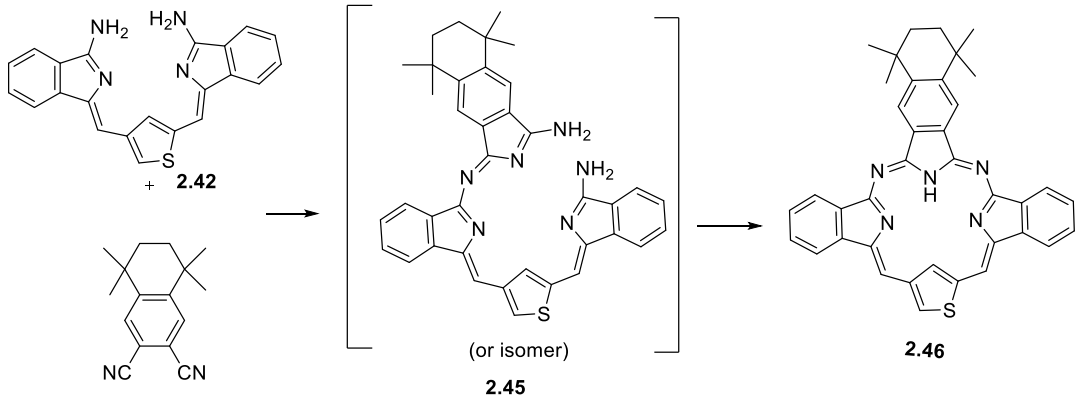

A mixture of bisaminoisoindoline thiophene **2.42** (0.1 g, 0.271 mmol) and 6,7-dicyano-1,2,3,4-tetrahydro-1,1,4,4-tetramethylnaphthalene (0.064 g, 0.271 mmol) was stirred in refluxing methanol in the presence of $NaOCH_3$ (approximately 3 mg) under an argon atmosphere overnight. After cooling, the solvent was evaporated, and the solid was purified by column chromatography using a solvent system 2:1 PE to THF then 1:1 PE to THF to yield the open compound **2.45**. The open compound **2.45** was precipitated from THF: PE then the dried solid was refluxed in *p*-xylene (3 mL) overnight. Upon completion, the solvent was removed under an argon atmosphere while cooling. The crude product was purified by column chromatography eluting with THF/ PE (1:5) then recrystallised by slow evaporation from DCM: MeOH to obtain the title compound **2.46** as a red solid (17 mg, 11%).

MP > 300°C

^{1}H NMR (500 MHz, Chloroform-*d*) δ 9.13 (s, 1H, NH), 8.48 (s, 2H), 8.37 – 8.32 (m, 2H), 8.12 (s, 1H), 8.06 – 7.99 (m, 2H), 7.78 (s, 1H), 7.74 (s, 1H), 7.62 – 7.57 (m, 4H), 7.19 (s, 1H), 1.89 (s, 4H), 1.57 (s, 12H).

MALDI-TOF-MS $(C_{38}H_{31}N_5S)^+$ m/z $[M]^+$ calcd: 589.22 found 589.71.

UV-vis (DCM): λ_{max} (nm) (ε (dm^3. mol^{-1} .cm^{-1})) = 268 (0.308 x10^5), 340 (0.345 x10^5), 357 (0.327 x10^5), 373 (0.304 x10^5), 408 (0.135 x10^5), 433 (0.129 x10^5), 507 (0.113 x10^5), 550 (0.862 x10^4).

Fluorescence (CH_2Cl_2, Excitation at 509 nm): 599 nm.

3.49 *S*-confused *cis*-diazatribenzothiaporphyrin (2.48a)

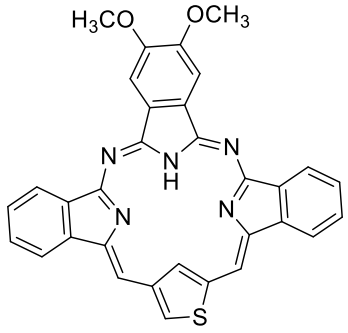

2.48a

A mixture of **2.42** (100 mg, 0.272 mmol, 1 eq) and 4,5-bis(methyloxy)benzene-1,2-dicarbonitrile (100 mg, 0.543 mmol, 2 eq) was stirred in refluxing xylene (3 ml) under an argon atmosphere and monitored by TLC (around 4 days). The solvent was then removed under vacuum, and the product was purified by column chromatography using THF: PE (1:4) as eluent. Recrystallisation from DCM and methanol gave the title compound as a red solid (31 mg, 21%).

MP > 300°C

^{1}H NMR (500 MHz, TCE-d_2) δ 8.39 – 8.32 (m, 2H), 8.20 (s, 1H), 8.11 – 8.02 (m, 2H), 7.96 (s, 2H), 7.82 (s, 1H), 7.78 (s, 1H), 7.68 – 7.57 (m, 4H), 6.92 (s, 1H), 4.21 (s, 6H).

MALDI-TOF-MS $(C_{32}H_{21}N_5O_2S)^+$ m/z $[M]^+$ calcd: 539.14 found 538.95.

UV-vis (DCM): λ_{max} (nm) (ε (dm^3. mol^{-1} .cm^{-1})) = 271 (0.262 x10^5), 340 (0.308 x10^5), 359 (0.276 x10^5), 375 (0.266 x10^5), 406 (0.127 x10^5), 431 (0.110 x10^5), 515 (0.875 x10^4), 554 (0.661 x10^4).

Fluorescence (CH_2Cl_2, Excitation at 515 nm): 605 nm.

3.50 *S*-confused *cis*-diazatribenzothiaporphyrin (2.48b)

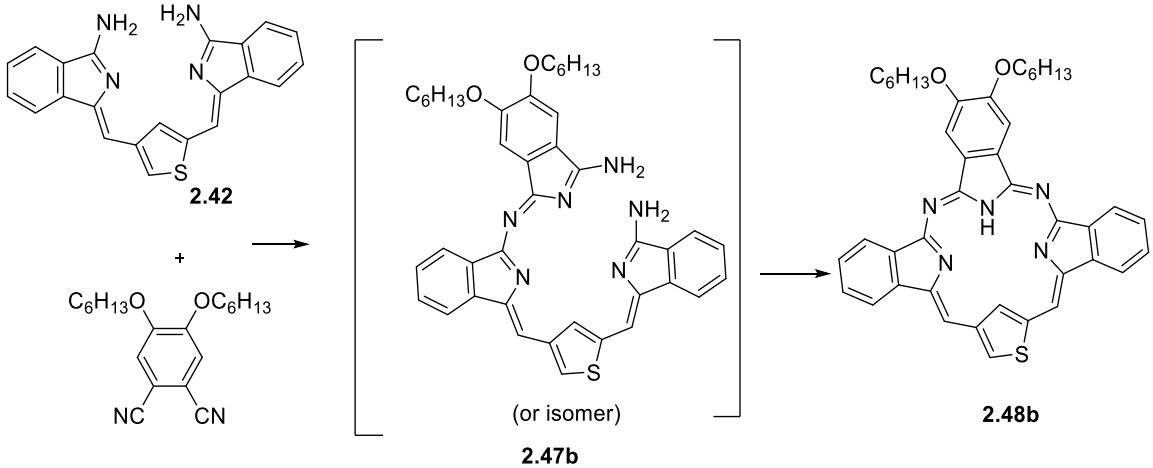

2.42

2.47b

2.48b

A mixture of compound **2.42** (100 mg, 0.27 mmol, 1eq) and 1,2-dicyano-4,5-bis(hexyloxy)benzene (90 mg, 0.27 mmol, 1 eq) was stirred in refluxing methanol (10 mL) in the presence of sodium methoxide (approximately 3 mg) overnight. After evaporation of the solvent under reduced pressure, the resulting crude was subjected to a column chromatography in silica gel using (1:1) THF/PE as a solvent system to yield the intermediate compound **2.47b** as deep red solid. Then, the product **2.47b** was precipitated with THF/PE and filtered. The resulting deep red solid **2.47b** was refluxed in *p*-xylene (3 mL) overnight. After that, the solid was purified by column chromatography in (3:1) DCM/PE. The product was recrystallised by slow evaporation from DCM/ MeOH to give the title compound as a red solid (12 mg, 7%).

MP 218°C

^{1}H NMR (500 MHz, TCE-d_2**)** δ 8.99 (s, 1H, NH), 8.41 – 8.35 (m, 2H), 8.24 (s, 1H), 8.16 – 8.09 (m, 2H), 7.99 (s, 2H), 7.92 (s, 1H), 7.87 (s, 1H), 7.70 – 7.58 (m, 4H), 7.17 (s, 1H), 4.37 (t, J = 6.4 Hz, 4H), 2.08 – 1.97 (m, 4H), 1.71 – 1.62 (m, 4H), 1.54 – 1.48 (m, 8H), 1.02 (t, J = 7.1 Hz, 6H).

^{13}C NMR (126 MHz, $C_2Cl_4D_2$) δ 68.06, 31.78, 29.35, 25.79, 22.85, 14.35 (Aliphatic region)

MALDI-TOF-MS $(C_{42}H_{41}N_5O_2S)^+$ m/z $[M]^+$ calcd: 679.29 found : 679.99.

UV-vis (DCM): λ_{max} (nm) (ε (dm^3. mol^{-1} .cm^{-1})) = 271 (0.362 x10^5), 340 (0.402 x10^5), 360 (0.371 x10^5), 377 (0.364 x10^5), 407 (0.175 x10^5), 432 (0.152 x10^5), 513 (0.117 x10^5), 552 (0.918 x10^4).

Fluorescence (CH_2Cl_2, Excitation at 514 nm): 604 nm.

3.51 *S*-confused *cis*-diazatribenzothiaporphyrin (2.48c)

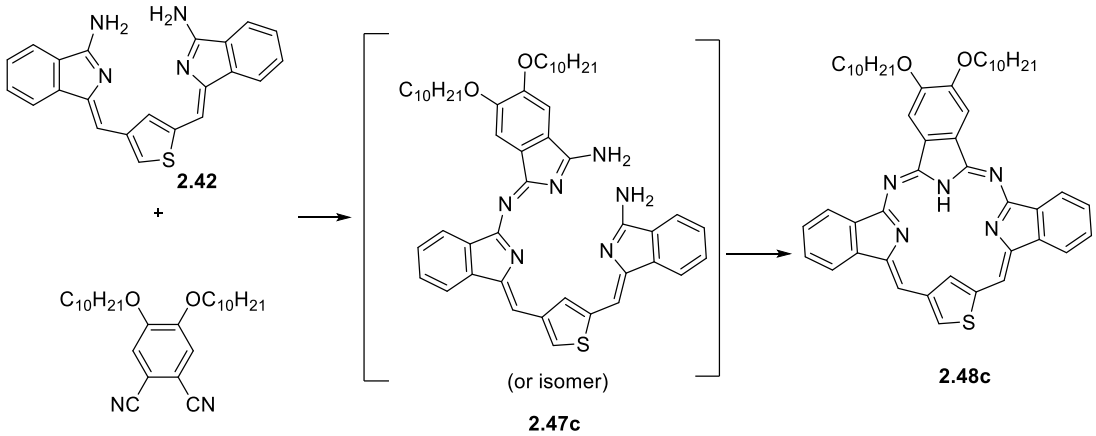

A mixture of **2.42** (100 mg, 0.272 mmol, 1 eq) and 4,5-bis(decyloxy)benzene-1,2-dicarbonitrile (120 mg, 0.272 mmol, 1eq) was stirred in refluxing methanol (10 mL) in the presence of $NaOCH_3$ (approximately 3 mg) under an argon atmosphere overnight. The solvent was removed under vacuum, and the crude mixture was purified by column chromatography using

(THF: PE (1:4)) to yield the intermediate compound **2.47c,** precipitated with THF/PE, and filtered. The solid was heated to reflux in *p*-xylene (3 mL) overnight. The solvent was removed under an argon stream while cooling. The resulting solid was separated by column chromatography through silica gel using THF: PE (1:8) as eluent and recrystallised by slow evaporation from DCM and methanol to give the title compound as a red solid (18 mg, 9%).

MP 184°C

^{1}H NMR (400 MHz, Chloroform-*d*) δ 8.77 (s, 1H, NH), 8.32 – 8.26 (m, 2H), 8.13 (s, 1H), 8.06- 7.98 (m, 2H), 7.85 (s, 2H), 7.78 (s, 1H), 7.74 (s, 1H), 7.63 – 7.54 (m, 4H), 6.96 (s, 1H), 4.31 (t, *J* = 6.6 Hz, 4H), 2.07 – 1.94 (m, 4H), 1.68 – 1.58 (m, 4H), 1.50 – 1.43 (m, 4H), 1.42 – 1.27 (m, 20H), 0.95 – 0.75 (m, 6H).

^{13}C NMR (126 MHz, Chloroform-*d*) δ 166.82, 166.31, 153.97, 153.67, 153.04, 147.92, 141.97, 141.59, 137.88, 137.76, 128.97, 128.65, 128.53, 127.50, 127.38, 121.95, 121.81, 119.35, 119.23, 106.13, 69.61, 32.13, 29.90, 29.83, 29.71, 29.59, 29.41, 26.32, 22.89, 14.30.

MALDI-TOF-MS $(C_{50}H_{57}N_5O_2S)^+$ m/z $[M]^+$ calcd: 791.42 found 791.74.

UV-vis (DCM): λ_{max} (nm) (ε (dm^3. mol^{-1} .cm^{-1})) = 269 (0.461 x10^5), 339 (0.483 x10^5), 360 (0.431 x10^5), 377 (0.423 x10^5), 406 (0.195 x10^5), 432 (0.169 x10^5), 513 (0.13387 x10^5), 551 (0.104 x10^5).

Fluorescence (CH_2Cl_2, Excitation at 512 nm): 609 nm.

3.52 *S*-confused *cis*-diazatribenzothiaporphyrin (2.48d)

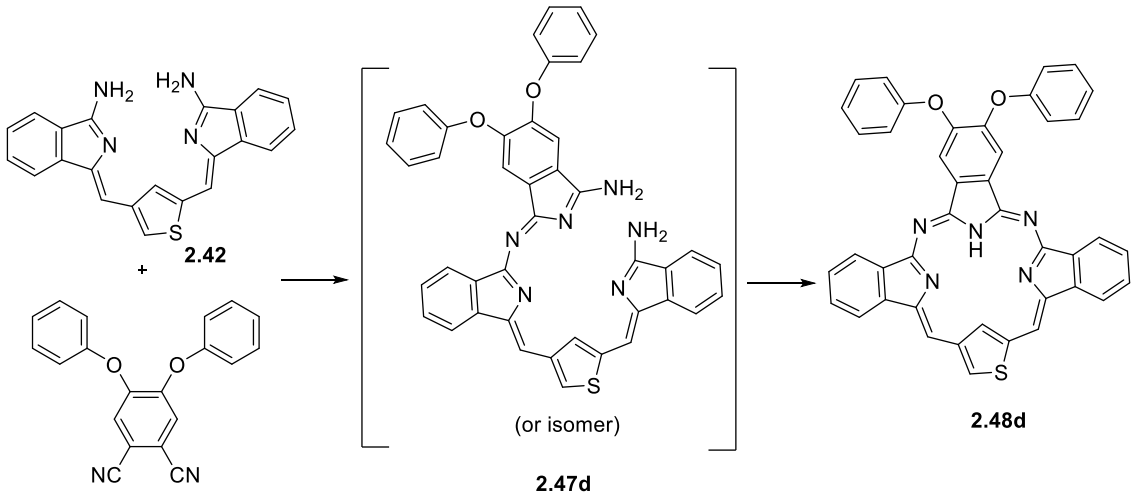

A mixture of compound **2.42** (100 mg, 0.271 mmol, 1 eq) and 4,5-bis-phenoxy-phthalonitrile (80 mg, 0.271 mmol, 1 eq) was stirred in refluxing methanol (10 mL) in the presence of sodium methoxide (approximately 3 mg) for 24 h. The solvent was removed under reduced pressure. The crude product was purified using column chromatography using DCM, then DCM: triethylamine (10:1) to afford the open compound **2.47d** which was precipitated with THF/PE (1:3). After that, the intermediate **2.47d** was refluxed in *p*-xylene (3 mL) overnight.

The solvent was removed under an argon stream while cooling. The resulting solid was purified by column chromatography using DCM/Triethylamine (20:1) and recrystallised by slow evaporation from DCM: MeOH to afford the title product as a red solid (14 mg, 8%).

MP > 300°C
^{1}H NMR (500 MHz, TCE-d_2) δ 8.30 – 8.22 (m, 4H), 8.20 (s, 1H), 8.15-8.08 (m 2H), 7.95 (s, 1H), 7.90 (s, 1H), 7.61 (m, 4H), 7.48 (t, *J* = 7.8 Hz, 4H), 7.26 (t, *J* = 7.5 Hz, 2H), 7.21 (d, *J* = 8.0 Hz, 4H), 7.09 (s, 1H).

MALDI-TOF-MS($C_{42}H_{25}N_5O_2S$)$^+$ m/z $[M]^+$ calcd: 663.17 found: 663.78.

UV-vis (DCM): λ_{max} (nm) (ε (dm^3. mol^{-1} .cm^{-1})) = 271 (0.226 x10^5), 314 (0.234 x10^5), 341 (0.258 x10^5), 357 (0.235 x10^5), 373 (0.219 x10^5), 407 (0.10545 x10^5), 433 (0.912 x10^4), 516 (0.775 x10^4), 560 (0.605 x10^4).

Fluorescence (CH_2Cl_2, Excitation at 514 nm): 610 nm.

3.53 *S*-confused *cis*-diazatribenzothiaporphyrin (2.48e)

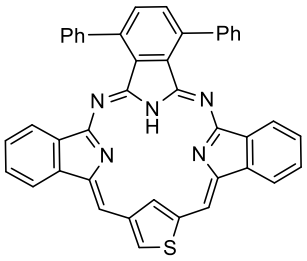

2.48e

A mixture of **2.42** (100 mg, 0.27 mmol, 1 eq) and 3,6-diphenylbenzene-1,2-dicarbonitrile (114 mg, 0.27 mmol, 1.5 eq) was heated in refluxing toluene (10 mL) for 3 days. TLC showed starting material in addition to the desired compound. The solvent was changed to xylene (3 mL) and refluxed two days until no starting material was left. The solvent was removed under an argon stream while cooling. Then, the crude product was purified by column chromatography eluting with THF/PE (1:2) then recrystallised by slow evaporation from DCM: MeOH to give the title product as a red solid (24 mg, 14%).

MP > 300°C
^{1}H NMR (400 MHz, Methylene Chloride-d_2) δ 8.88 (s, 1H, NH), 8.14 (s, 1H), 7.96-7.89 (m, 2H), 7.81 (s, 1H), 7.78 – 7.70 (m, 5H), 7.61 – 7.42 (m, 10H), 7.33 (t, *J* = 7.3 Hz, 2H), 7.25 – 7.16 (m, 2H), 6.97 (s, 1H).
MALDI-TOF-MS ($C_{42}H_{25}N_5S$)$^+$ m/z $[M]^+$ calcd: 631.18 found 631.82.
UV-vis (DCM): λ_{max} (nm) (ε (dm^3. mol^{-1} .cm^{-1})) = 266 (0.353 x10^5), 341 (0.285 x10^5), 409 (0.135 x10^5), 435 (0.119 x10^5), 520 (0.999 x10^4), 561 (0.826 x10^4).
Fluorescence (CH_2Cl_2, Excitation at 519 nm): 614 nm.

3.54 *S*-confused *cis*-diazatribenzothiaporphyrin (2.49)

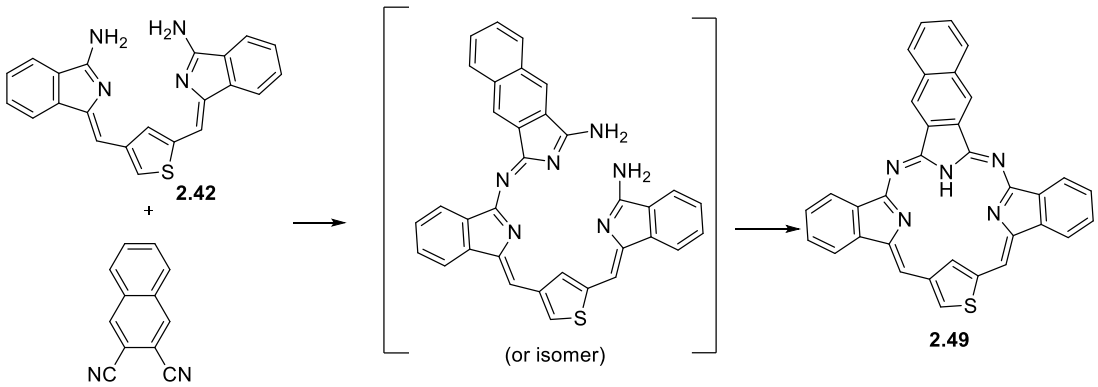

Compound **2.42** (160 mg, 0.434 mmol, 1 eq) and 2,3-dicyanonaphthalene (77 mg, 0.434 mmol, 1eq) were stirred in refluxing methanol (10 mL) in the presence of sodium methoxide (approximately 3 mg) under an argon atmosphere for 48h. The solvent was removed under vacuum, and the crude product was purified by column chromatography using DCM/TEA (20:1) to collect a red fraction (MALDI-MS: m/z 549) that is assumed to be the open compound. The red fraction was precipitated with THF/MeOH and filtered off. Then, the solid was heated overnight in refluxing xylene (3 mL). The solvent was removed under an argon atmosphere while cooling. The crude material was purified by column chromatography eluting with THF/ PE (1:4) and the title product was isolated as a red solid (17 mg, 7%).

MP > 300°C

^{1}H& ^{13}C NMR The compound is poorly soluble, even in THF solvent.

MALDI-TOF-MS($C_{34}H_{19}N_5S$)$^+$ m/z $[M]^+$ calcd: 529.13 found:529.85.

UV-vis (THF): λ_{max} (nm) (ε (dm^3. mol^{-1} .cm^{-1})) = 322 (0.180 x10^5), 367 (0.182 x10^5), 382 (0.168 x10^5), 444 (0.825 x10^4), 504 (0.777 x10^4), 542 (0.639 x10^4).

Fluorescence (CH_2Cl_2, Excitation at 504 nm): 592 nm.

3.55 Compound (2.50)

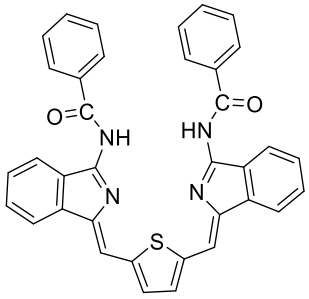

2.50

Benzoyl chloride (76 mg, 0.54 mmol) was added to a solution of **2.2** (100 mg, 0.27 mmol) in dry DCM (6 mL) and TEA (1 mL), and the reaction mixture was stirred at room temperature overnight. Upon completion, the solvent was removed, and the reaction mixture was finally purified by column chromatography using THF: PE (1:4) as the eluent to afford a red compound. The product was then recrystallised from DCM: MeOH to yield the product as a red solid (40 mg, 26%).

MP 220°C

^{1}H NMR (500 MHz, Chloroform-*d*) δ 12.59 (s, 2H, NH), 8.41 (d, *J* = 7.7 Hz, 4H), 8.14 (d, *J* = 7.6 Hz, 2H), 7.79 (d, *J* = 7.7 Hz, 2H), 7.63 (t, *J* = 7.5 Hz, 2H), 7.54 – 7.45 (m, 4H), 7.45 – 7.36 (m, 6H), 6.92 (s, 2H).

MALDI-TOF-MS $(C_{36}H_{24}N_4O_2S)^+$ m/z $[M]^+$ calcd: 576.16 found 575.87.

UV-vis (DCM): λ_{max} (nm) (ε (dm^3. mol^{-1} .cm^{-1})) = 312 (0.182 x10^5), 510 (0.205 x10^5), 548 (0.182 x10^5).

Fluorescence (CH_2Cl_2, Excitation at 511 nm): 573 nm.

3.56 Compound (2.51)

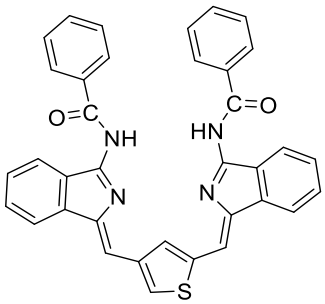

2.51

Benzoyl chloride (76 mg, 0.54 mmol) was added to a solution of **2.42** (100 mg, 0.27 mmol) in dry DCM (6 mL) and TEA (1 mL), and the reaction mixture was stirred at room temperature overnight. Upon completion, the solvent was removed, and the residue was finally purified by column chromatography using THF: PE (1:2) as the eluent to afford a yellow compound. The

product was recrystallised by slow evaporation from DCM: methanol to yield the product as a yellow solid (68 mg, 45%).

MP 160°C
^{1}H NMR (400 MHz, Chloroform-*d*) δ 8.57 – 8.43 (m, 4H), 8.22 (d, *J* = 7.4 Hz, 2H), 7.95 – 7.84 (m, 2H), 7.76 – 7.69 (m, 2H), 7.65 – 7.49 (m, 10H), 6.86 – 6.77 (m, 2H).
MALDI-TOF-MS $(C_{36}H_{24}N_4O_2S)^+$ m/z $[M]^+$ calcd: 576.16 found 576.71.
UV-vis (DCM): λ_{max} (nm) (ε (dm^3. mol^{-1} .cm^{-1})) = 421 (0.197 x10^5).
Fluorescence (CH_2Cl_2, Excitation at 417 nm): 502 nm.

3.57 Compound (2.53)

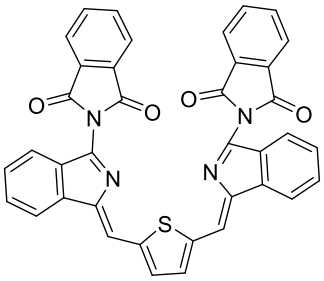

2.53

Phthaloyl chloride (55 mg, 0.27 mmol) was added to a solution of compound **2.2** (100 mg, 0.27 mmol) in dry THF (6 mL) and TEA (1 mL). The reaction mixture was stirred at room temperature and followed by TLC. Upon completion, the solvent was removed, and the mixture was finally purified by column chromatography using DCM: PE: EtOAc (1:1:0.1) as the eluent to afford a red compound. The product was then recrystallised by slow evaporation from DCM: PE to yield the product as a red solid (40 mg, 24%).

MP 240°C
^{1}H NMR (500 MHz, Methylene Chloride-d_2) δ 7.91 – 7.87 (m, 6H), 7.86 – 7.82 (m, 4H), 7.73 (s, 2H), 7.62 (s, 2H), 7.56 (d, *J* = 7.8 Hz, 2H), 7.50 (td, *J* = 7.5, 1.0 Hz, 2H), 7.42 – 7.38 (m, 2H).
^{13}C NMR (126 MHz, Methylene Chloride-d_2) δ 206.79, 165.91, 146.37, 146.23, 141.18, 135.21, 134.99, 133.63, 132.54, 129.60, 128.02, 124.43, 123.15, 122.03, 120.30.
MALDI-TOF-MS $(C_{38}H_{20}N_4O_4S)^+$ m/z $[M]^+$ calcd: 628.12 found 628.66.
UV-vis (DCM): λ_{max} (nm) (ε (dm^3. mol^{-1} .cm^{-1})) = 346 (0.120 x105), 508 (0.364 x10^5), 539 (0.314 x10^5).

Fluorescence (CH_2Cl_2, Excitation at 509 nm): 575 nm.

3.58 Compound (2.54)

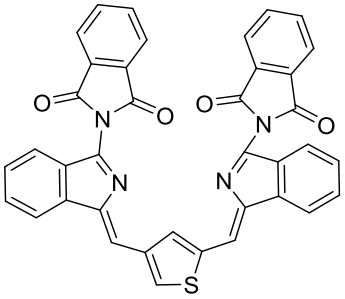

2.54

Phthaloyl chloride (55 mg, 0.27 mmol) was added to a solution of compound **2.42** (100 mg, 0.27 mmol) in dry THF (6 mL) and TEA (1 mL). The reaction mixture was stirred at room temperature and followed by TLC. Upon completion, the solvent was removed, and the crude product was finally purified by using column chromatography, eluting the product with DCM: PE: EtOAc (1:2:0.1). The product than was recrystallised by slow evaporation from DCM: PE to yield the product as a yellow solid (60 mg, 35%).

MP > 300°C
^{1}H NMR (500 MHz, Chloroform-*d*) δ 8.55 (s, 1H), 8.25 (s, 1H), 8.10 – 8.03 (m, 4H), 7.91 – 7.84 (m, 6H), 7.70 (s, 1H), 7.59 (d, *J* = 7.6 Hz, 2H), 7.51 – 7.45 (m, 2H), 7.42 – 7.35 (m, 3H).
MALDI-TOF-MS $(C_{38}H_{20}N_4O_4S)^+$ m/z $[M]^+$ calcd: 628.12 found 628.87.
UV-vis (DCM): λ_{max} (nm) (ε (dm^3. mol^{-1} .cm^{-1})) = 379 (0.340 x10^5), 426 (0.373 x10^5).

Fluorescence (CH_2Cl_2, Excitation at 419nm): 519 nm.

3.59 Compound (2.55)

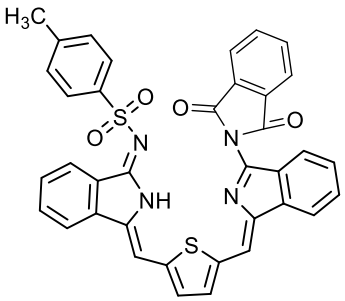

2.55

The mixture of compound **2.33** (30 mg, 0.057 mmol) and phthaloyl chloride (19 mg, 0.057 mmol) was stirred in dry DCM (24 mL) in the presence of TEA (3 mL) for 4 hours. The solvents were removed under reduced pressure, and the product was separated by column chromatography (DCM: EtOAc (4:1)). It was then recrystallised by slow evaporation from DCM: PE to yield the title compound as a red solid (10 mg, 27%).

MP 135℃

^{1}H NMR (400 MHz, Methylene Chloride-d_2) δ 10.69 (s, 1H, NH), 7.91 (d, *J* = 8.2 Hz, 1H), 7.87 – 7.81 (m, 3H), 7.79 – 7.74 (m, 3H), 7.73–7.67 (m, 3H), 7.66 – 7.60 (m, 1H), 7.57 – 7.45 (m, 4H), 7.43 – 7.37 (m, 1H), 7.27 (d, *J* = 4.7 Hz, 1H), 7.16 (d, *J* = 7.9 Hz, 2H), 6.92 (s, 1H), 2.32 (s, 3H).

MALDI-TOF-MS $(C_{37}H_{25}N_4O_4S_2)^+$ m/z $[M+H]^+$ calcd: 653.12 found 653.39.

UV-vis (DCM): λ_{max} (nm) (ε (dm^3. mol^{-1} .cm^{-1})) = 513 (0.277 x10^5).

Fluorescence (CH_2Cl_2, Excitation at 513 nm): 571 nm.

3.60 Compound (2.56)

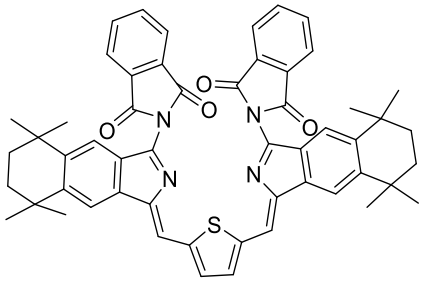

2.56

A solution of phthaloyl chloride (17 mg, 0.084 mmol) in dry DCM was added to a solution of bisaminoisoindoline **2.29** (50 mg, 0.084 mmol) in dry DCM (10 mL) and TEA (1 mL), and the mixture was stirred at room temperature, and followed by TLC. Upon completion, the solvents were removed, and the product was finally purified by column chromatography using DCM (100%) as the eluent to afford a red compound that was recrystallised from DCM: PE to yield the product as a red solid (20 mg, 28%).

MP 102℃

^{1}H NMR (400 MHz, Chloroform-*d*) δ 7.96- 7.92 (m, 4H), 7.80 (s, 2H), 7.80-7.76 (m, 4H), 7.69 (s, 2H), 7.44 (s, 2H), 7.40 (s, 2H), 1.67 (s, 8H), 1.31 (s, 12H), 1.26 (s, 12H).

MALDI-TOF-MS $(C_{54}H_{48}N_4O_4S)^+$ m/z $[M]^+$ calcd: 848.33 found : 848.84.

UV-vis (DCM): λ_{max} (nm) (ε (dm^3. mol^{-1} .cm^{-1})) = 510 (0.431 x10^5).

Fluorescence (CH_2Cl_2, Excitation at 508 nm): 572 nm.

3.61 Compound (2.58)

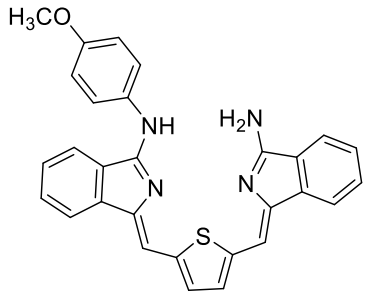

2.58

A mixture of **2.2** (100 mg, 0.27 mmol) and *p*-Anisidine (66.8 mg, 0.54 mmol) was refluxed in *p*-xylene (6 mL) for three days under an argon atmosphere. Then, the solvent was removed under an argon stream while cooling. The crude product was purified by column chromatography using DCM/EtOAc (10:0.1) and then DCM/EtOAc (1:1) as the eluent to afford a red compound that was recrystallised by slow evaporation from DCM and hexane to yield the product as a red solid (trace amount as a side product).

MP > 300℃

^{1}H NMR (400 MHz, Acetone-d_6) δ 9.21 (s, 1H, NH), 8. 39 (d, *J*= 9.1 Hz, 2H), 7.99 – 7.83 (m, 4H), 7.51 – 7.32 (m, 6H), 7.28 (s, 1H), 7.15 (s, 1H), 7.06 (d, *J* = 9.1 Hz, 2H), 6.75 (br-s, 2H, NH_2), 3.83 (s, 3H).

MALDI-TOF-MS $(C_{29}H_{22}N_4OS)^+$ m/z $[M]^+$ calcd: 474.15 found 474.55.
UV-vis (DCM): λ_{max} (nm) (ε (dm^3. mol^{-1} .cm^{-1})) = 367 (0.118 x10^5), 509 (0.114 x10^5).

Fluorescence (CH_2Cl_2, Excitation at 508 nm): 570 nm.

3.62 5,5'-Bis(trimethylsilylethynyl)-2,2'-bithiophene[135]

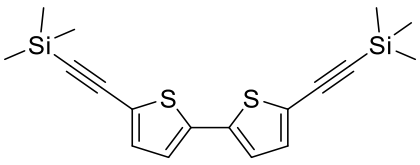

2.62

(Trimethylsilyl)acetylene (1.8 g, 18.5 mmol) was added to a mixture of 5,5-dibromo-2,2-bithiophene (1.2 g, 3.7 mmol), CuI (0.2 g, 0.74 mmol), and $[Pd(PPh_3)_2Cl_2]$ (0.1 g, 0.37 mmol) in triethylamine (10 mL) and THF (20 mL) under an argon atmosphere, and the mixture was heated for 10 h at 60 °C. The cold solution was filtered through a bed of Celite. The filtrate was evaporated under reduced pressure, and the residue was finally purified by silica- gel

column chromatography using 100% petroleum ether to obtain the product as a yellow solid (1.19 g, 91%).

^{1}H NMR (400 MHz, Chloroform-*d*) δ 7.11 (d, *J* = 3.9 Hz, 2H), 7.00 (d, *J* = 3.8 Hz, 2H), 0.25 (s, 18H).

3.63 Compound (2.63)

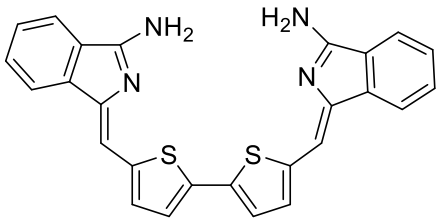

2.63

A mixture of amidine **2.1** (0.5 g, 2.1 mmol, 2 eq), BINAP (0.0727 g, 0.12 mmol), $PdCl_2(MeCN)_2$ (0.0275 g, 0.11 mmol) and 5,5'-bis(trimethylsilylethynyl)-2,2'-bithiophene (0.38 g, 1.1 mmol, 1 eq) was sealed in a microwave vessel with a magnetic bar and then purged and refilled with N_2. Then, DBU (0.8 mL) in dry DMF (6 mL) was added and the reaction mixture was stirred under N_2 for 5 min. Finally, the mixture was irradiated in a microwave reactor at 120 ℃ for 1 h. The mixture was then poured in water (20 mL) and a red precipitate formed which was filtered and washed with water. The reaction mixture was purified by column chromatography using THF: PE (2:1). The product then was recrystallised by slow evaporation from THF/ PE to give the title compound as a red powder (0.2 g, 40%).

MP > 300℃

^{1}H NMR (400 MHz, Methanol-d_4) δ 7.83 (d, *J* = 7.6 Hz, 2H), 7.77 (d, *J* = 7.4 Hz, 2H), 7.49 (t, *J* = 7.4 Hz, 2H), 7.40 (t, *J* = 7.4 Hz, 2H), 7.23 (s, 4H), 7.01 (s, 2H).

MALDI-TOF-MS $(C_{26}H_{18}N_4S_2)^+$ m/z $[M]^+$ calcd: 450.09 found 450.14.

UV-vis (DCM): λ_{max} (nm) (ε (dm^3. mol^{-1} .cm^{-1})) = 502 (0.309 x10^5), 540 (0.230 x10^5).

Fluorescence (THF, Excitation at 502 nm): 569 nm.

3.64 Compound (2.64)

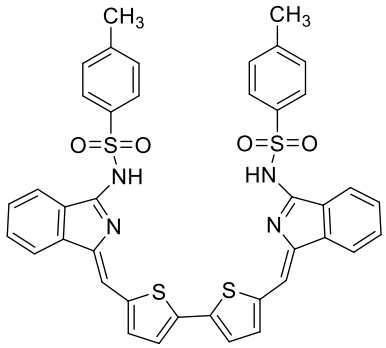

2.64

A mixture of **2.63** (100 mg, 0.22 mmol, 1 eq) with 4-toluenesulfonyl chloride (84 mg, 0.44 mmol, 2 eq) was stirred in dry DCM (10 mL) and TEA (0.3 mL) overnight at room temperature. The reaction mixture was diluted with H_2O, extracted by DCM, dried over $MgSO_4$, and filtered. Then, the solvents were removed under reduced pressure, and the resulting solid was purified by column chromatography using DCM: EtOAc (5:1). The product was recrystallised by slow evaporation from DCM and hexane to afford the product as a red solid (60 mg, 37%).

MP > 300°C

^{1}H NMR (400 MHz, Methylene Chloride-d_2) δ 10.70 (s, 2H, NH), 7.93 (d, *J* = 8.3 Hz, 4H), 7.81 (d, *J* = 7.7 Hz, 2H), 7.75 (d, *J* = 7.9 Hz, 2H), 7.67 – 7.59 (m, 2H), 7.45 (t, *J* = 7.5 Hz, 2H), 7.36 – 7.30 (m, 6H), 7.26 (d, *J* = 3.9 Hz, 2H), 6.89 (s, 2H), 2.40 (s, 6H).

^{13}C NMR (101 MHz, Methylene Chloride-d_2) δ 158.62, 143.63, 139.00, 138.45, 137.40, 135.99, 132.90, 132.25, 130.73, 130.67, 129.53, 129.17, 126.48, 125.72, 123.76, 119.85, 102.90, 21.25.

MALDI-TOF-MS $(C_{40}H_{30}N_4O_4S_4)^+$ m/z $[M]^+$ calcd: 758.11 found 757.68.

UV-vis (DCM): λ_{max} (nm) (ε (dm^3. mol^{-1} .cm^{-1})) = 301 (0.335 x10^5), 395 (0.168 x10^5), 503 (0.514 x10^5).

Fluorescence (CH_2Cl_2, Excitation at 500 nm): 567 nm.

3.65 Compound (2.69)

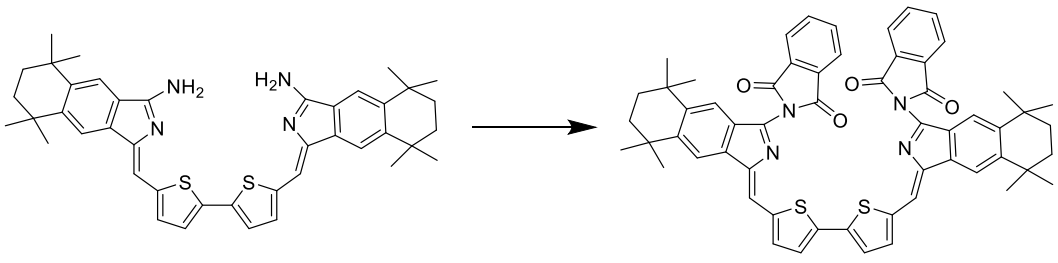

2.67 **2.69**

A mixture of 2-bromobenzimidamide hydrochloride **2.26** (0.37 g, 1.32 mmol, 2 eq), BINAP (0.0427 g, 0.073 mmol), $PdCl_2(MeCN)_2$ (0.0175 g, 0.066 mmol) and 5,5'-

bis(trimethylsilylethynyl)-2,2'-bithiophene (0.25 g, 0.66 mmol, 1 eq) was sealed in a microwave vessel with a magnetic bar and then purged with N_2. Then, DBU (0.5 mL) in dry DMF (6 mL) was added, and the reaction mixture was stirred under N_2 for 5 min. Finally, the mixture was irradiated in a microwave reactor at 120 ℃ for 1 h. The mixture was then poured in water (20 mL), and a red precipitate formed, which was then filtered and washed with water. The residue was purified by column chromatography using THF: PE (3:1) and then recrystallised from THF/ PE to give the title compound as a red powder (0.3 g) (MALDI-MS: m/z 670.32), which was used in the next step.

A solution of phthaloyl chloride (0.06 g, 0.29 mmol) in dry DCM was added to a solution of compound **2.67** (0.1 g) in dry DCM (10 mL) and TEA (1 mL). The reaction mixture was stirred at room temperature and followed by TLC. Upon completion, the solvents were removed, and the reaction mixture was finally purified by column chromatography using DCM: PE (1:1) as the eluent to afford a red compound. The product was recrystallised by slow evaporation from DCM: PE to yield a red solid product (0.02 g, 10% over two steps).

MP 123℃

^{1}H NMR (400 MHz, Methylene Chloride-d_2) δ 8.09- 8.04 (m, 4H), 7.95- 7.90 (m, 4H), 7.85 (s, 2H), 7.58 (s, 2H), 7.52 (s, 2H), 7.46 (d, *J* = 4.1 Hz, 2H), 7.36 (d, *J* = 4.0 Hz, 2H), 1.79 (s, 8H), 1.43 (s, 12H), 1.35 (s, 12H).

MALDI-TOF-MS $(C_{58}H_{51}N_4O_4S_2)^+$ m/z $[M+H]^+$ calcd: 931.33 found 931.44.

UV-vis (DCM): λ_{max} (nm) (ε (dm^3. mol^{-1} .cm^{-1})) = 414 (0.946 x10^4), 536 (0.334 10^5).

Fluorescence (CH_2Cl_2, Excitation at 537 nm): 615 nm.

3.66 Compound (2.71)

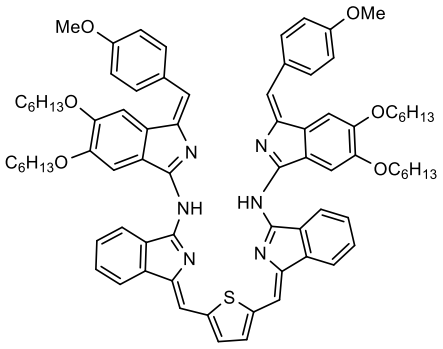

2.71

A mixture of **2.2** (100 mg, 0.271 mmol, 1 eq) and dihexyloxyaminoisoindoline (122 mg, 0.271 mmol, 1 eq) was refluxed in *p*-xylene (10 mL) under a N_2 atmosphere and monitored by TLC (3 days). Then, the solvent was removed under an argon stream while cooling. The crude

product was purified by column chromatography using PE/EtOAc (6:1) as the eluent to afford a green compound that was recrystallised by slow evaporation from DCM and MeOH to yield the product as a green solid (16 mg, 4%).

MP 149°C

^{1}H NMR (400 MHz, Chloroform-*d*) δ 9.96 (s, 2H, NH), 8.27 – 8.23 (m, 2H), 7.98 – 7.93 (m, 2H), 7.74 (s, 2H), 7.69 (s, 2H), 7.59 (s, 2H), 7.57 – 7.53 (m, 4H), 6.55 (d, *J* = 8.6 Hz, 4H), 6.28 (s, 2H), 5.95 (s, 2H), 5.42 (d, *J* = 8.7 Hz, 4H), 4.31 – 4.21 (m, 4H), 3.91 – 3.79 (m, 4H), 3.32 (s, 6H), 1.99 – 1.89 (m, 8H), 1.66 – 1.60 (m, 8H), 1.49 – 1.42 (m, 16H), 1.01 – 0.95 (m, 12H).

^{13}C NMR (101 MHz, Chloroform-*d*) δ 167.73, 157.93, 157.80, 152.82, 149.84, 146.52, 143.82, 141.46, 139.04, 132.67, 132.34, 129.90, 129.79, 128.12, 127.31, 126.42, 124.51, 121.65, 119.16, 112.89, 111.80, 106.44, 105.38, 100.87, 69.78, 68.42, 54.67, 32.14, 31.98, 29.72, 26.06, 22.93, 22.86, 14.27, 14.26.

MALDI-TOF-MS $(C_{78}H_{86}N_6O_6S)^+$ m/z $[M]^+$ calcd: 1234.63 found 1234.89.
UV-vis (DCM): λ_{max} (nm) (ε (dm^3. mol^{-1} .cm^{-1})) = 267 (0.358 x10^5), 336 (0.434 x10^5) 397 (0.451 x10^5), 489 (0.117 x10^5), 640 (0.604 x10^4), 703 (0.512 x10^4).

3.67 2,6-bis((trimethylsilyl)ethynyl)pyridine (2.74) [136]

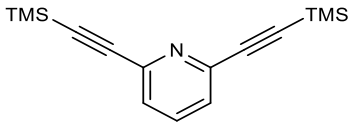

2.74

(Trimethylsilyl)acetylene (2.5 g, 2.5 mmol) was added to a mixture of 2,6-dibromopyridine (1.2 g, 5 mmol), CuI (0.2 g, 10 mmol), and $[Pd(PPh_3)_2Cl_2]$ (0.4 g, 0.51 mmol) in triethylamine (5 mL) and THF (10 mL) under an argon atmosphere, and the mixture was heated to reflux overnight. The cold solution was filtered through a bed of Celite. The filtrate was evaporated under reduced pressure and the residue was finally purified by silica-gel column chromatography using 100% petroleum ether to afford the product as a yellow solid (1.24 g, 91%).

^{1}H NMR (500 MHz, Chloroform-*d*) δ 7.61 – 7.55 (m, 1H), 7.38 (d, *J* = 7.8 Hz, 2H), 0.25 (s, 18H).
^{13}C NMR (126 MHz, Chloroform-*d*) δ 143.48, 136.38, 126.83, 103.23, 95.58, -0.19.

3.68 Compound (2.75)

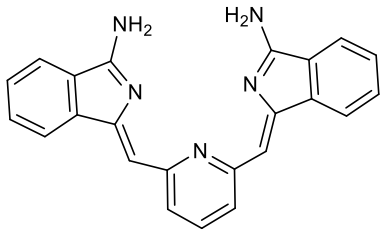

2.75

A solution of 2,6-bis [2-(trimethylsilyl) ethynyl] pyridine (0.58 g, 2.12 mmol, 1 eq) and DBU (1.62 mL) in dry DMF (12 mL) was added to a mixture of amidine **2.1** (1 g, 4.25 mmol, 2 eq), BINAP (0.16 g, 0.23 mmol) and $PdCl_2(MeCN)_2$ (0.056 g, 0.21 mmol). The reaction mixture was irradiated in a microwave reactor at 120°C for 1 h. After cooling, the solution was poured into water, and a yellow precipitate formed, which was filtered and washed with water. The dried solid was dissolved in acetone, the solution filtered through a bed of Celite, then 2-3 drops of conc. HCl was added, causing a precipitate. The solid was filtered off, and CH_3OH (10 mL)/ CH_3ONa (3 mg) were added to the solid. The product was stirred for 5 min and then poured into water to give the title compound as a yellow powder (0.26 g, 33%).

MP > 300°C

^{1}H NMR (500 MHz, Methanol-*d*$_4$) δ 7.88 (d, *J* = 7.6 Hz, 2H), 7.83 (d, *J* = 7.4 Hz, 2H), 7.62 – 7.53 (m, 4H), 7.48 (t, *J* = 7.4 Hz, 2H), 7.12 (d, *J* = 7.7 Hz, 2H), 6.53 (s, 2H).
MALDI-TOF-MS $(C_{23}H_{17}N_5)^+$ m/z $[M]^+$ calcd: 363.14 found 362.93.
UV-vis (THF): λ_{max} (nm) (ε (dm^3. mol^{-1} .cm^{-1})) = 353 (0.206 x105), 438 (0.603 x104).
Fluorescence (THF, Excitation at 440 nm): 499

3.69 Compound (2.77)

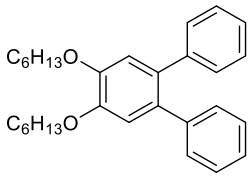

2.77

Following the method reported in the literature,[126] 1,2-dibromo-4,5-bis(hexyloxy)benzene (5.92 g, 13.5 mmol, 1 eq), benzene boronic acid (4.96 g, 40.7 mmol, 3 eq), and sodium carbonate (4.96 g, 40.7 mmol, 3 eq) were stirred in toluene (50 mL) and water (30 mL). Nitrogen was bubbled into the mixture and stirred at 60°C for 2 h. The catalyst ($Pd(PPh_3)_4$ (0.627 g, 0.8 mmol) was then added, and the reaction mixture was stirred overnight at reflux. Toluene was removed under reduced pressure and the crude residue was extracted with DCM

(50 mL) three times. The organic layers were combined and evaporated. The reaction mixture was purified by column chromatography which was eluted using 1:4 dichloromethane to petroleum ether. The product was obtained as bright white crystals (5.61 g, 96%).

^{1}H NMR (500 MHz, Chloroform-*d*) δ 7.53 – 7.41 (m, 10H), 7.26 (s, 2H), 4.38 (t, *J* = 6.7 Hz, 4H), 2.21 – 2.11 (m, 4H), 1.84 – 1.77 (m, 4H), 1.71 – 1.61 (m, 8H), 1.27 – 1.19 (m, 6H).
MALDI-TOF-MS $(C_{30}H_{38}O_2)^+$ m/z $[M]^+$ calcd: 430.28 found 429.92.

3.70 Compound (2.78)

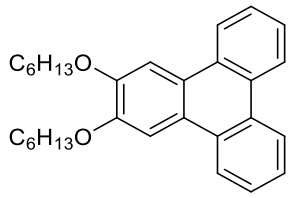

2.78

Following the method reported in the literature,[126] a solution of 1,2-bis(hexyloxy)-4,5-diphenylbenzene (2.32 g, 5.38 mmol, 1eq), iron (III) chloride (2.18 g, 13.5 mmol, 2.5 eq) and nitromethane (5 mL) in dry dichloromethane (130 mL) was stirred at room temperature for 5 hours. Methanol (80 mL) and water (80 mL) were added and stirred for 5 min. The organic solvents were evaporated, and the resulting mixture was extracted three times with DCM. The organic layers were combined, dried over magnesium sulphate, filtered and evaporated under reduced pressure. The reaction mixture was purified by column chromatography which was eluted using dichloromethane/petroleum ether (1:3) and then recrystallised in toluene to afford the product as a white solid (1.9 g, 82%).

^{1}H NMR (400 MHz, Chloroform-*d*) δ 8.66 (dd, *J* = 7.6, 2.0 Hz, 2H), 8.50 (dd, *J* = 7.8, 1.9 Hz, 2H), 8.04 (s, 2H), 7.70 – 7.56 (m, 4H), 4.26 (t, *J* = 6.7 Hz, 4H), 2.01 – 1.91 (m, 4H), 1.64 – 1.56 (m, 4H), 1.46 – 1.35 (m, 8H), 0.99 – 0.92 (m, 6H).

MALDI-TOF-MS $(C_{30}H_{36}O_2)^+$ m/z $[M]^+$ calcd: 428.27 found 428.09.

3.71 Compound (2.79) [127]

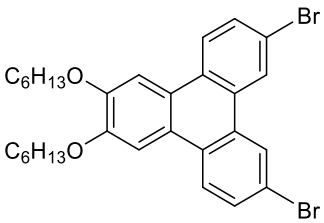

2.79

2,3-Bis(hexyloxy)triphenylene (1 g, 2.33 mmol, 1 eq) was stirred in DCM (60 mL) at 0°C. Bromine (0.26 mL, 0.79 g, 5 mmol, 2.14 eq.) was then added dropwise and the mixture stirred for 2 h at 0°C. The reaction mixture was washed with sodium metabisulphite solution (20%, 50 mL), and the crude product was extracted with DCM. The organic layer was dried over $MgSO_4$, and the solvent was removed under reduced pressure. The crude product was recrystallised from methanol, giving the product as a white powder (1.3 g, 95%).

^{1}H NMR (500 MHz, Chloroform-*d*) δ 8.62 (d, *J* = 2.0 Hz, 2H), 8.30 (d, *J* = 8.9 Hz, 2H), 7.90 (s, 2H), 7.72 (dd, *J* = 8.8, 2.0 Hz, 2H), 4.23 (t, *J* = 6.6 Hz, 4H), 1.99 – 1.91 (m, 4H), 1.62 – 1.55 (m, 4H), 1.46 – 1.34 (m, 8H), 0.94 (t, *J* = 7.0 Hz, 6H).

MALDI-TOF-MS $(C_{30}H_{35}Br_2O_2)^+$ m/z $[M+H]^+$ calcd: 585.09 found 585.82.

3.72 Compound (2.80)

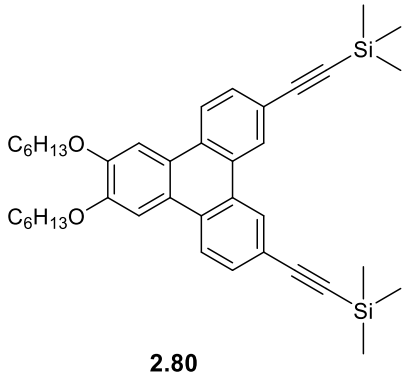

2.80

In a dry round bottomed flask, (trimethylsilyl)acetylene (0.083 g, 0.845 mmol) was added to a mixture of 2,11- dibromo-6,7-bis(hexyloxy)triphenylene **2.79** (0.1 g, 0.170 mmol), CuI (0.0064 g, 0.033 mmol), and $[Pd(PPh_3)_2Cl_2]$ (0.011 g, 0.015 mmol) in triethylamine (2 mL) and THF (4 mL) under an argon atmosphere, and the mixture was heated to reflux overnight. The cold solution was filtered through a bed of Celite. Then, the filtrate was evaporated under reduced pressure, and the residue was finally purified by silica-gel column chromatography using DCM: Hexane (1:4) and then recrystallised by slow evaporation from DCM: Methanol to afford the product as yellow crystals (0.07g, 70%).

MP 94°C

^{1}H NMR (400 MHz, Chloroform-*d*) δ 8.73 (s, 2H), 8.35 (d, *J* = 8.7 Hz, 2H), 7.90 (s, 2H), 7.69 (dd, *J* = 8.5, 1.6 Hz, 2H), 4.22 (t, *J* = 6.6 Hz, 4H), 2.01 – 1.87 (m, 4H), 1.66 – 1.51 (m, 4H), 1.48 – 1.35 (m, 8H), 1.01 – 0.89 (m, 6H), 0.34 (s, 18H).
^{13}C NMR (101 MHz, Chloroform-*d*) δ 149.94, 130.21, 129.56, 128.08, 127.30, 124.01, 122.67, 120.69, 106.60, 105.42, 94.80, 69.21, 31.56, 29.17, 25.71, 22.56, 13.96, 0.28.

MALDI-TOF-MS $(C_{40}H_{52}O_2Si_2)^+$ m/z $[M]^+$ calcd: 620.35 found 620.49.

3.73 Compound (2.82)

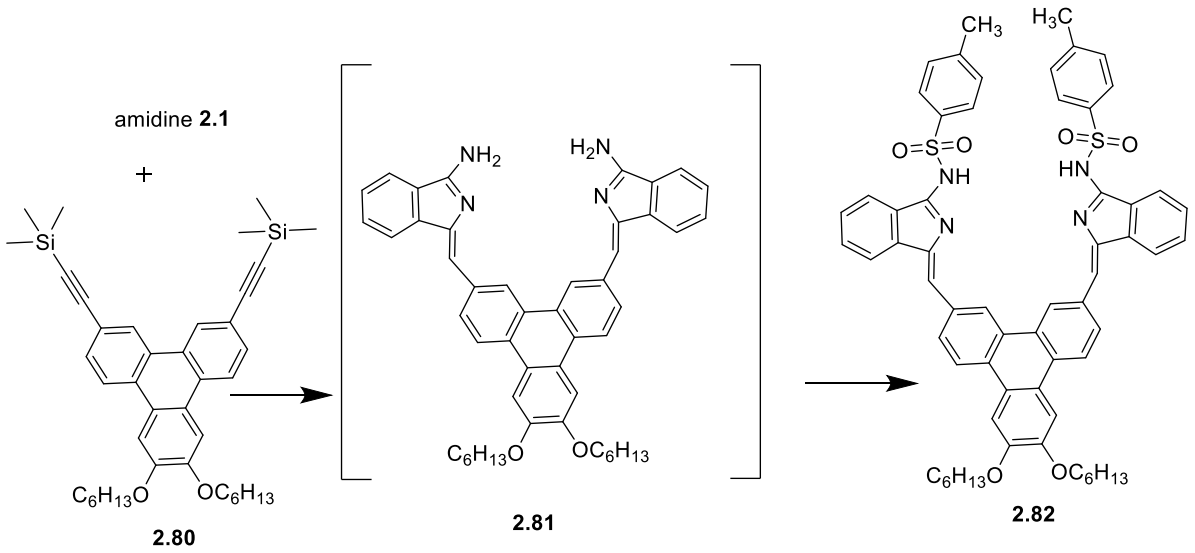

A mixture of amidine **2.1** (0.1 g, 0.424 mmol), BINAP (0.014 g, 0.0233 mmol), $PdCl_2(MeCN)_2$ (0.0055 mg, 0.0212 mmol), and compound **2.80** (0.13 g, 0.212 mmol) was sealed in a microwave vessel with a magnetic bar and then purged with N_2. Then, DBU (0.16 mL) in dry DMF (2 mL) was added, and the reaction mixture was stirred under N_2 for 5 min. Finally, the mixture was irradiated in a microwave reactor at 120 ˚C for 1 h. The mixture was then poured into water (20 mL), and a yellow precipitate formed, which was filtered and washed with water. The title compound as a yellow powder (0.11 g) (MALDI-MS: m/z 712.36) was used without further purification.

A mixture of compound **2.81** (100 mg) and 4-toluenesulfonyl chloride (53 mg, 0.28 mmol) was stirred in dry THF (6 mL) and TEA (0.6 mL) overnight at room temperature. The reaction mixture was diluted with H_2O, extracted by DCM, dried over $MgSO_4$, and filtered. The solvent was removed under reduced pressure, and the resulting solid was purified by column chromatography using DCM: EtOAc (4:1). The product was recrystallised by slow evaporation from DCM and hexane to afford the product as an orange solid (60 mg, 31% over two steps).

MP 188°C

^{1}H NMR (400 MHz, Chloroform-*d*) δ 10.84 (s, 2H, NH), 8.70 (s, 2H), 8.37 (d, *J* = 8.7 Hz, 2H), 7.98 (d, *J* = 8.3 Hz, 4H), 7.77 (d, *J* = 7.6 Hz, 2H), 7.73 (s, 2H), 7.66 (d, *J* = 10.2 Hz, 2H), 7.60 (d, *J* = 7.7 Hz, 2H), 7.42 (t, *J* = 7.5 Hz, 2H), 7.34 (t, *J* = 7.7 Hz, 2H), 7.25 (d, *J* = 8.9 Hz, 4H), 6.88 (s, 2H), 4.17 (t, *J* = 6.6 Hz, 4H), 2.35 (s, 6H), 2.00 – 1.90 (m, 4H), 1.60 – 1.56 (m, 4H), 1.45 – 1.37 (m, 8H), 0.99 – 0.92 (m, 6H).

^{13}C NMR (101 MHz, Chloroform-*d*) δ 159.23, 150.05, 143.20, 139.38, 136.69, 133.35, 132.62, 131.99, 130.30, 129.64, 129.48, 129.04, 128.71, 127.13, 126.62, 124.22, 124.11, 123.97, 123.64, 120.13, 110.38, 106.29, 69.15, 31.71, 29.35, 25.84, 22.66, 21.46, 14.03.
MALDI-TOF-MS $(C_{62}H_{60}N_4O_6S_2)^+$ m/z $[M]^+$ calcd: 1020.39 found 1020.36.
UV-vis (DCM): λ_{max} (nm) (ε (dm^3. mol^{-1} .cm^{-1})) = 291 (0.6188 x10^5), 394 (0.577 x10^5).

Fluorescence (CH_2Cl_2, Excitation at 393 nm): 530 nm.

3.74 Compound (2.85)

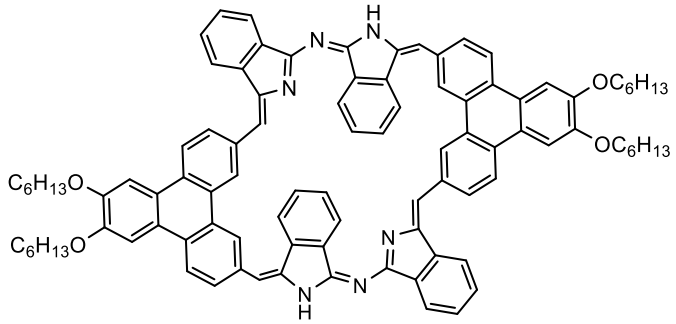

The compound **2.81** (50 mg) was refluxed in *p*-xylene (3 mL) overnight. The solvent was removed under pressure, and the resulting solid was purified using column chromatography with DCM as eluent. The product was recrystallised by slow evaporation from DCM and methanol to afford the product as a brown solid (20 mg, 14% over two steps).

MP 173℃

^{1}H NMR (500 MHz, Chloroform-*d*) δ 14.38 (s, 2H, NH), 10.09 (s, 2H), 8.44 (d, *J* = 8.5 Hz, 2H), 8.22 – 8.12 (m, 8H), 7.92 (d, *J* = 7.4 Hz, 2H), 7.68 – 7.54 (m, 6H), 7.48 (t, *J* = 7.4 Hz, 2H), 7.28 (s, 2H), 7.16 (d, *J* = 8.8 Hz, 2H), 7.08 – 7.01 (m, 4H), 6.90 (d, *J* = 7.6 Hz, 2H), 6.80 (s, 2H), 6.64 (s, 2H), 4.24 – 4.16 (m, 4H), 4.11 – 3.95 (m, 4H), 2.06 – 1.96 (m, 8H), 1.79 – 1.65 (m, 8H), 1.55 – 1.43 (m, 16H), 1.05 (t, *J* = 7.1 Hz, 6H), 1.00 (t, *J* = 7.0 Hz, 6H).
^{13}C NMR (126 MHz, Chloroform-*d*) δ 168.43, 165.02, 149.18, 148.82, 143.74, 140.54, 139.58, 138.67, 135.57, 133.80, 133.25, 133.06, 130.65, 130.00, 129.48, 129.44, 129.02, 128.79, 128.25, 128.00, 125.90, 125.52, 124.51, 123.53, 123.45, 123.07, 122.96, 122.41, 122.32, 120.05, 119.50, 115.88, 115.13, 105.19, 104.28, 68.59, 68.48, 32.04, 31.96, 29.62, 29.59, 26.31, 26.00, 22.97, 22.90, 14.36, 14.25.
MALDI-TOF-MS $(C_{96}H_{90}N_6O_4)^+$ m/z $[M]^+$ calcd: 1390.70 found 1391.45.
UV-vis (DCM): λ_{max} (nm) (ε (dm^3. mol^{-1} .cm^{-1})) = 271(0.510 x10^5), 339 (0.635 x10^5), 379 (0.523 x10^5), 419 (0.357 x10^5), 564 (0.5187 x10^4).

Fluorescence (CH_2Cl_2, Excitation at 400): 506, 663 nm.

4 References

(1) Milgrom, L. R. The Colours of Life: Anintroduction to the Chemistry of Porphyrins and Related Compound. Oxford University Press; 1997.

(2) Moss, G. P. Nomenclature of Tetrapyrroles: Recommendations 1986. Eur J Biochem **1988**, 178 (2), 277–328.

(3) Arnold, W.; Azzi, J. R. Chlorophyll Energy Levels and Electron Flow in Photosynthesis. Proc Natl Acad Sci USA **1968**, 61 (1), 29–35.

(4) Chiabrando, D.; Vinchi, F.; Fiorito, V.; Mercurio, S.; Tolosano, E. Heme in Pathophysiology: A Matter of Scavenging, Metabolism and Trafficking across Cell Membranes. Front Pharmacol **2014**, 5, 1–24.

(5) Rothemund, P.; Menotti, A. R. Porphyrin Studies. IV.1 The Synthesis of α, β, γ, δ-Tetraphenylporphine. J Am Chem Soc **1941**, 63 (1), 267–270.

(6) Adler, A. D.; Longo, F. R.; Finarelli, J. D.; Goldmacher, J.; Assour, J.; Korsakoff, L. A Simplified Synthesis for Meso-Tetraphenylporphin. J Org Chem **1967**, 32 (2), 476–476.

(7) Lindsey, J. S.; SChreiman, I. C.; Hsc, H. C.; Marguerettaz, A. M. Rothemund and Alder-Longo Reaction Revisited: Synthesis of Tetraphenylporphyrins under Equilibrium Conditions. J Org Chem **1987**, 52 (5), 827–836.

(8) Zhou, Z.; Shen, Z. The Development of Artificial Porphyrinoids Embedded with Functional Building Blocks. J Mater Chem C **2015**, 3 (14), 3239–3251.

(9) Abdulaeva, I. A.; Birin, K. P.; Bessmertnykh-Lemeune, A.; Tsivadze, A. Y.; Gorbunova, Y. G. Heterocycle-Appended Porphyrins: Synthesis and Challenges. Coord Chem Rev **2020**, 407, 213108.

(10) Higashino, T.; Imahori, H. Porphyrins as Excellent Dyes for Dye-Sensitized Solar Cells: Recent Developments and Insights. Dalton Trans **2015**, 44 (2), 448–463.

(11) Dent, C. E.; Linstead, R. P. 217. Phthalocyanine.Part VI. The Structure of the Phthalocyanine. J Chem Soc **1934**, 1033–1039.

(12) Shimizu, S.; Furuta, H. Core-Modified Phthalocyanines and Subphthalocyanines: A Synthetic Strategy towards Core-Modification and Novel Properties Arising from the Inner Ring-Expansion. Macroheterocycles **2015**, 8 (4), 332–342.

(13) Brothers, P. J.; Senge, M. O.; John Wiley& Sons. Phthalocyanines and Porphyrazines. In Fundamentals of Porphyrin Chemistry; 2022.

(14) Sakamoto, K.; Ohno-Okumura, E. Syntheses and Functional Properties of Phthalocyanines. Materials **2009**, 2 (3), 1127–1179.

(15) Nemykina, V. N.; Lukyanets, E. A. Synthesis of Substituted Phthalocyanines. Arkivoc **2010**, 136–208.

(16) A Barrett, B. P.; Linstead, R. P.; P Tuey, G. A.; M Robertson, B. J. 371. Phthalocyanines and Related Compounds. Part XV. Tetrabenzaporphin: Its Preparation from Phthalonitrile and a Proof of Its Structure. With a Note on a Preliminary X-Ray Investigation. J Chem Soc (Resumed) **1939**, 1809–1820.

(17) Tomoda, H.; Saito, S.; Ogawa, S.; Shiraishi, S. Synthesis of Phthalocyanines from Phthalonitrile with Organic Strong Bases. Chem Lett **1980**, 9 (10), 1277–1280.

(18) Tomoda, H.; Saito, S.; Shiraishi, S. Synthesis of Metallophthalocyanines from Phthalonitrile with Strong Organic Bases. Chem Lett **1983**, 12 (3), 313–316.

(19) Cammidge, A. N.; Chambrier, I.; Cook, M. J.; Hughes, D. L.; Rahman, M.; Sosa-Vargas, L. Phthalocyanine Analogues: Unexpectedly Facile Access to Non-Peripherally Substituted Octaalkyl Tetrabenzotriazaporphyrins, Tetrabenzodiazaporphyrins, Tetrabenzomonoazaporphyrins and Tetrabenzoporphyrins. Chem Eur J **2011**, 17 (11), 3136–3146.

(20) Díaz-Moscoso, A.; Tizzard, G. J.; Coles, S. J.; Cammidge, A. N. Synthesis of Meso-Substituted Tetrabenzotriazaporphyrins: Easy Access to Hybrid Macrocycles. Angew Chem Int Ed **2013**, 52 (41), 10784–10787.

(21) Cammidge, A. N.; Chembrier, I.; Cook, M. J.; Sosa-vargas, Lydia. 75 Synthesis and Properties of the Hybrid Phthalocyanine-Tetrabenzoporphyrin Macrocycles. In Handbook of Porphyrin Science: With Application to Chemistry, Physics, Materials Science, Engineering, Biology and Medicine; 2012; Vol. 16, 331-404.

(22) Dent, C. E. Preparation of Phthalocyanine-like Pigments Related to the Porphyrins. J Chem Soc (Resumed) **1938**, 1–6.

(23) A Barrett, B. P.; Linstead, R. P.; P Tuey, G. A.; M Robertson, B. J. 371. Phthalocyanines and Related Compounds. Part XV. Tetrabenztriazaporphin: Its Preparation from Phthalonitrile and a Proof of Its Structure. With a Note on a Preliminary X-Ray Investigation. J Chem Soc (Resumed) **1939**, 1809–1820.

(24) Remiro-Buenamañana, S.; Díaz-Moscoso, A.; Hughes, D. L.; Bochmann, M.; Tizzard, G. J.; Coles, S. J.; Cammidge, A. N. Synthesis of Meso-Substituted Subphthalocyanine-Subporphyrin Hybrids: Boron Subtribenzodiazaporphyrins. Angew Chem Int Ed **2015**, 54 (26), 7510–7514.

(25) Hellal, M.; Cuny, G. D. Microwave Assisted Copper-Free Sonogashira Coupling/5-Exo-Dig Cycloisomerization Domino Reaction: Access to 3-

(Phenylmethylene)Isoindolin-1- Ones and Related Heterocycles. Tetrahedron Lett **2011**, 52 (42), 5508–5511.

(26) Alkorbi, F.; Díaz-Moscoso, A.; Gretton, J.; Chambrier, I.; Tizzard, G. J.; Coles, S. J.; Hughes, D. L.; Cammidge, A. N. Complementary Syntheses Giving Access to a Full Suite of Differentially Substituted Phthalocyanine-Porphyrin Hybrids. Angew Chem Int Ed **2021**, 60 (14), 7632–7636.

(27) Sugano, Y.; Matsuo, K.; Hayashi, H.; Aratani, N.; Yamada, H. Synthesis and Properties of 10,20-Bis(Triisopropylsilylethynyl)-Tetrabenzo-5,15-Diazaporphine. J Porphyr Phthalocyanines **2023**, 27 (1–4), 136–144.

(28) Claessens, C. G.; Hahn, U.; Torres, T. Phthalocyanines: From Outstanding Electronic Properties to Emerging Applications. Chem Rec **2008**, 8 (2), 75–97.

(29) Lo, P. C.; Leng, X.; Ng, D. K. P. Hetero-Arrays of Porphyrins and Phthalocyanines. Coord Chem Rev **2007**, 251 (17–20), 2334–2353.

(30) Singh, K.; Sharma, A.; Sharma, S. Heteroporphyrins: Synthesis and Structural Modifications. In Advances in Heterocyclic Chemistry; Academic Press, 2012; Vol. 106, 111-184.

(31) Chatterjee, T.; Shetti, V. S.; Sharma, R.; Ravikanth, M. Heteroatom-Containing Porphyrin Analogues. Chem Rev **2017**, 117 (4), 3254–3328.

(32) a) Latos-Grazynski, L.; Smith, K. M.; Karl M, K.; Guilard, R. The Porphyrin Handbook.; Elsevier, 2000; Vol. 2. b) Latos-Graiyfiski, L.; Lisowski, J.; Szterenberg, L.; Olmstead, M. M.; Balch, A. L. Crystal and molecular structure of 21-thia-5, 20-diphenyl-10, 15-bis (p-nitrophenyl)-porphyrin and 21, 23-dithiatetraphenylporphyrin. The influence of sulfur on the π-delocalization pattern. J Org Chem **1991**; 56(12), 4043-4045.

(33) Gupta, I.; Ravikanth, M. Recent Developments in Heteroporphyrins and Their Analogues. Coord Chem Rev **2006**, 250 (3–4), 468–518.

(34) Yedukondalu, M.; Ravikanth, M. Core-Modified Porphyrin Based Assemblies. Coord Chem Rev **2011**, 255 (5–6), 547–573.

(35) Kuznetsov, A. Core-Modified Porphyrins: Novel Building Blocks in Chemistry. Phys Sci Rev **2023**, 8 (8), 1513–1543.

(36) Singh, G.; Chandra, S. Unravelling the Structural-Property Relations of Porphyrinoids with Respect to Photo- and Electro-Chemical Activities. Electrochem Sci Adv **2023**, 3 (1), e2100149.

(37) Kumaresan, D.; Gupta, I.; Ravikanth, M. Synthesis of 21-Oxoporphyrin Building Blocks and Energy Donor Appended Systems. Tetrahedron lett **2001**, 42 (48), 8547–8550.

(38) Ulman, A.; Manassen, J.; Frolow, F.; Rabinovich, D. Synthesis and Properties of Tetraphenylporphyrin Molecules Containing Heteroatoms

Other Than Nitrogen. 6. Electrochemical Studies. Inorg Chem **1981**, 20 (7), 1987–1990.

(39) Gouterman, M. Spectra of Porphyrins. J Mol Spectroscopy **1961**, 6, 138–163.

(40) Josefsen, L. B.; Boyle, R. W. Unique Diagnostic and Therapeutic Roles of Porphyrins and Phthalocyanines in Photodynamic Therapy, Imaging and Theranostics. Theranostics **2012**, 2 (9), 916–966.

(41) Pareek, Y.; Ravikanth, M. Thiaporphyrins: From Building Blocks to Multiporphyrin Arrays. RSC Adv **2014**, 4 (16), 7851–7880.

(42) Abraham, R. J.; Leonard, P.; Ulman, A. Tetraphenylporphyrin Molecules Containing Heteroatoms Other than Nitrogen: 8—A Carbon-13 NMR Study. Org Magn Res **1984**, 22 (9), 561–564.

(43) Gupta, I.; Ravikanth, M. Synthesis of Meso-Furyl Porphyrins with N4, N3S, N2S2 and N3O Porphyrin Cores. Tetrahedron **2003**, 59 (32), 6131–6139.

(44) Broadhurst, M. J.; Johnson, A. W. Synthesis of Porphin Analogues Containing Furan and/or Thiophen Rings. J Chem SOC C **1971**, 3681-3690.

(45) Latham, A. N.; Lash, T. D. Synthesis and Characterization of N-Methylporphyrins, Heteroporphyrins, Carbaporphyrins, and Related Systems. J Org Chem **2020**, 85 (20), 13050–13068.

(46) Lash, T. D. Modification of the Porphyrin Chromophore by Ring Fusion: Identifying Trends Due to Annelation of the Porphyrin Nucleus. J Porphyr Phthalocyanines **2001**, 5 (3), 267–288.

(47) Lash, T. D.; Rauen, P. J. Extended Porphyrinoid Chromophores: Heteroporphyrins Fused to Phenanthrene and Acenaphthylene. Tetrahedron **2021**, 100, 132481.

(48) Ujah, V. C.; AbuSalim, D. I.; Lash, T. D. Synthesis, Protonation and Aromatic Characteristics of a Series of 1,10-Phenanthroline-Fused Porphyrinoids. J Org Chem **2025**, 90 (1), 8–29.

(49) Ulman, A.; Manassen, J. Synthesis of New Tetraphenylporphyrin Molecules Containing Heteroatoms Other than Nitrogen. I. Tetraphenyl-21,23-Dithiaporphyrin. J Am Chem Soc **1975**, 97 (22), 6540–6544.

(50) Lash, T. D. Recent Developments in the Chemistry of Heteroporphyrins and Heterocarbaporphyrins. In Advances in Heterocyclic Chemistry; 2022; Vol. 138, 243–334.

(51) Yedukondalu, M.; Ravikanth, M. Mono-Functionalized Heteroporphyrin Building Blocks and Unsymmetrical Covalent and Non-Covalent Porphyrin Dyads. J Chin Chem Soc **2011**, 58 (1), 1–14.

(52) Punidha, S.; Agarwal, N.; Burai, R.; Ravikanth, M. Synthesis of N3S, N3O, N2S2, N2O2, N2SO and N2OS Porphyrins with One Meso-Unsubstituted Carbon. Eur J Org Chem **2004**, 2004 (10), 2223–2230.

(53) Gupta, I.; Ravikanth, M. One-Flask Synthesis of Mono- and Trifunctionalized 21-Thia and 21-Oxaporphyrin Building Blocks and Their Application in the Synthesis of Covalent and Noncovalent Unsymmetrical Porphyrin Arrays. J Org Chem **2004**, 69 (20), 6796–6811.

(54) Gupta, I.; Neeraj, A.; Ravikanth, M. Novel and Rapid Synthetic Routes to A3B- and AB3-Type 21-Thiaporphyrins and Their Use in the Construction of Unsymmetrical Covalent and Non- Covalent Porphyrin Arrays. Eur J Org Chem **2004**, 2004 (8), 1693–1697.

(55) Janaagal, A.; Kushwaha, A.; Jhaldiyal, P.; Kumar, T. J. D.; Gupta, I. Photoredox Catalysis by 21-Thiaporphyrins: A Green and Efficient Approach for C-N Borylation and C-H Arylation. Chem Eur J **2024**, 30 (46), e202401623.

(56) Lee, J.; Papatzimas, J. W.; Bromby, A. D.; Gorobets, E.; Derksen, D. J. Thiaporphyrin-Mediated Photocatalysis Using Red Light. RSC Adv **2016**, 6 (64), 59269–59272.

(57) e Silva, R. C; da Silva, L. O.; de Andrade Bartolomeu, A.; Brocksom, T. J.; de Oliveira, K. T. Recent Applications of Porphyrins as Photocatalysts in Organic Synthesis: Batch and Continuous Flow Approaches. Beilstein J Org Chem **2020**, 16 (1), 917–955.

(58) Mane, S. B.; Hung, C. H. Synthesis of Carboxylate Functionalized A3B and A 2B2 Thiaporphyrins and Their Application in Dye-Sensitized Solar Cells. New J Chem **2014**, 38 (8), 3960–3972.

(59) Shi, Y.; Zhang, F.; Linhardt, R. J. Porphyrin-Based Compounds and Their Applications in Materials and Medicine. Dyes Pigm **2021**, 188, 109136.

(60) Mane, S. B.; Luo, L.; Chang, G. F.; Diau, E. W. G.; Hung, C. H. Effects of Core-Modification on Porphyrin Sensitizers to the Efficiencies of Dye-Sensitized Solar Cells. J Chin Chem Soc **2014**, 61 (5), 545–555.

(61) Hajizadeh, F.; Reisi-Vanani, A.; Azar, Y. T. Theoretical Design of Zn-Dithiaporphyrins as Sensitizer for Dye-Sensitized Solar Cells. Curr Appl Phys **2018**, 18 (10), 1122–1133.

(62) Arnold, L.; Müllen, K. Modifying the Porphyrin Core - A Chemist's Jigsaw. J Porphyr Phthalocyanines **2011**, 15 (09n10), 757–779.

(63) Heo, P. Y.; Shin, K.; Lee, C. H. Stepwise Syntheses of Core-Modified, Meso-Substituted Porphyrins. Tetrahedron Lett **1996**, 37 (2), 197–200.

(64) Srinivasan, A.; Sridevi, B.; Reddy, M. V. R.; Narayanan, S. J.; Chandrashekar, T. K. Improved Synthesis of Meso Substituted 21-Oxa and 2l-Thia Tetra Phenyl Porphyrins. Tetrahedron Lett **1997**, 38 (23), 4149–4152.

(65) Cho, W. S.; Kim, H. J.; Littler, B. J.; Miller, M. A.; Lee, C. H.; Lindsey, J. S. Rational Synthesis of Trans-Substituted Porphyrin Building Blocks Containing One Sulfur or Oxygen Atom in Place of Nitrogen at a Designated Site. J Org Chem **1999**, 64 (21), 7890–7901.

(66) Kaur, T.; Lee, W. Z.; Ravikanth, M. N-Methyl-21-Thiaporphyrins. Eur J Org Chem **2014**, 2014 (11), 2261–2267.

(67) Hilmey, D. G.; Abe, M.; Nelen, M. I.; Stilts, C. E.; Baker, G. A.; Baker, S. N.; Bright, F. V.; Davies, S. R.; Gollnick, S. O.; Oseroff, A. R.; Gibson, S. L.; Hilf, R.; Detty, M. R. Water-Soluble, Core-Modified Porphyrins as Novel, Longer-Wavelength-Absorbing Sensitizers for Photodynamic Therapy. II. Effects of Core Heteroatoms and Meso-Substituents on Biological Activity. J Med Chem **2002**, 45 (2), 449–461.

(68) Pandian, R. P.; Chandrashekar, T. K. Water-Soluble Thiaporphyrins and Metallothiaporphyrins; Synthesis, Characterization, Ground-and Excited-State Properties. J Chem Soc, Dalton Trans **1993**, (1), 119–125.

(69) Minnes, R.; Weitman, H.; You, N.; Detty, M. R.; Ehrenberg, B. Dithiaporphyrin Derivatives as Photosensitizers in Membranes and Cells. J Phys Chem B **2008**, 112 (10), 3268–3276.

(70) Stilts, C. E.; Nelen, M. I.; Hilmey, D. G.; Davies, S. R.; Gollnick, S. O.; Oseroff, A. R.; Gibson, S. L.; Hilf, R.; Detty, M. R. Water-Soluble, Core-Modified Porphyrins as Novel, Longer-Wavelength- Absorbing Sensitizers for Photodynamic Therapy. J Med Chem **2000**, 43 (12), 2403–2410.

(71) Chmielewski, P. J.; Latos-Grazyński, L. Core Modified Porphyrins - A Macrocyclic Platform for Organometallic Chemistry. Coord Chem Rev **2005**, 249 (21–22), 2510–2533.

(72) Latos-Grazyñski, L.; Lisowskv, J.; Olmstead, M. M.; Balch, A. L. Five-Coordinate Complexes of 21-Thiaporphyrin. Preparations, Spectra, and Structures of Iron(II), Nickel(II), and Copper(II) Complexes. Inorg Chem **1989**, 28 (6), 1183–1188.

(73) Lash, T. D. Carbaporphyrinoid Systems. Chem Rev **2017**, 117 (4), 2313–2446.

(74) Colby, D. A.; Lash, T. D. Adaptation of the Rothemund Reaction for Carbaporphyrin Synthesis: Preparation of Meso-Tetraphenylazuliporphyrin and Related Benzocarbaporphyrins. Chem Eur J **2002**, 8 (23), 5397–5402.

(75) Lash, T. D. Recent Advances on the Synthesis and Chemistry of Carbaporphyrins and Related Porphyrinoid Systems. Eur J Org Chem **2007**, 2007 (33), 5461–5481.

(76) Lash, T. D. Metal Complexes of Carbaporphyrinoid Systems. Chem Asian J **2014**, 9 (3), 682–705.

(77) Lash, T. D. Heteroporphyrins and Carbaporphyrins. In Fundamentals of Porphyrin Chemistry: A 21st Century Approach; 2022, Vol. 1, 385-451.

(78) Lash, T. D.; Hayes, M. J. Carbaporphyrine. Angew Chem **1997**, 109 (8), 868–870.

(79) Stepien, M.; Latos-Grazynski, L.; Ste¸pien, S. Benziporphyrins: Exploring Arene Chemistry in a Macrocyclic Environment. Acc Chem Res **2005**, 38 (2), 88–98.

(80) Stępień, M.; Latos-Grazyński, L. Tetraphenyl-p-Benziporphyrin: A Carbaporphyrinoid with Two Linked Carbon Atoms in the Coordination Core. J Am Chem Soc **2002**, 124 (15), 3838–3839.

(81) Chmielewski, P. J.; Latos-Grażyński, L.; Rachlewicz, K.; Glowiak, T. Tetra-p-tolylporphyrin with an Inverted Pyrrole Ring: A Novel Isomer of Porphyrin. Angew Chem Int Ed Engl **1994**, 33 (7), 779–781.

(82) Furuta, H.; Asano, T.; Ogawa, T. "N-Confused Porphyrin": A New Isomer of Tetraphenylporphyrin. J Am Chem Soc **1994**, 116 (2), 767–768.

(83) Mukherjee, A. K.; Singha, D.; Pal, N. Review on N-Confused Porphyrin. Int J Exp Res Rev **2022**, 29, 55–66.

(84) Harvey, J. D.; Ziegler, C. J. Developments in the Metal Chemistry of N-Confused Porphyrin. Coord Chem Rev **2003**, 247 (1–2), 1–19.

(85) Geier, G. R.; Haynes, D. M.; Lindsey, J. S. An Efficient One-Flask Synthesis of N-Confused Tetraphenylporphyrin. Org Lett **1999**, 1 (9), 1455–1458.

(86) Muckey, M. A.; Szczepura, L. F.; Ferrence, G. M.; Lash, T. D. Silver(III) Carbaporphyrins: The First Organometallic Complexes of True Carbaporphyrins. Inorg Chem **2002**, 41 (19), 4840–4842.

(87) Lash, T. D.; Colby, D. A.; Szczepura, L. F. New Riches in Carbaporphyrin Chemistry: Silver and Gold Organometallic Complexes of Benzocarbaporphyrins. Inorg Chem **2004**, 43 (17), 5258–5267.

(88) Toganoh, M.; Furuta, H. Blooming of Confused Porphyrinoids—Fusion, Expansion, Contraction, and More Confusion. Chem Commun **2012**, 48 (7), 937–954.

(89) Sprutta, N.; Latos-Grazyński, L. A Tetraphenylthiaporphyrin with an Inverted Thiophene Ring. Tetrahedron Lett **1999**, 40 (48), 8457–8460.

(90) Chmielewski, M. J.; Pawlicki, M.; Sprutta, N.; Szterenberg, L.; Latos-Grazyński, L. Cadmium(II) and Zinc(II) Complexes of S-Confused Thiaporphyrin. Inorg Chem **2006**, 45 (21), 8664–8671.

(91) Białek, M. J.; Hurej, K.; Furuta, H.; Latos-Grażyński, L. Organometallic Chemistry Confined within a Porphyrin-like Framework. Chem Soc Rev **2023**, 52 (6), 2082–2144.

(92) Pacholska, E.; Latos-Grazynski, L.; Szterenberg, L.; Ciunik, Z. Pyrrole-Inverted Isomer of 5,10,15,20-Tetraaryl-21-Selenaporphyrin. J Org Chem **2000**, 65 (24), 8188–8196.

(93) Latos-Graz, L.; Pacholska, E.; Chmielewski, P. J.; Olmstead, M. M.; Balch, A. L. 5,20-Diphenyl-10,15-Bis(p-Tolyl)-21-Selenaporphyrin and Its Nickel(II) Complexes 1. Inorg Chem **1996**, 35 (3), 566–573.

(94) Pushpan, S. K.; Srinivasan, A.; Anand, V. R. G.; Chandrashekar, T. K.; Subramanian, A.; Roy, R.; Sugiura, K.; Sakata, Y. Inverted Meso-Aryl Porphyrins with Heteroatoms; Characterization of Thia, Selena, and Oxa N-Confused Porphyrins. J Org Chem **2001**, 66 (1), 153–161.

(95) Saito, S.; Osuka, A. Expanded Porphyrins: Intriguing Structures, Electronic Properties, and Reactivities. Angew Chem Int Ed **2011**, 50 (19), 4342–4373.

(96) Anguera, G.; Brewster, J. T.; Sánchez-García, D.; Sessler, J. L. Functionalized 2,2'-Bipyrroles: Building Blocks for Pyrrolic Macrocycles. Macroheterocycles **2018**, 11 (3), 227–245.

(97) Sessler, J. L.; Davis, J. M. Sapphyrins: Versatile Anion Binding Agents. Acc Chem Res **2001**, 34 (12), 989–997.

(98) Wang, Z.; Lecane, P. S.; Thiemann, P.; Fan, Q.; Cortez, C.; Ma, X.; Tonev, D.; Miles, D.; Naumovski, L.; Miller, R. A.; Magda, D.; Cho, D. G.; Sessler, J. L.; Pike, B. L.; Yeligar, S. M.; Karaman, M. W.; Hacia, J. G. Synthesis and Biologic Properties of Hydrophilic Sapphyrins, a New Class of Tumor-Selective Inhibitors of Gene Expression. Mol Cancer **2007**, 6, 1–12.

(99) Hooker, J. D.; Nguyen, V. H.; Taylor, V. M.; Cedeño, D. L.; Lash, T. D.; Jones, M. A.; Robledo, S. M.; Vélez, I. D. New Application for Expanded Porphyrins: Sapphyrin and Heterosapphyrins as Inhibitors of Leishmania Parasites. Photochem Photobiol **2012**, 88 (1), 194–200.

(100) Judy, M. M.; Maithews, J. L.; Newman, J. T.; Skiles, H. L.; Boriack, R. L.; Sessler, J. L.; Cyr, M.; Maiya, B. G.; Nichol, S. T. In Vitro Photodynamic Inactivation of Herpes Simplex Virus with Sapphyrins: 22 π-Electron Porphyrin-like Macrocycles. Photochem Photobiol **1991**, 53 (1), 101–107.

(101) Sessler, J. L.; Cyr, M.; Burrell, A. K. Sapphyrins and Heterosapphyrins. Tetrahedron **1992**, 48 (44), 9661–9672.

(102) Shevchuk, S. V; Davis, J. M.; Sessler, J. L. Synthesis of Sapphyrins via a "3+1+1" Procedure. Tetrahedron Lett **2001**, 42 (13), 2447–2450.

(103) Chatterjee, T.; Srinivasan, A.; Ravikanth, M.; Chandrashekar, T. K. Smaragdyrins and Sapphyrins Analogues. Chem Rev **2017**, 117 (4), 3329–3376.

(104) Sessler, J. L.; Seidel, D. Synthetic Expanded Porphyrin Chemistry. Angew Chem Int Ed **2003**, 42 (42), 5134–5175.

(105) Chandrashekar, T. K.; Venkatraman, S. Core-Modified Expanded Porphyrins: New Generation Organic Materials. Acc Chem Res **2003**, 36 (9), 676–691.

(106) Broadhurst, M. J.; Grigg, R.; Johnson, A. W. New Macrocyclic Aromatic Systems Related to Porphins. J Chem Soc D, Chem Commun **1969**, (1), 23–24.

(107) Sessler, J. L.; Cyr, M. J.; Lynch, V.; Ibers, J. A. Synthetic and Structural Studies of Sapphyrin, a 22-π-Electron Pentapyrrolic "Expanded Porphyrin". J Am Chem Soc **1990**, 112 (7), 2810–2813.

(108) Kuznetsov, A. E. Phthalocyanines Core-Modified by P and S and Their Complexes with Fullerene C60: DFT Study. Phys Sci Rev **2019**, 4 (10), 20190001.

(109) Dalai, S.; Belov, V. N.; Nizamov, S.; Rauch, K.; Finsinger, D.; De Meijere, A. Access to Variously Substituted 5,6,7,8-Tetrahydro-3H-Quinazolin-4-Ones via Diels-Alder Adducts of Phenyl Vinyl Sulfone to Cyclobutene-Annelated Pyrimidinones. Eur J Org Chem **2006**, 2753–2765.

(110) Liu, W. X.; Yan, F.; Qian, S. L.; Ye, J. Y.; Liu, X.; Yu, M. X.; Wu, X. H.; Le, M. L.; Zhou, Z. Y.; Liu, S. H.; Low, P. J.; Jin, S. Electronic Structures of Divinylchalcogenophene-Bridged Biruthenium Complexes: Exploring Trends from O to Te. Eur J Inorg Chem **2017**, 2017 (43), 5015–5026.

(111) Chambrier, I.; Cook, M. J. Reaction of Phthalonitrile with Alkoxide Ions. J Chem Res, Synopses (print) **1990**, (10), 322–323.

(112) Bruson, H. A.; Kroeger, J. W. Cycli-Alkylation of Aromatic Compounds by the Friedel and Crafts Reaction. J Am Chem Soc **1940**, 62 (1), 36–44.

(113) Lamei, N.; Foroumadi, A.; Emami, S.; Amini, M.; Shafiee, A. Heterocycle-Bridged and Conformationally Constrained Retinoids: Synthesis of 4- (7, 8, 9, 10-Tetrahydro-7, 7, 10, 10-Tetramethyl-4H-Benzo [6, 7] Chromeno-[4, 3-d] Thiazole-2-Yl) Benzoic Acid. Chin J Chem **2010**, 28 (10), 1951–1956.

(114) Schareina, T.; Zapf, A.; Cotté, A.; Müller, N.; Beller, M. A Bio-Inspired Copper Catalyst System for Practical Catalytic Cyanation of Aryl Bromides. Synthesis **2008**, 2008 (20), 3351–3355.

(115) Schareina, T.; Zapf, A.; Mägerlein, W.; Müller, N.; Beller, M. A State-of-the-Art Cyanation of Aryl Bromides: A Novel and Versatile Copper Catalyst System Inspired by Nature. Chem Eur J **2007**, 13 (21), 6249–6254.

(116) Ellis, G. P.; Romney-Alexander, T. M. Cyanation of Aromatic Halides. Chem Rev **1987**, 87 (4), 779–794.

(117) McKeown, N. B. Phthalocynine Meterials: Synthesis, Structure and Function; Cambridge University Press; 1998.

(118) Sprutta, N.; Latos-Grayhski, L. A Tetraphenyithiaporphyrin with an Inverted Thiophene Ring. Tetrahedron Lett **1999**, 40 (48), 8457–8460.

(119) Chmielewski, P. J. Synthesis and Characterization of a Directly Linked N-Confused Porphyrin Dimer. Angew Chem **2004**, 116 (42), 5773–5776.

(120) Lash, T. D. Benziporphyrins, a Unique Platform for Exploring the Aromatic Characteristics of Porphyrinoid Systems. Org Biomol Chem **2015**, 13 (29), 7846–7878.

(121) Jasat, A.; Dolphin, D. Expanded Porphyrins and Their Heterologs. Chem Rev **1997**, 97 (6), 2267–2340.

(122) Han, P.; Han, M.; Sessler, J. L.; Lei, C. Resolution of Expanded Porphyrinoids: A Path to Persistent Chirality and Appealing Chiroptical Properties. Chem Eur J **2023**, 29 (72).

(123) Buess, C. M.; Lawson, D. D. The Preparation, Reactions, and Properties of Triphenylenes. Chem Rev **1960**, 60 (4), 313–330.

(124) Kumar, S. Recent Developments in the Chemistry of Triphenylene-Based Discotic Liquid Crystals. Liq Cryst **2004**, 31 (8), 1037–1059.

(125) Gopee, H.; Kong, X.; He, Z.; Chambrier, I.; Hughes, D. L.; Tizzard, G. J.; Coles, S. J.; Cammidge, A. N. Expanded Porphyrin-like Structures Based on Twinned Triphenylenes. J Org Chem **2013**, 78 (18), 9505–9511.

(126) Reynes, M.; Dautel, O. J.; Virieux, D.; Flot, D.; Moreau, J. J. E. Synthesis and Crystal Structure of Tris(2,3-Triphenylenedioxy) Cyclotriphosphazene: A New Clathration System. CrystEngComm **2011**, 13 (20), 6050–6056.

(127) Cammidge, A. N.; Gopee, H. Structural Factors Controlling the Transition between Columnar-Hexagonal and Helical Mesophase in Triphenylene Liquid Crystals. J Mater Chem **2001**, 11 (11), 2773–2783.

(128) Stępień, M.; Latos-Grażyński, L.; Sprutta, N.; Chwalisz, P.; Szterenberg, L. Expanded Porphyrin with a Split Personality: A Hückel–Möbius Aromaticity Switch. Angew Chem **2007**, 119 (41), 8015–8019.

(129) Ashton, P. R.; Girreser, U.; Giuffrida, D.; Kohnke, F. H.; Mathias, J. P.; Raymo, F. M.; Slawin, A. Z.; Stoddart, J. F.; Williams, D. J. Molecular Belts. 2. Substrate-Directed Syntheses of Belt-Type and Cage-Type Structure. J Am Chem Soc **1993**, 115 (13), 5422–5429.

(130) Wenderski, T.; Light, K. M.; Ogrin, D.; Bott, S. G.; Harlan, C. J. Pd Catalyzed Coupling of 1,2-Dibromoarenes and Anilines: Formation of N,N-Diaryl-o-Phenylenediamines. Tetrahedron Lett **2004**, 45 (37), 6851–6853.

(131) Metz, J.; Schneider, O.; Hanack, M. Synthesis and Properties of Substituted (Phthalocyaninato)Iron and-Cobalt Compounds and Their Pyridine Adducts. Inorg Chem **1984**, 23 (8), 1065–1071.

(132) Sauer, T.; Wegner, G. Control of the Discotic to Isotropic Transition in Alkoxy-Substituted Silicondihydroxo-Phthalocyanines by Axial Substituents. Mol Cryst Liq Cryst **1988**, 162 (2), 97–118.

(133) Devadoss, T. Synthetic Applications of P-Toluenesulfonyl Chloride: A Recent Update. J Mol Struct **2023**, 1289, 135850.

(134) Seidler, A.; Svoboda, J.; Dekoj, V.; Chocholoušová, J. V.; Vacek, J.; Stará, I. G.; Starý, I. The Synthesis of π-Electron Molecular Rods with a Thiophene or Thieno[3,2-b]Thiophene Core Unit and Sulfur Alligator Clips. Tetrahedron Lett **2013**, 54 (22), 2795–2798.

(135) Ou, Y. P.; Xia, J.; Zhang, J.; Xu, M.; Yin, J.; Yu, G. A.; Liu, S. H. Experimental and Theoretical Studies of Charge Delocalization in Biruthenium-Alkynyl Complexes Bridged by Thiophenes. Chem Asian J **2013**, 8 (9), 2023–2032.

(136) Ou, Y.-P.; Yang, X.; Lin, Z.; Kong, L.; Liu, S. H. Binuclear Metal Ruthenium Complexes Bridged by Isomeric Bis(Ethynyl)Pyridine: Syntheses, Characterization and Electronic Coupling Properties. J Organomet Chem **2022**, 980, 122491.

5 Appendix

1-Crystal data and structure refinement for *cyclo*-(thiophene-CH-isoindole-N-isoindole(CMe_2-$CH_2CH_2CMe_2$)-N-isoindole-CH-), CH_2Cl_2

Identification code	**2.18 (Figure 2.8)**
Elemental formula	C38 H31 N5 S, C H2 Cl2
Formula weight	674.66
Crystal system, space group	Monoclinic, $P2_1/c$ (no. 14)
Unit cell dimensions	a = 12.9705(2) Å α = 90 ° b = 8.23402(15) Å β = 91.1200(17) ° c = 29.5821(5) Å γ = 90 °
Volume	3158.75(9) $Å^3$
Z, Calculated density	4, 1.419 Mg/m^3
F(000)	1408
Absorption coefficient	2.766 mm^{-1}
Temperature	100.01(10) K
Wavelength	1.54184 Å
Crystal colour, shape	purple plate
Crystal size	0.21 x 0.09 x 0.03 mm
Crystal mounting:	on a small loop, in oil, fixed in cold N_2 stream
On the diffractometer:	
Theta range for data collection	7.760 to 69.957 °
Limiting indices	-15<=h<=15, -6<=k<=9, -35<=l<=35
Completeness to theta = 67.684	88.9 %
Absorption correction	Semi-empirical from equivalents
Max. and min. transmission	1.00000 and 0.23329
Reflections collected (not including absences)	11728
No. of unique reflections	5215 [R(int) for equivalents = 0.043]
No. of 'observed' reflections ($I > 2\sigma_I$)	4310
Structure determined by:	dual methods, in SHELXT
Refinement:	Full-matrix least-squares on F^2, in SHELXL

Data / restraints / parameters	5215 / 0 / 449
Goodness-of-fit on F^2	1.068
Final R indices ('observed' data)	R_1 = 0.055, wR_2 = 0.151
Final R indices (all data)	R_1 = 0.067, wR_2 = 0.158
Reflections weighted: $w = [\sigma^2(Fo^2)+(0.0978P)^2+1.8379P]^{-1}$ where $P=(Fo^2+2Fc^2)/3$	
Extinction coefficient	n/a
Largest diff. peak and hole	0.62 and -0.58 e.Å^{-3}
Location of largest difference peak	near H(71b)

Table 1. Atomic coordinates (x 10^4) and equivalent isotropic displacement parameters ($Å^2$ x 10^4). U(eq) is defined as one third of the trace of the orthogonalized Uij tensor. E.s.ds are in parentheses.

	x	y	z	U(eq)	S.o.f.#
S(1)	3271.7(5)	4198.1(8)	4700.5(2)	187(2)	
C(2)	2643(2)	3792(3)	5199.0(9)	190(6)	
C(3)	1686(2)	4586(3)	5204.1(9)	214(6)	
C(4)	1485(2)	5483(3)	4814.0(9)	232(6)	
C(5)	2282(2)	5409(3)	4499.4(9)	206(6)	
C(6)	2348(2)	6200(3)	4073.8(9)	201(6)	
N(7)	4066.6(16)	5243(3)	3919.0(7)	182(5)	
C(8)	3197(2)	6124(3)	3801.0(9)	188(5)	
C(9)	3347(2)	6944(3)	3366.0(9)	189(5)	
C(10)	2751(2)	7987(3)	3097.0(9)	221(6)	
C(11)	3175(2)	8567(3)	2699.8(9)	253(6)	
C(12)	4153(2)	8093(3)	2565.9(9)	250(6)	
C(13)	4752(2)	7043(3)	2829.9(9)	211(6)	
C(14)	4342(2)	6498(3)	3234.3(9)	185(5)	
C(15)	4747(2)	5452(3)	3594.9(8)	170(5)	
N(16)	5719.2(16)	4821(3)	3580.3(7)	179(5)	
N(17)	5733.6(16)	3374(2)	4307.6(7)	170(5)	
C(18)	6121.5(19)	3921(3)	3900.9(9)	174(5)	
C(19)	7164(2)	3255(3)	3873.0(9)	185(5)	
C(20)	7939(2)	3479(3)	3564.3(9)	201(6)	
C(21)	8891(2)	2705(3)	3628.7(9)	207(6)	
C(211)	9759(2)	3049(4)	3297.4(10)	257(6)	
C(212)	10796(3)	2365(5)	3497.9(14)	298(13)	0.772(10)
C(213)	10699(3)	664(7)	3676.0(14)	280(12)	0.772(10)
C(214)	9995(6)	598(12)	4093(3)	254(17)	0.772(10)
C(215)	10519(9)	1613(15)	3265(4)	200(30)*	0.228(10)
C(216)	10955(11)	1440(20)	3732(5)	230(40)*	0.228(10)
C(217)	10140(20)	820(40)	4042(11)	220(70)*	0.228(10)
C(21A)	9486(3)	2405(7)	2834.7(13)	642(14)	
C(21B)	9958(4)	4860(4)	3275.2(14)	551(11)	
C(21C)	10581(2)	1235(4)	4516.8(10)	314(7)	
C(21D)	9734(3)	-1166(4)	4145.7(12)	388(8)	
C(22)	9036(2)	1639(3)	4002.3(9)	216(6)	
C(23)	8255(2)	1458(3)	4315.6(9)	215(6)	
C(24)	7337.3(19)	2283(3)	4253.5(8)	181(5)	
C(25)	6425(2)	2373(3)	4535.3(8)	176(5)	
N(26)	6391.3(17)	1607(3)	4921.2(7)	183(5)	
N(27)	4695.2(17)	2455(3)	5138.9(7)	194(5)	
C(28)	5575(2)	1653(3)	5201.2(8)	172(5)	
C(29)	5590(2)	744(3)	5628.4(9)	193(5)	
C(30)	6300(2)	-284(3)	5829.7(9)	213(6)	
C(31)	6054(2)	-979(3)	6243.9(9)	250(6)	
C(32)	5113(2)	-649(3)	6446.2(9)	238(6)	
C(33)	4385(2)	372(3)	6240.8(9)	217(6)	
C(34)	4633(2)	1079(3)	5826.5(9)	192(5)	
C(35)	4085(2)	2151(3)	5508.7(9)	192(5)	
C(36)	3108(2)	2805(3)	5539.0(9)	200(6)	
C(41)	2878(3)	4328(4)	2310.2(11)	350(7)	
Cl(42)	3056.2(6)	3131.4(10)	2799.0(3)	375(2)	
Cl(43)	2023.6(7)	3399.9(14)	1921.5(3)	549(3)	

- site occupancy, if different from 1.
* - U(iso) ($Å^2$ x 10^4)

Table 2. Molecular dimensions. Bond lengths are in Ångstroms, angles in degrees. E.s.ds are in parentheses.

S(1)-C(5)	1.722(3)	C(211)-C(215)	1.544(12)
S(1)-C(2)	1.731(2)	C(211)-C(212)	1.564(5)
C(2)-C(3)	1.404(4)	C(212)-C(213)	1.503(7)
C(2)-C(36)	1.418(4)	C(213)-C(214)	1.550(8)
C(3)-C(4)	1.390(4)	C(214)-C(21D)	1.501(11)
C(4)-C(5)	1.406(3)	C(214)-C(22)	1.530(8)
C(5)-C(6)	1.422(4)	C(214)-C(21C)	1.544(9)
C(6)-C(8)	1.379(4)	C(215)-C(216)	1.49(2)
C(6)-H(6)	1.02(4)	C(216)-C(217)	1.50(3)
N(7)-C(15)	1.327(3)	C(217)-C(21C)	1.54(3)
N(7)-C(8)	1.380(3)	C(217)-C(22)	1.59(3)
C(8)-C(9)	1.469(4)	C(22)-C(23)	1.395(4)
C(9)-C(10)	1.395(4)	C(23)-C(24)	1.380(4)
C(9)-C(14)	1.404(4)	C(24)-C(25)	1.463(3)
C(10)-C(11)	1.391(4)	C(25)-N(26)	1.306(3)
C(11)-C(12)	1.393(4)	N(26)-C(28)	1.357(3)
C(12)-C(13)	1.391(4)	N(27)-C(28)	1.328(3)
C(13)-C(14)	1.393(4)	N(27)-C(35)	1.386(3)
C(14)-C(15)	1.461(4)	C(28)-C(29)	1.469(4)
C(15)-N(16)	1.365(3)	C(29)-C(30)	1.377(4)
N(16)-C(18)	1.304(3)	C(29)-C(34)	1.410(4)
N(17)-C(25)	1.383(3)	C(30)-C(31)	1.395(4)
N(17)-C(18)	1.388(3)	C(31)-C(32)	1.396(4)
C(18)-C(19)	1.463(3)	C(32)-C(33)	1.396(4)
C(19)-C(20)	1.384(4)	C(33)-C(34)	1.400(4)
C(19)-C(24)	1.396(4)	C(34)-C(35)	1.464(4)
C(20)-C(21)	1.399(4)	C(35)-C(36)	1.381(4)
C(21)-C(22)	1.421(4)	C(36)-H(36)	0.95(3)
C(21)-C(211)	1.534(3)		
C(211)-C(21A)	1.504(5)	C(41)-Cl(43)	1.756(4)
C(211)-C(21B)	1.515(5)	C(41)-Cl(42)	1.761(3)

C(5)-S(1)-C(2)	92.63(13)	C(13)-C(14)-C(15)	132.8(2)
C(3)-C(2)-C(36)	128.5(2)	C(9)-C(14)-C(15)	105.7(2)
C(3)-C(2)-S(1)	110.5(2)	N(7)-C(15)-N(16)	127.0(2)
C(36)-C(2)-S(1)	120.94(19)	N(7)-C(15)-C(14)	111.6(2)
C(4)-C(3)-C(2)	113.0(2)	N(16)-C(15)-C(14)	121.4(2)
C(3)-C(4)-C(5)	113.5(2)	C(18)-N(16)-C(15)	123.3(2)
C(4)-C(5)-C(6)	128.6(3)	C(25)-N(17)-C(18)	111.9(2)
C(4)-C(5)-S(1)	110.4(2)	N(16)-C(18)-N(17)	131.9(2)
C(6)-C(5)-S(1)	120.92(19)	N(16)-C(18)-C(19)	121.9(2)
C(8)-C(6)-C(5)	124.1(3)	N(17)-C(18)-C(19)	106.2(2)
C(8)-C(6)-H(6)	117.6(18)	C(20)-C(19)-C(24)	120.1(2)
C(5)-C(6)-H(6)	118.3(18)	C(20)-C(19)-C(18)	132.2(2)
C(15)-N(7)-C(8)	107.5(2)	C(24)-C(19)-C(18)	107.7(2)
C(6)-C(8)-N(7)	122.2(2)	C(19)-C(20)-C(21)	120.0(3)
C(6)-C(8)-C(9)	127.8(2)	C(20)-C(21)-C(22)	119.4(2)
N(7)-C(8)-C(9)	110.0(2)	C(20)-C(21)-C(211)	119.1(2)
C(10)-C(9)-C(14)	120.3(2)	C(22)-C(21)-C(211)	121.5(2)
C(10)-C(9)-C(8)	134.5(2)	C(21A)-C(211)-C(21B)	110.2(3)
C(14)-C(9)-C(8)	105.1(2)	C(21A)-C(211)-C(21)	110.7(2)
C(11)-C(10)-C(9)	118.0(3)	C(21B)-C(211)-C(21)	109.7(2)
C(10)-C(11)-C(12)	121.4(3)	C(21A)-C(211)-C(215)	79.2(6)
C(13)-C(12)-C(11)	121.1(2)	C(21B)-C(211)-C(215)	129.9(5)
C(12)-C(13)-C(14)	117.7(2)	C(21)-C(211)-C(215)	112.1(5)
C(13)-C(14)-C(9)	121.5(2)	C(21A)-C(211)-C(212)	113.8(3)

C(21B)-C(211)-C(212)	103.0(3)	N(26)-C(25)-N(17)	133.0(2)
C(21)-C(211)-C(212)	109.1(2)	N(26)-C(25)-C(24)	121.0(2)
C(213)-C(212)-C(211)	113.1(3)	N(17)-C(25)-C(24)	106.1(2)
C(212)-C(213)-C(214)	111.5(4)	C(25)-N(26)-C(28)	124.0(2)
C(21D)-C(214)-C(22)	112.1(6)	C(28)-N(27)-C(35)	107.7(2)
C(21D)-C(214)-C(21C)	110.6(6)	N(27)-C(28)-N(26)	127.4(2)
C(22)-C(214)-C(21C)	109.8(5)	N(27)-C(28)-C(29)	111.7(2)
C(21D)-C(214)-C(213)	104.7(5)	N(26)-C(28)-C(29)	120.9(2)
C(22)-C(214)-C(213)	109.3(6)	C(30)-C(29)-C(34)	121.8(2)
C(21C)-C(214)-C(213)	110.2(6)	C(30)-C(29)-C(28)	133.1(2)
C(216)-C(215)-C(211)	104.3(10)	C(34)-C(29)-C(28)	105.1(2)
C(215)-C(216)-C(217)	110.0(18)	C(29)-C(30)-C(31)	118.0(3)
C(216)-C(217)-C(21C)	103.4(19)	C(30)-C(31)-C(32)	120.9(3)
C(216)-C(217)-C(22)	117(2)	C(33)-C(32)-C(31)	121.4(2)
C(21C)-C(217)-C(22)	106.7(19)	C(32)-C(33)-C(34)	117.8(2)
C(216)-C(217)-C(21D)	130(2)	C(33)-C(34)-C(29)	120.2(3)
C(21C)-C(217)-C(21D)	99.0(17)	C(33)-C(34)-C(35)	134.1(2)
C(22)-C(217)-C(21D)	97.6(15)	C(29)-C(34)-C(35)	105.7(2)
C(23)-C(22)-C(21)	119.7(2)	C(36)-C(35)-N(27)	121.3(2)
C(23)-C(22)-C(214)	115.0(4)	C(36)-C(35)-C(34)	128.9(2)
C(21)-C(22)-C(214)	125.3(4)	N(27)-C(35)-C(34)	109.8(2)
C(23)-C(22)-C(217)	124.9(11)	C(35)-C(36)-C(2)	123.7(2)
C(21)-C(22)-C(217)	115.2(11)	C(35)-C(36)-H(36)	118.1(17)
C(24)-C(23)-C(22)	119.7(3)	C(2)-C(36)-H(36)	118.1(17)
C(23)-C(24)-C(19)	121.0(2)		
C(23)-C(24)-C(25)	130.9(2)	Cl(43)-C(41)-Cl(42)	111.42(18)
C(19)-C(24)-C(25)	108.1(2)		

Table 3. Anisotropic displacement parameters ($Å^2$ x 10^4) for the expression:

$$\exp\{-2\pi^2(h^2a^{*2}U_{11} + \ldots + 2hka^*b^*U_{12})\}$$

E.s.ds are in parentheses.

	U_{11}	U_{22}	U_{33}	U_{23}	U_{13}	U_{12}
S(1)	202(3)	180(3)	179(3)	9(2)	30(2)	40(2)
C(2)	220(13)	164(13)	189(12)	-43(10)	38(11)	-3(10)
C(3)	213(13)	217(13)	215(13)	-25(11)	41(11)	16(10)
C(4)	235(13)	196(13)	266(14)	-14(11)	31(12)	36(11)
C(5)	215(13)	174(13)	230(13)	-32(11)	20(11)	16(10)
C(6)	213(13)	174(13)	216(13)	-4(11)	-25(11)	34(10)
N(7)	202(11)	151(10)	193(10)	-3(9)	-8(9)	35(8)
C(8)	217(13)	168(13)	177(12)	3(10)	-33(10)	34(10)
C(9)	231(13)	149(12)	185(12)	-15(10)	-13(10)	6(10)
C(10)	283(14)	181(13)	197(13)	-12(11)	-38(11)	50(11)
C(11)	362(16)	182(13)	213(13)	3(11)	-73(12)	41(11)
C(12)	410(17)	162(13)	177(13)	-3(11)	5(12)	-25(12)
C(13)	299(14)	148(12)	185(12)	-10(10)	6(11)	-9(11)
C(14)	213(13)	169(13)	175(12)	-18(10)	-6(10)	-14(10)
C(15)	206(12)	129(12)	174(12)	-13(10)	-13(10)	-4(10)
N(16)	187(10)	171(11)	178(10)	-14(9)	-9(9)	11(8)
N(17)	185(10)	163(10)	161(10)	-14(9)	20(9)	13(8)
C(18)	187(12)	157(13)	178(12)	-16(10)	16(10)	-11(10)
C(19)	194(13)	169(13)	192(12)	-27(10)	9(11)	14(10)
C(20)	197(13)	211(13)	194(12)	-11(11)	9(11)	-4(10)
C(21)	203(13)	193(13)	226(13)	-56(11)	17(11)	5(10)
C(211)	179(13)	272(15)	323(15)	9(12)	51(12)	10(11)
C(212)	216(19)	380(30)	300(20)	20(19)	75(16)	11(17)
C(213)	213(19)	380(30)	250(20)	5(18)	65(16)	100(20)
C(214)	160(30)	430(40)	170(30)	40(30)	40(20)	90(30)
C(21A)	410(20)	1180(40)	339(19)	-290(20)	172(17)	-270(20)
C(21B)	740(30)	370(20)	550(20)	-10(18)	330(20)	-207(19)
C(21C)	213(14)	444(18)	284(15)	30(14)	-44(12)	-15(13)
C(21D)	427(18)	330(18)	402(17)	-117(14)	-122(15)	219(15)
C(22)	209(13)	243(14)	194(13)	-62(11)	-9(11)	42(11)
C(23)	245(14)	209(13)	188(12)	-18(11)	-21(11)	47(11)
C(24)	186(13)	170(13)	187(12)	-32(10)	4(10)	12(10)
C(25)	195(12)	146(12)	189(12)	-36(10)	10(10)	10(10)
N(26)	232(11)	154(11)	162(10)	-14(9)	-6(9)	16(9)
N(27)	237(11)	176(11)	168(10)	-12(9)	21(9)	7(9)
C(28)	194(13)	156(12)	163(12)	-32(10)	-22(10)	14(10)
C(29)	245(13)	151(12)	184(12)	-20(10)	-9(11)	-17(10)
C(30)	247(13)	163(13)	229(13)	-4(11)	-42(11)	10(10)
C(31)	349(16)	172(13)	225(13)	16(11)	-84(12)	-19(11)
C(32)	387(16)	169(13)	157(12)	-11(10)	-26(11)	-60(11)
C(33)	315(14)	166(13)	171(12)	-7(11)	14(11)	-17(11)
C(34)	260(13)	149(12)	168(12)	-23(10)	1(11)	-28(10)
C(35)	271(14)	142(12)	164(12)	-27(10)	31(11)	-8(10)
C(36)	258(14)	160(13)	183(12)	-21(10)	45(11)	-18(10)
C(41)	372(17)	292(16)	384(17)	-14(14)	-13(14)	-14(13)
Cl(42)	384(4)	403(4)	342(4)	56(3)	72(3)	-32(3)
Cl(43)	416(5)	773(7)	456(5)	-9(5)	-63(4)	-111(5)

Table 4. Hydrogen coordinates (x 10^4) and isotropic displacement parameters (Å^2 x 10^3). All hydrogen atoms were included in idealised positions with U(iso)'s set at 1.2*U(eq) or, for the methyl group hydrogen atoms, 1.5*U(eq) of the parent carbon atoms.

	x	y	z	U(iso)	S.o.f.#
H(3)	1224	4518	5449	26	
H(4)	869	6086	4765	28	
H(10)	2076	8293	3182	26	
H(11)	2788	9302	2516	30	
H(12)	4417	8493	2290	30	
H(13)	5417	6711	2738	25	
H(17)	5121	3633	4408	20	
H(20)	7825	4158	3309	24	
H(21A)	11322	2380	3260	36	0.772(10)
H(21B)	11039	3084	3746	36	0.772(10)
H(21C)	11392	247	3761	34	0.772(10)
H(21D)	10409	-46	3435	34	0.772(10)
H(21E)	10156	610	3168	24	0.228(10)
H(21F)	11069	1853	3047	24	0.228(10)
H(21G)	11211	2503	3842	27	0.228(10)
H(21H)	11544	672	3731	27	0.228(10)
H(71A)	10082	2509	2639	96	
H(71B)	8906	3027	2706	96	
H(71C)	9291	1259	2858	96	
H(71D)	10044	5292	3582	83	
H(71E)	9372	5398	3124	83	
H(71F)	10586	5062	3105	83	
H(81A)	11195	567	4573	47	
H(81B)	10130	1177	4779	47	
H(81C)	10788	2364	4467	47	
H(81D)	9337	-1536	3880	58	
H(81E)	9324	-1316	4417	58	
H(81F)	10372	-1800	4174	58	
H(23)	8354	770	4571	26	
H(30)	6937	-514	5691	26	
H(31)	6533	-1686	6390	30	
H(32)	4966	-1130	6730	29	
H(33)	3741	581	6378	26	
H(36)	2740(20)	2620(30)	5809(9)	12(6)	
H(6)	1740(30)	6890(40)	3966(11)	30(8)	
H(41A)	2603	5403	2396	42	
H(41B)	3552	4500	2166	42	

- site occupancy, if different from 1.

Table 5. Torsion angles, in degrees. E.s.ds are in parentheses.

C(5)-S(1)-C(2)-C(3)	0.1(2)	C(22)-C(21)-C(211)-C(212)	-11.5(4)
C(5)-S(1)-C(2)-C(36)	-178.7(2)	C(21A)-C(211)-C(212)-C(213)	-77.1(4)
C(36)-C(2)-C(3)-C(4)	178.8(3)	C(21B)-C(211)-C(212)-C(213)	163.6(3)
S(1)-C(2)-C(3)-C(4)	0.1(3)	C(21)-C(211)-C(212)-C(213)	47.1(4)
C(2)-C(3)-C(4)-C(5)	-0.3(4)	C(211)-C(212)-C(213)-C(214)	-66.2(6)
C(3)-C(4)-C(5)-C(6)	-178.3(3)	C(212)-C(213)-C(214)-C(21D)	164.3(4)
C(3)-C(4)-C(5)-S(1)	0.3(3)	C(212)-C(213)-C(214)-C(22)	44.0(7)
C(2)-S(1)-C(5)-C(4)	-0.2(2)	C(212)-C(213)-C(214)-C(21C)	-76.7(6)
C(2)-S(1)-C(5)-C(6)	178.5(2)	C(21A)-C(211)-C(215)-C(216)	-169.3(10)
C(4)-C(5)-C(6)-C(8)	175.9(3)	C(21B)-C(211)-C(215)-C(216)	83.4(10)
S(1)-C(5)-C(6)-C(8)	-2.6(4)	C(21)-C(211)-C(215)-C(216)	-61.1(11)
C(5)-C(6)-C(8)-N(7)	0.7(4)	C(211)-C(215)-C(216)-C(217)	69.5(19)
C(5)-C(6)-C(8)-C(9)	-177.7(3)	C(215)-C(216)-C(217)-C(21C)	-162.0(15)
C(15)-N(7)-C(8)-C(6)	-178.3(2)	C(215)-C(216)-C(217)-C(22)	-45(3)
C(15)-N(7)-C(8)-C(9)	0.3(3)	C(215)-C(216)-C(217)-C(21D)	84(3)
C(6)-C(8)-C(9)-C(10)	-0.1(5)	C(20)-C(21)-C(22)-C(23)	-4.2(4)
N(7)-C(8)-C(9)-C(10)	-178.6(3)	C(211)-C(21)-C(22)-C(23)	174.9(3)
C(6)-C(8)-C(9)-C(14)	178.7(3)	C(20)-C(21)-C(22)-C(214)	174.4(5)
N(7)-C(8)-C(9)-C(14)	0.2(3)	C(211)-C(21)-C(22)-C(214)	-6.5(6)
C(14)-C(9)-C(10)-C(11)	-0.3(4)	C(20)-C(21)-C(22)-C(217)	179.7(13)
C(8)-C(9)-C(10)-C(11)	178.3(3)	C(211)-C(21)-C(22)-C(217)	-1.2(14)
C(9)-C(10)-C(11)-C(12)	1.7(4)	C(21D)-C(214)-C(22)-C(23)	53.5(6)
C(10)-C(11)-C(12)-C(13)	-1.2(4)	C(21C)-C(214)-C(22)-C(23)	-69.9(7)
C(11)-C(12)-C(13)-C(14)	-0.6(4)	C(213)-C(214)-C(22)-C(23)	169.1(4)
C(12)-C(13)-C(14)-C(9)	2.0(4)	C(21D)-C(214)-C(22)-C(21)	-125.1(5)
C(12)-C(13)-C(14)-C(15)	-178.0(3)	C(21C)-C(214)-C(22)-C(21)	111.5(5)
C(10)-C(9)-C(14)-C(13)	-1.6(4)	C(213)-C(214)-C(22)-C(21)	-9.5(8)
C(8)-C(9)-C(14)-C(13)	179.4(2)	C(216)-C(217)-C(22)-C(23)	-166.7(15)
C(10)-C(9)-C(14)-C(15)	178.4(2)	C(21C)-C(217)-C(22)-C(23)	-52(2)
C(8)-C(9)-C(14)-C(15)	-0.6(3)	C(21D)-C(217)-C(22)-C(23)	50(2)
C(8)-N(7)-C(15)-N(16)	178.7(2)	C(216)-C(217)-C(22)-C(21)	9(3)
C(8)-N(7)-C(15)-C(14)	-0.7(3)	C(21C)-C(217)-C(22)-C(21)	124.3(12)
C(13)-C(14)-C(15)-N(7)	-179.2(3)	C(21D)-C(217)-C(22)-C(21)	-133.9(9)
C(9)-C(14)-C(15)-N(7)	0.8(3)	C(21)-C(22)-C(23)-C(24)	1.7(4)
C(13)-C(14)-C(15)-N(16)	1.4(4)	C(214)-C(22)-C(23)-C(24)	-177.0(4)
C(9)-C(14)-C(15)-N(16)	-178.6(2)	C(217)-C(22)-C(23)-C(24)	177.4(15)
N(7)-C(15)-N(16)-C(18)	-1.3(4)	C(22)-C(23)-C(24)-C(19)	2.3(4)
C(14)-C(15)-N(16)-C(18)	178.0(2)	C(22)-C(23)-C(24)-C(25)	-176.8(3)
C(15)-N(16)-C(18)-N(17)	0.5(4)	C(20)-C(19)-C(24)-C(23)	-3.8(4)
C(15)-N(16)-C(18)-C(19)	179.6(2)	C(18)-C(19)-C(24)-C(23)	178.6(2)
C(25)-N(17)-C(18)-N(16)	177.2(3)	C(20)-C(19)-C(24)-C(25)	175.4(2)
C(25)-N(17)-C(18)-C(19)	-2.0(3)	C(18)-C(19)-C(24)-C(25)	-2.2(3)
N(16)-C(18)-C(19)-C(20)	6.1(5)	C(18)-N(17)-C(25)-N(26)	179.6(3)
N(17)-C(18)-C(19)-C(20)	-174.7(3)	C(18)-N(17)-C(25)-C(24)	0.6(3)
N(16)-C(18)-C(19)-C(24)	-176.7(2)	C(23)-C(24)-C(25)-N(26)	1.0(4)
N(17)-C(18)-C(19)-C(24)	2.5(3)	C(19)-C(24)-C(25)-N(26)	-178.1(2)
C(24)-C(19)-C(20)-C(21)	1.3(4)	C(23)-C(24)-C(25)-N(17)	-179.8(3)
C(18)-C(19)-C(20)-C(21)	178.2(3)	C(19)-C(24)-C(25)-N(17)	1.0(3)
C(19)-C(20)-C(21)-C(22)	2.6(4)	N(17)-C(25)-N(26)-C(28)	0.3(4)
C(19)-C(20)-C(21)-C(211)	-176.5(2)	C(24)-C(25)-N(26)-C(28)	179.2(2)
C(20)-C(21)-C(211)-C(21A)	-66.4(4)	C(35)-N(27)-C(28)-N(26)	179.8(2)
C(22)-C(21)-C(211)-C(21A)	114.5(4)	C(35)-N(27)-C(28)-C(29)	0.2(3)
C(20)-C(21)-C(211)-C(21B)	55.4(4)	C(25)-N(26)-C(28)-N(27)	-0.2(4)
C(22)-C(21)-C(211)-C(21B)	-123.7(3)	C(25)-N(26)-C(28)-C(29)	179.4(2)
C(20)-C(21)-C(211)-C(215)	-152.8(6)	N(27)-C(28)-C(29)-C(30)	177.6(3)
C(22)-C(21)-C(211)-C(215)	28.1(6)	N(26)-C(28)-C(29)-C(30)	-2.0(4)
C(20)-C(21)-C(211)-C(212)	167.6(3)	N(27)-C(28)-C(29)-C(34)	-0.6(3)

N(26)-C(28)-C(29)-C(34)	179.8(2)	C(28)-C(29)-C(34)-C(35)	0.7(3)
C(34)-C(29)-C(30)-C(31)	-1.0(4)	C(28)-N(27)-C(35)-C(36)	-179.1(2)
C(28)-C(29)-C(30)-C(31)	-178.9(3)	C(28)-N(27)-C(35)-C(34)	0.2(3)
C(29)-C(30)-C(31)-C(32)	0.5(4)	C(33)-C(34)-C(35)-C(36)	0.6(5)
C(30)-C(31)-C(32)-C(33)	0.5(4)	C(29)-C(34)-C(35)-C(36)	178.6(3)
C(31)-C(32)-C(33)-C(34)	-0.9(4)	C(33)-C(34)-C(35)-N(27)	-178.6(3)
C(32)-C(33)-C(34)-C(29)	0.4(4)	C(29)-C(34)-C(35)-N(27)	-0.6(3)
C(32)-C(33)-C(34)-C(35)	178.2(3)	N(27)-C(35)-C(36)-C(2)	1.4(4)
C(30)-C(29)-C(34)-C(33)	0.6(4)	C(34)-C(35)-C(36)-C(2)	-177.8(3)
C(28)-C(29)-C(34)-C(33)	179.0(2)	C(3)-C(2)-C(36)-C(35)	-176.3(3)
C(30)-C(29)-C(34)-C(35)	-177.8(2)	S(1)-C(2)-C(36)-C(35)	2.3(4)

Table 6. Hydrogen bonds, in Ångstroms and degrees.

D-H...A	d(D-H)	d(H...A)	d(D...A)	<(DHA)
N(17)-H(17)...S(1)	0.88	2.61	3.486(2)	176.2
N(17)-H(17)...N(7)	0.88	2.38	2.875(3)	116.2
N(17)-H(17)...N(27)	0.88	2.44	2.926(3)	115.2

Crystal structure analysis of a *cyclo*-thiophene-tris-isoindole derivative

Crystal data: $C_{38}H_{31}N_5S$, CH_2Cl_2, M = 674.66. Monoclinic, space group $P2_1/c$ (no. 14), a = 12.9705(2), b = 8.23402(15), c = 29.5821(5) Å, β = 91.1200(17) °, V = 3158.74(8) $Å^3$. Z = 4, Dc = 1.419 g cm^{-3}, F(000) = 1408, T = 100.01(10) K, μ(Cu-Kα) = 27.66 cm^{-1}, λ(Cu-Kα) = 1.54184 Å.

The crystal was a purple plate. From a sample under oil, one, *ca* 0.21 x 0.09 x 0.03 mm, was mounted on a small loop and fixed in the cold nitrogen stream on a Rigaku Oxford Diffraction XtaLAB Synergy diffractometer, equipped with Cu-Kα radiation, HyPix detector and mirror monochromator. Intensity data were measured by thin-slice ω-scans. Total no. of reflections recorded, to θ_{max} = 70.0 °, was 11,728 of which 5215 were unique (Rint = 0.043); 4310 were 'observed' with $I > 2\sigma_I$.

Data were processed using the CrysAlisPro-CCD and -RED (1) programs. The structure was determined by the intrinsic phasing routines in the SHELXT program (2A) and refined by full-matrix least-squares methods, on F^2's, in SHELXL (2B). There is disorder in the tetramethylene group of the central isoindole residue. The non-hydrogen atoms were refined with anisotropic thermal parameters. The hydrogen atoms on C(6) and C(36) were located in a difference map and were refined freely; no hydrogen atoms were found on N(16) and N(26). The remaining hydrogen atoms were included in idealised positions and their Uiso values were set to ride on the Ueq values of the parent carbon atoms. At the conclusion of the refinement, wR_2 = 0.158 and R_1 = 0.067 (2B) for all 5215 reflections weighted $w = [\sigma^2(F_o^2) + (0.0978\ P)^2 + 1.8739\ P]^{-1}$ with $P = (F_o^2 + 2F_c^2)/3$; for the 'observed' data only, R_1 = 0.055.

In the final difference map, the highest peak (*ca* 0.6 e$Å^{-3}$) was near H(71b).

Scattering factors for neutral atoms were taken from reference (3). Computer programs used in this analysis have been noted above, and were run through WinGX (4) on a Dell Optiplex 780 PC at the University of East Anglia.

References

1) Programs CrysAlisPro, Rigaku Oxford Diffraction Ltd., Abingdon, UK (2018).

2) G. M. Sheldrick, Programs for crystal structure determination (SHELXT), Acta Cryst. (2015) A71, 3-8, and refinement (SHELXL), Acta Cryst. (2008) A64, 112-122 and (2015) C71, 3-8.

3)'International Tables for X-ray Crystallography', Kluwer Academic Publishers, Dordrecht (1992). Vol. C, pp. 500, 219 and 193.

4) L. J. Farrugia, *J. Appl. Cryst.* (2012) **45**, 849–854.

Legends for Figures

Figure 1. View of a molecule of the *cyclo*-thiophene-tris-isoindole derivative, indicating the atom numbering scheme. Thermal ellipsoids are drawn at the 50% probability level.

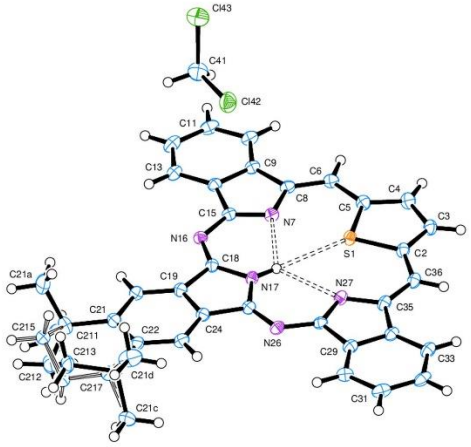

Figure 2. View of the packing/stacking of molecules, parallel to the *b* axis.

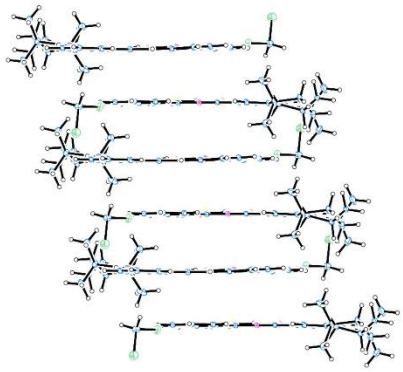

Figure 3. Packing of the molecules, viewed along the *b* axis.

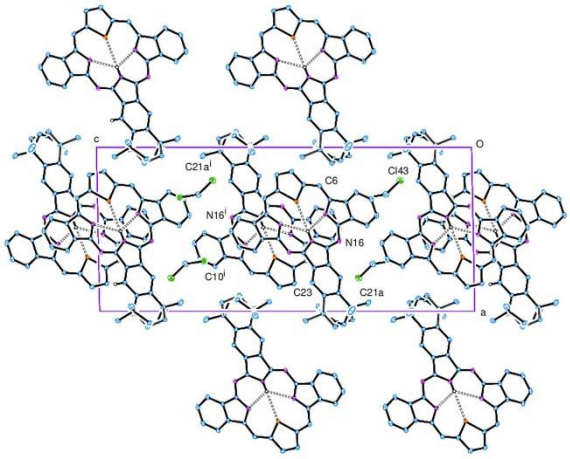

Notes on the structure

The principal molecule is a porphyrin derivative in which one of the pyrrole rings is replaced by a thiophene ring and the three remaining groups are isoindole derivatives. These four groups are linked by CH or N bridges, Figure 1.

The molecule is essentially planar except for the Me_2C-CH_2-CH_2-CMe_2 extension to the central isoindole residue; the atoms of this extension are disordered on either side of the molecular plane. The hydrogen atom of this central pyrrole ring was clearly identified in a difference map; it forms hydrogen bonds with the hetero atoms of the other two isoindole groups and S(1) of the thiophene group.

This molecule lies over an inverted molecule, with C(3) lying over C(24') at a distance of 3.278 Å. This dimer unit lies adjacent to, and *ca* 3.315 Å from its neighbour in a stack that runs parallel to the *b* axis, Figures 2 and 3.

A solvent molecule, CH_2Cl_2, is included in the crystal lattice.

2-Crystal data and structure refinement for Tol-SO_2-N-C_8H_5-CH-C_4H_2S-CH-C_8H_4-NH_2

Identification code	**2.33 (Figure (2.22))**
Elemental formula	C29 H22 N4 O2 S2, C H2 Cl2
Formula weight	607.55
Crystal system, space group	Triclinic, P-1 (no. 2)
Unit cell dimensions	a = 10.9621(3) Å α = 85.967(2) ° b = 11.1731(3) Å β = 84.032(2) ° c = 11.9243(3) Å γ = 75.335(2) °
Volume	1403.79(7) $Å^3$
Z, Calculated density	2, 1.437 Mg/m^3
F(000)	628
Absorption coefficient	3.766 mm^{-1}
Temperature	99.99(10) K
Wavelength	1.54184 Å
Crystal colour, shape	red block
Crystal size	0.15 x 0.17 x 0.29 mm
Crystal mounting:	on a small loop, in oil, fixed in cold N_2 stream
On the diffractometer:	
Theta range for data collection	8.209 to 72.499 °
Limiting indices	-13<=h<=12, -13<=k<=13, -14<=l<=14
Completeness to theta = 67.684	99.5 %
Absorption correction	Semi-empirical from equivalents
Max. and min. transmission	1.00000 and 0.66863
Reflections collected (not including absences)	17894
No. of unique reflections	5396 [R(int) for equivalents = 0.040]
No. of 'observed' reflections ($I > 2\sigma_I$)	4879

Structure determined by:	dual methods, in SHELXT
Refinement:	Full-matrix least-squares on F^2, in SHELXL
Data / restraints / parameters	5396 / 0 / 362
Goodness-of-fit on F^2	1.067
Final R indices ('observed' data)	R_1 = 0.036, wR_2 = 0.092
Final R indices (all data)	R_1 = 0.039, wR_2 = 0.094
Reflections weighted: $w = [\sigma^2(Fo^2)+(0.0443P)^2+0.6515P]^{-1}$ where $P=(Fo^2 + Fc^2)/3$	
Extinction coefficient	n/a
Largest diff. peak and hole	0.40 and -0.47 e.Å^{-3}
Location of largest difference peak	near C(31)

Table 1. Atomic coordinates (x 10^5) and equivalent isotropic displacement parameters ($Å^2$ x 10^4). U(eq) is defined as one third of the trace of the orthogonalized Uij tensor. E.s.ds are in parentheses.

	x	y	z	U(eq)
N(1)	11205(13)	38275(13)	35496(12)	182(3)
C(2)	3150(15)	45595(15)	28435(14)	180(3)
C(3)	-9648(15)	46476(15)	33728(14)	186(3)
C(4)	-21337(16)	52607(16)	30050(15)	220(3)
C(5)	-31989(16)	51688(17)	36978(16)	252(4)
C(6)	-31064(17)	44890(17)	47337(16)	260(4)
C(7)	-19395(16)	38672(16)	50946(15)	223(4)
C(8)	-8590(15)	39517(15)	43973(14)	186(3)
C(9)	4795(15)	34094(16)	45249(14)	187(3)
C(10)	10160(15)	26698(16)	53783(14)	192(3)
C(11)	23346(16)	21368(16)	54965(14)	195(3)
C(12)	28545(16)	15050(16)	64413(14)	211(3)
C(13)	41786(16)	11622(16)	63280(14)	213(3)
C(14)	47071(16)	15305(15)	52961(14)	191(3)
S(1)	35219(4)	22938(4)	44567(3)	193(1)
C(15)	60239(15)	13096(16)	49107(15)	199(3)
N(21)	57257(13)	25244(14)	31521(12)	204(3)
C(22)	64926(15)	17538(16)	39154(14)	190(3)
C(23)	78272(15)	15480(16)	34751(14)	188(3)
C(24)	89519(16)	8526(16)	38711(15)	220(4)
C(25)	100736(16)	8786(17)	32276(16)	241(4)
C(26)	100800(16)	15659(17)	22013(15)	236(4)
C(27)	89574(16)	22607(16)	17986(15)	212(3)
C(28)	78346(15)	22391(15)	24474(14)	186(3)
C(29)	64874(15)	28248(16)	23114(14)	194(3)
N(30)	60704(14)	35855(15)	14377(13)	248(3)
N(20)	5860(13)	51055(13)	18661(12)	206(3)
S(2)	20311(4)	47974(4)	12967(3)	195(1)
O(21)	20569(12)	56878(12)	3670(11)	268(3)
O(22)	29531(11)	46951(12)	21118(10)	236(3)
C(31)	22840(15)	33196(16)	7498(14)	198(3)
C(32)	32059(16)	23203(17)	11433(15)	218(4)
C(33)	33759(16)	11742(17)	6832(15)	243(4)
C(34)	26390(18)	10064(18)	-1474(15)	263(4)
C(35)	17060(17)	20269(18)	-5087(15)	260(4)
C(36)	15278(16)	31806(18)	-768(14)	230(4)
C(37)	28320(20)	-2320(20)	-6395(18)	365(5)
C(41)	38503(18)	71553(18)	24550(16)	274(4)
Cl(42)	50026(5)	71881(5)	13139(4)	401(1)
Cl(43)	24390(5)	83112(5)	22881(5)	440(2)

Table 2. Molecular dimensions. Bond lengths are in Ångstroms, angles in degrees. E.s.ds are in parentheses.

N(1)-C(2)	1.360(2)	C(22)-C(23)	1.468(2)
N(1)-C(9)	1.409(2)	C(23)-C(24)	1.390(2)
C(2)-N(20)	1.319(2)	C(23)-C(28)	1.402(2)
C(2)-C(3)	1.460(2)	C(24)-C(25)	1.386(2)
C(3)-C(4)	1.391(2)	C(25)-C(26)	1.399(3)
C(3)-C(8)	1.400(2)	C(26)-C(27)	1.391(2)
C(4)-C(5)	1.380(2)	C(27)-C(28)	1.389(2)
C(5)-C(6)	1.403(3)	C(28)-C(29)	1.477(2)
C(6)-C(7)	1.388(3)	C(29)-N(30)	1.340(2)
C(7)-C(8)	1.394(2)	N(20)-S(2)	1.6193(14)
C(8)-C(9)	1.458(2)	S(2)-O(21)	1.4395(12)
C(9)-C(10)	1.351(2)	S(2)-O(22)	1.4523(13)
C(10)-C(11)	1.435(2)	S(2)-C(31)	1.7637(18)
C(11)-C(12)	1.382(2)	C(31)-C(36)	1.393(2)
C(11)-S(1)	1.7353(17)	C(31)-C(32)	1.393(2)
C(12)-C(13)	1.399(2)	C(32)-C(33)	1.390(3)
C(13)-C(14)	1.386(2)	C(33)-C(34)	1.392(3)
C(14)-C(15)	1.433(2)	C(34)-C(35)	1.401(3)
C(14)-S(1)	1.7340(16)	C(34)-C(37)	1.498(3)
C(15)-C(22)	1.356(2)	C(35)-C(36)	1.382(3)
N(21)-C(29)	1.317(2)	C(41)-Cl(42)	1.7628(19)
N(21)-C(22)	1.400(2)	C(41)-Cl(43)	1.7656(19)
C(2)-N(1)-C(9)	112.48(13)	C(15)-C(22)-C(23)	127.32(15)
N(20)-C(2)-N(1)	128.69(15)	N(21)-C(22)-C(23)	109.67(14)
N(20)-C(2)-C(3)	124.60(15)	C(24)-C(23)-C(28)	120.65(15)
N(1)-C(2)-C(3)	106.71(14)	C(24)-C(23)-C(22)	133.35(16)
C(4)-C(3)-C(8)	121.93(15)	C(28)-C(23)-C(22)	106.00(14)
C(4)-C(3)-C(2)	130.57(16)	C(25)-C(24)-C(23)	117.97(16)
C(8)-C(3)-C(2)	107.49(14)	C(24)-C(25)-C(26)	121.34(16)
C(5)-C(4)-C(3)	117.31(16)	C(27)-C(26)-C(25)	120.96(16)
C(7)-C(6)-C(5)	121.27(16)	C(28)-C(27)-C(26)	117.62(16)
C(6)-C(7)-C(8)	117.71(16)	C(27)-C(28)-C(23)	121.44(15)
C(7)-C(8)-C(3)	120.41(15)	C(27)-C(28)-C(29)	133.79(16)
C(7)-C(8)-C(9)	131.08(16)	C(23)-C(28)-C(29)	104.76(14)
C(3)-C(8)-C(9)	108.51(14)	N(21)-C(29)-N(30)	123.01(15)
C(10)-C(9)-N(1)	126.41(15)	N(21)-C(29)-C(28)	112.61(14)
C(10)-C(9)-C(8)	128.78(15)	N(30)-C(29)-C(28)	124.37(15)
N(1)-C(9)-C(8)	104.81(13)	C(2)-N(20)-S(2)	119.67(12)
C(9)-C(10)-C(11)	128.46(15)	O(21)-S(2)-O(22)	116.89(7)
C(12)-C(11)-C(10)	126.59(16)	O(21)-S(2)-N(20)	106.10(7)
C(12)-C(11)-S(1)	110.30(13)	O(22)-S(2)-N(20)	112.96(7)
C(10)-C(11)-S(1)	123.01(13)	O(21)-S(2)-C(31)	108.48(8)
C(11)-C(12)-C(13)	113.44(15)	O(22)-S(2)-C(31)	106.88(8)
C(14)-C(13)-C(12)	113.73(15)	N(20)-S(2)-C(31)	104.84(8)
C(13)-C(14)-C(15)	127.55(15)	C(36)-C(31)-C(32)	121.15(17)
C(13)-C(14)-S(1)	110.02(12)	C(36)-C(31)-S(2)	118.04(13)
C(15)-C(14)-S(1)	122.40(13)	C(32)-C(31)-S(2)	120.81(14)
C(14)-S(1)-C(11)	92.51(8)	C(33)-C(32)-C(31)	118.79(16)
C(22)-C(15)-C(14)	125.05(15)	C(32)-C(33)-C(34)	121.44(16)
C(29)-N(21)-C(22)	106.92(14)	C(33)-C(34)-C(35)	118.21(17)
C(15)-C(22)-N(21)	123.00(15)	C(33)-C(34)-C(37)	121.01(18)

C(35)-C(34)-C(37)	120.77(18)	C(35)-C(36)-C(31)	118.83(16)
C(36)-C(35)-C(34)	121.56(17)	Cl(42)-C(41)-Cl(43)	112.06(10)

Table 3. Anisotropic displacement parameters ($Å^2$ x 10^4) for the expression:

$$\exp\{-2\pi^2(h^2a^{*2}U_{11} + \ldots + 2hka^*b^*U_{12})\}$$

E.s.ds are in parentheses.

	U_{11}	U_{22}	U_{33}	U_{23}	U_{13}	U_{12}
N(1)	135(6)	230(7)	175(7)	27(5)	7(5)	-56(5)
C(2)	172(8)	181(8)	189(8)	-2(6)	-11(6)	-54(6)
C(3)	172(8)	182(8)	204(8)	-13(6)	11(6)	-53(6)
C(4)	201(8)	205(8)	239(8)	8(7)	-6(7)	-32(7)
C(5)	170(8)	243(9)	316(10)	1(7)	-12(7)	-8(7)
C(6)	179(8)	265(9)	305(10)	-4(7)	71(7)	-38(7)
C(7)	196(8)	227(8)	230(9)	15(7)	34(7)	-52(7)
C(8)	169(8)	189(8)	195(8)	-12(6)	15(6)	-46(6)
C(9)	177(8)	206(8)	179(8)	-2(6)	28(6)	-70(6)
C(10)	169(8)	223(8)	188(8)	6(6)	26(6)	-76(6)
C(11)	193(8)	213(8)	182(8)	17(6)	15(6)	-75(7)
C(12)	216(8)	236(8)	175(8)	33(6)	13(6)	-68(7)
C(13)	212(8)	236(9)	187(8)	35(7)	-18(6)	-62(7)
C(14)	187(8)	204(8)	183(8)	23(6)	-25(6)	-53(6)
S(1)	148(2)	256(2)	164(2)	44(2)	3(1)	-53(2)
C(15)	173(8)	213(8)	211(8)	23(6)	-24(6)	-54(6)
N(21)	171(7)	250(7)	193(7)	44(6)	-20(5)	-68(6)
C(22)	146(7)	210(8)	214(8)	14(6)	-26(6)	-48(6)
C(23)	166(8)	209(8)	195(8)	-6(6)	5(6)	-64(6)
C(24)	194(8)	236(9)	220(8)	38(7)	-24(7)	-46(7)
C(25)	176(8)	257(9)	267(9)	16(7)	-27(7)	-17(7)
C(26)	176(8)	269(9)	253(9)	-19(7)	49(7)	-61(7)
C(27)	197(8)	242(9)	203(8)	17(7)	3(7)	-80(7)
C(28)	172(8)	196(8)	199(8)	4(6)	-18(6)	-63(6)
C(29)	174(8)	218(8)	197(8)	11(6)	-10(6)	-70(6)
N(30)	176(7)	324(8)	230(7)	98(6)	-30(6)	-63(6)
N(20)	172(7)	232(7)	203(7)	37(6)	3(5)	-51(6)
S(2)	169(2)	222(2)	190(2)	53(2)	6(2)	-68(2)
O(21)	256(6)	277(7)	257(6)	109(5)	13(5)	-87(5)
O(22)	206(6)	273(6)	243(6)	36(5)	-19(5)	-99(5)
C(31)	178(8)	239(9)	167(8)	32(6)	39(6)	-67(7)
C(32)	169(8)	285(9)	193(8)	51(7)	10(6)	-69(7)
C(33)	202(8)	251(9)	243(9)	41(7)	34(7)	-31(7)
C(34)	285(9)	297(10)	199(8)	2(7)	70(7)	-98(7)
C(35)	256(9)	370(10)	166(8)	1(7)	5(7)	-112(8)
C(36)	185(8)	317(9)	167(8)	44(7)	11(6)	-49(7)
C(37)	484(12)	321(11)	287(10)	-32(8)	21(9)	-111(9)
C(41)	269(9)	280(9)	265(9)	27(7)	21(7)	-79(7)
Cl(42)	306(2)	555(3)	311(3)	55(2)	60(2)	-104(2)
Cl(43)	356(3)	440(3)	404(3)	103(2)	36(2)	60(2)

Table 4. Hydrogen coordinates (x 10^4) and isotropic displacement parameters ($Å^2$ x 10^3). All hydrogen atoms were included in idealised positions with U(iso)'s set at 1.2*U(eq) or, for the methyl group hydrogen atoms, 1.5*U(eq) of the parent carbon atoms.

	x	y	z	U(iso)
H(1)	1950	3636	3412	22
H(4)	-2197	5724	2305	26
H(5)	-4012	5574	3469	30
H(6)	-3857	4454	5197	31
H(7)	-1879	3400	5793	27
H(10)	446	2477	5979	23
H(12)	2361	1321	7103	25
H(13)	4670	718	6905	26
H(15)	6614	814	5390	24
H(24)	8952	374	4562	26
H(25)	10854	420	3489	29
H(26)	10863	1558	1773	28
H(27)	8959	2733	1105	25
H(30A)	5254	3909	1408	30
H(30B)	6613	3761	894	30
H(32)	3709	2420	1716	26
H(33)	4009	491	941	29
H(35)	1184	1923	-1064	31
H(36)	900	3867	-339	28
H(37A)	3294	-231	-1389	55
H(37B)	2008	-399	-705	55
H(37C)	3321	-875	-146	55
H(41A)	4194	7276	3163	33
H(41B)	3659	6332	2521	33

Table 5. Torsion angles, in degrees. E.s.ds are in parentheses.

C(9)-N(1)-C(2)-N(20)	179.92(17)	C(15)-C(22)-C(23)-C(24)	2.9(3)
C(9)-N(1)-C(2)-C(3)	0.00(19)	N(21)-C(22)-C(23)-C(24)	-178.35(18)
N(20)-C(2)-C(3)-C(4)	1.2(3)	C(15)-C(22)-C(23)-C(28)	-177.36(17)
N(1)-C(2)-C(3)-C(4)	-178.85(17)	N(21)-C(22)-C(23)-C(28)	1.43(19)
N(20)-C(2)-C(3)-C(8)	-179.64(16)	C(28)-C(23)-C(24)-C(25)	0.8(3)
N(1)-C(2)-C(3)-C(8)	0.29(19)	C(22)-C(23)-C(24)-C(25)	-179.41(18)
C(8)-C(3)-C(4)-C(5)	0.6(3)	C(23)-C(24)-C(25)-C(26)	-1.0(3)
C(2)-C(3)-C(4)-C(5)	179.66(17)	C(24)-C(25)-C(26)-C(27)	0.8(3)
C(3)-C(4)-C(5)-C(6)	0.3(3)	C(25)-C(26)-C(27)-C(28)	-0.5(3)
C(4)-C(5)-C(6)-C(7)	-0.9(3)	C(26)-C(27)-C(28)-C(23)	0.3(3)
C(5)-C(6)-C(7)-C(8)	0.7(3)	C(26)-C(27)-C(28)-C(29)	-179.40(18)
C(6)-C(7)-C(8)-C(3)	0.2(3)	C(24)-C(23)-C(28)-C(27)	-0.5(3)
C(6)-C(7)-C(8)-C(9)	-179.37(18)	C(22)-C(23)-C(28)-C(27)	179.67(15)
C(4)-C(3)-C(8)-C(7)	-0.9(3)	C(24)-C(23)-C(28)-C(29)	179.27(16)
C(2)-C(3)-C(8)-C(7)	179.88(15)	C(22)-C(23)-C(28)-C(29)	-0.54(18)
C(4)-C(3)-C(8)-C(9)	178.78(16)	C(22)-N(21)-C(29)-N(30)	-178.21(16)
C(2)-C(3)-C(8)-C(9)	-0.45(19)	C(22)-N(21)-C(29)-C(28)	1.4(2)
C(2)-N(1)-C(9)-C(10)	179.86(17)	C(27)-C(28)-C(29)-N(21)	179.19(18)
C(2)-N(1)-C(9)-C(8)	-0.27(19)	C(23)-C(28)-C(29)-N(21)	-0.6(2)
C(7)-C(8)-C(9)-C(10)	-0.1(3)	C(27)-C(28)-C(29)-N(30)	-1.2(3)
C(3)-C(8)-C(9)-C(10)	-179.70(17)	C(23)-C(28)-C(29)-N(30)	179.09(17)
C(7)-C(8)-C(9)-N(1)	-179.94(18)	N(1)-C(2)-N(20)-S(2)	7.7(3)
C(3)-C(8)-C(9)-N(1)	0.44(19)	C(3)-C(2)-N(20)-S(2)	-172.38(13)
N(1)-C(9)-C(10)-C(11)	-0.3(3)	C(2)-N(20)-S(2)-O(21)	-169.76(13)
C(8)-C(9)-C(10)-C(11)	179.82(17)	C(2)-N(20)-S(2)-O(22)	-40.46(16)
C(9)-C(10)-C(11)-C(12)	171.79(18)	C(2)-N(20)-S(2)-C(31)	75.55(15)
C(9)-C(10)-C(11)-S(1)	-4.2(3)	O(21)-S(2)-C(31)-C(36)	-51.74(15)
C(10)-C(11)-C(12)-C(13)	-176.11(17)	O(22)-S(2)-C(31)-C(36)	-178.59(12)
S(1)-C(11)-C(12)-C(13)	0.3(2)	N(20)-S(2)-C(31)-C(36)	61.27(14)
C(11)-C(12)-C(13)-C(14)	0.4(2)	O(21)-S(2)-C(31)-C(32)	128.88(14)
C(12)-C(13)-C(14)-C(15)	-178.98(17)	O(22)-S(2)-C(31)-C(32)	2.03(15)
C(12)-C(13)-C(14)-S(1)	-0.9(2)	N(20)-S(2)-C(31)-C(32)	-118.11(14)
C(13)-C(14)-S(1)-C(11)	0.90(14)	C(36)-C(31)-C(32)-C(33)	1.0(2)
C(15)-C(14)-S(1)-C(11)	179.08(15)	S(2)-C(31)-C(32)-C(33)	-179.68(13)
C(12)-C(11)-S(1)-C(14)	-0.66(14)	C(31)-C(32)-C(33)-C(34)	-0.7(3)
C(10)-C(11)-S(1)-C(14)	175.86(15)	C(32)-C(33)-C(34)-C(35)	-0.4(3)
C(13)-C(14)-C(15)-C(22)	-175.97(18)	C(32)-C(33)-C(34)-C(37)	179.85(17)
S(1)-C(14)-C(15)-C(22)	6.2(3)	C(33)-C(34)-C(35)-C(36)	1.3(3)
C(14)-C(15)-C(22)-N(21)	2.0(3)	C(37)-C(34)-C(35)-C(36)	-178.97(17)
C(14)-C(15)-C(22)-C(23)	-179.40(16)	C(34)-C(35)-C(36)-C(31)	-1.0(3)
C(29)-N(21)-C(22)-C(15)	177.09(17)	C(32)-C(31)-C(36)-C(35)	-0.1(2)
C(29)-N(21)-C(22)-C(23)	-1.77(19)	S(2)-C(31)-C(36)-C(35)	-179.50(13)

Table 6. Hydrogen bonds, in Ångstroms and degrees.

D-H...A	d(D-H)	d(H...A)	d(D...A)	<(DHA)
N(1)-H(1)...S(1)	0.88	2.38	3.0139(14)	129.6
N(1)-H(1)...O(22)	0.88	2.25	2.8197(18)	122.3
N(30)-H(30A)...O(22)	0.88	2.53	3.3592(19)	158.4
N(30)-H(30B)...O(21)#1	0.88	2.15	3.0305(19)	175.6
C(36)-H(36)...N(20)#2	0.95	2.58	3.434(2)	149.5
C(41)-H(41B)...O(22)	0.99	2.26	3.210(2)	160.6

Symmetry transformations used to generate equivalent atoms:
#1 : 1-x, 1-y, -z #2 : -x, 1-y, -z

Crystal structure analysis of Tol-SO_2-N-C_8H_5-CH-C_4H_2S-CH-C_8H_4-NH_2

Crystal data: $C_{29}H_{22}N_4O_2S_2$, CH_2Cl_2, M = 607.55. Triclinic, space group P-1 (no. 2), a = 10.9621(3), b = 11.1731(3), c = 11.9243(3) Å, α = 85.967(2), β = 84.032(2), γ = 75.335(2) °, V = 1403.79(7) $Å^3$. Z = 2, Dc = 1.437 g cm^{-3}, F(000) = 628, T = 99.99(10) K, μ(Cu-Kα) = 37.7 cm^{-1}, λ(Cu-Kα) = 1.54184 Å.

The crystal was a red block. From a sample under oil, one, *ca* 0.15 x 0.17 x 0.29 mm, was mounted on a small loop and fixed in the cold nitrogen stream on a Rigaku Oxford Diffraction XtaLAB Synergy diffractometer, equipped with Cu-Kα radiation, HyPix detector and mirror monochromator. Intensity data were measured by thin-slice ω-scans. Total no. of reflections recorded, to θ_{max} = 72.5°, was 17,894 of which 5396 were unique (Rint = 0.040); 4879 were 'observed' with $I > 2\sigma_I$.

Data were processed using the CrysAlisPro-CCD and -RED (1) programs. The structure was determined by the intrinsic phasing routines in the SHELXT program (2A) and refined by full-matrix least-squares methods, on F^2's, in SHELXL (2B). The non-hydrogen atoms were refined with anisotropic thermal parameters. Many hydrogen atoms were clear in difference maps, but all were included in idealised positions and their Uiso values were set to ride on the Ueq values of the parent carbon or nitrogen atoms. At the conclusion of the refinement, wR_2 = 0.094 and R_1 = 0.039 (2B) for all 5396 reflections weighted w = $[\sigma^2(F_o^2) + (0.0443\ P)^2 + 06515\ P]^{-1}$ with P = $(F_o^2 + 2F_c^2)/3$; for the 'observed' data only, R_1 = 0.036.

In the final difference map, the highest peak (*ca* 0.4 e$Å^{-3}$) was near C(31).

Scattering factors for neutral atoms were taken from reference (3). Computer programs used in this analysis have been noted above, and were run through WinGX (4) on a Dell Optiplex 780 PC at the University of East Anglia.

References

1) Programs CrysAlisPro, Rigaku Oxford Diffraction Ltd., Abingdon, UK (2018).

2) G. M. Sheldrick, Programs for crystal structure determination (SHELXT), *Acta Cryst.* (2015) A**71**, 3-8, and refinement (SHELXL), *Acta Cryst.* (2008) A**64**, 112-122 and (2015) C**71**, 3-8.

3) 'International Tables for X-ray Crystallography', Kluwer Academic Publishers, Dordrecht (1992). Vol. C, pp. 500, 219 and 193.

4) L. J. Farrugia, *J. Appl. Cryst.* (2012) **45**, 849–854.

Legends for Figures

Figure 1.View of the tosyl molecule with hydrogen-bonded contacts, and solvent (CH_2Cl_2) molecule, indicating the atom numbering scheme. Thermal ellipsoids are drawn at the 50% probability level.

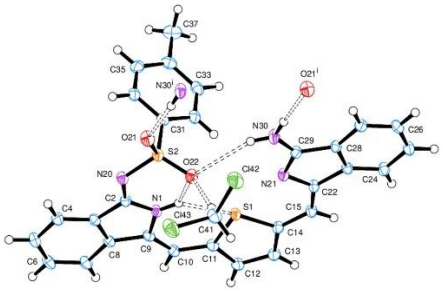

Figure 2.View of the stacking of four molecules. Molecules are linked through hydrogen bonds and π–π interactions.

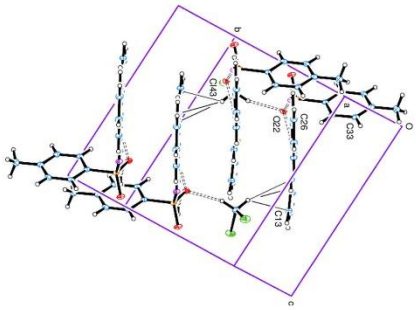

Figure 3.The packing of molecules, viewed along the *b* axis, showing the overlaying of aromatic rings.

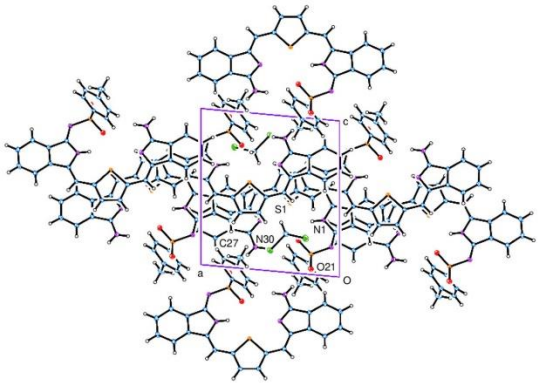

Notes on the structure

The atoms of the isoindole-thiophene-isoindole unit (ITI) of the molecule, from N(20), through N(1), S(1) and N(21) to N(30), form a good plane; the phenyl ring of C(31-36) is planar, with its normal 87.9 ° from that of the normal to the ITI unit, Figure 1. Within the ITI unit, there are two notably short bond distances, *viz.* C(2)–N(20) (1.319 Å) and C(29)–N(21) (1.317 Å); both are double-bonds. The isoindole H atom, H(1), forms a bifurcated pair of hydrogen bonds with S(1) and O(22); the two hydrogen atoms of the N(30) amine group each form good, approximately linear hydrogen bonds, intramolecularly with O(22) and intermolecularly with O(21'). The solvent molecule, CH_2Cl_2, is bound through a C–H…O(22) hydrogen bond to the main molecule.

The principal intermolecular bonding feature is, however, the stacking of the planar ITI units, Figure 2; four units are stacked with overlapping rings. Each of the isoindole, thiophene and isoindole-H rings of an ITI unit is involved in a separate stack.

3-Crystal data and structure refinement for Iso-thiophenylDAP-*op*-tetralin.CH_2Cl_2

Identification code	**2.46 (Figure 2.40)**
Elemental formula	C38 H31 N5 S, C H2 Cl2
Formula weight	674.66
Crystal system, space group	Monoclinic, P $2_1/c$ (no. 14)
Unit cell dimensions	a = 13.1271(4) Å α = 90 ° b = 8.2386(2) Å β = 91.789(2) ° c = 29.3880(7) Å γ = 90 °
Volume	3176.73(15) Å3
Z, Calculated density	4, 1.411 Mg/m3
F(000)	1408
Absorption coefficient	0.309 mm-1
Temperature	112(18) K
Wavelength	0.71073 Å
Crystal colour, shape	red plate
Crystal size	0.667 x 0.354 x 0.086 mm
Crystal mounting:	on a small loop, in oil, fixed in cold N_2 stream
On the diffractometer:	
Theta range for data collection	3.557 to 27.500 °
Limiting indices	-16<=h<=17, -10<=k<=10, -38<=l<=37
Completeness to theta = 25.242	99.7 %
Absorption correction	Semi-empirical from equivalents
Max. and min. transmission	1.00000 and 0.40573
Reflections collected (not including absences)	61008
No. of unique reflections	7256 [R(int) for equivalents = 0.048]
No. of 'observed' reflections ($I > 2\sigma_I$)	6183
Structure determined by:	dual methods, in SHELXT
Refinement:	Full-matrix least-squares on F^2, in SHELXL
Data / restraints / parameters	7256 / 0 / 442

Goodness-of-fit on F^2	1.012
Final R indices ('observed' data)	R_1 = 0.048, wR_2 = 0.115
Final R indices (all data)	R_1 = 0.059, wR_2 = 0.119
Reflections weighted: $w = 1/[\sigma^2(Fo^2)+(0.0504P)^2+3.526P]^{-1}$ where $P=(Fo^2+2Fc^2)/3$	
Extinction coefficient	n/a
Largest diff. peak and hole	0.81 and -0.72 e.Å^{-3}
Location of largest difference peak	near Cl(52)

Table 1. Atomic coordinates (x 10^5) and equivalent isotropic displacement parameters ($Å^2$ x 10^4). U(eq) is defined as one third of the trace of the orthogonalized Uij tensor. E.s.ds are in parentheses.

	x	y	z	U(eq)	S.o.f.#
N(1)	58404(11)	66783(18)	42986(5)	162(3)	
C(2)	65322(13)	76910(20)	45274(6)	169(3)	
C(3)	74231(13)	77830(20)	42385(6)	177(3)	
C(4)	83351(14)	86020(20)	43012(6)	203(4)	
C(5)	91017(14)	83970(20)	39850(6)	216(4)	
C(6)	100842(15)	93750(30)	40636(6)	284(4)	
C(61)	97680(30)	112540(40)	41405(12)	238(7)	0.706(5)
C(62)	106320(15)	88110(30)	45060(6)	266(4)	
C(7)	107290(20)	93540(50)	36585(9)	257(7)	0.706(5)
C(8)	108160(20)	76300(40)	34878(10)	283(8)	0.706(5)
C(9)	97829(15)	69550(30)	32762(7)	274(4)	
C(91)	95380(20)	76730(50)	28277(9)	297(8)	0.706(5)
C(92)	99930(30)	51480(30)	32718(10)	590(8)	
C(611)	99970(70)	109380(110)	40030(30)	290(20)#	0.294(5)
C(71)	109900(60)	86140(110)	36970(20)	198(16)#	0.294(5)
C(81)	105360(50)	83620(80)	32240(20)	233(17)#	0.294(5)
C(911)	92950(60)	68500(100)	27240(20)	264(17)#	0.294(5)
C(10)	89407(14)	73320(20)	36111(6)	202(4)	
C(11)	79927(13)	65600(20)	35473(6)	188(3)	
C(12)	72433(13)	68070(20)	38595(6)	171(3)	
C(13)	62108(13)	61340(20)	38898(5)	156(3)	
N(14)	57883(11)	52334(18)	35746(5)	166(3)	
N(15)	41826(11)	48685(18)	39408(5)	160(3)	
C(16)	48179(13)	46350(20)	36074(5)	157(3)	
C(17)	43840(14)	35940(20)	32463(6)	169(3)	
C(18)	47677(15)	30280(20)	28398(6)	199(4)	
C(19)	41571(16)	19880(20)	25781(6)	231(4)	
C(20)	31924(16)	15430(20)	27195(6)	246(4)	
C(21)	28003(15)	21400(20)	31217(6)	211(4)	
C(22)	34120(14)	31760(20)	33865(6)	174(3)	
C(23)	32897(13)	40060(20)	38253(6)	166(3)	
C(24)	24516(13)	39320(20)	40837(6)	181(3)	
C(25)	29931(14)	57140(20)	47536(6)	193(4)	
C(26)	23182(13)	47050(20)	45191(6)	186(3)	
S(27)	12654(5)	43483(8)	48162(2)	231(2)	0.632(3)
C(28)	15383(8)	55302(12)	52830(3)	295(3)	0.632(3)
C(27)	12654(5)	43483(8)	48162(2)	231(2)	0.368(3)
S(28)	15383(8)	55302(12)	52830(3)	295(3)	0.368(3)
C(29)	26581(14)	62130(20)	51805(6)	185(3)	
C(30)	32045(14)	72240(20)	55071(6)	195(4)	
N(31)	48021(11)	75089(18)	51006(5)	175(3)	
C(32)	41652(14)	78070(20)	54706(6)	182(3)	
C(33)	46980(14)	88920(20)	57986(6)	189(4)	
C(34)	44343(16)	95780(20)	62124(6)	226(4)	
C(35)	51347(17)	106190(20)	64262(6)	256(4)	
C(36)	60641(16)	109820(20)	62327(6)	251(4)	
C(37)	63269(15)	103040(20)	58188(6)	220(4)	
C(38)	56356(14)	92460(20)	56109(6)	188(4)	
C(39)	56479(14)	83410(20)	51818(6)	172(3)	
N(40)	64822(12)	84363(18)	49128(5)	180(3)	
C(51)	29127(18)	57070(30)	22918(7)	317(5)	

Cl(52)	30537(4)	69308(7)	27785(2)	370.4(14)
Cl(53)	20461(5)	65598(11)	18900(2)	565(2)

- site occupancy, if different from 1.
* - U(iso) ($Å^2$ x 10^4)

Table 2. Molecular dimensions. Bond lengths are in Ångstroms, angles in degrees. E.s.ds are in parentheses.

N(1)-C(13)	1.385(2)	C(16)-C(17)	1.466(2)
N(1)-C(2)	1.391(2)	C(17)-C(18)	1.391(2)
C(2)-N(40)	1.292(2)	C(17)-C(22)	1.396(2)
C(2)-C(3)	1.469(2)	C(18)-C(19)	1.389(3)
C(3)-C(4)	1.381(3)	C(19)-C(20)	1.394(3)
C(3)-C(12)	1.388(2)	C(20)-C(21)	1.394(3)
C(4)-C(5)	1.401(3)	C(21)-C(22)	1.393(2)
C(5)-C(10)	1.417(3)	C(22)-C(23)	1.473(2)
C(5)-C(6)	1.532(3)	C(23)-C(24)	1.357(2)
C(6)-C(611)	1.304(9)	C(24)-C(26)	1.445(2)
C(6)-C(7)	1.482(3)	C(25)-C(26)	1.383(3)
C(6)-C(62)	1.538(3)	C(25)-C(29)	1.404(2)
C(6)-C(61)	1.621(4)	C(26)-S(27)	1.6835(18)
C(6)-C(71)	1.746(8)	S(27)-C(28)	1.7111(12)
C(7)-C(8)	1.512(5)	C(28)-C(29)	1.611(2)
C(8)-C(9)	1.576(3)	C(29)-C(30)	1.444(3)
C(9)-C(91)	1.471(3)	C(30)-C(32)	1.357(3)
C(9)-C(92)	1.514(3)	N(31)-C(39)	1.320(2)
C(9)-C(81)	1.534(7)	N(31)-C(32)	1.414(2)
C(9)-C(10)	1.535(3)	C(32)-C(33)	1.475(2)
C(9)-C(911)	1.727(8)	C(33)-C(34)	1.394(2)
C(71)-C(81)	1.508(9)	C(33)-C(38)	1.395(3)
C(10)-C(11)	1.405(3)	C(34)-C(35)	1.393(3)
C(11)-C(12)	1.381(2)	C(35)-C(36)	1.395(3)
C(12)-C(13)	1.470(2)	C(36)-C(37)	1.392(3)
C(13)-N(14)	1.298(2)	C(37)-C(38)	1.386(3)
N(14)-C(16)	1.372(2)	C(38)-C(39)	1.466(2)
N(15)-C(16)	1.321(2)	C(39)-N(40)	1.373(2)
N(15)-C(23)	1.403(2)		

C(13)-N(1)-C(2)	111.84(14)	C(92)-C(9)-C(8)	101.3(2)
N(40)-C(2)-N(1)	131.20(16)	C(10)-C(9)-C(8)	107.70(17)
N(40)-C(2)-C(3)	123.07(16)	C(81)-C(9)-C(911)	99.5(4)
N(1)-C(2)-C(3)	105.73(14)	C(10)-C(9)-C(911)	111.1(3)
C(4)-C(3)-C(12)	120.99(16)	C(81)-C(71)-C(6)	111.2(5)
C(4)-C(3)-C(2)	130.58(16)	C(71)-C(81)-C(9)	104.5(5)
C(12)-C(3)-C(2)	108.39(15)	C(11)-C(10)-C(5)	119.61(17)
C(3)-C(4)-C(5)	119.36(17)	C(11)-C(10)-C(9)	118.39(17)
C(4)-C(5)-C(10)	119.73(16)	C(5)-C(10)-C(9)	121.98(16)
C(4)-C(5)-C(6)	117.10(17)	C(12)-C(11)-C(10)	119.41(17)
C(10)-C(5)-C(6)	123.17(17)	C(11)-C(12)-C(3)	120.76(16)
C(611)-C(6)-C(5)	115.4(4)	C(11)-C(12)-C(13)	131.47(16)
C(7)-C(6)-C(5)	111.84(18)	C(3)-C(12)-C(13)	107.70(15)
C(7)-C(6)-C(62)	114.3(2)	N(14)-C(13)-N(1)	130.59(16)
C(5)-C(6)-C(62)	109.76(15)	N(14)-C(13)-C(12)	123.15(15)
C(7)-C(6)-C(61)	106.1(2)	N(1)-C(13)-C(12)	106.25(14)
C(5)-C(6)-C(61)	107.77(19)	C(13)-N(14)-C(16)	122.16(15)
C(62)-C(6)-C(61)	106.60(19)	C(16)-N(15)-C(23)	106.79(14)
C(611)-C(6)-C(71)	109.2(5)	N(15)-C(16)-N(14)	127.52(15)
C(5)-C(6)-C(71)	107.7(3)	N(15)-C(16)-C(17)	112.47(15)
C(6)-C(7)-C(8)	109.2(2)	N(14)-C(16)-C(17)	120.00(15)
C(7)-C(8)-C(9)	112.9(2)	C(18)-C(17)-C(22)	121.97(16)
C(91)-C(9)-C(92)	115.0(2)	C(18)-C(17)-C(16)	132.44(17)
C(91)-C(9)-C(10)	110.56(18)	C(22)-C(17)-C(16)	105.59(15)
C(92)-C(9)-C(10)	109.86(18)	C(19)-C(18)-C(17)	117.65(17)
C(81)-C(9)-C(10)	113.0(3)	C(18)-C(19)-C(20)	120.72(17)
C(91)-C(9)-C(8)	111.9(2)	C(21)-C(20)-C(19)	121.54(17)

C(22)-C(21)-C(20)	117.93(18)	C(39)-N(31)-C(32)	106.55(14)
C(21)-C(22)-C(17)	120.17(16)	C(30)-C(32)-N(31)	124.94(16)
C(21)-C(22)-C(23)	134.18(17)	C(30)-C(32)-C(33)	125.87(16)
C(17)-C(22)-C(23)	105.64(15)	N(31)-C(32)-C(33)	109.16(15)
C(24)-C(23)-N(15)	124.94(16)	C(34)-C(33)-C(38)	120.42(17)
C(24)-C(23)-C(22)	125.56(16)	C(34)-C(33)-C(32)	133.63(18)
N(15)-C(23)-C(22)	109.50(15)	C(38)-C(33)-C(32)	105.93(15)
C(23)-C(24)-C(26)	126.76(16)	C(35)-C(34)-C(33)	117.69(18)
C(26)-C(25)-C(29)	114.05(16)	C(34)-C(35)-C(36)	121.44(17)
C(25)-C(26)-C(24)	127.79(16)	C(37)-C(36)-C(35)	120.95(18)
C(25)-C(26)-S(27)	111.71(13)	C(38)-C(37)-C(36)	117.44(19)
C(24)-C(26)-S(27)	120.44(14)	C(37)-C(38)-C(33)	122.04(17)
C(26)-S(27)-C(28)	99.31(8)	C(37)-C(38)-C(39)	132.42(17)
C(29)-C(28)-S(27)	102.61(9)	C(33)-C(38)-C(39)	105.51(15)
C(25)-C(29)-C(30)	126.84(17)	N(31)-C(39)-N(40)	127.38(15)
C(25)-C(29)-C(28)	112.21(14)	N(31)-C(39)-C(38)	112.83(15)
C(30)-C(29)-C(28)	120.95(14)	N(40)-C(39)-C(38)	119.79(16)
C(32)-C(30)-C(29)	126.53(16)	C(2)-N(40)-C(39)	122.75(15)
C(51)-Cl(52)	1.755(2)	Cl(52)-C(51)-Cl(53)	111.54(12)
C(51)-Cl(53)	1.760(2)		

Table 3. Anisotropic displacement parameters ($Å^2$ x 10^4) for the expression:

$$\exp\{-2\pi^2(h^2a^{*2}U_{11} + \ldots + 2hka^*b^*U_{12})\}$$

E.s.ds are in parentheses.

	U_{11}	U_{22}	U_{33}	U_{23}	U_{13}	U_{12}
N(1)	167(7)	175(7)	143(7)	4(5)	6(5)	-27(6)
C(2)	183(8)	165(8)	158(8)	27(6)	-18(6)	-24(7)
C(3)	187(8)	188(8)	156(8)	36(6)	-7(6)	-13(7)
C(4)	232(9)	215(9)	161(8)	38(7)	-31(7)	-70(7)
C(5)	204(9)	249(9)	191(8)	89(7)	-43(7)	-63(7)
C(6)	231(10)	416(12)	202(9)	70(8)	-28(7)	-163(9)
C(61)	261(15)	205(14)	246(15)	11(13)	-9(13)	-116(12)
C(62)	188(9)	391(11)	215(9)	-6(8)	-33(7)	-6(8)
C(7)	205(14)	336(19)	231(14)	16(12)	26(11)	-94(14)
C(8)	166(13)	433(19)	253(14)	-24(13)	61(10)	-2(12)
C(9)	163(9)	309(11)	354(11)	-22(8)	58(8)	-9(8)
C(91)	242(15)	470(20)	179(13)	11(13)	78(11)	-31(14)
C(92)	900(20)	433(15)	459(15)	-8(12)	305(15)	240(15)
C(10)	161(8)	217(9)	228(9)	65(7)	8(7)	1(7)
C(11)	176(8)	212(9)	177(8)	9(7)	7(6)	-10(7)
C(12)	163(8)	191(8)	157(8)	40(6)	-10(6)	-31(7)
C(13)	163(8)	167(8)	139(7)	24(6)	9(6)	-1(6)
N(14)	175(7)	178(7)	145(6)	4(5)	5(5)	-12(6)
N(15)	164(7)	158(7)	159(7)	-1(5)	0(5)	-18(6)
C(16)	174(8)	155(8)	140(7)	11(6)	-3(6)	-2(6)
C(17)	213(9)	130(8)	164(8)	11(6)	-22(6)	4(6)
C(18)	260(9)	171(8)	164(8)	14(7)	7(7)	6(7)
C(19)	376(11)	170(9)	147(8)	-4(7)	-6(7)	4(8)
C(20)	365(11)	180(9)	187(8)	-5(7)	-84(8)	-47(8)
C(21)	253(9)	184(9)	192(8)	25(7)	-45(7)	-51(7)
C(22)	214(9)	145(8)	161(8)	19(6)	-21(6)	6(7)
C(23)	185(8)	140(8)	172(8)	5(6)	-28(6)	-13(6)
C(24)	170(8)	170(8)	204(8)	-1(7)	-21(7)	-42(6)
C(25)	175(8)	211(9)	195(8)	-5(7)	49(7)	-21(7)
C(26)	162(8)	190(9)	207(8)	24(7)	24(6)	-15(7)
S(27)	212(3)	284(4)	200(3)	-21(2)	33(2)	-28(3)
C(28)	387(6)	274(5)	222(5)	7(4)	-12(4)	-25(4)
C(27)	212(3)	284(4)	200(3)	-21(2)	33(2)	-28(3)
S(28)	387(6)	274(5)	222(5)	7(4)	-12(4)	-25(4)
C(29)	200(9)	178(8)	178(8)	31(7)	30(7)	16(7)
C(30)	256(9)	192(9)	139(8)	16(6)	45(7)	32(7)
N(31)	214(8)	175(7)	136(7)	8(5)	15(6)	-4(6)
C(32)	261(9)	156(8)	128(7)	17(6)	10(7)	23(7)
C(33)	277(10)	153(8)	136(8)	19(6)	-16(7)	36(7)
C(34)	339(10)	196(9)	144(8)	15(7)	16(7)	57(8)
C(35)	415(12)	198(9)	151(8)	-34(7)	-31(8)	86(8)
C(36)	372(11)	180(9)	195(9)	-39(7)	-97(8)	30(8)
C(37)	285(10)	183(9)	189(8)	-3(7)	-54(7)	14(7)
C(38)	264(9)	152(8)	144(8)	14(6)	-34(7)	28(7)
C(39)	233(9)	146(8)	133(7)	18(6)	-23(6)	-1(7)
N(40)	212(8)	172(7)	154(7)	8(6)	-18(6)	-23(6)
C(51)	373(12)	246(10)	330(11)	-10(8)	-12(9)	6(9)
Cl(52)	346(3)	472(3)	298(3)	-74(2)	92(2)	46(2)
Cl(53)	350(3)	896(6)	441(3)	22(3)	-109(3)	69(3)

Table 4. Hydrogen coordinates (x 10^4) and isotropic displacement parameters (Å^2 x 10^3). All hydrogen atoms were included in idealised positions with U(iso)'s set at 1.2*U(eq) or, for the methyl group hydrogen atoms, 1.5*U(eq) of the parent carbon atoms.

	x	y	z	U(iso)	S.o.f.#
H(1)	5253	6421	4399	19	
H(4)	8439	9282	4551	24	
H(61A)	9347	11335	4401	36	0.706(5)
H(61B)	10372	11896	4190	36	0.706(5)
H(61C)	9398	11646	3876	36	0.706(5)
H(62A)	10168	8858	4752	40	
H(62B)	10866	7717	4470	40	
H(62C)	11204	9508	4572	40	
H(7A)	11400	9777	3738	31	0.706(5)
H(7B)	10427	10036	3422	31	0.706(5)
H(8A)	11038	6937	3738	34	0.706(5)
H(8B)	11333	7588	3259	34	0.706(5)
H(91A)	9416	8815	2862	45	0.706(5)
H(91B)	10098	7510	2631	45	0.706(5)
H(91C)	8939	7163	2698	45	0.706(5)
H(92A)	10145	4782	3577	88	
H(92B)	9403	4585	3152	88	
H(92C)	10563	4931	3084	88	
H(61D)	10647	11446	4060	43	0.294(5)
H(61E)	9768	11152	3696	43	0.294(5)
H(61F)	9513	11366	4210	43	0.294(5)
H(71A)	11556	9367	3683	24	0.294(5)
H(71B)	11250	7589	3814	24	0.294(5)
H(81A)	11060	8082	3012	28	0.294(5)
H(81B)	10187	9333	3117	28	0.294(5)
H(91D)	8798	5998	2702	40	0.294(5)
H(91E)	8981	7866	2643	40	0.294(5)
H(91F)	9837	6628	2521	40	0.294(5)
H(11)	7871	5889	3297	23	
H(18)	5410	3335	2747	24	
H(19)	4394	1584	2306	28	
H(20)	2801	831	2541	30	
H(21)	2150	1856	3211	25	
H(24)	1907	3321	3968	22	
H(25)	3614	6034	4639	23	
H(28)	1140	5729	5533	35	0.632(3)
H(27)	702	3700	4747	28	0.368(3)
H(30)	2864	7502	5769	23	
H(34)	3812	9348	6341	27	
H(35)	4979	11082	6704	31	
H(36)	6515	11687	6382	30	
H(37)	6943	10551	5687	26	
H(51A)	2673	4642	2379	38	
H(51B)	3570	5575	2155	38	

- site occupancy, if different from 1.

Table 5. Torsion angles, in degrees. E.s.ds are in parentheses.

C(13)-N(1)-C(2)-N(40)	-179.89(18)	C(3)-C(12)-C(13)-N(14)	176.34(16)
C(13)-N(1)-C(2)-C(3)	-0.48(19)	C(11)-C(12)-C(13)-N(1)	174.01(18)
N(40)-C(2)-C(3)-C(4)	0.2(3)	C(3)-C(12)-C(13)-N(1)	-2.91(19)
N(1)-C(2)-C(3)-C(4)	-179.30(18)	N(1)-C(13)-N(14)-C(16)	-0.1(3)
N(40)-C(2)-C(3)-C(12)	178.06(16)	C(12)-C(13)-N(14)-C(16)	-179.14(16)
N(1)-C(2)-C(3)-C(12)	-1.41(19)	C(23)-N(15)-C(16)-N(14)	-179.40(16)
C(12)-C(3)-C(4)-C(5)	-2.2(3)	C(23)-N(15)-C(16)-C(17)	-0.01(19)
C(2)-C(3)-C(4)-C(5)	175.44(18)	C(13)-N(14)-C(16)-N(15)	0.7(3)
C(3)-C(4)-C(5)-C(10)	-1.2(3)	C(13)-N(14)-C(16)-C(17)	-178.67(16)
C(3)-C(4)-C(5)-C(6)	178.17(17)	N(15)-C(16)-C(17)-C(18)	-179.74(18)
C(4)-C(5)-C(6)-C(611)	-69.2(5)	N(14)-C(16)-C(17)-C(18)	-0.3(3)
C(10)-C(5)-C(6)-C(611)	110.2(5)	N(15)-C(16)-C(17)-C(22)	-0.6(2)
C(4)-C(5)-C(6)-C(7)	-166.8(2)	N(14)-C(16)-C(17)-C(22)	178.86(15)
C(10)-C(5)-C(6)-C(7)	12.6(3)	C(22)-C(17)-C(18)-C(19)	-1.5(3)
C(4)-C(5)-C(6)-C(62)	65.2(2)	C(16)-C(17)-C(18)-C(19)	177.54(18)
C(10)-C(5)-C(6)-C(62)	-115.4(2)	C(17)-C(18)-C(19)-C(20)	0.4(3)
C(4)-C(5)-C(6)-C(61)	-50.5(2)	C(18)-C(19)-C(20)-C(21)	1.0(3)
C(10)-C(5)-C(6)-C(61)	128.9(2)	C(19)-C(20)-C(21)-C(22)	-1.4(3)
C(4)-C(5)-C(6)-C(71)	168.5(3)	C(20)-C(21)-C(22)-C(17)	0.3(3)
C(10)-C(5)-C(6)-C(71)	-12.1(4)	C(20)-C(21)-C(22)-C(23)	-178.32(18)
C(5)-C(6)-C(7)-C(8)	-47.4(3)	C(18)-C(17)-C(22)-C(21)	1.2(3)
C(62)-C(6)-C(7)-C(8)	78.1(3)	C(16)-C(17)-C(22)-C(21)	-178.09(16)
C(61)-C(6)-C(7)-C(8)	-164.6(2)	C(18)-C(17)-C(22)-C(23)	-179.86(16)
C(6)-C(7)-C(8)-C(9)	68.9(3)	C(16)-C(17)-C(22)-C(23)	0.87(18)
C(7)-C(8)-C(9)-C(91)	73.5(3)	C(16)-N(15)-C(23)-C(24)	179.61(17)
C(7)-C(8)-C(9)-C(92)	-163.5(2)	C(16)-N(15)-C(23)-C(22)	0.58(19)
C(7)-C(8)-C(9)-C(10)	-48.2(3)	C(21)-C(22)-C(23)-C(24)	-1.2(3)
C(611)-C(6)-C(71)-C(81)	-80.9(7)	C(17)-C(22)-C(23)-C(24)	-179.96(17)
C(5)-C(6)-C(71)-C(81)	45.1(6)	C(21)-C(22)-C(23)-N(15)	177.81(19)
C(6)-C(71)-C(81)-C(9)	-68.3(6)	C(17)-C(22)-C(23)-N(15)	-0.93(19)
C(10)-C(9)-C(81)-C(71)	60.2(6)	N(15)-C(23)-C(24)-C(26)	-0.2(3)
C(911)-C(9)-C(81)-C(71)	178.0(5)	C(22)-C(23)-C(24)-C(26)	178.65(17)
C(4)-C(5)-C(10)-C(11)	3.5(3)	C(29)-C(25)-C(26)-C(24)	-177.17(17)
C(6)-C(5)-C(10)-C(11)	-175.88(17)	C(29)-C(25)-C(26)-S(27)	0.0(2)
C(4)-C(5)-C(10)-C(9)	-174.96(17)	C(23)-C(24)-C(26)-C(25)	2.4(3)
C(6)-C(5)-C(10)-C(9)	5.7(3)	C(23)-C(24)-C(26)-S(27)	-174.47(15)
C(91)-C(9)-C(10)-C(11)	70.7(3)	C(25)-C(26)-S(27)-C(28)	2.00(15)
C(92)-C(9)-C(10)-C(11)	-57.3(3)	C(24)-C(26)-S(27)-C(28)	179.38(14)
C(81)-C(9)-C(10)-C(11)	151.8(3)	C(26)-S(27)-C(28)-C(29)	-2.90(11)
C(8)-C(9)-C(10)-C(11)	-166.81(19)	C(26)-C(25)-C(29)-C(30)	178.11(17)
C(911)-C(9)-C(10)-C(11)	41.0(4)	C(26)-C(25)-C(29)-C(28)	-2.2(2)
C(91)-C(9)-C(10)-C(5)	-110.9(2)	S(27)-C(28)-C(29)-C(25)	3.32(15)
C(92)-C(9)-C(10)-C(5)	121.2(2)	S(27)-C(28)-C(29)-C(30)	-177.00(14)
C(81)-C(9)-C(10)-C(5)	-29.7(4)	C(25)-C(29)-C(30)-C(32)	-3.7(3)
C(8)-C(9)-C(10)-C(5)	11.7(3)	C(28)-C(29)-C(30)-C(32)	176.67(15)
C(911)-C(9)-C(10)-C(5)	-140.5(3)	C(29)-C(30)-C(32)-N(31)	-0.3(3)
C(5)-C(10)-C(11)-C(12)	-2.3(3)	C(29)-C(30)-C(32)-C(33)	177.40(17)
C(9)-C(10)-C(11)-C(12)	176.21(17)	C(39)-N(31)-C(32)-C(30)	177.16(17)
C(10)-C(11)-C(12)-C(3)	-1.1(3)	C(39)-N(31)-C(32)-C(33)	-0.89(19)
C(10)-C(11)-C(12)-C(13)	-177.72(17)	C(30)-C(32)-C(33)-C(34)	1.4(3)
C(4)-C(3)-C(12)-C(11)	3.5(3)	N(31)-C(32)-C(33)-C(34)	179.39(18)
C(2)-C(3)-C(12)-C(11)	-174.67(16)	C(30)-C(32)-C(33)-C(38)	-176.74(17)
C(4)-C(3)-C(12)-C(13)	-179.22(16)	N(31)-C(32)-C(33)-C(38)	1.29(19)
C(2)-C(3)-C(12)-C(13)	2.65(19)	C(38)-C(33)-C(34)-C(35)	0.2(3)
C(2)-N(1)-C(13)-N(14)	-177.10(18)	C(32)-C(33)-C(34)-C(35)	-177.70(18)
C(2)-N(1)-C(13)-C(12)	2.07(19)	C(33)-C(34)-C(35)-C(36)	0.7(3)
C(11)-C(12)-C(13)-N(14)	-6.7(3)	C(34)-C(35)-C(36)-C(37)	-0.4(3)

C(35)-C(36)-C(37)-C(38)	-0.7(3)	C(37)-C(38)-C(39)-N(31)	-177.25(18)
C(36)-C(37)-C(38)-C(33)	1.6(3)	C(33)-C(38)-C(39)-N(31)	0.7(2)
C(36)-C(37)-C(38)-C(39)	179.20(18)	C(37)-C(38)-C(39)-N(40)	2.2(3)
C(34)-C(33)-C(38)-C(37)	-1.4(3)	C(33)-C(38)-C(39)-N(40)	-179.93(15)
C(32)-C(33)-C(38)-C(37)	177.05(16)	N(1)-C(2)-N(40)-C(39)	-0.5(3)
C(34)-C(33)-C(38)-C(39)	-179.54(16)	C(3)-C(2)-N(40)-C(39)	-179.81(16)
C(32)-C(33)-C(38)-C(39)	-1.13(18)	N(31)-C(39)-N(40)-C(2)	0.6(3)
C(32)-N(31)-C(39)-N(40)	-179.20(17)	C(38)-C(39)-N(40)-C(2)	-178.77(16)
C(32)-N(31)-C(39)-C(38)	0.16(19)		

Table 6. Hydrogen bonds, in Ångstroms and degrees.

D-H...A	d(D-H)	d(H...A)	d(D...A)	<(DHA)
N(1)-H(1)...N(15)	0.86	2.30	2.815(2)	118.2
N(1)-H(1)...N(31)	0.86	2.34	2.843(2)	117.5
C(25)-H(25)...N(15)	0.93	2.40	2.977(2)	119.7
C(25)-H(25)...N(31)	0.93	2.37	2.952(2)	120.4
C(27)-H(27)...S(28)#1	0.93	3.01	3.6842(13)	131.0

Symmetry transformations used to generate equivalent atoms:
#1 : -x, 1-y, 1-z

Crystal structure analysis of Iso-thiophenylDAP-*op*-tetralin.CH_2Cl_2

Crystal data: $C_{38}H_{31}N_5S$, CH_2Cl_2, M = 674.66. Monoclinic, space group $P2_1/c$ (no. 14), a = 13.1271(4), b = 8.2386(2), c = 29.3880(7) Å, β = 91.789(2) °, V = 3176.73(15) $Å^3$. Z = 4, Dc = 1.411 g cm^{-3}, F(000) = 1408, T = 112(18) K, μ(Mo-Kα) = 3.09 cm^{-1}, λ(Mo-Kα) = 0.71073 Å.

The crystal was a red plate. From a sample under oil, one, *ca* 0.086 x 0.354 x 0.667 mm, was mounted on a small loop and fixed in the cold nitrogen stream on a Rigaku Oxford Diffraction XtaLAB Synergy diffractometer, equipped with Mo-Kα radiation, HyPix detector and mirror monochromator. Intensity data were measured by thin-slice ω-scans. Total no. of reflections recorded, to θ_{max} = 27.5°, was 61008 of which 7256 were unique (Rint = 0.048); 6183 were 'observed' with $I > 2\sigma_I$.

Data were processed using the CrysAlisPro-CCD and -RED (1) programs. The structure was determined by the intrinsic phasing routines in the SHELXT program (2A) and refined by full-matrix least-squares methods, on F^2's, in SHELXL (2B). There is disorder in the aliphatic ring and, in the thiophene ring, the sulfur atom is disordered over the two symmetry-related positions. The non-hydrogen atoms (except those in the minor components of disordered groups) were refined with anisotropic thermal parameters. The hydrogen atoms were included in idealised positions and their Uiso values were set to ride on the Ueq values of the parent carbon or nitrogen atoms. At the conclusion of the refinement, wR_2 = 0.119 and R_1 = 0.0589 (2B) for all 7256 reflections weighted $w = [\sigma^2(F_o^2) + (0.0504\ P)^2 + 3.53\ P]^{-1}$ with $P = (F_o^2 + 2F_c^2)/3$; for the 'observed' data only, R_1 = 0.0484.

In the final difference map, the highest peak (*ca* 0.8 $eÅ^{-3}$) was near Cl(52).

Scattering factors for neutral atoms were taken from reference (3). Computer programs used in this analysis have been noted above, and were run through WinGX (4) on a Dell Optiplex 780 PC at the University of East Anglia.

References

1) Programs CrysAlisPro, Rigaku Oxford Diffraction Ltd., Abingdon, UK (2018).

2) G. M. Sheldrick, Programs for crystal structure determination (SHELXT), *Acta Cryst.* (2015) A**71**, 3-8, and refinement (SHELXL), *Acta Cryst.* (2008) A**64**, 112-122 and (2015) C**71**, 3-8.

3) 'International Tables for X-ray Crystallography', Kluwer Academic Publishers, Dordrecht (1992). Vol. C, pp. 500, 219 and 193.

4) L. J. Farrugia, *J. Appl. Cryst.* (2012) **45**, 849–854.

Legends for Figures

Figure 1. View of a molecule of Iso-thiophenylDAP-*op*-tetralin, indicating the atom numbering scheme. Thermal ellipsoids are drawn at the 50% probability level.

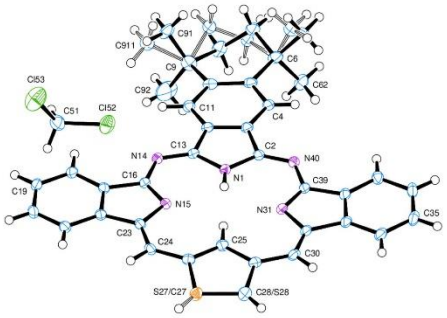

Figure 2. View of the stacking of molecules, parallel to the *b* axis. Molecules are drawn with the normal to the molecular plane vertical in the plane of the paper.

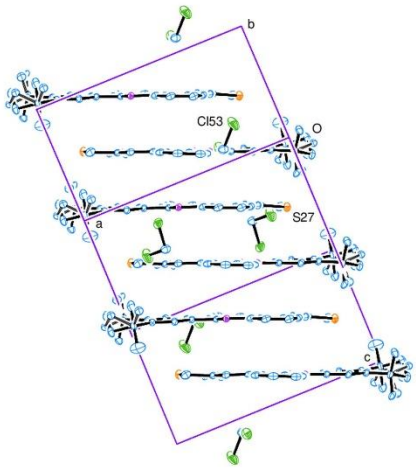

Figure 3. View of the stacking of molecules, showing the overlapping of five parallel ring systems. Molecules are drawn looking along the normal to the molecular plane.

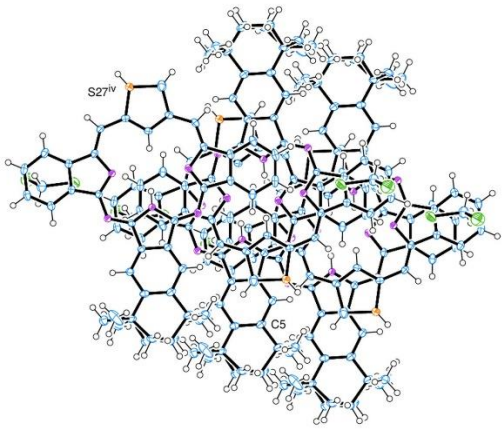

Notes on the structure

This essentially is a planar molecule; the only significant deviations from the central 16-membered ring are in the cyclohexenyl ring C(5)-C(10), Figure 1.

This ring C(5)-C(10) is disordered in two orientations, with an occupation ratio 0.71:0.29. The rings in both orientations have half-chair conformations, but with opposing forms; in the major form C(7) and C(8) are above and below (respectively) the molecular plane, while C(71) and C(81) are below and above that plane. There is also disorder in the thiophene ring, where the sulfur atom is in either the S(27) or S(28) site; the occupation ratio here is 0.63:0.37.

Bond lengths in the 16-membered ring indicate clearly the double-bonds in the C(13)-N(14), C(16)-N(15) and C(23)-C(24) bonds and in the corresponding bonds in the opposite side of the ring; the bonds about N(1) and C(25) are all quite similar at *ca* 1.39 Å, as in the aromatic rings.

The hydrogen atoms on N(1) and C(25) both form shared weak hydrogen bonds to both N(15) and N(31) within the 16-membered ring.

The planar molecules are stacked along the *b* axis, related about centres of symmetry and *ca* 3.4 Å apart, Figures 2 and 3.

There is also a well-ordered solvent, dichloromethane, molecule; H(51a) of this molecule is directed towards the centre of the phenyl ring of C(17-22).

4-Crystal data and structure refinement for tolyl-SO_2-N-isoindole-CH-thiophene-CH-isoindole-isoindole-dione

Identification code	**2.55 (Figure 2.49)**
Elemental formula	C37 H24 N4 O4 S2, O0.16
Formula weight	655.20
Crystal system, space group	Monoclinic, $P2_1/c$ (no.14)
Unit cell dimensions	a = 10.7839(2) Å α = 90 ° b = 15.0075(3) Å β = 94.9500(13) ° c = 18.9381(3) Å γ = 90 °
Volume	3053.49(8) $Å^3$
Z, Calculated density	4, 1.425 Mg/m^3
F(000)	1357
Absorption coefficient	1.996 mm^{-1}
Temperature	100(2) K
Wavelength	1.54184 Å
Crystal colour, shape	orange block
Crystal size	0.16 x 0.05 x 0.04 mm
Crystal mounting:	on a small loop, in oil, fixed in cold Nstream
On the diffractometer:	
Theta range for data collection	7.684 to 72.482 deg.
Limiting indices	-13<=h<=13, -17<=k<=18, -13<=l<=22
Completeness to theta = 67.684	99.5 %
Absorption correction	Semi-empirical from equivalents
Max. and min. transmission	1.00000 and 0.75172
Reflections collected (not including absences)	22487
No. of unique reflections	5872 [R(int) for equivalents = 0.042]
No. of 'observed' reflections ($I > 2\sigma_I$)	5177
Structure determined by:	dual methods, in SHELXT
Refinement:	Full-matrix least-squares on F^2, in SHELXL
Data / restraints / parameters	5872 / 0 / 429
Goodness-of-fit on F^2	1.072

Final R indices ('observed' data)	R_1 = 0.049, wR_2 = 0.120
Final R indices (all data)	R_1 = 0.056, wR_2 = 0.123
Reflections weighted: $w = [\sigma^2(Fo^2)+(0.0469P)^2+2.8667P]^{-1}$ where $P=(Fo^2+2Fc^2)/3$	
Extinction coefficient	n/a
Largest diff. peak and hole	0.49 and -0.36 e.A-3
Location of largest difference peak	close to C(31)–S(3) bond

Table 1. Atomic coordinates (x 10^5) and equivalent isotropic displacement parameters ($Å^2$ x 10^4). U(eq) is defined as one third of the trace of the orthogonalized Uij tensor. E.s.ds are in parentheses.

	x	y	z	U(eq)	S.o.f.#
C(1)	1230(20)	69111(16)	52858(12)	313(5)	
N(2)	-5517(18)	63799(13)	56415(10)	315(4)	
C(3)	1950(20)	56224(16)	58090(12)	293(5)	
C(4)	14130(20)	57478(16)	55360(12)	306(5)	
C(5)	25090(20)	52591(17)	56006(13)	359(5)	
C(6)	35280(20)	56072(19)	52909(14)	421(6)	
C(7)	34610(20)	64156(19)	49293(14)	417(6)	
C(8)	23780(20)	69165(18)	48736(13)	366(5)	
C(9)	13590(20)	65717(16)	51884(12)	310(5)	
C(10)	-2000(20)	49095(16)	61626(12)	320(5)	
S(1)	-24966(5)	56100(4)	64842(3)	323(2)	
C(11)	-13570(20)	47961(16)	64658(12)	318(5)	
C(12)	-17250(20)	40294(17)	67923(13)	373(6)	
C(13)	-28910(20)	40979(17)	70516(14)	386(6)	
C(14)	-34470(20)	49197(17)	69362(12)	337(5)	
C(15)	-46500(20)	51579(17)	71496(12)	336(5)	
N(21)	-49097(18)	67022(13)	67183(10)	284(4)	
C(22)	-52980(20)	59174(16)	70442(12)	304(5)	
C(23)	-65790(20)	60894(16)	72006(12)	310(5)	
C(24)	-74270(20)	55660(18)	75326(13)	360(5)	
C(25)	-86060(20)	59128(18)	75820(13)	384(6)	
C(26)	-89570(20)	67412(18)	72969(13)	377(6)	
C(27)	-81220(20)	72607(17)	69621(12)	329(5)	
C(28)	-69220(20)	69251(15)	69284(11)	287(5)	
C(29)	-58280(20)	73307(15)	66479(11)	281(5)	
N(30)	-57874(18)	81520(13)	64153(10)	299(4)	
S(3)	-44671(5)	85855(4)	62205(3)	294(2)	
O(4)	-34549(16)	82538(12)	66934(8)	358(4)	
O(5)	-46593(18)	95308(11)	61894(9)	381(4)	
C(31)	-42360(20)	82056(15)	53613(11)	268(5)	
C(32)	-34390(20)	74921(15)	52840(12)	282(5)	
C(33)	-32560(20)	71958(16)	46094(12)	314(5)	
C(34)	-38470(20)	76000(16)	40134(12)	334(5)	
C(35)	-46250(20)	83285(17)	41071(12)	348(5)	
C(36)	-48220(20)	86371(16)	47764(12)	309(5)	
C(37)	-36240(30)	72790(20)	32827(14)	490(7)	
N(41)	-3303(18)	77576(14)	50535(11)	343(4)	
C(42)	-7080(20)	84470(17)	55095(14)	351(5)	
O(42)	-5892(18)	84235(12)	61414(10)	425(4)	
C(43)	-12280(20)	91605(17)	50227(14)	367(6)	
C(44)	-17590(20)	99652(17)	51771(15)	396(6)	
C(45)	-21900(20)	104919(18)	46010(16)	440(6)	
C(46)	-20930(30)	102226(18)	39120(16)	444(6)	
C(47)	-15510(30)	94108(18)	37629(16)	430(6)	
C(48)	-11210(20)	88885(17)	43328(14)	364(6)	
C(49)	-5540(20)	79899(17)	43374(14)	368(6)	
O(49)	-3482(18)	75115(13)	38444(10)	462(5)	
O(99)	88800(200)	64310(150)	25550(120)	1000(60) *	0.155

- site occupancy, if different from 1.
* - U(iso) (Å^2 x 10^4)

Table 2. Molecular dimensions. Bond lengths are in Ångstroms, angles in degrees. E.s.ds are in parentheses.

C(1)-N(2)	1.305(3)	C(26)-C(27)	1.385(4)
C(1)-N(41)	1.418(3)	C(27)-C(28)	1.395(3)
C(1)-C(9)	1.453(3)	C(28)-C(29)	1.467(3)
N(2)-C(3)	1.413(3)	C(29)-N(30)	1.311(3)
C(3)-C(10)	1.351(3)	N(30)-S(3)	1.636(2)
C(3)-C(4)	1.464(3)	S(3)-O(5)	1.4343(17)
C(4)-C(5)	1.388(3)	S(3)-O(4)	1.4396(18)
C(4)-C(9)	1.400(3)	S(3)-C(31)	1.762(2)
C(5)-C(6)	1.391(4)	C(31)-C(36)	1.388(3)
C(6)-C(7)	1.392(4)	C(31)-C(32)	1.389(3)
C(7)-C(8)	1.385(4)	C(32)-C(33)	1.383(3)
C(8)-C(9)	1.394(3)	C(33)-C(34)	1.387(3
C(10)-C(11)	1.427(3)	C(34)-C(35)	1.398(4)
S(1)-C(14)	1.734(2)	C(34)-C(37)	1.504(3)
S(1)-C(11)	1.736(2)	C(35)-C(36)	1.383(3)
C(11)-C(12)	1.381(3)	N(41)-C(49)	1.401(3)
C(12)-C(13)	1.393(4)	N(41)-C(42)	1.429(3)
C(13)-C(14)	1.380(3)	C(42)-O(42)	1.193(3)
C(14)-C(15)	1.437(3)	C(42)-C(43)	1.490(3)
C(15)-C(22)	1.343(3)	C(43)-C(44)	1.379(4)
N(21)-C(29)	1.366(3)	C(43)-C(48)	1.383(4)
N(21)-C(22)	1.410(3)	C(44)-C(45)	1.394(4)
C(22)-C(23)	1.460(3)	C(45)-C(46)	1.379(4)
C(23)-C(28)	1.394(3)	C(46)-C(47)	1.390(4)
C(23)-C(24)	1.396(3)	C(47)-C(48)	1.381(4)
C(24)-C(25)	1.384(4)	C(48)-C(49)	1.480(3)
C(25)-C(26)	1.395(4)	C(49)-O(49)	1.213(3)
N(2)-C(1)-N(41)	121.0(2)	C(15)-C(14)-S(1)	125.19(18)
N(2)-C(1)-C(9)	114.2(2)	C(22)-C(15)-C(14)	129.8(2)
N(41)-C(1)-C(9)	124.8(2)	C(29)-N(21)-C(22)	112.29(19)
C(1)-N(2)-C(3)	105.95(19)	C(15)-C(22)-N(21)	127.1(2)
C(10)-C(3)-N(2)	123.4(2)	C(15)-C(22)-C(23)	127.5(2)
C(10)-C(3)-C(4)	127.4(2)	N(21)-C(22)-C(23)	105.24(19)
N(2)-C(3)-C(4)	109.16(19)	C(28)-C(23)-C(24)	120.6(2)
C(5)-C(4)-C(9)	120.6(2)	C(28)-C(23)-C(22)	108.0(2)
C(5)-C(4)-C(3)	133.2(2)	C(24)-C(23)-C(22)	131.3(2)
C(9)-C(4)-C(3)	106.1(2)	C(25)-C(24)-C(23)	117.4(2)
C(4)-C(5)-C(6)	117.5(2)	C(24)-C(25)-C(26)	122.0(2)
C(5)-C(6)-C(7)	121.7(2)	C(27)-C(26)-C(25)	120.9(2)
C(8)-C(7)-C(6)	121.2(2)	C(26)-C(27)-C(28)	117.4(2)
C(7)-C(8)-C(9)	117.2(2)	C(23)-C(28)-C(27)	121.7(2)
C(8)-C(9)-C(4)	121.8(2)	C(23)-C(28)-C(29)	108.1(2)
C(8)-C(9)-C(1)	133.6(2)	C(27)-C(28)-C(29)	130.1(2)
C(4)-C(9)-C(1)	104.5(2)	N(30)-C(29)-N(21)	129.6(2)
C(3)-C(10)-C(11)	128.2(2)	N(30)-C(29)-C(28)	124.3(2)
C(14)-S(1)-C(11)	92.24(12)	N(21)-C(29)-C(28)	106.08(19)
C(12)-C(11)-C(10)	125.1(2)	C(29)-N(30)-S(3)	120.30(17)
C(12)-C(11)-S(1)	110.25(18)	O(5)-S(3)-O(4)	117.82(11)
C(10)-C(11)-S(1)	124.69(18)	O(5)-S(3)-N(30)	106.09(11)
C(11)-C(12)-C(13)	113.6(2)	O(4)-S(3)-N(30)	110.50(10)
C(14)-C(13)-C(12)	113.7(2)	O(5)-S(3)-C(31)	108.27(10)
C(13)-C(14)-C(15)	124.6(2)	O(4)-S(3)-C(31)	107.59(10)
C(13)-C(14)-S(1)	110.21(18)	N(30)-S(3)-C(31)	105.97(10)

C(36)-C(31)-C(32)	121.3(2)	N(41)-C(42)-C(43)	105.0(2)
C(36)-C(31)-S(3)	119.67(17)	C(44)-C(43)-C(48)	121.9(2)
C(32)-C(31)-S(3)	119.02(17)	C(44)-C(43)-C(42)	129.7(3)
C(33)-C(32)-C(31)	119.0(2)	C(48)-C(43)-C(42)	108.3(2)
C(32)-C(33)-C(34)	121.3(2)	C(43)-C(44)-C(45)	116.6(3)
C(33)-C(34)-C(35)	118.5(2)	C(46)-C(45)-C(44)	121.8(3)
C(33)-C(34)-C(37)	120.6(2)	C(45)-C(46)-C(47)	121.1(3)
C(35)-C(34)-C(37)	120.8(2)	C(48)-C(47)-C(46)	117.2(3)
C(36)-C(35)-C(34)	121.3(2)	C(47)-C(48)-C(43)	121.4(2)
C(35)-C(36)-C(31)	118.7(2)	C(47)-C(48)-C(49)	129.2(3)
C(49)-N(41)-C(1)	123.3(2)	C(43)-C(48)-C(49)	109.3(2)
C(49)-N(41)-C(42)	111.7(2)	O(49)-C(49)-N(41)	124.8(2)
C(1)-N(41)-C(42)	124.8(2)	O(49)-C(49)-C(48)	129.6(2)
O(42)-C(42)-N(41)	125.0(2)	N(41)-C(49)-C(48)	105.6(2)
O(42)-C(42)-C(43)	130.1(2)		

Table 3. Anisotropic displacement parameters ($Å^2$ x 10^4) for the expression:

$$\exp\{-2\pi^2(h^2a^{*2}U_{11} + \ldots + 2hka^*b^*U_{12})\}$$

E.s.ds are in parentheses.

	U_{11}	U_{22}	U_{33}	U_{23}	U_{13}	U_{12}
C(1)	268(11)	330(13)	342(12)	36(9)	31(9)	13(9)
N(2)	287(10)	319(11)	343(10)	58(8)	48(8)	21(8)
C(3)	289(11)	296(12)	294(11)	-4(9)	20(9)	28(9)
C(4)	284(11)	311(12)	323(12)	-50(9)	32(9)	26(9)
C(5)	319(12)	363(13)	395(13)	-74(10)	26(10)	54(10)
C(6)	289(12)	509(16)	470(15)	-132(12)	55(11)	100(11)
C(7)	302(13)	490(16)	470(15)	-93(12)	103(11)	-23(11)
C(8)	303(12)	393(14)	411(13)	-25(11)	76(10)	-47(10)
C(9)	279(11)	330(12)	322(12)	-29(9)	39(9)	-11(9)
C(10)	321(12)	317(12)	321(12)	-1(9)	20(9)	65(10)
S(1)	310(3)	300(3)	372(3)	82(2)	93(2)	48(2)
C(11)	334(12)	315(12)	306(11)	46(9)	28(9)	33(10)
C(12)	378(13)	325(13)	423(14)	86(10)	81(11)	74(11)
C(13)	410(14)	348(13)	412(14)	137(11)	114(11)	46(11)
C(14)	365(13)	342(13)	311(12)	87(10)	66(10)	29(10)
C(15)	343(12)	353(13)	321(12)	96(10)	80(10)	10(10)
N(21)	278(10)	290(10)	293(9)	28(8)	78(7)	35(8)
C(22)	328(12)	339(12)	251(11)	47(9)	62(9)	17(10)
C(23)	328(12)	350(13)	256(11)	8(9)	54(9)	-4(10)
C(24)	350(13)	416(14)	322(12)	49(10)	73(10)	-19(11)
C(25)	332(13)	471(15)	359(13)	-1(11)	79(10)	-51(11)
C(26)	293(12)	461(15)	381(13)	-71(11)	57(10)	6(11)
C(27)	310(12)	350(13)	327(12)	-58(10)	31(9)	21(10)
C(28)	304(12)	309(12)	254(11)	-33(9)	46(9)	-3(9)
C(29)	309(11)	313(12)	224(10)	-22(9)	32(8)	32(9)
N(30)	330(10)	275(10)	298(10)	-11(8)	65(8)	19(8)
S(3)	352(3)	284(3)	252(3)	-16(2)	59(2)	-10(2)
O(4)	360(9)	446(10)	268(8)	37(7)	22(7)	-56(8)
O(5)	541(11)	252(9)	364(9)	-47(7)	128(8)	-23(8)
C(31)	302(11)	235(11)	272(11)	19(8)	59(9)	-10(9)
C(32)	292(11)	269(11)	288(11)	47(9)	48(9)	12(9)
C(33)	337(12)	268(12)	352(12)	-6(9)	116(10)	26(9)
C(34)	397(13)	324(13)	289(12)	-31(9)	70(10)	-34(10)
C(35)	401(13)	359(13)	277(12)	61(10)	-9(10)	10(10)
C(36)	317(12)	284(12)	328(12)	31(9)	43(9)	22(9)
C(37)	611(18)	540(18)	326(13)	-59(12)	81(12)	16(14)
N(41)	310(10)	334(11)	392(11)	88(9)	75(8)	36(8)
C(42)	271(12)	351(13)	440(15)	49(10)	72(10)	-15(10)
O(42)	426(10)	413(10)	439(11)	4(8)	45(8)	23(8)
C(43)	255(11)	306(13)	543(15)	95(11)	56(10)	-10(9)
C(44)	316(13)	333(13)	544(16)	22(11)	65(11)	-19(10)
C(45)	335(13)	322(14)	671(18)	115(12)	81(12)	44(11)
C(46)	370(14)	362(14)	605(17)	177(12)	70(12)	28(11)
C(47)	378(14)	404(15)	517(16)	101(12)	92(12)	10(11)
C(48)	310(12)	309(13)	486(15)	94(11)	111(11)	-4(10)
C(49)	344(13)	348(13)	429(14)	74(11)	142(10)	36(10)
O(49)	504(11)	470(11)	427(10)	67(9)	127(8)	105(9)

Table 4. Hydrogen coordinates (x 10^4) and isotropic displacement parameters ($Å^2$ x 10^3). All hydrogen atoms were included in idealised positions with U(iso)'s set at 1.2*U(eq) or, for the methyl group hydrogen atoms, 1.5*U(eq) of the parent carbon atoms.

	x	y	z	U(iso)
H(5)	2562	4707	5847	43
H(6)	4289	5285	5327	51
H(7)	4171	6628	4717	50
H(8)	2332	7471	4631	44
H(10)	362	4422	6216	38
H(12)	-1230	3505	6836	45
H(13)	-3270	3623	7286	46
H(15)	-5047	4710	7404	40
H(21)	-4161	6778	6576	34
H(24)	-7204	4994	7717	43
H(25)	-9193	5576	7817	46
H(26)	-9780	6952	7333	45
H(27)	-8357	7823	6763	39
H(32)	-3025	7212	5688	34
H(33)	-2716	6706	4553	38
H(35)	-5025	8617	3703	42
H(36)	-5349	9134	4835	37
H(37A)	-3149	7729	3045	73
H(37B)	-4424	7178	3008	73
H(37C)	-3152	6720	3319	73
H(44)	-1827	10151	5652	48
H(45)	-2562	11051	4686	53
H(46)	-2400	10598	3533	53
H(47)	-1480	9223	3289	52

Table 5. Torsion angles, in degrees. E.s.ds are in parentheses.

N(41)-C(1)-N(2)-C(3)	-177.7(2)	C(22)-N(21)-C(29)-C(28)	-1.8(2)
C(9)-C(1)-N(2)-C(3)	-0.5(3)	C(23)-C(28)-C(29)-N(30)	-173.0(2)
C(1)-N(2)-C(3)-C(10)	-178.2(2)	C(27)-C(28)-C(29)-N(30)	5.4(4)
C(1)-N(2)-C(3)-C(4)	1.4(3)	C(23)-C(28)-C(29)-N(21)	4.1(2)
C(10)-C(3)-C(4)-C(5)	-6.6(4)	C(27)-C(28)-C(29)-N(21)	-177.5(2)
N(2)-C(3)-C(4)-C(5)	173.8(2)	N(21)-C(29)-N(30)-S(3)	-5.3(3)
C(10)-C(3)-C(4)-C(9)	177.8(2)	C(28)-C(29)-N(30)-S(3)	171.15(17)
N(2)-C(3)-C(4)-C(9)	-1.8(3)	C(29)-N(30)-S(3)-O(5)	-163.44(17)
C(9)-C(4)-C(5)-C(6)	-1.8(3)	C(29)-N(30)-S(3)-O(4)	-34.7(2)
C(3)-C(4)-C(5)-C(6)	-176.9(2)	C(29)-N(30)-S(3)-C(31)	81.61(19)
C(4)-C(5)-C(6)-C(7)	0.1(4)	O(5)-S(3)-C(31)-C(36)	-31.5(2)
C(5)-C(6)-C(7)-C(8)	1.2(4)	O(4)-S(3)-C(31)-C(36)	-159.79(18)
C(6)-C(7)-C(8)-C(9)	-0.6(4)	N(30)-S(3)-C(31)-C(36)	82.0(2)
C(7)-C(8)-C(9)-C(4)	-1.1(4)	O(5)-S(3)-C(31)-C(32)	146.81(18)
C(7)-C(8)-C(9)-C(1)	175.2(3)	O(4)-S(3)-C(31)-C(32)	18.5(2)
C(5)-C(4)-C(9)-C(8)	2.4(4)	N(30)-S(3)-C(31)-C(32)	-99.74(19)
C(3)-C(4)-C(9)-C(8)	178.7(2)	C(36)-C(31)-C(32)-C(33)	-1.7(3)
C(5)-C(4)-C(9)-C(1)	-174.8(2)	S(3)-C(31)-C(32)-C(33)	-179.90(17)
C(3)-C(4)-C(9)-C(1)	1.4(2)	C(31)-C(32)-C(33)-C(34)	0.3(3)
N(2)-C(1)-C(9)-C(8)	-177.4(3)	C(32)-C(33)-C(34)-C(35)	0.9(4)
N(41)-C(1)-C(9)-C(8)	-0.2(4)	C(32)-C(33)-C(34)-C(37)	179.0(2)
N(2)-C(1)-C(9)-C(4)	-0.7(3)	C(33)-C(34)-C(35)-C(36)	-1.0(4)
N(41)-C(1)-C(9)-C(4)	176.5(2)	C(37)-C(34)-C(35)-C(36)	-179.1(2)
N(2)-C(3)-C(10)-C(11)	-4.2(4)	C(34)-C(35)-C(36)-C(31)	-0.3(4)
C(4)-C(3)-C(10)-C(11)	176.2(2)	C(32)-C(31)-C(36)-C(35)	1.6(3)
C(3)-C(10)-C(11)-C(12)	176.7(3)	S(3)-C(31)-C(36)-C(35)	179.86(18)
C(3)-C(10)-C(11)-S(1)	-4.0(4)	N(2)-C(1)-N(41)-C(49)	-115.8(3)
C(14)-S(1)-C(11)-C(12)	0.5(2)	C(9)-C(1)-N(41)-C(49)	67.2(3)
C(14)-S(1)-C(11)-C(10)	-178.8(2)	N(2)-C(1)-N(41)-C(42)	58.9(3)
C(10)-C(11)-C(12)-C(13)	179.2(2)	C(9)-C(1)-N(41)-C(42)	-118.1(3)
S(1)-C(11)-C(12)-C(13)	-0.2(3)	C(49)-N(41)-C(42)-O(42)	-178.0(2)
C(11)-C(12)-C(13)-C(14)	-0.5(3)	C(1)-N(41)-C(42)-O(42)	6.7(4)
C(12)-C(13)-C(14)-C(15)	179.8(2)	C(49)-N(41)-C(42)-C(43)	0.9(3)
C(12)-C(13)-C(14)-S(1)	0.9(3)	C(1)-N(41)-C(42)-C(43)	-174.4(2)
C(11)-S(1)-C(14)-C(13)	-0.8(2)	O(42)-C(42)-C(43)-C(44)	-3.3(5)
C(11)-S(1)-C(14)-C(15)	-179.7(2)	N(41)-C(42)-C(43)-C(44)	177.9(2)
C(13)-C(14)-C(15)-C(22)	-177.3(3)	O(42)-C(42)-C(43)-C(48)	177.7(3)
S(1)-C(14)-C(15)-C(22)	1.5(4)	N(41)-C(42)-C(43)-C(48)	-1.1(3)
C(14)-C(15)-C(22)-N(21)	-3.5(4)	C(48)-C(43)-C(44)-C(45)	0.3(4)
C(14)-C(15)-C(22)-C(23)	172.3(2)	C(42)-C(43)-C(44)-C(45)	-178.6(2)
C(29)-N(21)-C(22)-C(15)	175.5(2)	C(43)-C(44)-C(45)-C(46)	0.0(4)
C(29)-N(21)-C(22)-C(23)	-1.1(2)	C(44)-C(45)-C(46)-C(47)	-0.3(4)
C(15)-C(22)-C(23)-C(28)	-172.9(2)	C(45)-C(46)-C(47)-C(48)	0.1(4)
N(21)-C(22)-C(23)-C(28)	3.7(2)	C(46)-C(47)-C(48)-C(43)	0.2(4)
C(15)-C(22)-C(23)-C(24)	4.9(4)	C(46)-C(47)-C(48)-C(49)	177.4(3)
N(21)-C(22)-C(23)-C(24)	-178.5(2)	C(44)-C(43)-C(48)-C(47)	-0.4(4)
C(28)-C(23)-C(24)-C(25)	-0.4(3)	C(42)-C(43)-C(48)-C(47)	178.7(2)
C(22)-C(23)-C(24)-C(25)	-177.9(2)	C(44)-C(43)-C(48)-C(49)	-178.2(2)
C(23)-C(24)-C(25)-C(26)	1.7(4)	C(42)-C(43)-C(48)-C(49)	0.9(3)
C(24)-C(25)-C(26)-C(27)	-1.3(4)	C(1)-N(41)-C(49)-O(49)	-2.6(4)
C(25)-C(26)-C(27)-C(28)	-0.6(4)	C(42)-N(41)-C(49)-O(49)	-177.9(2)
C(24)-C(23)-C(28)-C(27)	-1.4(3)	C(1)-N(41)-C(49)-C(48)	175.0(2)
C(22)-C(23)-C(28)-C(27)	176.6(2)	C(42)-N(41)-C(49)-C(48)	-0.3(3)
C(24)-C(23)-C(28)-C(29)	177.1(2)	C(47)-C(48)-C(49)-O(49)	-0.5(5)
C(22)-C(23)-C(28)-C(29)	-4.8(3)	C(43)-C(48)-C(49)-O(49)	177.0(3)
C(26)-C(27)-C(28)-C(23)	1.9(3)	C(47)-C(48)-C(49)-N(41)	-177.9(3)
C(26)-C(27)-C(28)-C(29)	-176.3(2)	C(43)-C(48)-C(49)-N(41)	-0.4(3)
C(22)-N(21)-C(29)-N(30)	175.1(2)		

Table 6. Hydrogen bonds, in Ångstroms and degrees.

D-H...A	d(D-H)	d(H...A)	d(D...A)	<(DHA)
N(21)-H(21)...S(1)	0.88	2.53	3.1390(19)	127.4
N(21)-H(21)...O(4)	0.88	2.35	2.810(3)	113.1
C(32)-H(32)...S(1)	0.95	2.87	3.712(2)	148.5

Crystal structure analysis of a derivative of a thiophene bisindole derivative

Crystal data: $C_{37}H_{24}N_4O_4S_2$, $O_{0.16}$, M = 655.20. Monoclinic, space group $P2_1/c$ (no. 14), a = 10.7839(2), b = 15.0075(3), c = 18.9381(3) Å, β = 94.9500(13) °, V = 3053.49(8) $Å^3$. Z = 4, Dc = 1.425 g cm^{-3}, F(000) = 1357, T = 100(2) K, μ(Cu-Kα) = 20.0 cm^{-1}, λ(Cu-Kα) = 1.54184 Å.

The crystal was an orange block. From a sample under oil, one, *ca* 0.16 x 0.05 x 0.04 mm, was mounted on a small loop and fixed in the cold nitrogen stream on a Rigaku Oxford Diffraction XtaLAB Synergy diffractometer, equipped with Cu-Kα radiation, HyPix detector and mirror monochromator. Intensity data were measured by thin-slice ω-scans. Total no. of reflections recorded, to θ_{max} = 72.5°, was 22,487 of which 5,872 were unique (Rint = 0.042); 5,177 were 'observed' with $I > 2\sigma_I$.

Data were processed using the CrysAlisPro-CCD and -RED (1) programs. The structure was determined by the intrinsic phasing routines in the SHELXT program (2A) and refined by full-matrix least-squares methods, on F^2's, in SHELXL (2B). The non-hydrogen atoms of the thiophene derivative molecule were refined with anisotropic thermal parameters. The hydrogen atoms were included in idealised positions and their Uiso values were set to ride on the Ueq values of the parent carbon atoms. A single difference peak, 0.83 $eÅ^{-3}$ was considered as a solvent molecule and was included in the refinement process as a partially occupied oxygen atom (water molecule). At the conclusion of the refinement, wR_2 = 0.123 and R_1 = 0.056 (2B) for all 5872 reflections weighted $w = [\sigma^2(F_o^2) + (0.0469\ P)^2 + 2.87\ P]^{-1}$ with $P = (F_o^2 + 2F_c^2)/3$; for the 'observed' data only, R_1 = 0.049.

In the final difference map, the highest peak (*ca* 0.5 $eÅ^{-3}$) was close to the S(3)–C(31) bond..

Scattering factors for neutral atoms were taken from reference (3). Computer programs used in this analysis have been noted above, and were run through WinGX (4) on a Dell Optiplex 780 PC at the University of East Anglia.

References

1) Programs CrysAlisPro, Rigaku Oxford Diffraction Ltd., Abingdon, UK (2018).

2) G. M. Sheldrick, Programs for crystal structure determination (SHELXT), *Acta Cryst.* (2015) A**71**, 3-8, and refinement (SHELXL), *Acta Cryst.* (2008) A**64**, 112-122 and (2015) C**71**, 3-8.

3) 'International Tables for X-ray Crystallography', Kluwer Academic Publishers, Dordrecht (1992). Vol. C, pp. 500, 219 and 193.

4) L. J. Farrugia, *J. Appl. Cryst.* (2012) **45**, 849–854.

Legends for Figures

Figure 1. View of the thiophene bisindole derivative, indicating the atom numbering scheme. Thermal ellipsoids are drawn at the 50% probability level.

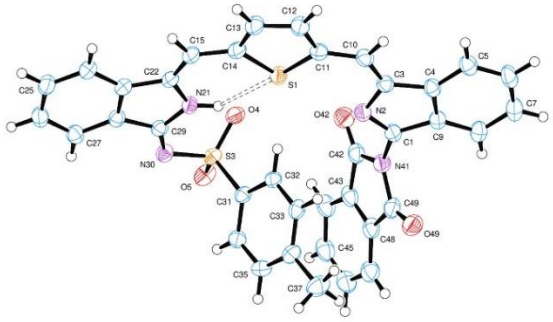

Figure 2. Alternative view of the molecule, suggesting the parallel arrangement of the tolyl group and the isoindole group of N(41).

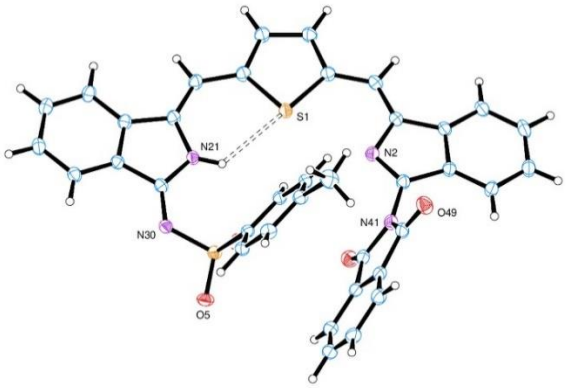

Figure 3. View of the molecule showing the partial overlap of the phenyl group of C(31) and the isoindole group of N(41).

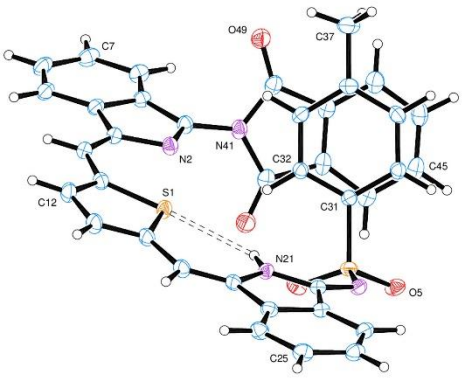

Figure 3. The packing of molecules, viewed along the *b* axis.

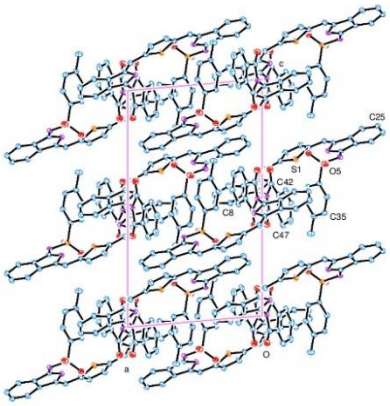

Notes on the structure

The molecule, with principal atoms labelled, is shown in Figure 1. The central portion of the molecule, from the isoindole group of N(21), through the thiophene ligand to the isoindole group of N(2), is approximately planar, but there are rotations about the C(29)-N(30) and C(1)-N(41) bonds which take the tosyl group of S(3) and the isoindole group of N(41) out-of-plane and into an almost parallel arrangement of these aromatic groups, Figure 2; the overlapping of these rings is indicated in Figure 3.

There is also extensive intermolecular π-π stacking involving all the aromatic rings, e.g. (i) two molecules, related by a centre of symmetry, overlap along the length of the N(2)-isoindole and thiophene groups, and (ii) on the opposite side of the N(2) isoindole group, a neighbouring N(21) group is overlapping.

The N(21)-H(21) group appears to form intramolecular, bifurcated hydrogen bonds with close neighbours (O4) and S(1); the H…O and H…S distances, 2.35 and 2.53 Å are both short, within the normal values for hydrogen bonds but the N-H…O angle, at 113.1°, is tighter than normal.

The packing of molecules is shown in Figure 4.

5-Crystal data and structure refinement for thiophene-{(CH-NC_8H_4)-NH-($NC_8H_2(OC_6H_{13})_2$)-CH-C_6H_4-OMe}$_2$

Identification code	**2.71 (Figure 2.56)**
Elemental formula	C71.65 H64.64 N6 O6 S (averaged over four molecules)
Formula weight	1137.79
Crystal system, space group	Orthorhombic, $Pna2_1$ (no. 33)
Unit cell dimensions	a = 31.3301(4) Å α = 90 ° b = 26.1402(4) Å β = 90 ° c = 32.5934(6) Å γ = 90 °
Volume	26,693.2(7) $Å^3$
Z, Calculated density	16, 1.132 Mg/m^3
F(000)	9609
Absorption coefficient	0.858 mm^{-1}
Temperature	100(2) K
Wavelength	1.54184 Å
Crystal colour, shape	blue block
Crystal size	0.43 x 0.17 x 0.05 mm
Crystal mounting:	on a small loop, in oil, fixed in cold N_2 stream
On the diffractometer:	
Theta range for data collection	7.684 to 70.000 °
Limiting indices	-32<=h<=38, -31<=k<=31, -39<=l<=39
Completeness to theta = 67.684	99.3 %
Absorption correction	Semi-empirical from equivalents
Max. and min. transmission	1.00000 and 0.24705
Reflections collected (not including absences)	107,970
No. of unique reflections	42,351 [R(int) for equivalents = 0.050]
No. of 'observed' reflections ($I > 2\sigma_I$)	2,6458
Structure determined by:	dual methods, in SHELXT
Refinement:	Full-matrix-block least-squares on F^2, in SHELXL
Data / restraints / parameters	4,2351 / 1 / 3097
Goodness-of-fit on F^2	0.985

Final R indices ('observed' data)	R_1 = 0.091, wR_2 = 0.248
Final R indices (all data)	R_1 = 0.128, wR_2 = 0.277
Reflections weighted: $w = [\sigma^2(Fo^2)+(0.1966P)^2]^{-1}$ where $P=(Fo^2+2Fc^2)/3$	
Absolute structure parameter	0.49(2)
Extinction coefficient	n/a
Largest diff. peak and hole	0.52 and -0.28 e.Å^{-3}
Location of largest difference peak	near H(63a)

Table 1. Atomic coordinates (x 10^5) and equivalent isotropic displacement parameters ($Å^2$ x 10^4). U(eq) is defined as one third of the trace of the orthogonalized Uij tensor. E.s.ds are in parentheses.

	x	y	z	U(eq)	S.o.f.#
S(1)	22927(5)	69097(6)	44531(6)	813(4)	
C(2)	18840(20)	70750(30)	47900(20)	837(17)	
C(3)	16050(20)	66590(30)	48470(30)	940(20)	
C(4)	17120(20)	62450(30)	46080(20)	871(19)	
C(5)	20770(20)	63000(30)	43780(30)	848(19)	
C(6)	22504(19)	59400(30)	40960(20)	824(18)	
N(7)	29621(15)	62880(20)	39567(18)	772(14)	
C(8)	26272(19)	59380(20)	38970(20)	772(16)	
C(9)	27366(19)	55750(30)	35780(20)	841(19)	
C(10)	25310(20)	51650(30)	33980(30)	960(20)	
C(11)	27200(20)	49190(30)	30810(30)	1090(30)	
C(12)	31250(20)	50690(30)	29190(30)	1090(30)	
C(13)	33350(20)	54740(30)	31110(30)	1000(20)	
C(14)	31412(19)	57230(20)	34310(20)	815(17)	
C(15)	32637(19)	61650(20)	36780(20)	775(16)	
N(16)	36526(15)	63950(20)	36203(19)	815(14)	
N(17)	36070(15)	68783(19)	42485(17)	744(13)	
C(18)	38010(20)	67190(20)	38880(20)	770(16)	
C(19)	42094(19)	69790(30)	38610(20)	793(17)	
C(20)	45360(20)	69320(30)	35630(20)	844(18)	
C(21)	48932(19)	72600(30)	36200(30)	857(19)	
C(22)	49053(19)	76100(30)	39480(20)	825(18)	
C(23)	45923(18)	76290(20)	42410(20)	756(16)	
C(24)	42381(18)	73170(20)	41900(20)	766(16)	
C(25)	38629(17)	72430(20)	44470(20)	760(17)	
C(26)	37750(20)	74780(20)	48090(20)	796(17)	
C(27)	34200(20)	73750(30)	50840(20)	803(17)	
C(28)	32580(40)	77600(30)	53310(20)	1120(30)	
C(29)	29250(40)	76840(40)	55820(20)	1370(40)	1
C(30)	27320(30)	71990(40)	55970(20)	1080(30)	
C(31)	28850(20)	68060(30)	53700(20)	890(20)	
C(32)	32292(19)	68980(30)	51040(20)	802(17)	
O(33)	23840(30)	71570(40)	58530(20)	1640(40)	
C(34)	22010(30)	66760(70)	58970(40)	1620(60)	
C(36)	18610(30)	75480(30)	50010(20)	930(20)	
N(37)	24520(20)	79820(20)	46719(18)	919(16)	
C(38)	21140(30)	79530(30)	49600(20)	980(20)	
C(39)	21040(30)	84190(40)	52180(20)	1060(30)	
C(40)	18560(40)	85980(40)	55270(30)	1230(30)	
C(41)	19300(50)	90600(50)	57070(30)	1650(60)	
C(42)	22760(50)	93360(60)	55890(30)	1650(60)	
C(43)	25550(40)	91630(40)	52620(30)	1420(40)	
C(44)	24730(40)	87060(40)	50820(20)	1200(30)	
C(45)	26510(30)	84140(30)	47500(20)	970(20)	
N(46)	30190(20)	85770(20)	45570(20)	971(18)	
N(47)	29703(18)	79560(20)	40146(18)	809(14)	
C(48)	31630(20)	83480(30)	42330(20)	849(18)	
C(49)	35570(20)	84650(20)	40180(20)	842(18)	
C(50)	38540(20)	88450(20)	41000(30)	855(18)	
C(51)	41940(20)	88950(30)	38440(30)	890(20)	
C(52)	42390(20)	85600(30)	35020(30)	880(20)	

C(53)	39480(20)	81850(30)	34180(30)	900(20)	
C(54)	36010(20)	81510(30)	36890(30)	880(20)	
C(55)	32130(20)	78190(30)	36740(30)	860(20)	
C(56)	31390(20)	74810(20)	33610(20)	801(17)	
C(57)	27520(20)	71920(20)	32610(20)	775(16)	
C(58)	23490(20)	73200(30)	33970(20)	827(17)	
C(59)	19960(20)	70570(30)	32630(20)	903(19)	
C(60)	20380(20)	66420(30)	29930(30)	940(20)	
C(61)	24430(30)	65090(30)	28660(30)	960(20)	
C(62)	27880(20)	67800(30)	29880(30)	920(20)	
O(63)	16977(18)	63730(20)	28680(20)	1200(19)	
C(64)	13120(60)	65610(80)	29050(60)	1600(60)	0.7
C(65)	17130(90)	60250(110)	25730(90)	1020(70)	0.3
O(101)	52317(13)	72755(19)	33738(17)	920(13)	
C(102)	52540(20)	69380(30)	30400(30)	1010(20)	
C(103)	56790(30)	70430(40)	28460(30)	1160(30)	
C(104)	57560(40)	67380(50)	24630(40)	1570(50)	
C(105)	62190(60)	68380(60)	22920(50)	1730(70)	0.8
C(106)	64610(80)	64810(100)	20040(70)	1670(80)	0.6
C(107)	61250(70)	65120(100)	16900(70)	1640(80)	0.6
O(111)	52588(13)	79223(17)	39467(18)	915(14)	
C(112)	52850(20)	83210(30)	42470(30)	901(19)	
C(113)	56620(30)	86530(30)	41580(40)	1190(30)	
C(114)	56470(30)	89150(40)	37560(40)	1410(40)	
C(115)	60310(40)	92730(50)	36710(50)	1700(60)	
C(116)	59010(60)	96570(100)	32870(100)	2180(150)	0.6
C(117)	63250(90)	99840(120)	30950(100)	1900(100)	0.6
C(118)	59670(130)	97550(170)	39030(130)	2030(140)	0.45
C(119)	62560(130)	101320(180)	34050(150)	2040(140)	0.45
O(121)	45165(15)	92577(18)	38790(20)	1021(16)	
C(122)	44770(30)	96120(30)	41910(40)	1160(30)	
C(123)	48450(40)	99690(60)	42020(70)	2030(80)	
C(124)	48120(40)	103540(50)	45680(70)	1970(70)	
C(125)	51950(110)	106930(150)	45710(120)	1950(120)	0.5
C(126)	54700(180)	108400(200)	41530(180)	1900(200)	0.3
C(127)	58020(190)	113100(200)	42310(190)	2000(200)	0.3
O(131)	45988(15)	86322(18)	32656(19)	963(14)	
C(132)	46490(30)	83080(30)	29200(30)	1020(20)	
C(133)	50380(30)	84500(40)	26950(30)	1170(30)	
C(134)	50810(40)	81500(50)	22940(40)	1420(40)	
C(135)	54580(50)	82520(60)	20550(50)	1790(60)	
C(136)	54920(80)	80090(100)	16430(60)	1910(110)	0.65
C(137)	58230(100)	79830(130)	13860(100)	1840(110)	0.5
S(2)	71292(7)	46655(8)	44098(7)	1047(6)	
C(202)	68030(30)	48840(40)	47970(30)	1220(30)	
C(203)	67470(40)	45350(50)	50940(40)	1560(50)	
C(204)	69990(40)	40690(50)	50280(40)	1560(50)	
C(205)	72020(30)	40880(40)	46600(30)	1210(30)	
C(206)	74740(30)	36820(40)	44990(40)	1260(30)	
N(207)	76090(20)	39850(20)	38020(20)	986(18)	
C(208)	76590(30)	36400(30)	41270(30)	1130(30)	
C(209)	79600(30)	32420(30)	40100(30)	1100(30)	
C(210)	81400(30)	28230(30)	42180(40)	1240(30)	
C(211)	84540(30)	25460(30)	40240(40)	1250(30)	
C(212)	86050(30)	26810(30)	36210(40)	1180(30)	
C(213)	84280(20)	30890(30)	34270(30)	950(20)	
C(214)	81110(20)	33700(30)	36220(30)	980(20)	
C(215)	78670(20)	38260(30)	35030(30)	940(20)	
N(216)	79444(16)	40510(20)	31390(20)	849(15)	

N(217)	73504(16)	46390(20)	31820(20)	883(16)	
C(218)	77116(19)	44230(20)	30030(30)	860(20)	
C(219)	77787(18)	46850(20)	26160(20)	775(17)	
C(220)	80940(20)	46090(30)	23210(30)	867(19)	
C(221)	80710(20)	49200(30)	19730(30)	940(20)	
C(222)	77590(20)	52980(30)	19290(30)	880(20)	
C(223)	74560(20)	53720(30)	22260(30)	853(18)	
C(224)	74660(17)	50630(20)	25700(20)	778(17)	
C(225)	71855(19)	50370(20)	29290(20)	821(18)	
C(226)	68428(19)	53370(30)	29870(30)	850(18)	
C(227)	65140(20)	53520(30)	33030(30)	873(19)	
C(228)	64410(20)	49810(40)	35880(30)	980(20)	
C(229)	61220(20)	50330(40)	38870(30)	1120(30)	
C(230)	58630(20)	54800(40)	38800(30)	1160(30)	
C(231)	59140(20)	58420(40)	35770(30)	1040(20)	
C(232)	62320(20)	57900(30)	33000(30)	950(20)	
O(233)	55601(18)	54880(30)	41910(20)	1390(30)	
C(234)	52580(30)	59090(50)	41530(40)	1500(50)	
C(236)	66140(30)	53860(40)	47950(30)	1150(30)	
N(237)	69812(17)	57630(20)	42169(17)	837(14)	
C(238)	66750(30)	57620(30)	45290(20)	1000(20)	
C(239)	64270(20)	62490(30)	44950(20)	910(19)	
C(240)	60740(30)	64460(40)	47070(30)	1110(30)	
C(241)	59140(30)	69030(40)	45800(30)	1140(30)	
C(242)	60700(20)	71560(30)	42310(30)	1080(30)	
C(243)	64110(20)	69560(30)	40110(20)	857(18)	
C(244)	65910(20)	64960(30)	41560(20)	809(17)	
C(245)	69350(20)	61810(30)	39950(20)	755(15)	
N(246)	71524(15)	63220(20)	36577(16)	718(12)	
N(247)	76852(15)	56703(19)	37413(16)	734(12)	
C(248)	74904(18)	60590(20)	35420(20)	742(15)	
C(249)	77366(18)	61580(20)	31773(19)	691(14)	
C(250)	76759(19)	65240(20)	28678(19)	719(14)	
C(251)	79710(20)	65330(20)	25540(20)	750(15)	
C(252)	83150(20)	61830(30)	25370(20)	874(19)	
C(253)	83700(20)	58220(20)	28450(20)	780(16)	
C(254)	80722(19)	58130(20)	31660(20)	743(15)	
C(255)	80521(18)	54960(20)	35300(20)	713(14)	
C(256)	83290(20)	51330(20)	36350(20)	773(16)	
C(257)	83830(20)	48350(30)	40150(30)	910(20)	
C(258)	82180(30)	49910(30)	43950(30)	1010(20)	
C(259)	82760(30)	46810(40)	47400(30)	1210(30)	
C(260)	85160(30)	42390(30)	47110(30)	1140(30)	
C(261)	86870(30)	40910(30)	43470(40)	1140(30)	
C(262)	86250(20)	43870(30)	39940(30)	1020(20)	
O(263)	85700(30)	39490(30)	50650(30)	1510(30)	
C(264)	87940(60)	35460(60)	51040(60)	1390(70)	0.6
C(265)	84580(110)	40900(140)	54230(120)	1600(110)	0.4
O(301)	83538(17)	49000(20)	16460(20)	1129(18)	
C(302)	86080(50)	44820(60)	15780(50)	1780(80)	0.8
C(303)	88760(70)	45900(80)	12600(60)	1590(80)	0.7
C(304)	87770(60)	46240(60)	9180(70)	1940(70)	
C(305)	88640(90)	46400(110)	4250(90)	1950(100)	0.6
O(311)	77786(17)	55770(20)	15701(18)	1001(14)	
C(312)	74730(30)	59640(40)	15030(30)	1160(30)	
C(313)	75720(50)	62020(60)	10980(40)	1730(60)	
C(314)	80740(70)	64420(80)	10790(60)	1840(70)	0.8
C(315)	81850(110)	69040(140)	7200(110)	1970(120)	0.5
C(316)	86640(120)	70460(160)	7540(120)	1980(140)	0.45
O(321)	79513(18)	68720(20)	22246(16)	987(14)	

C(322)	76070(30)	72180(30)	22100(30)	1050(20)	
C(323)	76770(50)	75830(50)	18730(30)	1680(60)	
C(324)	72190(60)	79320(110)	17920(70)	1920(120)	0.6
C(325)	72490(130)	82020(160)	13550(110)	1900(130)	0.45
C(326)	71140(110)	77210(140)	8650(100)	1910(110)	0.5
C(327)	72010(150)	78560(190)	4450(150)	1860(160)	0.35
C(329)	78630(120)	74000(170)	14960(120)	1790(130)	0.4
O(331)	85765(16)	62420(20)	22084(17)	983(14)	
C(332)	89200(20)	58690(30)	21600(20)	930(20)	
C(333)	91480(30)	59850(40)	17750(30)	1100(20)	
C(334)	95230(40)	56390(60)	17160(30)	1490(40)	
C(335)	97570(40)	57340(90)	12970(50)	2060(80)	
C(336)	101230(60)	53570(130)	12490(60)	1750(130)	0.5
C(337)	103230(90)	52930(160)	8450(110)	1950(150)	0.45
C(339)	88940(90)	60670(120)	14590(90)	1690(90)	0.5
S(3)	52652(7)	53102(8)	15300(7)	1000(5)	
C(402)	51850(30)	59000(50)	12950(30)	1220(30)	
C(403)	53890(50)	58900(40)	9170(40)	1410(40)	
C(404)	55870(40)	54550(60)	8220(30)	1350(40)	
C(405)	55650(30)	50700(30)	11290(30)	1110(30)	
C(406)	57720(30)	45860(50)	11280(30)	1280(40)	
N(407)	54358(18)	42140(20)	17317(18)	875(15)	
C(408)	57360(30)	41840(30)	14190(20)	930(20)	
C(409)	59840(30)	37350(30)	14430(30)	1060(30)	
C(410)	63250(30)	35310(40)	12260(30)	1180(30)	
C(411)	65140(30)	30950(40)	13700(40)	1280(40)	
C(412)	63840(20)	28540(40)	17290(40)	1220(30)	
C(413)	60340(20)	30400(30)	19610(30)	1010(20)	
C(414)	58510(20)	34770(30)	18080(30)	990(20)	
C(415)	55090(20)	38020(30)	19730(30)	869(19)	
N(416)	53016(16)	36660(20)	23217(19)	821(14)	
N(417)	47529(17)	43040(20)	22290(20)	846(14)	
C(418)	49600(20)	39260(30)	24350(20)	809(17)	
C(419)	47240(20)	38150(20)	28100(20)	800(17)	
C(420)	47780(20)	34640(30)	31130(20)	889(19)	
C(421)	44920(30)	34330(30)	34250(30)	940(20)	
C(422)	41330(20)	37750(30)	34400(20)	869(18)	
C(423)	40840(20)	41340(30)	31370(30)	940(20)	
C(424)	43797(19)	41630(20)	28170(20)	796(16)	
C(425)	43900(20)	44770(30)	24450(20)	843(18)	
C(426)	41150(20)	48410(30)	23410(30)	970(20)	
C(427)	40580(30)	51180(30)	19660(30)	1060(20)	
C(428)	41990(30)	49580(40)	15720(40)	1180(30)	
C(429)	41470(40)	52370(50)	12300(40)	1400(40)	
C(430)	38980(50)	56990(50)	12710(50)	1610(60)	
C(431)	37500(40)	58570(40)	16320(50)	1570(50)	
C(432)	38150(30)	55760(30)	19750(40)	1250(30)	
O(433)	38710(40)	59650(30)	8920(30)	2070(50)	
C(434)	35100(70)	64110(100)	9780(80)	1900(80)	0.7
C(435)	42400(200)	54900(300)	4100(200)	2200(200)	0.3
C(436)	49420(30)	63080(30)	14670(40)	1160(30)	
N(437)	48040(20)	60190(20)	21560(20)	956(17)	
C(438)	47580(30)	63660(30)	18330(30)	1080(30)	
C(439)	44530(30)	67590(30)	19560(30)	980(20)	
C(440)	42870(40)	72020(30)	17610(30)	1210(30)	
C(441)	39880(40)	74820(40)	19710(40)	1270(30)	
C(442)	38420(40)	73420(40)	23440(40)	1290(30)	
C(443)	40000(30)	69180(30)	25550(30)	1160(30)	
C(444)	43160(30)	66330(30)	23390(30)	1020(20)	

C(445)	45490(20)	61550(30)	24500(30)	906(19)	
N(446)	44865(18)	59370(20)	28150(20)	937(16)	
N(447)	50878(18)	53650(20)	27530(20)	871(15)	
C(448)	47350(20)	55600(30)	29460(30)	890(20)	
C(449)	46800(20)	52990(30)	33290(30)	849(18)	
C(450)	43760(20)	53600(30)	36510(30)	879(19)	
C(451)	44020(20)	50680(30)	39840(30)	879(19)	
C(452)	47290(20)	46850(30)	40120(30)	960(20)	
C(453)	50270(20)	46220(30)	36980(30)	879(19)	
C(454)	50010(20)	49310(30)	33550(20)	835(17)	
C(455)	52710(20)	49700(30)	29860(20)	841(18)	
C(456)	56210(20)	46900(30)	29200(20)	871(18)	
C(457)	59400(20)	46930(30)	25920(30)	920(20)	
C(458)	59910(20)	50890(40)	23120(30)	1050(20)	
C(459)	62830(30)	50940(40)	20040(30)	1100(30)	
C(460)	65580(30)	46700(50)	19780(30)	1270(40)	
C(461)	65320(20)	42680(40)	22570(40)	1260(40)	
C(462)	62120(20)	42930(40)	25670(30)	1030(20)	
O(463)	68500(20)	46680(30)	16640(20)	1460(30)	
C(464)	71600(40)	42630(60)	16650(50)	1900(70)	
O(501)	45010(19)	30860(20)	37410(18)	1073(16)	
C(502)	48500(30)	27430(40)	37510(30)	1170(30)	
C(503)	47710(40)	23500(50)	40850(40)	1500(40)	
C(504)	51590(120)	20650(100)	41710(80)	1800(130)	0.45
O(511)	38647(17)	37080(20)	37569(19)	1074(17)	
C(512)	35340(30)	40630(30)	38090(30)	1230(30)	
C(513)	32680(40)	39100(40)	41720(40)	1330(40)	
C(514)	28330(60)	42360(80)	41470(60)	1480(70)	0.6
C(515)	25570(60)	41410(80)	45020(60)	1420(60)	0.6
C(516)	21480(90)	43920(130)	45350(100)	1750(100)	0.5
C(517)	18840(160)	43500(200)	48930(160)	2020(180)	0.35
C(518)	35330(70)	38040(60)	45640(70)	1420(80)	0.6
C(519)	32620(70)	35950(90)	49440(70)	1570(70)	0.6
C(520)	35260(80)	35090(100)	53490(80)	1770(80)	0.6
C(521)	36870(130)	29870(160)	52630(130)	2060(140)	0.45
O(521)	41541(18)	50870(20)	43325(19)	1100(16)	
C(522)	38120(30)	54440(40)	43330(30)	1060(20)	
C(523)	36020(50)	53740(70)	47470(60)	1950(70)	
C(524)	32090(70)	53820(100)	47560(50)	1920(80)	0.8
C(525)	29430(60)	52930(70)	52430(120)	1950(160)	0.5
C(526)	25360(100)	53630(130)	52790(100)	1990(110)	0.55
O(531)	47260(20)	44270(30)	43680(20)	1230(19)	
C(532)	50420(50)	40720(60)	44180(40)	1580(50)	
C(533)	49480(70)	37750(100)	48260(70)	1880(80)	0.7
C(534)	53500(90)	34160(110)	49060(90)	1860(90)	0.6
C(535)	54040(100)	31030(120)	53270(100)	1770(100)	0.5
S(4)	-1865(5)	68717(7)	65459(7)	922(5)	
C(602)	-5800(20)	70640(30)	62020(30)	1000(20)	
C(603)	-8710(20)	66710(40)	61600(30)	1040(20)	
C(604)	-7840(30)	62290(40)	63830(30)	1170(30)	
C(605)	-4140(20)	62740(30)	66180(30)	960(20)	
C(606)	-2700(20)	58980(30)	68920(30)	970(20)	
N(607)	4428(15)	62240(20)	70279(19)	839(15)	
C(608)	1180(20)	58850(30)	70930(20)	874(19)	
C(609)	2400(19)	55220(20)	74220(30)	890(20)	
C(610)	390(20)	51190(30)	76240(30)	900(20)	
C(611)	2440(20)	48890(30)	79290(30)	1000(20)	
C(612)	6360(20)	50350(30)	80640(30)	1000(20)	
C(613)	8440(20)	54350(30)	78730(30)	940(20)	

C(614)	6419(18)	56770(30)	75540(20)	836(18)	
C(615)	7606(19)	61110(30)	72910(20)	814(17)	
N(616)	11400(15)	63470(20)	73350(19)	811(14)	
N(617)	10504(17)	68280(20)	67117(18)	822(14)	
C(618)	12609(19)	66820(30)	70550(20)	825(17)	
C(619)	16560(20)	69730(20)	70630(20)	824(17)	
C(620)	20067(19)	69450(20)	73380(30)	880(20)	
C(621)	23360(20)	72740(30)	72740(30)	930(20)	
C(622)	23370(20)	76240(20)	69410(30)	910(20)	
C(623)	20020(20)	76380(30)	66610(30)	980(20)	
C(624)	16660(20)	73000(20)	67260(30)	884(19)	
C(625)	12800(20)	72000(30)	64810(30)	912(19)	
C(626)	11870(20)	73770(30)	61090(30)	960(20)	
C(627)	8370(30)	71960(30)	58470(20)	940(20)	
C(628)	6720(30)	66970(40)	58600(30)	1170(30)	
C(629)	3280(30)	65420(40)	56290(30)	1110(30)	
C(630)	1350(30)	69020(40)	53770(30)	1080(20)	
C(631)	2930(30)	73650(30)	53340(30)	1020(20)	
C(632)	6420(20)	75210(30)	55650(20)	930(20)	
O(633)	-2310(20)	67870(30)	51560(20)	1280(20)	
C(634)	-4100(40)	63020(60)	51880(40)	1450(40)	
C(636)	-5800(20)	75250(40)	59880(20)	980(20)	
N(637)	270(20)	79570(30)	63029(19)	941(17)	
C(638)	-2950(30)	79300(30)	60090(20)	950(20)	
C(639)	-2740(30)	83580(40)	57340(30)	1080(30)	
C(640)	-4950(30)	85230(40)	53820(30)	1150(30)	
C(641)	-3500(30)	89770(50)	51840(30)	1250(30)	
C(642)	40(30)	92450(40)	53120(30)	1210(30)	
C(643)	2260(30)	90510(40)	56460(30)	1150(30)	
C(644)	890(30)	86370(30)	58530(30)	990(20)	
C(645)	2620(20)	83730(30)	62080(20)	912(19)	
N(646)	6180(20)	85380(20)	64010(20)	959(17)	
N(647)	5501(19)	79390(20)	69716(19)	896(15)	
C(648)	7460(20)	83240(30)	67450(30)	919(19)	
C(649)	11410(20)	84720(30)	69660(20)	868(18)	
C(650)	14280(20)	88440(30)	68900(30)	894(18)	
C(651)	17550(20)	89140(30)	71630(30)	910(20)	
C(652)	18010(20)	85760(30)	75070(30)	930(20)	
C(653)	14930(20)	81950(30)	75770(20)	878(18)	
C(654)	11620(20)	81490(30)	73120(20)	877(18)	
C(655)	7870(20)	78180(30)	73240(20)	847(18)	
C(656)	6910(20)	74790(30)	76170(20)	874(18)	
C(657)	3150(20)	71930(30)	77050(20)	876(19)	
C(658)	-910(20)	73270(30)	75630(30)	970(20)	
C(659)	-4500(30)	70480(30)	76600(40)	1160(30)	
C(660)	-4080(30)	66220(30)	79220(40)	1260(30)	
C(661)	-180(20)	64760(30)	80810(30)	1060(20)	
C(662)	3310(20)	67720(30)	79670(30)	930(20)	
O(663)	-7482(19)	63210(30)	80310(40)	1870(50)	
C(664)	-11510(60)	64590(80)	77620(60)	1550(60)	0.7
O(701)	27047(14)	72915(18)	74970(20)	1038(16)	
C(702)	27670(20)	69420(30)	78120(40)	1140(30)	
C(703)	32090(20)	70160(30)	79670(40)	1180(30)	
C(704)	33280(30)	66880(40)	83370(40)	1310(40)	
C(705)	37910(30)	67780(40)	84730(50)	1500(40)	
C(706)	39620(40)	64140(60)	87790(70)	1820(60)	
C(707)	37070(50)	64390(70)	91710(60)	1880(60)	
O(711)	26809(14)	79353(18)	69240(20)	1055(17)	
C(712)	26790(20)	83440(30)	66410(30)	1060(30)	
C(713)	30690(40)	86520(40)	67110(60)	1520(60)	

C(714)	30790(50)	88730(60)	71040(110)	2230(150)	0.8
C(715)	34610(70)	92720(90)	71570(70)	1740(70)	0.7
C(716)	34400(80)	95660(110)	76070(80)	1820(90)	0.6
C(717)	38590(110)	98380(140)	77150(110)	1920(110)	0.5
C(719)	31360(90)	91060(110)	64880(90)	1570(80)	0.5
O(721)	20538(16)	92841(19)	71442(19)	1001(14)	
C(722)	20380(30)	96310(30)	68000(30)	1090(30)	
C(723)	23450(30)	100590(40)	68810(50)	1450(40)	
C(724)	23960(60)	103800(50)	64980(60)	1550(70)	0.7
C(725)	26740(120)	109140(160)	65740(130)	1860(140)	0.4
O(731)	21438(14)	86559(19)	77491(19)	987(15)	
C(732)	22130(20)	82990(30)	80810(30)	1040(20)	
C(733)	26310(30)	84270(40)	82750(40)	1490(40)	
C(734)	27060(40)	80870(50)	86540(40)	1520(40)	
C(735)	31110(70)	81350(90)	88760(80)	1740(100)	0.6
C(736)	31490(90)	77980(110)	92510(80)	1780(120)	0.5
C(737)	34790(160)	78100(200)	94900(160)	1520(160)	0.25

- site occupancy, if different from 1.
* - U(iso) ($Å^2$ x 10^4)

Table 2. Molecular dimensions. Bond lengths are in Ångstroms, angles in degrees. E.s.ds are in parentheses.

S(1)-C(2)	1.741(8)	C(30)-O(33)	1.376(12)
S(1)-C(5)	1.748(7)	C(31)-C(32)	1.402(10)
C(2)-C(3)	1.408(10)	O(33)-C(34)	1.390(18)
C(2)-C(36)	1.417(11)	C(36)-C(38)	1.329(11)
C(3)-C(4)	1.375(11)	N(37)-C(45)	1.314(9)
C(4)-C(5)	1.375(10)	N(37)-C(38)	1.418(11)
C(5)-C(6)	1.422(11)	C(38)-C(39)	1.480(13)
C(6)-C(8)	1.347(9)	C(39)-C(40)	1.357(14)
N(7)-C(15)	1.351(9)	C(39)-C(44)	1.450(13)
N(7)-C(8)	1.407(8)	C(40)-C(41)	1.361(15)
C(8)-C(9)	1.449(10)	C(41)-C(42)	1.358(15)
C(9)-C(10)	1.380(10)	C(42)-C(43)	1.450(16)
C(9)-C(14)	1.408(10)	C(43)-C(44)	1.354(13)
C(10)-C(11)	1.353(12)	C(44)-C(45)	1.437(13)
C(11)-C(12)	1.430(13)	C(45)-N(46)	1.383(10)
C(12)-C(13)	1.396(10)	N(46)-C(48)	1.296(10)
C(13)-C(14)	1.372(11)	N(47)-C(48)	1.386(9)
C(14)-C(15)	1.458(9)	N(47)-C(55)	1.392(10)
C(15)-N(16)	1.372(8)	C(48)-C(49)	1.451(11)
N(16)-C(18)	1.302(8)	C(49)-C(54)	1.358(11)
N(17)-C(18)	1.387(9)	C(49)-C(50)	1.388(9)
N(17)-C(25)	1.404(8)	C(50)-C(51)	1.360(11)
C(18)-C(19)	1.452(9)	C(51)-O(121)	1.390(8)
C(19)-C(24)	1.393(9)	C(51)-C(52)	1.424(11)
C(19)-C(20)	1.416(10)	C(52)-C(53)	1.366(10)
C(20)-C(21)	1.423(9)	C(52)-O(131)	1.380(9)
C(21)-O(101)	1.331(9)	C(53)-C(54)	1.403(11)
C(21)-C(22)	1.407(10)	C(54)-C(55)	1.494(9)
C(22)-C(23)	1.371(10)	C(55)-C(56)	1.368(10)
C(22)-O(111)	1.375(7)	C(56)-C(57)	1.466(9)
C(23)-C(24)	1.387(8)	C(57)-C(58)	1.379(10)
C(24)-C(25)	1.456(9)	C(57)-C(62)	1.401(10)
C(25)-C(26)	1.359(10)	C(58)-C(59)	1.373(9)
C(26)-C(27)	1.451(10)	C(59)-C(60)	1.400(11)
C(27)-C(32)	1.385(10)	C(60)-O(63)	1.342(8)
C(27)-C(28)	1.386(10)	C(60)-C(61)	1.377(11)
C(28)-C(29)	1.343(15)	C(61)-C(62)	1.354(10)
C(29)-C(30)	1.404(16)	O(63)-C(64)	1.310(19)
C(30)-C(31)	1.357(11)	O(63)-C(65)	1.32(3)
O(101)-C(102)	1.402(9)	C(116)-C(118)	2.04(5)
C(102)-C(103)	1.500(12)	C(117)-C(119)	1.10(4)
C(103)-C(104)	1.501(15)	O(121)-C(122)	1.381(11)
C(104)-C(105)	1.575(18)	C(122)-C(123)	1.484(14)
C(105)-C(106)	1.53(3)	C(123)-C(124)	1.56(2)
C(106)-C(107)	1.47(3)	C(124)-C(125)	1.49(4)
O(111)-C(112)	1.430(9)	C(125)-C(126)	1.65(6)
C(112)-C(113)	1.495(11)	C(126)-C(127)	1.63(8)
C(113)-C(114)	1.479(15)	O(131)-C(132)	1.417(10)
C(114)-C(115)	1.550(14)	C(132)-C(133)	1.470(12)
C(115)-C(118)	1.48(4)	C(133)-C(134)	1.532(16)
C(115)-C(116)	1.65(3)	C(134)-C(135)	1.439(16)
C(116)-C(117)	1.70(3)	C(135)-C(136)	1.49(2)
C(116)-C(119)	1.71(5)	C(136)-C(137)	1.34(3)

S(2)-C(202)	1.722(9)	C(230)-O(233)	1.388(10)
S(2)-C(205)	1.731(10)	C(231)-C(232)	1.352(11)
C(202)-C(203)	1.342(13)	O(233)-C(234)	1.457(14)
C(202)-C(236)	1.441(13)	C(236)-C(238)	1.323(12)
C(203)-C(204)	1.465(16)	N(237)-C(245)	1.318(9)
C(204)-C(205)	1.362(14)	N(237)-C(238)	1.399(9)
C(205)-C(206)	1.457(13)	C(238)-C(239)	1.496(12)
C(206)-C(208)	1.348(14)	C(239)-C(244)	1.380(10)
N(207)-C(215)	1.333(10)	C(239)-C(240)	1.401(11)
N(207)-C(208)	1.399(11)	C(240)-C(241)	1.360(14)
C(208)-C(209)	1.454(12)	C(241)-C(242)	1.404(13)
C(209)-C(214)	1.390(13)	C(242)-C(243)	1.390(10)
C(209)-C(210)	1.409(13)	C(243)-C(244)	1.409(10)
C(210)-C(211)	1.372(14)	C(244)-C(245)	1.454(9)
C(211)-C(212)	1.442(15)	C(245)-N(246)	1.345(8)
C(212)-C(213)	1.358(12)	N(246)-C(248)	1.318(8)
C(213)-C(214)	1.391(10)	N(247)-C(248)	1.352(8)
C(214)-C(215)	1.468(10)	N(247)-C(255)	1.416(8)
C(215)-N(216)	1.344(10)	C(248)-C(249)	1.440(9)
N(216)-C(218)	1.296(9)	C(249)-C(254)	1.385(9)
N(217)-C(218)	1.392(8)	C(249)-C(250)	1.403(9)
N(217)-C(225)	1.426(9)	C(250)-C(251)	1.380(9)
C(218)-C(219)	1.449(11)	C(251)-O(321)	1.393(8)
C(219)-C(220)	1.392(9)	C(251)-C(252)	1.415(10)
C(219)-C(224)	1.401(9)	C(252)-O(331)	1.358(8)
C(220)-C(221)	1.400(12)	C(252)-C(253)	1.388(10)
C(221)-O(301)	1.386(10)	C(253)-C(254)	1.403(9)
C(221)-C(222)	1.397(11)	C(254)-C(255)	1.448(9)
C(222)-C(223)	1.371(11)	C(255)-C(256)	1.329(9)
C(222)-O(311)	1.380(10)	C(256)-C(257)	1.474(10)
C(223)-C(224)	1.381(10)	C(257)-C(262)	1.395(10)
C(224)-C(225)	1.463(10)	C(257)-C(258)	1.402(12)
C(225)-C(226)	1.343(9)	C(258)-C(259)	1.398(12)
C(226)-C(227)	1.458(10)	C(259)-C(260)	1.385(13)
C(227)-C(228)	1.362(11)	C(260)-C(261)	1.357(14)
C(227)-C(232)	1.446(10)	C(260)-O(263)	1.390(11)
C(228)-C(229)	1.402(11)	C(261)-C(262)	1.399(13)
C(229)-C(230)	1.423(14)	O(263)-C(265)	1.27(4)
C(230)-C(231)	1.378(14)	O(263)-C(264)	1.274(15)
O(301)-C(302)	1.370(13)	C(323)-C(324)	1.72(3)
C(302)-C(303)	1.37(2)	C(324)-C(325)	1.59(4)
C(303)-C(304)	1.16(2)	C(325)-C(326)	2.08(5)
C(304)-C(305)	1.63(3)	C(326)-C(327)	1.44(5)
O(311)-C(312)	1.409(10)	O(331)-C(332)	1.461(9)
C(312)-C(313)	1.491(15)	C(332)-C(333)	1.476(11)
C(313)-C(314)	1.69(2)	C(333)-C(339)	1.32(3)
C(314)-C(315)	1.72(4)	C(333)-C(334)	1.495(14)
C(315)-C(316)	1.55(4)	C(334)-C(335)	1.569(17)
O(321)-C(322)	1.408(10)	C(335)-C(336)	1.52(3)
C(322)-C(323)	1.469(13)	C(336)-C(337)	1.47(4)
C(323)-C(329)	1.44(4)		
S(3)-C(405)	1.727(10)	C(404)-C(405)	1.420(14)
S(3)-C(402)	1.741(12)	C(405)-C(406)	1.424(15)
C(402)-C(403)	1.388(15)	C(406)-C(408)	1.418(14)
C(402)-C(436)	1.426(15)	N(407)-C(415)	1.354(10)
C(403)-C(404)	1.331(16)	N(407)-C(408)	1.389(9)

C(408)-C(409)	1.412(13)	N(437)-C(438)	1.396(10)
C(409)-C(410)	1.387(12)	C(438)-C(439)	1.459(13)
C(409)-C(414)	1.430(13)	C(439)-C(444)	1.360(12)
C(410)-C(411)	1.366(16)	C(439)-C(440)	1.420(12)
C(411)-C(412)	1.390(15)	C(440)-C(441)	1.372(15)
C(412)-C(413)	1.420(11)	C(441)-C(442)	1.349(15)
C(413)-C(414)	1.371(12)	C(442)-C(443)	1.397(13)
C(414)-C(415)	1.470(10)	C(443)-C(444)	1.423(14)
C(415)-N(416)	1.356(9)	C(444)-C(445)	1.493(12)
N(416)-C(418)	1.322(8)	C(445)-N(446)	1.332(10)
N(417)-C(418)	1.360(9)	N(446)-C(448)	1.327(9)
N(417)-C(425)	1.411(9)	N(447)-C(448)	1.371(9)
C(418)-C(419)	1.458(10)	N(447)-C(455)	1.406(9)
C(419)-C(420)	1.360(10)	C(448)-C(449)	1.431(11)
C(419)-C(424)	1.411(9)	C(449)-C(454)	1.395(10)
C(420)-C(421)	1.358(10)	C(449)-C(450)	1.428(10)
C(421)-O(501)	1.374(9)	C(450)-C(451)	1.331(10)
C(421)-C(422)	1.436(10)	C(451)-O(521)	1.377(9)
C(422)-O(511)	1.344(9)	C(451)-C(452)	1.435(11)
C(422)-C(423)	1.372(11)	C(452)-O(531)	1.343(10)
C(423)-C(424)	1.396(10)	C(452)-C(453)	1.393(11)
C(424)-C(425)	1.463(10)	C(453)-C(454)	1.382(10)
C(425)-C(426)	1.330(10)	C(454)-C(455)	1.475(11)
C(426)-C(427)	1.431(13)	C(455)-C(456)	1.335(10)
C(427)-C(432)	1.421(13)	C(456)-C(457)	1.463(11)
C(427)-C(428)	1.422(15)	C(457)-C(462)	1.353(11)
C(428)-C(429)	1.339(14)	C(457)-C(458)	1.389(12)
C(429)-C(430)	1.445(19)	C(458)-C(459)	1.359(12)
C(430)-C(431)	1.33(2)	C(459)-C(460)	1.407(15)
C(430)-O(433)	1.421(16)	C(460)-O(463)	1.373(11)
C(431)-C(432)	1.353(16)	C(460)-C(461)	1.394(16)
O(433)-C(434)	1.65(2)	C(461)-C(462)	1.422(13)
C(436)-C(438)	1.333(14)	O(463)-C(464)	1.433(17)
N(437)-C(445)	1.299(10)		

O(501)-C(502)	1.415(11)	C(519)-C(520)	1.57(3)
C(502)-C(503)	1.519(14)	C(520)-C(521)	1.48(4)
C(503)-C(504)	1.45(3)	O(521)-C(522)	1.420(10)
O(511)-C(512)	1.400(11)	C(522)-C(523)	1.511(19)
C(512)-C(513)	1.502(13)	C(523)-C(524)	1.23(2)
C(513)-C(518)	1.55(3)	C(524)-C(525)	1.81(4)
C(513)-C(514)	1.61(2)	C(525)-C(526)	1.29(3)
C(514)-C(515)	1.47(2)	O(531)-C(532)	1.366(13)
C(515)-C(516)	1.44(3)	C(532)-C(533)	1.57(3)
C(516)-C(517)	1.44(5)	C(533)-C(534)	1.59(3)
C(518)-C(519)	1.60(3)	C(534)-C(535)	1.60(4)

S(4)-C(605)	1.734(9)	C(610)-C(611)	1.329(11)
S(4)-C(602)	1.739(8)	C(611)-C(612)	1.359(11)
C(602)-C(603)	1.381(12)	C(612)-C(613)	1.380(10)
C(602)-C(636)	1.395(13)	C(613)-C(614)	1.371(10)
C(603)-C(604)	1.392(13)	C(614)-C(615)	1.471(10)
C(604)-C(605)	1.393(11)	C(615)-N(616)	1.346(8)
C(605)-C(606)	1.401(12)	N(616)-C(618)	1.321(9)
C(606)-C(608)	1.385(10)	N(617)-C(618)	1.353(9)
N(607)-C(615)	1.348(8)	N(617)-C(625)	1.424(9)
N(607)-C(608)	1.365(9)	C(618)-C(619)	1.454(9)
C(608)-C(609)	1.481(11)	C(619)-C(624)	1.395(10)
C(609)-C(614)	1.391(9)	C(619)-C(620)	1.418(10)
C(609)-C(610)	1.393(10)	C(620)-C(621)	1.360(10)

C(621)-O(701)	1.365(9)	C(644)-C(645)	1.453(11)
C(621)-C(622)	1.419(11)	C(645)-N(646)	1.351(10)
C(622)-O(711)	1.350(8)	N(646)-C(648)	1.318(10)
C(622)-C(623)	1.394(11)	N(647)-C(648)	1.391(10)
C(623)-C(624)	1.390(10)	N(647)-C(655)	1.404(9)
C(624)-C(625)	1.470(11)	C(648)-C(649)	1.483(11)
C(625)-C(626)	1.330(11)	C(649)-C(650)	1.347(10)
C(626)-C(627)	1.470(12)	C(649)-C(654)	1.408(10)
C(627)-C(632)	1.394(10)	C(650)-C(651)	1.368(11)
C(627)-C(628)	1.403(13)	C(651)-O(721)	1.349(9)
C(628)-C(629)	1.377(13)	C(651)-C(652)	1.433(11)
C(629)-C(630)	1.385(12)	C(652)-O(731)	1.351(9)
C(630)-C(631)	1.316(13)	C(652)-C(653)	1.403(10)
C(630)-O(633)	1.389(11)	C(653)-C(654)	1.357(10)
C(631)-C(632)	1.389(12)	C(654)-C(655)	1.459(11)
O(633)-C(634)	1.389(14)	C(655)-C(656)	1.337(10)
C(636)-C(638)	1.387(12)	C(656)-C(657)	1.423(10)
N(637)-C(645)	1.349(11)	C(657)-C(662)	1.393(11)
N(637)-C(638)	1.392(9)	C(657)-C(658)	1.399(10)
C(638)-C(639)	1.436(13)	C(658)-C(659)	1.379(12)
C(639)-C(644)	1.403(13)	C(659)-C(660)	1.410(14)
C(639)-C(640)	1.407(12)	C(660)-O(663)	1.370(11)
C(640)-C(641)	1.426(15)	C(660)-C(661)	1.382(13)
C(641)-C(642)	1.374(15)	C(661)-C(662)	1.391(11)
C(642)-C(643)	1.387(13)	O(663)-C(664)	1.58(2)
C(643)-C(644)	1.348(13)		

O(701)-C(702)	1.388(11)	C(716)-C(717)	1.53(4)
C(702)-C(703)	1.484(11)	O(721)-C(722)	1.444(10)
C(703)-C(704)	1.528(14)	C(722)-C(723)	1.501(13)
C(704)-C(705)	1.535(12)	C(723)-C(724)	1.51(2)
C(705)-C(706)	1.480(19)	C(724)-C(725)	1.66(4)
C(706)-C(707)	1.51(2)	O(731)-C(732)	1.444(10)
O(711)-C(712)	1.412(10)	C(732)-C(733)	1.494(12)
C(712)-C(713)	1.480(15)	C(733)-C(734)	1.543(16)
C(713)-C(714)	1.41(3)	C(734)-C(735)	1.46(2)
C(713)-C(719)	1.41(3)	C(735)-C(736)	1.51(3)
C(714)-C(715)	1.60(3)	C(736)-C(737)	1.29(5)
C(715)-C(716)	1.66(3)		

C(2)-S(1)-C(5)	91.7(4)	C(14)-C(13)-C(12)	119.5(7)
C(3)-C(2)-C(36)	125.4(7)	C(13)-C(14)-C(9)	121.8(6)
C(3)-C(2)-S(1)	110.4(6)	C(13)-C(14)-C(15)	132.6(6)
C(36)-C(2)-S(1)	124.0(5)	C(9)-C(14)-C(15)	105.5(6)
C(4)-C(3)-C(2)	112.4(7)	N(7)-C(15)-N(16)	127.4(6)
C(5)-C(4)-C(3)	115.4(6)	N(7)-C(15)-C(14)	112.1(5)
C(4)-C(5)-C(6)	126.8(6)	N(16)-C(15)-C(14)	120.4(6)
C(4)-C(5)-S(1)	109.9(6)	C(18)-N(16)-C(15)	120.7(6)
C(6)-C(5)-S(1)	123.1(5)	C(18)-N(17)-C(25)	110.1(5)
C(8)-C(6)-C(5)	130.4(6)	N(16)-C(18)-N(17)	127.4(6)
C(15)-N(7)-C(8)	105.8(5)	N(16)-C(18)-C(19)	125.4(7)
C(6)-C(8)-N(7)	125.7(6)	N(17)-C(18)-C(19)	107.3(6)
C(6)-C(8)-C(9)	123.9(6)	C(24)-C(19)-C(20)	122.6(6)
N(7)-C(8)-C(9)	110.4(6)	C(24)-C(19)-C(18)	107.9(6)
C(10)-C(9)-C(14)	119.3(7)	C(20)-C(19)-C(18)	129.6(7)
C(10)-C(9)-C(8)	134.6(7)	C(19)-C(20)-C(21)	115.1(7)
C(14)-C(9)-C(8)	106.1(5)	O(101)-C(21)-C(22)	114.6(6)
C(11)-C(10)-C(9)	119.3(7)	O(101)-C(21)-C(20)	124.5(7)
C(10)-C(11)-C(12)	122.7(7)	C(22)-C(21)-C(20)	120.9(7)
C(13)-C(12)-C(11)	117.4(8)	C(23)-C(22)-O(111)	123.8(7)

C(23)-C(22)-C(21)	122.2(6)	N(46)-C(45)-C(44)	120.0(7)
O(111)-C(22)-C(21)	113.9(7)	C(48)-N(46)-C(45)	121.2(6)
C(22)-C(23)-C(24)	117.9(7)	C(48)-N(47)-C(55)	111.2(6)
C(23)-C(24)-C(19)	121.1(7)	N(46)-C(48)-N(47)	127.6(7)
C(23)-C(24)-C(25)	130.9(7)	N(46)-C(48)-C(49)	126.2(6)
C(19)-C(24)-C(25)	107.9(5)	N(47)-C(48)-C(49)	106.2(7)
C(26)-C(25)-N(17)	126.3(6)	C(54)-C(49)-C(50)	121.1(8)
C(26)-C(25)-C(24)	127.1(5)	C(54)-C(49)-C(48)	109.8(6)
N(17)-C(25)-C(24)	106.6(6)	C(50)-C(49)-C(48)	129.0(7)
C(25)-C(26)-C(27)	127.3(6)	C(51)-C(50)-C(49)	118.5(7)
C(32)-C(27)-C(28)	117.9(8)	C(50)-C(51)-O(121)	125.8(7)
C(32)-C(27)-C(26)	121.9(6)	C(50)-C(51)-C(52)	119.8(6)
C(28)-C(27)-C(26)	120.2(7)	O(121)-C(51)-C(52)	114.3(7)
C(29)-C(28)-C(27)	122.0(9)	C(53)-C(52)-O(131)	122.2(8)
C(28)-C(29)-C(30)	119.5(8)	C(53)-C(52)-C(51)	122.2(7)
C(31)-C(30)-O(33)	123.5(11)	O(131)-C(52)-C(51)	115.7(6)
C(31)-C(30)-C(29)	120.7(9)	C(52)-C(53)-C(54)	115.9(8)
O(33)-C(30)-C(29)	115.8(9)	C(49)-C(54)-C(53)	122.5(6)
C(30)-C(31)-C(32)	118.7(9)	C(49)-C(54)-C(55)	107.2(7)
C(27)-C(32)-C(31)	121.1(7)	C(53)-C(54)-C(55)	130.3(8)
C(30)-O(33)-C(34)	117.5(8)	C(56)-C(55)-N(47)	131.9(6)
C(38)-C(36)-C(2)	128.1(8)	C(56)-C(55)-C(54)	122.5(7)
C(45)-N(37)-C(38)	105.7(7)	N(47)-C(55)-C(54)	105.6(6)
C(36)-C(38)-N(37)	123.6(8)	C(55)-C(56)-C(57)	129.8(7)
C(36)-C(38)-C(39)	125.9(8)	C(58)-C(57)-C(62)	117.8(6)
N(37)-C(38)-C(39)	110.4(6)	C(58)-C(57)-C(56)	124.0(6)
C(40)-C(39)-C(44)	120.3(8)	C(62)-C(57)-C(56)	118.0(7)
C(40)-C(39)-C(38)	136.0(8)	C(59)-C(58)-C(57)	120.7(7)
C(44)-C(39)-C(38)	103.7(8)	C(58)-C(59)-C(60)	120.9(7)
C(39)-C(40)-C(41)	122.0(9)	O(63)-C(60)-C(61)	120.5(7)
C(42)-C(41)-C(40)	119.1(12)	O(63)-C(60)-C(59)	121.4(7)
C(41)-C(42)-C(43)	121.4(10)	C(61)-C(60)-C(59)	118.1(6)
C(44)-C(43)-C(42)	118.8(10)	C(62)-C(61)-C(60)	121.0(7)
C(43)-C(44)-C(45)	136.3(10)	C(61)-C(62)-C(57)	121.5(7)
C(43)-C(44)-C(39)	118.3(10)	C(64)-O(63)-C(65)	110.9(15)
C(45)-C(44)-C(39)	105.2(7)	C(64)-O(63)-C(60)	120.6(11)
N(37)-C(45)-N(46)	125.0(8)	C(65)-O(63)-C(60)	123.5(13)
N(37)-C(45)-C(44)	114.8(7)		

C(21)-O(101)-C(102)	119.3(5)	C(119)-C(116)-C(118)	68(2)
O(101)-C(102)-C(103)	104.9(6)	C(119)-C(117)-C(116)	72(3)
C(102)-C(103)-C(104)	113.3(8)	C(115)-C(118)-C(116)	53.3(16)
C(103)-C(104)-C(105)	110.7(10)	C(117)-C(119)-C(116)	70(3)
C(106)-C(105)-C(104)	125.0(16)	C(122)-O(121)-C(51)	116.8(7)
C(107)-C(106)-C(105)	92.3(18)	O(121)-C(122)-C(123)	111.7(11)
C(22)-O(111)-C(112)	118.4(6)	C(122)-C(123)-C(124)	111.9(14)
O(111)-C(112)-C(113)	109.6(7)	C(125)-C(124)-C(123)	109.6(19)
C(114)-C(113)-C(112)	114.6(8)	C(124)-C(125)-C(126)	123(3)
C(113)-C(114)-C(115)	114.5(9)	C(127)-C(126)-C(125)	112(5)
C(118)-C(115)-C(114)	109(2)	C(52)-O(131)-C(132)	116.9(6)
C(118)-C(115)-C(116)	81(2)	O(131)-C(132)-C(133)	109.7(8)
C(114)-C(115)-C(116)	108.1(9)	C(132)-C(133)-C(134)	111.8(9)
C(115)-C(116)-C(117)	113.0(15)	C(135)-C(134)-C(133)	116.1(12)
C(115)-C(116)-C(119)	96(2)	C(134)-C(135)-C(136)	117.8(17)
C(117)-C(116)-C(119)	37.7(15)	C(137)-C(136)-C(135)	130(3)
C(115)-C(116)-C(118)	46.0(14)		
C(117)-C(116)-C(118)	103(2)	Etc, etc, etc.	

Table 3. Anisotropic displacement parameters ($Å^2$ x 10^4) for the expression:

$$\exp\{-2\pi^2(h^2a^{*2}U_{11} + \ldots + 2hka^*b^*U_{12})\}$$

E.s.ds are in parentheses.

	U_{11}	U_{22}	U_{33}	U_{23}	U_{13}	U_{12}
S(1)	76.4(9)	78.3(9)	89.3(10)	14.4(8)	-17.2(8)	-16.7(7)
C(2)	79(4)	93(4)	79(4)	8(4)	-14(3)	-13(3)
C(3)	90(4)	95(5)	98(5)	6(4)	-2(4)	-12(4)
C(4)	68(4)	88(4)	105(5)	20(4)	-3(3)	-22(3)
C(5)	69(4)	68(3)	117(5)	14(4)	-18(4)	-10(3)
C(6)	64(3)	76(4)	107(5)	15(4)	-25(3)	-9(3)
N(7)	58(3)	72(3)	101(4)	7(3)	-18(3)	-8(2)
C(8)	64(3)	61(3)	107(5)	9(3)	-20(3)	-3(3)
C(9)	67(3)	71(3)	114(5)	14(4)	-30(3)	-12(3)
C(10)	63(3)	74(4)	152(7)	-1(5)	-24(4)	1(3)
C(11)	80(4)	75(4)	173(8)	-24(5)	-33(5)	-3(3)
C(12)	69(4)	94(5)	165(8)	-39(5)	-18(4)	9(3)
C(13)	65(3)	87(4)	148(7)	-18(5)	-24(4)	-11(3)
C(14)	64(3)	71(3)	109(5)	-13(4)	-23(3)	3(3)
C(15)	62(3)	72(3)	98(4)	2(3)	-19(3)	-4(3)
N(16)	64(3)	78(3)	102(4)	-5(3)	-14(3)	-8(2)
N(17)	66(3)	68(3)	89(3)	0(3)	-16(3)	-3(2)
C(18)	75(3)	62(3)	94(5)	7(3)	-22(3)	-10(3)
C(19)	64(3)	78(4)	95(4)	12(4)	-21(3)	2(3)
C(20)	72(4)	79(4)	103(5)	2(4)	-25(4)	-8(3)
C(21)	60(3)	77(4)	120(5)	18(4)	-17(4)	-5(3)
C(22)	64(3)	72(4)	111(5)	12(4)	-27(4)	-12(3)
C(23)	63(3)	63(3)	100(4)	9(3)	-23(3)	-10(3)
C(24)	66(3)	68(3)	96(4)	11(3)	-25(3)	-1(3)
C(25)	58(3)	68(3)	102(5)	11(3)	-30(3)	-8(3)
C(26)	80(4)	69(3)	90(4)	-5(3)	-32(4)	-5(3)
C(27)	83(4)	74(4)	84(4)	-2(3)	-28(3)	7(3)
C(28)	200(9)	77(4)	61(4)	-3(4)	-23(5)	27(5)
C(29)	245(13)	112(7)	55(4)	9(4)	7(6)	83(8)
C(30)	122(6)	133(7)	70(4)	15(5)	4(4)	67(6)
C(31)	73(4)	112(5)	84(4)	-10(4)	-11(3)	28(4)
C(32)	65(3)	95(4)	81(4)	-7(3)	-12(3)	5(3)
O(33)	204(8)	197(8)	92(4)	51(5)	66(5)	127(7)
C(34)	108(7)	253(16)	123(8)	74(10)	41(6)	97(9)
C(36)	106(5)	100(5)	75(4)	10(4)	-13(4)	-26(4)
N(37)	116(4)	84(3)	76(3)	6(3)	-21(3)	-26(3)
C(38)	110(5)	106(5)	78(4)	14(4)	-19(4)	-27(4)
C(39)	133(6)	114(6)	70(4)	14(4)	-10(4)	-43(5)
C(40)	169(8)	134(7)	65(5)	6(5)	7(5)	-51(6)
C(41)	236(13)	187(12)	72(5)	-23(7)	13(7)	-99(11)
C(42)	234(13)	179(11)	83(6)	-47(7)	34(7)	-96(11)
C(43)	217(11)	116(7)	91(6)	-18(5)	9(7)	-73(7)
C(44)	182(9)	116(6)	64(4)	0(4)	-21(5)	-39(6)
C(45)	122(6)	97(5)	72(4)	10(4)	-14(4)	-47(4)
N(46)	115(4)	93(4)	84(4)	-1(3)	-23(3)	-28(3)
N(47)	91(3)	73(3)	78(3)	7(3)	-17(3)	-18(3)
C(48)	98(5)	70(4)	86(5)	10(4)	-20(4)	-22(3)
C(49)	94(4)	65(3)	94(5)	8(4)	-32(4)	-14(3)
C(50)	83(4)	65(3)	108(5)	9(3)	-27(4)	-11(3)
C(51)	84(4)	68(4)	114(5)	18(4)	-36(4)	-6(3)
C(52)	63(3)	86(4)	114(5)	31(4)	-18(4)	-5(3)

C(53)	85(4)	74(4)	112(5)	22(4)	-28(4)	-6(3)
C(54)	80(4)	65(3)	120(6)	19(4)	-30(4)	-11(3)
C(55)	73(4)	75(4)	110(5)	25(4)	-28(4)	-10(3)
C(56)	87(4)	58(3)	96(4)	5(3)	-29(3)	-9(3)
C(57)	86(4)	70(3)	76(4)	6(3)	-20(3)	-6(3)
C(58)	93(4)	74(4)	81(4)	0(3)	-18(3)	-12(3)
C(59)	89(4)	81(4)	101(5)	-4(4)	-5(4)	-11(3)
C(60)	85(4)	86(4)	111(5)	-15(4)	-20(4)	-8(4)
C(61)	105(5)	79(4)	106(5)	-14(4)	-30(4)	1(4)
C(62)	86(4)	82(4)	109(5)	-2(4)	-19(4)	4(3)
O(63)	95(3)	118(4)	147(5)	-30(4)	-24(3)	-26(3)
O(101)	63(2)	93(3)	119(4)	0(3)	-2(2)	-14(2)
C(102)	87(5)	107(5)	110(6)	-7(5)	-5(4)	-16(4)
C(103)	120(6)	100(5)	128(7)	5(5)	4(5)	-26(5)
C(104)	176(10)	129(8)	165(10)	-16(8)	41(9)	-71(8)
C(105)	209(16)	142(11)	168(13)	-4(10)	114(13)	-5(11)
C(107)	140(14)	180(20)	169(18)	2(16)	4(14)	-27(14)
O(111)	64(2)	78(3)	133(4)	14(3)	-21(2)	-17(2)
C(112)	73(4)	80(4)	117(5)	2(4)	-18(4)	-7(3)
C(113)	88(5)	95(5)	173(9)	0(6)	-24(5)	-20(4)
C(114)	106(6)	128(7)	188(11)	35(8)	-43(7)	-24(5)
C(115)	131(8)	134(8)	244(15)	61(10)	-40(9)	-62(7)
C(116)	116(12)	230(20)	300(30)	150(20)	-78(17)	-116(15)
O(121)	83(3)	68(2)	155(5)	5(3)	-34(3)	-15(2)
C(122)	99(5)	85(5)	163(8)	3(6)	-36(5)	-20(4)
C(123)	142(9)	139(9)	330(20)	-41(13)	-78(12)	-38(8)
C(124)	146(10)	147(10)	300(20)	-59(13)	-39(12)	-38(8)
O(131)	86(3)	77(3)	127(4)	11(3)	-20(3)	0(2)
C(132)	100(5)	87(5)	117(6)	22(5)	-6(5)	4(4)
C(133)	84(5)	118(6)	148(8)	24(6)	-2(5)	8(4)
C(134)	141(8)	122(7)	163(10)	39(8)	25(8)	19(6)
C(135)	195(13)	175(12)	167(12)	13(10)	69(11)	12(10)
C(136)	220(20)	210(20)	139(15)	38(15)	91(16)	83(18)
S(2)	114.6(13)	95.0(12)	104.5(14)	17.2(11)	33.0(12)	9.6(10)
C(202)	129(7)	107(6)	130(7)	28(6)	48(6)	16(5)
C(203)	199(11)	138(8)	132(8)	46(7)	88(8)	33(8)
C(204)	174(10)	140(9)	153(9)	48(8)	72(8)	31(8)
C(205)	143(7)	108(6)	111(6)	24(5)	41(6)	5(5)
C(206)	138(7)	95(5)	145(8)	35(6)	44(7)	20(5)
N(207)	101(4)	71(3)	123(5)	10(4)	24(4)	1(3)
C(208)	105(5)	86(5)	150(8)	14(5)	29(6)	-3(4)
C(209)	108(5)	78(4)	146(7)	6(5)	22(5)	12(4)
C(210)	135(7)	87(5)	149(8)	18(6)	17(6)	-6(5)
C(211)	141(7)	67(4)	166(9)	10(5)	-4(7)	22(5)
C(212)	111(6)	93(5)	149(8)	3(6)	3(6)	15(5)
C(213)	94(5)	71(4)	120(6)	-8(4)	7(4)	7(3)
C(214)	89(4)	73(4)	132(7)	1(4)	14(4)	5(3)

Etc, etc, etc.

Table 4. Hydrogen coordinates (x 10^4) and isotropic displacement parameters ($Å^2$ x 10^3). All hydrogen atoms were included in idealised positions with U(iso)'s set at 1.2*U(eq) or, for the methyl group hydrogen atoms, 1.5*U(eq) of the parent carbon atoms.

	x	y	z	U(iso)	S.o.f.#
H(3)	1369	6663	5030	113	
H(4)	1545	5942	4601	105	
H(6)	2071	5656	4039	99	
H(10)	2260	5057	3496	116	
H(11)	2577	4635	2962	131	
H(12)	3247	4899	2689	131	
H(13)	3610	5578	3020	120	
H(20)	4517	6698	3340	101	
H(23)	4617	7849	4472	91	
H(26)	3967	7740	4892	96	
H(28)	3387	8089	5322	135	
H(29)	2820	7955	5748	165	
H(31)	2762	6475	5389	107	
H(32)	3333	6628	4936	96	
H(34A)	1958	6697	6086	242	
H(34B)	2101	6555	5629	242	
H(34C)	2413	6437	6006	242	
H(36)	1638	7580	5196	112	
H(40)	1625	8396	5622	147	
H(41)	1742	9187	5911	198	
H(42)	2337	9650	5724	199	
H(43)	2790	9366	5176	170	
H(50)	3820	9066	4329	103	
H(53)	3978	7961	3191	108	
H(58)	2315	7594	3586	99	
H(59)	1721	7157	3354	108	
H(61)	2479	6223	2690	116	
H(62)	3062	6689	2886	111	
H(64A)	1308	6817	3124	240	0.7
H(64B)	1227	6722	2645	240	0.7
H(64C)	1112	6285	2971	240	0.7
H(65A)	2004	5890	2552	153	0.3
H(65B)	1516	5746	2637	153	0.3
H(65C)	1631	6183	2312	153	0.3
H(10A)	5019	7004	2844	122	
H(10B)	5237	6578	3134	122	
H(10C)	5907	6966	3046	139	
H(10D)	5697	7412	2778	139	
H(10E)	5543	6835	2252	188	
H(10F)	5721	6370	2523	188	
H(10G)	6208	7174	2153	208	0.8
H(10H)	6404	6884	2536	208	0.8
H(10I)	6738	6622	1911	200	0.6
H(10J)	6499	6132	2116	200	0.6
H(10K)	6205	6302	1453	246	0.6
H(10L)	5856	6386	1804	246	0.6
H(10M)	6091	6868	1603	246	0.6
H(11A)	5313	8169	4524	108	
H(11B)	5021	8528	4241	108	
H(11C)	5684	8915	4376	142	

H(11D)	5923	8440	4169	142	
H(11E)	5381	9118	3741	169	
H(11F)	5635	8652	3537	169	
H(11G)	6208	9986	3852	305	0.45
H(11H)	5702	9919	3813	305	0.45
H(11I)	5950	9679	4197	305	0.45
H(12A)	4456	9431	4457	139	
H(12B)	4210	9810	4151	139	
H(12C)	4857	10162	3941	244	
H(12D)	5112	9770	4228	244	
H(12E)	4551	10563	4540	236	
H(12F)	4795	10163	4830	236	
H(13A)	4397	8341	2738	122	
H(13B)	4669	7948	3011	122	
H(13C)	5290	8383	2870	140	
H(13D)	5030	8821	2633	140	
H(13E)	5076	7780	2360	170	
H(13F)	4828	8224	2121	170	
H(13G)	5709	8144	2219	215	
H(13H)	5480	8627	2018	215	
H(13I)	5406	7649	1687	229	0.65
H(13J)	5260	8166	1480	229	0.65
H(13K)	5740	7795	1138	276	0.5
H(13L)	5913	8330	1310	276	0.5
H(13M)	6061	7805	1520	276	0.5
H(203)	6564	4584	5323	188	
H(204)	7017	3793	5217	187	
H(206)	7528	3408	4682	151	
H(210)	8048	2733	4486	148	
H(211)	8574	2258	4160	150	
H(212)	8825	2489	3493	141	
H(213)	8520	3181	3159	114	
H(220)	8312	4360	2355	104	
H(223)	7244	5629	2197	102	
H(226)	6808	5590	2781	102	
H(228)	6610	4679	3584	118	
H(229)	6080	4776	4089	134	
H(231)	5727	6128	3563	125	
H(232)	6272	6048	3098	114	
H(23A)	5053	5895	4380	225	
H(23B)	5412	6235	4162	225	
H(23C)	5105	5881	3892	225	
H(236)	6422	5458	5013	138	
H(240)	5950	6266	4931	133	
H(241)	5690	7056	4733	136	
H(242)	5941	7466	4144	130	
H(243)	6519	7122	3774	103	
H(250)	7442	6755	2874	86	
H(253)	8603	5589	2838	94	
H(256)	8529	5051	3426	93	
H(258)	8067	5305	4417	121	
H(259)	8150	4775	4994	145	
H(261)	8850	3785	4331	137	
H(262)	8747	4283	3741	123	
H(26A)	8886	3427	4833	209	0.6
H(26B)	9046	3621	5272	209	0.6
H(26C)	8624	3279	5237	209	0.6
H(26D)	8285	4401	5403	241	0.4
H(26E)	8291	3818	5553	241	0.4
H(26F)	8713	4160	5588	241	0.4

H(30A)	8775	4401	1827	214	0.8
H(30B)	8429	4181	1509	214	0.8
H(30C)	9016	4918	1330	190	0.7
H(30D)	9103	4326	1268	190	0.7
H(30E)	8613	4947	940	233	
H(30F)	8553	4356	918	233	
H(30G)	8592	4688	280	292	0.6
H(30H)	9056	4925	360	292	0.6
H(30I)	8995	4318	338	292	0.6
H(31A)	7488	6223	1724	139	
H(31B)	7182	5816	1501	139	
H(31C)	7365	6481	1045	207	
H(31D)	7537	5942	880	207	
H(31E)	8272	6153	1032	220	0.8
H(31F)	8141	6585	1353	220	0.8
H(31G)	8121	6774	442	236	0.5
H(31H)	8007	7210	771	236	0.5
H(31I)	8732	7310	550	297	0.45
H(31J)	8724	7176	1030	297	0.45
H(31K)	8838	6741	702	297	0.45
H(32A)	7585	7405	2473	126	
H(32B)	7337	7030	2165	126	
H(32C)	6967	7704	1801	231	0.6
H(32D)	7188	8194	2009	231	0.6
H(32E)	7541	8341	1319	227	0.45
H(32F)	7048	8494	1349	227	0.45
H(32G)	7266	7396	919	229	0.5
H(32H)	6805	7643	881	229	0.5
H(32I)	7112	7575	265	279	0.35
H(32J)	7042	8166	374	279	0.35
H(32K)	7507	7918	412	279	0.35
H(32L)	7890	7685	1302	269	0.4
H(32M)	8147	7258	1553	269	0.4
H(32N)	7681	7134	1378	269	0.4
H(33A)	8801	5518	2150	111	
H(33B)	9119	5890	2395	111	
H(33C)	9425	5279	1727	179	
H(33D)	9727	5691	1944	179	
H(33E)	9553	5692	1068	247	
H(33F)	9868	6088	1289	247	
H(33G)	10350	5460	1444	210	0.5
H(33H)	10019	5018	1338	210	0.5
H(33I)	10552	5039	864	293	0.45
H(33J)	10108	5176	647	293	0.45
H(33K)	10441	5621	754	293	0.45
H(33L)	9066	6141	1215	253	0.5
H(33M)	8720	5761	1409	253	0.5
H(33N)	8707	6358	1518	253	0.5
H(403)	5388	6176	737	170	
H(404)	5733	5406	569	162	
H(406)	5960	4523	905	154	
H(410)	6425	3691	983	141	
H(411)	6744	2952	1219	154	
H(412)	6533	2559	1821	146	
H(413)	5934	2875	2203	122	
H(420)	5017	3239	3107	107	
H(423)	3850	4364	3145	113	
H(426)	3921	4933	2552	116	
H(428)	4339	4637	1549	142	
H(429)	4267	5136	975	168	

H(431)	3597	6170	1650	188	
H(432)	3696	5688	2228	150	
H(43A)	3470	6616	729	285	0.7
H(43B)	3239	6250	1054	285	0.7
H(43C)	3607	6632	1202	285	0.7
H(436)	4904	6591	1288	140	
H(440)	4380	7301	1496	145	
H(441)	3879	7786	1850	152	
H(442)	3622	7539	2468	155	
H(443)	3905	6826	2822	139	
H(450)	4156	5609	3627	105	
H(453)	5244	4370	3720	105	
H(456)	5673	4441	3126	104	
H(458)	5808	5377	2337	126	
H(459)	6301	5371	1815	132	
H(461)	6722	3985	2242	151	
H(462)	6190	4022	2760	123	
H(46A)	7350	4302	1428	285	
H(46B)	7328	4280	1919	285	
H(46C)	7013	3933	1650	285	
H(50A)	5117	2933	3808	140	
H(50B)	4880	2571	3482	140	
H(50C)	4673	2525	4338	180	
H(50D)	4543	2111	3997	180	
H(50E)	5103	1813	4387	270	0.45
H(50F)	5253	1889	3921	270	0.45
H(50G)	5382	2301	4262	270	0.45
H(51A)	3354	4074	3560	148	
H(51B)	3655	4409	3854	148	
H(51C)	2904	4605	4133	177	0.6
H(51D)	2678	4144	3892	177	0.6
H(51E)	2505	3768	4514	171	0.6
H(51F)	2723	4232	4750	171	0.6
H(51G)	2199	4761	4491	210	0.5
H(51H)	1974	4272	4300	210	0.5
H(51I)	1622	4545	4853	303	0.35
H(51J)	1812	3987	4939	303	0.35
H(51K)	2039	4480	5132	303	0.35
H(51L)	3677	4125	4647	171	0.6
H(51M)	3758	3551	4498	171	0.6
H(51N)	3030	3841	5003	189	0.6
H(51O)	3128	3267	4865	189	0.6
H(52A)	3761	3760	5377	212	0.6
H(52B)	3343	3518	5596	212	0.6
H(52C)	3864	2871	5493	309	0.45
H(52D)	3446	2753	5228	309	0.45
H(52E)	3859	2992	5012	309	0.45
H(52F)	3609	5370	4108	127	
H(52G)	3920	5798	4301	127	
H(52H)	3698	5043	4861	234	
H(52I)	3708	5647	4931	234	
H(52J)	3104	5114	4567	230	0.8
H(52K)	3114	5716	4643	230	0.8
H(52L)	3003	4938	5333	234	0.5
H(52M)	3084	5523	5443	234	0.5
H(52N)	2450	5298	5564	298	0.55
H(52O)	2466	5717	5206	298	0.55
H(52P)	2385	5129	5096	298	0.55
H(53A)	5323	4243	4435	190	
H(53B)	5045	3833	4183	190	

H(53C)	4685	3567	4798	226	0.7
H(53D)	4909	4017	5057	226	0.7
H(53E)	5608	3632	4876	223	0.6
H(53F)	5358	3162	4681	223	0.6
H(53G)	5669	2906	5318	266	0.5
H(53H)	5413	3343	5558	266	0.5
H(53I)	5161	2870	5361	266	0.5
H(603)	-1116	6701	5990	125	
H(604)	-956	5930	6375	140	
H(606)	-460	5623	6944	117	
H(610)	-239	5011	7545	108	
H(611)	110	4607	8060	120	
H(612)	766	4864	8289	120	
H(613)	1120	5539	7960	113	
H(620)	2011	6706	7557	106	
H(623)	2002	7868	6436	117	
H(626)	1362	7643	6004	115	
H(628)	804	6455	6037	141	
H(629)	226	6201	5641	133	
H(631)	167	7595	5144	123	
H(632)	750	7858	5530	112	
H(63A)	-665	6282	5015	217	
H(63B)	-202	6046	5099	217	
H(63C)	-490	6237	5474	217	
H(636)	-809	7569	5799	117	
H(640)	-734	8338	5280	138	
H(641)	-504	9100	4954	150	
H(642)	92	9550	5178	145	
H(643)	482	9215	5730	138	
H(650)	1404	9053	6653	107	
H(653)	1517	7973	7806	105	
H(656)	918	7417	7803	105	
H(658)	-120	7621	7393	116	
H(659)	-721	7141	7552	139	
H(661)	10	6190	8259	127	
H(662)	602	6680	8076	111	
H(66A)	-1391	6241	7843	233	0.7
H(66B)	-1226	6819	7804	233	0.7
H(66C)	-1085	6402	7472	233	0.7
H(70A)	2730	6589	7709	137	
H(70B)	2559	7002	8035	137	
H(70C)	3246	7380	8041	142	
H(70D)	3411	6939	7741	142	
H(70E)	3289	6322	8268	157	
H(70F)	3134	6770	8568	157	
H(70G)	3976	6766	8226	179	
H(70H)	3812	7128	8588	179	
H(70I)	4265	6498	8838	219	
H(70J)	3951	6063	8667	219	
H(70K)	3825	6196	9370	225	
H(70L)	3722	6786	9284	225	
H(70M)	3409	6351	9114	282	0.3
H(71A)	2422	8559	6682	128	
H(71B)	2676	8211	6357	128	
H(71C)	3110	8598	7311	267	0.8
H(71D)	2805	9049	7156	267	0.8
H(71E)	3447	9530	6935	208	0.7
H(71F)	3737	9090	7133	208	0.7
H(71G)	3206	9821	7602	218	0.6
H(71H)	3373	9313	7823	218	0.6

H(71I)	3140	9029	6194	236	0.5
H(71J)	2905	9348	6547	236	0.5
H(71K)	3410	9258	6568	236	0.5
H(72A)	1745	9767	6766	131	
H(72B)	2118	9449	6544	131	
H(72C)	2625	9917	6964	174	
H(72D)	2237	10274	7108	174	
H(72E)	2109	10472	6393	186	0.7
H(72F)	2540	10173	6285	186	0.7
H(72G)	2695	11104	6315	279	0.4
H(72H)	2529	11126	6779	279	0.4
H(72I)	2961	10827	6671	279	0.4
H(73A)	2217	7945	7975	125	
H(73B)	1980	8328	8285	125	
H(73C)	2634	8792	8357	178	
H(73D)	2864	8373	8074	178	
H(73E)	2473	8156	8852	183	
H(73F)	2677	7726	8567	183	
H(73G)	3147	8496	8961	209	0.6
H(73H)	3347	8051	8685	209	0.6
H(73I)	2898	7871	9425	214	0.5
H(73J)	3119	7440	9156	214	0.5
H(73K)	3441	7564	9713	228	0.25
H(73L)	3735	7721	9332	228	0.25
H(73M)	3512	8154	9604	228	0.25

- site occupancy, if different from 1.

Table 5. Torsion angles, in degrees. E.s.ds are in parentheses.

C(5)-S(1)-C(2)-C(3)	2.0(6)	C(22)-C(23)-C(24)-C(25)	178.6(6)
C(5)-S(1)-C(2)-C(36)	177.0(6)	C(20)-C(19)-C(24)-C(23)	0.3(9)
C(36)-C(2)-C(3)-C(4)	-178.3(7)	C(18)-C(19)-C(24)-C(23)	-178.7(5)
S(1)-C(2)-C(3)-C(4)	-3.4(8)	C(20)-C(19)-C(24)-C(25)	-176.5(6)
C(2)-C(3)-C(4)-C(5)	3.4(10)	C(18)-C(19)-C(24)-C(25)	4.6(6)
C(3)-C(4)-C(5)-C(6)	-177.7(7)	C(18)-N(17)-C(25)-C(26)	-179.5(6)
C(3)-C(4)-C(5)-S(1)	-1.8(8)	C(18)-N(17)-C(25)-C(24)	0.4(6)
C(2)-S(1)-C(5)-C(4)	-0.2(5)	C(23)-C(24)-C(25)-C(26)	0.4(10)
C(2)-S(1)-C(5)-C(6)	175.9(6)	C(19)-C(24)-C(25)-C(26)	176.7(6)
C(4)-C(5)-C(6)-C(8)	-171.3(7)	C(23)-C(24)-C(25)-N(17)	-179.5(6)
S(1)-C(5)-C(6)-C(8)	13.2(10)	C(19)-C(24)-C(25)-N(17)	-3.2(6)
C(5)-C(6)-C(8)-N(7)	6.1(11)	N(17)-C(25)-C(26)-C(27)	5.6(10)
C(5)-C(6)-C(8)-C(9)	-171.8(6)	C(24)-C(25)-C(26)-C(27)	-174.3(6)
C(15)-N(7)-C(8)-C(6)	-176.1(6)	C(25)-C(26)-C(27)-C(32)	27.7(10)
C(15)-N(7)-C(8)-C(9)	2.0(7)	C(25)-C(26)-C(27)-C(28)	-151.4(7)
C(6)-C(8)-C(9)-C(10)	-1.2(12)	C(32)-C(27)-C(28)-C(29)	-0.6(11)
N(7)-C(8)-C(9)-C(10)	-179.3(7)	C(26)-C(27)-C(28)-C(29)	178.5(7)
C(6)-C(8)-C(9)-C(14)	176.1(6)	C(27)-C(28)-C(29)-C(30)	0.0(13)
N(7)-C(8)-C(9)-C(14)	-2.1(7)	C(28)-C(29)-C(30)-C(31)	1.8(13)
C(14)-C(9)-C(10)-C(11)	-1.0(10)	C(28)-C(29)-C(30)-O(33)	-178.2(7)
C(8)-C(9)-C(10)-C(11)	176.0(7)	O(33)-C(30)-C(31)-C(32)	177.2(7)
C(9)-C(10)-C(11)-C(12)	-0.7(12)	C(29)-C(30)-C(31)-C(32)	-2.9(11)
C(10)-C(11)-C(12)-C(13)	2.5(13)	C(28)-C(27)-C(32)-C(31)	-0.5(9)
C(11)-C(12)-C(13)-C(14)	-2.6(12)	C(26)-C(27)-C(32)-C(31)	-179.6(6)
C(12)-C(13)-C(14)-C(9)	1.0(11)	C(30)-C(31)-C(32)-C(27)	2.2(9)
C(12)-C(13)-C(14)-C(15)	-176.6(8)	C(31)-C(30)-O(33)-C(34)	3.9(12)
C(10)-C(9)-C(14)-C(13)	0.9(10)	C(29)-C(30)-O(33)-C(34)	-176.1(9)
C(8)-C(9)-C(14)-C(13)	-176.9(6)	C(3)-C(2)-C(36)-C(38)	-180.0(8)
C(10)-C(9)-C(14)-C(15)	179.0(6)	S(1)-C(2)-C(36)-C(38)	5.8(11)
C(8)-C(9)-C(14)-C(15)	1.3(7)	C(2)-C(36)-C(38)-N(37)	2.9(13)
C(8)-N(7)-C(15)-N(16)	-179.2(6)	C(2)-C(36)-C(38)-C(39)	-173.5(8)
C(8)-N(7)-C(15)-C(14)	-1.2(7)	C(45)-N(37)-C(38)-C(36)	-174.3(8)
C(13)-C(14)-C(15)-N(7)	177.8(7)	C(45)-N(37)-C(38)-C(39)	2.5(9)
C(9)-C(14)-C(15)-N(7)	-0.1(7)	C(36)-C(38)-C(39)-C(40)	-4.3(16)
C(13)-C(14)-C(15)-N(16)	-4.1(11)	N(37)-C(38)-C(39)-C(40)	178.9(10)
C(9)-C(14)-C(15)-N(16)	178.0(6)	C(36)-C(38)-C(39)-C(44)	172.9(8)
N(7)-C(15)-N(16)-C(18)	11.6(10)	N(37)-C(38)-C(39)-C(44)	-3.8(9)
C(14)-C(15)-N(16)-C(18)	-166.2(6)	C(44)-C(39)-C(40)-C(41)	3.3(16)
C(15)-N(16)-C(18)-N(17)	-0.2(10)	C(38)-C(39)-C(40)-C(41)	-179.7(11)
C(15)-N(16)-C(18)-C(19)	179.1(6)	C(39)-C(40)-C(41)-C(42)	-4(2)
C(25)-N(17)-C(18)-N(16)	-178.2(6)	C(40)-C(41)-C(42)-C(43)	3(2)
C(25)-N(17)-C(18)-C(19)	2.3(6)	C(41)-C(42)-C(43)-C(44)	-2(2)
N(16)-C(18)-C(19)-C(24)	176.2(6)	C(42)-C(43)-C(44)-C(45)	176.9(12)
N(17)-C(18)-C(19)-C(24)	-4.3(7)	C(42)-C(43)-C(44)-C(39)	1.6(16)
N(16)-C(18)-C(19)-C(20)	-2.6(11)	C(40)-C(39)-C(44)-C(43)	-2.2(15)
N(17)-C(18)-C(19)-C(20)	176.8(6)	C(38)-C(39)-C(44)-C(43)	-180.0(9)
C(24)-C(19)-C(20)-C(21)	-0.9(9)	C(40)-C(39)-C(44)-C(45)	-178.8(8)
C(18)-C(19)-C(20)-C(21)	177.8(6)	C(38)-C(39)-C(44)-C(45)	3.4(9)
C(19)-C(20)-C(21)-O(101)	-179.8(6)	C(38)-N(37)-C(45)-N(46)	175.5(7)
C(19)-C(20)-C(21)-C(22)	-1.5(9)	C(38)-N(37)-C(45)-C(44)	-0.2(9)
O(101)-C(21)-C(22)-C(23)	-176.9(6)	C(43)-C(44)-C(45)-N(37)	-177.9(12)
C(20)-C(21)-C(22)-C(23)	4.6(9)	C(39)-C(44)-C(45)-N(37)	-2.2(10)
O(101)-C(21)-C(22)-O(111)	2.4(8)	C(43)-C(44)-C(45)-N(46)	6.2(17)
C(20)-C(21)-C(22)-O(111)	-176.0(6)	C(39)-C(44)-C(45)-N(46)	-178.1(8)
O(111)-C(22)-C(23)-C(24)	175.6(5)	N(37)-C(45)-N(46)-C(48)	11.2(12)
C(21)-C(22)-C(23)-C(24)	-5.1(9)	C(44)-C(45)-N(46)-C(48)	-173.4(7)
C(22)-C(23)-C(24)-C(19)	2.7(8)	C(45)-N(46)-C(48)-N(47)	5.7(11)

```
C(45)-N(46)-C(48)-C(49)    -176.3(7)
C(55)-N(47)-C(48)-N(46)     177.7(7)
C(55)-N(47)-C(48)-C(49)      -0.6(7)
N(46)-C(48)-C(49)-C(54)    -179.3(7)
N(47)-C(48)-C(49)-C(54)      -0.9(7)
N(46)-C(48)-C(49)-C(50)      -2.1(12)
N(47)-C(48)-C(49)-C(50)     176.3(6)
C(54)-C(49)-C(50)-C(51)      -0.6(10)
C(48)-C(49)-C(50)-C(51)    -177.5(6)
C(49)-C(50)-C(51)-O(121)    179.1(6)
C(49)-C(50)-C(51)-C(52)       0.0(9)
C(50)-C(51)-C(52)-C(53)       0.1(9)
O(121)-C(51)-C(52)-C(53)   -179.0(6)
C(50)-C(51)-C(52)-O(131)   -178.7(6)
O(121)-C(51)-C(52)-O(131)     2.1(8)
O(131)-C(52)-C(53)-C(54)    179.0(6)
C(51)-C(52)-C(53)-C(54)       0.2(9)
C(50)-C(49)-C(54)-C(53)       1.0(10)
C(48)-C(49)-C(54)-C(53)     178.4(6)
C(50)-C(49)-C(54)-C(55)    -175.6(6)
C(48)-C(49)-C(54)-C(55)       1.9(7)
C(52)-C(53)-C(54)-C(49)      -0.8(9)
C(52)-C(53)-C(54)-C(55)     174.9(6)
C(48)-N(47)-C(55)-C(56)    -175.2(6)
C(48)-N(47)-C(55)-C(54)       1.7(7)
C(49)-C(54)-C(55)-C(56)     175.1(6)
C(53)-C(54)-C(55)-C(56)      -1.1(10)
C(49)-C(54)-C(55)-N(47)      -2.2(7)
C(53)-C(54)-C(55)-N(47)    -178.4(6)
N(47)-C(55)-C(56)-C(57)       7.6(11)
C(54)-C(55)-C(56)-C(57)    -168.9(6)
C(55)-C(56)-C(57)-C(58)      20.0(11)
C(55)-C(56)-C(57)-C(62)    -164.5(7)
C(62)-C(57)-C(58)-C(59)      -1.0(10)
C(56)-C(57)-C(58)-C(59)     174.5(6)
C(57)-C(58)-C(59)-C(60)       1.8(11)
C(58)-C(59)-C(60)-O(63)     178.2(7)
C(58)-C(59)-C(60)-C(61)      -0.3(12)
O(63)-C(60)-C(61)-C(62)     179.6(8)
C(59)-C(60)-C(61)-C(62)      -1.9(12)
C(60)-C(61)-C(62)-C(57)       2.7(12)
C(58)-C(57)-C(62)-C(61)      -1.2(11)
C(56)-C(57)-C(62)-C(61)    -177.0(7)
C(61)-C(60)-O(63)-C(64)    -163.7(12)
C(59)-C(60)-O(63)-C(64)      17.9(16)
C(61)-C(60)-O(63)-C(65)     -11.1(19)
C(59)-C(60)-O(63)-C(65)     170.5(16)

C(22)-C(21)-O(101)-C(102)    179.3(6)
C(20)-C(21)-O(101)-C(102)     -2.3(10)
C(21)-O(101)-C(102)-C(103)  -177.5(7)
O(101)-C(102)-C(103)-C(104) -176.6(9)
C(102)-C(103)-C(104)-C(105) -176.0(11)
C(103)-C(104)-C(105)-C(106)  158.8(17)
C(104)-C(105)-C(106)-C(107)   59(2)
C(23)-C(22)-O(111)-C(112)     -5.8(9)
C(21)-C(22)-O(111)-C(112)    174.9(5)
C(22)-O(111)-C(112)-C(113)  -172.7(6)
O(111)-C(112)-C(113)-C(114)   61.4(10)
C(112)-C(113)-C(114)-C(115)  178.1(10)
C(113)-C(114)-C(115)-C(118)  -78(2)
C(113)-C(114)-C(115)-C(116) -163.5(16)
C(118)-C(115)-C(116)-C(117)   86(3)
C(114)-C(115)-C(116)-C(117) -168(2)
C(118)-C(115)-C(116)-C(119)   50(3)
C(114)-C(115)-C(116)-C(119)  157(2)
C(114)-C(115)-C(116)-C(118)  107(2)
C(115)-C(116)-C(117)-C(119)  -69(4)
C(118)-C(116)-C(117)-C(119)  -22(4)
C(114)-C(115)-C(118)-C(116) -106.1(12)
C(115)-C(116)-C(119)-C(117)  120(3)
C(118)-C(116)-C(119)-C(117)  157(4)
C(50)-C(51)-O(121)-C(122)     -2.8(10)
C(52)-C(51)-O(121)-C(122)    176.3(6)
C(51)-O(121)-C(122)-C(123)   178.5(9)
O(121)-C(122)-C(123)-C(124) -177.2(11)
C(122)-C(123)-C(124)-C(125)  178.5(19)
C(123)-C(124)-C(125)-C(126)   27(4)
C(124)-C(125)-C(126)-C(127)  167(4)
C(53)-C(52)-O(131)-C(132)     1.9(9)
C(51)-C(52)-O(131)-C(132)   -179.3(6)
C(52)-O(131)-C(132)-C(133)   177.8(6)
O(131)-C(132)-C(133)-C(134) -173.9(7)
C(132)-C(133)-C(134)-C(135) -178.5(10)
C(133)-C(134)-C(135)-C(136) -173.9(13)
C(134)-C(135)-C(136)-C(137) -170(3)

C(205)-S(2)-C(202)-C(203)     -1.1(11)
C(205)-S(2)-C(202)-C(236)    179.0(10)
C(236)-C(202)-C(203)-C(204) -176.4(12)
S(2)-C(202)-C(203)-C(204)      3.7(17)
C(202)-C(203)-C(204)-C(205)   -5.1(19)
C(203)-C(204)-C(205)-C(206) -179.1(12)
C(203)-C(204)-C(205)-S(2)      4.2(16)
C(202)-S(2)-C(205)-C(204)     -2.0(10)
C(202)-S(2)-C(205)-C(206)   -178.7(11)
C(204)-C(205)-C(206)-C(208)  173.5(13)
S(2)-C(205)-C(206)-C(208)    -10.2(18)
C(205)-C(206)-C(208)-N(207)   -2.9(19)
C(205)-C(206)-C(208)-C(209)  173.5(11)
C(215)-N(207)-C(208)-C(206)  175.5(10)
C(215)-N(207)-C(208)-C(209)   -1.3(10)
C(206)-C(208)-C(209)-C(214) -173.2(10)
N(207)-C(208)-C(209)-C(214)    3.7(10)
C(206)-C(208)-C(209)-C(210)   -0.6(18)
```

Etc, etc, etc.

Table 6. 'Weak' hydrogen bonds, in Ångstroms and degrees.

D-H...A	d(D-H)	d(H...A)	d(D...A)	<(DHA)
C(20)-H(20)...N(446)	0.95	2.63	3.568(8)	170.8
C(23)-H(23)...O(633)#3	0.95	2.47	3.394(7)	164.6
C(220)-H(220)...N(616)#4	0.95	2.52	3.465(7)	171.2
C(302)-H(30A)...N(616)#4	0.99	2.58	3.378(14)	138.1
C(450)-H(450)...N(16)	0.95	2.59	3.530(7)	169.8

Symmetry transformations used to generate equivalent atoms:
#1 -x+1,-y+2,z-1/2 #2 -x+1,-y+2,z+1/2
#3 x+1/2,-y+3/2,z #4 -x+1,-y+1,z-1/2

Crystal structure analysis of

thiophene-{(CH-NC_8H_4)-NH-($NC_8H_2(OC_6H_{13})_2$)-CH-C_6H_4-OMe}$_2$

Crystal data: $C_{71.65}H_{64.64}N_6O_6S$, M = 1137.79. Orthorhombic, space group $Pna2_1$ (no. 33), a = 31.3301(4), b = 26.1402(4), c = 32.5934(6) Å, V = 26,693.2(7) Å^3. Z = 16, Dc = 1.132 g cm^{-3}, F(000) = 9609, T = 100(2) K, μ(Cu-Kα) = 0.858 mm^{-1}, λ(Cu-Kα) = 1.54184 Å.

The crystal was a blue block. From a sample under oil, one, *ca* 0.43 x 0.17 x 0.05 mm, was mounted on a small loop and fixed in the cold nitrogen stream on a Rigaku Oxford Diffraction XtaLAB Synergy diffractometer, equipped with Cu-Kα radiation, HyPix detector and mirror monochromator. Intensity data were measured by thin-slice ω-scans. Total no. of reflections recorded, to θ_{max} = 70°, was 107,970 of which 42,351 were unique (Rint = 0.050); 26,458 were 'observed' with $I > 2\sigma_I$.

Data were processed using the CrysAlisPro-CCD and -RED (1) programs. The structure was determined by the intrinsic phasing routines in the SHELXT program (2A) and refined by full-matrix least-squares methods, on F^2's, in SHELXL (2B). There are four almost identical molecules in the asymmetric unit. Each molecule may be described in parts – the head (the thiophene ring), the body (the two bis-isoindole chains) and the tails (the four hexyloxy chains dangling off the ends). The head and body parts were well-defined with all non-hydrogen atoms refined anisotropicacally. Some of the tail chains were less well-defined, with disordered groups; some of these were refined anisotropically, others isotropically; others appeared to be merging into a sea of indistinct chain units. Few hydrogen atoms were located in the difference maps; many were included where possible in idealised positions and were set to ride on the parent carbon atoms; no amino hydrogen atoms were located or included. At the conclusion of the refinement, wR_2 = 0.277 and R_1 = 0.128 (2B) for all 42,351 reflections weighted $w = [\sigma^2(F_o^2) + (0.1966\ P)^2]^{-1}$ with $P = (F_o^2 + 2F_c^2)/3$; for the 'observed' data only, R_1 = 0.091.

In the final difference map, the highest peak (*ca* 0.5 eÅ^{-3}) was near H(63a).

Scattering factors for neutral atoms were taken from reference (3). Computer programs used in this analysis have been noted above, and were run through WinGX (4) on a Dell Optiplex 780 PC at the University of East Anglia.

References

1) Programs CrysAlisPro, Rigaku Oxford Diffraction Ltd., Abingdon, UK (2018).

2) G. M. Sheldrick, Programs for crystal structure determination (SHELXT), Acta Cryst. (2015) A71, 3-8, and refinement (SHELXL), Acta Cryst. (2008) A64, 112-122 and (2015) C71, 3-8.

3) 'International Tables for X-ray Crystallography', Kluwer Academic Publishers, Dordrecht (1992). Vol. C, pp. 500, 219 and 193.

4) L. J. Farrugia, J. Appl. Cryst. (2012) 45, 849–854.

Legends for Figures

Figure 1. View of the one of the four independent molecules of the thiophene derivative molecules, indicating the atom numbering scheme. Thermal ellipsoids are drawn at the 10% probability level.

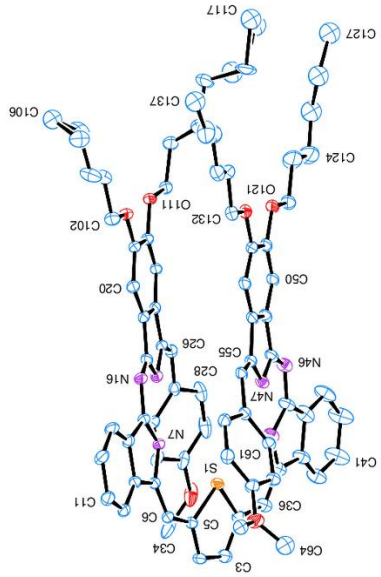

Figure 2. Showing the overlap of parallel isoindole groups, with the C(24)…C(54) distance of 3.377 Å.

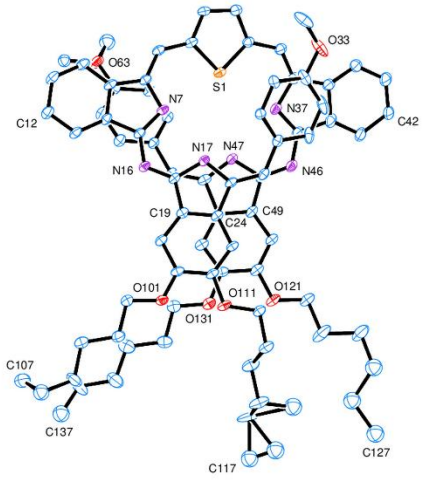

Figure 3. View along the pseudo twofold symmetry axis through S(1)/

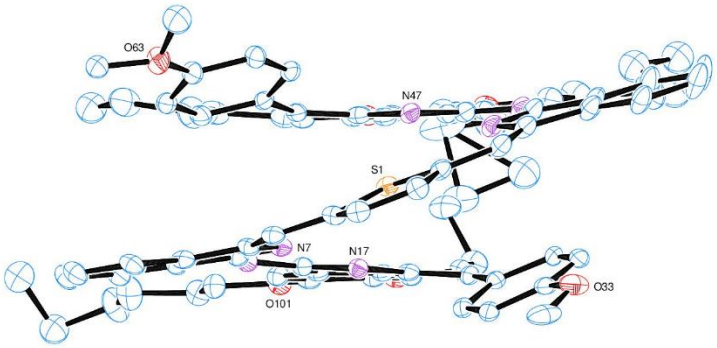

Notes on the structure

This is a large structure! Each molecule comprises $C_{78}H_{84}N_6O_6$, as Figure 1; there are four independent, very similar, molecules in the asymmetric unit; and four units in the cell… Not all of the C and H atoms are accounted for – there is disorder in some of the hexyl chains, some of these atoms appearing to float away with little evidence of anything left in the difference map.

However, the major part of the molecule, i.e. all but the hexyl chains, is well defined and was refined anistropically. A pseudo twofold symmetry axis passes through the sulphur atom, and shows the bis-isoindole chains curving away from the central thiophene plane in a spiralling fashion so that there is overlap of the isoindole planes of N(17) and N(47), Figure 2; C(24) is directly above C(54) at a distance of 3.377 Å. Figure 3 shows the three major planes in the molecule, with the thiophene ring tilted about 19 ° from each of the parallel isoindole ring planes.

There is evidence of further π…π bonding where the phenyl groups of C(27) and C(57) overlap the isoindole groups of N(37) and N(7) respectively, but the pairs of rings are rather distorted from parallel.

There are also several examples of π…π interactions between molecules, e.g. the furan rings of N(47) and N(247') are almost overlapping, parallel and *ca* 3.4 Å apart. And I am sure there are many similar intermolecular interactions in this structure…

6-Crystal data and structure refinement for $(OC_6H_{13})_2$,$(C{\equiv}CSiMe_3)_2$-triphenylene

Identification code	**2.80 (scheme 2.44)**
Elemental formula	C40 H52 O2 Si2
Formula weight	620.99
Crystal system, space group	Triclinic, P-1 (no. 2)
Unit cell dimensions	a = 8.75513(11) Å α = 74.6548(10) ° b = 18.8397(2) Å β = 80.5590(10) ° c = 23.9779(2) Å γ = 76.6264(11) °
Volume	3688.22(7) $Å^3$
Z, Calculated density	4, 1.118 Mg/m^3
F(000)	1344
Absorption coefficient	1.104 mm^{-1}
Temperature	100(2) K
Wavelength	1.54184 Å
Crystal colour, shape	yellow block
Crystal size	0.19 x 0.17 x 0.07 mm
Crystal mounting:	on a small loop, in oil, fixed in cold N_2 stream
On the diffractometer:	
Theta range for data collection	7.710 to 72.498 °
Limiting indices	-10<=h<=10, -23<=k<=23, -29<=l<=25
Completeness to theta = 67.684	99.3 %
Absorption correction	Semi-empirical from equivalents
Max. and min. transmission	1.00000 and 0.67421
Reflections collected (not including absences)	49253
No. of unique reflections	14251 [R(int) for equivalents = 0.070]
No. of 'observed' reflections ($I > 2\sigma_I$)	12219
Structure determined by:	dual methods, in SHELXT
Refinement:	Full-matrix-block least-squares on F^2, in SHELXL
Data / restraints / parameters	14251 / 0 / 797
Goodness-of-fit on F^2	1.039
Final R indices ('observed' data)	R_1 = 0.070, wR_2 = 0.199

Final R indices (all data)	R_1 = 0.078, wR_2 = 0.204
Reflections weighted: $w = [\sigma^2(Fo^2)+(0.1034P)^2+4.4588P]^{-1}$ where $P=(Fo^2+2Fc^2)/3$	
Extinction coefficient	n/a
Largest diff. peak and hole	1.22 and -0.60 e.Å^{-3}
Location of largest difference peak	near C(101)

Table 1. Atomic coordinates (x 10^5) and equivalent isotropic displacement parameters ($Å^2$ x 10^4). U(eq) is defined as one third of the trace of the orthogonalized Uij tensor. E.s.ds are in parentheses.

	x	y	z	U(eq)
C(1)	76250(30)	-15447(14)	36768(11)	276(5)
C(101)	79160(30)	-21520(17)	33564(11)	328(6)
C(102)	81620(40)	-25705(17)	30611(14)	381(7)
Si(1)	85339(10)	-32535(5)	26027(4)	458(2)
C(103)	104540(50)	-38930(30)	27590(30)	1030(20)
C(104)	69120(40)	-37825(17)	27938(15)	426(7)
C(105)	86050(70)	-27340(30)	18298(18)	930(20)
C(2)	84070(30)	-16473(14)	41694(12)	284(5)
C(3)	81100(30)	-10909(14)	44679(11)	257(5)
C(4)	70490(30)	-4096(13)	42950(10)	226(5)
C(5)	67700(30)	1913(13)	46049(10)	208(5)
C(6)	75290(30)	942(14)	51041(10)	226(5)
C(7)	73210(30)	6598(14)	53916(10)	230(5)
O(71)	79930(20)	5979(10)	58793(7)	252(4)
C(72)	90170(30)	-1076(14)	60935(10)	240(5)
C(73)	95690(30)	-792(14)	66522(10)	244(5)
C(74)	107120(30)	-8024(14)	68892(11)	252(5)
C(75)	113300(30)	-7872(14)	74443(11)	258(5)
C(76)	124120(30)	-15167(16)	77044(12)	326(6)
C(77)	131330(40)	-14730(20)	82278(13)	454(8)
C(8)	63430(30)	13614(14)	51755(10)	235(5)
O(81)	62460(20)	18976(10)	54744(8)	284(4)
C(82)	52410(30)	26101(15)	52728(12)	306(6)
C(83)	53060(30)	31177(16)	56562(13)	348(6)
C(84)	69510(40)	32556(18)	56482(14)	407(7)
C(85)	70180(40)	37700(20)	60383(17)	506(8)
C(86)	61810(50)	45700(20)	58370(20)	654(11)
C(87)	61360(60)	50480(30)	62670(30)	841(15)
C(9)	55730(30)	14570(14)	46981(10)	230(5)
C(10)	57510(30)	8762(13)	44043(10)	208(5)
C(11)	49170(30)	9853(13)	38998(10)	210(5)
C(12)	38250(30)	16491(14)	37034(10)	231(5)
C(13)	30970(30)	17728(14)	32107(11)	246(5)
C(14)	34600(30)	12291(14)	28799(10)	231(5)
C(141)	27820(30)	13829(12)	22989(11)	191(5)
C(142)	23930(30)	15310(15)	18677(14)	324(6)
Si(2)	19813(8)	17595(4)	10942(3)	295(2)
C(143)	6070(40)	26800(20)	9262(15)	511(9)
C(144)	39060(40)	17990(20)	6365(13)	445(7)
C(145)	11710(40)	10000(20)	9636(14)	468(8)
C(15)	44780(30)	5551(14)	30803(10)	236(5)
C(16)	52000(30)	4128(13)	35902(10)	216(5)
C(17)	62710(30)	-2981(13)	37962(10)	223(5)
C(18)	65710(30)	-8831(14)	35020(11)	262(5)
C(21)	71130(30)	60594(14)	77444(10)	249(5)
C(211)	81510(30)	61632(11)	71514(10)	190(5)
C(212)	87830(30)	62792(15)	67208(14)	361(6)
Si(3)	98941(9)	64373(4)	59783(3)	343(2)
C(213)	105080(40)	73581(18)	58123(14)	445(7)
C(214)	85690(50)	64690(20)	54376(16)	574(9)

C(215)	115860(40)	56338(19)	59746(14)	469(8)
C(22)	67010(30)	66209(14)	80599(11)	275(5)
C(23)	57270(30)	65166(14)	85712(11)	264(5)
C(24)	51170(30)	58576(14)	88020(10)	231(5)
C(25)	40010(30)	57653(13)	93285(10)	227(5)
C(26)	34400(30)	63557(14)	96168(11)	243(5)
C(27)	23700(30)	62888(14)	101060(11)	242(5)
O(271)	17460(20)	68449(10)	103962(8)	282(4)
C(272)	23260(30)	75305(15)	101776(12)	304(6)
C(273)	15580(40)	80513(16)	105683(13)	353(6)
C(274)	23280(40)	87478(18)	104214(14)	423(7)
C(275)	20340(40)	92708(17)	98327(14)	405(7)
C(276)	28270(50)	99508(19)	96906(17)	531(9)
C(277)	24130(60)	104890(20)	91210(20)	698(12)
C(28)	18290(30)	56065(14)	103401(10)	240(5)
O(281)	8060(20)	55796(10)	108355(7)	266(4)
C(282)	2970(30)	48780(14)	110828(11)	255(5)
C(283)	-7650(30)	49253(14)	116427(10)	246(5)
C(284)	-13320(30)	41840(14)	118915(11)	268(5)
C(285)	-24160(30)	41397(15)	124603(11)	291(5)
C(286)	-28340(40)	33616(18)	126861(13)	401(7)
C(287)	-39460(40)	32680(20)	132405(14)	506(8)
C(29)	23580(30)	50313(14)	100609(10)	240(5)
C(30)	34350(30)	50972(14)	95467(10)	229(5)
C(31)	39430(30)	44871(13)	92457(10)	235(5)
C(32)	33620(30)	38140(14)	94378(11)	284(5)
C(33)	38490(30)	32401(15)	91549(11)	310(6)
C(34)	49890(30)	33046(14)	86668(11)	296(5)
C(341)	55890(30)	26780(15)	83773(11)	329(6)
C(342)	61580(40)	21943(17)	81428(13)	399(7)
Si(4)	70621(10)	14309(4)	77667(3)	372(2)
C(343)	67970(70)	17970(20)	69870(16)	771(15)
C(344)	91700(40)	11320(19)	78811(15)	462(8)
C(345)	59990(50)	6480(20)	80760(20)	609(10)
C(35)	55500(30)	39689(14)	84636(11)	267(5)
C(36)	50310(30)	45721(14)	87372(11)	244(5)
C(37)	55950(30)	52732(14)	85027(11)	237(5)
C(38)	65680(30)	53950(14)	79726(11)	251(5)

Table 2. Molecular dimensions. Bond lengths are in Ångstroms, angles in degrees. E.s.ds are in parentheses.

C(1)-C(18)	1.378(4)	C(21)-C(38)	1.386(4)
C(1)-C(2)	1.409(4)	C(21)-C(22)	1.407(4)
C(1)-C(101)	1.493(4)	C(21)-C(211)	1.548(3)
C(101)-C(102)	1.156(4)	C(211)-C(212)	1.081(4)
C(102)-Si(1)	1.846(3)	C(212)-Si(3)	1.868(3)
Si(1)-C(104)	1.849(3)	Si(3)-C(214)	1.857(4)
Si(1)-C(105)	1.851(5)	Si(3)-C(215)	1.858(3)
Si(1)-C(103)	1.857(4)	Si(3)-C(213)	1.858(3)
C(2)-C(3)	1.374(4)	C(22)-C(23)	1.370(4)
C(3)-C(4)	1.405(3)	C(23)-C(24)	1.407(3)
C(4)-C(17)	1.417(3)	C(24)-C(37)	1.417(3)
C(4)-C(5)	1.467(3)	C(24)-C(25)	1.461(3)
C(5)-C(10)	1.404(3)	C(25)-C(30)	1.400(3)
C(5)-C(6)	1.413(3)	C(25)-C(26)	1.414(3)
C(6)-C(7)	1.379(3)	C(26)-C(27)	1.373(3)
C(7)-O(71)	1.360(3)	C(27)-O(271)	1.370(3)
C(7)-C(8)	1.417(3)	C(27)-C(28)	1.416(4)
O(71)-C(72)	1.440(3)	O(271)-C(272)	1.435(3)
C(72)-C(73)	1.514(3)	C(272)-C(273)	1.506(4)
C(73)-C(74)	1.525(3)	C(273)-C(274)	1.545(4)
C(74)-C(75)	1.526(3)	C(274)-C(275)	1.515(5)
C(75)-C(76)	1.521(4)	C(275)-C(276)	1.530(5)
C(76)-C(77)	1.523(4)	C(276)-C(277)	1.511(6)
C(8)-O(81)	1.366(3)	C(28)-O(281)	1.362(3)
C(8)-C(9)	1.373(3)	C(28)-C(29)	1.374(4)
O(81)-C(82)	1.435(3)	O(281)-C(282)	1.438(3)
C(82)-C(83)	1.507(4)	C(282)-C(283)	1.513(3)
C(83)-C(84)	1.517(4)	C(283)-C(284)	1.528(3)
C(84)-C(85)	1.531(4)	C(284)-C(285)	1.523(3)
C(85)-C(86)	1.504(6)	C(285)-C(286)	1.529(4)
C(86)-C(87)	1.529(6)	C(286)-C(287)	1.509(4)
C(9)-C(10)	1.418(3)	C(29)-C(30)	1.420(3)
C(10)-C(11)	1.458(3)	C(30)-C(31)	1.462(3)
C(11)-C(12)	1.408(3)	C(31)-C(32)	1.411(3)
C(11)-C(16)	1.420(3)	C(31)-C(36)	1.416(3)
C(12)-C(13)	1.374(3)	C(32)-C(33)	1.375(4)
C(13)-C(14)	1.406(4)	C(33)-C(34)	1.406(4)
C(14)-C(15)	1.390(4)	C(34)-C(35)	1.389(4)
C(14)-C(141)	1.535(3)	C(34)-C(341)	1.476(4)
C(141)-C(142)	1.087(4)	C(341)-C(342)	1.168(4)
C(142)-Si(2)	1.866(3)	C(342)-Si(4)	1.853(3)
Si(2)-C(145)	1.851(3)	Si(4)-C(344)	1.844(4)
Si(2)-C(143)	1.855(3)	Si(4)-C(343)	1.847(4)
Si(2)-C(144)	1.859(3)	Si(4)-C(345)	1.850(4)
C(15)-C(16)	1.403(3)	C(35)-C(36)	1.409(3)
C(16)-C(17)	1.462(3)	C(36)-C(37)	1.457(3)
C(17)-C(18)	1.414(3)	C(37)-C(38)	1.405(3)
C(18)-C(1)-C(2)	119.1(2)	C(102)-Si(1)-C(103)	107.56(18)
C(18)-C(1)-C(101)	120.6(2)	C(104)-Si(1)-C(103)	110.7(2)
C(2)-C(1)-C(101)	120.3(2)	C(38)-C(21)-C(22)	118.8(2)
C(102)-C(101)-C(1)	173.5(3)	C(38)-C(21)-C(211)	119.3(2)
C(101)-C(102)-Si(1)	178.7(3)	C(22)-C(21)-C(211)	122.0(2)
C(102)-Si(1)-C(104)	108.41(14)	C(212)-C(211)-C(21)	174.4(3)
C(102)-Si(1)-C(105)	108.60(19)	C(211)-C(212)-Si(3)	177.6(3)
C(104)-Si(1)-C(105)	110.61(19)	C(214)-Si(3)-C(215)	109.76(18)

C(214)-Si(3)-C(213)	108.61(17)	C(4)-C(17)-C(16)	120.2(2)
C(215)-Si(3)-C(213)	113.23(16)	C(1)-C(18)-C(17)	121.9(2)
C(214)-Si(3)-C(212)	109.04(16)	C(213)-Si(3)-C(212)	108.59(14)
C(215)-Si(3)-C(212)	107.54(13)	C(23)-C(22)-C(21)	119.9(2)
C(105)-Si(1)-C(103)	110.9(3)	C(22)-C(23)-C(24)	122.3(2)
C(3)-C(2)-C(1)	119.9(2)	C(23)-C(24)-C(37)	118.0(2)
C(2)-C(3)-C(4)	122.0(2)	C(23)-C(24)-C(25)	122.3(2)
C(3)-C(4)-C(17)	118.5(2)	C(37)-C(24)-C(25)	119.7(2)
C(3)-C(4)-C(5)	121.9(2)	C(30)-C(25)-C(26)	118.8(2)
C(17)-C(4)-C(5)	119.6(2)	C(30)-C(25)-C(24)	120.5(2)
C(10)-C(5)-C(6)	119.1(2)	C(26)-C(25)-C(24)	120.7(2)
C(10)-C(5)-C(4)	120.2(2)	C(27)-C(26)-C(25)	121.9(2)
C(6)-C(5)-C(4)	120.8(2)	O(271)-C(27)-C(26)	124.8(2)
C(7)-C(6)-C(5)	121.7(2)	O(271)-C(27)-C(28)	115.5(2)
O(71)-C(7)-C(6)	124.6(2)	C(26)-C(27)-C(28)	119.6(2)
O(71)-C(7)-C(8)	116.2(2)	C(27)-O(271)-C(272)	116.21(19)
C(6)-C(7)-C(8)	119.2(2)	O(271)-C(272)-C(273)	108.0(2)
C(7)-O(71)-C(72)	116.46(18)	C(272)-C(273)-C(274)	110.9(2)
O(71)-C(72)-C(73)	108.35(19)	C(275)-C(274)-C(273)	114.4(3)
C(72)-C(73)-C(74)	110.8(2)	C(274)-C(275)-C(276)	113.7(3)
C(73)-C(74)-C(75)	112.4(2)	C(277)-C(276)-C(275)	112.3(3)
C(76)-C(75)-C(74)	113.4(2)	O(281)-C(28)-C(29)	125.2(2)
C(75)-C(76)-C(77)	112.9(2)	O(281)-C(28)-C(27)	115.9(2)
O(81)-C(8)-C(9)	125.1(2)	C(29)-C(28)-C(27)	118.9(2)
O(81)-C(8)-C(7)	115.4(2)	C(28)-O(281)-C(282)	115.78(19)
C(9)-C(8)-C(7)	119.6(2)	O(281)-C(282)-C(283)	109.4(2)
C(8)-O(81)-C(82)	116.72(19)	C(282)-C(283)-C(284)	108.8(2)
O(81)-C(82)-C(83)	108.3(2)	C(285)-C(284)-C(283)	115.3(2)
C(82)-C(83)-C(84)	113.5(2)	C(284)-C(285)-C(286)	110.9(2)
C(83)-C(84)-C(85)	113.5(3)	C(287)-C(286)-C(285)	114.9(3)
C(86)-C(85)-C(84)	114.5(3)	C(28)-C(29)-C(30)	122.2(2)
C(85)-C(86)-C(87)	112.9(4)	C(25)-C(30)-C(29)	118.5(2)
C(8)-C(9)-C(10)	121.9(2)	C(25)-C(30)-C(31)	120.2(2)
C(5)-C(10)-C(9)	118.5(2)	C(29)-C(30)-C(31)	121.3(2)
C(5)-C(10)-C(11)	120.3(2)	C(32)-C(31)-C(36)	118.2(2)
C(9)-C(10)-C(11)	121.2(2)	C(32)-C(31)-C(30)	122.2(2)
C(12)-C(11)-C(16)	118.0(2)	C(36)-C(31)-C(30)	119.6(2)
C(12)-C(11)-C(10)	122.0(2)	C(33)-C(32)-C(31)	122.0(2)
C(16)-C(11)-C(10)	120.0(2)	C(32)-C(33)-C(34)	120.1(2)
C(13)-C(12)-C(11)	122.4(2)	C(35)-C(34)-C(33)	118.7(2)
C(12)-C(13)-C(14)	119.7(2)	C(35)-C(34)-C(341)	120.4(2)
C(15)-C(14)-C(13)	118.9(2)	C(33)-C(34)-C(341)	120.9(2)
C(15)-C(14)-C(141)	120.4(2)	C(342)-C(341)-C(34)	175.7(3)
C(13)-C(14)-C(141)	120.7(2)	C(341)-C(342)-Si(4)	179.7(3)
C(142)-C(141)-C(14)	173.8(2)	C(344)-Si(4)-C(343)	111.6(2)
C(141)-C(142)-Si(2)	173.2(3)	C(344)-Si(4)-C(345)	111.08(18)
C(145)-Si(2)-C(143)	111.70(18)	C(343)-Si(4)-C(345)	109.4(2)
C(145)-Si(2)-C(144)	108.24(16)	C(344)-Si(4)-C(342)	108.75(15)
C(143)-Si(2)-C(144)	110.49(17)	C(343)-Si(4)-C(342)	107.89(16)
C(145)-Si(2)-C(142)	109.81(14)	C(345)-Si(4)-C(342)	107.99(16)
C(143)-Si(2)-C(142)	109.52(14)	C(34)-C(35)-C(36)	122.0(2)
C(144)-Si(2)-C(142)	106.96(13)	C(35)-C(36)-C(31)	118.8(2)
C(14)-C(15)-C(16)	122.0(2)	C(35)-C(36)-C(37)	120.9(2)
C(15)-C(16)-C(11)	118.8(2)	C(31)-C(36)-C(37)	120.3(2)
C(15)-C(16)-C(17)	121.5(2)	C(38)-C(37)-C(24)	118.8(2)
C(11)-C(16)-C(17)	119.7(2)	C(38)-C(37)-C(36)	121.4(2)
C(18)-C(17)-C(4)	118.5(2)	C(24)-C(37)-C(36)	119.8(2)
C(18)-C(17)-C(16)	121.3(2)	C(21)-C(38)-C(37)	122.0(2)

Table 3. Anisotropic displacement parameters (Å^2 x 10^4) for the expression:

$$\exp\{-2\pi^2(h^2a^{*2}U_{11} + \ldots + 2hka^*b^*U_{12})\}$$

E.s.ds are in parentheses.

	U_{11}	U_{22}	U_{33}	U_{23}	U_{13}	U_{12}
C(1)	340(13)	194(12)	327(13)	-112(10)	-25(10)	-69(10)
C(101)	295(13)	446(17)	243(12)	-185(12)	-60(10)	66(11)
C(102)	385(15)	308(15)	455(16)	-85(13)	-59(12)	-72(12)
Si(1)	405(4)	472(5)	619(6)	-369(5)	38(4)	-117(4)
C(103)	440(20)	960(40)	2060(70)	-1160(40)	-290(30)	180(20)
C(104)	493(17)	292(15)	542(19)	-166(14)	-102(14)	-66(13)
C(105)	1310(40)	1340(50)	520(20)	-480(30)	290(30)	-1000(40)
C(2)	320(13)	182(12)	342(13)	-74(10)	-62(10)	-6(10)
C(3)	307(12)	201(12)	271(12)	-65(10)	-62(10)	-37(10)
C(4)	242(11)	188(12)	257(12)	-71(9)	-4(9)	-58(9)
C(5)	231(11)	174(11)	234(11)	-63(9)	-2(9)	-67(9)
C(6)	230(11)	188(12)	261(12)	-57(9)	-28(9)	-40(9)
C(7)	253(11)	236(12)	225(11)	-72(10)	-25(9)	-76(9)
O(71)	304(9)	219(9)	254(8)	-77(7)	-95(7)	-27(7)
C(72)	259(11)	210(12)	254(12)	-66(10)	-45(9)	-26(9)
C(73)	246(11)	247(13)	250(12)	-72(10)	-46(9)	-39(10)
C(74)	261(11)	228(12)	267(12)	-68(10)	-20(9)	-43(10)
C(75)	266(12)	238(13)	273(12)	-72(10)	-51(9)	-24(10)
C(76)	324(13)	281(14)	338(14)	-51(11)	-52(11)	-2(11)
C(77)	419(16)	499(19)	368(16)	-79(14)	-137(13)	95(14)
C(8)	278(12)	200(12)	254(12)	-101(10)	-20(9)	-56(9)
O(81)	377(10)	201(9)	314(9)	-120(7)	-110(7)	-15(7)
C(82)	373(14)	234(13)	327(13)	-112(11)	-100(11)	5(11)
C(83)	419(15)	263(14)	390(15)	-157(12)	-91(12)	3(12)
C(84)	448(16)	377(17)	444(17)	-180(14)	11(13)	-122(13)
C(85)	523(19)	470(20)	630(20)	-283(17)	-4(16)	-159(16)
C(86)	640(20)	470(20)	960(30)	-360(20)	-30(20)	-130(18)
C(87)	810(30)	660(30)	1230(40)	-560(30)	50(30)	-240(20)
C(9)	256(11)	183(12)	271(12)	-83(9)	-39(9)	-39(9)
C(10)	220(11)	179(11)	235(11)	-64(9)	-13(9)	-53(9)
C(11)	226(11)	172(11)	243(11)	-58(9)	-11(9)	-62(9)
C(12)	269(11)	195(12)	244(11)	-67(9)	-42(9)	-49(9)
C(13)	270(11)	194(12)	279(12)	-59(10)	-52(9)	-40(9)
C(14)	260(11)	227(12)	235(11)	-64(10)	-53(9)	-78(9)
C(141)	220(10)	39(9)	276(13)	-23(9)	52(9)	-26(8)
C(142)	290(13)	202(13)	518(19)	-148(12)	-2(12)	-78(10)
Si(2)	309(4)	306(4)	288(4)	-89(3)	-80(3)	-41(3)
C(143)	560(20)	480(20)	438(18)	-116(15)	-230(15)	132(16)
C(144)	405(16)	590(20)	348(15)	-101(14)	-16(12)	-140(15)
C(145)	529(18)	590(20)	407(16)	-226(15)	-60(14)	-215(16)
C(15)	271(11)	210(12)	256(12)	-83(10)	-36(9)	-68(9)
C(16)	234(11)	189(12)	241(11)	-61(9)	-22(9)	-62(9)
C(17)	242(11)	185(12)	259(12)	-84(9)	-13(9)	-50(9)
C(18)	303(12)	209(12)	304(13)	-97(10)	-53(10)	-54(10)
C(21)	225(11)	245(13)	252(12)	-66(10)	-10(9)	-1(9)
C(211)	289(11)	48(10)	245(12)	40(8)	-143(10)	-65(8)
C(212)	310(13)	229(14)	549(19)	-124(13)	-122(13)	29(11)
Si(3)	329(4)	331(4)	306(4)	-44(3)	-9(3)	1(3)
C(213)	388(15)	376(17)	474(18)	-29(14)	40(13)	-26(13)
C(214)	600(20)	650(20)	436(18)	-55(17)	-166(16)	-71(18)

C(215)	509(18)	434(18)	363(16)	-86(14)	40(13)	39(14)
C(22)	296(12)	203(12)	323(13)	-75(10)	-20(10)	-37(10)
C(23)	289(12)	201(12)	304(13)	-93(10)	-30(10)	-14(10)
C(24)	232(11)	197(12)	263(12)	-74(10)	-47(9)	-2(9)
C(25)	226(11)	198(12)	253(12)	-66(10)	-58(9)	3(9)
C(26)	264(11)	178(12)	298(12)	-79(10)	-45(9)	-29(9)
C(27)	261(11)	210(12)	273(12)	-114(10)	-53(9)	-1(9)
O(271)	321(9)	218(9)	322(9)	-133(7)	15(7)	-37(7)
C(272)	346(13)	248(13)	333(13)	-106(11)	-12(11)	-67(11)
C(273)	439(15)	304(15)	348(14)	-162(12)	-3(12)	-66(12)
C(274)	501(17)	383(17)	447(17)	-200(14)	-34(13)	-105(14)
C(275)	419(16)	316(16)	509(18)	-187(14)	-40(13)	-31(13)
C(276)	610(20)	364(18)	650(20)	-228(16)	14(17)	-103(16)
C(277)	760(30)	440(20)	770(30)	-80(20)	90(20)	-79(19)
C(28)	221(11)	256(13)	238(11)	-69(10)	-36(9)	-16(9)
O(281)	295(9)	231(9)	271(9)	-88(7)	16(7)	-49(7)
C(282)	270(12)	242(13)	261(12)	-80(10)	-26(9)	-45(10)
C(283)	258(11)	227(12)	267(12)	-86(10)	-27(9)	-47(9)
C(284)	291(12)	250(13)	283(12)	-94(10)	-41(10)	-53(10)
C(285)	316(13)	293(14)	293(13)	-84(11)	-34(10)	-99(11)
C(286)	470(17)	382(17)	392(15)	-50(13)	-58(13)	-206(14)
C(287)	534(19)	610(20)	419(17)	-15(16)	-46(14)	-332(17)
C(29)	260(11)	192(12)	266(12)	-60(10)	-39(9)	-26(9)
C(30)	231(11)	213(12)	239(11)	-55(9)	-59(9)	-8(9)
C(31)	263(11)	184(12)	258(12)	-61(9)	-72(9)	-3(9)
C(32)	362(13)	223(13)	266(12)	-61(10)	-27(10)	-55(10)
C(33)	452(15)	187(12)	301(13)	-62(10)	-60(11)	-66(11)
C(34)	402(14)	200(12)	287(13)	-78(10)	-87(11)	-5(11)
C(341)	387(14)	247(14)	250(12)	-34(11)	2(10)	85(11)
C(342)	563(18)	287(15)	355(15)	-26(12)	-140(13)	-94(13)
Si(4)	529(5)	241(4)	359(4)	-134(3)	-93(3)	1(3)
C(343)	1230(40)	560(20)	420(20)	-239(18)	-300(20)	300(30)
C(344)	502(18)	388(17)	538(19)	-228(15)	-4(15)	-73(14)
C(345)	600(20)	420(20)	910(30)	-350(20)	-90(20)	-76(17)
C(35)	318(12)	198(12)	274(12)	-85(10)	-23(10)	0(10)
C(36)	262(11)	200(12)	268(12)	-68(10)	-61(9)	-5(9)
C(37)	225(11)	206(12)	278(12)	-78(10)	-62(9)	11(9)
C(38)	240(11)	219(12)	280(12)	-89(10)	-34(9)	19(9)

Table 4. Hydrogen coordinates (x 10^4) and isotropic displacement parameters ($Å^2$ x 10^3). All hydrogen atoms were included in idealised positions with U(iso)'s set at 1.2*U(eq) or, for the methyl group hydrogen atoms, 1.5*U(eq) of the parent carbon atoms.

	x	y	z	U(iso)
H(10A)	10685	-4263	2521	155
H(10B)	11293	-3601	2667	155
H(10C)	10398	-4152	3172	155
H(10D)	7092	-4148	2554	64
H(10E)	6880	-4046	3206	64
H(10F)	5905	-3434	2723	64
H(10G)	8803	-3090	1581	139
H(10H)	7595	-2388	1761	139
H(10I)	9457	-2449	1739	139
H(2)	9138	-2100	4295	34
H(3)	8638	-1169	4801	31
H(6)	8200	-373	5245	27
H(72A)	9937	-195	5801	29
H(72B)	8441	-524	6168	29
H(73A)	8645	-6	6945	29
H(73B)	10098	353	6578	29
H(74A)	11616	-881	6589	30
H(74B)	10169	-1231	6970	30
H(75A)	11914	-372	7357	31
H(75B)	10421	-682	7736	31
H(76A)	13272	-1646	7402	39
H(76B)	11802	-1925	7824	39
H(77A)	13640	-1037	8124	68
H(77B)	13922	-1931	8345	68
H(77C)	12302	-1424	8551	68
H(82A)	4143	2544	5291	37
H(82B)	5604	2834	4864	37
H(83A)	4915	2891	6061	42
H(83B)	4590	3606	5528	42
H(84A)	7342	3483	5244	49
H(84B)	7668	2768	5776	49
H(85A)	6547	3563	6436	61
H(85B)	8139	3766	6061	61
H(86A)	5085	4575	5778	79
H(86B)	6719	4797	5457	79
H(87A)	5509	4857	6631	126
H(87B)	5657	5570	6101	126
H(87C)	7215	5022	6345	126
H(9)	4903	1926	4560	28
H(12)	3583	2025	3919	28
H(13)	2351	2223	3094	29
H(14A)	1072	3068	1000	77
H(14B)	419	2808	516	77
H(14C)	-397	2651	1173	77
H(14D)	4354	2199	700	67
H(14E)	4634	1317	743	67
H(14F)	3743	1903	226	67
H(14G)	1926	524	1057	70
H(14H)	171	959	1211	70
H(14I)	987	1116	554	70

H(15)	4691	179	2865	28
H(18)	6029	-818	3174	31
H(21A)	11209	7349	6095	67
H(21B)	11068	7455	5419	67
H(21C)	9572	7756	5835	67
H(21D)	7679	6894	5441	86
H(21E)	9158	6530	5049	86
H(21F)	8171	6001	5538	86
H(21G)	12282	5619	6260	70
H(21H)	11191	5165	6075	70
H(21I)	12178	5694	5587	70
H(22)	7097	7072	7918	33
H(23)	5454	6903	8777	32
H(26)	3813	6812	9468	29
H(27A)	2065	7763	9775	36
H(27B)	3488	7428	10175	36
H(27C)	1664	7781	10979	42
H(27D)	418	8214	10521	42
H(27E)	1922	9033	10725	51
H(27F)	3482	8577	10435	51
H(27G)	881	9451	9821	49
H(27H)	2426	8985	9528	49
H(27I)	2495	10219	10008	64
H(27J)	3987	9775	9671	64
H(27K)	2796	10234	8802	105
H(27L)	2912	10923	9056	105
H(27M)	1265	10657	9135	105
H(28A)	1227	4467	11162	31
H(28B)	-284	4768	10804	31
H(28C)	-1683	5344	11566	29
H(28D)	-177	5021	11926	29
H(28E)	-1895	4096	11598	32
H(28F)	-395	3773	11954	32
H(28G)	-3395	4524	12398	35
H(28H)	-1885	4247	12754	35
H(28I)	-3318	3253	12381	48
H(28J)	-1846	2984	12753	48
H(28K)	-3467	3358	13551	76
H(28L)	-4151	2756	13353	76
H(28M)	-4943	3629	13178	76
H(29)	1991	4574	10217	29
H(32)	2612	3756	9773	34
H(33)	3415	2799	9289	37
H(34A)	5667	1951	6942	116
H(34B)	7306	2231	6828	116
H(34C)	7276	1405	6777	116
H(34D)	9268	941	8298	69
H(34E)	9666	735	7677	69
H(34F)	9696	1561	7728	69
H(34G)	4884	821	8010	91
H(34H)	6467	233	7887	91
H(34I)	6081	474	8495	91
H(35)	6307	4018	8130	32
H(38)	6861	5011	7764	30

Table 5. Torsion angles, in degrees. E.s.ds are in parentheses.

C(18)-C(1)-C(2)-C(3)	0.1(4)	C(5)-C(4)-C(17)-C(18)	179.4(2)
C(101)-C(1)-C(2)-C(3)	-178.8(2)	C(3)-C(4)-C(17)-C(16)	-177.9(2)
C(1)-C(2)-C(3)-C(4)	-0.6(4)	C(38)-C(21)-C(22)-C(23)	-2.5(4)
C(2)-C(3)-C(4)-C(17)	-0.1(4)	C(211)-C(21)-C(22)-C(23)	177.3(2)
C(2)-C(3)-C(4)-C(5)	-178.2(2)	C(21)-C(22)-C(23)-C(24)	0.4(4)
C(3)-C(4)-C(5)-C(10)	177.3(2)	C(22)-C(23)-C(24)-C(37)	2.9(4)
C(17)-C(4)-C(5)-C(10)	-0.8(3)	C(22)-C(23)-C(24)-C(25)	-176.2(2)
C(3)-C(4)-C(5)-C(6)	-2.0(3)	C(23)-C(24)-C(25)-C(30)	-179.4(2)
C(17)-C(4)-C(5)-C(6)	179.9(2)	C(37)-C(24)-C(25)-C(30)	1.6(3)
C(10)-C(5)-C(6)-C(7)	-1.4(3)	C(23)-C(24)-C(25)-C(26)	2.5(4)
C(4)-C(5)-C(6)-C(7)	178.0(2)	C(37)-C(24)-C(25)-C(26)	-176.5(2)
C(5)-C(6)-C(7)-O(71)	178.7(2)	C(30)-C(25)-C(26)-C(27)	0.6(4)
C(5)-C(6)-C(7)-C(8)	-1.1(3)	C(24)-C(25)-C(26)-C(27)	178.8(2)
C(6)-C(7)-O(71)-C(72)	1.5(3)	C(25)-C(26)-C(27)-O(271)	-178.1(2)
C(8)-C(7)-O(71)-C(72)	-178.6(2)	C(25)-C(26)-C(27)-C(28)	1.3(4)
C(7)-O(71)-C(72)-C(73)	-176.91(19)	C(26)-C(27)-O(271)-C(272)	-2.8(3)
O(71)-C(72)-C(73)-C(74	-177.85(19)	C(28)-C(27)-O(271)-C(272)	177.7(2)
C(72)-C(73)-C(74)-C(75)	178.5(2)	C(27)-O(271)-C(272)-C(273)	-177.5(2)
C(73)-C(74)-C(75)-C(76)	177.3(2)	O(271)-C(272)-C(273)-C(274)	170.6(2)
C(74)-C(75)-C(76)-C(77)	175.1(2)	C(272)-C(273)-C(274)-C(275)	67.7(3)
O(71)-C(7)-C(8)-O(81)	2.3(3)	C(273)-C(274)-C(275)-C(276)	-179.1(3)
C(6)-C(7)-C(8)-O(81)	-177.8(2)	C(274)-C(275)-C(276)-C(277)	-175.9(3)
O(71)-C(7)-C(8)-C(9)	-177.4(2)	O(271)-C(27)-C(28)-O(281)	-2.4(3)
C(6)-C(7)-C(8)-C(9)	2.4(3)	C(26)-C(27)-C(28)-O(281)	178.1(2)
C(9)-C(8)-O(81)-C(82)	0.8(4)	O(271)-C(27)-C(28)-C(29)	177.7(2)
C(7)-C(8)-O(81)-C(82)	-178.9(2)	C(26)-C(27)-C(28)-C(29)	-1.8(4)
C(8)-O(81)-C(82)-C(83)	-179.7(2)	C(29)-C(28)-O(281)-C(282)	1.8(3)
O(81)-C(82)-C(83)-C(84)	60.4(3)	C(27)-C(28)-O(281)-C(282)	-178.1(2)
C(82)-C(83)-C(84)-C(85)	-179.9(3)	C(28)-O(281)-C(282)-C(283)	177.3(2)
C(83)-C(84)-C(85)-C(86)	-67.6(4)	O(281)-C(282)-C(283)-C(284)	178.48(19)
C(84)-C(85)-C(86)-C(87)	174.4(3)	C(282)-C(283)-C(284)-C(285)	179.8(2)
O(81)-C(8)-C(9)-C(10)	179.0(2)	C(283)-C(284)-C(285)-C(286)	-176.8(2)
C(7)-C(8)-C(9)-C(10)	-1.2(4)	C(284)-C(285)-C(286)-C(287)	-178.3(3)
C(6)-C(5)-C(10)-C(9)	2.6(3)	O(281)-C(28)-C(29)-C(30)	-179.6(2)
C(4)-C(5)-C(10)-C(9)	-176.8(2)	C(27)-C(28)-C(29)-C(30)	0.3(4)
C(6)-C(5)-C(10)-C(11)	-178.3(2)	C(26)-C(25)-C(30)-C(29)	-2.1(3)
C(4)-C(5)-C(10)-C(11)	2.3(3)	C(24)-C(25)-C(30)-C(29)	179.7(2)
C(8)-C(9)-C(10)-C(5)	-1.3(3)	C(26)-C(25)-C(30)-C(31)	177.5(2)
C(8)-C(9)-C(10)-C(11)	179.6(2)	C(24)-C(25)-C(30)-C(31)	-0.6(3)
C(5)-C(10)-C(11)-C(12)	176.7(2)	C(28)-C(29)-C(30)-C(25)	1.7(4)
C(9)-C(10)-C(11)-C(12)	-4.2(3)	C(28)-C(29)-C(30)-C(31)	-178.0(2)
C(5)-C(10)-C(11)-C(16)	-3.4(3)	C(25)-C(30)-C(31)-C(32)	-177.8(2)
C(9)-C(10)-C(11)-C(16)	175.7(2)	C(29)-C(30)-C(31)-C(32)	1.9(4)
C(16)-C(11)-C(12)-C(13)	-3.4(3)	C(25)-C(30)-C(31)-C(36)	1.0(3)
C(10)-C(11)-C(12)-C(13)	176.5(2)	C(29)-C(30)-C(31)-C(36)	-179.4(2)
C(11)-C(12)-C(13)-C(14)	-1.1(4)	C(36)-C(31)-C(32)-C(33)	1.6(4)
C(12)-C(13)-C(14)-C(15)	4.1(3)	C(30)-C(31)-C(32)-C(33)	-179.7(2)
C(12)-C(13)-C(14)-C(141)	-174.4(2)	C(31)-C(32)-C(33)-C(34)	1.6(4)
C(13)-C(14)-C(15)-C(16)	-2.5(4)	C(32)-C(33)-C(34)-C(35)	-2.9(4)
C(141)-C(14)-C(15)-C(16)	175.9(2)	C(32)-C(33)-C(34)-C(341)	176.6(3)
C(14)-C(15)-C(16)-C(11)	-1.9(3)	C(33)-C(34)-C(35)-C(36)	1.1(4)
C(14)-C(15)-C(16)-C(17)	-179.9(2)	C(341)-C(34)-C(35)-C(36)	-178.5(2)
C(12)-C(11)-C(16)-C(15)	4.8(3)	C(34)-C(35)-C(36)-C(31)	2.1(4)
C(10)-C(11)-C(16)-C(15)	-175.1(2)	C(34)-C(35)-C(36)-C(37)	-177.8(2)
C(12)-C(11)-C(16)-C(17)	-177.2(2)	C(32)-C(31)-C(36)-C(35)	-3.4(3)
C(10)-C(11)-C(16)-C(17)	2.9(3)	C(30)-C(31)-C(36)-C(35)	177.9(2)
C(3)-C(4)-C(17)-C(18)	1.3(3)	C(32)-C(31)-C(36)-C(37)	176.5(2)

C(30)-C(31)-C(36)-C(37)	-2.3(3)	C(25)-C(24)-C(37)-C(38)	175.0(2)
C(23)-C(24)-C(37)-C(38)	-4.1(3)	C(23)-C(24)-C(37)-C(36)	178.0(2)

C(5)-C(4)-C(17)-C(16)	0.3(3)
C(15)-C(16)-C(17)-C(18)	-2.6(3)
C(11)-C(16)-C(17)-C(18)	179.5(2)
C(15)-C(16)-C(17)-C(4)	176.5(2)
C(11)-C(16)-C(17)-C(4)	-1.4(3)
C(2)-C(1)-C(18)-C(17)	1.2(4)
C(101)-C(1)-C(18)-C(17)	-180.0(2)
C(4)-C(17)-C(18)-C(1)	-1.8(4)
C(16)-C(17)-C(18)-C(1)	177.3(2)
C(25)-C(24)-C(37)-C(36)	-2.9(3)
C(35)-C(36)-C(37)-C(38)	5.3(4)
C(31)-C(36)-C(37)-C(38)	-174.5(2)
C(35)-C(36)-C(37)-C(24)	-176.9(2)
C(31)-C(36)-C(37)-C(24)	3.3(3)
C(22)-C(21)-C(38)-C(37)	1.2(4)
C(211)-C(21)-C(38)-C(37)	-178.6(2)
C(24)-C(37)-C(38)-C(21)	2.1(4)
C(36)-C(37)-C(38)-C(21)	180.0(2)

Crystal structure analysis $(OC_6H_{13})_2$,$(C{\equiv}CSiMe_3)_2$-triphenylene

Crystal data: $C_{40}\,H_{52}\,O_2\,Si_2$, M = 620.99. Triclinic, space group P-1(no. 2), a = 8.75513(11), b = 18.8397(2), c = 23.9779(2) Å,α = 74.6548(10), β = 80.5590(10), γ = 76.6264(11) °, V = 3688.22(7) $Å^3$. Z = 4, Dc = 1.118 g cm^{-3}, F(000) = 1344, T = 100(2) K, μ(Cu-Kα) = 11.04 cm^{-1}, λ(Cu-Kα) = 1.54184 Å.

The crystal was a yellow block. From a sample under oil, one, *ca* 0.07 x 0.17 x 0.19 mm, was mounted on a small loop and fixed in the cold nitrogen stream on a Rigaku Oxford Diffraction XtaLAB Synergy diffractometer, equipped with Cu-Kα radiation, HyPix detector and mirror monochromator. Intensity data were measured by thin-slice ω-scans. Total no. of reflections recorded, to θ_{max} = 72.5°, was 49,253 of which 14,251 were unique (Rint = 0.070); 12,219 were 'observed' with $I > 2\sigma_I$.

Data were processed using the CrysAlisPro-CCD and -RED (1) programs. The structure was determined by the intrinsic phasing routines in the SHELXT program (2A) and refined by full-matrix least-squares methods, on F^2's, in SHELXL (2B). There are two almost identical molecules in this crystal. The non-hydrogen atoms were refined with anisotropic thermal parameters. The hydrogen atoms were included in idealised positions and their Uiso values were set to ride on the Ueq values of the parent carbon atoms. At the conclusion of the refinement, wR_2 = 0.204 and R_1 = 0.078 (2B) for all 14,251 reflections weighted $w = [\sigma^2(F_o^2) + (0.1034\,P)^2 + 4.4588\,P]^{-1}$ with $P = (F_o^2 + 2F_c^2)/3$; for the 'observed' data only, R_1 = 0.070.

In the final difference map, the highest peak (*ca* 1.2 $eÅ^{-3}$) was near C(101).

Scattering factors for neutral atoms were taken from reference (3). Computer programs used in this analysis have been noted above, and were run through WinGX (4) on a Dell Optiplex 780 PC at the University of East Anglia.

References

1) Programs CrysAlisPro, Rigaku Oxford Diffraction Ltd., Abingdon, UK (2018).

2) G. M. Sheldrick, Programs for crystal structure determination (SHELXT), Acta Cryst. (2015) A71, 3-8, and refinement (SHELXL), Acta Cryst. (2008) A64, 112-122 and (2015) C71, 3-8.

3) A. J. C. Wilson (Ed.), 'International Tables for X-ray Crystallography', Kluwer Academic Publishers, Dordrecht (1992). Vol. C, pp. 500, 219 and 193.

4) L. J. Farrugia, J. Appl. Cryst. (2012) 45, 849–854.

Legends for Figures

Figure 1. View of the two independent molecules of the triphenylene derivative. Thermal ellipsoids are drawn at the 50% probability level.

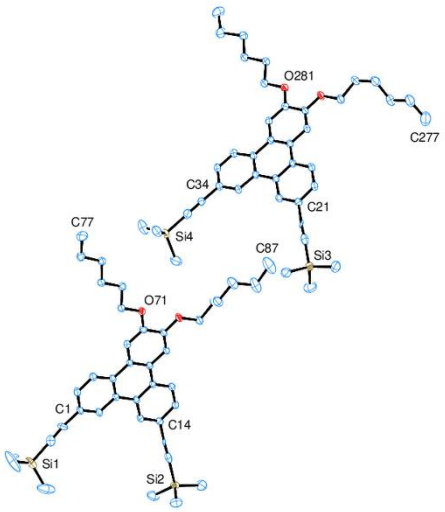

Figure 2. View of one of the independent molecules of the triphenylene derivative, showing the atom numbering scheme.

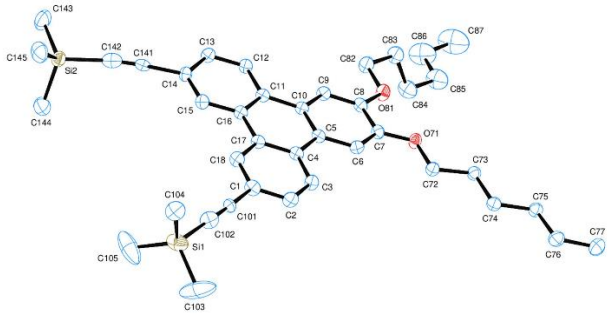

Figure 3. Side views of the two molecules along the C(2)…C(13) and C(22)…C(33) vectors, showing the pseudo-mirror symmetry between the two molecules.

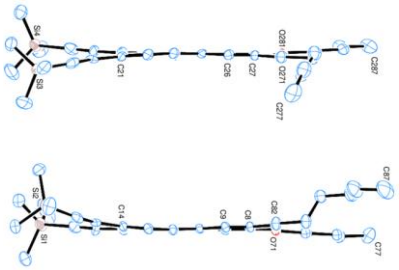

Figure 4. Views of the stacking of the molecules of C(1-18); the triphenylene rings of the O(71) and O(71^{ii}) molecules show good π…π overlap, but the rings in the O(71) and O(71^{i}) molecules are not overlapping. Note: the perpendicular axes to the triphenylene rings are vertical in the plane of the paper; and rotation about these axes gives the views in Figures 4a and 4b.

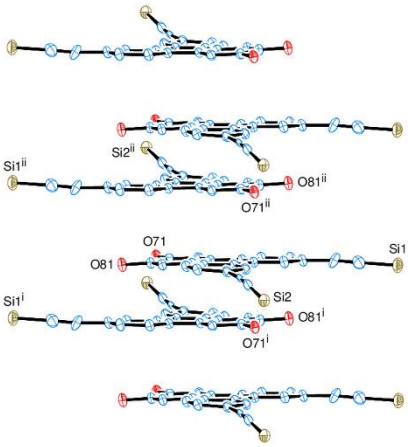

Figure 5. The overall packing, viewed along the *a* axis.

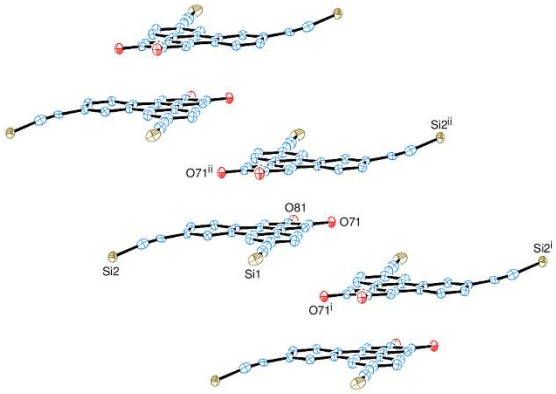

Notes on the structure

There are two very similar molecules in this crystal, Figures 1 and 2. Both molecules, except for the $SiMe_3$ groups and one of the O-hexyl groups in each molecule, are essentially planar, and their orientations are related by pseudo mirror symmetry, Figure 3. The O-hexyl groups of O(71) and O(281) show all-*trans* conformations, but those of O(81) and O(271) have a mixture of *cis* and *trans* conformations, and the fragments of chains C(83-87) and C(273-277) are quite different.

Each molecule of C(1-18) lies face-to-face with another about a centre of symmetry; the closest interactions between the two planes are between C(5) and C(5') at 3.478 Å. These dimer units are stacked parallel to the *a* axis, with the parallel planes *ca* 3.5 A apart, but with a considerable shift from overlap, Figures 4a and 4b. A very similar pattern is found in the molecules of C(21-38).